AD A027358

DDC
REPRODUCED
JUL 26 1976
B

Air Force Combat Climatology Center

REPORT ON RESEARCH

For the Period July 1975 - June 1976

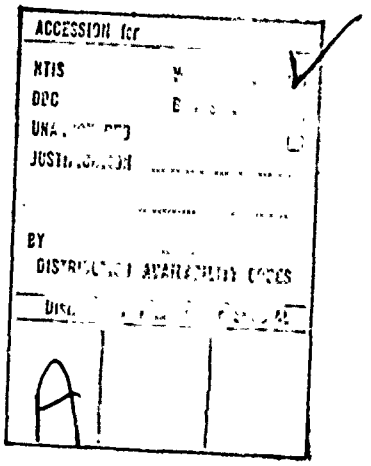

NOTE

While this document was being prepared for publication, the Department of Defense announced 111 organizational changes on November 22, 1974. Consequently, the Air Force announced plans to reorganize and realign the mission and programs of the Air Force Cambridge Research Laboratories (AFCRL). Intended was a redesignation of the AFCRL as the Air Force Geophysics Laboratory (AFGL), with the consolidation of its geophysics research, which formed the major part of AFCRL, to form the new Laboratory. AFCRL electronics research was to be transferred to a new element to be established to perform Command, Control, and Communications (C^3) research. In conjunction with ongoing programs at the Rome Air Development Center (RADC), this new organization was subsequently named the Office of the Deputy for Electronic Technology, and located at Hanscom AFB. This organization, established on January 1, 1976, was assigned to the Rome Air Development Center, to be responsive to the C^3 needs of the Electronic Systems Division at Hanscom AFB. The Air Force Cambridge Research Laboratories were redesignated as the Air Force Geophysics Laboratory on January 15, 1976.

This document has been approved for public release and sale; its distribution is unlimited.

Qualified requestors may obtain additional copies from the Defense Documentation Center. All others should apply to the Clearinghouse for Federal Scientific and Technical Information.

AFCRL-TR-75-0288

Report on Research at AFCRL

JULY 1972 – JUNE 1974

DDC
RECEIVED
JUL 26 1976
B

SURVEY OF
PROGRAMS AND
PROGRESS

THE AIR FORCE CAMBRIDGE
RESEARCH LABORATORIES
AIR FORCE
SYSTEMS COMMAND
BEDFORD, MASSACHUSETTS

MAY 1975

1972 - 1974 AIR FORCE (1) 31 JULY 1975 - 2500

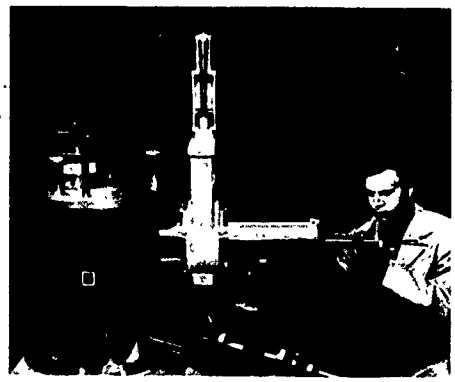

Foreword

The first *Report on Research* at the Air Force Cambridge Research Laboratories covered research during the period January 1961 through June 1962. This, the seventh report in this series, covers the period July 1972 through June 1974. The research laboratory begun as the Cambridge Field Station on September 20, 1945, has grown through almost 30 years, and has made contributions to Air Force operations, to technology, and to scientific knowledge out of all proportion to its size and to the Air Force investment in its programs. The broad span of research covered by this book has a single unifying theme — the Air Force missions of surveillance, detection, communication, and navigation. During the past few years, the Laboratories have responded to the combination of increasing demands and declining resources faced by the entire Air Force by focusing their research programs more and more closely on the operational needs of user commands. Although only a few of the programs involve operational hardware, they are all closely related to present or foreseen problems of the operational Air Force.

Bernard S. Morgan Jr.

BERNARD S. MORGAN, JR.
Colonel, USAF
Commander

Contents

I **The Air Force Cambridge Research Laboratories** 1

Organization and People ... Annual Budgets ... AFCRL Computation Center ... Field Sites ... Research Vehicles ... The AFCRL Research Library ... The Classified Program

II **Aeronomy Laboratory** 8

Atmospheric Composition ... Stratospheric Environment ... ALADDIN '74 Rocket Program ... Atmospheric Density and Structure ... Chemical Release Studies ... Solar Ultraviolet Radiation ... Design Climatology

III **Microwave Physics Laboratory** 49

Radar Systems ... Antennas ... Tropospheric Propagation ... Rotation Rate Sensors ... Hypersonic Electromagnetics ... Microwave Acoustics

IV **Aerospace Instrumentation Laboratory** 85

Free Balloons ... Tethered Balloons ... Powered Balloons ... Aircraft-Launched High-Altitude Balloon System ... Balloon Instrumentation ... High-Altitude Balloon Sampling Program ... Research Rockets ... Research Satellites

V **Space Physics Laboratory** 100

Energetic Particle Research ... Electrical Processes Research ... Geomagnetism ... Polar Upper Atmospheric Research ... Auroral Substorm Activity

VI **Meteorology Laboratory** 134

Short-Range Forecasting ... Atmospheric Modeling ... Atmospheric Boundary Layer ... Satellite Meteorology ... Weather Radar Techniques ... Warm Fog Dissipation ... Thunderstorm Electricity ... Meteorological Instrumentation ... Measurement of Ceiling and Visibility ... Aerosol Techniques

VII **Sacramento Peak Observatory** 165

The Sun ... New Instruments at Sacramento Peak ... Research Results

VIII **Terrestrial Sciences Laboratory** 192

Geodesy and Gravity ... Geokinetics ... Seismology ... Geology ... Spectroscopic Studies

IX **Optical Physics Laboratory** 213

Atmospheric Optics ... Infrared Physics ... Infrared Horizon Studies ... Radiation Effects ... Laser Physics

X **Ionospheric Physics Laboratory** 245

Trans-Ionospheric Propagation Studies . . . Solar Radio Astronomy Research . . . Global Ionospheric Fluctuations . . . Auroral Investigations . . . Propagation Studies . . . Lightning Warning and Suppression . . . Ionospheric Waveguide

XI **Solid State Sciences Laboratory** 283

Electromagnetic Materials . . . Infrared Spectroscopy and Laser Calorimetry . . . Radiation Effects and Device Hardening . . . Infrared Detector Research . . . Device Processing Technology

Appendices

A **AFCRL Projects by Program Element** 317

B **AFCRL Rocket and Satellite Program: July 1972 — June 1974** 319

C **AFCRL Organization Chart** 323

1 Air Force Cambridge Research Laboratories

The Air Force Cambridge Research Laboratories (AFCRL) has served the United States Air Force for more than 25 years by conducting basic and applied research to meet known and anticipated military needs and requirements. This report describes the programs, activities, and accomplishments of AFCRL for the period July 1, 1972 to June 30, 1974.

The largest research laboratory in the Air Force, AFCRL conducts technical programs covering a broad spectrum of disciplines in the environmental sciences and selected areas of electronics. AFCRL is an in-house laboratory with a professional staff of almost 600 scientists and engineers. Its in-house programs are supported by contractual research in universities and industry.

The research programs of AFCRL are summarized in the mission statement: *Conducts research in those areas of the environmental, physical and engineering sciences offering the greatest potential to the continued superiority of the Air Force's operational capability; conducts specifically assigned exploratory development efforts involving the environmental, physical and engineering sciences; participates in establishing advanced technologies whose exploitation will lead to new Air Force capabilities.*

ORGANIZATION AND PEOPLE: AFCRL's former headquarters organization, the Office of Aerospace Research (OAR), was deactivated on July 1, 1970, when AFCRL became a part of the Air Force Systems Command (AFSC). AFCRL became one of 12 laboratories under the Director of Science and Technology, Headquarters Air

Force Systems Command, at Andrews AFB, Maryland.

The merger of AFCRL into the Air Force Systems Command was intended to focus the research and development activities of the Laboratories more directly on evolving Air Force systems, technology, and research requirements. AFCRL's previous efforts were coupled with both immediate and long range Air Force needs, and a firm and extensive data and technology base was developed. The continuing pressure on the Air Force budget resulted in a need to utilize AFCRL's expertise in solving user-command problems, concentrating on those areas where technology can have the largest and most rapid impact on the operational Air Force.

To achieve and maintain this tight coupling, the AFCRL annual Laboratory Technical Program Reviews were reinstated to give management an overview of Laboratory programs, and two new annual reviews were begun to review the programs on finer scales. Each unit of work which can be described as a separate entity and which justifies an annual report on progress is reported separately as an In-House Work Unit. This system is designed to give management the best and most timely information possible on work unit, project, and program objectives, progress and plans.

Reductions in number of employees were directed by Systems Command Headquarters. The number of officers and airmen authorized was cut from 175 on July 1, 1972, to 156 on June 30, 1973 and to 155 on June 30, 1974. Civilian employment was reduced more sharply, from 981 on July 1, 1972 to 904 on June 30, 1974. Including the loss of 80 positions effective June 30, 1972, this amounts to a cut of more than 14 percent in the last four years.

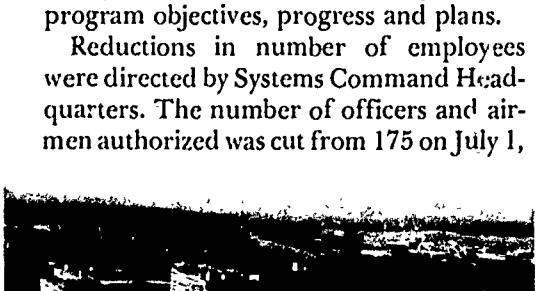

AFCRL's main laboratory complex is located at L. G. Hanscom AFB, Bedford, Mass., approximately 20 miles west of Boston.

These reductions in manpower authorizations led to the termination of the Energy Conversion, Plasma Physics, Solar Plasma Dynamics, and Space Forecasting Branches of the Space Physics Laboratory and of the Vertical Sounding Techniques Branch of the Meteorology Laboratory.

In other organizational changes, the Applications Branch of the Technical Plans and Operations Directorate was abolished, and its functions, including the AFCRL Environmental Consultation Service, were consolidated with the Technical Programs Branch. Responsibility for the Space Forecasting Program was also transferred to the Technical Programs Branch to increase management emphasis on this program. Other branches in other Laboratories were assigned revised missions, or had their names changed to emphasize their mission of greatest importance to the Air Force.

The ten Laboratories comprising AFCRL are the Aeronomy Laboratory, Aerospace Instrumentation Laboratory, Ionospheric Physics Laboratory, Meteorology Laboratory, Microwave Physics Laboratory, Optical Physics Laboratory, Sacramento Peak Observatory, Space Physics Laboratory, Solid State Sciences Laboratory, and the Terrestrial Sciences Laboratory. In addition, AFCRL operates a small West Coast Office to focus AFCRL support to the technology requirements and system development efforts of the AFSC Space and Missile Systems Organization (SAMSO) near Los Angeles.

The main AFCRL laboratory complex is located at L. G. Hanscom AFB, Bedford, Massachusetts, 20 miles west of Boston. At Hanscom AFB, AFCRL is a tenant of the Electronic Systems Division of the Air Force Systems Command.

Colonel Bernard S. Morgan, Jr., assumed command of AFCRL in January 1974, succeeding Colonel William K. Moran, Jr. Colonel Morgan came to AFCRL from the position of Chief, Command Control and Reconnaissance Division, Assistant Chief of Staff, Studies and Analysis, Hq USAF. Colonel Donald R. Wippermann, Vice Commander, reported to AFCRL on July 31, 1973.

In June 1974, 183 AFCRL employees held the doctor's degree, 202 held master's degrees, and 211 bachelor's degrees. AFCRL scientists are active in their respective professional societies. One scientist served as Editor of *Applied Optics* during the reporting period, and two other AFCRL scientists served as Associate Editor of the *IEEE Transactions on Antennas and Propagation* and the *Journal of Crystal Growth.* AFCRL scientists also served as editorial advisors and referees for various professional journals, served on professional committees, and chaired professional meetings and symposia. Examples of this type of activity include Chairman of the Wave Propagation Standards Committee on the IEEE, Executive Secretary of the U.S. Committee on Extension of the Standard Atmosphere, and President of the Professional Group on Antennas and Propagation of the IEEE, and the Commander, who served on the editorial boards of the *Journal of Dynamic Systems, Measurement and Control,* and *Computers in Mathematical Sciences with Applications.*

Of the 1059 employees at AFCRL, nearly 600 are scientists or engineers, and 183 hold the Ph.D. degree.

During the two years of this Report, AFCRL sponsored or cosponsored eight scientific conferences. AFCRL scientists and engineers authored 581 articles in scientific and professional journals. Reflecting the squeeze on travel funds, the number of papers presented at technical meetings declined by about 50 to 538, while the number of in-house reports increased by nearly 100 to 323. These publications and presentations are listed at the conclusion of each laboratory chapter.

ANNUAL BUDGETS: The annual budgets for the two years covered in this report are shown in the accompanying tables. The indicated totals cover salaries, equipment, travel, supplies, computer rental, service contracts, and those funds going into contract research. The largest expenditure is for salaries which accounted for approximately $21 million of the FY-1974 budget of $56.02 million. The annual budget decreased from $59 million in FY-1972 to $55 million in FY-1973, then increased to $56 million in FY-1974.

Funds received from AFCRL's higher headquarters, the AFSC Director of Science and Technology (DL), and, to a lesser extent, those received from AFSC organizations other than DL, are used to conduct continuing long-range programs.

AFCRL receives much support from other elements of the Air Force. The Electronic Systems Division, the host organization at Hanscom AFB, provides support such as accounting, personnel, procurement, and housekeeping to the laboratory complex. Holloman AFB, New Mexico, provides services to the Sacramento Peak Observatory and the AFCRL Balloon Detachment No. 1. Funds from other agencies are earmarked for specific research projects.

Nearly half of the AFCRL budget during the reporting period was spent for contract

TABLE 1
SOURCES OF FY-1973 FUNDS

Air Force Systems Command - DL	$42,700,000
Advanced Research Projects Agency	3,864,720
Defense Nuclear Agency	3,793,000
Air Force Systems Command Other than DL	1,988,989
National Aeronautics and Space Administration	1,009,500
Air Weather Service	588,109
Defense Mapping Agency	350,580
Atomic Energy Commission	232,210
Navy	176,640
Department of Transportation	135,000
Defense Communications Agency	50,000
Army	43,000
Air Force Technical Applications Center	14,920
TOTAL	$54,916,668

TABLE 2
SOURCES OF FY-1974 FUNDS

Air Force Systems Command - DL	$42,268,000
Defense Nuclear Agency	4,890,000
Advanced Research Projects Agency	3,850,000
Air Force Systems Command Other than DL	2,698,000
Air Weather Service	927,000
National Aeronautics and Space Administration	806,000
Atomic Energy Commission	259,000
Army	92,000
Defense Mapping Agency	85,000
Department of Transportation	48,000
Air Force Technical Applications Center	40,000
Defense Communications Agency	32,000
Navy	24,000
TOTAL	$56,019,000

research. Of the $56.02 million FY-1974 budget, $23.98 million was devoted to contract research. As of June 30, 1974, AFCRL had 370 contracts in effect. Of these, 149 were with U. S. industrial concerns, 130 were with U.S. universities, and 28 were with foreign universities and companies. The remainder were with research foundations and other government agencies.

AFCRL contracts almost always call for work in direct support of research carried out within AFCRL. They are monitored by scientists who are themselves active, participating researchers, and who plan the research, organize the program, interpret the results and share the workload of the actual research.

AFCRL COMPUTATION CENTER: A 43,000 square foot, two-story structure was occupied in November 1970 by the AFCRL Computation Center. The AFCRL Command Section, the Director of Technical Plans and Operations, and the Director of Research Services were also moved to this building at that time. One CDC 6600 computer system was installed in December 1970 and a second 6600 was installed in July 1972.

The CDC 6600 systems consist of a modular designed multiprocessor operation with extensive input-output devices, peripheral equipment and communications equipment. The systems provide remote batch, interactive graphics and con-

The AFCRL computer center was completed in November 1970. In July 1972, a second CDC-6600 computer was installed, making it one of the most powerful computer facilities in the Air Force.

versational capabilities through a network of approximately 50 remote stations located within the laboratory complex and at off-base locations. The decommutation facility processes data from satellites, rockets, aircraft, balloons and from laboratory data collection systems, using two special purpose Honeywell computer systems.

The Computation Center also provides mathematical analysis and scientific programmer services and operates a large-scale analog/hybrid computation facility in support of simulation studies.

FIELD SITES: In addition to the 90 acres which it occupies at Hanscom AFB, AFCRL operates several off-base sites, locally and at distant locations. The largest local site is the Sagamore Hill Radio Observatory in Hamilton, Massachusetts, which includes two large radio telescopes, one with an 84-foot dish, the other with a 150-foot dish. Other local sites are the Weather Radar Research Facility at Sudbury, Massachusetts, and a 350-acre Antenna Range in Ipswich, Massachusetts. A high precision millimeter wave radio telescope (15 to 100 GHz) is located on Prospect Hill in Waltham, Massachusetts.

AFCRL has large permanent sites in New Mexico and California. Balloon launch facilities are located at Holloman AFB, New Mexico, and at Chico, California. At Sunspot, New Mexico, overlooking Holloman AFB from its 9200-foot elevation, stands the Sacramento Peak Solar Observatory, perhaps the most completely instrumented facility in the world for solar optical astronomy. Its vacuum tower telescope began operating in October 1969.

The most remote permanent facility is the Geopole Observatory at Thule Air Base, Greenland, which began observations in 1958 and has yielded a 14-year continuous record of Arctic magnetic activity, auroral phenomena and ionospheric variations. Another remote station is the Goose Bay Ionospheric Observatory at Goose Bay Air Station, Labrador where studies of a variety of sub-arctic events are made, including polar cap absorption of high frequency waves.

AFCRL field programs utilize a number of military installations including the Fort Churchill, Canada, rocket range; Fort Wainwright and Eielson AFB, Alaska; Albrooke AFB, Canal Zone; Eglin AFB, Florida; Travis AFB, California; Vandenberg AFB, California, and the White Sands Missile Range, New Mexico. In addition to these military sites, AFCRL has used other locations on a temporary basis. Trailers were transported from Hanscom AFB to a 15-acre field site near Donaldson, Minnesota, for studies of small-scale meteorological phenomena. Existing facilities at Roswell, New Mexico, and Sioux Falls, South Dakota, commercial airports, and the Poker Flat, Alaska, range are also used.

RESEARCH VEHICLES: From its permanent balloon launch sites in New Mexico and California, and from temporary sites in several other locations, AFCRL launched

AFCRL scientists utilize facilities all over the world. An experiment to determine the infrared emission from high-altitude atmospheric layers required a rocket launch from the Barriero do Inferno Rocket Range in northern Brazil.

118 large research balloons during the two-year period. Of these, 73 were launched in FY-1973. In addition, 107 tethered flights were conducted. These balloons carried test and experimental payloads for the Space and Missile Systems Organization (SAMSO), the Defense Nuclear Agency (DNA), National Aeronautics and Space Administration (NASA), the Army, and university scientists with military contracts. AFCRL scientists themselves are, however, the largest users.

Rockets are used to examine almost every aspect of the earth's upper atmosphere and near-space environment—winds, temperatures and densities; the electrical structure of the ionosphere; solar ultraviolet radiation; atmospheric composition; the earth's radiation belts; cosmic ray activity; and airglow and aurora. The rockets most frequently used have been the Nike Iroquois (NIRO), the Nike Tomahawk, the Black Brant, and the Aerobee.

During the past two years, AFCRL launched a total of 93 large research rockets, which were fired from Wallops Island (20), Eglin AFB, Florida (19), Fort Churchill, Canada (16), White Sands Missile Range, New Mexico (15), and Poker Flat, Alaska (18).

During this reporting period, AFCRL-designed packages were carried aboard the Air Force S72-1 satellite and the NASA Atmosphere Explorer-C satellites.

Five research instrumented aircraft—two NKC-135's and three C-130's—gather data for various projects. The NKC-135's have been part of the AFCRL inventory for more than a decade, and two of the C-130's for almost as long. One NKC-135 and one C-130 are instrumented for measuring the transmission, scattering and reflectance of optical/IR radiation in the atmosphere. The other NKC-135 is used for performing ionospheric and associated observations all over the world, with recent emphasis on the Arctic auroral zone. Two other C-130's are instrumented for meteorological observations.

THE AFCRL RESEARCH LIBRARY: The breadth and quality of the technical collection maintained by the AFCRL Research Library are surpassed by few libraries in the country.

Available to AFCRL scientists are the scientific journals of Bulgaria, Czechoslovakia, Holland, France, Germany, Hungary, Italy, Japan, Poland, Russia and Swe-

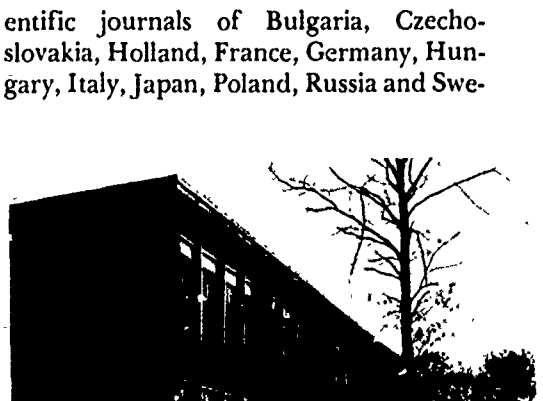

The extensive collection of the AFCRL Research Library is an important ingredient of the research environment.

den. The collection of Chinese science journals and monographs is one of the most comprehensive in the U.S. Associated with the foreign periodical collection are translation services.

CLASSIFIED PROGRAM: A portion of the research program is classified because of its relation to operational systems. Publications or presentations resulting from this classified research have not been included in the listings at the end of each chapter.

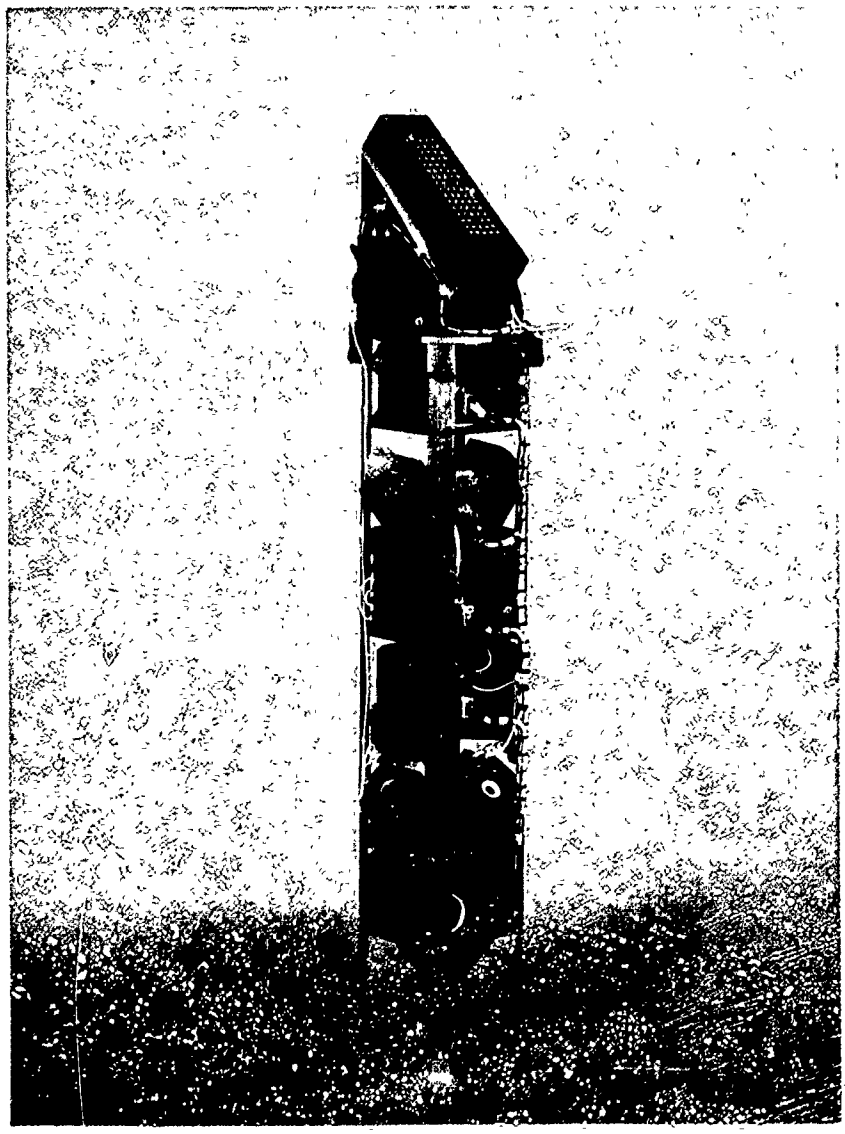

Rocket payload experiment package showing X-ray and UV sensors.

II Aeronomy Laboratory

Aeronomy is the study of the physical and chemical properties of the earth's upper atmosphere. It deals principally with the atoms, molecules, ions and photons present in the atmosphere and how they interact with one another. The lowest region of the atmosphere, the troposphere, which extends from the ground to about 10 to 15 km, is investigated primarily by the Meteorology Laboratory. The Aeronomy Laboratory's principal investigations are in the regions above this—namely, the stratosphere, mesosphere and thermosphere.

A major area of activity of the Laboratory is the study of the stratospheric environment. The National Environmental Policy Act of 1969 requires the Air Force to provide environmental impact statements for its operations such as flying the B-1 and F-15 aircraft. Questions which must be answered include: What will aircraft emissions do to the ozone content of the stratosphere? how will this affect the amount of ultraviolet radiation reaching the earth? what will this do to the incidence of skin cancer? how will agriculture and marine life be affected? will the temperature of the earth change? and if so, how much? (A temperature change of even one degree can have tremendous effects on the earth's climate.)

Recently, the Arms Control and Disarmament Agency has raised the possibility that a nuclear war, involving many explosions, could destroy the ozone layer in the stratosphere, thereby permitting the lethal solar ultraviolet radiation to reach the ground. The Laboratory is investigating this problem so that the Department of De-

fense will have quantitative answers as to the magnitude of this problem.

Another major area of activity is the study of ultraviolet radiations. The Laboratory is engaged in a joint program with the Space and Missile Systems Organization (SAMSO) on investigating these radiations for missile surveillance purposes. The atmospheric background radiations in the ultraviolet region of the spectrum are being investigated, as they pose a limit on surveillance capabilities. The ultraviolet radiations from the sun are being studied because they are a major source of energy for the earth's upper atmosphere.

Another major area is the development of models of the properties of the earth's atmosphere for use in systems design and in systems operations. For example, the Laboratory has had a major role in the development of the U.S. Standard Atmosphere, 1975, a cooperative effort involving the Air Force, the National Aeronautics and Space Administration and the National Oceanic and Atmospheric Administration. In systems operations, the Laboratory is working on atmospheric density models for the Aerospace Defense Command to be used in its tracking operations of all space objects, both friendly and unfriendly.

Another major area is the study of disturbed atmospheres. Systems operating in or through the earth's upper atmosphere may be affected by both natural disturbances such as polar cap absorption events, aurora. events, sudden ionospheric disturbances, etc., and by atmospheric nuclear detonations. The Laboratory is measuring atmospheric properties and developing models which are used as inputs to computer codes such as OPTIR, RANC IV and ROSCOE which are used in the determination of nuclear weapons effects.

The Laboratory is also involved in climatology studies for systems design. For example, the Laboratory recently completed Military Standard 210B which describes climatic extremes for military equipment and is used by all three services.

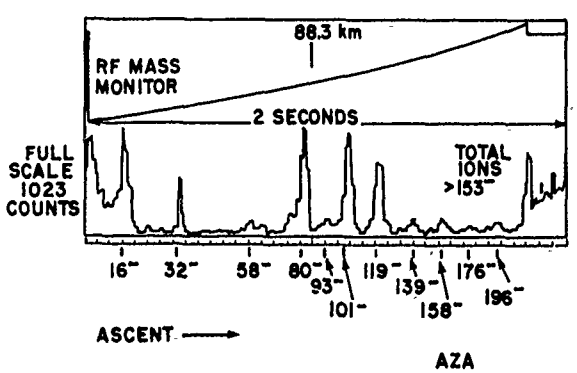

An example of a negative ion mass spectrum taken in a rocket flight showing the presence of very heavy negative ions in the D region. The mass numbers are in atomic mass units.

ATMOSPHERIC COMPOSITION

The Atmospheric Composition Branch has conducted a number of programs aimed at measuring and predicting the positive ion, negative ion and neutral composition of the upper atmosphere for various Air Force and Department of Defense systems.

ROCKET MEASUREMENTS: Several rocket programs were conducted in a continuing intensive effort to elucidate disturbed ionospheric processes for Air Force communications and detection systems. A coordinated auroral studies program designated ICECAP '73 was carried out from Poker Flat, Alaska, in March 1973 by AFCRL and the Defense Nuclear Agency. A dual-mode quadrupole mass spectrometer that was programmed to measure the positive ion and neutral composition on alternate mass scans was launched into a strong auroral arc on the night of March 26, and measurements were obtained between 82 and 182 km. The ion concentrations between 101 and 123 km exceeded 10^6 per cubic centimeter and the NO^+/O_2 ratio was about 2.3. Using the ion composition measurements, it was possible to deduce a maximum neutral nitric oxide concentration of 3×10^9 per cubic centimeter in

the vicinity of 100 km. Concentration profiles of N_2, O_2, O and Ar were obtained between 110 and 182 km and these exhibited a superimposed wave-like structure above 130 km for which no direct experimental cause is apparent. If real, these oscillations may reflect the effects of auroral heating but this requires further study.

A program was conducted at Fort Churchill, Canada, to study lower ionospheric processes during daytime auroral zone absorption (AZA) events. A recurrent magnetic storm caused several AZA's during the week of June 11, 1973. This storm was predicted to re-occur from measurements by Pioneer 9, traveling eight days ahead of the earth, which showed moderate increases in the solar wind. Two Ute Tomahawk rockets were launched on two successive days. The first rocket, containing a cryopumped positive ion mass spectrometer, plasma frequency probe and electron energy deposition scintillator was launched on June 12, 1973 during a 2.5 dB absorption event. The Churchill ionosonde indicated complete absorption during the flight. Composition measurements were obtained between 73 and 132 km. Water cluster ions were predominant below 83 km. Ion concentrations were similar to concentrations measured during a polar cap absorption (PCA) event. Ionized molecular oxygen was the major ion between about 83 and 93 km, giving way to NO^+ at higher altitudes. The NO^+/O_2^+ ratio attained an unusually high value of about 8 near 106 km and diminished to a relatively steady value of 2.7 ±'0.3 above 120 km. This indicates an enhanced neutral nitric oxide concentration near 106 km. Meteoric ions were measured in the typical broad layer near 92 km and in submerged thin layers at higher altitudes. The scintillator showed an electron energy deposition of 3 ergs per square cm per second for electrons with greater than 7 keV energy. They enhanced the ionization considerably between about 80 and 100 km which, in turn, was responsible for the complete HF absorption.

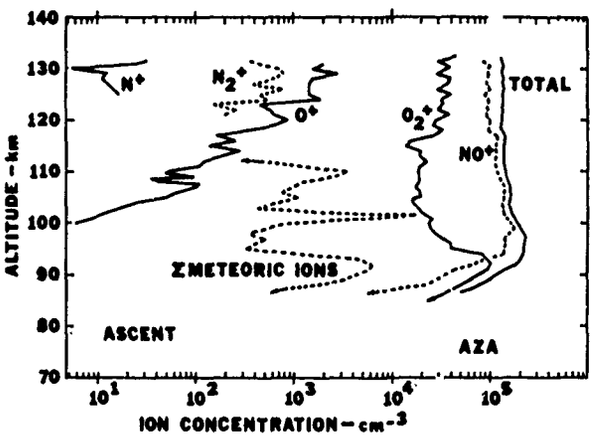

The E-region composition during the daytime 2.5 dB auroral absorption event. The ionization between 80 and 105 km is considerably enhanced above normal by the influx of energetic electrons.

The second rocket, instrumented with a cryopumped negative ion mass spectrometer, plasma frequency probe and electron energy deposition scintillator, was launched on June 13, 1973 during a 2 dB absorption event. The ionosonde indicated nearly complete absorption during the flight. The electron concentration was enhanced between about 80 and 105 km, showing a maximum of 2.2×10^5 per cubic cm from 94 to 98 km. Composition measurements were obtained between 68 and 132 km. Atomic oxygen and molecular oxygen, each with one excess electron, were the predominant E-region ions, and these, along with the heavy cluster ions, diminished sharply above 92 km. The negative ion cluster layer centered near 88 km was again measured and contained ions as heavy as 197 ±'3 amu. Ionized molecular oxygen may have been produced in the sampling process by the reaction $O_2 + e \rightarrow O^- + O$. Negatively charged molecular oxygen is believed to be an ambient ion, but its relatively large abundance is inexplicable if the rate constant for the associative detachment reaction with atomic oxygen is correct. Above 100 km the major ions were

NO_2^- and Cl^-; both of these species may have resulted from contaminants.

Another rocket program was conducted at Fort Churchill, Canada, in March and April 1974 to obtain quiescent polar lower ionosphere data for ionospheric modeling purposes and to study auroral processes. A rocket carrying a cryopumped positive ion mass spectrometer and Langmuir probes obtained nighttime undisturbed measurements between 75 and 130 km. The ionization of polar nighttime lower ionosphere was enhanced compared to the mid-latitude nighttime ionosphere indicating that a drizzle of energetic ionizing particles is present at polar latitudes during seemingly quiescent periods. A second rocket, containing a negative ion mass spectrometer, was launched during daytime quiescent conditions. Surprisingly large amounts of O^- and O_2^- ions were measured between 72 and 100 km. This finding is contrary to present theories and points out that negative ion processes are still not well understood. This is presently hampering the development of communications computer codes.

Two Ute Tomahawk rockets were launched into Class II and Class III auroral events, respectively. The payloads contained a dual-mode positive ion/neutral mass spectrometer, plasma frequency probe and electron energy deposition scintillator. Measurements were obtained between 95 and 170 km. These data are presently being analyzed; their excellent quality promises an elucidation of the ionospheric E- and lower F-region processes during moderate and strong auroral events.

Rocket experiments were also conducted to study the neutral composition of the mesosphere and lower thermosphere. The *N*eutral *A*tmospheric *C*omposition *S*pectrometer (NACS) was designed to measure the major and minor neutral atmospheric constituents between 60 and 140 km. Two high latitude experiments were flown on December 7 and 10, 1972 from Fort Churchill, Canada, during nights of auroral disturbance and quiet atmospheric conditions, respectively. Several general conclusions can be drawn from these and earlier results. First, the character of the turbopause region between 90 and 120 km changes considerably with time. Up to the turbopause, all of the major constituents, N_2, O_2, Ar, and CO_2 are measured in their ground level mixing ratio. Above the turbopause these constituents generally follow the expected diffusion profiles. However, the species profiles are changed because the turbopause changes in altitude and frequently consists of a region of alternating laminar and turbulent layers. It is certainly more accurate to characterize the turbopause as a region rather than as a level or a boundary. Second, the atomic oxygen profile varies substantially from one time to another. This profile is even more strongly dependent on the distribution and intensity of turbulent layers in the region between 90 and 120 km. A third important point which has been demonstrated by the ALADDIN experiments is that when the relevant structural and dynamical parameters are meas-

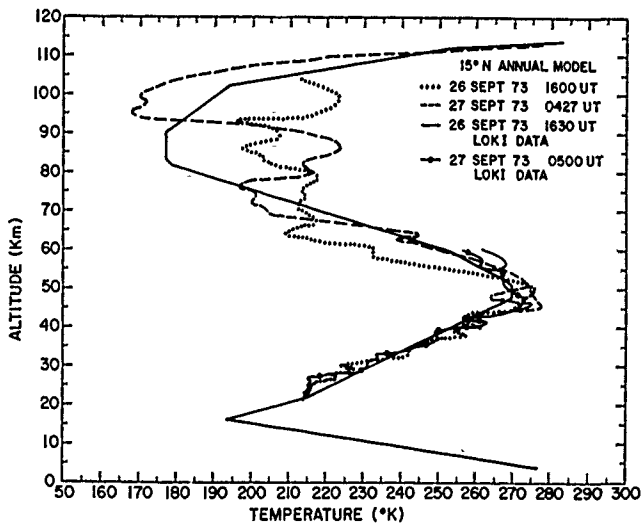

Diurnal Variation in Molecular Temperature at Natal, Brazil, on September 26 and 27, 1973.

ured, a suitable mathematical model calculation based on chemical and transport processes can be developed which is in good agreement with mid-latitude measurements.

SATELLITE MEASUREMENTS: The small research satellite program was begun in 1972 to provide a relatively inexpensive way of studying atmospheric, ionospheric and magnetospheric phenomena. The intent was to further the investigations begun with the OV3-6 (ATCOS II), OV1-15 (SPADES), and OV1-16 (Cannon Ball) satellites. The program expense was reduced by making use of excess payload capability of various launches. AFCRL scientists are supplying most of the experiments that instrument the satellites.

The satellites will be launched during the later part of 1974. The orbit will be highly elliptical to have sufficient orbital energy for a low perigee, near 150 km. The satellites will study the properties of the atmosphere and ionosphere between 150 and 500 km. The experiment complement includes two types of mass spectrometers to measure atmospheric and ionospheric composition and species densities. One satellite will be launched during 1975 to further study these parameters with additional ionospheric and magnetospheric measurements. The satellites include magnetic torquing systems to properly orient them for data collection.

The unique *V*elocity *M*ass *S*pectrometer (VMS) which was first developed several years ago at AFCRL has been further improved and included on two satellites. The new version combines the concept of the velocity mass spectrometer with the RF quadrupole instrument. The advantage of the VMS is that it can distinguish between the atmospheric species and those that come from spacecraft outgassing and surface effects in the measuring instrument. The first flight of this combined VMS/RF quadrupole mass spectrometer will be in late 1974.

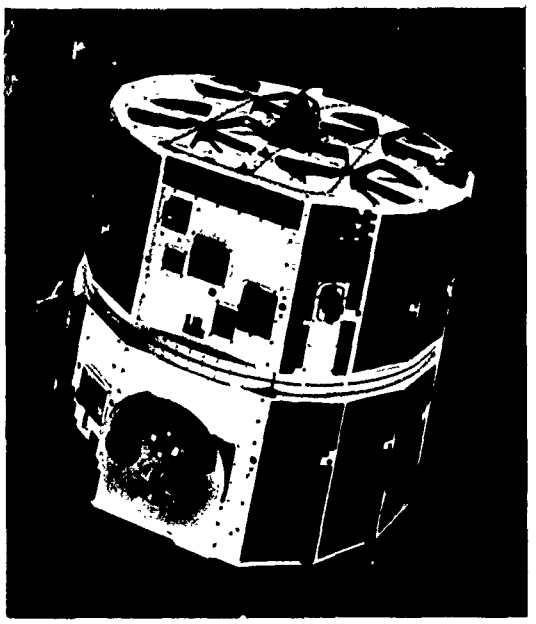

The Atmosphere Explorer-C satellite.

IONOSPHERIC MODELS: Two unique models were developed for disturbed ionospheric conditions. A nighttime PCA D-region model was formulated which agrees well with the ion composition, charged particle densities and proton flux measured during a PCA event. The PCA model can be easily adapted to calculate the D-region ionization following atmospheric nuclear explosions, but only for nighttime periods. It was further possible to derive mesospheric distributions of H_2O, O, NO_2 and NO. Except for the latter, no reliable measurements of these critical species exist.

Another model was developed for a steady Class II aurora and shown to be in good agreement with the ion composition measurements. It was possible to deduce the nitric oxide concentration in the E region, the maximum being 4×10^8 molecules per cubic centimeter near 110 km. Considerable controversy prevails over the amount of the enhancement of nitric oxide

(a strong IR emitter) and the processes which produce the increased concentrations. These models serve as critical inputs for both communictions and optical computer codes for Department of Defense systems.

CLUSTER STUDIES: AFCRL rocket-borne mass spectrometer measurements indicate that the ionospheric D region is predominantly composed of positive and negative cluster ions, especially water cluster ions. The propagation of electromagnetic energy, particularly in the VLF and HF spectrums important to Air Force communications, depends critically on the mass of these ions and their photochemistry. Additionally, clustering reactions may serve as sinks for jet engine and missile exhaust pollutants in the stratosphere by agglomeration of the pollutants into particulates which then fall to the troposphere where they are washed out by rain. Studies of pollutant clustering processes were conducted to determine the stratospheric effects caused by the Air Force B-1 and F-15 aircraft and also by a fleet of SST aircraft in an effort sponsored under the Department of Transportation's Climatic Impact Assessment Program (CIAP).

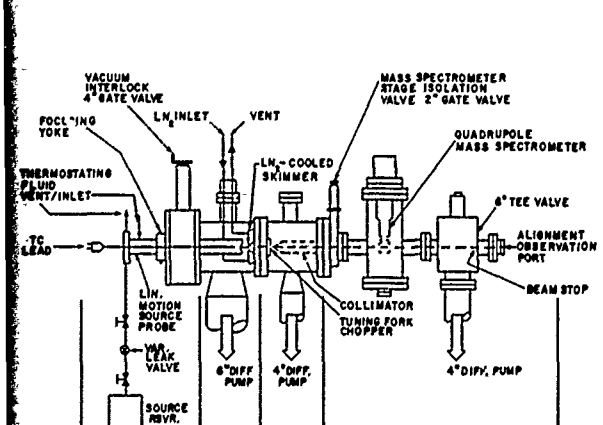

Schematic of the AFCRL molecular beam apparatus.

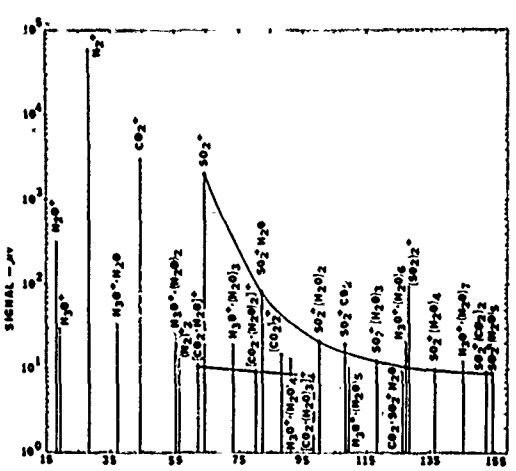

Heteromolecular clusters observed in a fully expanded jet composed of 10 percent water, 2.5 percent carbon dioxide, and 0.25 percent sulfur dioxide in nitrogen. The $SO_2 + (H_2O)_n$ and $[CO_2(H_2O)_n]^+$ series are connected by curves.

During the past two years, the molecular beam/free-jet apparatus used to generate and study clustering processes has been made fully operational. This equipment includes a phase-sensitive pulse counting method that allows near-simultaneous monitoring of mass peaks of interest by fast mass scanning while retaining the advantages of phase-sensitive detection. An experimental and theoretical study of dimer formation in supersonic water vapor molecular beams was completed. Heteromolecular or mixed clusters of engine exhaust pollutants of H_2O, SO_2, CO_2, CO and NO were produced and observed for the first time. A theoretical method was developed for the calculation of equilibrium concentrations of polar-polar, nonpolar-polar and ion dimers.

STRATOSPHERIC ENVIRONMENT

Planning and documentation have been completed for a new Stratospheric Environment Project with an official start date

of July 1, 1974. The goal of this effort is to provide the necessary stratospheric data and models from which environmental impact statements may be written for aircraft such as the B-1 and F-15. This effort will also make it possible for the Air Force to present its inputs when standards for stratospheric pollution are being established.

The composition of stratospheric gases, especially the minor species, will be measured using cryogenic whole air samplers installed on balloons and aircraft. Quantitative analysis of the retrieved samples will be performed in the Laboratory. Measurements will be made of the ambient composition in the region behind a stratospheric aircraft. Stratospheric sampling programs will be conducted on balloon and aircraft platforms and a mass spectrometer will be developed for the measurement of positive and negative ions in the stratosphere. In addition, an infrared interferometer will be adapted for coordinated flight measurements.

The chemical composition of stratospheric aerosols and the dependence of composition on particle size, altitude, spatial location and season will be investigated. Of particular importance are the processes by which aerosols are formed, and a particular area of interest will be the aerosol composition in the region behind a stratospheric aircraft. Balloon flights will be made for the accurate determination of aerosol composition in the stratosphere.

Stratospheric winds, temperature and turbulence will be measured and models will be developed to predict the dispersion, spreading and lifetime of aircraft and missile exhaust products in the stratosphere. The principal techniques are: adding appropriate chemicals to an aircraft exhaust to make it visible and then photographing it from the ground, the emission from a small sounding rocket of a smoke trail which also is photographed from the ground, and balloon measurements of temperature and microscale dynamics.

The intensity of solar ultraviolet radiation between 1800 and 3500 angstroms as a function of altitude in the stratosphere will be measured by means of a spectrometer mounted on a biaxial solar pointing control and carried aloft by a balloon. From these measurements, photon absorption rates and the vertical distribution of ozone will be determined.

Laboratory chemistry experiments will be performed to measure the reactions and properties of species important in the stratosphere, both as normal constituents and as pollutants from aircraft operations. Measurements include photoabsorption cross sections, neutral and ion chemical reaction rates, and clustering and nucleation rates.

Theoretical determinations will be made of the species and thermal distributions of the normal stratosphere and of the effect on these distributions caused by aircraft traversing this region. One-dimensional, time-dependent dynamical model atmosphere calculations will begin using the coupled set of equations of motion and continuity. A one-dimensional calculation will be made to determine the effects on the stratosphere of the nitrogen oxide emission from stratospheric aircraft. The energy equation with heat sources, sinks and transfer coefficients will be added to the models.

By means of global modeling, the long-term and short-term climatic effects of stratospheric perturbations will be determined. A limited test model will be developed which will incorporate sufficient physics to test a range of photochemical rate parameters and turbulent diffusion coefficients. The test model will be multilevel and time dependent but it will be zonally averaged. Work will begin on constructing a three-dimensional, time-dependent dynamical model of the global atmospheric circulation which will include all of the important stratospheric constituents and processes.

ALADDIN '74 ROCKET PROGRAM

The ALADDIN '74 (*A*tmospheric *L*ayering and *D*ensity *D*istributions of *I*ons and *N*eutrals) program was launched during a 24-hour period on June 29 and 30, 1974. The objective of the program was to study in detail the structure and dynamics in the upper atmosphere between 70 and 160 km. Selected parameters necessary for studying the physical and chemical processes in this region of the atmosphere and ionosphere were measured through the 24-hour period. The measurements included density, temperature and composition of the neutral and ionized atmosphere together with wind, shear, and turbulence measurements to allow improvements of atmospheric models. A second objective was to measure and compare atomic oxygen profiles from several different experimental techniques. The program consisted of 54 rocket payloads launched from Wallops Island, Virginia, together with measurements from several ground-based instruments and the measurements of the Atmosphere Explorer-C satellite. The program was a cooperative effort of many scientists from the United States, Germany, England, and Canada. The program was sponsored by AFCRL and the National Aeronautics and Space Administration (NASA), and was coordinated by AFCRL.

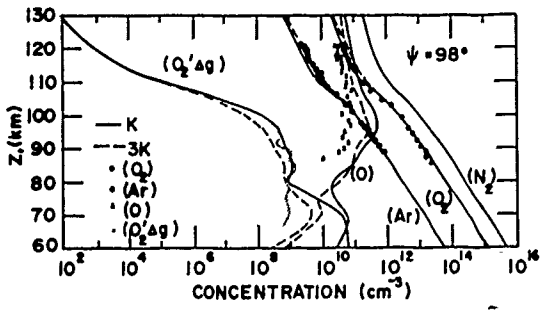

Comparison of the ALADDIN I theoretical time-dependent model atmospheres incorporating measured turbulent diffusion coefficients with the simultaneously determined neutral species distributions. The continuous and dashed curves are the theoretical results at a solar zenith angle of 98 degrees utilizing the measured turbulent diffusion coefficients (K) and an arbitrary diffusion profile three times as large (3K).

The rocket measurements made during the program included: chemical release measurements of wind, shear, turbulence, diffusion coefficients, density and temperature (AFCRL; Georgia Technological Institute; NASA Ames Research Center, Moffett Field, California; Geophysics Corporation of America; University College London); accelerometer instrumented and non-instrumented falling sphere measurements of atmospheric density and temperature (AFCRL; White Sands Missile Range, New Mexico); pitot probe measurement of atmospheric density and temperature (University of Michigan/NASA); mass spectrometer measurements of atmospheric composition (University of Bonn, West Germany; University of Pittsburgh, Pennsylvania; NASA); ultraviolet spectrometer measurements of solar radiations and atmospheric profiles of N_2, O_2 and O by absorption technique (AFCRL); nitric oxide chemiluminescent release to determine atomic oxygen profile (AFCRL); photometer measurements of species profiles from airglow emissions and solar attenuation (AFCRL; White Sands Missile Range, New Mexico; University of Colorado; University of Saskatchewan, Canada); probe and radio propagation measurements of electron and ion density and electron temperature (University of Illinois; University of Bonn, West Germany; Pennsylvania State University); electric field measurements (University College London; NASA Goddard Space Flight Center, Greenbelt, Maryland); ground-based ionospheric sounders (National Oceanic and Atmospheric Administration (NOAA), Lowell Technological Institute Research Foundation, Mass.; AFCRL); Millstone Radar ionospheric measurements (Massachusetts Institute of Technology); and ground-based optical measure-

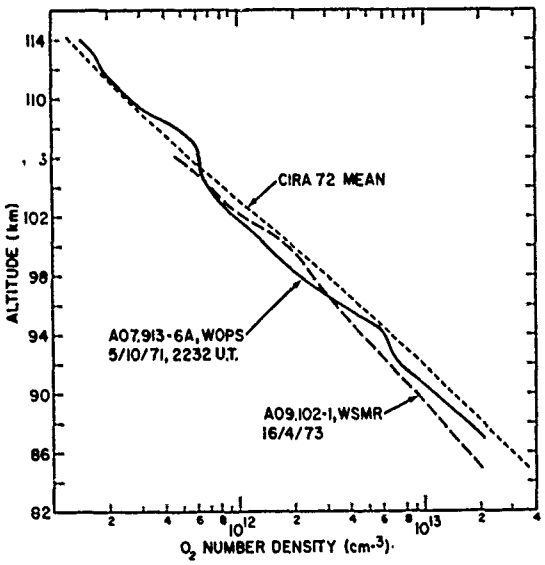

Molecular oxygen densities deduced from 1450 angstrom absorption measurements and mean model values.

ments (AFCRL; PhotoMetrics, Inc., Waltham, Mass.; University College London; NASA Goddard Space Flight Center, Greenbelt, Maryland).

The wealth of new data collected during the ALADDIN '74 experiment will be studied and analyzed during the coming months. The results of this experiment should provide a baseline comparison of atmospheric measurements with which both past and future measurements can be compared.

ATMOSPHERIC DENSITY AND STRUCTURE

Neutral atmospheric density and temperature have been obtained from falling spheres launched by rocket, accelerometers aboard satellites, and ionization gauges on satellites. A parallel Laboratory effort in theoretical density studies, atmospheric modeling, and measurements of ion-neutral reaction rates has improved understanding of the chemical processes in the upper atmosphere, and enabled us to assist in preparing environmental impact statements for the B-1 bomber, which will spend part of the time flying in the stratosphere.

ROCKET DENSITY MEASUREMENTS: New rocket-borne falling sphere measurements of neutral atmospheric density and temperature have been obtained during several coordinated field programs conducted by AFCRL, the Defense Nuclear Agency (DNA), and the National Aeronautics and Space Administration (NASA). Four sets of data were obtained at Churchill Research Range, Canada, in December 1971 and December 1972. Results acquired in December 1971 from two daytime measurements made four hours apart under quiescent conditions revealed no significant short-term structure variations in the altitude range 30 to 105 km. In fact, the data suggested that there may be some correlation between low geomagnetic activity (e.g., $K_p=2^-$) and the cold model from the *U.S. Standard Atmosphere Supplements, 1966.* Analysis of results obtained from two measurements made in December 1973 led to the conclusion that structure variations in the atmosphere may be induced by relatively intense geomagnetic disturbances,

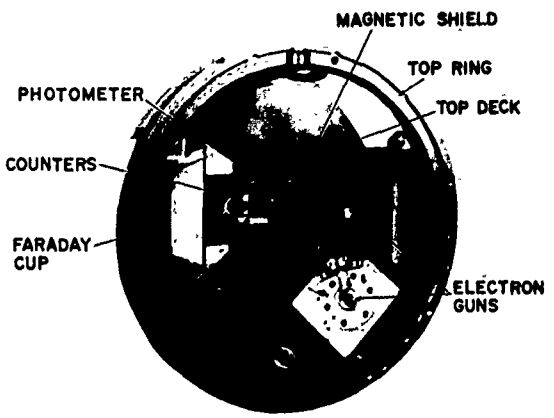

End view of payload used for density Bremsstrahlung measurements.

particle precipitation or lower atmosphere dynamics.

Falling sphere data obtained during the Winter Anomaly field program at Wallops Island, Virginia, in January 1972, ALADDIN II at Eglin AFB, Florida, in April 1972, and ALADDIN '74 at Wallops Island in June 1974 provided valuable comparisons and correlations between different rocket-borne techniques and ground-based measurements. For example, a temperature profile obtained at Wallops Island on January 31, 1972 exhibited considerable enhancement at approximately 70 km. The measurement corresponded to a time (1745 GMT)when low frequency radio absorption had shown a rapid increase from about 3 dB to 25 dB and then a decrease to the original value. The falling sphere temperature data are supported by one other near-simultaneous measurement (WSMR instrument). The temperature enhancement may be related to a winter anomaly.

Two falling sphere rockets were launched at Natal, Brazil, on September 26 and 27, 1973 to determine the diurnal variation of neutral density and temperature at equatorial latitudes (5 degrees, 52 minutes south latitude). Below 60 km, the temperature-height profiles are characterized by wave structures which show phase differences that vary up to 180 degrees. Preliminary analysis of the data in this region indicate that mean nighttime temperatures are about 4° K warmer than corresponding daytime values. Above 60 km the differences become significantly larger and at 100 km the nighttime value is cooler by more than 50° K.

Several rocket payloads have been flown which have provided data on mesospheric ozone, and mesospheric and lower thermospheric molecular oxygen.

Densities obtained from Lyman-alpha ion chambers during spring and fall show wave motion. The relative accuracy of the data is typically 4 to 8 percent, as determined from independent sensors in the same payload. The absolute accuracy below about 95 km is questionable due to the uncertainties in the temperature dependence of the molecular oxygen cross sections at Lyman-alpha. The lower densities in spring near 90 km are opposite to the Groves seasonal model and may be an interdiurnal fluctuation.

Molecular oxygen density profiles were obtained from 1450 angstrom ion chambers with an absolute error estimated to be less than 12 percent over the entire altitude range. The density scale heights, and hence the temperatures are less than the CIRA 72 and proposed U. S. Standard Atmosphere, 1974 above about 160 km, but the densities agree well with these two models from 140 to 160 km. The exospheric temperature of 960° K calculated from the Jacchia 1971 model for the time of measurement is close to the 1000° K value assumed by these models.

A rocket payload for the measurement of atmospheric density utilizing an electron beam has been successfully designed, built, calibrated, and flown. Atmospheric density was determined from measurements of the X-ray continuum Bremsstrahlung, created by the interaction of the electron beam with the gas surrounding the payload. The atmospheric content of molecular nitrogen was also determined from measurements of the luminescence at 3914 angstroms produced by the electron beam. Measurements were made from 120 km to 168 km during the rocket ascent, and from 168 km to 80 km during the rocket descent. By using two electron beams the density and nitrogen content were measured at two different distances from the rocket payload. A comparison was made of the effect on electron beam density measurements of using collimated and uncollimated electron beams.

Of particular importance to the success of the measurements was the testing and improvement of the techniques of magnetically shielding X-ray detectors from energetic beam electrons, and the utiliza-

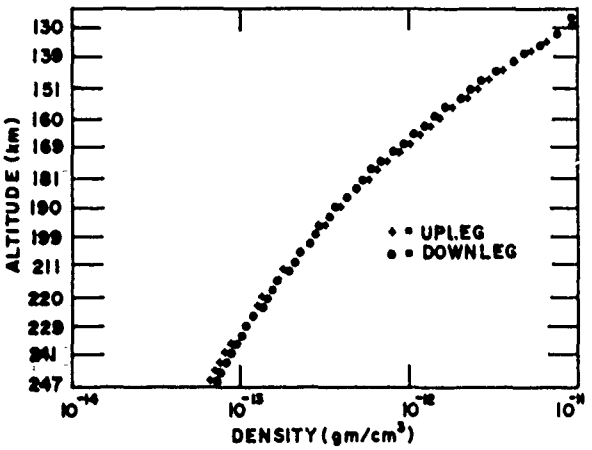

Density measurements from the MESA accelerometer on Atmosphere Explorer-C, orbit 1437, April 24, 1974.

tion of low Z number material in the detector collimator. The rocket payload was calibrated in a laboratory vacuum chamber where gas densities and nuclei composition similar to those expected in flight were maintained. This calibration was made possible by the use of carbon-coated target materials in the chamber which reduced both the number of scattered high energy electrons and the background continuous and line X-ray photon flux.

SATELLITE DENSITY MEASUREMENTS: Analysis of results from the Miniature Electrostatic Accelerometer (MESA) experiment on the low-orbiting SPADES (OVI-15) satellite has been completed. These results comprise the first set of *in situ* density measurements to be obtained below 200 km at all latitudes. A compendium of the density profiles and their ratio to model values was prepared in a format suitable for use by other investigators. In addition, a study of accelerometer results obtained at high northern latitudes during August 6-8, 1968, a period of moderate geomagnetic activity, was made. Density enhancements of 15-30 percent were found in the auroral zone in conjunction with increased auroral electrojet currents. These results indicate that joule heating of the thermosphere occurs in agreement with Cole's theory.

Data from the MESA triaxial accelerometer system on the Cannon Ball II satellite have been reduced. Eighty orbits of data were obtained to as low as 132 km during August 6-14, 1971 before the spacecraft tape recorder failed. The measured density values were acquired mainly under moderately quiet geomagnetic conditions and at low and middle Northern Hemisphere latitudes. Results were found to be generally within 10 percent of the Jacchia 1971 models. The observed scale heights were about 10 percent larger than the models predicted. The average density at perigee was 7 percent less than the model value.

A major effort has been the development of three improved MESA triaxial accelerometer systems for flight on the three NASA Atmosphere Explorer satellites. These satellites, with nominal one-year lifetimes, have the capability to fly despun or with a selected spin rate. They will have low perigee elliptical orbits. Perigee and apogee can be adjusted by an on-board propulsion system. A different inclination for each satellite is planned, ranging from near equatorial to polar. These three satellites comprise an integrated effort with the objective of significantly improving our understanding of lower thermospheric variations. The first launch (AE-C) was on December 16, 1973. Inclination of the satellite is 68.1 degrees. Perigee heights as low as 130 km have been reached. The triaxial accelerometer system is working perfectly. Data are being acquired typically on six to ten orbits per day. High accuracy density profiles are being derived ten days after acquisition on a routine basis using a local terminal tied to the NASA central computer. An extensive data base, required for development of accurate models, is being collected. Analysis of these results is in the early stages. Instrumentation for the two following launches is fabricated and tested. AE-D will be launched into a near-polar

orbit in March 1975 and AE-E will be launched into a near-equatorial orbit in June 1975.

Two types of accelerometers will be flown on an Air Force satellite scheduled for launch in late 1974 into a low perigee, high inclination orbit. In addition to a single axis MESA instrument, a triaxial piezoelectric accelerometer will be flight tested. This instrument, while inherently less accurate than the MESA, has the advantage of low cost, weight and power requirement. By flight calibration with the MESA its usefulness for future flights can be evaluated. A triaxial piezoelectric accelerometer will also be flown on a satellite scheduled for launch in late 1975.

Data obtained from ionization gauge measurements on board the OV3-6 satellite have been further analyzed and results are being compiled for publication. The report will examine, in more detail, the latitudinal structure of atmospheric density at middle latitudes. In general, the results are in agreement with model predictions (Jacchia 71) and measurements obtained by means of orbital analysis, particularly during periods of high solar activity. Where differences do occur, they are most pronounced during the equinoctial period and in the early morning hours, suggesting that the diurnal bulge may not simply migrate in unison with the sub-solar point. Some indication of geomagnetic coupling of the neutral atmosphere is indicated by a data correlation with the Dst index.

LABORATORY MEASUREMENTS OF ION-NEUTRAL REACTION RATES: Reactions of ions with neutral species are important processes in gases exposed to ionizing radiation. In the ionosphere, such reactions affect the rates of decay of electron density following sunset or following a nuclear detonation. These atmospheric perturbations influence the propagation of radio and radar signals, leading in some cases to the occurrence of blackout and to errors from refraction and scintillation. In order to predict the magnitude and persistence of these effects upon communications and radar systems, large computer codes have been developed. These codes require as input parameters such data as the rate constants for the reactions of important ions with the atmospheric neutral species. Double mass spectrometer systems have been developed in the Aeronomy Laboratory to study these reactions.

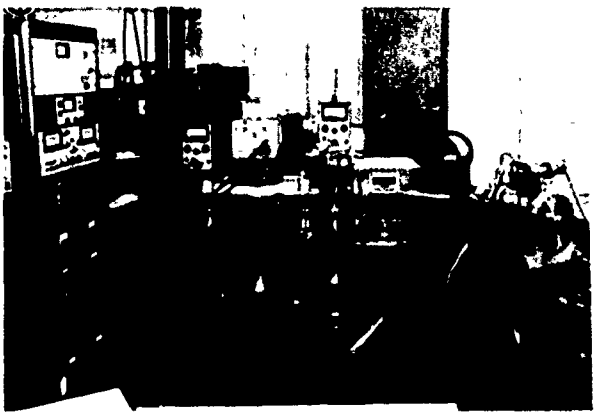

Double mass spectrometer system for ion-neutral reaction measurements.

Clustered ions, such as $H^+ (H_2O)_2$, and $H^+ (H_2O)_3$, are important species in the lower ionosphere, and their reactions are of interest. Under normal conditions, these species are stable. Under the perturbed conditions resulting from a nuclear detonation, the temperature is greatly increased, and collision-induced dissociation reactions may occur. Using a double mass spectrometer system, cross sections and translational energy thresholds were measured for the dissociation of $H^+ (H_2O)_2$, $H^+ (H_2O)_3$, and CO_3^- in collisions with N_2 and O_2. The existence of long lived excited states of each of these ions was also observed. Ion kinetic energies ranged from about 0.5 eV to 30 eV in these experiments.

Sulfur is a minor atmospheric species but is of potential interest because of its relatively large electron affinity in comparison with major atmospheric components. Cross sections were measured for several

reactions of S with N_2, O_2, N_2O, and CO_2. Information on bond dissociation enegies and electron affinities was obtained from the translational energy thresholds of the cross sections. In all of the reactions of S^- observed in this work, the cross sections were small at low energies, and it was concluded that the principal sink for S^- ions in the atmosphere is the associative detachment reaction with oxygen, i.e. $S^- + O_2 \rightarrow SO_2 + e$.

The double mass spectrometer system can also be operated as a device for determining the kinetic energies of ionic species from measurements of their times-of-flight over a known distance. Such studies on the important charge transfer reaction, $N_2^+ + O_2 \rightarrow O_2^+$ showed that, over the range of N_2 kinetic energies from 2.5 to 30 eV, the kinetic energy of the O_2^+ produced in the reaction is thermal. This result indicates that no transfer of energy occurred between internal and translational modes and therefore that the reaction is virtually resonant. The energy levels of the $N_2^+ + O_2$ system are such that, for resonant charge transfer to occur between reactants in their ground states, the products can only be formed in their ground electronic states. In fact, the reaction is exactly resonant for the $v = 13$ vibrational level of the ground electron state of N_2, and much of the N_2 produced in this reaction is probably in that level. Such studies as this indicate possible sources of reactive species and of optical radiation in the perturbed atmosphere.

ENVIRONMENTAL IMPACT STATEMENT FOR THE B-1 BOMBER: The Air Force is required by law to prepare an Environmental Impact Statement for those of its systems and operations which may have an effect on the environment. The Aeronautical Systems Division (ASD) has the responsibility for preparing the Environmental Impact Statement for the B-1 bomber. ASD came to AFCRL for assistance in assessing the effects of engine exhaust products upon ozone and transmitted ultraviolet, upon visible and infrared absorption, and upon local and global changes in climate. This study involved a coordinated effort by the Aeronomy, Optical Physics, and Meteorology Laboratories.

Although water and carbon dioxide are the major components of jet engine exhaust, the principal effects upon atmospheric ozone and transmitted ultraviolet radiation are caused, not by these major products, but by nitric oxide produced when air is heated in the combustion process. The nitric oxide is a catalyst in a series of reactions which destroy ozone. It is planned that the proposed B-1 fleet of 241 aircraft will spend a total of 650 hours per year in the stratosphere, injecting about 500 tons of nitric oxide during that time. From knowledge of the rates of the ozone destruction reactions and by comparison with the effects of normal ambient atmospheric nitric oxide upon ozone, it is possible to calculate the effects of this injected nitric oxide. On the assumption of uniform mixing, these calculations show that the ozone column density would be reduced by less than 0.002 percent. This would lead to an increase of about 0.01 percent in the ground level intensity of that component of

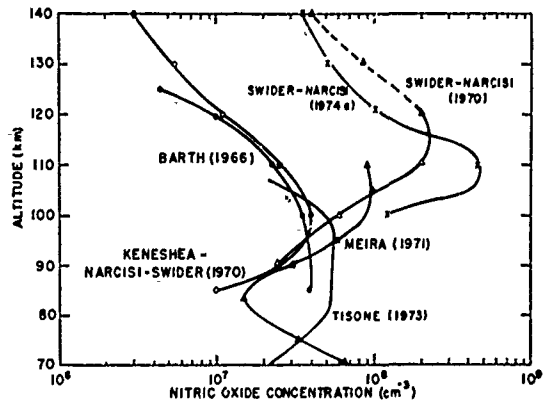

Mid-latitude optical observations of nitric oxide by Barth, Meira and Tisone and a model (Keneshea et al) are compared to auroral estimates from ion-composition analysis by Swider and Narcisi (1970-Class I aurora, 1974a-Class II aurora).

ultraviolet radiation which is responsible for sunburn and ultimately for skin cancers.

The amounts of water, carbon dioxide, carbon monoxide, and particulates emitted by the planned B-1 fleet are three to five orders of magnitude less than the amounts of these substances naturally occurring in the stratosphere. Absorption of solar infrared and visible radiation by these injected species is therefore a similarly small fraction of that from the naturally occurring abundances. Comparison of the absorption effects of other exhaust products, such as sulfur dioxide, nitric oxide, and hydrocarbons, with the natural absorption of the 6.3 micrometer band of water shows that the emitted species have absorptions at least seven orders of magnitude smaller. The contribution of the projected B-1 fleet to absorption and scattering of visible and infrared radiation is therefore expected to add less than one half of 1 percent to the natural levels.

There is presently no completely reliable means of determining the impact of jet engine exhaust products upon local and global weather. However, some mathematical models have been developed which incorporate the kinds of chages in heat balance and temperature distribution that the operation of a B-1 fleet might produce. However, the net sources and sinks of energy used in computer experiments with these models have been substantially greater than those likely to result from the B-1 fleet. These experiments showed that the differences between control and perturbed conditions are at first local but that appreciable differences are observed world-wide after about one month. These effects are differences in detail only, e.g. the timing or phase of a major cyclone development, and the means, variances, and spectral distributions of the principal meteorological elements (pressure, temperature, wind) remain virtually unchanged. The conclusion of these studies is that there is little likelihood of any long-term global effect of B-1 operations upon the climate, although there might be some small and transient local effects.

CHEMISTRY OF THE UPPER ATMOSPHERE: Analysis of auroral ion composition results have yielded estimates of nitric oxide concentrations for the E-layer which are higher than mid-latitude values. Computational studies indicate that these higher levels of nitric oxide are apparently present before the start of an aurora because only the larger auroras, Class III or better, can apparently perturb this initial nitric oxide distribution. A previous theoretical study of the normal mid-latitude E region is in harmony with mid-latitude nitric oxide observations. Nitric oxide is an important ionizable gas at twilight and at night for the E region. Furthermore this gas is involved in the reaction $O_2^+ + NO \rightarrow NO^+ + O_2$ which may leave O_2 in the singlet delta state and be an important 1.27 micrometer radiation source in the auroral region.

Studies of the solar proton event of November 2-5, 1969 have led to a more precise definition of the daytime electron loss factor as a function of altitude. Ozone observations during this event have been interpreted as indicating that excess OH plus H generated in ion-chemical processes during the enhanced levels of the SPE result in a lowering of O_3 and O densities in the lower mesosphere.

Laboratory work concerning ion-molecule reactions of interest with regard to atmospheric nuclear bursts has been continued. The cross section for the process $O^+ + CO \rightarrow CO^+ + O$ has been measured. The dissociation energy (8.78 ±'0. 13 eV) and ionization potential (> 6 eV) of thorium monoxide as well as the ionization potential of thorium dioxide, 8 ±'1 eV have been determined.

THEORETICAL DENSITY STUDIES: Derivation of density values from radar observations of the orbital motions of satellites has continued. Cannon Ball II, Musket Ball

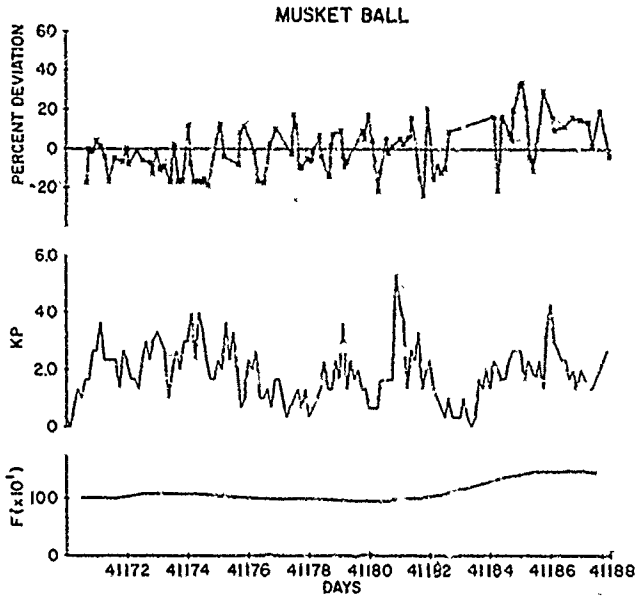

Orbital drag density departures from the Jacchia 1971 models for Musket Ball, for the period August 7-24, 1971. K_p and $F_{10.7}$ are shown for the same period.

and low altitude Air Force satellites have been used to derive density data. As a result of the extensive data from these satellites the models have been revised.

The model and the supporting data for the new U.S. Standard Atmosphere have been completed and the text material is in an advanced state of preparation for publication. The Standard is prepared by the Committee on the Extension of the Standard Atmosphere (COESA) and is sponsored by the Air Force, NASA and NOAA.

ATMOSPHERIC MODELS: The accomplishments to date include the measurement of turbulent diffusion coefficients and turbulent rates of dissipation from the chemical releases of the ALADDIN programs, and the incorporation of these diffusion coefficients into the one-dimensional photochemical-transport time-dependent theoretical model atmosphere calculations. Comparison of the resultant theoretical species distributions with the experimental measurements from the ALADDIN programs gave excellent agreement with the measured species [O_2], [Ar], [Na], [O_2 ($^1\Delta_g$)] and fair agreements with [O]. These excellent comparisons show conclusively that vertical motions in the mid-latitude mesosphere and lower thermosphere are the dominant mechanism controlling the vertical distribution of major and minor atmospheric species.

These same theoretical calculations incorporating the measured turbulent diffusion coefficients of ALADDIN I were utilized in developing the portion of the proposed U.S. Standard Atmosphere, 1974 for altitudes between 80 and 250 km.

CHEMICAL RELEASE STUDIES

From June 1972 to June 1974 three major field experiments were carried out to determine the dynamics of natural and man-made disturbances in the upper atmosphere and their effects on atmospheric characteristics and Air Force systems. Dynamic natural disturbances (solar flares, magnetic storms, etc.) or nuclear events degrade or black out Air Force missile detection, tracking and communications systems.

The first was HAVE GENIE II (*G*eophysical *E*xperiments for *N*eutral Species in the *I*onospheric *E*-Region) conducted at Eglin AFB, Florida, in October 1972. The program objectives were the development of tracers and techniques to define atmospheric motions and turbulence and to study the oxidation-reduction mechanisms and radiation characteristics of metallic vapors for defense applications.

The second was HAVE MERLIN II (*M*ultiple *E*xploratory *R*eleases for *L*ayering of *I*ons and *N*eutrals) in October 1973 at Eglin AFB, Florida. This exploratory program continued the objectives of the October 1972 program and combined measurements by chemical releases with instrumented probe measurements for composition and density.

The third program was HAVE ALADDIN '74 (*A*tmospheric *L*ayering and *D*ensity *D*istributions of *I*ons and *N*eutrals). The ALADDIN '74 program was planned to measure the transport properties, structure, composition and optical emission of the upper atmosphere. This program was conducted on June 29 and 30, 1974 at Wallops Island, Virginia, where 54 sounding rockets were launched during a 24-hour period in the largest coordinated scientific rocket program to date. ALADDIN '74 combined Air Force, NASA, and Army rockets into a single program with measurements timed to coincide with nearby passes of the Atmosphere Explorer-C aeronomy satellite. The results, when used as inputs for theoretical calculations, will provide the most complete understanding ever achieved of the upper atmosphere.

ATOMIC OXYGEN PROFILES: Nitric oxide (NO) releases were conducted as part of the GENIE, MERLIN and ALADDIN programs. The released NO reacts with ambient atomic oxygen and produces a headglow. The brightness of the headglow, as measured with on-board photometers, is directly related to the atomic oxygen density. This technique for measurement of atomic oxygen profiles has been qualified for both night and daytime measurements. MERLIN data show a peak in atomic oxygen density at 97 km, a trough at 105 km, and another peak at 110 km. Similar double peaks have been observed on other occasions and indicate a discontinuity in the turbulent structure of the upper atmosphere. Thus, the atomic oxygen and the related ionic species densities cannot be represented by a simple, smooth profile. Such unusual profiles will affect the RF propagation characteristics of the lower ionosphere, the optical emission intensity of the natural airglow, and artificial glows associated with missile exhaust gases.

DAYTIME WINDS AND RF CLOUDS: Development of instrumentation to provide a real-time day-and-night capability to track vapor clouds in the upper atmosphere was completed and validated during the ALADDIN series by measuring winds during the day. This exercise provided the first measurement of upper atmospheric winds during a 24-hour period. This series and further measurements can provide a better understanding of the diurnal effects involved in the dynamic interactions of upper atmosphere processes and motions. This technique provides the capability for determining E-region winds in real time for the placement of ion clouds at an optimum altitude in the weapons reentry region for use as radar targets and as radio wave reflectors for emergency communications links. Another application is the capability to provide optical calibration (position and structure) of artificial ion clouds released during daytime to determine radar system susceptibility in perturbed environments.

MESOSPHERE WINDS: A chemical smoke tracer was developed and flight tested during GENIE. This tracer provides the only current valid technique for defining D-region winds and turbulence. These parameters are important to an understanding of the water vapor profile and its impact on weapons effects and radio propagation characteristics.

OPTICAL WEAPONS EFFECTS: Chemical releases have direct bearing on existing and planned defense systems and on understanding of high altitude missile and nuclear effects. In this category belong the metal oxide vapor releases, such as lithium, sodium, cesium, barium, aluminum, iron, nickel, lead and their oxides. Sodium and aluminum vapors are ubiquitous ingredients of missile exhaust and contribute to their photoluminescent and chemiluminescent radiation characteristics. Certain oxides of metals form in nuclear explosions and radiate in a portion of the optical spectrum where advanced tracking and homing systems may operate. These metal oxide clouds can also be reproduced by chemical

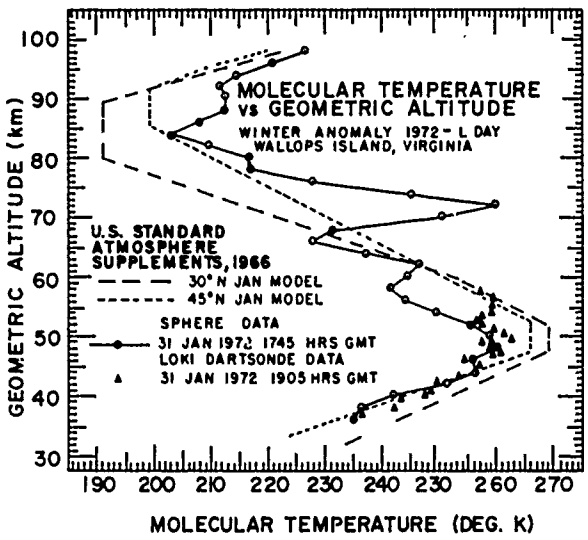

Molecular Temperature versus Geometric Altitude for January 31, 1972 at Wallops Island, Virginia.

releases in the upper atmosphere, permitting the study of their lifetime and radiation characteristics.

Metallic vapor releases of sodium, lithium, barium, aluminum, iron, nickel and lead were performed during the GENIE and MERLIN programs. It was determined that the minimum altitude where free metal vapors of their oxides can be maintained for appreciable periods is about 90 km. Below this altitude, the metallic vapors condense. Aluminum, barium and lead form the oxides, AlO, BaO, and PbO, respectively, which are not readily reduced by atomic oxygen. Other metal oxides quickly disappear and then the free metal resonance lines become evident when illuminated by sunlight. An interesting phenomenon was observed when sodium was released at night without solar fluorescence; the released vapor emitted the sodium D lines. Clearly, a chemiluminescent reaction must have occurred between the released sodium gas and some ambient species-probably atomic oxygen. This phenomenon may have some bearing on the natural sodium nightglow and on missile plume sodium emission. Releases of iron and nickel compounds demonstrated that the vapor and oxides of these metals are not significant sources of radiation in nuclear afterglows. Data were obtained to permit definition of the Al - O - AlO - AlO_2 - hν system for E- and F-regions during an evaluation of IR emitters.

CHEMICAL RELEASES AS AIRCRAFT DECOYS: There is a need for improved infrared flares to protect advanced aircraft against heat-seeking missiles. Exploratory flight tests have previously shown the promise of pyrophorics as infrared countermeasures when relatively high radiant intensities were obtained per unit mass of released material. Intensity levels and spectral characteristics have been confirmed in controlled laboratory experiments. These tests confirmed that the materials burn at altitudes to 60,000 feet and that radiation is independent of altitude. The effects of aerodynamic drag on the mass and volume of material released have been studied with a co-flowing air stream at simulated altitudes. The significance of these laboratory tests have led to the adoption of this concept for further development work by the Avionics Laboratory.

CHEMICAL RELEASES FOR STRATOSPHERIC PERTURBATIONS: In February and June 1973, the first extensive measurements of stratospheric dynamics were completed at White Sands Missile Range, New Mexico. The experiments consisted of producing and photographing sets of vertical and horizontal smoke trails in the stratosphere. Each of the vertical trails, 14 to 23 km, was produced by dispensing $TiCl_4$ from Nike rocket payloads. The horizontal trails were made by fuel dumps and $TiCl_4$ from a WB-57F flown by the 258th Weather Reconnaissance Squadron. These trails served as dye markers for both the motion of the winds and the turbulent mixing. By continually photographing the trails for some ten minutes, a time history is obtained from

which wind shears are measured. Telescopic photographs of the trails clearly show the increase of trail diameter and the action of turbulence in dispersing the smoke. This information along with the measurement of ozone densities obtained simultaneously provide a necessary bench mark for evaluating dynamic models of the stratosphere. The models will be used to predict the behavior of emission products, supersonic bombers and missiles in the stratosphere. These and other weapons-produced perturbations can also have an effect in the stratosphere, such as the possible reduction of the ozone layer. These possible effects can result in a higher incidence of cancer, and loss of food crop production in farms and oceans. A computer model of stratospheric transport has been developed which, in conjunction with published wind profiles, predicts a half residence time of three years for emissions deposited 10 km above the tropopause. The corresponding vertical effective diffusivity of 0.3 meter per second was obtained. Thus, clear air turbulence is a major contributor to the removal of pollutants.

CHEMILUMINESCENT STUDIES: Large missiles produce characteristic missile plume signatures as they pass through the earth's upper atmosphere. AFCRL developed a program to simulate in a laboratory the exhaust gas interaction with the upper atmosphere. The laboratory simulation was needed to vary parameters under controlled conditions in order to determine the chemical reactions and mechanisms producing the observed chemiluminescence.

A small-scale, one-pound thrust engine was fired in the AEDC 10V aerospace chamber against a supersonic airsteam containing atomic oxygen. The rocket exhaust gas and the flowstream interacted simulating the upper atmosphere interaction. The chemiluminescence of this region was studied over a broad spectral region, and was observed to increase in the presence of atomic oxygen. The results of these measurements are being used to define new systems for the determination of the thrust and payload capabilities of ICBM's.

THEORETICAL STUDIES: The Keneshea-MacLeod dynamic model of the ionosphere was significantly improved by including the effects of neutral wind-induced transport on the long-lived metallic ions deposited in the lower E region by meteors. Using neutral wind data obtained in the ALADDIN II (April 1972) rocket program, it was shown that the sporadic E layer found experimentally was due to the compression of metallic ions by the neutral winds. Furthermore, the strength of this mechanism is so great that the layer can be generated from a constant background profile in a half hour.

An analysis of the errors induced by neglecting vertical winds in deriving upper atmospheric winds from chemical trail releases was carried out. This study showed that serious errors in deriving such "pseudohorizontal" winds could be made if the observation period were as long as a few hundred seconds. This led to the recommendation that the errors could be minimized by assuming a constant wind over short observation times (less than 100 seconds) or a wind varying linearly with time for longer observation times (100-1000 seconds).

A scale autocorrelation coefficient was developed that compares a function of time with itself when the scale of times is "stretched." It was shown that this scale autocorrelation can be used to determine ratios of frequencies which occur in phenomena with periodicities. The properties of the scale autocorrelation coefficient were developed and applied to the finding of some of the ratios of the frequencies in atmospheric pressures measured daily for 8,766 days. It was also applied to measurements of the International Magnetic Character Figure, C_i, which was measured daily for 27,258 days. These applications are regarded as the first test of the utility of

the scale autocorrelation coefficient. The results indicate that the scale autocorrelation coefficient may prove to be a valuable supplement to the use of the usual autocorrelation coefficient and the Fourier transformation of time-dependent functions.

Cross sections were calculated for the resonance scattering of Lyman-alpha radiation by spinless, non-relativistic hydrogen atoms in the ground state using a two-level model. A slight generalization of Dirac's resonance scattering theory was used to take into account the degeneracy of the upper state, together with the *exact* matrix elements for the electromagnetic interaction. In contrast to the usual treatments in which only the dipole approximation for the matrix element is taken, the shift in position of resonance is *finite.* No renormalization is needed to obtain the finite result. Moreover, if the shift is interpreted as an electromagnetic shift in the energy of the ground state relative to the first excited state, this shift is close in value to the Lamb shift. The differential cross section was given as a function of the scattering angle for both polarized and unpolarized radiation. The total cross section was shown to be equal to that obtained by detailed balancing using the Einstein A and B coefficients. In addition, the radiation pattern of the scattered radiation was found.

Detailed measurements of the vertical wind profile at SST altitudes were made to evaluate atmospheric transport processes of importance in establishing dispersal rates of SST emissions. To obtain the necessary high spatial resolution, dense tracer trails of $TiCl_4$ were deposited from rockets in the altitude range, 13 to 21 km. The trails were photographed at regular intervals from three different locations to provide position and time information from which the wind parameters are computed. The trail positions on the photographs were measured on a digital scanning densitometer which read x and y coordinates of points along the trails with errors of the order of one to two microns per centimeter. These

Adjusting a double grazing-incidence spectrometer prior to an Aerobee launch at Wallops Island, Virginia.

data were digitized and recorded on magnetic tape that was subsequently analyzed and processed by the CRL 6600 computer.

SOLAR ULTRAVIOLET RADIATION

Models of the earth's upper atmosphere and ionosphere, constructed to aid our understanding of such features as the observed temperature-altitude profile and the neutral and charged particle density distribution, depend upon detailed considerations of the many photoabsorption and photochemical processes occurring as a result of solar irradiation. Quantitative models require accurate experimental determinations of the absolute intensity and spectral distribution, as well as the temporal variability, of the solar radiation reaching the earth and the rate at which this energy is absorbed and subsequently dissipated within the atmosphere. Research in the Ultraviolet Radiation Branch provides such solar flux measurements for the wavelength range between 30 and 3500 angstroms, spanning the soft X-ray, extreme ultraviolet, vacuum ultraviolet and ultraviolet spectral regions, as radiation of these wavelengths interacts strongly with

the atmospheric constituents. The basic radiometric measurements, made with calibrated spectrometers mated with solar pointing controls, are carried by rockets and satellites to altitudes well above 100 km.

ROCKET MEASUREMENTS OF SOLAR UV: This phase of the solar ultraviolet program uses high performance sounding rockets to carry spectrometric instruments to altitudes essentially outside the earth's atmosphere. Measurements made at the top of the rocket trajectory reflect, with little correction, the incident solar flux, and measurements made at lower altitudes allow a determination of the rate of absorption of the radiation as it progresses through the atmosphere. During this reporting period, the development of new instrumentation has increased the spectral range of measurement from the previous limits, 30 to 1250 angstroms, to include wavelengths as long as 1950 angstroms and with the further instrumental capability to extend the range to 3500 angstroms.

Of the five rocket experiments described in this report, only one, on July 15, 1972, failed completely. A grazing-incidence spectrometer to measure the solar flux throughout the 230 to 1260 angstrom region could not take any data because the rocket exploded shortly after launch.

On August 23, 1972, an Aerobee 170 rocket was launched from White Sands Missile Range, New Mexico, carrying a double, grazing-incidence spectrometer to measure fluxes in two bands, 55 to 300 angstroms and 230 to 1220 angstroms. The measurement phase of the experiment was highly successful, but failure of the recovery system resulted in loss of the spectrometer which, at the time, was making a second flight. Calibration throughout the spectral range allowed precise determination of the absolute flux levels for this date. These measured fluxes taken together with known photoabsorption cross sections and photochemical reaction rates have been used to determine computationally the electron density as a function of altitude. The densities so determined, when compared with simultaneous ionosonde measurements of the electron density, show agreement to within 30 percent.

A new spectroradiometric instrument has been designed and fabricated to extend the measurement capability into the vacuum ultraviolet, covering the range from 1250 to 1950 angstroms. The instrument, machined mainly from beryllium, is of the Ebert-Fastie type. The design is modular and allows either two long wavelength or one long and one short wavelength spectrometers to be combined into a single payload. An experiment of the latter configuration was launched on an Aerobee 170 from White Sands Missile Range on November 2, 1973 allowing for the first time simultaneous coverage of the spectral regions 220 to 1250 angstroms and 1250 to 1950 angstroms. The flight was largely successful, suffering only from occasional data dropouts on the short wavelength channel. The recovered instrumentation was refurbished with a slight modification and launched a second time on April 23, 1974. On this date, the two spectrometers operated flawlessly but were lost because of a recovery failure. Data from these two flights are currently being analyzed. Initial indications are that the new spectrometer operated with the design resolution (0.1 angstrom) and efficiency (about 3 percent) and is a generally satisfactory instrument. Eventual determination of the continuum radiation levels in the 1300 to 1600 angstrom region is of particular interest since previously reported values by other investigators are discrepant by as much as a factor of 3. Preliminary results from the AFCRL measurements indicate flux values near the larger limit of the range of existing measurements.

As a part of the ALADDIN III program, an Aerobee 170 rocket was launched on June 29, 1974 from Wallops Island, Virginia. This double, grazing-incidence spectrometer was designed primarily to acquire

data relevant to the determination of atmospheric composition. Throughout the flight, eight pre-selected wavelengths in the range between 284 and 1206 angstroms were scanned repeatedly. Underperformance of the rocket limited the data coverage to about 50 percent that of a normal flight. The available data are currently being analyzed to give the composition in terms of number densities of atomic oxygen and of molecular oxygen and nitrogen which can be compared with mass spectrometric measurements made with another rocket of the ALADDIN program at approximately the same time.

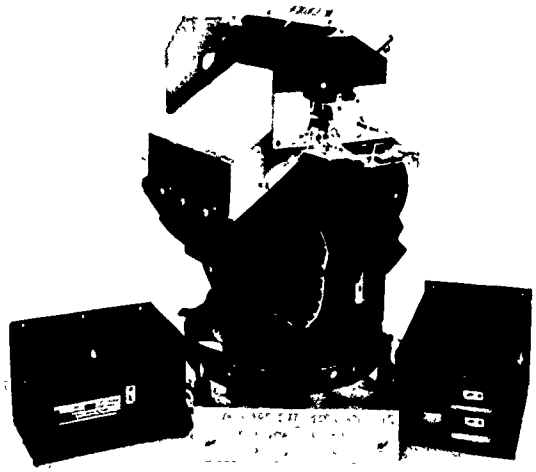

The AFCRL solar ultraviolet spectrometer and solar pointing subsystem for the NASA Atmosphere Explorer series satellites.

SATELLITE MEASUREMENT OF SOLAR UV: Satellite-borne instrumentation affords the opportunity for nearly continuous solar flux measurements over extended periods of time. Such extensive data allow a study of long-term temporal variations in the flux levels which are associated with the relatively slow changes in solar activity occurring over one or more solar rotations. The nearly continuous time coverage increases the probability of observing those unpredictable impulsive events of a few minutes duration which are associated with eruptive phenomena such as solar flares. In a manner similar to a rocket experiment, measurements of atmospheric attenuation can also be made from a satellite spectrometer over those portions of an earth orbit during which the satellite penetrates deeply into the atmosphere as well as during periods of solar occultation occurring at satellite sunrise and sunset. The Ultraviolet Radiation Branch has designed and supplied spectrophotometric experiments as part of three payloads of the present NASA Atmosphere Explorer series. The first spacecraft of the series was launched on December 16, 1973 and will be followed by two additional launches in 1975.

The satellite spectrophotometer is composed of 24 grazing-incidence monochromators and provides flux measurements throughout the 140 to 1850 angstrom region. Of the 24 monochromators, 12 are stationary at fixed wavelengths, while the remaining 12 scan, in segments, the total wavelength range. The spacecraft orbits the earth 11 times each day, with a perigee altitude of 135 km and an inclination of 65 degrees. This orbit, which is maintained by occasional firings of an onboard engine, allows a sequence of operations which is significant for the aeronomical purposes of the mission. At altitudes between 400 and 1000 km, below the high energy radiation belts, measurements are made of the unattenuated or incident fluxes. During the perigee-near portions of the orbit, down to 135 km, the observed flux levels show attenuation resulting from atmospheric absorption. Additional observations made near satellite sunrise and sunset extend the attenuation measurements to altitudes as low as 100 km. In one respect the perigee pass of the satellite differs from the vertical probing of a sounding rocket in that the satellite in passing through perigee sweeps through a much larger range in latitude and tends to blend atmospheric attenuation features which show a latitudinal dependence. This shortcoming can be tol-

erated since the satellite instrument provides the equivalent in data of 11 rocket experiments each day. Because of the motion of perigee and the precession of the orbit, eventually attenuation measurements will be made over a wide range of latitudes and local times during the planned one-year lifetime of the mission.

During the first six months of operation, approximately 2,000 orbits have been logged. In this time period there have been seven solar rotations. Preliminary results show notably different behavior between wavelengths longer than 1200 angstroms and shorter wavelengths, both in amplitude and phasing, with regard to the variations associated with changing solar activity. Spectrally, those emissions originating in different regions of the solar atmosphere—that is, coronal, chromospheric or near-photospheric—exhibit variations of widely differing magnitude ranging from a few percent for photospheric-like radiation to several hundred percent for coronal excitations. One impulsive event chronologically associated with a solar sub-flare has been found to exhibit remarkable similarity to the simultaneous sudden increase in radio emission at 10.7 centimeter wavelength. A great many attenuation profiles have been recorded by the spectrophotometer. The stability and low background achieved by the instrument are making the determination of optical depths computationally straightforward.

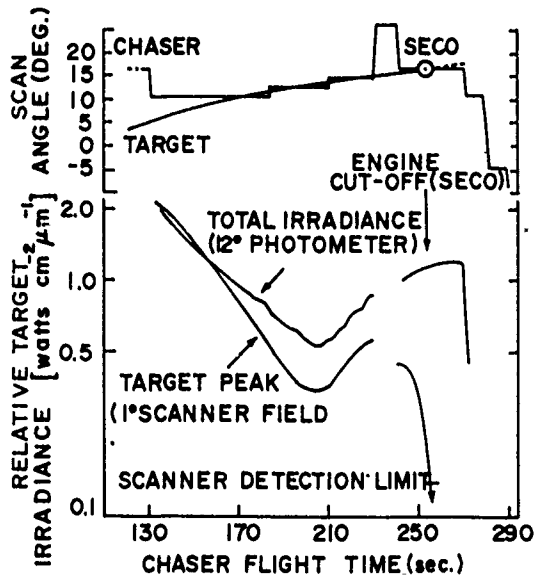

Irradiance measurements made during Chaser flight number 4.

MISSILE PLUME OPTICAL RADIATION MEASUREMENTS: The final rocket probe flight of Project Chaser occurred during October 1972. This program measured missile plume signatures of ICBM launches on the Western Test Range, Vandenberg AFB, California. Measurements were obtained of the radiant intensities of the missile during the upper stage burns for use in systems development. This program was supported by the Space and Missile Systems Organization (SAMSO) and was a joint effort with the Optical Physics Laboratory and Aerospace Instrumentation Laboratory of AFCRL. Missiles using three representative propellant combinations were observed during the project. Data analysis and systems studies using the Chaser data are continuing both at AFCRL and elsewhere. Interest in further, similar measurements led to program direction for an Advanced Development Plan in mid-1973. The proposed "Multiband Technology" program was approved and received initial funding in July 1974. However, to meet the requested program milestones, considerable prior effort was expended to plan and establish the technical requirements of the measurements. In contrast to the previous Chaser measurements, which were only at night, it is planned to have several measurements during daytime. Two general types of measurements will be made: target engine measurements of test rocket engines carried with the sensors on one large rocket probe, and high probe measurements observing missile test flights on the Western Test Range. The Project Chaser

measurements have shown that chemical reactions both within the exhaust gases and following mixture of the exhaust with the ambient atomic oxygen produce chemiluminescent emission. Further field observations with improved spatial and spectral resolution and associated directed research in this laboratory will provide the necessary information for application of this ultraviolet emission to a wide range of systems missions.

ATMOSPHERIC ULTRAVIOLET MEASUREMENTS: Surveillance satellites for detection, tracking, attack assessment and other missions must continually be upgraded to respond to changing military situations. This work will provide detailed information on the earth atmospheric emission which forms the background radiation environment within which missile targets must be observed. Work on a satellite experiment entitled "Vacuum Ultraviolet Backgrounds" has been initiated, and the experiment is partly fabricated. The experiment will measure global UV levels with spectral resolution up to 1 angstrom using an Ebert-Fastie spectrometer and spatial resolution to 1 km using a broad-band photometer. The experiment is planned for launch in 1977. This work is closely related to our missile plume radiation measurements, and the results of the two efforts will allow a complete and reasonably definitive statement on surveillance uses of the ultraviolet. The primary unknown is the strength and global distribution of the Lyman-Birge-Hopfield bands of N_2, which occur in a region which otherwise has an extremely low atmospheric radiance, due to photoabsorption by molecular oxygen in the Schumann-Runge continuum. In addition, the intensities and distribution of the oxygen emission lines at 1304 and 1356 angstroms will be correlated with atmospheric, ionospheric, and auroral parameters in an effort to develop passive sensors of quantities such as the electron density profile. Where feasible, missile target measurements will be conducted.

ULTRAVIOLET PHOTON CROSS SECTIONS: Knowledge of the interaction of ultraviolet photons with atmospheric gas molecules is essential to a wide class of Air Force interests, such as atmospheric characteristics, both ionospheric and stratospheric, and the extent and severity of blackouts from atmospheric nuclear detonations. Progress has continued in an effort to obtain values on all the earth atmospheric gases for the total absorption cross section, the total photoionization cross section, and partial photoionization cross sections. During this period, the first two types of cross sections were reported for water vapor in the VUV region. The oscillator strengths of atomic oxygen were also measured and reported. These observations provide a measure of the total absorption at strong lines. Partial cross sections will be measured with a photoelectron spectrometer, which was built and partly tested during this period. Finally, special reports of cross-section values at solar emission lines and at emission lines produced by nuclear detonations have been prepared for the Defense Nuclear Agency and other user groups. The photon cross sections obtained by this research are especially important in predicting the effects of high altitude nuclear bursts, and they are primary inputs to computer codes such as ROSCOE, RANC IV, and OPTIR which model the perturbation and return to ambient conditions. The results define the environment within which Air Force equipment must operate. In addition, all other atmospheric model atmospheres or ionospheres must use cross-section data to account for the initial energy input.

ANALYSIS OF MOLECULAR NITROGEN SPECTRA: Knowledge of the high energy (14.3-15.5 eV) Rydberg States of N_2 has long been incomplete and unsatisfactory, primarily because of the lack of detailed

high resolution spectroscopic studies. The present work remedies this situation by providing high quality, rotationally resolved and analyzed absorption spectra in the difficult wavelength region 900-870 angstroms, where wavelength resolution of 0.005 angstrom was achieved. The excited states reached by photon absorption from the ground state are Rydberg states converging on the lowest state of the molecular ion N_2^+. From the two Rydberg series photographed, accurate molecular constants, coupling constants, and band origins were derived. A marked change in the coupling condition occurs as the principal quantum number of the excited Rydberg orbital increases. Numerous spectral perturbations were observed and analyzed.

ABSORPTION SPECTRA OF MOLECULAR CLUSTERS: Molecules held together by weak forces not involving chemical bonding are called clusters. Cluster ions occur in the upper atmosphere, and neutral clusters are an intermediate step in the nucleation process of gas-to-particle conversion in a free jet expansion. Little is presently known about the energetics of formation of clusters or their radiative properties. The simplest neutral clusters are the rare gas dimers such as Ne_2 or Kr_2. These are important not only as cluster prototypes but also in their own right as the working medium in high intensity vacuum ultraviolet (VUV) sources, including the recently discovered rare gas VUV lasers which are among the shortest wavelength coherent sources currently available. Detailed characterization of the ground and excited electronic states involved is required to effect improved efficiency and greater intensity of VUV emission. A possible application for intense VUV sources is in the area of satellite-to-satellite communications.

The present high resolution VUV absorption studies on Ne_2 and Kr_2 reveal the ground-state vibrational structures of these van der Waals dimers in sufficient detail to permit definitive determination of dissociation energies and of potential well depths and shapes. For example, the ground electronic states of Ne_2 and Kr_2 respectively contain 2 and 16 bound vibrational levels and have dissociation energies of 0.0021 and 0.0157 eV. Information is also obtained on the long-range parts of many excited electronic states by observing the effects on the spectra of increased gas pressure; almost every atomic transition then gives rise to molecular bands of the dimer. Heteronuclear molecules such as HeNe, ArKr, and ArXe have also been detected, as have the corresponding heteronuclear ions, and the analyses of these band systems are in progress.

DESIGN CLIMATOLOGY

Military materiel must have year-round world-wide endurance capability and operational utility. Equipment that is overdesigned could be costly, yet ineffective. But underdesign could cause failure and loss of life. Climatological studies, therefore, have been continued to improve our knowledge of the risks of weather extremes as they relate to the Air Force's design of equipment and operational planning.

CLIMATIC EXTREMES: Department of Defense Military Standard 210, Climatic Extremes for Military Equipment, is the document used by the three Services to specify climatic design criteria for equipment destined for world-wide usage. When AFCRL was given technical responsibility for this Standard in 1967, it was realized that the criteria in the then current version were obsolescent. A major DOD effort was spearheaded to revise MIL-STD-210A, an effort which culminated in December 1973 with DOD acceptance of MIL-STD-210B. Since 1967, numerous scientific studies were accomplished to revise criteria in MIL-STD-210A; and during the last two years, studies dealing with thermodynamic properties of the atmosphere between 3 and 80 km, diurnal cycles of high absolute

humidity, extremes of low density for surface elevations to 15,000 feet, extreme rainfall rates for one minute, and 1, 12 and 24 hours, and extremes of surface and upper air wind speed were completed. The study on rainfall rates was particularly useful in an investigation to determine whether F-111 engine flameouts over Southeast Asia could be due to water ingestion. Also prepared under one cover was a synthesis of all studies, including Army and Navy inputs, which establish and support the criteria in MIL-STD-210B. In the standards field, this is unique since most standards lack verifying supporting documentation.

Several presentations at national meetings and at the Office of the Assistant Secretary of Defense and the publication of AFCRL technical reports resulted in numerous requests for consultation with Air Force designers in the area of climatic extremes.

WINDS AND GUSTS: Wind studies related to design and operational problems have long occupied the attention of climatologists. Studies currently underway include winds for Air Force paradrop operations, gustiness and range of wind speed during periods of strong winds, and upper air mean winds for reentry vehicles.

Air Weather Service expressed a need for knowledge of winds at altitudes up to 1,500 feet for support of Tactical Air Command low level paradrop missions. Often the most important factor in TAC's frequent inability to paradrop men or materiel on a particular target is insufficient specification of the mean wind between drop altitude and the surface. An AWS special study in 1971 pointed to the strong need for studies of such winds. Accordingly, a study was initiated specifically aimed at examining the nature and variability of paradrop winds. The study was just recently completed.

Knowledge of surface wind gustiness during periods of strong winds is important to all exposed Air Force systems. Research in the area of strong surface winds had been conducted in the past at AFCRL, but the relationship between short period winds (gusts) and winds averaged for a minute or more had not been explored. It is this spectrum of gusts associated with a strong wind that is needed for planning, design and operation.

A recently published comprehensive report on extreme wind speeds, gustiness, and variations with height was the culmination of a three-year study using original wind records. Nomograms of gust factor versus gust duration and steady wind speed were used to assign the most dynamically effective gust according to equipment dimensions. Also, a power-law relationship was developed for adjusting wind speed to a common height.

A follow-on study is currently being conducted to determine a statistical description of the wind speed range (difference between maximum and minimum) as a func-

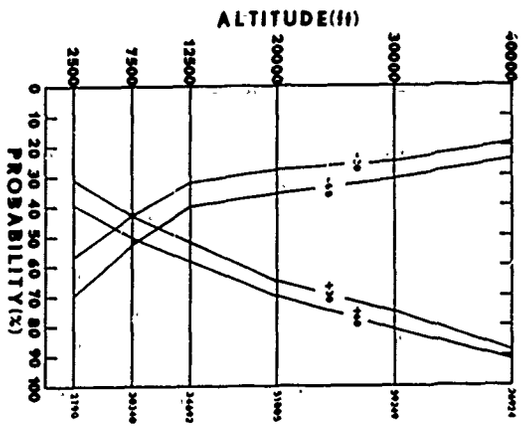

Probability of having a clear line-of-sight from various altitudes to the ground at 30- and 60-degree depression angles (labeled -30 and -60) and to the sky at 30- and 60-degree elevation angles (labeled +30 and +60) based on 205,000 inflight observations taken over the Northern Hemisphere between 1968 and 1974. Values along the right abscissa indicate the number of observations taken at the indicated heights.

tion of time interval and mean wind speed. Such relationships are important in the design and operation of aircraft, especially VSTOL aircraft, during takeoff and landing. Some of the results of this study are currently being used in the design of an undergraduate pilot trainer.

A third investigation, also related to Air Force design or operational problems, is concerned with upper air mean winds for reentry vehicles. In this study, observed mean monthly winds at altitudes 5,000 to 80,000 feet are being compared to the currently used gradient winds to determine their accuracies.

SEEABILITY: The increased use of optical, infrared and laser sensors in detection, lock-on and tracking systems, many of which cannot see through heavy haze or clouds, has resulted in the need for more information on the probability of haze- or cloud-free lines of sight. Also, there are many military operations which are inhibited and often terminated by hydrometeor interference, such as erosion effects on hypersonic vehicles and millimeter-wavelength communication outages due to precipitation.

In order to determine how often haze or clouds would limit operations, two efforts were conducted: an in-flight observation program and the development of a cloud-free line-of-sight (CFLOS) model based on observed cloud-cover statistics. A third effort was initiated to determine the probability and amount of precipitation that would occur along ray paths through the atmosphere.

A six-year collection of more than 250,000 in-flight line-of-sight observations over much of the Northern Hemisphere was concluded in July 1974. Analysis of these observations will provide probabilities of clear, cloud-free or haze-free lines of sight from an aircraft at various altitudes to the sky, horizon, and surface of the earth.

A model for estimating CFLOS probabilities was developed by correlating cloud-cover observations with whole-sky photographs. The model will give CFLOS probabilities through the atmosphere for any desired elevation angle based on the cloud-cover statistics for a given location. Because signals transmitted through the atmosphere in the visible and infrared portions of the electromagnetic spectrum can be seriously degraded by clouds, the utility of such systems can be greatly enhanced by placing ground receivers at several locations. Therefore, the CFLOS model was extended to estimate joint probabilities of cloud-free lines of sight from n of m observing sites by using a climatic record of sky-cover observations taken simultaneously from each of the m sites.

The objective of the third effort is to develop a climatology of precipitation occurrence along atmospheric ray paths. Virtually no quantitative information exists on how often attenuation, due to precipitation, will affect microwave transmission at various elevation angles. Since July 1973, special photographic observations have been taken at 17 National Weather Service radar sites. The radar scope is photographed every three hours with the antenna in each of four elevation angles—0, 15, 30 and 45 degrees. These photographs will be used to determine the slant range thickness of precipitation echoes. These data will provide probabilities of precipitation interference not only from the surface outward, but also between levels and from any level out through the atmosphere or to the ground. Data collection for this program will continue through December 1975.

STANDARD AND REFERENCE ATMOSPHERES: A proposed revision to the U.S. Standard Atmosphere for levels between 50 and 85 km was adopted by the U.S. Committee on Extension to the Standard Atmosphere (COESA). It is being incorporated into the U.S. Standard Atmosphere developed by COESA for levels up to 1,000

km. The same revision has also been adopted by the International Standards Organization for the ISO Standard Atmosphere which extends to 80 km.

As part of a continuing investigation of the distribution and variability of atmospheric properties between 30 and 120 km, the *U.S. Standard Atmosphere Supplements, 1966* are being revised and expanded in scope. Monthly models for each 15 degrees latitude from equator to pole are being completed for altitudes up to 90 km. Specialized winter models are also being developed to describe warm and cold stratospheric and mesospheric conditions typical of arctic and subarctic regions. As a result, these reference atmospheres will depict the horizontal and vertical distributions of the thermodynamic properties of the atmosphere that would be encountered by aerospace vehicles.

INSTANTANEOUS PRECIPITATION: Research on instantaneous precipitation rates was continued and expanded because of its importance in the development of ground approach control radars, satellite communication systems, search radars, etc. A generalized relationship was developed to specify the rates that would be exceeded with any desired probability of occurrence from 2 percent to 1/10 percent at any place in the world. The calculations can be made from standard climatological data. Research on the relationship between instantaneous rates at a point and along a horizontal path has begun. Preliminary results indicate that the average intensity along the path increases with path length for light rainfalls, and diminishes with increasing path length for high rates of fall.

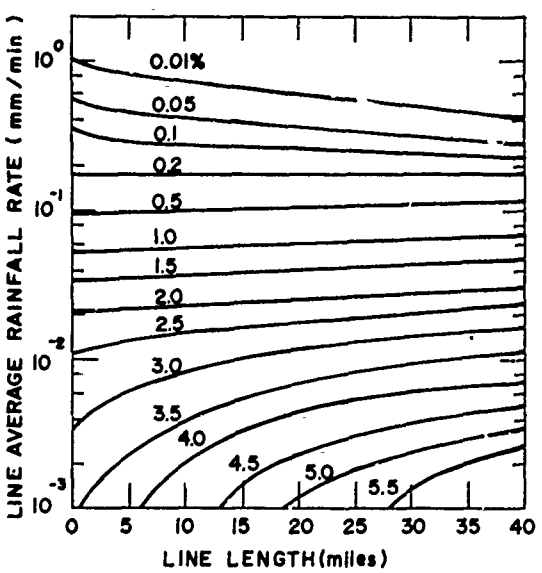

Variation with horizontal path length of the probability of rainfall rates being exceeded.

CONDITIONAL PROBABILITY: The work to produce an analytical model of the conditional probability of an event following a previous event of the same kind was begun several years ago as a basic form of short-range prediction. While many elements in the physical process must enter into the development of a cloudy condition, it is nevertheless apparent that the initial condition of the cloud cover, simply by itself, implies a determinable probability of that cloud cover persisting, rising, lowering or dissipating.

The approach has been to transform the weather element into a normalized variable. Two normalized values, the initial and the subsequent, separated by an interval of time, have joint probability of occurrence which is greater, the greater the correlation between them. An equation yielding the conditional probability that a later event will not exceed any desired threshold value was derived in terms of the cumulative probability distribution of the subsequent initial value.

The next phase will introduce an additional predictor. In the case of cloud cover, the additional element will be wind direction or moisture content as revealed by dew point.

STOCHASTIC MODELING: This investigation is aimed at relating the probability of a

single-point event, like rainfall at the Boston, Massachusetts, rain gauge, to the corresponding probability of the event extending over a larger area. The work was undertaken as a parallel effort to the previously successful modeling of the time frequency and duration of weather events. Modeling for simultaneous occurrences in a horizontal field, however, proved to be much more difficult since there were very few guidelines from previous authors.

With the use of electronic computers, this present effort has produced a stochastic model by Monte Carlo simulation. In its application, estimates are made of the probability of threshold conditions of the weather. In July, in a New England area centered near Worcester, Massachusetts, the probability of no rain, on any day, is 62 percent, of less than 1 inch is 97.5 percent, and of less than 3 inches is 99.9 percent. For an area of (90 nm)², the frequency of no rainfall averaged only two days of the month, but the frequency of a heavy rainfall of 3 inches or more, somewhere in the area, was as high as 3 percent, making it expected at least once during July.

Application of the model made possible such estimates of rainfall as the following: the probability is 9 percent that one tenth of the 8,100 square nautical mile area will receive 1.0 inches or more of rainfall in 24 hours, the probability is ½ percent that as much as one half of the area will receive 1.0 inches of rain. When it rains at the rain-recording station, the probability is 58 percent that it will be raining simultaneously over an entire large city (11 square nautical miles).

Since the stochastic model has proved effective for the probability estimates of 24-hour rainfall in New England, it is expected to apply to other elements of the weather, such as cloud cover, the horizontal extent of fog, warm temperatures, or cold waves. Future work will be devoted to adaptation of the model, as required by the applications.

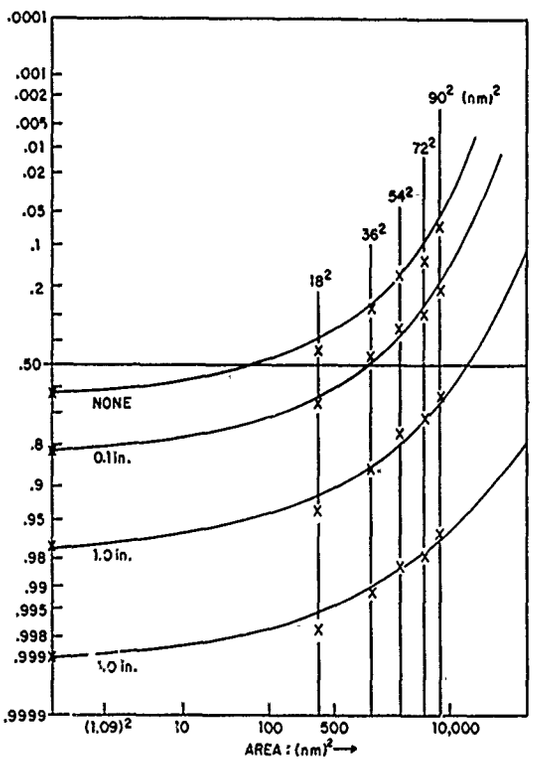

Normal Probability Plot of New England July 24-hour Rainfall. Based on 20 years of data (1952-1971), the X's on the ordinate give the single-point frequency of no rain, <0.1 inch, <1.0 inch, <3.0 inches. The remaining X's give the frequencies of the same amounts as maxima in areas of 18², 36², 54², 72², and 90² nm². The curves give model estimates of the probability of each amount as maximum in the area.

JOURNAL ARTICLES
JULY 1972 - JUNE 1974

BEST, G. T.
Dispersion of Plane Grating Spectrometers
Appl. Opt., Vol. 12, No. 8 (August 1973)
New High Altitude Vapor Trail Tracking Techniques
J. of Atm. and Terrestrial Phys., Vol. 36, No. 3 (1974

BEST, G. T., and FORSBERG, C. A.
Wide-Angle Narrowband Interference Filter Photography
Appl. Opt., Vol. 12, No. 4 (April 1973)

BEST, G. T., and HOFFMAN, H. S.
The Electronic Transition Moment of the $A^1\Sigma - X^1\Sigma$ Band System of BaO

J. of Quantitative Spectroscopy and Radiative Transfer, Vol. 13, No. 1 (January 1973)

CALO, J. M., CAPT.
Heteromolecular Clusters of H_2O, SO_2, CO_2, CO, and NO
Nature, Vol. 248, No. 5450 (1974)

CHAMPION, K. S. W.
The Properties of the Neutral Atmosphere
Space Res. XII, Akademie-Verlag, Berlin, Ger. (1972)
Co-Ed. of Book, *COSPAR International Reference Atmosphere 1972*
Akademie-Verlag, Berlin, Ger. (1972)
Review of Physics of the Atmosphere
Bull. of the Am. Met. Soc., Vol. 54, No. 1 (January 1973)
1968: Composition of the Mesosphere and Lower Thermosphere
Selected Met. Papers, No. 18, Upper Atm. (Compiled by The Met. Soc. of Japan) (August 1973)

CHAMPION, K. S. W., GILLETTE, D. F., and HUSSEY, I. M. (Off. of Res. Svc.)
Atmospheric Densities from Cannon Ball II and Musket Ball Satellite Orbital Observations
Space Res. XIV, Akademie-Verlag, Berlin, Ger. (June 1974)

CHAMPION, K. S. W., and MARCOS, F. A
The Triaxial Accelerometer System on AE
Sp. Ed. of Radio Sci. for Atm. Explorer, Vol. 8, No. 4 (May 1973)
Lower Thermosphere Density Variations Determined from Accelerometers on the Cannon Ball II Satellite
Space Res. XIII, Akademie-Verlag, Berlin, Ger. (May 1973)

CHAMPION, K. S. W., MARCOS, F. A., and SCHWEINFURTH, R. A.
Atmospheric Density Values from Orbital Drag on the Cannon Ball II and Musket Ball Satellites
Space Res. XIII, Akademie-Verlag, Berlin, Ger. (May 1973)

CORBIN, V. L., and KLEIN, M. M.
Scattering of HF Radio Waves by Elliptical Electron Density Distributions
Radio Sci., Vol. 8, No. 8-9 (August-September 1973)

CORBIN, V. L., MOSES, H. E., and QUESADA, A. F.
The Application of the Scale Autocorrelation Coefficient to the Determination of the Harmonic Content of Periodic Phenomena - A Meteorological and a Geophysical Example
J. of Geophys. Res., Vol. 78, No. 27 (20 September 1973)

CORMIER, R. V.
Low Density Extremes for Ground Elevations Up to 15,000 Ft.
J. of Appl. Met., Vol. 12, No. 5 (August 1973)

DANDEKAR, B. S.
Atomic Oxygen Concentration from the (OI) 5577 Å Line Emission at the Auroral Zone Latitude
Planetary and Space Sci., Vol. 20, No. 10 (November 1972)
Simplified Formula for the Determination of the Altitude of an Auroral Arc from a Single Station
J. of Atm. and Terrestrial Phys., Vol. 36, No. 5 (1974)

DANDEKAR, B. S., and DAVIS, D. J., JR.
Photometric Observations of the March Aurora
Sky and Telescope, Vol. 44, No. 9 (September 1972)
Calibration of the Airglow Photometers and Spectrometers
Appl. Opt., Vol. 12, No. 4 (April 1973)
Errata to: Calibrations of the Airglow Photometers and Spectrometers
Appl. Opt., Vol. 12, No. 7 (July 1973)

DEWAN, E. M.
Harmonic Entrainment of Van Der Pol Oscillations: Phaselocking Vs. Asynchronous Quenching
IEEE Trans. on Auto. Control, Vol. 17, No. 5 (October 1972)
Ltr. to the Editor, *Author's Reply to Comments by Buis*
IEEE Trans.., Vol. AC-18, No. 2 (April 1973)
Comments on the Remarks of A. Le Pourheit
IEEE Trans., Vol. AC-18, No. 4 (August 1973)

DONNELLY, R. G. (NOAA, Boulder, Colo.), and HALL, L. A.
Extreme Ultraviolet Spectrum of the Solar Flare of 2114 UT March 27, 1967
Solar Phys., Vol. 31 (August 1973)

FAIRE, A. C., CHAMPION, K. S. W., and MURPHY, E. A.
Variability in Density and Temperature Measurements at White Sands During the 1971 Winter
Space Res. XIII, Akademie-Verlag, Berlin, Ger. (May 1973)

FAIRE, A. C., and MURPHY, E. A.,
Structure Variations in the Winter Polar Atmosphere
Space Res. XIV, Akademie-Verlag, Berlin, Ger. (June 1974)

FAIRE, A. C., MURPHY, E. A., and OLSEN, R. O. (Atm. Sci. Lab., White Sands Missile Range, N. M.)
Atmospheric Density, Temperature and Winds Measured During ALADDIN II
Neutral Atmospheric Density, Temperature and Winds
Space Res. XIV, Akademie-Verlag, Berlin, Ger. (June 1974)

FONTIJN, A. (Aerochem., Inc., Princeton, N. J.), GOLOMB, D., and HODGESON, J. A. (Envmt. Protection Agcy., Res. Triangle Pk., N. C.)
A Review of Experimental Measurement Methods Based on Gas-Phase Chemiluminescence
Chemiluminescence and Bioluminescence, Plenum Pub. Co. (1973)

FORBES, J. M., and MARCOS, F. A.
Thermospheric Density Variations Associated with Auroral Electrojet Activity
J. of Geophys. Res., Vol. 78, No. 19 (July 1973)

FREEMAN, D. E.
Derivatives of Molecular Vibrational Force Constants with a Singular Jacobian
Chem. Phys. Ltrs., Vol. 18, No. 3 (1 February 1973)

GOLOMB, D., GOOD, R. E., and BAILEY, A. B., BUSBY, M. R., DAWBARN, R. (Aro/Arnold Engrg. Dev. Ctr., Tenn.)
Dimers, Clusters and Condensation in Free Jets. II
J. of Chem. Phys., Vol. 57, No. 9 (1972)

GOOD, R. E., and GOLOMB, D.
Atmospheric Oxygen Profiles in the Lower Thermosphere
Space Res. XIII, Akademie-Verlag, Berlin, Ger. (1973)
Dimerization in Free Jets, First Step Towards Condensation
Rarefied Gas Dyn., Eighth Symp., Academic Press (1974)

GRINGORTEN, I. I.
A Square Equal-Area Map of the World
J. of Appl. Met., Vol. 11, No. 5 (August 1972)
Conditional Probability for an Exact Noncategorized Initial Condition
Mo. Wea. Rev., Vol. 100 (November 1972)

HALL, W. N.
3914 A, 5577 A and 6300 A Intensity Measurements at Thule During January 24-29, 1971
World Data Ctr. A Rpt. UAG-24, H. E Coffey and J. V. Lincoln, Eds. (December 1972)

HEROUX, L. J., and MALINOVSKY, M. (Lab. de Phys. Stellaire et Planetaire, Fr.)
An Analysis of the Solar Spectrum Between 50 and 300 A
Astrophys. J., Vol. 181, No. 3, Pt. 1 (1 May 1973)

HINTEREGGER, H. E., BEDO, D. E., and MANSON, J. E.
The Extreme Ultraviolet Spectrophotometer on AE
Radio Sci., Vol. 8, No. 4 (April 1973)

HOFFMAN, H. S., and MOSES, H. E.
The Ultraviolet Convergence of the Electromagnetic Correction to the Ground State Energy of Hydrogen
Lettere al Nuovo Cimento, Vol. 4, No. 2 (1972)

KATAYAMA, D. H., HUFFMAN, R. E., and O'BRYAN, C. L.
The Absorption and Photoionization Cross Sections For H_2O and D_2O in the Vacuum Ultraviolet
J. of Chem. Phys., Vol. 59, No. 8 (1973)

KENESHEA, T. J., and SWIDER, W.
Diurnal D-Region Models Using the Keneshea Code and Present Reaction Rates
J. of Atm. and Terrestrial Phys., Vol. 34, No. 10 (October 1972)

KLEIN, F. S., LEMPERT, G. D. (Weizmann Inst., Israel), MURAD, E., and PERSKY, A. (Weizmann Inst., Israel)
Product Distribution in Ion-Neutral Collisions
Adv. in Mass Spectrometry, Vol. 6 (1974)

LENHARD, R. W
A Revised Assessment of Radiosonde Accuracy
Bull. of the Am. Met. Soc., Vol. 54, No. 7 (July 1973)
Variability of Wind Over a Distance of 16.25 Km
J. of Appl. Met., Vol. 12, No. 6 (September 1973)
Precipitation Intensity and Extent
J. de Recherches Atmospheriques (May 1974)

LUND, I. A.
A Model for Estimating Joint Probabilities of Cloud-Free Lines-of-Sight Through the Atmosphere
J. of Appl. Met., Vol. 12, No. 6 (September 1973)
Persistence and Recurrence Probabilities of Cloud-Free and Cloudy Lines-of-Sight Through the Atmosphere
J. of Appl. Met., Vol. 12, No. 7 (October 1973)

LUND, I. A., and SHANKLIN, M. D. (Univ. of Mo.)
Photogrammetrically Determined Cloud-Free Lines-of-Sight Through the Atmosphere
J. of Appl. Met., Vol. 11, No. 5 (August 1972)
Universal Methods for Estimating Probabilities of Cloud-Free Lines-of-Sight Through the Atmosphere
J. of Appl. Met., Vol. 12, No. 1 (February 1973)

MAC LEOD, M. A.
Improved Computation of Cubic Natural Splines with Equi-Spaced Knots
Math. of Comp., Vol. 27, No. 121 (1973)

MALINOVSKY, M. (Lab. de Phys. Stellaire et Planetaire, Fr.), HEROUX, L. J., and SAHAL-BRECHOT, S. (Obsv. of Meudon, Fr.)
Simultaneous Determination of the Electron Temperature and Density in the Chromospheric-Coronal Transition Region of the Sun
Astron. and Astrophys., Vol. 23 (1973)

MANSON, J. E.
Measurements of the Solar Spectrum Between 30 and 128 A
Solar Phys., Vol. 27 (1972)
A Light Source and Filters for Use in the 130 to 280 A Region
Appl. Opt., Vol. 12, No. 7 (July 1973)

MAPLETON, R. A., and DOHERTY, R. W., MEEHAN, P. E. (RDP, Inc., Bedford, Mass.)
Electron Capture from $He(1s^2)$ by Protons, III
Phys. Rev. A, Vol. 9, No. 2 (February 1974)

MAPLETON, R. A., DOHERTY, R. W., RUSSEL, J. F., MEEHAN, P. E. (RDP, Inc., Boston, Mass.)

Electron Capture from Argon by Multiply Charged Atomic Oxygen Ions
Phys. Rev., Vol. 7, No. 9 (September 1973)

MARCOS, F. A., and CHAMPION, K. S. W.
Gravity Waves Observed in High Latitude Neutral Density Profiles
Space Res. XII, Akademie-Verlag, Berlin, Ger. (1972)

MC ISAAC, J. P., and CHAMPION, K. S. W.
Direct Measurement of the Semi-Annual Variation During 1968
Space Res. XII, Akademie-Verlag, Berlin, Ger. (1972)

MC MAHON, W. J., and HEROUX, L. J.
Measurement of Energy and Angular Distribution of Extreme Ultraviolet Photoelectrons
Appl. Opt., Vol. 13, No. 2 (February 1974)

MOORE, J. G.
Zenith Intensities of the (O I) 5577 Å and 6300 Å Radiation Inside the Polar Cap During the January 1971 Solar Particle Event
World Data Ctr. A Rpt. UAG-24, H. E. Coffey and J. V. Lincoln, Eds. (December 1972)

MOSES, H. E.
Exact Electromagnetic Matrix Elements and Exact Selection Rules for Hydrogenic Atoms
Lettere al Nuovo Cimento, Vol. 4, No. 2 (1972)
Exact Vorticity Solutions of the Incompressible Navier-Stokes Equations
J. de Mecanique (Paris, Fr.), No. 3 (September 1972)
An Exact Solution of Euler's Equations for the Motion of a Gas on a Rotating Sphere
Phys. of Fluids, Vol. 16, No. 8 (August 1973)
An Exact Solution for the Rotation of the Atmosphere About the Spheroidal Earth
J. of Geophys. Res., Vol. 78, No. 27 (20 September 1973)
The Expansion of Electromagnetic Fields and Potentials in the Wave Functions of the Photon. The Exact Electromagnetic Matrix Elements and Selection Rules of Hydrogenic Atoms
Phys. Rev. A, Vol. 8, No. 4 (October 1973)
The Use of Vector Spherical Harmonics in Global Meteorology and Aeronomy
J. of Atm. Sci., Vol. 31 (1974)

MOSES, H. E., and QUESADA, A. F.
The Expansion of Physical Quantities in Terms of the Irreducible Representations of the Scale Euclidean Group and Application to the Construction of Scale-Invariant Correlation Functions. Part II - Three Dimensional Problems
Archive for Rational Mech., Vol. 50, No. 3 (1973)
The Power Spectrum of the Mellin Transformation with Application to Scaling of Physical Quantities
J. of Math. Phys., Vol. 15, No. 6 (June 1974)

MULLEN, E. G., and DAVIS, D. J., JR.
Photometric Observations of Auroras During August 1972
Sky and Telescope, Vol. 45, No. 2 (February 1973)

MURAD, E.
The Apparent Charge Transfer Reaction $O^+ + CO \rightarrow CO^+ + O$
Chem. Phys. Ltrs., Vol. 16, No. 3 (15 October 1972)
The Reaction of O^+ with CO
J. of Chem. Phys., Vol. 58, No. 10 (15 May 1973)

NARCISI, R. S.
O_2^+ as a Source of Water Cluster Ions in the D Region and Negative Ion Composition Measurements in the D and Lower E Region
COSPAR Symp. on D- and E-Region Ion Chem., Aeron. Rpt. No. 48, C. F. Sechrist, Jr., and M. A. Geller, Eds., Univ. of Ill., Urbana, Ill. (1972)
Mass Spectrometer Measurements in the Ionosphere
Chap. in Phys. and Chem. of Upper Atm., Proc. of the Summer Advanced Inst., Orleans, Fr., 31 July - 11 Aug. 1972; B. M. McCormac, Ed.; D. Reidel Pub. Co., Dordrecht, Holl. (1973)
Ion and Neutral Composition Measurements in the Lower Ionosphere
Space Res. XIV, Akademie-Verlag, Berlin, Ger. (June 1974)

NARCISI, R. S., PHILBRICK, C. R., MAC LEOD, M. A., and ROSENBERG, N. W.
Composition Measurements of Sporadic E and Ions from a Chemical Release
Space Res. XIII, Akademie-Verlag, Berlin, Ger. (1973)

PAULSON, J. F.
Negative Ion-Neutral Reactions
Chap. in Book, Ion-Molecule Reactions (1972)

PHILBRICK, C. R.
Satellite Measurements of Atmospheric Composition in the Altitude Range 150 to 450 Km
Space Res. XIV, Akademie-Verlag, Berlin, Ger. (June 1974)

PHILBRICK, C. R., GOLOMB, D., ZIMMERMAN, S. P., KENESHEA, T. J., MAC LEOD, M. A., GOOD, R. E., DANDEKAR, B. S., and REINISCH, B. W. (Lowell Technol. Inst. Res. Fdn., Mass.)
The ALADDIN Experiment - Part II, Composition (Preliminary Results)
Space Res. XIV, Akademie-Verlag, Berlin, Ger. (June 1974)

ROSENBERG, N. W., GOLOMB, D., ZIMMERMAN, S. P., VICKERY, W. K., and THEON, J. S. (NASA Goddard Space Flt. Ctr., Greenbelt, Md.)
The ALADDIN Experiment, Part I - Dynamics

Space Res. XIII, Akademie-Verlag, Berlin, Ger. (1973)

SILVERMAN, S. M., KRASSA, R. F. K., and TURTLE, J. P.
Measurements at the AFCRL Geopole Observatory During August 1972
World Data Ctr. A Rpt. UAG-28, H. E. Coffey, Ed. (July 1973)

SILVERMAN, S. M., and MULLEN, E. G.
Eclipses: A Literature of Misadventures
Natural Hist., Vol. 81, No. 6 (June - July 1972)

SILVERMAN, S. M., and TUAN, T. F. (Univ. of Cincinnati, Ohio)
Auroral Audibility
Adv. in Geophys., Vol. 16 (August 1973)

SWIDER, W.
E-Region Model Parameters
J. of Atm. and Terrestrial Phys., Vol. 34, No. 10 (October 1972)

SWIDER, W., and KENESHEA, T. J.
Decrease of Ozone and Atomic Oxygen in the Lower Mesosphere During a PCA Event
Planetary and Space Sci., Vol. 21, No. 11 (1973)

TANAKA, Y., and YOSHINO, K.
Absorption Spectra of Ne_2 and HeNe Molecules in the Vacuum-UV Region
J. of Chem. Phys., Vol. 57, No. 7 (1 October 1972)

TANAKA, Y., YOSHINO, K., and FREEMAN, D. E.
On the Determination of the Ground State Potential Energy of Ne_2 from Its Vacuum Ultraviolet Spectrum
J. of Chem. Phys., Vol. 59, No. 1 (1 July 1973)
Vacuum Ultraviolet Absorption Spectra of the Van Der Waals Molecules Kr_2 and ArKr
J. of Chem. Phys., Vol. 59, No. 9 (1 November 1973)
Low-Lying Excited Electronic States of Diatomic Krypton
Bull. of the Am. Phys. Soc., Vol. 19, No. 2 (1974)

TURTLE, J. P.
Effects of the January 1971 Solar Particle Event on Polar VLF Propagation
World Data Ctr. A Rpt. UAG-24, H. E. Coffey and J. V. Lincoln, Eds. (December 1972)
Effects of the September 1971 Solar Particle Event on Polar VLF Propagation
World Data Ctr. A Rpt. UAG-24, H. E. Coffey and J. V. Lincoln, Eds. (December 1972)

VAN TASSEL, R. A., HUFFMAN, R. E., and ROEBBER, J. C. (Northeastern Univ., Boston, Mass.)
Atomic Oxygen Oscillator Strengths in the Autoionization Region. I. The Absolute Strength of the 5s Lines
J. of Chem. Phys., Vol. 59, No. 11 (1973)

YOSHINO, K., and CARROLL, P. K. (Univ. Coll., Dublin, Ire.)
The $Cn'\pi\mu$ and $Cn'\ ^1\Sigma\mu$ + Rydberg States of N_2 High Resolution Studies
J. of Phys. B, Atomic and Mol. Phys., Vol. 5, No. 8 (August 1972)

ZIMMERMAN, S. P.
Meteor Trails and Atmospheric Turbulence
J. of Geophys. Res., Vol 78, No. 19 (1 July 1973)
The Effective Vertical Turbulent Viscosity as Measured from Radio Meteor Trails
J. of Geophys. Res., Vol. 79, No. 7 (1 March 1974)

ZIMMERMAN, S. P., and LOVING, N. V. (AF Flt. Dyn. Lab., Wright-Patterson AFB, Oh.)
Turbulent Dissipation and Diffusivities in the Stratosphere
CIAP Monograph I, "The Natural Strato." (1974)

ZIMMERMAN, S. P., and PAO, M. Y. H. (Flow Res., Inc., Seattle, Wash.)
Lagrangian Description of Turbulent Diffusion
CIAP Monograph I, "The Natural Strato." (1974)

ZIMMERMAN, S. P., PEREIRA, G. P., MURPHY, E. A., and THEON, J. (NASA Goddard Space Flt. Ctr., Greenbelt, Md.)
Internal Gravity Waves and Turbulence in Simultaneous Upper Atmosphere Temperature and Wind Measurements
Space Res. XIII, Akademie-Verlag, Berlin, Ger. (1973)

ZIMMERMAN, S. P., ROSENBERG, N. W., FAIRE, A. C., GOLOMB, D., and TROWBRIDGE, C. A. (PhotoMet., Inc., Lexington, Mass.), MURPHY, E. A., VICKERY, W. K., and REES, D. (Univ. Coll., London, Eng.), SMITH, L. B. (Sandia Corp., Albuquerque, N. M.)
The ALADDIN II Experiment - Part I. Dynamics
Space Res. XIV, Akademie-Verlag, Berlin, Ger. (June 1974)

ZIMMERMAN, S. P., and TROWBRIDGE, C. A. (PhotoMet., Inc., Lexington, Mass.)
The Measurement of Turbulent Spectra and Diffusion Coefficients in the Altitude Region 90 to 105 Km
Space Res. XIII, Akademie-Verlag, Berlin, Ger. (1973)

PAPERS PRESENTED AT MEETINGS JULY 1972 - JUNE 1974

CALO, J. M., CAPT.
Cluster Formation from SST Pollutants
(Inv. Paper) Mtg. on Strato. Aerosols, Dept. of Trnsp., Wash., D. C. (5 October 1972)

CHAMPION, K. S. W.

COSPAR International Reference Atmospheres 1972
2nd Conf. of Appl. of Chem. to Nuc. Wpn Eff., Inst. for Def. Analys., Arlington, Va. (12-14 September 1972)

Achievements of ALADDIN II
1973 Ann. Am. Geophys. Union Mtg., Wash., D. C. (16-20 April 1973)

Dynamics and Structure of the Quiet Thermosphere
1974 Intl. Symp. on Solar Terrestrial Phys./17th Plenary Mtg. of COSPAR, Sao Paulo, Brazil (17 June - 1 July 1974)

CHAMPION, K. S. W., GILLETTE, D. F., and HUSSEY, I. M. (Off. of Res. Svc.)

Drag Density from the Cannon Ball II and Musket Ball Satellites
16th Plenary Mtg. of COSPAR, Konstanz, Fed. Rep. of Ger. (23 May - 6 June 1973)

CHERNOSKY, E. J.

Relation of SKp to the Direction of the Interplanetary Magnetic Field as Inferred from Polar Cap Observations
1973 Ann. Am. Geophys. Union Mtg., Wash., D. C. (16-20 April 1973)

COHEN, H. A., and WILSON, P. S.

Laboratory Measurements of the Effectiveness of a Magnetic Shield
12th Symp. on Elect., Ion and Laser Beam Technol., Mass. Inst. of Technol., Cambridge, Mass. (21-23 May 1973)

A Measurement of the Gas Density Near a Rocket Using Electron Beam Induced Bremsstrahlung and Luminescence
55th Ann. Spring Mtg. of the Am. Geophys. Union, Wash., D. C. (8-12 April 1974)

COLE A. E.

International Standards Organization (ISO) Reference Atmospheres
ISO Com. on Std. and Ref. Atm. Mtg., Paris, Fr. (5-8 October 1973)

Periodic Oscillations in the Stratosphere and Mesosphere
1974 Intl. Symp. on Solar Terrestrial Phys./17th Plenary Mtg. of COSPAR, Sao Paulo, Brazil (17 June - 1 July 1974)

CORMIER, R. V.

Realism in Environmental Design Criteria - MIL-STD-210B
Ann. Mtg. of the Inst. of Envmt. Sci., Anaheim, Calif. (2-5 April 1973)

The Temporal and Spatial Variability of Integrated Boundary Layer Winds
5th AMS Conf. on Wea. Forecasting and Analys., St. Louis, Mo. (4-8 March 1974)

Climatic Extremes for the Design of World-Wide Military Equipment – MIL-STD-210B
20th Ann. Mtg. of the Inst. of Envmt. Sci., Wash., D. C. (28 April - 1 May 1974)

Climatic Extremes for the World-Wide Environment to 80 Km
11th Natl. Conf. on Envmt. Eff. on Acft. and Prpln. Sys., Trenton, N. J. (21-23 May 1974)

DANDEKAR, B. S.

Determination of the Atomic Oxygen Concentration from the Rocket Measurement of the (OI) 5577 Å Line Emission of the Airglow
1973 Ann. Am. Geophys. Union Mtg., Wash., D. C. (16-20 April 1973)

DEWAN, E. M

Thermally Stratified Compressible Fluid Motion on a Rotating Sphere with Gravitation
Am. Phys. Soc. Mtg., Wash., D. C. (23-26 April 1973)

The Stratosphere as Protector of the Global Biological System
Govt. Microcircuit Appl. Conf., Boulder, Colo. (25-27 June 1974)

DRAPER, J. S., BIEN, F. (Aerodyne Res., Inc., Burlington, Mass.), HUFFMAN, R. E., and PAULSEN, D. E.

Effect of the State of the Thermosphere on Man-Made Flowfields
1973 Ann. Fall Mtg. of the Am. Geophys. Union, San Francisco, Calif. (10-14 December 1973)

FAIRE, A. C., and CHAMPION, K. S. W.

Rocketborne Measurements of Atmospheric Perturbations in a Nuclear Environment
Jt. Strat. Sci. Mtg., San Diego, Calif. (7-9 January 1974)

FAIRE, A. C., and MURPHY, E. A.

Neutral Density and Temperature Results Obtained at Wallops Island on 31 January 1972
Fall Ann. Mtg. of the Am. Geophys. Union, San Francisco, Calif. (4-7 December 1972)

Structure Variations in the Winter Polar Atmosphere
16th Plenary Mtg. of COSPAR, Konstanz, Fed. Rep. of Ger. (23 May - 6 June 1973)

FAIRE, A. C., MURPHY, E. A., and OLSEN, R. O. (Atm. Sci. Lab., White Sands, N. M.)

Neutral Atmospheric Density, Temperature and Winds
1973 Ann. Am. Geophys. Union Mtg., Wash., D. C. (16-20 April 1973)

Atmospheric Density Temperature and Winds Measured During ALADDIN II
16th Plenary Mtg. of COSPAR, Konstanz, Fed. Rep. of Ger. (23 May - 6 June 1973)

FONTIJN, A. (Aerochem., Inc., Princeton, N. J.), GOLOMB, D., and HODGESON, J. A. (Envmt. Protection Agcy., Res. Triangle Pk., N. C.)

A Review of Experimental Measurement Methods Based on Gas-Phase Chemiluminescence
Intl. Chemiluminescence Symp., Univ. of Ga., Athens, Ga. (13-14 October 1972)

FORBES, J. M., CAPT.
Thermospheric Response to Joule Heating in the Auroral Electrojet
ARPA Iono. Modeling Mtg., NOAA, Boulder, Colo. (31 October - 2 November 1972)

FREEMAN, D. E., YOSHINO, K., and TANAKA, Y.
Vacuum Ultraviolet Absorption Spectrum of the Van der Waals Molecule Xe_2 Part II. Ground State Vibrational Structure and Potential Well Depth
29th Ann. Symp. on Mol. Structure and Spectroscopy, Ohio State Univ., Columbus, Ohio (10-14 June 1974)

GOLOMB, D.
Metallic Vapor Releases - A Status Report
DNA Atm. Eff. Symp., San Diego, Calif. (9-13 April 1973)

GOLOMB, D., and BEST, G. T.
Photoluminescence of PbO in the Upper Atmosphere
55th Ann. Spring Mtg. of the Am. Geophys. Union, Wash., D. C. (8-12 April 1974)

GOLOMB, D., and GOOD, R. E.
Atomic Oxygen Densities from Nitric Oxide Headglow
1973 Ann. Am. Geophys. Union Mtg., Wash., D. C. (16-20 April 1973)

GOOD, R. E., BEST, G. T., and HARPELL, G. F. (Off. of Res. Svc.)
Rocket Measurement of Ozone at Twilight
1975 Ann. Am. Geophys. Union Mtg., Wash., D. C. (16-20 April 1973)

GOOD, R. E., and GOLOMB, D.
Dimerization in Free Jets, First Step Toward Condensation
8th Intl. Symp. on Rarefied Gas Dyn., Stanford Univ., Menlo Pk., Calif. (10-14 July 1972)
NO Release in Sunlight and Measurement of Atomic Oxygen from Chemiluminescence
55th Ann. Spring Mtg. of the Am. Geophys. Union, Wash., D. C. (8-12 April 1974)

GRINGORTEN, I. I.
A Stochastic Model of Areal Persistence
3rd Conf. on Prob. and Stat. in Atm. Sci., Boulder, Colo. (19-22 June 1973)
A Study of the Horizontal Extent of Rainfall by Stochastic Modeling
1973 Ann. Fall Mtg. of the Am. Geophys. Union, San Francisco, Calif. (10-14 December 1973)

HALL, W. N.
Low Latitude Pulsating Auroras
1973 Ann. Am. Geophys. Union Mtg., Wash., D. C. (16-20 April 1973)

HOFFMAN, H. S., GOLOMB, D., and BEST, G. T.
Chemiluminescence of Sodium Vapor Released at Night
55th Ann. Spring Mtg. of the Am. Geophys. Union, Wash., D. C. (8-12 April 1974)

HUFFMAN, R. E.
Vacuum Ultraviolet Spectroscopy and the Earth's Atmosphere
(Inv. Sem.) Atomic and Mol. Phys. Gp., Dept. of Phys., Univ. of Tex., Austin, Tex. (20 October 1972)
Vacuum Ultraviolet Problems Related to Weapons Effects Codes
DNA Atm. Eff. Symp., San Diego, Calif. (9-13 April 1973)
Vacuum Ultraviolet Instrumentation
Sem., Univ. of Calif., Santa Barbara, Calif. (11 April 1973)

INNES, F. R.
The Classical Adjoint for Spherical Tensors and Products
Am. Phys. Soc. Mtg., Wash., D. C. (23-26 April 1973)
The Operators of Angular Momentum Theory and their Adjoints
Am. Phys. Soc. Mtg., New England Sec., Providence, R. I. (5-6 April 1974)

KATAYAMA, D. H., HUFFMAN, R. E., and TANAKA, Y.
The Absorption Spectrum of O_2 in the Vacuum Ultraviolet Region
Symp. on Mol. Structure and Spectroscopy, Ohio State Univ., Columbus, Ohio (11-15 June 1973)
O_2 ($a\,^1\Delta g$) Absorption Bands in the Vacuum Ultraviolet
29th Ann. Symp. on Mol. Structure and Spectroscopy, Ohio State Univ., Columbus, Ohio (10-14 June 1974)

KENESHEA, T. J.
Numerical Model of the ALADDIN I Experiment
2nd Conf. of Appl. of Chemistry to Nuc. Wpn. Eff., Inst. for Def. Analys., Arlington, Va. (12-14 September 1972)

KENESHEA, T. J., and ZIMMERMAN, S. P.
Modeling the ALADDIN II Experiment
1973 Ann. Am. Geophys. Union Mtg., Wash., D. C. (16-20 April 1973)

KITROSSER, D. F., GOLOMB, D., and REES, D. (Univ. Coll., London, Eng.)
Temperatures, Diffusion Coefficients and Densities from Photoluminescent AlO Clouds
1973 Ann. Am. Geophys. Union Mtg., Wash., D. C. (16-20 April 1973)

KLEIN, F. S., LEMPERT, G. D. (Weizmann Inst., Israel), MURAD, E., and PERSKY, A. (Weizmann Inst., Israel)
Product Distribution in Ion-Neutral Collisions
6th Intl. Conf. on Mass Spectrometry, Edinburgh, Scot. U. K. (10-14 September 1973)

LENHARD, R. W.
Precipitation Intensity and Extent
IUCRM Colloq. on the Fine Scale Structure of

Precipitation and EM Propagation, Nice, Fr. (23-31 October 1973)

LUND, I. A.
An Objective Procedure for Alerting Forecasters of Potential Low Visibilities at Travis AFB, California
5th AMS Conf. on Wea. Forecasting and Analys., St. Louis, Mo. (4-8 March 1974)

MAC LEOD, M. A., KENESHEA, T. J., and REINISCH, B. W. (Lowell Technol. Inst. Res. Fdn., Lowell, Mass.)
The ALADDIN II Ionosphere: A Comparison of Theoretical Calculations with Digisonde Observations
1973 Ann. Am. Geophys. Union Mtg., Wash., D. C. (16-20 April 1973)

MANSON, J. E.
Calibration Techniques Between 30 and 200 Angstroms
NBS-Sponsored Sec. Wkshp. on VUV Radiometric Calibrations of Space Exper., Univ. of Colo., Boulder, Colo. (28-29 November 1972)

MARCOS, F. A., MC INERNEY, R. (Off. of Res. Svc.), and DELOREY, D., RICHARDS, E. (Boston Coll., Mass.)
Satellite Density Measurements of the Lower Thermosphere Summer Northern Hemisphere
55th Ann. Spring Mtg. of the Am. Geophys. Union, Wash., D. C. (8-12 April 1974)

MOSES, H. E.
A Simple Exact Solution for the Motion of the Atmosphere About the Rotating Earth
Fall Ann. Mtg. of the Am. Geophys. Union, San Francisco, Calif. (4-7 December 1972)

MURPHY, E. A., FAIRE, A. C., and CHAMPION, K. S. W.
Density and Temperature Measurements in the Polar Winter Atmosphere During Quiet and Disturbed Conditions
55th Ann. Spring Mtg. of the Am. Geophys. Union, Wash., D. C. (8-12 April 1974)

MURPHY, E. A., FAIRE, A. C., ZIMMERMAN, S. P., and ROSENBERG, N. W.
Atmospheric Instabilities Measured During ALADDIN II
1973 Ann. Am. Geophys. Union Mtg., Wash., D. C. (16-20 April 1973)

NARCISI, R. S.
Mass Spectrometer Measurements in the Ionosphere
Summer Adv. Inst. on Phys. and Chem. of Upper Atm., Univ. of Orleans, Orleans, Fr. (31 July - 11 August 1972)
A Potpourri on the Lower Ionosphere, D and E Region Composition During PCA and Auroral Disturbances
2nd Conf. of Appl. of Chem. to Nuc. Wpn. Eff., Inst. for Def. Analys., Arlington, Va. (12-14 September 1972)
Ion and Neutral Composition Measurements in the Lower Ionosphere
16th Plenary Mtg. of COSPAR, Konstanz, Fed. Rep. of Ger. (23 May - 6 June 1973)
The Lower Ionosphere - Its Composition, Structure and Phenomenology
Colloq., Worcester Polytech., Worcester, Mass. (8 May 1974)

NARCISI, R. S., BAILEY, A. D., THOMAS, D. M., and WLODYKA, L. E.
D and E Region Positive Ion Composition During an Auroral Absorption Event
55th Ann. Spring Mtg. of the Am. Geophys. Union, Wash., D. C. (8-12 April 1974)

NARCISI, R. S., and SWIDER, W.
Mesospheric Neutral Constituents Deduced from PCA Ion Composition Measurements
DNA Atm. Eff. Symp., San Diego, Calif. (9-13 April 1973); 1973 Ann. Am. Geophys. Union Mtg., Wash., D. C. (16-20 April 1973)

PAULSEN, D. E. LARRABEE, J. C., LE BLANC, F. J., and HUFFMAN, R. E.
Measurement of the Night Ultraviolet Airglow Layer Near 100 Kilometers
1973 Ann. Fall Mtg. of the Am. Geophys. Union, San Francisco, Calif. (10-14 December 1973)

PAULSON, J. F.
Laboratory Studies on Ion-Neutral Reactions
2nd Conf. of Appl. of Chem. to Nuc. Wpn. Eff., Inst. for Def. Analys., Arlington, Va. (12-14 September 1972)
Charge Transfer and Collisional Dissociation Reactions in Ion Beam Studies
DNA Atm. Eff. Symp., San Diego, Calif. (9-13 April 1973)

PAULSON, J. F., and GALE, J., HENCHMAN, M. J., MASSON, A. J. (Brandeis Univ., Waltham, Mass.)
Accidentally Resonant Charge Transfer Reactions
22nd Ann. Conf. on Mass Spectrometry and Allied Topics, Philadelphia, Pa. (13-17 May 1974)

PHILBRICK, C. R.
Satellite Measurements of Atmospheric Composition in the Altitude Range 150 to 450 Km
16th Plenary Mtg. of COSPAR, Konstanz, Fed. Rep. of Ger. (23 May - 6 June 1973)

PHILBRICK, C. R., FAUCHER, G. A., and TRZCINSKI, E.
Composition Measurements During the ALADDIN II Program
1973 Ann. Am. Geophys. Union Mtg., Wash., D. C. (16-20 April 1973)

PHILBRICK, C. R., GOLOMB, D., ZIMMERMAN, S. P., KENESHEA, T. J., MAC LEOD, M. A., GOOD, R. E., DANDEKAR, B. S., and REINISCH, B. W. (Lowell Technol. Inst. Res. Fdn., Lowell, Mass.)
The ALADDIN Experiment - Part II. Composition (Preliminary Results)

16th Plenary Mtg. of COSPAR, Konstanz, Fed. Rep. of Ger. (23 May - 6 June 1973)

PORTER, H. S. (Univ. of Cincinnati, Ohio), SILVERMAN, S. M., and TUAN, T. F. (Univ. of Cincinnati, Ohio)
The Effect of Gravity Waves on 6300 Å and 5200 Å Airglow
1973 Ann. Am. Geophys. Union Mtg., Wash., D. C. (16-20 April 1973)

REES, D. (Univ. Coll., London, Eng.), KITROSSER, D. F., and GOLOMB, D.
Combined Temperature, Diffusion Coefficient and Density Measurements of Photoluminescent AlO Releases
16th Plenary Mtg. of COSPAR, Konstanz, Fed. Rep. of Ger. (23 May - 6 June 1973)

REINISCH, B. W. (Lowell Technol. Inst. Res. Fdn., Lowell, Mass.), and MAC LEOD, M. A.
Chemical Releases at Sunset Trigger Sporadic E
1973 Ann. Am. Geophys. Union Mtg., Wash., D. C. (16-20 April 1973)

ROSENBERG, N. W., and DEWAN, E. M., JR.
Stratospheric Turbulence and Vertical Effective Diffusion Coefficients
CIAP Mtg., Dept. of Trnsp., Cambridge, Mass. (26 February 1974)

ROSENBERG, N. W., GOOD, R. E., and DEWAN, E. M.
Wind Determined Atmospheric Turbulence: Smoke Trails, Jimspheres, Radiosonde
55th Ann. Spring Mtg. of the Am. Geophys. Union, Wash., D.C. (8-12 April 1974)

ROSENBERG, N. W. GOOD, R. E., VICKERY, W. K., and DEWAN, E. M., JR.
Experimental Determination of Small Scale Transport Mechanisms in the Stratosphere
Mtg. of AIAA and AMS, Denver, Colo. (12 June 1973)

ROSENBERG, N. W., GOOD, R. E., and ZIMMERMAN, S. P.
Transport Measurements in the Stratosphere
Dept. of Trnsp.-CIAP Sys. Ctr., Cambridge, Mass. (14 November 1972)

ROSENBERG, N. W., and ROPER, R. G. (Ga. Inst. of Technol., Atlanta, Ga.)
ALADDIN II Winds and Shears
1973 Ann. Am. Geophys. Union Mtg., Wash., D. C. (16-20 April 1973)

SECHRIST, C. F., JR. (Univ. of Ill.), and NARCISI, R. S.
Nitric Oxide and the Winter D Region
55th Ann. Spring Mtg. of the Am. Geophys. Union, Wash., D. C. (8-12 April 1974)

SHERMAN, C., SWIDER, W., and NARCISI, R. S.
Auroral Ion Composition Measurements and Model
DNA Atm. Eff. Symp., San Diego, Calif. (9-13 April 1973)

1973 Ann. Am. Geophys. Union Mtg., Wash., D. C. (16-20 April 1973)

SWIDER, W.
Chemistry of the E- and F-Regions
2nd Conf. of Appl. of Chem. to Nuc. Wpn. Eff., Inst. for Def. Analys., Arlington, Va. (12-14 September 1972)
E and F Region Chemistry
Iono. Modeling Mtg., NOAA, Boulder, Colo. (31 October - 2 November 1972)

SWIDER, W., and KENESHEA, T. J.
Diurnal Variation of the D-Region During a PCA Event
Iono. Modeling Mtg., NOAA, Boulder, Colo. (31 October - 2 November 1972)
Decrease of Ozone with Increasing Ionization During a PCA Event
1973 Ann. Am. Geophys. Union Mtg., Wash., D. C. (16-20 April 1973)

SWIDER, W., KENESHEA, T. J., and FOLEY, C. I. (Boston Coll., Mass.)
Nitric Oxide and Atomic Nitrogen in the Auroral E-Region
55th Ann. Spring Mtg. of the Am. Geophys. Union, Wash., D.C. (8-12 April 1974)

SWIDER, W., KENESHEA, T. J., and ULWICK, J. C. (Iono. Phys. Lab.)
Photodetachment During a PCA Event
DNA Atm. Eff. Symp., San Diego, Calif. (9-13 April 1973)

SWIDER, W., KENESHEA, T. J., and WEEKS, L. H.
Decline of Ozone and Atomic Oxygen During a PCA Event
DNA Atm. Eff. Symp., San Diego, Calif. (9-13 April 1973)

TAKEZAWA, S.
The Absorption Spectrum of NO in the VUV Region: Rydberg Bands, $3s\,\sigma \leftarrow 1\pi$
29th Ann. Symp. on Mol. Structure and Spectroscopy, Ohio State Univ., Columbus, Ohio (10-14 June 1974)

TANAKA, Y.
The Absorption and Emission Spectra of Rare Gas Molecules
Am. Phys. Soc. Mtg., Univ. of So. Calif., Los Angeles, Calif. (27-29 December 1972)

TANAKA, Y., YOSHINO, K., and FREEMAN, D. E.
The Absorption Spectrum of Kr_2 in the Vacuum Ultraviolet Region
Symp. on Mol. Structure and Spectroscopy, Ohio State Univ., Columbus, Ohio (11-15 June 1973)
Low-Lying Excited Electronic States of Diatomic Krypton
26th Ann. Gaseous Elect. Conf., Univ. of Wis. (17-19 October 1973)
Vacuum Ultraviolet Absorption Spectrum of the van der Waals Molecule Xe_2 Part I. Excited Electronic States
29th Ann. Symp. on Mol. Structure and Spectroscopy, Ohio State Univ., Columbus, Ohio (10-14 June 1974)

TATTELMAN, P., and GRINGORTEN, I. I.
Estimated Glaze Ice and Wind Loads at the Earth's Surface for the Contiguous United States
5th AMS Conf. on Wea. Forecasting and Analys., St. Louis, Mo. (4-8 March 1974)

THOMAS, D. M., NARCISI, R. S., BAILEY, A. D., and WLODYKA, L. E.
D and E Region Negative Ion Composition During an Auroral Absorption Event
55th Ann. Spring Mtg. of the Am. Geophys. Union, Wash., D. C. (8-12 April 1974)

VAN TASSEL, R. A., HUFFMAN, R. E., and ROEBBER, J. L. (Northeastern Univ., Boston, Mass.)
Oscillator Strength of the Autoionized Transition: O $I^3 P_2 \rightarrow 5s^3 D^\circ$ (775.3Å)
1st Intl. Conf. on Spectral Lines, Univ. of Tenn., Knoxville, Tenn. (28 August - 1 September 1972)
Oscillator Strengths of Atomic Oxygen Autoionized Lines
2nd Conf. of Appl. of Chem. to Nuc. Wpn. Eff., Inst. for Def. Analys., Arlington, Va. (12-14 September 1972)

WEEKS, L. H.
Ozone and Molecular Oxygen
2nd Conf. of Appl. of Chem. to Nuc. Wpn. Eff., Inst. for Def. Analys., Arlington, Va. (12-14 September 1972)
Molecular Oxygen Observations from UV Absorption
1973 Ann. Fall Mtg. of the Am. Geophys. Union, San Francisco, Calif. (10-14 December 1973)

YOSHINO, K., and TANAKA, Y.
Homogeneous Perturbation between the o $^1\pi u$ State and the $b^1\pi u$ State of the Nitrogen Molecule
Symp. on Mol. Structure and Spectroscopy, Ohio State Univ., Columbus, Ohio (11-15 June 1973)
Homogeneous Perturbation Between the c^14 (v=0) $^1\Sigma^+u$ (or p^1) and the b(v=1) $^1\Sigma_u^+$ Levels of N_2
29th Ann. Symp. on Mol. Structure and Spectroscopy, Ohio State Univ., Columbus, Ohio (10-14 June 1974)

ZIMMERMAN, S. P., and KENESHEA, T. J.
Models and Atmospheres
Am. Inst. of Aero. and Astro., Wash., D. C. (29-30 January 1974)

ZIMMERMAN, S. P., and LOVING, N. V. (AF Flt. Dyn. Lab., Wright-Patterson AFB, Ohio)
Turbulent Dissipation and Diffusivities in the Stratosphere
Mtg. of the Sci. Panel on the Nat. Strato., Ft. Lauderdale, Fla. (28 November - 2 December 1972)

ZIMMERMAN, S. P., and PAO, M. Y. H. (Flow Res., Inc., Seattle, Wash.)
La Grangian Description of Turbulent Diffusion
Mtg. of the Sci. Panel of the Nat. Strato., Ft. Lauderdale, Fla. (28 November - 2 December 1972)

ZIMMERMAN, S. P., ROSENBERG, N. W., FAIRE, A. C., GOLOMB, D., and TROWBRIDGE, C. A. (PhotoMet., Inc., Lexington, Mass.), MURPHY, E. A., VICKERY, W. K., and REES, D. (Univ. Coll., London, Eng.), and SMITH, L. B. (Sandia Labs., Albuquerque, N. M.)
The ALADDIN II Experiment - Part I. Dynamics
16th Plenary Mtg of COSPAR, Konstanz, Fed. Rep. of Ger. (23 May - 6 June 1973)

ZIMMERMAN, S. P., and TROWBRIDGE, C. A. (PhotoMet., Inc., Lexington, Mass.)
The Turbulence Spectra of Dissipation Rates and Diffusion Coefficients Measured During the ALADDIN II Experiment
1973 Ann. Am. Geophys. Union Mtg., Wash., D. C. (16-20 April 1973)

ZIMMERMAN, S. P., and WALLACE, J. M. (Univ. of Wash.), DANIELSEN, E. (NCAR, Boulder, Colo.), LIST, R. (NOAA, Boulder, Colo.), ELLSAEESER, H. (Lawrence Livermore Lab., Calif.), LILL, D. (NCAR, Boulder, Colo.), LOVING, N. (AF Flt. Dyn. Lab., Wright-Patterson AFB, Ohio), PAO, M. Y. H. (Flow Res., Inc., Seattle, Wash.)
The Description of the Natural Stratosphere in Its Present State
Mtg. of the Sci. Panel of the Nat. Strato., Ft. Lauderdale, Fla. (28 November - 2 December 1972)

TECHNICAL REPORTS
JULY 1972 - JUNE 1974

CHAMPION, K. S. W., and SCHWEINFURTH, R. A.
A New Mean Reference Atmosphere for 25 to 500 Km
AFCRL-72-0579 (2 October 1972)

CHERNOSKY, E. J.
Dichotomy in Geomagnetic Disturbance and Its Solar Origin
AFCRL-TR-73-0097 (8 February 1973)

COLE, A. E.
Distribution of Thermodynamic Properties of the Atmosphere Between 30 and 80 Km
AFCRL-72-0477 (10 August 1972)

COLE, A. E., and KANTOR, A. J.
COESA Task Group I Report on Proposed 50 to 100 Km Revision to U. S. Standard Atmosphere 1962
AFCRL-72-0692 (27 November 1972)

CORBIN, V. L., and QUESADA, A. F.
Least Squares Cubic Splines
AFCRL-TR-73-0661 (29 October 1973)

CORMIER, R. V.
Extremes of Low Atmospheric Density Near the Ground for Elevations up to 15, 000 Feet for MIL-STD-210B

AFCRL-72-0711 (6 December 1972)
An Annotated Listing-Tall Towers Instrumented for Wind Observations
AFCRL-TR-73-0179 (23 March 1973)
The Nature and Variability of Integrated Boundary Layer Winds
AFCRL-TR-74-0264 (12 June 1974)

DANDEKAR, B. S.
Factors Involved in Optical Programs for the Polar Cap
AFCRL-72-0746 (29 December 1972)

DEWAN, E. M.
Thermally Stratified Compressible Fluid Motion on a Rotating Sphere with Gravitation
AFCRL-TR-73-0225 (12 April 1973)

FAIRE, A. C., and MURPHY, E. A.
Neutral Density and Temperature Measurements
Proc. of COSPAR Symp. on Solar Particle Event of Nov. 1969, AFCRL-72-0474 (11 August 1972)

FORBES, J. M., CAPT.
Advective Heating in the Thermosphere During Geomagnetic Storms
AFCRL-72-0552 (14 September 1972)
Propagation of Internal Gravity Waves in a Medium of Weak Random Vertical Shear
AFCRL-TR-73-0377 (21 June 1973)
Wind Estimates Near 150 Km from the Variation in Inclination of Low-Perigee Satellite Orbits
AFCRL-TR-73-0379 (21 June 1973)

FORBES, J. M., CAPT., and BRAMSON, A. S. (IBM Corp. Fed. Sys. Div., Burlington, Mass.)
A FORTRAN Program for Computing Steady-State Composition Models of the Upper Atmosphere
AFCRL-TR-73-0636 (9 October 1973)

FORBES, J. M., CAPT., and GILLETTE, D. F.
An Empirical Density Model for Predicting Low-Altitude Satellite Ephemerides. Part I: Data Analysis and Model Formulation
AFCRL-TR-74-0062 (1 February 1974)

FORBES, J. M., CAPT., and STRAKA, R. M. (Iono. Phys. Lab.)
Correlations Between Exospheric Temperature and Various Indicators of Solar Activity
AFCRL-TR-73-0378 (21 June 1973)

GRANTHAM, D. D., and KANTOR, A. J.
Probability of Encountering Thunderstorms at 50,000 and 60,000 Feet for Selected Routes Over the United States
AFCRL-72-0415 (14 July 1972)

GRINGORTEN, I. I.
Duration and Unusual Extremes of Cold - Supplement 1
AFCRL-72-0705 (1 December 1972)

A Polar Equal-Area Map of the World
AFCRL-TR-73-0349 (4 June 1973)
Stochastic Modeling of the Areal Extent of Weather Conditions
AFCRL-TR-73-0731 (30 November 1973)

HALL, W. N., and LLOYD, J. W. F.
Polar Cap Optical Intensities During the 2 November 1969 Solar Particle Event
Proc. of COSPAR Symp. on Solar Particle Event of Nov. 1969, AFCRL-72-0474 (11 August 1972)

JASPERSE, J. R.
Electron Transport in a Dilute Weakly Ionized Gas Application to a Model Ionosphere
AFCRL-TR-73-0600 (27 September 1973)

KANTOR, A. J., and COLE, A. E.
Abbreviated Tables of Thermodynamic Properties to 85 Km for the U. S. Standard Atmosphere, 1974
AFCRL-TR-73-0687 (6 November 1973)

KENESHEA, T. J., and HUFFMAN, R. E.
Solar Photoionization Rate Constants and Ultraviolet Intensities
AFCRL-72-0667 (16 November 1972)

KLEIN, M. M.
Deceleration and Vertical Motion of a Gas Puff Released into the Upper Atmosphere
AFCRL-TR-73-0046 (12 January 1973)

LENHARD, R. W., and SISSENWINE, N.
Extremes of 1, 12, and 24 Hour Rain for MIL-STD-210B
AFCRL-TR-73-0329 (18 May 1973)

LUND, I. A.
Haze-Free and Cloud-Free Lines-of-Sight Through the Atmosphere
AFCRL-72-0540 (13 September 1972)
Joint Probabilities of Cloud-Free Lines-of-Sight Through the Atmosphere at Grand Forks, Fargo, and Minot, North Dakota
AFCRL-TR-73-0178 (23 March 1973)

LUND, I. A., and NEEDLEMAN, S. M. (Terrestrial Sci. Lab.)
Tropical Soil Moisture Estimation from Meteorological Observations
AFCRL-TR-74-0064 (4 February 1974)

MARCOS, F. A., and BLOEMKER, C. F. (N. C. State Univ.), BEDINGER, J. F., CONSTANTINIDES, E. (GCA Corp., Bedford, Mass.)
Results from the PCA 69 Chemical Release Experiments
Proc. of COSPAR Symp. on Solar Particle Event of Nov. 1969, AFCRL-72-0474 (11 August 1972)

MARCOS, F. A., MC INERNEY, R., and CORBIN, J., FIORETTI, R., GROSSBARD, N. (Boston Coll, Mass.)
Atmospheric Density Results Derived from the SPADES Satellite Accelerometer Data
AFCRL-72-0608 (12 October 1972)

MOSES, H.E.
A Simple Exact Solution for the Motion of the Atmosphere About the Rotating Earth and Application to the Rotation of the Atmosphere
AFCRL-72-0609 (13 October 1972)
An Exact Solution for the Rotation of the Atmosphere About the Spheroidal Earth
AFCRL-TR-73-0275 (20 April 1973)
Resonance Scattering of Lyman-Alpha Radiation by Hydrogen in the Ground State
AFCRL-TR-73-0744 (6 December 1973)

MOSES, H. E., and QUESADA, A. F.
The Scaling of Physical Quantities and Its Relation to the Power Spectrum of the Mellin Transform
AFCRL-TR-73-0651 (16 October 1973)

MULLEN, E. G.
Solar-Geophysical Data for the 14 to 21 December 1971 Geophysical Event
AFCRL-TR-73-0160 (13 March 1973)

MULLEN, E G., LLOYD, J. W. F., and DAVIS, D. J., JR.
A Two-Channel Interference-Filter Photometer Digital Recording System at the AFCRL Geopole Observatory, Thule, Greenland
AFCRL-TR-73-0366 (18 June 1973)

NARCISI, R. S.
Aeronomical Implications from Ion Composition Measurements During a PCA
Proc. of COSPAR Symp. on Solar Particle Event of Nov. 1969, AFCRL-72-0474 (11 August 1972)

NARCISI, R. S., PHILBRICK, C. R., THOMAS, D. M., BAILEY, A. D., WLODYKA, L. E., BAKER, D., FEDERICO, G., WLODYKA, R., and GARDNER, M. E.
Positive Ion Composition of the D and E Regions During a PCA
Proc. of COSPAR Symp. on Solar Particle Event of Nov. 1969, AFCRL-72-0474 (11 August 1972)

NARCISI, R. S., SHERMAN, C., PHILBRICK, C. R., THOMAS, D. M., BAILEY, A. D., WLODYKA, L. E., WLODYKA, R. A., BAKER, D., and FEDERICO, G.
Negative Ion Composition of the D and E Regions During a PCA
Proc. of COSPAR Symp. on Solar Particle Event of Nov. 1969, AFCRL-72-0474 (11 August 1972)

PAULSON, J. F.
Effects of the B-1 on Ozone and on Transmitted UV
Envmt. Eff. of B-1 Emissions in the Strato., C. G. Stergis, Ed., AFCRL-TR-73-0608 (10 October 1973)

ROSENBERG, N. W.
Application of a Computer-Controlled Two-Dimensional Densitometer to Photograph Chemical Releases
AFCRL-TR-73-0155 (9 March 1973)

SALMELA, H. A., and GRANTHAM, D. D.
Diurnal Cycles of High Absolute Humidity at the Earth's Surface
AFCRL-72-0587 (5 October 1972)

SISSENWINE, N., and CORMIER, R. V.
Synopsis of Background Material for MIL-STD-210B, Climatic Extremes for Military Equipment
AFCRL-TR-74-0052 (24 January 1974)

SISSENWINE, N., TATTLEMAN, P., GRANTHAM, D. D., and GRINGORTEN, I. I.
Extreme Wind Speeds, Gustiness, and Variations with Height for MIL-STD-210B
AFCRL-TR-73-0560 (29 August 1973)

STERGIS, C. G., Editor
Environmental Impact of B-1 Emissions in the Stratosphere
AFCRL-TR-73-0608 (10 October 1973)

SWIDER, W.
Charged Particle Reactions Involving Oxygen and Nitrogen in the E- and F-Regions
AFCRL-TR-73-0361 (13 June 1973)

SWIDER, W., and FOLEY, C.I. (Boston, Coll., Mass.)
D-Region Ionization Rates for the 2 to 5 November 1969 PCA Event as Determined from Satellite Proton Flux Measurements
AFCRL-TR-74-0190 (12 April 1974)

SWIDER, W., and GARDNER, M. E.
Atmospheric Ionization by Precipitating Protons and Alpha Particles
Proc. of COSPAR Symp. on Solar Particle Event of Nov. 1969, AFCRL-72-0474 (11 August 1972)

SWIDER, W., and KENESHEA, T. J.
Diurnal Variations in the D Region During PCA Events
Proc. of COSPAR Symp. on Solar Particle Event of Nov. 1969, AFCRL-72-0474 (11 August 1972)

TATTELMAN, P., and GRINGORTEN, I. I.
Estimated Glaze Ice and Wind Loads at the Earth's Surface for the Contiguous United States
AFCRL-TR-73-0646 (16 October 1973)

TATTELMAN, P., and SISSENWINE, N.
Extremes of Hydrometeors at Altitude for MIL-STD-210B. Supplement - Drop-Size Distributions
AFCRL-TR-73-0008 (9 January 1973)

TSIPOURAS, P. (Off. of Res. Svc.), and CORMIER, R. V.
Hermite Interpolation Algorithm for Constructing Reasonable Analytic Curves Through Discrete Data Points
AFCRL-TR-73-0400 (6 July 1973)

TURTLE, J. P., and OELBERMANN, E. J., JR. (Ordnance Res. Lab., Penn. State Univ.)
Discussion of Polar VLF and Particle Precipitation Data for the 2 November 1969 Solar Particle Event
Proc. of COSPAR Symp. on Solar Particle Event of Nov. 1969, AFCRL-72-0474 (11 August 1972)

WEEKS, L. H.
Molecular Oxygen Measurements from UV Absorption
AFCRL-TR-74-0109 (27 February 1974)

WEEKS, L. H., and CUIKAY, R. S. (Raytheon Co., Norwood, Mass.), CORBIN, J. R.
Ozone Measurements in the Mesosphere During the Solar Proton Event of 2 November 1969
Proc. of COSPAR Symp. on Solar Particle Event of Nov. 1969, AFCRL-72-0474 (11 August 1972)

III Microwave Physics Laboratory

The Microwave Physics Laboratory is committed to research and development in the fields of electromagnetic radiation, control and propagation, to enhance the ability of the tactical and strategic forces of the USAF to meet present and future requirements. Laboratory scientists are presently at work in such critical problem areas as all-weather battlefield surveillance, the detection of stationary and slow-moving targets in heavy ground clutter, electronic countermeasures, and penetration aid technology for both aircraft and missiles. Research goals are achieved by specializing in such technical areas as antennas, microwave acoustics and magnetics, tropospheric propagation, radar systems, laser physics and target scattering phenomena.

Most problems are approached from the basic physics appropriate to the particular electromagnetic system or device. Laboratory personnel have an in-depth competence in electromagnetic diffraction, radar, antennas, propagation in turbulent media, surface and bulk wave propagation of acoustic waves in the gigahertz frequency range, the physics of ionized media produced by hypersonic reentry vehicles, and laser beam interactions.

Laboratory accomplishments also merit discussion. During a recent two-year interval, the Microwave Physics Laboratory was the recipient of five AFSC Technical Achievement Awards, given for: Tropospheric Range Error Correction for the Global Positioning System; An Interference Rejection Antenna with Variable Polarization; UHF Frequency Synthesizer Using Acoustic Surface Waves; Fast Response Frequency Analyzer — Using

Dielectric Resonators; and Low Profile Antenna for Aircraft Station-Keeping Applications.

Research by this laboratory has also led to the design and development of the Synthetic Aperture Dual Frequency Radar (SADFRAD), an Air Force sensor system capable of detecting stationary targets concealed in heavy foliage, presently being implemented by the Air Force Avionics Laboratory (AFAL).

In 1973 a new radar concept called NFMRAD (Null Filter Mobile Radar) was invented that combines antenna nulling with doppler filtering to achieve an economical, improved AWACS-type radar. The Laboratory has also studied air-to-air radar problems and, for the Air Force Weapons Laboratory, demonstrated by computer that the number of missiles fired from one aircraft toward another can be determined by simple processing of signals from existing radars. Methods for the modification of the radar cross section of reentry vehicles and for the rapid recovery of ECM capabilities during the reentry phase of flight have been developed to satisfy the requirements of the Space and Missile Systems Organization (SAMSO) ABRES Program.

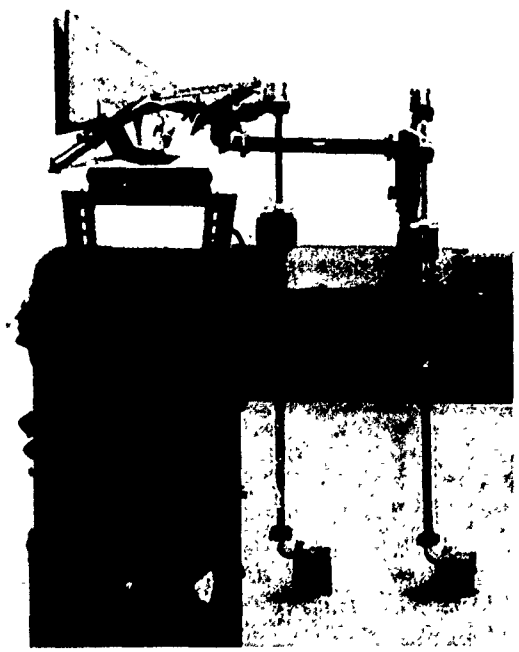

This two element horn array was used for the Null Filter Mobile Radar (NFMRAD) tests. A null was formed in the antenna pattern in the direction of the maximum clutter response and it substantially improved the target-to-clutter ratio.

Research in laser propagation phenomena, performed at the request of the Air Force Weapons Laboratory, has resulted in technological advances that may provide the basis for the future development of reliable and highly effective antimissile defensive systems for aircraft. New techniques using ionizable coatings to protect against lasers have been successfully tested.

Methods for suppressing and controlling reentry plasma sheath effects on ballistic missile antennas have been invented. New techniques using minute quantities of chemical injectants or special laminated ablative heat shields have been demonstrated on rocket flights. These advances are now being applied to high power laser problems for the Air Force Weapons Laboratory and the Aeronautical Systems Division.

There have been many requests for support in tropospheric propagation systems. Range error corrections have been provided to SAMSO for the NAVSTAR Global Positioning System and to Aeronautical Systems Division (ASD) for the Pave Nickel Demonstration System. Our scientists were able to show that the loss of target during Airborne Warning and Control System (AWACS) flight tests was caused by sharp negative gradients in tropospheric refraction.

Perhaps the Microwave Physics Laboratory's strongest contribution to Air Force technology needs has been in antenna design. A new method of phased array design which eliminates grating lobes and allows the use of much larger aperture horns in antenna arrays has been demonstrated. This invention substantially re-

duces the cost of phased arrays by eliminating 90 percent of the ferrite phase shifters formerly needed for such limited angle scanning. During this period, our scientists completed the first rigorous handling of the log periodic array and showed how to improve the gains of these giant antennas used for OHD applications. Important advances were also made on conformal arrays, and rigorous analysis of a finite sized array on a curved surface was carried out. These studies find use in aircraft-to-satellite communications.

Microwave acoustics research supports AFAL (Countermeasures), RADC (Communications), ESD (SEEKBUS), and SAMSO (ABRES). Of primary importance has been the in-house discovery of the minimum diffraction (practically zero) loss orientation of acoustic materials. This and other recent advances in the theory of low loss acoustic devices have resulted in in-house fabrication and demonstration of the best filters and delay lines extant. New advances have been made in the theory of acoustic filters and how to excite them efficiently. The research results of this group have been widely disseminated in response to requests for this information by thousands of workers in the field, in the form of a special handbook series developed and published by members of the Laboratory.

Technical consultation services have been performed for the TPN-19 Precision Approach Radar, the Airborne Multiwire VLF Antenna, AN/FPS-85 Air Defense radar, AN/GRN-27 ILS system now in field use, acoustic wave technology application for the Advanced Power Management Program of AFAL, passive microwave radiometry for meteorological application and SAMSO's Reentry Antenna Test Program (RANT).

RADAR SYSTEMS

The last *Report on Research* pointed out that the Microwave Physics Laboratory had developed novel radar systems that used the lower radar frequencies and the resonant region as new means for airborne detection of stationary or slowly moving military targets near the earth's surface. Continued pressing interest in such practical problems has motivated a number of in-house investigations leading directly to improved Air Force systems. The Laboratory has continued to exploit the long wavelength radar technique because such wavelengths provide a natural filtering action that has several distinct advantages over more conventional microwave radar detection techniques. These advantages include lower data rates, radar returns that are almost independent of the aspect angle, and lower reradiated energy from ground clutter. This latter effect gives long wavelength radars a higher signal-to-clutter ratio than their microwave counterparts and this is an important asset in target detection. Lower data rates reduce the size and memory requirements of the digital signal processors

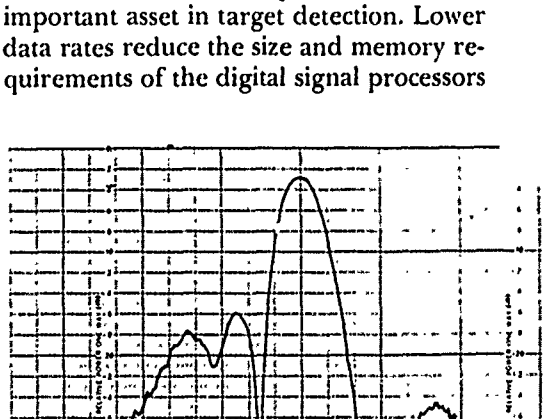

The measured antenna pattern is for an eight element optimum signal-to-clutter ratio antenna array developed for the NFMRAD radar. The deep broad null on the right of the main beam cancels out ground clutter that would normally appear in a doppler velocity filter. Control of radiation levels in a narrow angular sector such as this allows the maximization of main beam antenna gain as well as the optimization of clutter and jammer rejection.

used with modern radar systems. Aspect angle invariance is an advantage in that target classification schemes have one less ambiguous parameter to contend with. In Airborne Moving Target Indicator (AMTI) Radars, a high signal-to-clutter ratio reduces the amount of processing that must be done and thereby simplifies the entire detection process.

AIRBORNE MOVING TARGET INDICATOR (AMTI) RADARS: The Laboratory has capitalized on the experience in the Resonant Region Radar and the Synthetic Aperture Dual Frequency Radar (both of which were long wavelength radars, developed, built and flight tested in-house) to develop three new AMTI radar systems: the Null Filter Mobile Radar (NFMRAD), the Arrested Synthetic Aperture Radar (ASAR), and the Tuned Synthetic Aperture Radar (TUSAR). The NFMRAD concept uses an airborne flush mounted, fixed, phased array antenna as the basic building block of an AMTI radar. The system uses several techniques to enhance its performance; non-adaptive nulls placed in the antenna radiation pattern and complementary doppler velocity filters are two. This combination not only reduces clutter but also decreases the system sensitivity to the large stationary targets that must be rejected by an AMTI radar. The system concept also includes moving range gates to increase the dwell time on the target, and a two-stage detection process to further reduce false alarms. The antenna null placement (based on a Laboratory-developed technique) allows pattern control over a restricted sidelobe region and, at the same time, achieves the maximum antenna gain in the main beam. This provides a much more efficient use of the antenna aperture than an antenna in which all sidelobes are controlled. The antenna feeding coefficients are calculated by a computer technique to get the maximum target-to-clutter ratio for the overall radar system.

An X-band model of this AMTI radar system has been constructed in-house and mounted on a truck to test system concepts. The truck provides a moving platform that simulates aircraft motion while a riding lawnmower, equipped with a small radar reflector, is used to simulate a slowly moving target. The Hanscom Field runways and flight line serve as the test area. The first antenna system used was a two-element horn array which allowed placement of only one null. Test results showed that proper null placement enhanced the detection of targets that were buried in clutter when no null placement was used. The model now has an eight-horn antenna array and the testing program is continuing. This technique has promise for many future radar designs.

The Arrested Synthetic Aperture (ASAR) and Tuned Synthetic Aperture (TUSAR) Techniques have been developed to provide detection of slowly moving concealed ground targets by a long wavelength radar. Both techniques are compatible with the Laboratory's SADFRAD system (described in the previous *Report on Research*) in that all three can use the same transmitter-receiver system, the same antenna and the same type of digital processing. The basis for both new systems is the fact that at the low SADFRAD frequencies, one needs AMTI signal improvements of about only 20 dB to achieve reliable target detection.

In the ASAR system, two synthetic aperture beams, each formed from a separate antenna on board the same aircraft, are coherently subtracted to cancel ground clutter. The antennas are displaced along the flight path of the aircraft and the beam from the forward antenna is delayed by the time it takes the aircraft to fly the distance between the two antennas. Because synthetic aperture processing is used, the physical antenna patterns need not be closely matched. It is this feature that allows airborne operation at the long radar wavelengths. Any antenna pattern control at frequencies where the antennas must be

placed a portion of a wavelength from the aircraft is quite difficult. Computer simulations have shown that up to 40 dB of AMTI improvement is possible with this system. Future plans call for the field testing of an ASAR system model.

The Tuned Synthetic Aperture Radar (TUSAR) provides an alternate method for detecting and tracking slowly moving ground vehicles from an airborne reconnaissance platform. Slowly moving targets have doppler-doppler rate parameters which differ from those of stationary objects and ground clutter. TUSAR exploits this dissimilarity to improve moving target detectability against ground clutter and, with additional processing, to locate and track moving targets.

Studies conducted to date have begun to define the possible improvements in target detectability as a function of target speed, radar processing parameters and antenna design. Since the TUSAR concept requires extensive on-board, real-time signal processing, studies of the performance of various simple sub-optimum processors are underway.

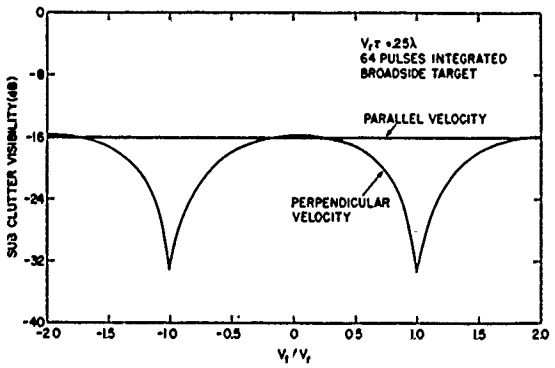

Subclutter visibility versus the target to radar platform velocity ratio for the Tuned Synthetic Aperture Radar (TUSAR). An outstanding feature of this new AMTI system is its sensitivity to targets traveling parallel to the radar platform as well as those traveling radially to the platform.

INTEGRATED MULTIPLE FREQUENCY RADAR (IMFRAD): The Integrated Multiple Frequency Radar (IMFRAD) is an advanced development version of the Laboratory's highly successful Synthetic Aperture Dual Frequency Radar (SADFRAD) system and is currently being developed by the Air Force Avionics Laboratory with the participation of Microwave Physics personnel. SADFRAD (described in detail in the last *Report on Research)* is an airborne, resonant region, dual-frequency, synthetic aperture surveillance radar built in-house by the Microwave Physics Laboratory. The system featured the first on-board, real-time digital processor ever flown and a three-channel color display. It was installed in an Air Force C-121 aircraft and tested jointly with AFAL. Test results showed that the system could detect tactical-sized targets in dense foliage. In fact, it is the only radar system ever built with a proven capability to detect concealed targets at operationally compatible distances. In addition to this extremely important military application, useful scientific data were gathered including well calibrated backscatter measurements from all types of terrain and the ocean at HF and UHF frequencies as well as backscatter measurements from a number of different target shapes.

The program resulted in a technology transfer to AFAL which is now building a longer range version with increased capability and a much lower false alarm rate. The system will use three frequencies and will be tested in a C141 aircraft. The Microwave Physics Laboratory is providing systems engineering support and is designing, building, and testing the three-frequency antenna system for IMFRAD. The antenna design is complicated by the fact that the aircraft becomes part of the radiating structure at these frequencies. By careful engineering, substantially better antenna patterns have been achieved than those used for SADFRAD. Because of this, the IMFRAD system is expected to have much

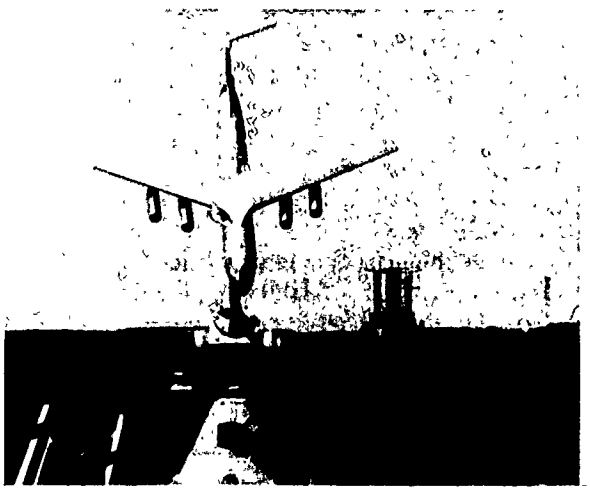

Reduced scale modeling is one way of designing antennas for eventual aircraft mounting. Here, a one-eighteenth scale model of the C-141 aircraft is shown mounted at the Laboratory's Ipswich test site. A scaled antenna system for IMFRAD is being developed and the model is used in taking antenna patterns. In the background is the antenna system for the Laboratory's original HF-UHF developmental radar.

greater protection against false alarms than was possible with the SADFRAD.

SPECIAL APPLICATION RADAR TECHNIQUES: In some radar sensing applications, the only important information is that a target is within a certain prespecified range limit, and detailed information on its location and velocity is not required. Proximity fuzes are an example of such an application. A new short range radar fuze, based on the temporal coherence properties of a quasimonochromatic noise-like signal is being studied by Laboratory scientists. Other applications of this type of signal were outlined in an earlier *Report on Research.*

In the fuzing application, a quasimonochromatic noise generator serves as a transmitting source. The signal reflected from the target is tested against a small sample of the noise source signal. If interference is observed, the round trip range to the target is less than the coherence length of the noise signal. If no interference is observed, the opposite is true. Since the coherence length of the noise signal is a known and controllable parameter, one has a unique way of deciding when the target is within range.

Such a fuzing system is simple in concept, requires a minimum of components, and is easily implemented. Target range is indicated by the existence of an interference signal. The fuze can be used against stationary or moving targets and, for the latter, results in a less complicated design with greater sensitivity.

In conjunction with the Meteorology Laboratory, Microwave Physics Laboratory personnel have been studying a satellite-borne radar system that will measure meteorological parameters not measurable by present optical, infrared or passive microwave systems. These parameters include cloud heights and rainfall rates. The study indicates that radar wavelengths on the order of 1 cm would be the most practical for this purpose. A high resolution antenna system would be needed to look at angles other than straight down. It appears at present that a practical radar system could be developed and flown in a satellite specifically designed for the system.

The rapid detection of air-to-air missile launches is an essential link in the defense of strategic and tactical aircraft. Early detection increases the available time for evasive maneuvers and deployment of countermeasures. Identification of the number of missiles launched and the type of missile air frame is necessary to insure the proper selection of effective countermeasures and defensive tactics. The Laboratory is currently studying improved airborne pulse doppler radar techniques for rapid single or salvo launch detection and air-frame identification. High resolution doppler spectra associated with the launch aircraft provide the necessary launch detection information. Effective methods for achieving

these high resolution spectra while simultaneously suppressing radar ground clutter are now under intensive investigation.

PHASE DERIVED NAVIGATION: If a CW transmitter moves in a straight line at constant speed relative to a triangular array of three receiving antennas, the signals received at these antennas can be used to determine the position and velocity of the transmitter with respect to the receivers. The method requires the measurement of total accumulated phase differences during two or more time intervals. This is one of several schemes considered under a project called Phase Derived Navigation. One application of this technique, currently being studied, is an aircraft instrument landing monitor (ILM) which would display CW beacon transmitters along the runway in perspective on a CRT in the aircraft, along with aircraft height, velocity, and distance from the runway.

RESONANT-REGION TARGET CLASSIFICATION: The resonant region in radar scattering is loosely defined as the frequency band for which the radar wavelength is approximately the same size as the radar target. Within this frequency band, the radar target has unique scattering properties that can lead both to new methods for characterizing it and to real-time methods for obtaining information about its gross physical size and shape.

The special characteristics of resonant region scattering arise because usually only one or two modes of surface current are excited by the incident radar beam, and the reradiated or scattered fields have a simple spatial structure. At higher frequencies, many modes of surface current combine algebraically to produce the fields. Thus, minor discontinuities and subsections of the scattering surface may produce sharp resonances and specular flare spots in higher frequency scattering, but are sufficiently small compared to the wavelength at resonant region frequencies to be unimportant. The scattering pattern at lower resonant-region frequencies is thus primarily determined by the overall size and shape of the scatterer.

Several of the special properties of resonant region scattering from targets that are thin compared to their length were discussed in the last *Report on Research.* It was pointed out that the phase of the backscattered fields from these targets does not vary with target aspect angle as long as the target is no more than about a half wavelength long. Similarly, to a first approximation, the shapes of the usual monostatic radar cross section curves (when viewed as a function of frequency) are also invariant to target rotation through the first resonant maximum.

New results for thick cylinders show that the aspect invariance of the phase exists only at frequencies in the very low resonant and Rayleigh regions. There are, however, specific higher frequencies at which the phase is aspect invariant or has minimum dispersion. Similar results but with much sharper resonances occur with hollow metallic tubes and hollow tubes having one end closed to form an internal cavity.

These aspect-invariant properties are important because they provide measurable information characteristic of the target without the seriously complicating influence of angular dependence. In particular, the frequency location of the first maximum of the monostatic radar cross section provides a measure of the length of thin scatterers; the width of the first resonant maximum will be related to the Q or thickness of the scatterer, and the aspect ratio of the target can be determined from the polarization characteristics. Similar possibilities exist for the phase.

To more fully exploit these characteristics, target classification techniques were used with multiple-frequency resonant region data. Radar cross section versus aspect angle data were obtained for several bodies of revolution at frequencies in the high Rayleigh and low resonance region. The

objects all had approximately the same volume and the shapes were two right circular cylinders, a cone, a step cylinder and a double step cylinder. The analysis showed that there was sufficient information to differentiate between the objects when five or more radar frequencies distributed over about an octave in frequency were used. In addition, the data were sufficiently aspect invariant in that they remained resonably constant over at least 20 degrees of aspect angle and in some cases, over 90 degrees. Results also showed that even if the objects were quite similar in shape as, for example, the double-step cylinder and the cone, higher resonance region frequencies could still be used to distinguish them at the expense, however, of less aspect angle invariance.

As part of this research, a new technique was developed for removing the uncertainties in the radar cross-section data caused by the interrelation between the radar polarization vector and the unknown target aspect angle. In addition, the dual-frequency phase signature technique (a Laboratory-developed technique explained in the previous *Report on Research)* was extended and used to measure phase shift of the target scattering. This technique is independent of the target range and its motion and provides an absolute rather than a differential phase shift. Each of these measurement techniques adds its share to reducing the enormous complexity of the target identification problem.

ANTENNAS

In the past two years the emphasis in the Laboratory's antenna research has shifted into a closer alignment with a number of ongoing Air Force programs, to shorten the time frame for application. A major reason for this foreshortening of the time frame is the increasing consultation services provided by the Laboratory. Scientists have participated in design reviews, evaluations, and technical studies throughout the Air Force.

As examples of the interaction with system project offices and user commands, the Laboratory has conducted studies in trailing wire LF antennas for aircraft, designed a variable polarization array for a gunship sensor, evaluated the ground effects on ILS antennas, developed new techniques for limited scan antennas and evaluated radar performance for GCA landing control systems.

The Laboratory research program in antennas has been oriented around a few major themes. The first is hemispherical coverage antennas. To maintain an effective communication link between an aircraft and a satellite, the antenna coverage must be essentially hemispherical, with particularly good performance near the horizon. Additionally, high performance aircraft require flush mounted antennas. This problem has been addressed in depth; mutual coupling and element-matching techniques have been studied, a novel corrugated surface for the low elevation coverage has been devised, and dual-band techniques are under investigation. A second category is limited scan antennas. These are used principally as geostationary satellite antennas and landing control radar antennas. System cost and complexity can be reduced by tailoring the antenna to the required coverage sector. New techniques for such limited scan antennas have been invented in the Laboratory. These fall into two areas: phased arrays with odd-mode control, and hybrid array-reflector antennas.

Moderate gain antennas for HF or UHF band usage also continue to receive attention for special applications. The Laboratory-developed short backfire array has been incorporated into a special design for gunship use, and new ideas for HF band antennas are under study. A detailed analysis of the log periodic array is being completed; the currents on the elements have been rigorously determined, permitting accurate calculation of the radiation pattern. In the following sections these efforts are described in detail.

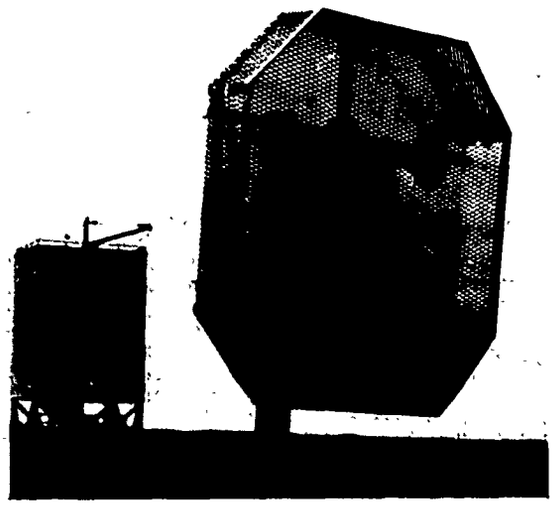

A four-element short backfire antenna array is currently being used by scientists at AFCRL for the reception of low level electrical discharges in atmospheric clouds. This antenna is characterized by low sidelobe levels and a directive gain of 19 dB.

SHORT BACKFIRE ANTENNAS: Short backfire antennas are efficient radiators of electromagnetic energy and are attractive to antenna systems designers because they are also simple and compact. A typical short backfire antenna is comprised of: 1) a planar reflector approximately two wavelengths in diameter with a rim along the edge approximately one-half wavelength deep; 2) a reflector disk approximately one-half wavelength in diameter, arranged parallel to the large reflector, and 3) a feed located between the two reflectors. The feed may be any radiator of small axial extension; for example, a dipole, pair of crossed dipoles, a loop, or a short helix or spiral. Such simple feeds are, however, impractical for frequencies above 1 GHz, because their small physical dimensions demand an extremely accurate feed design with close tolerances. In addition, such designs provide only limited power handling. During this reporting period, continuing research on this type of antenna has produced a new design that overcomes these limitations. The improvement is achieved by using the open end of a waveguide as the primary radiator in the antenna cavity. The waveguide intrudes into the cavity from behind the larger reflector plate of the backfire. Different types of waveguides may be used, and the polarization response of the antenna will be determined by the polarization characteristics and the energizing system of the waveguide. Use of such a feed structure with the short backfire antenna provides a high-frequency, high-gain, high-power antenna for ground, aircraft, and space applications. Flush-mounted antenna designs can also be provided for high-performance aircraft and space vehicles. There is also the possibility of using these structures in arrays for monopulse tracking and telemetry.

Most of the short backfire arrays already developed have reflector shapes that are symmetric with respect to the array center and are of equal dimensions in both major axes. Their E and H-plane radiation patterns therefore have about the same half-power beamwidth. Laboratory scientists have now gone a step further and shown that the technique of arraying short backfire elements may also be applied to reflectors with major-to-minor axis ratios significantly different from unity. Such designs include all types of fan beam arrays. An in-line eight-element array was constructed in the experimental phase of the laboratory program. By varying element parameters, the array was optimized and was capable of receiving or transmitting linear, elliptic, or circular polarization with a 7-degree half-power beamwidth in its azimuthal plane and a directive gain of 22.1 dB. With an area illumination efficiency of 0.84, this structure is very attractive for applications such as Instrument Landing Systems (ILS), where reduced antenna reflector dimensions are important design considerations.

A four-element short backfire array has also been designed, fabricated, and ex-

perimentally tested for use by scientists of the Ionospheric Physics Laboratory in the reception of low-level atmospheric noise at 920 MHz. This array, which uses an octagonal reflector, has low-sidelobe radiation patterns and a directive gain of approximately 19 dB. It serves as the tracking antenna for electrically active atmospheric clouds in a system being developed here at AFCRL for lightning warning applications.

FLUSH-MOUNTED PHASED ARRAY TECHNIQUES: A substantial laboratory effort is devoted to the study and development of techniques for improved-performance, flush-mounted and low-profile phased arrays. Arrays of this type are required on aircraft for communicating with satellites or other aircraft. Ideally, they should have a wide bandwidth and near-hemispherical scan with special emphasis on the coverage near the horizon. These requirements are stringent and therefore provide a strong stimulus for accelerated research in phased array technology. This, in turn, has resulted in a broad range of in-house and contractual developments in these areas. Recent contractual accomplishments have included development of novel stripline and waveguide radiators that operate over octave-bandwidth frequency ranges, and studies of dielectric clad arrays that provide scan coverage from horizon to zenith.

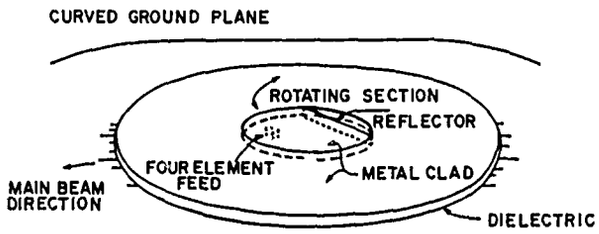

A flush mounted station keeping antenna. The design uses a two dimensional metal clad lens that actually conforms to the aircraft shape while only the inner section need be rotated for azimuthal coverage. This approach produces an antenna that is lighter and more easily streamlined than present designs.

In-house studies include the analysis of planar arrays of waveguide elements on curved surfaces such as cylinders and cones. These analyses include interelement mutual coupling and have resulted in a convenient analytical conformal array model based on the Geometrical Theory of Diffraction.

Other in-house studies include the development of a low-profile scanning lens for aircraft station-keeping, and also an array technique for zenith-to-horizon coverage. This latter array uses waveguide shorting switches to transform the array into a corrugated structure for end-fire (horizon) radiation, even though the antenna functions as a conventional array for moderate angles from zenith. Preliminary results indicate that this technique can provide efficient radiation from zenith to horizon while scanning in one plane. Hemispherical coverage is then provided by mechanically rotating the structure.

The multiplicity of satellite-to-aircraft communication links projected for future Air Force systems has provided impetus for

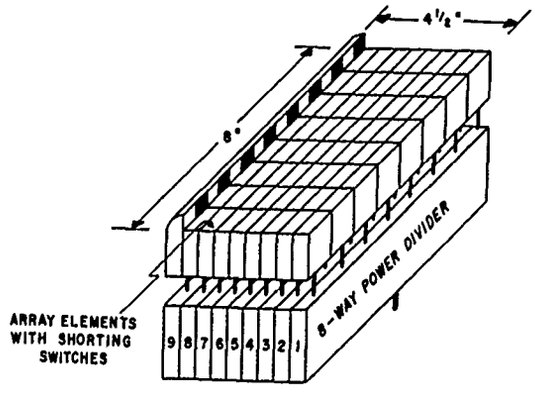

Efficient scanning from broadside to end fire can be achieved with this novel phased array for aircraft and satellite use. The elements are short circuited forming a corrugated surface for the end fire direction. At other scan angles, the array functions in a normal fashion.

an in-house study of a dual-band array technique for flush-mounted application. The development is based on a dielectric slab-loaded waveguide geometry that serves as a transmission medium for two signals, one at roughly double the frequency of the other. The technique is intended to maximize the aperture efficiency of the array while allowing completely independent beam-forming systems at the two frequencies Experimental testing is presently underway.

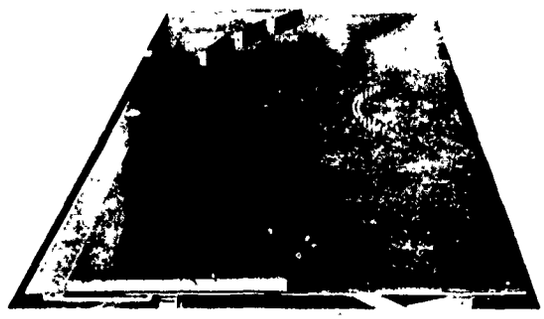

A Laboratory-developed hybrid reflector-array limited scan antenna. Sixteen monopoles, arranged in a circular arc, feed the specially shaped stepped reflector. Theoretical studies show that this pillbox antenna can provide an amount of off-axis scan (measured in beamwidths) that is nearly equal to the number of feed elements.

ANTENNAS FOR LIMITED SECTOR SCANNING: The previous *Report on Research* outlined several Laboratory efforts pertaining to antennas with restricted scanning ranges. These limited scan antennas find application in precision approach radars for airport Ground Control Approach systems, and also as scanned or multiple-beam antennas for satellite communication links. Due to the importance of the subject and the likelihood that substantial improvements over conventional technology would result from research in this area, the Laboratory has undertaken two in-house and two contractual studies in limited-scan antennas. The contractual studies have centered about techniques using a phased array or Butler matrix in combination with a dual-reflector or dual-lens system. The intermediate reflector or lens is oversized to allow use of a minimum-size final aperture and an extremely small feed array. Theoretical results indicate that this approach will reduce the number of phase controls required by as much as 40 percent in comparison with present state-of-the-art techniques. Another limited-scan antenna technique developed in-house consists of an array illuminating a single reflector or lens. This antenna provides parameter control of the scan performance, and efficiently uses the available number of terminals for scanning. A circular arc array generates a phase distribution that is linear in angle by producing an equal progressive phase increment on the elements. The shape of the reflector or lens surface is cho-

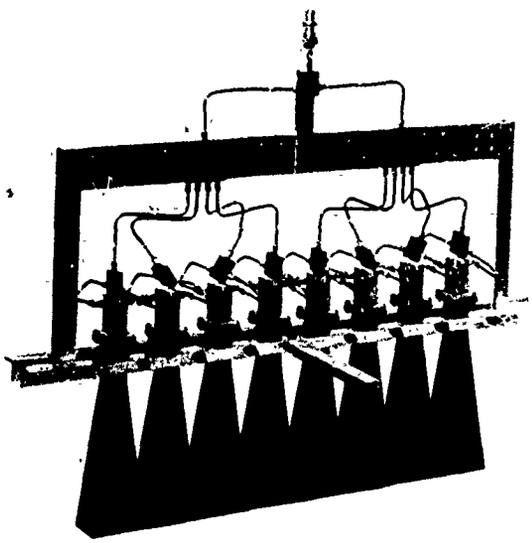

Another limited scan antenna design that uses eight, large aperture elements with multiple higher order modes to achieve cancellation of the dominant grating lobes. The array needs less active components (such as phase shifters) to achieve its scan than conventional arrays.

sen to translate this angular phase distribution into a linear phase front. A two-dimensional pillbox antenna, employing 16 monopole elements and a corporate feed, has been constructed to demonstrate this principle of limited scanning. Theoretical studies show that the amount of off-axis scan, measured in beamwidths, is nearly equal to the number of feed elements.

The second limited-scan antenna technique being developed in-house is a phased array that uses large array elements with relatively few phase controls. This approach depends on multiple higher order modes in the horn elements to achieve cancellation of the dominant grating lobes. Studies to date have included the design of an eight-element array with collimating lenses for one plane of scan, a study of stratified dielectric layer filters for grating lobe suppression, the design of a four-mode element for scanning in two planes, and theoretical scanning studies for one and two planes of scan. Results indicate that use of this large-element technique can reduce the number of active components required by nearly an order of magnitude as compared to conventional arrays.

LOG-PERIODIC ANTENNAS: Log-periodic dipole (LPD) antennas are widely used as broadband radiating and receiving devices. Arrays of such elements have been used for over-the-horizon backscatter detection radars. For any particular design, there are several parameters (more than in most other antenna arrays) that must be specified. In order to maximize some useful antenna property such as antenna gain over many combinations of the basic parametric design values, the designer must have a mathematical model of proven reliability, and it must be sufficiently simple so that large arrays of these dipoles can be handled. To date, several attempts at developing such a model have been made. None have really succeeded. Intrinsic to each is some restriction of the ranges over which the defining parameters can be varied. And even over common regions of validity, the theories often disagree with each other and with experiment by significant amounts. The purpose of the present in-house effort is to develop a mathematical model that eases these parametric limits, that agrees closely with experiment, and that can be reliably used in optimization studies of these antennas and arrays in which each element is itself an LPD antenna. This Laboratory model was used for numerous calculations over a wide range of most of the parameters defining the antenna, including the number of dipoles, the dipole length taper, the inter-dipole spacing factor, the transmission feed-line characteristic impedance, the terminating impedance, and dipole length to diameter ratio. Quantities calculated included the dipole current distributions, antenna gain, pattern front-to-back ratio, input impedance, E-plane and H-plane radiation patterns, the distribution of power among the dipoles and the load, self and mutual admittances, and the relative driving-point voltages and currents.

Special attention was given to the determination of the combinations of dipole length taper and inter-dipole spacing factors that lead to maximum gain. The new results differ from those obtained by other investigators, most of whom used a much simpler mathematical model. For example, higher values of gain were predicted by the new results. The ultimate test of any theory is a comparison with experiment. The new Laboratory theory has been compared with numerous experimental results and the agreement is usually quite satisfactory.

In a separate but related in-house effort, Laboratory scientists are looking at HF log-periodic arrays to satisfy a Tactical Air Command requirement for a short range (50-500 nautical miles) HF communication system that will provide reliable communications for simultaneous voice and data-link channels between a central command post and several scattered outposts. The

research is exploring several alternatives to provide an omni-directional azimuthal antenna pattern and a highly directional vertical antenna pattern. This latter will alleviate the problem of signal distortion caused by multi-path signal interference. Theoretical studies have been completed on vertical arrays of loops and crossed dipoles with log-periodic spacing. Experimental work based on the theoretical studies is presently being conducted.

INTERFERENCE REJECTION ANTENNA SYSTEM: The need to suppress interference signals in electromagnetic detection systems has led to the development of signal processing and pattern synthesis techniques that are usually complex and generally do not have a real-time response capability. A new Laboratory-developed method of variable polarization control discriminates between several incident signals of differing polarizations and selects the desired signal. The equipment required to convert a particular antenna so that it has a real-time interference rejection capability is quite simple and consists of a few phase shifters and delay lines. Laboratory scientists have developed a dual-plane monopulse sensor system utilizing short backfire elements with high-gain characteristics and the capability of rejecting interference signals several orders of magnitude stronger than the desired signal. The application of this interference rejection scheme to military sensor systems is obvious but commercial uses for GCA radars and microwave communication systems are also foreseen.

TROPOSPHERIC PROPAGATION

The Laboratory's tropospheric propagation research program has two principal objectives. The first is to investigate the limitations imposed by the atmosphere on the propagation of electromagnetic energy at microwave and millimeter wavelengths and to find techniques for removing these limitations. The second is to use the propagated wave as a diagnostic tool for obtaining information on both lower atmospheric structure and solar activity and then, to investigate the effects on Air Force electronic systems. Radar and radiometric systems are used for these studies with the primary instrument being the Laboratory's 29-foot millimeter wave antenna at Prospect Hill, Waltham, Mass.

Millimeter waves interact strongly with the lower atmosphere. Atmospheric oxygen, water vapor and precipitation all attenuate millimeter waves limiting the use of these wavelengths for communications and radar. Also, tropospheric refraction de-

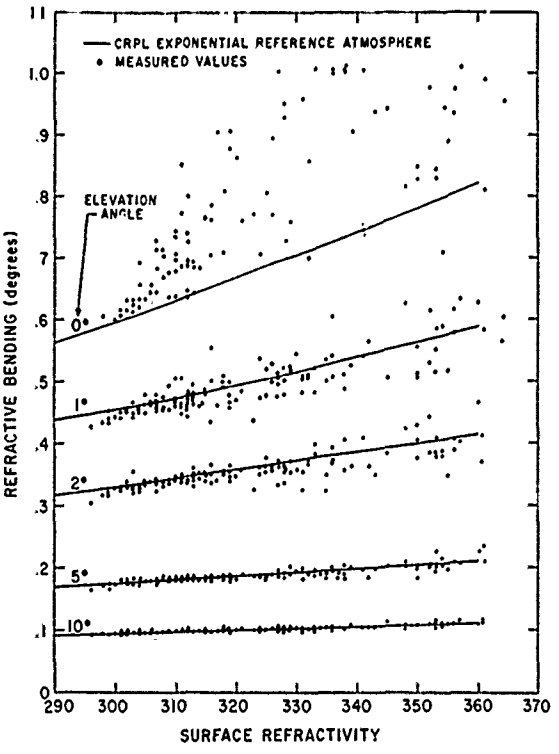

Tropospheric refractive bending measurements show that bending is reasonably well correlated with surface refractivity for elevation angles above 5°. At lower elevation angles accurate corrections cannot be obtained from surface refractivity alone.

grades the performance of systems operated at low elevation angles. On the positive side, however, this millimeter wave-atmosphere interaction has been partially responsible for the emergence of a new branch of science called microwave meteorology. Microwave measurements of atmospheric emission lead to estimates of temperature, pressure, and water vapor profiles. Through high-resolution doppler-shift and doppler-spread measurements, cross-path wind speeds can be measured and turbulent regions detected.

The Laboratory also monitors the millimeter wave emission from active regions on the sun. Large solar flares produce density changes in the upper atmosphere that, in turn, perturb satellite orbits. These solar flares also change the characteristics of the ionosphere and produce HF communications blackouts. Observations of the sun have been conducted for many years to derive criteria for predicting these solar events.

TROPOSPHERIC REFRACTION: The lower atmosphere has an index of refraction slightly larger than unity. It decreases approximately exponentially with height. As a result, radio waves travel more slowly than in free space and as they traverse layers of decreasing index of refraction, they are bent downward. Two types of errors arise from this atmospheric refraction: 1) space targets observed from the ground appear to be at a higher elevation angle than the true angle, and 2) if the distance to the target is based on a time delay measurement, the target will appear further away than it actually is. For a target on the horizon (the most extreme case), the pointing error will be about 0.7 degree and the range error, over 300 feet. As the elevation angle of the target increases, the pointing and range errors decrease approximately proportional to the cosecant of the angle.

To obtain accurate angle and range-error corrections, it is necessary to know the value of index of refraction along the ray path. Although this is possible in principle, it is not usually done in practice because of the large expense involved. More often, a vertical refractivity profile is obtained by either launching a radiosonde and calculating the index of refraction from temperature, pressure and humidity measurements, or by launching a microwave refractometer and obtaining the refractivity directly. A horizontally stratified atmosphere is assumed and the angle or range-error corrections are calculated using either ray-tracing or numerical integration techniques. If an actual profile is not available, then a representative refractivity model can be employed.

Angle and range-error corrections based on vertical refractivity profiles and, in some cases, even surface refractivity alone, have proved satisfactory for many applications, particularly those for which target elevation angles are above 5 degrees above the horizon and the region is horizontally stratified. For example, range-error corrections based on global average surface refractivities have been provided for the NAVSTAR Global Positioning System which is designed to operate at elevation angles above 5 degrees. A standard error of less than 4 percent of the total range error can be obtained from a polynomial regression on surface refractivity. Our analysis of refractivity profiles in Central Europe has shown that the atmosphere is so horizontally stratified and so stable that range-error corrections based on a single annual mean surface refractivity should be adequate for an airborne radar system. However, this correction method has not produced acceptable results when applied to an atmosphere with a horizontally varying index of refraction or for targets at very low elevation angles.

Targets of opportunity can be used to overcome this limitation. If the position of a satellite is accurately known and the satellite either rises or sets in the general direction of the target, then refraction corrections can be obtained using the satellite for

calibration. This has been done frequently for angle-error corrections but not for range error since the true range of the satellite is usually not accurately known. Natural radio sources can also be used as targets for angle corrections. The true positions of the sun, moon and many of the other strong radio sources are listed in the ephemerides and these sources can be detected with a microwave radiometer, i.e., a wide-band receiver designed to measure noise-type signals. Thus, for some locations, angle corrections can be accurately obtained using both artificial and natural targets.

However, these techniques are not always adequate. A technique based on atmospheric emission measurements with a microwave radiometer seems to have the potential of providing real-time angle and range-error corrections. Refractive bending, range error and atmospheric emission (sometimes referred to as apparent sky temperature) are functions of the same meteorological parameters: temperature, pressure and humidity. Ideally, one would like to relate angle and range error directly to atmospheric emission. However, the mathematical functions are so complex, it has not yet been possible to obtain either an analytical or numerical solution to this problem. It has, however, been investigated using a statistical approach and the initial results are very promising. Atmospheric emissions at several frequencies and elevation angles were calculated for a large sample of both stratified and non-stratified atmospheres. Refractive bending and range error were also calculated for the same atmospheres; results were correlated and regression lines were obtained. It was then shown, using statistical estimation methods, that more accurate corrections could be obtained by utilizing atmospheric emission measurements along with surface refractivity than by using surface refractivity alone.

If this technique proves feasible it could easily be implemented into many Air Force systems at low cost. It would provide correction data continually and might ultimately enable the user to forecast the onset of poor propagation conditions.

Scientists review tropospheric range error corrections for NAVSTAR Global Positioning System. Based on world wide statistics, it was shown that range error could be estimated from site latitude, height above sea level, season and elevation angle. This work received one of the Laboratory's five AFSC Technical Achievement Awards.

EARTH-TO-SATELLITE COMMUNICATIONS: Earth-to-satellite wide-band communications requirements require utilization of the millimeter wavelength region of the electromagnetic spectrum. It is now known that total atmospheric attenuation in the window regions is relatively low except for conditions of heavy cloud cover and precipitation. Long-term attenuation statistics for the region in which the ground terminal is to be located are needed for design data for communications links. Ideally these data could be obtained by placing a millimeter wave beacon on a satellite and conducting long-term measurements. This approach would be very expensive and to date there has been only one satellite which has transmitted signals above 10 GHz, the ATS-5. However, this laboratory has successfully obtained long-term rain attenua-

tion data using two types of radiometric techniques. In the first, attenuation through rain was obtained directly from an extinction measurement using the sun as a source. In the second, the attenuation was inferred from a measurement of atmospheric emission. The advantage of an extinction measurement is that losses as high as 30 dB can be obtained directly, whereas attenuations on the order of only 10 or 12 dB can be inferred from an emission measurement. The advantage of the second method is that data can be obtained continually at any angle, day or night, while the extinction measurement can obviously only be made during the day in the direction of the sun. Thus, the first method provides a limited amount of accurate attenuation data over a large dynamic range while the second method produces a larger sample of somewhat less accurate attenuations over a smaller dynamic range.

Rain attenuation statistics have been obtained for Hawaii at 15 and 35 GHz and for Boston at 35 GHz. It appears that attenuation and rain rate are reasonably well correlated for Hawaiian rain but are essentially uncorrelated for Boston rain.

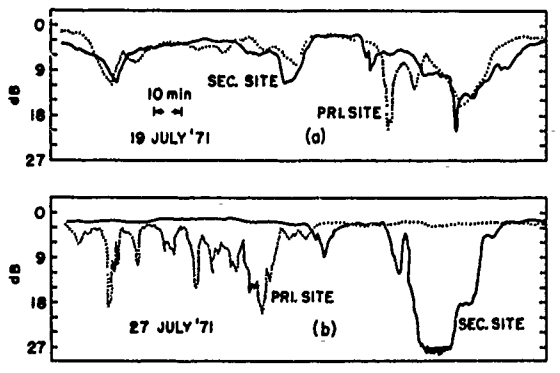

Simultaneous records of received mm signal level as a function of time for two ground stations having a separation of 9 miles. Upper trace is for light intermittent rain and shows that space diversity is not too effective. The lower trace however is for heavy rain and is a perfect illustration of the value of space diversity. The secondary site is badly affected while the primary site is operational.

Since heavy rain is generally quite localized, the possibility of using site diversity to improve the reliability of a communications link was investigated. Results based on a year of data showed that a site diversity system in the Boston area, with a 7-mile separation between sites, would improve system reliability significantly. Under the conditions of this experiment, it was found that for the proposed two-site diversity system, an 18-dB increase in the effective radiated power of the satellite (above that needed to overcome free-space loss) would be required for an outage time of one hour per year as opposed to over 33 dB for a single-site system.

Atmospheric scattering limits the data rate of millimeter communication channels. Several approaches to this important problem are currently being pursued in-house. One such study of this limitation has been carried out through investigation of the propagation in a random medium using a perturbation theory that assumes small fluctuations in the index of refraction. In order to cover the other extreme, the case of strong fluctuations, an approach that involves functional methods is being tried. The crucial factor in this approach is the characteristic functional from which the complete statistical description of the waves in a random medium can be derived. The goal of all these related approaches is to develop an accurate statistical model for atmospheric scattering which will enable the Air Force user organizations to predict realistic data rates for millimeter communication channels.

REMOTE SENSING OF LOWER ATMOSPHERIC STRUCTURE: Temperature and humidity data can be obtained from either ground-based or satellite-based radiometric measurements of atmospheric emission by inverting the radiative transfer integral. The accuracy to which the meteorological data can be inferred depends on the accuracies of the radiometric measurement, the absorption coefficients of water vapor and oxygen, the line breadth constants of

the absorption lines and the technique used to invert the radiative transfer integral equation. This laboratory has reviewed different inversion methods along with stabilization techniques. By introducing Bayesian estimation theory, a more intuitive and unified approach to the inversion problem results. One result of this approach was to show that several statistical inversion techniques are particular cases of the general Bayesian estimation and are identical under specified conditions.

A computer program to determine inversion accuracy has been written. The stabilization techniques and information processing of passive sensor data that have been developed are now being used in the Defense Meteorological Satellite Program.

TROPOSPHERIC FORWARD SCATTER PROPAGATION: Microwave signals in the near millimeter wave region have been used in a long-range forward scatter experiment conducted jointly by the laboratory and the Canadian Communications Research Center. The purpose of the experiment is to study both signal propagation and tropospheric parameters.

The increasing number of communication links above 10 GHz makes the allocation of shared frequency bands inevitable. The feasibility of frequency sharing between earth-space and terrestrial line-of-sight communications systems depends upon ability to predict the statistics of interference between these two systems over any given path. The experiment mentioned above has accumulated signal statistics at 15.7 GHz and a path length of 500 km for a one-year period and will be used to obtain better long-range propagation interference prediction in this frequency range. The narrow beam antennas (0.15 degrees beamwidth) used for transmission and reception limit the scattering to a well defined region in space. Computer control of antenna pointing was used to quickly probe received signal levels at a series of scatter locations. Some of these yielded additional information on propagation mechanisms previously not available, such as the distinction between hydrometeor and turbulent air scatter.

The precise definition of the scatter region in space is even more important when the forward scatter link is used as a remote meteorological sensing tool. A wealth of information on tropospheric scattering structure and motion has been obtained during the propagation experiments. This additional information was collected during routine spatial scans incorporated into the measurement programs. The signal used in such scatter experiments is highly coherent in transmission. When scatterers contributing to the received signal are in motion, they impose a doppler shift on the scattered signal. A long-range bistatic system has the property that the observed average doppler shift in the scatter volume is essentially due to the wind component across the propagation path. The observed frequency shift is proportional to the horizontal distance of the scatter volume from the line connecting the transmitter and receiver. Twenty doppler scans are recorded in the plane transverse to the propagation path and including the mid-path point. These are, in effect, a map of the vertical cross-path wind structure between 5 and 15 km height and covering a range of 30 km either side of the center. Under reasonably uniform crosspath winds over the 60-km horizontal range, the linear dependence of doppler shift in the off-path position is quite obvious, with a reversal in sign between the upwind and the downwind regions. Strong wind shears have been observed in this fashion and could be verified from routine radiosonde stations operating in the vicinity of the forward scatter path.

SOLAR ACTIVITY: Solar radiation is the prime energy source for the terrestrial environment. Variations in either the intensity or the spectral character of this energy produce corresponding changes in our

local environment referred to as aurora, HF communications blackouts, magnetic storms and polar cap absorptions. Because these effects disrupt communications systems, a world-wide program of solar observations has been in progress with the goal of developing a capability to forecast the occurrences of the major solar disturbance, the proton flare.

Laboratory scientists have recently completed an analysis of high-resolution radio observations at 9.1 cm (Stanford), 8.6 mm (AFCRL) and 3.4 mm (Aerospace) taken over the years 1968 to 1970. The purpose was to determine the spectral character of individual active regions during their passage across the solar disk. Positional comparison of enhanced regions demonstrated that the majority of active regions individually observed, at resolutions between 3 and 4 arc-minutes, have no corresponding feature at the other two wavelengths. For those centers which could be co-located, however, a catalogue was prepared and employed as a data base for determining mean characteristics of such regions. The catalogue provides mean values of region fluxes, sizes and spectral indices in the 9.1 cm to 3.4 mm wavelength range. A significant deviation from the mean characteristic of those active regions generating proton flares is suggested as a potential means of forecasting high energy events.

ROTATION RATE SENSORS

There is a continuing Air Force need for more sensitive and more reliable rotation sensors to be used in navigation and guidance systems for missiles and satellites. Devices sensitive to very low rotation rate are required to prevent significant navigation errors on a long flight. Rotation rate sensors based on interferometry of countercirculating waves in a circular configuration are being studied in the Laboratory. Optical waves in such a geometry lead to a phase shift proportional to the angular velocity of the ring and the area of the enclosed circuit. Elastic surface waves—both acoustic and magnetic—may also be used in similar ring interferometers, although there is not a one to one correspondence with the optical case owing to the non-constancy of elastic surface wave velocity in different frames of reference. This latter approach has been adopted and the theoretical principles of such rotation rate sensors, based on ring interferometry of acoustic and magnetic elastic surface waves, have been established. Such devices require relative motion between the transducer generating the waves and the medium on which the waves propagate. An advantage of these devices is that the calculated sensitivity is higher by several orders of magnitude than that for optical (Sagnac) ring interferometers. Acoustic and magnetic devices could be used both as tachometers and "pick-offs" for gyro readouts.

In establishing the theoretical foundations of the acoustic and magnetic rate sensors (ARS and MARS), much attention has been given to the differences between elastic surface waves and optical waves. These differences originate in the fact that the velocity of light *in vacuo* is a constant for all frames of reference. The ARS and MARS approaches are feasible because coupling between the transducer and the medium is possible without direct physical contact. The first ARS device uses a quartz cylinder as the sensing element and has been designed to operate at 100 MHz. A disk of 1 cm^2 area rotating at 1 rpm would give a phase shift of about 10 minutes at this frequency. The first experiment designed to demonstrate the MARS principle is being done with a film of yttrium iron garnet (YIG) grown epitaxially. This YIG film is the carrier for the magnetostatic waves that are generated at frequencies of 1 to 4 GHz. A 4-GHz wave traveling about a cylinder of 1-cm radius rotating at 1.5 rps would lead to a phase shift of about 1 degree.

HYPERSONIC ELECTROMAGNETICS

Shock-ionized flow fields produced by an aerospace vehicle during atmospheric reentry severely disrupt the operation of electromagnetic radiating and penetration aids on board the reentry vehicle. Research and development efforts range all the way from rocket flight tests to laboratory studies of plasma simulation techniques. The fourth and fifth rocket launches of the Laboratory's Trailblazer payloads occurred in July 1972 and December 1973. The rocket program is now in a period of transition. The Trailblazer series of flight tests, all five of which were successful, was completed and provided excellent data on the high-altitude (100 to 300 kilofeet) radio blackout effects on microwave systems. This altitude regime is primarily of importance for electronic countermeasures (ECM) systems on ballistic missiles. However, similar problems also occur at lower altitudes with the radar fuzing systems on reentry vehicles. A new series of rocket flights is now being planned and will investigate these low-altitude effects.

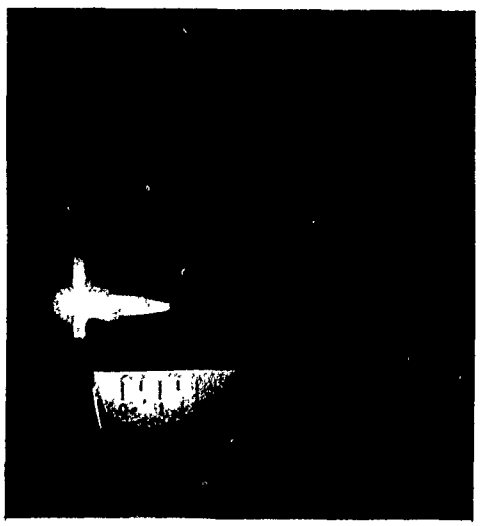

A plume of incandescent gas is produced by the intense heating of a ceramic specimen exposed to a beam of focused infrared laser radiation. Changes in the microwave propagation characteristics of the ceramic material are monitored during the irradiation period.

One task has been directed toward an analysis of the breakdown effects that are encountered when a high-power microwave signal is incident upon an ionized region of space. This problem is prominent during high-power transmissions from reentry spacecraft. A related study that grew out of the microwave analyses is that of laser-induced breakdown in the atmosphere. This phenomenon can be a limiting factor in high-energy laser propagation. One other experiment undertaken since the last reporting period is the analysis of the effects of high-power laser irradiation on dielectric materials.

TRAILBLAZER ROCKET FLIGHTS: The goals of the Laboratory's high-altitude experiments, using the Trailblazer II test vehicle, were to acquire data on the ionization occurring in the shock layer formed around a vehicle during reentry, and to develop techniques to suppress the electrons in the flow which cause the distortion and attenuation of microwave signal transmission. An associated objective was to develop diagnostic devices to measure the flow properties. All these goals have now been achieved.

The first three flights were used to determine the effects of the ionization on antenna performance. At low-power levels, the ionization causes antenna impedance mismatch, signal attenuation and antenna pattern distortion. The antennas placed at various positions on the vehicle experienced a variety of conditions and the levels of signal degradation changed as a function of altitude. At high-power transmission levels, additional effects are found. For example, the ionization reduces the antenna breakdown threshold and this places considerable constraint on the useful power levels of on-board ECM systems.

In the second phase of the program (Flights 4 and 5), the emphasis was on eliminating or greatly reducing the effects of the shock-induced ionization. The prob-

lems are caused by the presence of unattached electrons in the medium through which the signal propagates. The electrons are free to oscillate with the signal and produce distorting effects when their number becomes sufficiently large. The method selected to overcome this problem was to reduce the free electron concentration by introducing chemical additives into the flow, particularly substances that have a strong affinity for attaching electrons. Such electrophilic agents reduce the free electron concentrations by binding up the electrons as negative ions, and these heavier ions do not have a significant effect on the signal transmission. This alleviation technique is much more efficient than simply cooling the flow which would require the addition of much larger amounts of material.

In conjunction with the flight tests, Laboratory scientists developed computer models to provide numerical solutions to the combined Maxwell-flow field equations. In the absence of any additives, these models have given good agreement with previously obtained test data. Models that include the effects of additive materials are now being computed and the results will be compared to the flight test data.

Two quite different additive techniques were tested in the rocket flights. One technique was the localized injection of a liquid, Freon 114B2 (Flight 4); the other was use of an electrophilic material in the vehicle heat shield (Flight 5). On this fifth flight, a Teflon coating was effective in its dual role of providing heat protection to the vehicle and of reducing the electron density levels around the surface of the nose cone. Heat transfer from the external flow causes heat shield ablation releasing the alleviant material from the heat shield into the boundary layer. Both methods have, therefore, been shown to be effective and viable approaches for reducing electron concentrations in the shock layer. On these last two test flights, signal attenuation levels for the test antennas were improved by about 30 dB through the use of the alleviants.

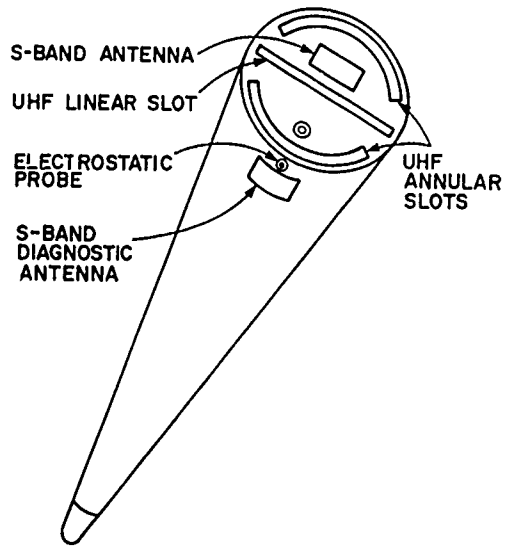

A typical nosecone designed to conduct flight experiments on the performance of base-mounted antennas. These antennas are exposed to electron density gradients in the near wake of the test vehicle during low altitude reentry and their performance can be severely degraded. In addition to the basic antenna measurement experiment, the payload contains diagnostic instrumentation to determine the ionization levels at the rear of the vehicle and in the near wake region. This information will be important in evaluating the actual transmission data during the flight.

The diagnostic measurements included in the flights are an additional information-gathering aspect of the program. Several extremely interesting devices were tested on these flights and some unique scientific results were obtained. The reentry vehicles for both alleviation flight tests were outfitted with a number of electrostatic probes that measured directly the charged particle densities over the vehicle surface. It was necessary to measure both the positive ion and the electron densities to determine the effectiveness of the alleviation material in reducing the concentration of free electrons. This was the first successful simultaneous measurement of both

positive- and negative-charged particle densities during flight tests. The probes were judiciously placed on the vehicles and measured the whole time history of the additive-plasma interaction as a function of the position on the vehicle, the spreading of the additive stream when local liquid injection was used, and any non-uniform ablation of the Teflon heat shield.

A number of effects were observed. Liquid injection reduced the measured free electron density by three orders of magnitude following each injection pulse. Secondly, from the measured changes in charged particle density, the liquid additive stream was seen to spread out as it flowed back over the vehicle. The Teflon heat shield reduced the electron density by a factor of 200 throughout the time interval that the probes were sensitive to the plasma. The probe results during that flight also showed no effects of uneven ablation.

Additional measurements served to confirm these significant diagnostic results. The electrostatic probes measure the electron density only within several millimeters of the vehicular surface, whereas the microwave signal attenuation depends upon the total integrated electron density throughout the entire thickness of the plasma sheath. This integrated effect was observed directly, using the on-board S-band test transmitter and antenna as a diagnostic device, as well as a signal source. The variations in the signal strength received at ground stations, the coupling to another on-board antenna, and other observed radiation characteristics could all be related to corresponding fluctuations in the properties of the reentry plasma sheath as a function of altitude and vehicular motion. These microwave transmission data were then used to compute electron density profiles for the reentry trajectory which agreed quite well with the electrostatic probe data and also with theoretical flow field predictions.

An additional validation of the electrostatic probe as a diagnostic tool was obtained through the close agreement of its response with that of a special stripline probe on the third Trailblazer rocket flight. Both plasma diagnostic devices measure the electron density close to the vehicle surface, but employ entirely different principles. Thus, one can be checked against the other.

The evaluation of the flight data indicates that both types of alleviation techniques (liquid injection and electrophilic heat shields) can be applied successfully and that differences in weight, penetration, and distribution will decide which approach would be most applicable for a given mission requirement.

ARMING AND FUZING ANTENNA MEASUREMENTS: Air Force interest in the performance of high-velocity missiles at low altitudes has opened up a new area of research centered about antennas and shock-induced ionization. As a result of the higher atmospheric densities involved, an entirely new spectrum of problems has emerged.

A new class of base-mounted antennas (windowless) is being considered for use on advanced reentry vehicle systems. The antennas are placed in the relatively protected base region of the nose cone. This antenna location leaves the nose-cone skin mechanically intact, and so it can operate at much higher aerodynamic stress levels.

Some preliminary research into the problems of antenna operation under these low-altitude, high-stress conditions has begun. The situation is complex because at these altitudes the boundary layer has become turbulent, and very little information is available on the properties of the flow in the near wake base region where the antennas are located. Thus, to evaluate the system performance, one must first obtain experimental data against which theoretical analyses can be tested.

Laboratory scientists are simulating the nose-cone environment using cloth made of a conducting fabric to represent the lossy medium associated with the near wake

flow. In addition, a contractual effort is being conducted for AFCRL in the MIT wind tunnel using a slightly more sophisticated approach to the problem of analyzing the wake properties for conical bodies. Finally, actual flight tests with a series of vehicles at velocities and altitudes approaching actual operational conditions are being planned. The combination of these various efforts should provide a range of information which will be useful in establishing the performance of such antennas for Air Force missions.

MICROWAVE ENERGY/PLASMA INTERACTIONS: The study of the ionized environment that exists in the vicinity of an aerospace vehicle requires a knowledge of the complex interactions between microwave energy and plasmas. Two such Laboratory studies centered about 1) the effect of preionization on microwave breakdown, and 2) the generation of harmonic emission from a plasma.

When a high-power microwave signal propagates along a path containing residual ionization, the breakdown level of the medium is markedly decreased. Such paths can occur naturally in transmission from hypersonic vehicles within the sensible atmosphere, or such paths can be artificially produced by nuclear detonations. A computer program has been written to calculate the electric field strength required to initiate microwave breakdown in a partially ionized gas. The breakdown field is found by calculating ionization rates and balancing them against the losses due to diffusion in the free and ambipolar modes. These analytical results were compared to experimental data obtained in neon and neon-argon mixtures. In certain pressure ranges, lowering of breakdown voltage by as much as a factor of 5 was confirmed when residual electron densities of 10^8 per cubic centimeter and greater were encountered. Simultaneous measurements of the electron density, metastable density, and the microwave breakdown field in a neon afterglow have also been made. Results show that electron collisional ionization of the neon metastable states tends to be the dominant electron production mechanism.

The interaction of a high-power microwave signal and a plasma can also produce non-linear effects. One such effect is the generation of second harmonic emission when a plasma is subjected to microwave absorption at plasma resonance. Laboratory scientists have confirmed this in experiments with neon and xenon plasmas. Measurements of the amplitude of the second harmonic emission as a function of input power and the neutral gas density were also made. Experiments such as these provide a better understanding of the signal loss and distortion that occur in a plasma environment.

LASER DIELECTRIC INTERACTIONS: Many classes of dielectric materials are relatively transparent to microwave energy. Under laser irradiation, however, certain of these materials can become less transmissive. The change may be permanent or transient. A study to characterize the altered dielectric properties and their effect on microwave signal transmission has recently been initiated.

A CW carbon dioxide laser is used to irradiate a variety of dielectric materials. Depending upon the sample absorption coefficient, thermal conductivity and specific heat, an increase in temperature will occur. This temperature change may be accompanied by changes in the sample's dielectric constant and loss tangent. Small samples of material under test have also been placed within a microwave cavity structure. The resonant frequency and quality factor are determined for the cavity and sample combination. By repetitively sweeping the cavity with a probing signal of sufficient bandwidth during the laser irradiation period, changes in resonant frequency and quality factor can be dynami-

The output of a 300-watt carbon dioxide laser, operating at 10.6 micrometers, is used to locally heat a dielectric sample held in a ground plane (bright spot). Effects of this irradiation on the sample properties can be determined by monitoring the microwave reflections in the waveguide section or by transmitting to a receiving horn.

cally monitored. This information yields a temporal history of the changes in dielectric constant and loss tangent of the illuminated samples. In other, more recent experiments, the dielectric sample was placed in the open end of a waveguide section terminated in a ground plane. In this configuration, using standard microwave diagnostic techniques, the complex impedance coefficient may be determined. The transmission, reflection, and absorption of microwave energy by a laser-irradiated sample may thus be measured. The laser power level is varied in successive tests and the dependence of the dielectric properties on incident laser power is thereby determined.

It has been found that dielectric materials containing organic components, such as epoxy impregnating resins, undergo thermal decomposition, leaving permanent conducting areas that, in turn, alter the microwave transmissive properties. Certain ceramic dielectrics, on the other hand, suffer changes only under actual high temperature conditions and rapidly recover to pre-test characteristics upon cessation of laser irradiation and subsequent cooling.

Having established that normally transmissive material may undergo changes during or after laser irradiation, the question arises as to the effect, if any, that such changes can produce in the radiation pattern of transmitted microwave signals. A two-fold effort is underway to answer this query. A computer code has been written to predict the effect on the far field antenna patterns of microwave systems whose radiating apertures are blocked by obstacles of arbitrary size, shape, position, and degree of transmissivity. Laboratory experiments have also been conducted to measure the changes in antenna pattern when laser damage is simulated by using patches of fully or partially reflecting materials placed near the radiating structure. The tests have shown that the degree of pattern distortion varies with the nature and placement of the patches, as well as the type of radiating structure under observation.

LASER PLASMA PRODUCTION: Power densities produced by readily available laser systems can alter the medium through which they pass. Heating of naturally occurring suspended particulate matter can produce diffraction effects due to density variations. At higher power densities, these aerosol particles can become ionized, and produce plasmas through cascade breakdown. Finally, in the gigawatt density region, the very molecules that compose the atmosphere can break down and produce dense plasmas.

Certain of these laser-plasma-producing regimes are under study using a CW CO_2 laser, as well as a pulsed, 15-joule, transversely excited atmospheric pressure CO_2 laser. In particular, the laser-supported combustion wave is of interest since it may be ignited at relatively low laser power levels. Once established, such a plasma extracts energy from the incoming laser wave to maintain itself. This mechanism suggests

a technique for reducing the energy delivered to a surface by an intense laser beam. The production of energy-absorbing plasmas adjacent to a surface is therefore under investigation. The influence of coatings containing readily ionized components, as well as the injection of solid particle aerosols, is under study. This effort attempts to produce a lowering of the characteristic power densities required to initiate a laser-supported absorption wave, and thereby protect the surface from further laser damage.

WAVE PROPAGATION IN AND SCATTERING FROM TURBULENT MEDIA: The index of refraction of the atmosphere varies from point to point in a random manner and this fact classifies it as a turbulent medium. Although the average value of the variations is zero, electromagnetic waves passing through the atmosphere can be strongly affected. This is an important consideration for communications and tracking systems working at millimeter and optical frequencies. The turbulence can lead to loss of coherence and spreading or scattering of the radiation, coupled with a fluctuation in the intensity of the signals. Such behavior is generally observed in the propagation of laser beams through the atmosphere.

The classical approach to this problem involves the Born or Rytov approximations. These approaches fail, however, when the turbulence is strong, which is true of long propagation paths in the lower atmosphere. In order to include strong turbulence effects, Laboratory scientists developed a new approach based on transport methods, and derived relations for the intensity distribution, mutual coherence function and frequency spectrum of a collimated or focussed beam. The effects of turbulence strength and the inner and outer scales of the turbulence are included. In addition, the intensity and phase fluctuations of the signal were derived. Scientists were able, for the first time, to theoretically predict the saturation of the amplitude fluctuations, a phenomenon observed by Soviet researchers.

A second aspect of this research is related to the scattering of electromagnetic waves from turbulent media (as opposed to the line-of-sight propagation discussed in the previous paragraph). This is of importance since reentry vehicles usually produce a turbulent plasma wake which often has a radar cross section larger than the vehicle itself. Since the properties of the wake can be used to discriminate decoys from reentry vehicles, it is important to be able to predict its cross section. The radar cross section is traditionally calculated using the Born approximation, but flight-test data show that this is often inadequate, since it neglects the multiple scattering of the incident radar signal and also does not properly include refraction effects. Laboratory scientists studied the effects of including both multiple scatter and refraction in the cross section predictions. First studied was the effect of including multiple scatter. Its inclusion leads to, at most, a 3 dB correction. However, other studies showed that the inclusion of refraction can lead to a correction of tens of dB's when the aspect angle at which the wake is viewed is small. The results of these studies are being used to develop improved wake cross-section models and as a corollary, more accurate predictions of the wake's electromagnetic scattering behavior.

MICROWAVE ACOUSTICS

Surface acoustic wave devices can now be used not only as delay lines but can also perform sophisticated signal processing functions, such as correlation and convolution, that previously required a computer. In addition, microwave acoustic components can perform many of the functions of purely electronic devices and they do this in smaller packages, since the acoustic velocity and wavelength are 100,000 times smaller than the electromagnetic velocity and wavelength.

In recent years, Laboratory scientists have performed basic measurements and

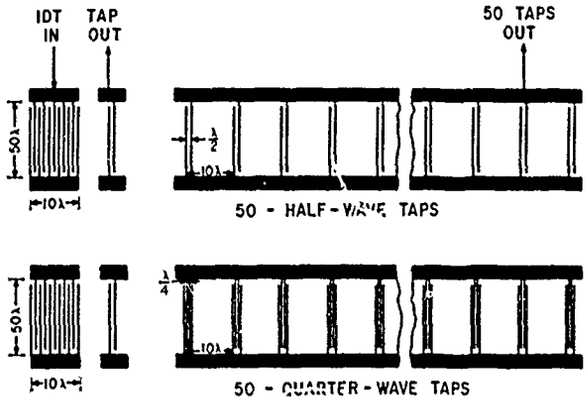

Reflections from tap lines are a source of signal distortion in surface acoustic wave transducers. A change in line spacing from half to quarter wavelength ensures that there are no net reflections at the input.

calculations of acoustic properties for device designs and made them available in the *Microwave Acoustics Handbook* and the *Acoustic Surface Wave Design Data Chart.* Both publications are much in demand. Moderate time-bandwidth surface acoustic wave pulse compressors are currently being used in Air Force radar systems and the Laboratory's present research is directed toward the development of compact, inexpensive, contiguous, surface acoustic wave filters. These will find use in command, control, and communications systems and also in electronic warfare applications.

IMPROVED SURFACE ACOUSTIC WAVE (SAW) TRANSDUCERS: SAW transducers are fabricated by depositing thin metal film lines on a piezoelectric substrate. Although the individual loading of each metal line is very small, the coherent addition of reflections from many lines spaced by one-half wavelength produces significant reflections and losses that cause signal distortion. Two approaches were taken to solve this problem. The first was experimental and required the development of a real-time laser probe to measure the magnitude of the reflections and losses. A theoretical transmission line model of the transducer was used to calculate the impedance mismatch between the deposited metal film and the substrate from the measured reflection. With this technique, metal-substrate combinations with minimum impedance discontinuities can be chosen.

The second novel solution to this limitation is to space the transducer lines by one-quarter wavelength so that the impedance discontinuities produce no net reflections. This scheme has proved very successful in building SAW filters with precise band-pass characteristics.

MINIMIZATION OF SURFACE ACOUSTIC WAVE DIFFRACTION: A major source of losses in microwave frequency surface wave devices is diffraction loss. Prediction of such diffraction effects is greatly complicated by the material anisotropy. Laboratory scientists have solved this difficult problem so that it is no longer a fundamen-

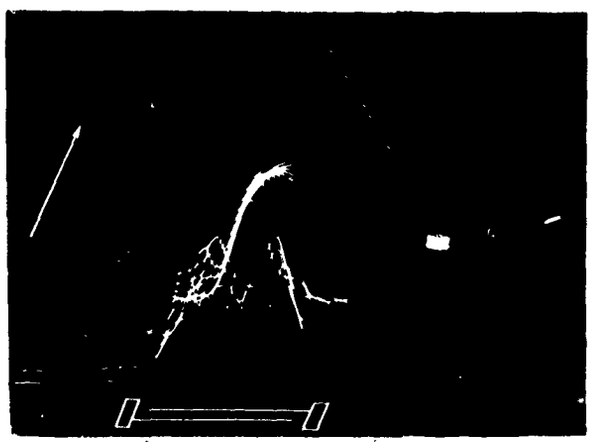

Computer simulated stop action view of surface acoustic wave diffraction from an interdigital transducer. Here the aperture is 40 wavelengths wide and the simulated radiation is into an anisotropic medium. Such displays were used by AFCRL scientists in their development of materials and crystal cuts that minimize diffraction spreading.

tal limitation. Tests have experimentally confirmed this new general theory and delineated the limits under which a simpler scaled isotropic theory can be used. These techniques have recently been used in the comprehensive, optimum design of uniform surface wave transducers. Both anisotropic diffraction and beam-steering effects are included in these designs.

In non-uniform or apodized transducers, the aperture width varies along the length of the transducer. Ideal transducer design procedures assume that the acoustic beam remains the same width as the finger pair from which it is sent. Anisotropic diffraction effects, however, cause each beam to spread at a different rate. Laboratory scientists have developed a general diffraction compensation synthesis procedure that corrects the original ideal design for diffraction variations for any anisotropic material. In addition, a new class of crystal has been discovered in which the inherent anisotropy of the material is used to continually refocus or reform the beam. This virtually eliminates diffraction spreading. One of these minimal diffraction cuts has been experimentally shown to have 100 times less beam spreading than isotropic materials. Such crystals are being used to make compact delay lines having hundreds of microseconds of delay without prohibitive diffraction losses. Another feature is that ideal transducer designs can be applied to these crystals without the need for further diffraction compensation. This advance is being applied to the highly apodized filter having rectangular bandpass characteristics required for fast spectral analysis.

FREQUENCY SYNTHESIS WITH ELASTIC SURFACE WAVES: Many electronic devices use a number of stable, equally spaced frequencies in their operation. The apparatus that provides such signals is called a frequency synthesizer. Surface acoustic wave technology has been applied to develop a novel, compact frequency synthesizer. The development is in response to an ESD requirement.

A single clock-controlled pulse generator produces a pulse train containing the required frequencies as harmonics. A surface acoustic wave filter band selects and filters the required signals. This approach inherently yields high reliability and low costs. The latter advantage stems from a fabrication technique of contact printing the entire filter bank from a single photolithographic master in much the same way as in integrated circuit production. Prototype filter banks with 21 channels have been fabricated on single 0.9 x 2 cm piezoelectric substrates. Each of the 21 filters consists of

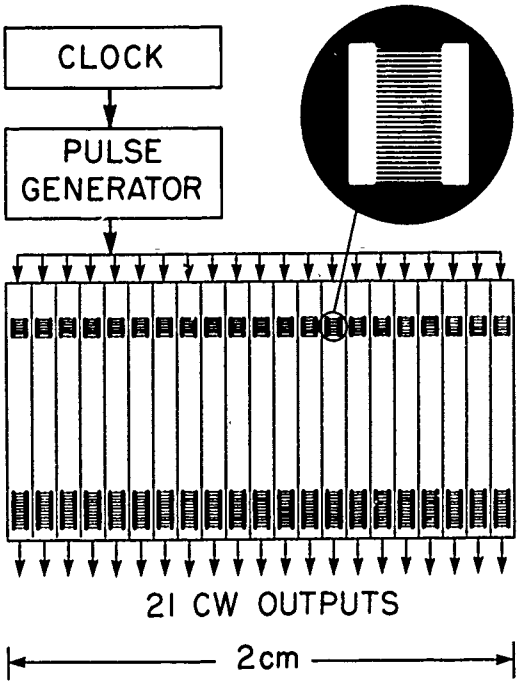

The 2 cm scale refers to the dimensions of the acoustic surface wave filter bank in this AFCRL-developed microwave frequency synthesizer. Each vertical column is a separate surface acoustic wave filter. The signal propagates as a Rayleigh (surface acoustic) wave from the small transducer at the top to the larger one at the bottom. Each visible line in the insert is composed of 4 1.5 μ wide lines. The spacing between the center of the lines determines the frequency of the filter.

an input and an output transducer, and the pairs of transducers are designed to constitute 21 filters, each tuned to a different frequency. In addition to the response peak that each filter has at its design frequency, each filter has a response null, or rejection notch, at all the other frequencies. Thus, the pass frequency of each channel corresponds to the nulls of all other channels. A spectrum of regularly spaced frequencies across the band is generated by repetitive sub-nanosecond pulses recurring at a rate equal to the null-spacing interval. When this signal is distributed to the 21 input transducers, the output transducers simultaneously yield the required 21 CW signals.

Test devices were contact printed on lithium tantalate, with an acoustic surface wave propagation velocity of 3230 m/sec, and aluminum-nitride-on-sapphire, which has a propagation velocity of about 6000 m/sec. The same 21-channel master was used in both cases. The tantalate yielded contiguous filters spaced by 5.3 MHz, with frequencies from 520 through 650 MHz, and relative center frequencies accurate to about 0.02 percent. The rejection ratio for the periodic frequency input was in excess of 40 dB, with an insertion loss of about 17 dB at the center frequency of single channels. The aluminum nitride thin film device had channels spaced by 10 MHz in the 970-1210 MHz band. Because of nonuniformities in the film, however, the performance was not as good as the lithium tantalate. However, no degradation of performance was found for the aluminum nitride filters with a CW input of 1 watt per channel.

Second-order effects have been minimized by the use of a "thinned" transducer configuration, i.e., periodically omitting groups of transducer lines. This allows one to retain the same overall transducer length and this determines the null spacing. At the same time, however, reducing the number of lines minimizes the effects of acoustic reflections. Without thinning, these reflections would badly distort the frequency response. Electromagnetic leakage has been decreased by a package design that minimizes feedthrough with minimum lead lengths and maximum shielding.

Computer calculations have been carried out to develop an optimized matching scheme for connecting all of the input transducers to the pulse source. By using a series-parallel connection of the input transducers to match the real part, and a single inductor to tune out the combined imaginary part, a satisfactory alternative to complicated and bulky matching networks has been developed. This approach preserves the simplicity, compactness, and reliability inherent in this SAW design of a multichannel filter bank. This work is being extended to fast spectral analysis application for electronic reconnaissance, warfare, and intelligence applications.

MICROWAVE DIELECTRIC RESONATORS AND FILTERS: Dielectric resonators have an advantage in microwave circuit applications at frequencies above 3 GHz because of their small size, simple coupling circuitry and high reliability. They are especially useful where multichannel filtering and high density packaging are required. One such application is a Laboratory-developed 96-channel, C-band Frequency Analyzer, which incorporates 96 individual contiguous filters, each having a 3 dB bandwidth of 10 MHz. The core of the filter module is of circular cross section, with eight radial separators and 12 disks formed into 96 individual cells. Each cell contains dielectric resonator-disk and detector circuitry which couples to a single common coaxial feed line in the center of the core. The signal processing circuitry is mounted on etched circuit boards mounted radially on the metallized core. The first such frequency analyzer was, of course, a hand-wired prototype. The operational version will have large-scale integrated (LSI) circuits, reducing the protruding radial boards to mere ¼-inch wide strips. This frequency analyzer was developed in response to a

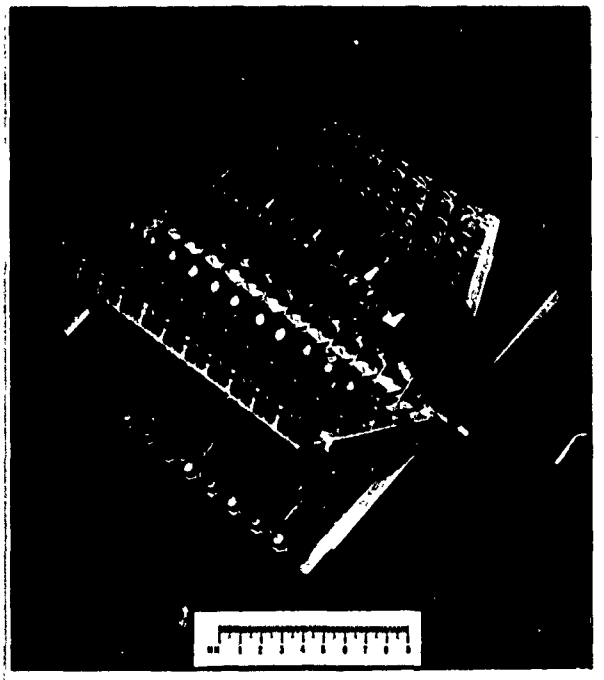

This 96-Channel C-Band frequency analyzer has 96 individual strontium titanate disk resonators arranged in a corn cob type core, coupling to a single coaxial feed line. The 10 MHz wide filters give contiguous coverage from 4000-4960 MHz. A parallel processing signal sorter supplies output voltages proportional to the detected frequencies in less than 1 microsecond. Such devices find use in electronic warfare applications.

SAMSO requirement. Another application of dielectric resonators, currently under study in the Laboratory, is a wideband electronically tunable filter for the AWACS and AABNCP Systems.

MAGNETIC SURFACE WAVES: A magnetically saturated ferrimagnet, such as yttrium iron garnet, will support many modes of propagation in the microwave frequency range. The modes include both surface and volume waves in which the energy carried by the waves is purely magnetic in character with the electric field component entirely negligible. The velocity of propagation is tunable and propagation velocities may be varied by several orders of magnitude. Most of these waves are reciprocal in the sense that energy can propagate between any two points in either direction. One type, however, is non-reciprocal.

Laboratory scientists have made significant advances in the generation, control and understanding of these magnetic surface waves. They find use in signal processing devices at frequencies above a few gigahertz, where acoustic surface wave losses are prohibitively high. Among other possibilities, tunable filters, variable delay lines, pulse compressors, and isolators can be constructed using these magnetic surface waves. In addition, they possess the unique features of non-reciprocity and electronic tunability and these are not possessed by their acoustic counterparts.

The practical use of magnetic surface waves at 15 GHz was demonstrated at AFCRL. Propagation losses were measured and figured to be a thousand times smaller than the best previously obtained. This was accomplished by reducing the surface losses with optical polishing followed by suitable chemical polishing. Measurements were also made of insertion, coupling, and propagation loss of tunable microwave magnetic delay lines. It was shown that electronically tunable delay lines, in the frequency range 4-12 GHz with zero to one microsecond delays, are indeed practical. As a result of these in-house efforts, Laboratory scientists feel that magnetic surface wave technology is ready for exploitation and utilization in microwave signal processing systems.

JOURNAL ARTICLES
JULY 1972 - JUNE 1974

ALTSHULER, E. E., WULFSBERG, K. N., and KALAGHAN, P. M.
Atmospheric Emission Statistics at 35 GHz
J. de Recherches Atmospheriques, Vol. 8, Nos. 1-2 (January-June 1974)

BUDREAU, A. J., CARR, P. H., and LAKER, K. R., 1st LT.
Frequency Synthesizer Using Acoustic Surface-Wave Filters
Microwave J., SAW Ser., No. 2 (March 1974/Feature Art.)

CARR, P. H.
Reduction of Reflections in Surface Wave Delay Lines with Quarter-Wave Taps
Proc. Ltrs. of the IEEE, Vol. 60, No. 9 (September 1972)
Elastic Surface Waves – Many New Applications
Astro. and Aero., Vol. 10, No. 11 (November 1972)

CARR, P. H., DE VITO, P. A., MAJ., and SZABO, T. L., CAPT.
The Effect of Temperature and Doppler Shift on the Performance of Elastic Surface Wave Encoders and Decoders
IEEE Trans. on Sonics and Ultrasonics, Vol. SU-19, No. 3 (July 1972)

DRANE, C. J., and MCILVENNA, J. E.
Anti-Jam Arrays with Maximum Gain
Proc. of the 22nd USAF Ant. Symp., Urbana, Ill. (October 1972)

EHRENSPECK, H. W.
A New Class of Medium-Size High-Efficiency Reflector Antennas
IEEE Trans. on Ant. and Propagation, Vol. AP-22, No. 2 (March 1974)

EHRENSPECK, H. W., and STROM, J. A.
Short-Backfire Antennas and Arrays
Proc. of the 23rd USAF Ant. Symp., Urbana, Ill. (October 1973)

FANTE, R. L.
Optical Propagation in Space-Time-Modulated Media Using Many-Space-Scale Perturbation Theory
J. of the Opt. Soc. of Am., Vol. 62, No. 9 (September 1972)
Propagation of Electromagnetic Waves in Media Which Vary Slowly with Position and Time
Rad. Sci., Vol. 7, No. 12 (December 1972)
On the Propagation of Electromagnetic Waves Through a Time-Varying Dielectric Layer
Appl. Sci. Res., Vol. 27, No. 4 (April 1973)
Wave Amplification and the Principle of Conservation of Wave Action
Proc. of the IEEE, Ltrs. Sec., Vol. 61, No. 8 (August 1973)
Propagation of Electromagnetic Waves Through Turbulent Plasma Using Transport Theory
IEEE Trans. on Ant. and Propagation, Vol. AP-21, No. 5 (September 1973)
Calculation of the Mutual Coherence Function for a Laser Beam in Atmospheric Turbulence
Appl. Opt., Vol. 12, No. 10 (October 1973)
Mutual Coherence Function and Frequency Spectrum of a Laser Beam Propagating Through Atmospheric Turbulence
J. of the Opt. Soc. of Am., Vol. 64, No. 5 (May 1974)

FANTE, R. L., and POIRIER, J. L.
Mutual Coherence Function of a Finite Optical Beam in a Turbulent Medium
Appl. Opt. (Ltr. to Ed.), Vol. 12, No. 10 (September 1973)

FANTE, R. L., and TAYLOR, R. L.
Effect of Losses in Transient Propagation in Dispersive Media – A Systems Study
IEEE Trans. on Ant. and Propagation, Vol. 21, No. 6 (November 1973)

GALLOP, M. A., JR., 1ST. LT., and TELFORD, L. E.
Estimation of Tropospheric Refractive Bending from Atmospheric Emission Measurements
Rad. Sci., Vol. 8, No. 10 (October 1973)

GOGGINS, W. B., JR., LT. COL., and SLETTEN, C. J.
New Concepts for AMTI Radar
Proc. of the 1973 Intl. IEEE/G-AP Symp. and USNC/URSI Mtg. (21-24 August 1973)

GOGGINS, W. B., JR., LT. COL., SLETTEN, C. J., and HOLT, F. S.
New Concepts in AMTI Radar
Microwave J., Vol. 17, No. 1 (January 1974)

GOGGINS, W. B., JR., LT. COL., BLACKSMITH, P., and SLETTEN, C. J.,
Phase Signature Radars
IEEE Trans. on Ant. and Propagation, Vol. AP22, No. 6 (November 1973)

HAYES, D. T.
Upper and Lower Bounds on Gas Breakdown in Inhomogeneous Fields
J. of Appl. Phys., Vol. 44, No. 10 (October 1973)

HAYES, D. T., HERSKOVITZ, S. B., LENNON, J. F., and POIRIER, J. L.
Enhancement of Microwave Antenna Performance in a Reentry Plasma: Flight Test Results of Chemical Alleviation
Proc. of the 1973 Intl., IEEE/G-AP Symp. and USNC/URSI Mtg. (21-24 August 1973)
Electrostatic Probe Measurements of Chemical Injection Effects During a Reentry Flight Test
J. of Spacecraft and Rockets, Vol. 11, No. 6 (June 1974)

HAYES, D. T., and ROTMAN, W.
Microwave and Electrostatic Probe Measurements on a Blunt Reentry Vehicle
AIAA J., Vol. 11, No. 5 (May 1973)

LAKER, K. R., 1ST LT., and GHAUSI, M. S. (Natl. Sci. Fdn., Wash., D. C.)
Synthesis of a Low-Sensitivity Multiloop Feedback Active RC Filter
IEEE Trans. on Circuits and Sys., CAS-21, No. 2 (March 1974)

LAMMERS, U. H. W.
Imaging Properties of Monostatic and Bistatic Troposcatter Radars
Rad. Sci., Vol. 8, No. 2 (February 1973)

LAMMERS, U. H. W., and OLSEN, R. L. (Comm. Res. Ctr., Ottawa, Can.)
Interference Measurements Over a Long 15.7 GHz Transhorizon Path
1973 AGARD Conf. Proc., Rome, Italy (7-11 May 1973)

MAILLOUX, R. J.
An Overlapped Sub-Array for Limited Scan Application
IEEE Trans. on Ant. and Propagation, Vol. AP-22, No. 3 (May 1974)

MAILLOUX, R. J., and BLACKSMITH, P.
Array and Reflector Techniques for Airport Precision Approach Radars
Proc. of AGARD Conf. on Ant. for Avionics, Munich, Ger., 23 Nov. - 3 Dec. 1973, Proc. No. 139 (June 1974)

MAILLOUX, R. J., and FORBES, G.
An Array Technique with Grating Lobe Suppression for Limited Scan Applications
IEEE Trans. on Ant. and Propagation, Vol. AP-21, No. 5 (September 1973)

MAILLOUX, R. J., and MAVROIDES, W. G.
A Metallized Channel Guide Antenna for Use Over a Cylindrical Ground Screen
IEEE Trans. on Ant. and Propagation, Vol. AP-20, No. 5 (September 1972)

MANO, K.
Hypergeometric Structure of the Generalized Veneziano Amplitudes
J. of Math. Phys., Vol. 13, No. 8 (August 1972)
Recurrence Formula for the Veneziano Model N-Point Functions
J. of Math. Phys., Vol. 13, No. 10 (October 1972)
A Binomial Expansion Identity
SIAM Rev. Vol. 15, No. 4 (October 1973)
Generalization of Two Binomial-Coefficient Identities of Rosenbaum
Bharata Ganita Parisad, Vol. 24, No. 2 (December 1973)

NEWBURGH, R. G.
Synchrotron Radiation as Evidence Against the Ritz Emission Theory
Am. J. of Phys., Vol. 40, No. 8 (August 1972)
Thomas Precession and Extended Structures
Il Nuovo Cimento, Vol. 5, No. 5 (30 September 1972)
Motional Effects in Retardation Plates and Mode Locking in Ring Lasers
Appl. Opt., Vol. 12, No. 1 (January 1973)
Comments on "The Incompatibility of Mach's Principle and the Principle of Equivalence in Current Gravitation Theory"
Brit. J. for the Philos. of Sci., Vol. 24, (October 1973)

PAPA, R. J.
Extension of Dougherty's Model Fokker-Planck Equation for a Plasma
J. of Plasma Phys., Vol. 11, (Pt. 1) (February 1974)

PAPA, R. J., and LINDSTROM, P.
Attenuation of Longitudinal Electroacoustic Waves in a Plasma
J. of Plasma Phys., Vol. 11 (Pt. 1) (February 1974)

PAPA, R. J., and TAYLOR, R. L.
The High Power Electromagnetic Transmission Characteristics of a Diffusing Reentry Plasma
J. of Appl. Phys., Vol. 45, No. 2 (February 1974)

POIRIER, J. L., and KORFF, D. (Lowell Technol. Inst., Lowell, Mass.)
Beam Spreading in a Turbulent Medium
J. of the Opt. Soc. of Am., Vol. 62, No. 7 (July 1972)

RAO, K. V. N., and HAYES, D. T.
Harmonic Emission from Tonks-Dattner Resonance Excited Afterglow Plasmas
IEEE Trans. on Plasma Sci. (Ltrs. Sec.), Vol. PS-2, Issue 2 (June 1974)

SETHARES, J. C., and MERRY, J. B.
Low Loss Magnetostatic Surface Waves at Frequencies Up to 15 GHz
Digest of the Intl. Mag. Conf., Wash., D. C., Apr. 24-27, 1973 (April 1973); IEEE MAG-9, No. 3 (September 1973)

SLETTEN, C. J.
AD COM Initiatives – 1973
Proc. of 1973 Intl. IEEE/G-AP Symp. and USNC/URSI Mtg. (21-24 August 1973)

SLOBODNIK, A. J., JR.
Attenuation of Microwave Acoustic Surface Waves Due to Gas Loading
J. of Appl. Phys., Vol. 43, No. 6 (August 1972)
You Too Can Design Microwave Acoustic Devices
Microwaves, Vol. 12, No. 9 (September 1973)
A Review of Material Tradeoffs in the Design of Acoustic Surface Wave Devices at Microwave Frequencies
Gp. on Sonics and Ultrasonics, Vol. SU-20, No. 4 (October 1973)
Surface Quality Effects on SAW Attenuation on YZ $LiNbO_3$
Elect. Ltrs., Vol. 10, No. 12 (June 1974)

SLOBODNIK, A. J., JR., and BUDREAU, A. J.
Acoustic Surface Wave Loss Mechanisms on $Bi_{12}GeO_{20}$ at Microwave Frequencies
J. of Appl. Phys., Vol. 43, No. 8 (August 1972)

SLOBODNIK, A. J., JR., and SILVA, J. H.
No More Scratches
Microwaves Notebook, Microwaves, Vol. 12, No. 3 (March 1973)

SLOBODNIK, A. J., JR., and SZABO, T. L., CAPT.
New Technique for Measuring Acoustic Surface Wave Propagation Loss
Elect. Ltrs., Vol. 8, No. 25 (14 December 1972)
Ultra-Low Diffraction Acoustic Surface Wave Propagation on $Bi_{12}GeO_{20}$
Elect. Ltrs (Eng.), Vol. 9, No. 6 (March 1973)
Minimal Diffraction Cuts for Acoustic Surface Wave Propagation on $Bi_{12}GeO_{20}$
J. of Appl. Phys., Vol. 44, No. 7 (July 1973)
Design of Optimum Acoustic Surface Wave Delay Lines at Microwave Frequencies
IEEE Trans. on Microwave Theory and Techniques, Vol. 22, No. 4 (April 1974)

STIGLITZ, M. R.
Response Curve Shaping of Coupled Dielectric Resonators
Proc. of the IEEE, Vol. 61, No. 3 (March 1973)

STIGLITZ, M. R., and KEARNS, W. J.
A Photoresist Film Applicator for Long and Fragile Crystal Substrates
Rev. of Sci. Instm., Vol. 44, No. 11 (November 1973)

SZABO, T. L., CAPT.
Surface Acoustic Wave Losses of Thin Film Gratings
Appl. Phys. Ltrs., Vol. 22 (15 May 1973)

SZABO, T. L., CAPT., and SLOBODNIK, A. J., JR.
The Effect of Diffraction on the Design of Acoustic Surface Wave Devices
IEEE Trans. on Sonics and Ultrasonics, Vol. SU-20, No. 3 (July 1973)
Diffraction Compensation in Periodic Apodized Acoustic Surface Wave Filters
IEEE Trans. on Sonics and Ultrasonics, Vol. SU-21, No. 2 (April 1974)

TELFORD, L. E.
Millimeter Wave Spectroheliograms Associated with the January 24, 1971 and September 1, 1971 Solar-Terrestrial Events
Data on Solar Geophys. Activity Assoc. with the Major Ground-Level Cosmic Ray Events of 24 Jan. and 1 Sep. 1971 (UAG Rpt., NOAA, Boulder, Colo.), UAG-24, Pts. I and II (December 1972)

WALTHER, F. G., BUDREAU, A. J., and CARR, P. H.
Multiple UHF Frequency Generation Using Acoustic Surface Wave Filters
Proc. of the IEEE, Vol. 61, No. 8 (August 1973)

WULFSBERG, K. N.
Path Diversity for Millimeter-Wave Earth-to-Satellite Links
Rad. Sci., Vol. 8, No. 1 (January 1973)

PAPERS PRESENTED AT MEETINGS JULY 1972 - JUNE 1974

ALTSHULER, E. E., WULFSBERG, K. N., and KALAGHAN, P. M.
Atmospheric Emission Statistics at 35 GHz
IUCRM Colloq. on the Fine Scale Structure of Precipitation and EM Propagation, Observatoire de Nice, Fr. (23-31 October 1973)

BUDREAU, A. J., and CARR, P. H.
Narrow Band Surface Wave Filters at 1 GHz
Ultrasonics Symp., IEEE Gp. on Sonics and Ultrasonics, Boston, Mass. (4 October 1972)

BUDREAU, A. J., CARR, P. H., and LAKER, K. R., 1ST LT.
Multiple-Channel UHF Frequency Synthesizer Using Acoustic Surface-Wave Filters
1973 Ultrasonics Symp., U. S. Naval Postgrad. Sch., Monterey, Calif. (5 November 1973)

BUDREAU, A. J., LAKER, K. R., 1ST. LT., and CARR, P. H.
Compact Microwave Acoustic Surface Wave Filter Bank for Frequency Synthesis
MRI Intl. Symp. XXIII on Opt. and Acoust. Micro-Elect., Polytech. Inst. of Brooklyn, N. Y. (16-18 April 1974)

CARL, J. W. (AMRL, Wright-Patterson AFB, Ohio), GILL, R. A. (AFIT, Wright-Patterson AFB, Ohio), GINSBURG, A. P., 1ST. LT., and HALL, C. F., KABRISKY, M. (AFIT, Wright-Patterson AFB, Ohio)
Psychological Aspects of a Model for the Classification of Visual Images
Intl. Cong. of Cybernetics and Sys., Oxford, Eng. (28 August - 1 September 1972)

CARR, P. H.
The Physics of Microwave Acoustic Devices and Their Uses in Military Systems
Sem., Naval Postgrad. Sch., Monterey. Calif. (22 January 1973)
The Role of Temperature in Acoustic Surface Wave Signal Processing Devices
Sem., Penn. State Univ., Univ. Pk., Pa. (27 March 1973)
Acoustic Surface Waves and Their Uses in AF Systems
Sem., AF Inst., of Technol., Wright-Patterson AFB, Ohio (7 June 1973)
Ultrasonic Rayleigh Surface Waves: Research to Applications
Sem., Univ. of Me., Orono, Me. (14 February 1974)

CARR, P. H. and BUDREAU, A. J.
Attenuation of Microwave Frequency Elastic Surface Waves
40th Mtg. of N. E. Sec. of Am. Phys. Soc., Univ. of Vt., Burlington, Vt. (13-14 October 1972)

DRANE, C. J., JR., and MCILVENNA, J. F.
Synthesis of Antenna Array Radiation Patterns with Anti-Jam Properties
1972 AFSC Sci. and Engrg. Symp., San Antonio, Tex. (17-19 October 1972)

EHRENSPECK, H. W., and STROM, J. A.
Short-Backfire Antennas and Arrays
23rd Ann. AF Ant. Symp., Univ. of Ill., Urbana, Ill. (10-12 October 1973)

FALCONE, V. J., JR.
Temperature Inferring by the Generalized Inverse
1973 Intl. IEEE/G-AP Symp. and USNC/URSI Mtg., Univ. of Colo., Boulder, Colo. (21-24 August 1973)

FANTE, R. L.
Propagation of Waves in Media Which Vary Slowly with Position and Time
Fall USNC/URSI Mtg., Williamsburg, Va. (11-15 December 1972)
Frequency Spectrum of a Wave Propagating Through the Turbulent Atmosphere
1974 IEEE G-MTT Intl. Symp. and USNC/URSI Mtg., Ga. Inst. of Technol., Atlanta, Ga. (11-13 June 1974)

FANTE, R. L., PAPA, R. J., and TAYLOR, R. L.
Effect of Losses and Nonlinearities on Transients in Dispersive Media – A Systems Study
1973 Intl. IEEE/G-AP Symp. and USNC/URSI Mtg., Univ. of Colo., Boulder, Colo. (21-24 August 1973)

GINSBURG, A. P., CAPT.
Psychological Aspects of a Model for the Classification of Visual Images
Intl. Cong. of Cybernetics and Sys., Oxford, Eng. (28 August - 1 September 1972)
Pattern Recognition Techniques Suggested from Psychological Correlates of a Model of the Human Visual System
1973 Natl. Aerosp. and Elect. Conf., Dayton, Ohio (14-16 May 1973)
Perceptual Correlates of a Two-Dimensional Spatial Frequency Model of the Human Visual System
1973 Ann. Mtg. of the Opt. Soc. of Am., Rochester, N. Y. (9-12 October 1973)

GITELSON, S., NEWBURGH, R. G., and SAKAI, H. (Opt. Phys. Lab.)
A Polarization Sagnac Interferometer
1972 Fall Mtg. of the Opt. Soc. of Am., San Francisco, Calif. (17-20 October 1972)

GOGGINS, W. B., JR., MAJ., and CENTOFANTI, J. J., LT. COL. (AFSC Andrews AFB, Md.)
Synthetic Aperture Dual Frequency Radar (SADFRAD)
19th Ann. Tri-Svc. Radar Symp., AF Acad., Colo. (10-12 July 1973)

GOGGINS, W. B., JR., MAJ., and SLETTEN, C. J.
New Concepts for AMTI Radar
1973 Intl. IEEE/G-AP Symp. and USNC/URSI Mtg., Univ. of Colo., Boulder, Colo. (21-24 August 1973)

GOGGINS, W. B., JR., LT. COL., SLETTEN, C. J., and HOLT, F. S.
New Concepts in AMTI Radar
Adaptive Ant. Sys. Wkshp., Naval Res. Lab., Wash., D. C. (11-13 March 1974)

HAYES, D. T.
The Calculation of Lower Bounds on the Breakdown Power Levels of Electromagnetic Structures
Fall USNC/URSI Mtg., Williamsburg, Va. (11-15 December 1972)
Electrostatic Probe Measurements of the Flow Field Characteristics of the Blunt Body Reentry Vehicle
5th AIAA Fluid and Plasma Dyn. Conf., Boston, Mass. (26-28 June 1973)

HAYES, D. T., HERSKOVITZ, S. B., LENNON, J. F., and POIRIER, J. L.
Inflight Electrostatic Probe Measurements of the Effect of Chemical Injection on the Properties of the Reentry Flow Field
AIAA 6th Fluid and Plasma Dyn. Conf., Palm Springs, Calif. (16-18 July 1973)
Enhancement of Microwave Antenna Performance in a Reentry Plasma: Flight Test Results of Chemical Alleviation
1973 Intl. IEEE/G-AP Symp. and USNC/URSI Mtg., Univ. of Colo., Boulder, Colo. (21-24 August 1973)

KALAGHAN, P. M.
Solar Limb Brightening at $\lambda = 8.6$ Mm
1973 Intl. IEEE/G-AP Symp. and USNC/URSI Mtg., Univ. of Colo., Boulder, Colo. (21-24 August 1973)

LAKER, K. R., 1ST LT.
Computer-Aided Analysis and Design of Multiple-Loop Feedback Active RC Networks
8th Ann. Princeton Conf. on Info. Sci. and Sys., Princeton Univ., Princeton, N. J. (28-29 March 1974)

LAKER, K. R., 1ST LT., BUDREAU, A. J., and CARR, P. H.
Compact Acoustic Surface Wave Frequency Multiplexer
1974 IEEE Intl. Symp. on Circuits and Sys. Theory, San Francisco, Calif. (22-25 April 1974)

LAKER, K. R., 1ST LT., and GHAUSI, M. S. (Natl. Sci. Fdn., Wash., D. C.), KELLY, J. J. (Univ. of Bridgeport, Conn.)
Minimum Sensitivity Leapfrog Active RC Filters
1974 IEEE Intl. Symp. on Circuits and Sys. Theory, San Francisco, Calif. (22-25 April 1974)

LAMMERS, U. H. W., and OLSEN, R. L. (Comm. Res. Ctr., Ottawa, Can.)
Measurements of Wind-Induced Doppler Shifts at 16 GHz Over a Long Range Bistatic Scatter Link
IEEE Conf. on Propagation of Rad. Waves at Freq. Above 10 GHz, London, Eng. (10-13 April 1973)
Interference Measurements Over a 15.7 GHz Transhorizon Path
AGARD Electmg. Wave Propagation Panel Specialists Mtg., Rome, Italy (7-11 May 1973)
Bistatic Measurement of Meteorological and Propagation Parameters with a High-Resolution Ku-Band Scatter System
1973 Intl. IEEE/G-AP Symp. and USNC/URSI Mtg., Univ. of Colo., Boulder, Colo. (21-24 August 1973)

LAMMERS, U. H. W., and STIGLITZ, M. R.
A One Microsecond Pulse Frequency Analyzer for Electronic Countermeasures
1972 AFSC Sci. and Engrg. Symp., San Antonio, Tex. (17-19 October 1972)

MACK, R. B.
Resonant Region Scattering
Boston Chap. Mtg. of the IEEE Gp. on Ant. and Propagation, Raytheon Co., Bedford, Mass. (19 September 1973)

MAILLOUX, R. J.
Array Techniques for Limited Scan Application
(Inv. Paper) Boston Chap. Mtg. of IEEE Gp. on Ant. and Propagation, Boston, Mass. (26 September 1972)
The "Blind Spot" Phenomenon in Phased Arrays
USAF Ant. Symp., Univ. of Ill., Urbana, Ill. (11-13 October 1972)

MAILLOUX, R. J., and BLACKSMITH, P.
Array and Reflector Techniques for Airport Precision Approach Radars
26th Mtg. of the Avionics Panel, Munich, Ger. (26-28 November 1973)

MAILLOUX, R. J., and FORBES, G. R.
An Array Technique with Grating Lobe Suppression for Limited Scan Applications
1972 Intl. IEEE/G-AP Symp., Williamsburg, Va. (11-15 December 1972)
An Experimental Array Program for Limited Scanning Studies
1973 Intl. IEEE/G-AP Symp. and USNC/URSI Mtg., Univ. of Colo., Boulder, Colo. (21-24 August 1973)

MAILLOUX, R. J., and MAVROIDES, W. G.
Design, Fabrication and Testing of a Low Profile Antenna for Aircraft Station Keeping Application
1972 AFSC Sci. and Engrg. Symp., San Antonio, Tex. (17-19 October 1972)

MERRY, J. B., and SETHARES, J. C.
Low Loss Magnetostatic Surface Waves at Frequencies up to 15 GHz
1973 INTERMAG (Intl. Mag.) Conf., Wash., D. C. (24-27 April 1973)

NEWBURGH, R. G.
Fresnel Drag and the Foundations of the Special Theory of Relativity
Boston Colloq. for the Philosophy of Science, Boston Univ. (27 February 1973); (Inv.) Colloq., Phys. Dept., Worcester Polytech, Inst., Mass. (9 October 1973); Colloq., Phys. Dept., Boston Coll., Mass. (31 October 1973)
Acoustic and Magnetic Surface Wave Ring Interferometers for Rotation Rate Sensing
Colloq., Naval Ordance Laboratory (26 April 1974)

OLSEN, R. L. (Comm. Res. Ctr., Ottawa, Can.), and LAMMERS, U. H. W.
Measurements of Wind-Induced Doppler Shifts at 16 GHz Over a Long Range Bistatic Scatter Link
IEEE Conf. on Propagation of Radiowaves Above 10 GHz, London, Eng. (10-13 April 1973)
Transhorizon Interference Measurements at 15.7 GHz
1974 IEEE G-MTT Intl. Symp. and USNC/URSI Mtg., Ga. Inst. of Technol., Atlanta, Ga. (11-13 June 1974)

PAPA, R. J.
Nonlinear Transmission of EM Waves Through a Diffusing Chemically Seeded Reentry Plasma
Fall USNC/URSI Mtg., Williamsburg, Va. (11-15 December 1972)

PAPA, R. J., and TAYLOR, R. L.
Effect of Losses and Nonlinearities on Transients in Dispersive Media – A System Study
1973 Intl. IEEE/G-AP Symp. and USNC/URSI Mtg., Univ. of Colo., Boulder, Colo. (21-24 August 1973)

RAO, K. V. N.
Nonlinear Electroacoustic Resonances in Afterglow Plasmas
Am. Phys. Soc. Plasma Phys. Mtg., Monterey, Calif. (13-16 November 1972)

ROTMAN, W., JACAVANCO, D., and HALDERMAN, C. (Mass. Inst. of Technol.)
Electrophilic Ablators for Reentry Antenna Systems
1972 Intl. IEEE/G-AP Symp., Williamsburg, Va. (11-15 December 1972)

SCHELL, A. C.
A Limited Sector Scanning Antenna
URSI/IEEE/G-AP Fall Symp., Williamsburg, Va. (12-15 December 1972)
Performance of a Reflector-Array Limited Scan Technique
1973 Intl. IEEE/G-AP Symp. and USNC/URSI Mtg., Univ. of Colo., Boulder, Colo. (21-24 August 1973)

SCHINDLER, J. K.
Resonant Region Radar Observables and Signatures
(Inv.) Tech. Coop. Prog. (TTCP) Action Gp. on Target Signature Characteristics, Naval Res. Lab., Wash., D. C. (3 June 1974)

SCHINDLER, J. K., and GOGGINS, W. B., JR., LT. COL.
A Novel Airborne Radar Technique for Moving Target Detection, Location and Tracking
1974 IEEE G-MTT Intl. Symp. and USNC/URSI Mtg., Ga. Inst of Technol., Atlanta, Ca. (11-13 June 1974)

SETHARES, J. C.
Low Loss Magnetostatic Surface Waves at Frequencies up to 15 GHz
1973 INTERMAG (Intl. Mag.) Conf., Wash., D. C. (24-27 April 1973)
Microwave Magnetic Surface Waves in Saturated Ferrimagnets
IEEE Mtg. on Mag., Sonics and Ultrasonics Microwave Theory and Techniques and Aerosp. and Elect. Sys., RCA, Burlington, Mass. (11 September 1973)

SETHARES, J. C., and STIGLITZ, M. R.
Propagation Loss and MSSW Delay Lines
Intl. Mag. Conf., Toronto, Can. (14-17 May 1974)
Magnetostatic Surface Wave Delay Lines
1974 IEEE G-MTT Intl. Symp. and USNC/URSI Mtg., Ga. Inst. of Technol., Atlanta, Ga. (12-14 June 1974)

SLETTEN, C. J.
Applications of Electromagnetic Technology in ttelecommunications
NSF Wkshp. on Electmg. Theory of Continuous Media, Williamsburg, Va. (12-15 December 1972); Univ. of Miss., University, Miss. (15 February 1973)
AD COM Initiatives – 1973
1973 Intl. IEEE/G-AP Symp. and USNC/URSI Mtg., Univ. of Colo., Boulder, Colo. (21-24 August 1973)

SLOBODNIK, A. J., JR.
Material Dependence of Acoustic Surface Wave Propagation Losses
Ultrasonics Symp., IEEE Gp. on Sonics and Ultrasonics, Boston, Mass. (4 October 1972)
The Effect of Surface Quality on Acoustic Surface Wave Attenuation on YZ $LiNbO_3$
1973 Ultrasonics Symp., U. S. Naval Postgrad. Sch., Monterey, Calif. (5 November 1973)
A Review of the Properties of Surface Acoustic Wave Materials
(Inv. Paper) MRI Intl. Symp. XXIII on Opt. and Acoust. Micro-Elect., Polytech. Inst. of Brooklyn, N. Y. (16-18 April 1974)

SLOBODNIK, A. J., JR., and SZABO, T. L., CAPT.
Synthesis of Periodic Apodized SAW Filters in the Presence of Diffraction
1974 IEEE G-MTT Intl. Symp. and USNC/URSI Mtg., Ga. Inst. of Technol., Atlanta, Ga. (11-13 June 1974)

SLOBODNIK, A. J., JR., SZABO, T. L., CAPT., KEARNS, W. J., and TIGHE, J. F., SSGT.
Minimal Diffraction Acoustic Surface Wave Orientations
1973 Ultrasonics Symp., U. S. Naval Postgrad. Sch., Monterey, Calif. (5 November 1973)

SZABO, T. L., CAPT., and SLOBODNIK, A. J., JR.
Methods for Determining Acoustic Surface Wave Diffraction
Ultrasonics Symp., IEEE Gp. on Sonics and Ultrasonics, Boston, Mass. (4 October 1972)
Transducer Design Including Beam Steering and Diffraction
85th Mtg. of Acoust. Soc. of Am., Boston, Mass. (10-13 April 1973)

WULFSBERG, K. N., and ALTSHULER, E. E.
Statistics on Apparent Sky Temperature at 35 GHz for the Boston Area
1973 Intl. IEEE/G-AP Symp. and USNC/URSI Mtg., Univ. of Colo., Boulder, Colo. (21-24 August 1973)

TECHNICAL REPORTS
JULY 1972 - JUNE 1974

ALTSHULER, E. E., and KALAGHAN, P. M.
Tropospheric Range Error Corrections for the NAVSTAR System
AFCRL-TR-74-0198 (16 April 1974)

DE VITO, P. A., MAJ.
Some Properties of an Injection-Locked Pulsed Magnetron
AFCRL-TR-73-0073 (16 January 1973)

DE VITO, P. A., MAJ., CARR, P. H., and SZABO, T. L., CAPT.
The Performance of 31 and 127 Bit Elastic Surface Wave Encoders and Decoders
AFCRL-72-0736 (19 December 1972)

DRANE, C. J., JR.
On the Three-Term Theory for Analyzing Thin Cylindrical Dipole Antennas
AFCRL-72-0744 (29 December 1972)
On Improving Approximations for Current and Charge Distributions of Cylindrical Dipole Antennas
AFCRL-TR-73-0752 (18 December 1973)
On the Long Cylindrical Antenna
AFCRL-TR-74-0080 (8 February 1974)

EHRENSPECK, H. W., and STROM, J. A.
A Sixteen-Element SBF Array
AFCRL-72-0500 (23 August 1972)
An Eight-Element SBF Fan-Beam Array
AFCRL-TR-74-0115 (4 March 1974)

FANTE, R. L.
Effect of Diffusion on Laser Induced Breakdown of Gases
AFCRL-72-0479 (15 August 1972)
Receiver Noise Due to R/V Plasma Sheath Turbulence
AFCRL-72-0735 (18 December 1972)
Propagation of Electromagnetic Waves Through Turbulent Media Using Transport Theory
AFCRL-72-0733 (18 December 1972)
Wave Amplification and the Principle of Conservation of Wave Action
AFCRL-TR-73-0156 (8 March 1973)
Change in Reflection Coefficient Induced by a Spot on the Surface of a Dielectric Inside a Rectangular Waveguide
AFCRL-TR-73-0365 (18 June 1973)
Mutual Coherence Function of a Beam Propagating in a Turbulent Medium
AFCRL-TR-73-0566 (7 September 1973)
Radar Cross Section of Underdense Turbulent Wakes
AFCRL-TR-73-0634 (11 October 1973)
Mutual Coherence Function and Frequency Spectrum of a Laser Beam Propagating Through Atmospheric Turbulence
AFCRL-TR-74-0079 (6 February 1974)
Frequency Spectrum of Optical Waves Propagating in a Moving Turbulent Atmosphere
AFCRL-TR-74-0135 (8 March 1974)

FANTE, R. L., and TAYLOR, R. L.
Transient Signal Propagation in Lossy Plasmas
AFCRL-TR-73-0277 (25 April 1973)

FOSTER, M. R., 1ST LT.
Microwave Breakdown Calculations that Include the Effects of Preionization in Neon and Neon-Argon Mixtures
AFCRL-TR-73-0562 (6 September 1973)

GOGGINS, W. B., JR. MAJ.
Identification of Radar Targets by Pattern Recognition
AFCRL-TR-73-0126 (26 February 1973)

HAYES, D. T.
The Calculation of Lower Bounds on the Breakdown Power Levels of Electromagnetic Structures
AFCRL-TR-73-0095 (7 February 1973)

HAYES, D. T., HERSKOVITZ, S. B., LENNON, J. F., and POIRIER, J. L.
Preliminary Report on the Trailblazer II Chemical Alleviation Flight of 28 July 1972
AFCRL-72-0640 (25 October 1972)

HOLT, F. S., PIERCE, J. N., and SCHINDLER, J. K.
Improved Spectrum Analysis Noise Radar Systems
AFCRL-TR-73-0279 (30 April 1973)

KALAGHAN, P. M., and ALTSHULER, E. E.
Tropospheric Refraction Corrections for Airborne Systems
AFCRL-TR-73-0376 (26 June 1973)

KARAS, N. V.
Microstrip Plasma Probe
AFCRL-72-0417 (17 July 1972)
Electroacoustic Probe Results Obtained in an Argon Afterglow Plasma for a Planar Geometry
AFCRL-TR-73-0665 (2 November 1973)

KEARNS, W. J., and SILVA, J. H., SGT.
Fabrication of Elastic Surface Devices by Chemical Etching
AFCRL-72-0731 (19 December 1972)

LENNON, J. F.
Trailblazer II Rocket Tests on the Reentry Plasma Sheath: Vehicle Performance and Plasma Predictions (Flights No. 1-3)
AFCRL-TR-73-0317 (16 May 1973)

LENNON, J. F., and HERSKOVITZ, S. B.
Design and Testing of a Chemical Injection System for Reentry Plasma Alleviation
AFCRL-TR-74-0113 (28 February 1974)

LINDSTROM, P., and PAPA, R. J.
Representation of the Electric Field of Longitudinal Waves in a Plasma
AFCRL-TR-73-0193 (29 March 1973)

MACK, R. B., WOJCICKI, A. W., and ANDRIOTAKIS, J. J.
An Implementation of Conventional Methods of Measuring the Amplitude and Phase of Backscatter Fields
AFCRL-TR-73-0418 (16 July 1973)

MAILLOUX, R. J.
Array Techniques for Limited Scan Application
AFCRL-72-0421 (19 July 1972)
An Overlapped Sub-Array for Limited Scan Application
AFCRL-TR-73-0598 (27 September 1973)

MAILLOUX, R. J., and FORBES, G. R.
Experimental Studies of a Multiple Mode Array Technique for Limited Scan Applications
AFCRL-TR-73-0685 (6 November 1973)

MAVROIDES, W. G., SCHOFIELD, R. A., and MAILLOUX, R. J.
A Lightweight, Low-Profile Antenna for Airborne Station-Keeping Application
AFCRL-TR-73-0047 (12 January 1973)

NEWBURGH, R. G., BLACKSMITH, P., BUDREAU, A. J., and SETHARES, J. C.
Novel Acoustic and Magnetic Rotation Rate Sensors
AFCRL-TR-74-0023 (10 January 1974)

PAPA, R. J.
Chemical Injection into a Reentry Plasma to Improve High Power EM Wave Transmission
AFCRL-72-0556 (18 September 1972)
Numerical Solution of the Dispersion Relations for a Hot Magnetoplasma with Collisions
AFCRL-72-0712 (6 December 1972)

PAPA, R. J., and LINDSTROM, P.
Attenuation of Longitudinal Electroacoustic Waves in a Plasma
AFCRL-TR-73-0123 (28 February 1973)

PAPA, R. J., and TAYLOR, R. L.
Comparison of the Effects of Different Transport Coefficients on the Nonlinear Reflection and Transmission Coefficients of a Reentry Plasma
AFCRL-TR-73-0362 (8 June 1973)
Effects of Different Flow Field Conditions on the High Power Transmission Properties of a Reentry Plasma
AFCRL-TR-73-0754 (14 December 1973)

POIRIER, J. L., ANTONUCCI, J. D., and TROPEA, D. H.
Performance of a Microwave Antenna System in the Shoulder Region of a Blunt Reentry Nose Cone
AFCRL-TR-73-0656 (24 October 1973)

POIRIER, J. L., and TROPEA, D. H.
A Simple Method of Simulating Motion and Plasma Induced Variations in the Attenuation of Signals Transmitted from Reentry Vehicles
AFCRL-TR-73-0650 (17 October 1973)

RAO, K. V. N.
Linear and Nonlinear Tonks-Dattner Resonances in Laboratory Afterglow Plasmas
AFCRL-TR-73-0094 (7 February 1973)

ROTMAN, W., and MALONEY, L. R., MAJ.
High Power Microwave Antenna Performance in the Stagnation Region of a Blunt Reentry Nose Cone
AFCRL-TR-73-0072 (16 January 1973)

SCHINDLER, J. K., and GOGGINS, W. B., LT. COL.
An Airborne Radar Technique for Moving-Target Detection, Location, and Tracking
AFCRL-TR-73-0719 (26 November 1973)

SETHARES, J. C., and MERRY, J. B.
Magnetostatic Surface Waves in Ferrimagnets Above 4 GHz
AFCRL-TR-74-0112 (28 February 1974)

SLOBODNIK, A. J., JR.
UHF and Microwave Frequency Acoustic Surface Wave Delay Lines: Design
AFCRL-TR-73-0538 (16 August 1973)

SLOBODNIK, A. J., JR., and CONWAY, E. D., DELMONICO, R. T. (ACSI, Inc., Burlington Mass.), Editors
Microwave Acoustics Handbook – Vol. 1A. Surface Wave Velocities
AFCRL-TR-73-0597 (1 October 1973)

SZABO, T. L., CAPT., and SLOBODNIK, A. J., JR.
Acoustic Surface Wave Diffraction and Beam Steering
AFCRL-TR-73-0302 (3 May 1973)

IV Aerospace Instrumentation Laboratory

AFCRL is concerned with investigations of the environment in which Air Force systems must operate, and its scientists use a variety of equipment and methods for obtaining their research data. It follows that atmospheric and space probes play an important role in this mission. The Aerospace Instrumentation Laboratory provides balloon, satellite and rocket support to other AFCRL laboratories and also conducts research and development programs to ensure that the scientist has the best vehicle and ancillary equipment within his budget to meet his objectives. To carry out this work, the Laboratory's professional manning is mainly composed of engineers, both military and civilian.

Permanent balloon launch facilities are located at Holloman AFB, New Mexico, (Detachment 1, AFCRL), and at Chico, California (Detachment 3, AFCRL). Both detachments have a remote operations capability for performing flights wherever a need may exist. The Holloman facility has access to the use of precision radar, optical instrumentation, telemetry and restricted airspace on the White Sands Missile Range, New Mexico, which provides the opportunity to conduct balloon operations involving free fall, explosives and high altitude tethering.

While the Laboratory's rocket branches provide support solely to AFCRL experimenters, the balloon branches are frequently called upon to support other Air Force organizations, the Army, Navy, and NASA. Additionally, the Atomic Energy Commission's air sampling program (Project Ash Can) receives its balloon support from the Laboratory with flight operations

conducted in Alaska and Panama as well as at Holloman and Chico. The operational aspects of this work are very similar to those proposed for AFCRL's newly instituted Stratospheric Environmental Quality program.

During this reporting period, the Laboratory launched 230 free and tethered balloons. Highlights of its tethered balloon operations were programs conducted for the Space and Missile Systems Organization (SAMSO) System 621B, a satellite system for precise navigation; a series that provided for the Department of Defense, on a quick-response basis, information on missile targeting and firing (Project Graduation Level); and a long series of flights conducted at Donaldson, Minnesota, in support of the Meteorology Laboratory's (AFCRL) research on boundary layer effects.

Alaska was visited by Laboratory launch crews twice in support of the Ash Can Program and twice in support of AFCRL scientists engaged in infrared emission studies being funded by the Defense Nuclear Agency. ICECAP '73B, conducted at Fairbanks and Poker Flat, Alaska, included both balloon and rocket vehicles. Significant data were obtained and are reported in the Optical Physics Laboratory chapter of this report.

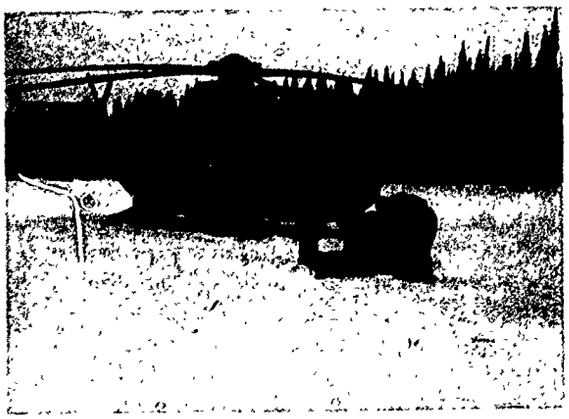

A recovery crew prepares to load the 700-pound ICECAP payload aboard the helicopter after lifting it from the forested area in the background.

During July and August 1972, the Laboratory launched four flights in support of the NASA Viking program which has as its objective the unmanned soft landing on the planet Mars in 1976. The Laboratory's participation in this national effort was to support balloon-launched decelerator tests which qualified the Mars descent parachute. This included not only launching the balloons but also designing the balloon system, and developing the necessary electronic equipment for command and control functions. The balloons used in this program had 34 million cubic foot volumes which enabled them to carry 6,000 pounds of payload to 120,000 feet. The four balloon flights for the Viking program were unqualified successes and provided crucial parachute data on simulated entry of the Martian atmosphere.

For years, the Laboratory has been flying extremely delicate optical equipment on its balloons. During November 1973 the largest balloon-borne telescope was successfully flown and recovered. Its 50-inch lens acquired significant measurements of infrared emissions from the planets Venus and Jupiter.

Four flights carrying a laser were made for NASA Goddard Space Flight Center, Greenbelt, Maryland. These were atmospheric propagation experiment designed to acquire data on the effects of the atmosphere on laser transmissions. Test results were provided to Rome Air Development Center, Rome, New York, and the Air Force Avionics Laboratory, Wright-Patterson AFB, Ohio, for use in their laser communications work.

On May 5, 1974, Project LACATE (Lower Atmospheric Composition and Temperature Experiment) was successfully launched and ascended to a float altitude of 41.4 km. The experiment, designed and fabricated by the NASA Langley Research Center, Virginia, was intended to remotely

infer temperature and the concentration of selected trace constituents in the 8 to 50 km altitude range. The experiment used limb radiance measurements taken in several bands of the infrared spectral region to infer vertical profiles of temperature, ozone, water vapor, atmospheric oxides, nitric acid, methane and aerosols. Carried by a large thin film (0.6 mil) polyethylene balloon, having a volume of 45 million cubic feet (500-foot diameter), the experiment successfully gathered data for a period of 5.5 hours at the float altitude.

The Laboratory is participating in Project GEST (Gaseous Explosive Simulation Tests) as balloon technical advisors to the Air Force Weapons Laboratory (AFWL), Kirtland AFB, New Mexico. The effort consists of developing a system to be used for simulating the gas entrainment and mixing processes present in a nuclear detonation. Thirty-two-foot diameter aluminized spherical balloons were designed and their fabrication and testing monitored. The balloons were ground-inflated with a detonable gas mixture of oxygen and methane (1.5 to 1 mixture ratio), raised to a height of approximately 150 feet and detonated, giving an equivalent TNT yield of 1,000 pounds. The Laboratory designed and supervised the fabrication and testing of the spherical balloons, in addition to assisting in formulating operational procedures and techniques. Three single detonations were successfully performed in November and December 1973, and a partially successful double detonation was executed in June 1974. A second double detonation is scheduled to take place in February 1975.

The strategic posture of the United States is extremely dependent upon the proper functioning of early warning sensors and the communications systems which link these sensors to commanders and, ultimately, the commanders to the nuclear strike force elements. The Aerospace Instrumentation Laboratory is participating in this AFWL program as balloon technical advisor. The program is designed to determine hardened alternative means of communications to existing ground-based C-cubed systems. Among the alternate systems being considered by a contractor team, two would employ balloons as a means of deploying selected communications hardware at prescribed operational altitudes. These balloon systems would be carried to altitude by rockets and aircraft and air-launched. The technical advisor role consists of reviewing contractor team development plans, observing development tests and sitting as a member on a Technical Advisory Group Panel, consisting of personnel of the various laboratories and divisions of the Air Force having expertise in the various disciplines involved.

FREE BALLOONS

Free balloon system technology has made progress on many fronts during the past two years: record altitudes, improved thin polyethylene film, better understanding of film properties under use conditions, improved launching methods, and advanced instrumentation, discussed under the section on Balloon Instrumentation.

A balloon, 47 million cubic feet in volume, fabricated from 0.35 mil polyethylene, was launched from AFCRL's Detachment 3, Chico, California. Its record size and record altitude reached (170,000 feet) although in themselves significant, were not as important as the demonstration that very thin polyethylene film could be made to survive the rigors of dynamic launch and ascent. The potentially catastrophic tendency of large balloons to develop massive sails which dynamically load the film during passage through the extremely cold tropopause was counteracted by a self-opening reefing sleeve. New reefing sleeve design information was gained and subsequently used on the NASA LACATE program.

Sleeved balloon in reeled-up position just prior to launch.

Very significant with respect to future high altitude balloon flights was the development of more uniformly balanced tensile properties in 0.35 mil polyethylene film. Continuous encouragement of the vendor toward this end resulted in a 0.35 mil film at least an order of magnitude superior to previous attempts.

Contracted research was successful in demonstrating the truth of an in-house postulation that polyethylene film cold brittleness is not a film property as such, but is a directionally sensitive film property. Examination of films from batches that were used in good balloons on the one hand and poorly performing balloons on the other hand showed the ductile brittle transition point of the latter film to be about 15 degrees warmer than the other, a significant distinction.

The principal problem associated with large gross load balloon systems is launching. The two usual techniques are the platform launcher (dynamic) and the tandem method (relatively quite static). The tandem method does not fully utilize inherent material and design strengths while the dynamic method introduces large, unpredictable (insofar as both orientation and magnitude are concerned) dynamic forces on the balloon structure. A method of inflation and static launch utilizing an unrestrained, cloth-sleeved balloon has been successfully demonstrated with a 1,000-pound payload. This method should significantly extend the potential payload-altitude capability of single-cell free balloons.

TETHERED BALLOONS

Today the altitude capability of tethered balloons which carry useful payload weights is on the order of 15,000 feet. This capability allows many scientific and military applications of these balloons. If the capability could be increased to much higher altitudes, say above 50,000 feet, and the balloon could survive the environment in getting there, the Air Force would have a station-keeping platform with many more scientific and military applications. With this as a goal, the research and development work in tethered ballooning is basically that of searching for and testing new materials, both for the balloon and for the tether cable, that have high strength, light weight and ability to withstand the environment. At the same time the Laboratory conducts many tethered balloon operations for Air Force and DOD purposes.

Fibers of Kevlar, a new synthetic material, are being woven in two different patterns for evaluation as the strength members for large balloons. A new concept in weaving, called triaxial or Doweave, has been laboratory tested and will be flight tested as the basic material for the hull of a 45,000 cubic foot aerodynamically shaped balloon. Also as part of this development

program, Kevlar fibers are being mixed with Dacron fibers to form a ripstop-type weave pattern. This material will be coated with polyurethane for use in the fins of the balloon. These materials offer high strength for minimum weight, the ideal combination for high altitude balloons.

The physical characteristics of various kinds of tether cables are continuously being investigated to optimize this important part of tethered balloon systems. Cables made of steel or synthetic fibers, such as Dacron, are currently in operational use. Short lengths of cable using Kevlar fibers have been laboratory tested, with excellent results, and will be flight evaluated in the near future. Studies have shown that if tether cables can be developed using the theoretical properties of Kevlar, it will overcome one of the limitations which prohibits flying tethered balloons to 50,000 feet and above.

Numerous instrumented flights have been made to determine the stability of tethered balloons and payloads under various wind conditions and suspension configurations. Reports are being written summarizing these test results.

A wide variety of projects using tethered balloons have been supported during this reporting period. Components of a satellite destined for use in a Global Navigation System (SAMSO System 621B) were flight tested from a tethered balloon. The tethered balloon proved to be an inexpensive test-bed which simulated satellite conditions, yet permitted recovery and repair of components as necessary. During the summer of 1973, the second phase of a project sponsored by the AFCRL Meteorology Laboratory was conducted at Donaldson, Minnesota. The purpose of these tests was to measure various parameters of the earth's boundary layer by suspending sensors at various levels along the cable of a balloon. The scientific results of this project are given in the chapter on the Meteorology Laboratory.

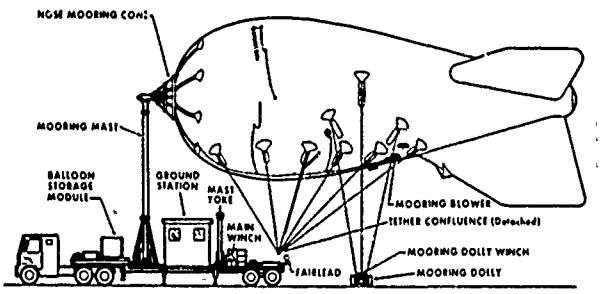

The Hugo II tethered balloon system in its moored configuration.

The HUGO II Wind Data System is one of the more interesting items developed in the tethered balloon area. It is a mobile, self-contained system which measures atmospheric temperature, pressure, wind speed and wind direction at selected altitude levels. Development was undertaken in support of the Air Force Weapons Laboratory's TORUS Electromagnetic Pulse Simulator Program.

HUGO II employs a 30,000 cubic foot helium-inflated, ballonet balloon of British manufacture. It is a rugged (Neoprene-coated Nylon) and aerodynamically stable balloon, sized to maintain a normal flight altitude of 2,000 feet above ground level while supporting over 400 pounds of payload. (Since ground level can be as high as 6,000 feet, the balloon may be flying as high as 8,000 feet above mean sea level.) The gross weight of the flying system (balloon, payload, tether) is 1,250 pounds.

The payload consists of a balloon control unit (BCU), three sensor stations, four high-intensity warning lights and numerous cloth pennants—all attached to the balloon or the tether line. The radio-equipped BCU relieves balloon overpressure automatically or on command, and, in case of emergency, will dump the helium and sever the tether line.

The HUGO II makes atmospheric measurements with three aerodynamically

shaped sensor units called Aerosondes. Battery-powered and hung from quick-disconnect mounting brackets, they can be moved to any desired tether line location. Sensor data are transmitted (upon interrogation) at 2280.5 MHz to the ground station for display and recording. (Ground level winds and temperature are measured by a separate pole-mounted sensing station.) The wind speed and direction sensor of the Aerosonde (developed at the University of Wisconsin) has a unique wind direction unit which senses changes in the earth's magnetic field as the anemometer cups rotate.

The HUGO II system is packed on a flatbed trailer for over-the-road transport. An all-weather shelter on the trailer contains the command transmitter, the recording instrumentation and a working area for the crew. The balloon and flight gear are stored in external compartments. Power to the ground station is supplied by a gasoline engine generator. The hydraulically controlled winch for the 3/16-inch-diameter, 6,000-foot steel tether cable is also powered by a gasoline engine.

A folding mooring mast is used, in combination with a dolly, to secure the system between flights. When moored in this way the HUGO II balloon successfully withstood gusts of over 45 knots, in December 1972 at Holloman AFB.

In the course of development the HUGO II System underwent three series of tests covering all of its intended functions. These tests, which saw the incorporation of several field-proven design improvements, were successfully concluded in December 1973.

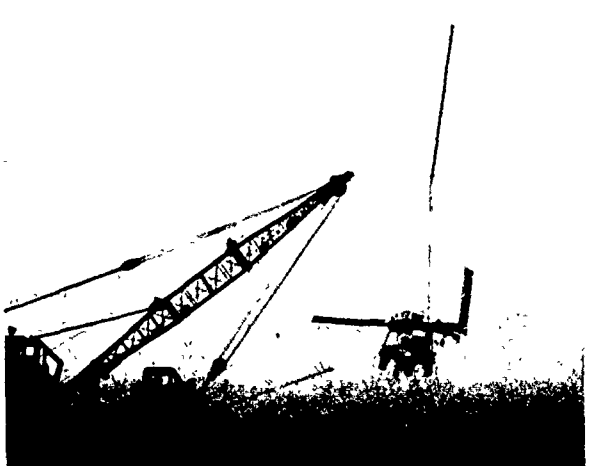

Launch of the powered balloon on its test flight.

POWERED BALLOONS

For several years, the Laboratory has been investigating the concept of adding a propulsion source to a free balloon so that high altitude station-keeping could be accomplished. Basic feasibility and parametric studies were completed which indicated that such a system was feasible, and a plan for a demonstration flight was submitted and approved under the AFCRL Laboratory Director's Fund. The powered balloon system (POBAL) was flown over White Sands Missile Range on September 16, 1972. The flight was partially successful with the system obtaining airspeeds in the range of 7 to 15 knots. It used batteries to power a 12-horsepower electric motor, a 30-foot diameter propeller, and a 711,000 cubic foot volume round balloon which flew at 60,000 feet. A structural failure in the 9-foot-high rudder, however, limited the flight duration to three hours. The system did demonstrate that it is feasible to power a balloon against the wind at high altitude.

Two follow-on contractual efforts are underway for an advanced powered balloon system known as POBAL-S. It uses a streamlined, stern propelled balloon which reduces drag to a value much less than that of POBAL. The system has a design speed of 16 knots at 60,000 feet for a seven-day duration with a 200-pound useful payload.

A fuel cell power source that can supply 30 volts and 96 amperes on a 100 percent duty cycle for seven days is required and the allowable weight for the entire system including tankage and fuel is 500 pounds. Such a system is available commercially, and will be adapted for use in the system.

The POBAL-S design effort is being completed under contract. Hull configurations, power sources, altitude change devices, navigation devices and launch techniques have been studied. Based on the results, drawings are being completed for the POBAL-S system.

AIRCRAFT-LAUNCHED HIGH-ALTITUDE BALLOON SYSTEM

In-house studi s and investigations leading to the preliminary design of a prototype aircraft-launched high-altitude balloon system (ALBS) were carried out. The ultimate goal of this research is an operational capability to deploy and inflate in mid-air balloon platforms capable of supporting payloads of up to 1,000 pounds for 24 hours at altitudes of 80,000 feet or higher. This capability will enhance the effectiveness of Air Force missions whose mode of operation requires the rapid availability of low cost substitute satellite systems, such as the TRI-TAC Multi-Mode Transmission System (478T). In the course of the investigations, certain technical problems were identified, whose solution is essential, such as designing the cryogenic storage system for maximum efficiency and safety, choosing the most effective and desirable method of vaporizing the cryogen and warming the gas quickly to ambient temperatures, determining optimum balloon materials and balloon deployment procedures, and sizing system decelerators. Work towards resolving these problems was initiated through additional in-house studies and laboratory experiments.

Meetings were held with representatives of the TRI-TAC SPO at ESD and with representatives of Headquarters Tactical Air Command (TAC) relative to the applicability of the ALBS and various other Lighter-Than-Air (LTA) systems to the Multi-Mode Transmission System airborne relay requirement. These meetings led to a jointly funded (ESD and AFCRL) project order to the Cryogenics Division of the National Bureau of Standards to conduct laboratory tests of cryogenic storage and heat transfer techniques advocated in an AFCRL in-house report (AFCRL-TR-73-0633). The National Bureau of Standards began work on the project order in May 1974 and will require one year for completion. In the meantime an analytical study was undertaken in-house at AFCRL to examine more critically the ability of air-launched balloon systems and other high-altitude LTA vehicles to meet the projected tri-service needs of the Multi-Mode Transmission System for an operationally useful backup relay platform.

BALLOON INSTRUMENTATION

Many improved specialty products were designed, developed and flight tested specifically for flight control and data systems associated with free, tethered and powered balloon operations. The scope of the design effort ranged from sub-miniature plug-in modules to circuit board sub-assemblies, to complete instrumentation systems and some independent piggy-back hardware.

Balloon-borne instrumentation for control of particulate-debris atmospheric samplers and for telemetry of in-flight performance has been developed. The major system modular components are a controller, frequency-sensitive data encoder and a backup controller. The controller is designed to handle the normal flight safety and balloon control functions as well as the operation of atmospheric sampling equipment.

Work has continued in updating and upgrading the performance capabilities of

routine flight equipment modules in an effort to expand functional utility and reliability. An example of this is the new 18-channel balloon command tone generator which provides time-sequenced command tone intelligence encoding for high frequency (HF) command transmissions from ground stations to remotely located free floating balloon instrument systems. The implementation of the new tone generator will expand and improve balloon command capability. Its 18 primary, sequenced commands and six backup, non-sequenced commands double the existing HF command capability.

A new in-house developed COS-MOS adjustable timer module for flight safety and ballast drop hold-off is another improved basic flight system component available for inclusion in special design applications. It can be set to any duration between 0 and 99 hours in one-hour increments for flight termination and 0 to 9 hours for safety and ballast hold-off by convenient miniature rotary switches on the timer case. The new timer uses a crystal-controlled oscillator for the basic clock with an accuracy of 50 ppm. Advantages of the digital timer are very low power drain, and it resets every time power is interrupted. Therefore, no test time has to be included in the programmed timer setting. The new timer weighs one pound, compared to the 4½ pounds of the previous timer design. High reliability, high noise immunity, low power integrated COS-MOS Medium Scale Integration (MSI) circuits are used throughout.

A pulse Morse Code modulation data-acquisition encoder was designed and developed. This eight-channel digital data system resolves a five-volt input signal into 512 equal parts. These 512 parts are transformed into a Morse Code. This makes a nine-bit binary word where a logical 1 represents a dash and a 0 represents a dot. The encoder output is transmitted back to the ground control station. Information such as altitude, pressure, temperature or any parameter that can be represented by a voltage or a resistance can be telemetered over sky wave distances.

Considerable effort has been expended in improving free-balloon tracking methods. Several types of beacon transponders for balloon flights have been investigated. In addition to meeting FAA flight safety requirements, the transponders, together with the FAA Air Traffic Control (ATC) radar network, have provided a valuable and accurate means of locating the position of balloons to within approximately one mile.

The primary problem encountered in the use of transponders is operation at high altitudes (to 160,000 feet). Small lightweight commercial aviation units require that a special pressurization case be built to house the entire receiver-transmitter unit. Heavier military units such as the RT-859

An interesting aspect of the sampling operations conducted at Panama and Alaska is that the equipment is "air snatched" by C-130 aircraft — otherwise recovery would be extremely difficult because of the surface features of the two locations. Here, a sampling payload is being winched into the aircraft. This particular payload consisted of a direct flow sampler, located at ten o'clock and a carbon 14 sampler located at nine o'clock.

/APX-72 which contain pressurized transmitter compartments have been successfully used. For comparison purposes, the weight of a commercial light aircraft ATC transponder system for balloon use including batteries for 24-hour continuous operation is approximately 15 pounds, while the weight of the military equipment is approximately 34 pounds. The military equipment has the obvious advantage of available maintenance and replacement support from the Air Force logistics system. Further investigations planned include the addition of mode C altitude reporting sensors to the balloon-borne transponder system.

A third generation balloon locating instrument using VHF Omnidirectional Range (VOR) navigation has been designed, developed, fabricated and tested by the Laboratory. The results have been outstanding and this design is destined to become a routine component of scientific free balloon systems that require positive in-flight position or track data over long durations for precision profile control. This instrument takes advantage of the latest technological advances, especially in the integrated circuits field. COS-MOS circuits are used wherever possible. This technology provides high noise immunity, micropower dissipation and MSI in a single package. The result is a low power drain instrument. The accuracy is 0.5 degree over a temperature range of −40° C to +55° C.

Plotting VOR fixes on aeronautical charts and triangulating a position is slow and tedious. It requires one person for the entire duration of a balloon flight. In its operational form, the new system will utilize an automatic plotter operating in conjunction with a mini-computer to automatically fix the position of the balloon. This capability is currently being developed. When put into operation, it will allow the code copier to feed the Morse Code bearing information directly into the computer. The computer will convert the Morse Code into bearing angles and compute the corresponding latitude-longitude position of the balloon. This position will be fed directly to the plotter and automatically marked on a map. Any type of map will be usable with this plotter as long as the scale is accounted for in the computer program.

In order to provide a world-wide balloon tracking capability at minimal cost, the VOR balloon locating system will be complemented by an Omega tracking system in areas where no VOR coverage exists. An Omega balloon tracking system has been developed and is ready for flight test as soon as the Omega network becomes usable over our major area of geographical interest.

The Omega System is a hyperbolic navigational aid which presently uses four stations located in the Northern Hemisphere. This system lays down a hyperbolic grid of lines of position that can be used for navigation, position fixing, and the establishment of time and frequency references. Four additional stations to complete the complement of eight Omega stations are planned, and with these installations, complete global coverage of the Omega System will be achieved. The present stations are located in Norway, North Dakota, and Trinidad and Hawaii. The expansion plans for the Omega System call for establishing stations in the West Pacific, South America, the Indian Ocean and in Australia.

Navigation is accomplished through the reception and phase comparison of signals from three or more stations with respect to each other, or three stations with respect to a stable oscillator. After obtaining phase differences between three stations, geographical position may be determined by plotting on an Omega chart, or through calculations.

HIGH-ALTITUDE BALLOON SAMPLING PROGRAM

The U.S. Atomic Energy Commission's program for measuring upper atmospheric

nuclear debris collected by balloon-borne filtering devices has been in continuous operation since 1956. Beginning in July 1972, these sampling operations were conducted by the Aerospace Instrumentation Laboratory.

In the spring of each year, an annual sampling cross section is made beginning at Albrook AFB, Canal Zone, in March, then proceeding to Holloman AFB, New Mexico, in April and concluding at Eielson AFB, Alaska, in May. Sampling is normally conducted at altitudes of 70,000, 80,000 and 90,000 feet above mean sea level (MSL.) However, in 1973 additional sampling was conducted at altitudes of 105, 000 and 120,000 feet MSL. At Holloman AFB, sampling is conducted on a quarterly basis at altitudes of 70,000, 80,000 and 90,000 feet MSL. Research and development flights to update the sampling hardware and to qualify a nitric oxide sensing system for flight were also accomplished during this reporting period.

RESEARCH ROCKETS

The Aerospace Instrumentation Laboratory participates in environmental research using rockets in two ways. First, the Laboratory has overall management of the research rocket probes and is directly involved in the vehicle selection, the design of payload packages, the launch and the data acquisition for each probe. Second, the Laboratory conducts engineering research in several disciplines to permit new or upgraded experiments to be conducted.

During the reporting period, the Laboratory was responsible for the launch of 93 rocket vehicles from various parts of the globe. Twenty vehicles were launched from the NASA Wallops Flight Center, Virginia; 19 from Eglin AFB, Florida; 18 from Poker Flat Research Range, Alaska; 16 from Churchill Research Range, Manitoba, Canada; 15 from White Sands Missile

The Hi Star payload in its flight configuration. The nosetip is ejected to expose the star tracker while the IR sensor is deployed for the mapping mission.

Range, New Mexico; four from Barriera do Inferno, Natal, Brazil, and one from Vandenberg AFB, California.

Sixty-nine of these rounds were complete successes and ten additional returned partial data, giving an overall 85 percent success rate in returning data. The 14 failures were equally divided between payload and vehicle problems. Thus, the overall vehicle system success was 92 percent.

Of the 93 rockets flown, 68 were of the small vehicle workhorse class—that is, payloads up to 250 pounds with apogees from 100 to 200 km. Nineteen were in the large vehicle class carrying 400 to 800 pounds from 150 to 250 km. Six missions used high-performance rockets. Two were reentry vehicles and four reached apogees greater than 500 km.

Many of the payloads were designed to a sophistication seldom encountered in years past. In the area of cleanliness alone, zero outgassing and zero pieces ejected became a reality for some payloads. Eleven payloads carried full inertial attitude control systems and achieved a 100 percent success record. Twenty payloads were recovered in 21 attempts, including two from water and eight under arctic conditions.

The versatility of the Laboratory's family of vehicles is indicated by the range of payloads carried—6-inch diameter, 26 pounds, to 22-inch diameter, 780 pounds —and the range of apogee achieved, 90 km to 625 km. Most of the payloads flown were in support of AFCRL scientists' in-house research projects. Highlights of these and other agency-funded programs show the scope of these efforts.

CHASER: The fourth and last vehicle of the Chaser program, reported on in our last period, was flown successfully from Vandenberg AFB, California, in October 1972. The Aerobee 170 vehicle flew a nominal trajectory, sensors were exposed and succeeded in tracking the target missile, after which the payload was retrieved from the Pacific. Because of the success of this program, a more sophisticated follow-on effort is now in the planning stage.

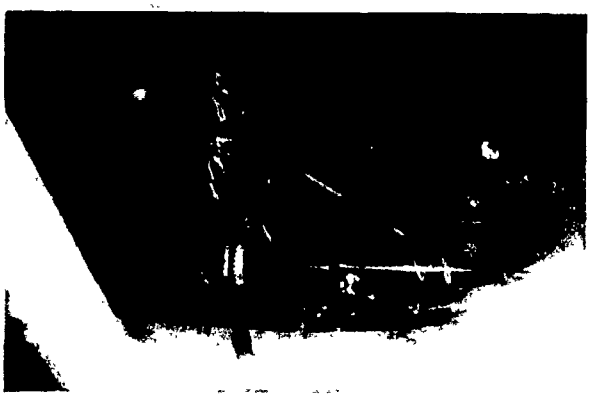

The Chaser payload aboard the recovery craft after retrieval from the sea at night.

HI STAR: Another program reported on in our last period continued with launches of Aerobee 170's from White Sands Missile Range, New Mexico, in August and December 1972, bringing the total launched to seven. Both of these IR mappings of the celestial sphere were successful and the payloads were recovered for re-flight. These flights completed the mapping in the Northern Hemisphere. Both payloads were refurbished and shipped along with three Aerobee 200 vehicles to Woomera Rocket Range, Australia. Launches are scheduled for September 1974. One of the first two payloads recovered will be field refurbished to fly the final mission. This field refurbishment will be a first for the Laboratory.

HI HI STAR: This program is an attempt to map the IR sources with greater sensitivity and accuracy than the earlier Hi Star. The large size of the liquid helium-cooled dewar necessitated packaging the instrument looking aft in a 22-inch diameter nose cone. After powered flight, the 780-pound payload is separated from the vehicle and oriented by the attitude control system for

its mapping mission. Following reentry into the atmosphere the recovery parachute is deployed from the nose cone. If the payload were allowed to impact in this configuration the aft pointing instrument would impact first, possibly suffering damage. Therefore, a payload inverter system was designed that inverts the payload end for end while it is descending on the parachute, insuring greater protection for the instrument. The first launch was conducted from White Sands Missile Range in February 1974. A propulsion problem in the Aerobee 350 caused this engine to shut down prematurely, resulting in a reduced apogee. However, some scientific data were recorded and all support systems functioned properly, resulting in an instrument recovered in excellent condition for reuse. Four additional flights are planned in this program.

HAVE MERLIN: HAVE MERLIN was a concentrated program to launch a series of chemical payloads in a short time span from Eglin AFB, Florida. The Armament Development Test Center at Eglin had phased out vertical probe activity and reassigned all launch support personnel. Although this Laboratory has on occasion launched its own rockets from expeditionary type sites, this was the first time the Laboratory was totally responsible for all preparation and launch activity at an established site. The Laboratory put together a crew that successfully launched nine vehicles in 48 hours, seven of these in a 24-hour period.

ICECAP: Eighteen payloads have been launched in this program conducted for the Defense Nuclear Agency at Poker Flat Rocket Range, Alaska. The majority of these have been concentrated in two series in February and March of both 1973 and 1974. Six vehicles were launched in ICECAP '73 including two 600-pound complex payloads. One contained an ultra clean LWIR spectrometer that featured an alligator-like recloseable nose cone enabling the sensor to be exposed without ejecting any hot pieces from the payload and providing protection from impact damage for the instrument during recovery. Both of these payloads employed an inertial ACS and were recovered.

ICECAP '74 saw these refurbished instruments flown again in a six-rocket program. A new instrument, HIRIS, a large helium-cooled IR sensor, was flown for the first time. Each of these three payloads had grown to over 700 pounds. In the time between these programs, the Laboratory developed a new soft-landing recovery system to insure undamaged return of the instruments. This system benefited greatly from the recovery system developed for Hi Hi Star, using the same final stage decelerator, a 46-foot diameter "Paraform" parachute. A payload inverter system was also developed for the HIRIS mission. The Laboratory coordinated and took an active part in the launch and successful recovery of all five payloads under the hostile arctic conditions. At present the Laboratory is involved in the planning of the ICECAP '75 program.

ALADDIN '74: In cooperation with the National Aeronautics and Space Administration (NASA), a program was conducted at Wallops Island, Virginia, on June 29-30, 1974 to permit correlative measurements of a number of environmental parameters by various techniques. Some 50 research probes were launched, of which 17 were the responsibility of AFCRL. This was the largest concentrated sounding rocket program ever conducted and AFCRL's participation was also its largest. The Laboratory was responsible for total integration of five payloads and provided flight telemetry systems for ten others. The only recovery system flown was provided by the Laboratory, employing a Sandia-developed ram air-filled, decelerator-flotation system. An AFCRL scientist was Project Scientist for the entire program while this Labora-

tory was assigned engineering coordination responsibilities in areas of launch schedule, data acquisition and build-up facilities requirements. Laboratory personnel worked closely with the NASA Wallops Flight Center over a period of two years culminating in the launch of 54 rockets in 24 hours.

CASTOR-LANCE: In support of an IR layering experiment, the Laboratory was required to provide a vehicle for a high altitude launch near the equator. Castor and Lance motors were selected from available hardware, modified for sounding rocket flight, and launched from Brazil on May 25, 1973, resulting in a successful experiment.

In-house aerodynamic analyses including performance, drag and loads were confirmed in the operational test.

NIKE-MALEMUTE AND TERRIER-MALEMUTE: NASA, Sandia Laboratories and AFCRL jointly funded the development of two new vehicles for studies requiring high altitude or a maximum of time out of the sensible atmosphere.

The requirements established jointly were to carry 68 kg to 500 km and 68 kg to 700 km. A new motor was developed using a flight-proven motor case from a military weapon and proven propellant from a different weapon program. The new motor, tagged Malemute, was static fired successfully. Vehicles using the Nike or the Terrier as boosters and the Malemute as an upper stage meet the design requirements. Flight tests will be accomplished after this report period.

DISPERSION CONTROL SYSTEM: The usual sounding rocket is a free-flight vehicle subject to variation from its predicted flight path as a result of atmospheric density and winds, thrust misalignments, and of air frame manufacturing errors. With due care, these variables can be held to reasonable limits, but the rocket impacts at some distance from the aiming point. This distance, defined as dispersion by the sounding rocket fraternity, is primarily due to rotation of the velocity vector in response to perturbations from the forecast values. This pointing error, generated early in flight, operates for the remainder of the vehicle flight time. With vehicles of high performance, the dispersion becomes too large to permit safe operation at some launch sites. A control system has been designed for the Paiute Tomahawk to minimize dispersion. In concept, an onboard gyroscope measures the difference between the actual flight path and the desired flight path. This error is electronically processed to give command signals to small fins projecting from the payload skin. The fins are driven to redirect the vehicle thus minimizing the dispersion. Studies and designs are complete, hardware is in procurement, and a flight test planned for February 1975.

RESEARCH SATELLITES

In recent years the Laboratory has been responsible for technical management of research satellites and has designed and fabricated the spacecraft. One of these, the OV5-6, a small satellite designed to measure solar radiation, was flown piggyback on a Titan III in May 1969 and achieved an orbit of 10,000 by 60,000 nautical miles. At the time of this report, all systems were still working well and the satellite had exceeded its 18-month design life by a factor of more than 3. This is the only research satellite collecting scientific data outside of the earth's magnetosphere. These data are being analyzed by scientists of the Space Physics Laboratory.

Present involvement in the satellite area is the provision of technical and engineering assistance to AFCRL scientists who conduct experiments on a piggyback basis. The Laboratory serves as technical focal point for these programs and interfaces

with the military program office and the spacecraft contractor. Laboratory engineers conduct environmental and electronic tests to certify the experiments and coordinate integration and test of the instruments at the satellite manufacturer's plant. Assistance is provided from experiment conception through data collection.

JOURNAL ARTICLES
JULY 1972 - JUNE 1974

CARTEN, A. S., JR.
The Aircraft Wake Turbulence Problem
AIAA Student J., Vol. 10, No. 4 (December 1972)
The HUGO II Tethered Balloon System
Atm. Technol., Pub., by Natl. Ctr. for Atm. Res., Boulder, Colo., No. 5 (March 1974)

COHN, A. (Space Phys. Lab.), and MARCUCCI, M., CAPT.
Stimulated Emission Cross-Section of H_2 Dissociation Transition
J. of Appl. Phys., Vol. 44, No. 4 (April 1973)

DOHERTY, F. X
The Use of Balloons in Blast Simulation at High Altitudes
Proc. of 3rd Intl. Symp. on Mil. Appl. of Blast Simulators, Schwetzingen, Ger. (September 1972)

KORN, A. O.
Development of a Powered Balloon System
Atm. Technol., Pub. by Natl. Ctr. for Atm. Res., Boulder Colo., No. 5 (March 1974)

PAPERS PRESENTED AT MEETINGS
JULY 1972 - JUNE 1974

CORBALIS, F. F., JR., CAPT., GIANNETTI, A. A., and RICE, C. (Wentworth Inst., Boston, Mass.)
The Opening Performance of 100-Ft. and 140-Ft. Diameter RSR (Recovery Systems Research) Parachutes Near 100,000 Ft. with Balloon-Borne Payloads
7th AFCRL Sci. Balloon Symp.,
Wentworth-By-The-Sea, Portsmouth, N.H.
(25-27 September 1972)

DANAHER, T. J.
AFCRL Balloon Operations
Symp. on Telescope Sys. for Balloon-Borne Res., NASA Ames Res. Ctr., Moffett Fld., Calif.
(21-22 February 1974)

DOHERTY, F. X.
The Use of Balloons in Blast Simulation at High Altitudes
3rd Intl. Symp. on Mil. Appl. of Blast Simulators, Schwetzingen, Ger. (19-21 September 1972)

FORD, J. S., MAJ. (Air Force Acad., Colo.), and JACKSON, D. E., CAPT.
A Study of NOLARO Cable for Use with Tethered Balloons
7th AFCRL Sci. Balloon Symp.,
Wentworth-By-The-Sea, Portsmouth, N.H.
(25-27 September 1972)

HARRINGTON, E. V., JR., CAPT., CARTEN, A. S., JR., and CORBIN, C. D (G. T. Schjeldahl Co., Northfield, Minn.)
The HUGO II Tethered Balloon System
7th AFCRL Sci. Balloon Symp.,
Wentworth-By-The-Sea, Portsmouth, N.H.
(25-27 September 1972)

LECLAIRE, R., 2nd LT., and KORN, A. O.
The Powered Balloon System
7th AFCRL Sci. Balloon Symp.,
Wentworth-By-The-Sea, Portsmouth, N.H.
(25-27 September 1972)

STELVES, R. G., and AMMONS, R. L., HEDBERG, J. H. (Space Gen. Corp., El Monte, Calif.)
Open-Loop Tracking of Moving Targets with an Aerobee Sounding Rocket
AIAA 3rd Sounding Rocket Technol. Conf., Albuquerque, N.M. (9 March 1973)

TECHNICAL REPORTS
JULY 1972 - JUNE 1974

CARTEN, A. S., JR.
An Investigation of Techniques for Launching Large Balloon Systems from Aircraft or Rockets in Flight
AFCRL-TR-73-0633 (9 October 1973)

CORBALIS, F., JR., CAPT., GIANNETTI, A., and RICE, C. (Emmanuel Coll. Phys. Res. Div., Lexington, Mass.)
The Opening Performance of 100-Foot and 140-Foot Diameter RSR Parachutes Near 100,000 Feet with Balloon Borne Payloads
Proc., 7th AFCRL Sci. Balloon Symp.,
AFCRL-TR-73-0071 (3 January 1973)

DWYER, J. F.
Balloon-Apex Pressure Differential
(A Simple Approximation of Pressure Differential at the Apex of Single Cell, Natural Shape Balloons)
AFCRL-TR-73-0633 (9 October 1973)

FORD, J. S., MAJ. (Air Force Acad., Colo.), and JACKSON, D. E., CAPT,
A Study of NOLARO Cable for Use with Tethered Balloons
Proc., 7th AFCRL Sci. Balloon Symp.,
AFCRL-TR-73-0071 (3 January 1973)

GILDENBERG, B. D.
Equations Derived for Computer Programming of Helium Inflations for Large Plastic Balloons
AFCRL-TR-74-0200 (22 April 1974)

HARRINGTON, E. V., JR., CAPT., CARTEN, A. S., JR., and CORBIN, C. D. (G. T. Schjeldahl Co., Northfield, Minn.)
The HUGO II Tethered Balloon System
Proc., 7th AFCRL Sci. Balloon Symp.,
AFCRL-TR-73-0071 (3 January 1973)

KORN, A. O., LECLAIRE, R. C., 1ST LT., and RICE, C. B. (Emmanuel Coll. Phys. Res. Div., Lexington, Mass.)
LDF Powered Balloon Program
AFCRL-TR-73-0424 (18 July 1973)

LAMB, T. M., CAPT.
A State of the Art Pulse Amplitude Decommutator Design
AFCRL-TR-73-0478 (31 July 1973)

LECLAIRE, R. C., 2ND LT., and KORN, A. O.
The Powered Balloon System
Proc., 7th AFCRL Sci. Balloon Symp.,
AFCRL-TR-73-0071 (3 January 1973)

LECLAIRE, R. C., 1ST LT., and RICE, C. B. (Emmanuel Coll. Phys. Res. Div., Lexington, Mass).
The Local Motions of a Payload Supported by a Tritethered Natural Shape Balloon
AFCRL-TR-73-0748 (12 December 1973)

NOLAN, G. F., Ed.
Proceedings, Seventh AFCRL Scientific Balloon Symposium
AFCRL-TR-73-0071 (3 January 1973)

NOLAN, G. F., and KEENEY, P. L.
Analysis of Factors Influencing Rate of Rise of Large Scientific Balloons
AFCRL-TR-73-0753 (18 December 1973)

PAYNE, J. C., YOUNG, E., MAJ., and RICE, C. (Emmanuel Coll. Phys. Res. Div., Lexington, Mass.)
Launching of Small Inflated Balloons from Cargo Aircraft
AFCRL-TR-73-0276 (20 April 1973)

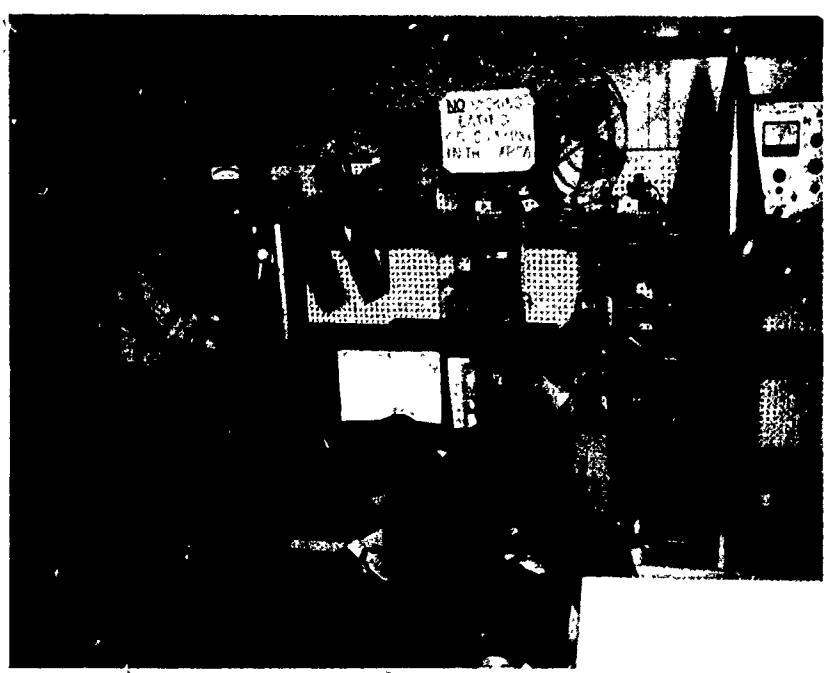

Assembly and checkout of a sounding rocket payload to measure the electric fields in an aurora.

V Space Physics Laboratory

Air Force systems which operate in the near-earth space environment are subject to a variety of effects as a result of their interaction with the environment. Near-earth space is a varying environment, and the fields and particles of which it is composed vary diurnally, seasonally, and, in particular, in response to activity on the sun. Such variations or disturbances disrupt and degrade communication systems, surveillance systems, detection and tracking systems, and interfere with the operation of electronic devices and detectors on satellites.

The Space Physics Laboratory conducts research on the near-earth space environment to understand the behavior of that environment and to define its parameters for the purpose of providing satellite design criteria, and of developing a capability to predict disruptive disturbances. Thus, this Laboratory's research program studies the varying magnetic and electric fields in the magnetosphere, and the particle fluxes and distributions occurring in that region of space in which Air Force satellites operate. The research involves experimental and theoretical efforts. Data are obtained through ground-based observations and from instrumentation on rockets and satellites. Considerable theoretical effort is applied to the development of a useful model of the magnetosphere which can be used to cope with the real problems experienced by Air Force systems operating in or using the near-earth space environment.

ENERGETIC PARTICLE RESEARCH

Energetic particle fluxes limit space operations. By depositing energy in the earth's atmosphere, ionizing and heating the ambient gases, particularly at high latitudes, they degrade, and sometimes inhibit, the operation of systems which rely on long-distance propagation of electromagnetic radiation. The increased Air Force utilization of space-borne sensor and communication systems has demonstrated requirements for better knowledge of particle data at all altitudes. Systems operate from orbits low enough to be affected by high atmosphere density changes (partially resulting from heating due to the energy deposited as particles are stopped) up to synchronous altitude where the mean free path of particles is so long that electric charging due to impact of particles permits sizable charge build-up which produces electrical interference.

The variety of effects which are of interest channels our investigations into the studies of a variety of particles of different types and energies. Studies during the reporting period have included proton and electron populations from 50 eV to hundreds of MeV, and to a lesser degree, alpha particles and heavy particles in the 1-100 MeV per nucleon range.

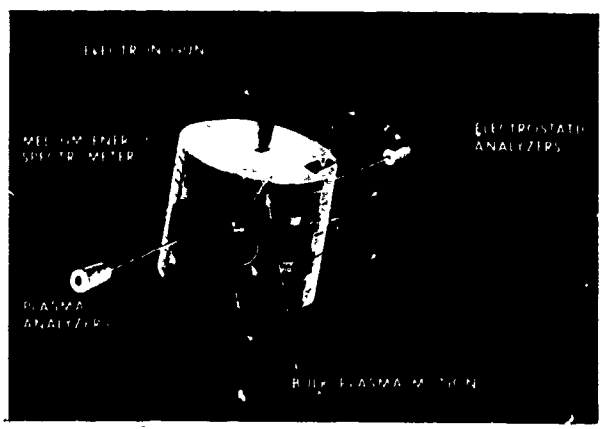

AFCRL components aboard the SCATHA (Spacecraft Charging at High Altitudes) satellite.

The motion of charged particles is affected by both electric and magnetic fields. Magnetic fields can only affect the direction of motion and thus deflect particles from some volumes and concentrate them in others, while electric fields can, in addition, modify their energy. The relatively stable terrestrial magnetic field consequently tends to exclude low energy in-flowing particles from equatorial regions and to contain those particles already in orbit near the earth in a restricted region, i.e., the so-called Van Allen belts.

High solar activity not only brings solar-produced particles to the earth but also changes the electromagnetic field configuration, which modifies the resident particle populations. Systems designed to operate properly in the average particle environment experience malfunctions or anomalous behavior during and after extreme solar activity. The malfunctions of DSCS satellites occurred predominately during magnetic substorms and were apparently caused by the influx of plasma from the earth's magnetotail to synchronous altitude.

AFCRL's program of solar energetic particle study includes both direct acquisition of solar particle data on USAF satellite-borne sensors and its subsequent analysis and theoretical model studies of solar particle propagation in the interplanetary space and in the magnetosphere. Models of solar proton events, particularly the intensity expected at the earth, are developed. These models are used by Global Weather Central-Air Weather Service (GWC-AWS) to predict the intensity of particles as a function of time from observables available to GWC either from satellite-borne or ground-based sensors.

Studies were continued of the energetic particle propagation through the magnetosphere and studies of particle access to the earth's surface, particularly the polar caps where they lead to Polar Cap Absorp-

tion (PCA) events, which disrupt communications. The geomagnetic field allows energetic charged particles to reach the earth only over limited regions, the extent of these regions being determined by the rigidity of the particle (i.e., momentum per unit charge). Early work in calculating the limit of particle rigidity accessibility (cutoff rigidity) used geomagnetic field models of the internal field alone; more recent work has used a magnetospheric model that includes external currents on the boundary of the magnetosphere and the magnetospheric tail. The newer model predicts the significant daily variation in cutoff rigidity which occurs in the polar regions. Since knowledge of cutoff rigidities in the polar regions is essential for the prediction of the distribution and extent of solar particle induced communication perturbations, a detailed study of cutoff rigidities in the polar regions was conducted. The studies led to the conclusion that even the newer magnetospheric models are not adequate for precise theoretical predictions of the cutoff rigidities in the polar caps, and this has since been verified by extensive satellite measurements which used the results of these calculations as a baseline for the analysis of the observational data.

Although a complete analysis of particle motion in the magnetosphere for different energies and different locations is still formidable, the available magnetospheric models are adequate for describing the particle motion at relativistic energies. From a study of ground-level solar cosmic-ray events, it was possible to determine the solar particle spectrum at relativistic energies, the solar particle intensity as a function of time, and the angular distribution (anisotropy) of these particles in the interplanetary medium. This knowledge is important because relativistic solar particles arrive at the earth prior to the slower non-relativistic particles. The abundance and depth of atmospheric penetration of the non-relativistic particles affect radio wave propagation. For this reason, data from the neutron monitor at the Geopole Station, Thule, Greenland, are used in real time by the Air Weather Service to provide a warning of the presence of extremely high energy solar particles. These data, in conjunction with the real-time VELA satellite data, are used operationally by AWS. Space Physics Laboratory personnel have provided computer programs to process these data, to identify solar particles at energies initiating PCA events, and affecting spaceborne operational systems.

The VELA satellite system is being phased out. To fill the gap in the data base required by the military, AFCRL is incorporating the appropriate particle instruments into the SOLRAD-HI satellite system. SOLRAD-HI will become operational in the last quarter of 1975, and will consist of two satellites located outside the magnetosphere at 19 earth radii, together with a dedicated read-out station operated by the U. S. Navy. These data will be sent to AWS/GWC in real time for operational use. Software now being prepared will allow various military users to get maximum utility from the data.

Research on prediction of solar particle events continues with the objective of improving the accuracy of the proton prediction system originally developed by the Space Physics Laboratory and currently used by the Air Weather Service. One of the problems addressed was the updating of initial prediction parameters from real-time satellite data to get a better answer to the question: "Once a solar proton event has been identified and the maximum in flux realized, when will the event end?" (i.e., when will the enhanced intensity recede to a background level?). This study showed that the maximum flux, which occurs early in a solar particle event, determines the equilibrium condition from which the future decay rate and the end of the event can be predicted. In practice, these predictions are continually updated as additional real-time data become available. These predictions are sufficiently accu-

rate to forecast the onset, duration, and end of PCA events.

Space Physics Laboratory scientists have been assembling data on all previous solar particle events with the objectives of ordering the data in a systematic, coherent manner, and classifying the events in accordance with the proton event classification system previously developed by this laboratory and accepted as an international standard by COSPAR. To date, over 500 particle increases for the period 1955 through 1969 have been identified. For each of these events, satellite, space probe, and ground-based data have been examined.

The onset time, time of maximum intensity, maximum flux, and duration of the event have been identified, along with the energy range of the detector making the observation. This catalog contains primarily proton data; however, for completeness, the associated solar electron data for the current solar cycle are also included.

Preliminary analysis of the data compiled has shown that the classical solar particle event is extremely rare. Much more probable is a multiple injection sequence where the background intensity may increase due to the presence of an active region on the sun, additional increases of various magnitudes may result from several discrete solar flare injections, and the particle intensity may also be modulated by transient phenomena also generated by solar activity — often originating from the same active region responsible for the particle enhancements. The separation and identification of each of these enhancements requires the examination of data at a number of energy levels from different positions in space.

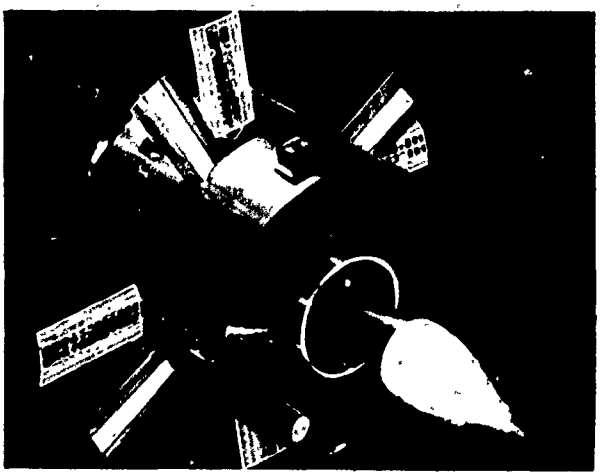

The SOLRAD-HI satellites. After orbital injection, the satellites will drift into widely separated positions even though they have almost the same orbit.

The solar flare phenomenon is, of course, of interest to the scientific community in general. Consequently, the International Astronomical Union and the Inter-Union Commission on Solar-Terrestrial Physics have sponsored a Campaign for Integrated Observations of Solar Flares (CINOF). Two scientists from the Energetic Particles Branch of the Space Physics Laboratory were named as coordinators for the energetic particle portion of this study in recognition of the activity of the Space Physics Laboratory in this field. The CINOF study was designed to conduct intensive observations of the sun during June 5-29, 1972 with the objective of studying small flares and related phenomena in the hope that the analyses of these flares might be somewhat simpler than the large, outstanding events. A summary of the available solar particle and interplanetary observations for June 1972 was edited and published as an AFCRL Special Report. The most significant conclusion of this special campaign was that even small subflares are extremely complex, and that there is no such phenomenon as a "simple flare."

The extremely strong solar proton storms during early weeks of August 1972 were characterized as one of the most intense ever recorded on earth. The AFCRL satellite OV5-6 observed the time history of the near-earth proton and alpha particle fluxes throughout the duration of these events. This satellite spends all but perigee outside the magnetosphere and is instrumented with a variety of detectors including a proton alpha telescope measuring protons from 1 to 100 MeV and alpha particles from 10 to 100 MeV. The data from this event increased our understand-

ing of such events and resulted in several significant publications.

A somewhat less intense solar event occurred October 30, 1972. Fortunately, during this period appropriate instruments were operating in two satellites. One of these, OV5-6, was observing outside the magnetosphere, while the other, S72-1, was taking data at lower altitude above the polar caps and within the magnetosphere. These data permitted us to study the transmission characteristics of particles from outside to inside of the magnetosphere. Analysis of the polar data resulted as well in the establishment of improved upper limits to the production of deuterons and tritons by the sun.

The S72-1 satellite, when traversing lower latitudes, was used to continue studies of high energy trapped proton fluxes in the South Atlantic anomaly. The omnidirectional fluxes averaged over the period October 1972 to February 1973 were found to be in agreement with nuclear emulsion data taken in 1961-1962 before the "Starfish" high altitude test. Since this time interval of 11 years is coincident with a solar cycle, this further supports earlier conclusions that the atmosphere controls particle lifetimes.

The narrow angular resolution of the instrument on the satellite permitted a more accurate mapping of particle flux as a function of energy. This is especially true in the area of the South Atlantic anomaly where trapped particle fluxes reach their maximum due to the geometry of the earth's field. These data made it possible to quantitatively relate peculiar blips observed by the DMSP satellite optical sensors with the energetic proton fluxes present in the earth's vicinity.

The proper interpretation of our data, both in the sensors flown as well as when the particles penetrate the earth's atmosphere, requires precise knowledge of energy-loss and range parameters of the incident particles. Significant improvement in our knowledge of these parameters for heavy particles was accomplished coincident with our instrument design. This knowledge was also applied to the high atmosphere to relate our measurements to the ionospheric parameters of interest to radar and radio propagation.

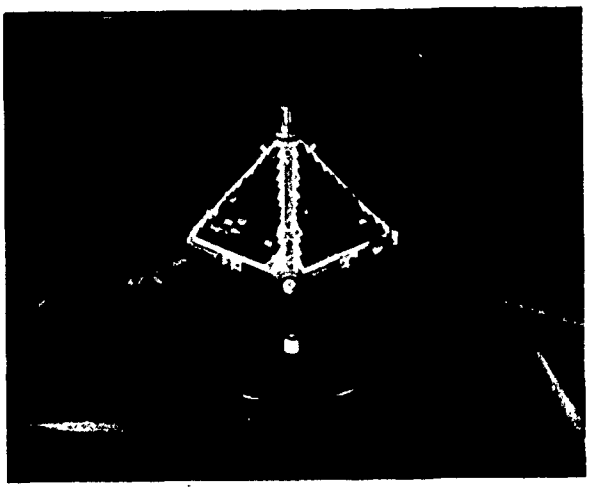

The OV5-6 satellite, launched in May 1969 to measure energetic particles emitted by the sun, was still in orbit and returning data at the end of the reporting period in 1974.

AFCRL also participated in a study carried out to establish the cause of anomalous behavior of the DSCS satellite system at times of geophysical activity. Our ability to analyze the data from our satellite sensors in a timely manner permitted us to make a significant contribution to this study. As a result of this study, spacecraft charging at synchronous orbit has been linked to the transport of high energy plasma particles from the magnetospheric tail to the synchronous regime. The charging process is a result of the complex interaction between a satellite and its environment. Secondary emission, photoelectron emission, and the ambient thermal plasma all act to mediate the satellite charge. Anisotropies in the plasma sheath created by spin, velocity, and shadowing complicate the interaction and influence the charge balance. During a magnetospheric substorm, a satellite,

wrapped in its thermal blanket, acts much like a capacitor immersed in a high temperature plasma.

Because of the anomalous behavior of military spacecraft at synchronous orbit, a research satellite has been initiated to investigate the phenomenon of Spacecraft Charging at High Altitude (SCATHA). Environmental monitors aboard the SCATHA satellite will provide data during magnetospheric quiet and storm times. Engineering experiments will detect and analyze in detail the electrical charging phenomena. Scientific data and engineering information will be correlated to relate cause and effect in satellite charging.

The Energetic Particles Branch will provide a complementary set of detectors to measure the fluxes and spectra of high energy particles. The instruments will obtain energy resolution from 50 eV to several MeV. A rapid time analysis of the fluxes is essential to an understanding of the transient charging effects, when the most damaging currents would flow. An ultimate time resolution of 2×10^{-1} sec is anticipated from our instruments. Design and construction of the SCATHA instruments is in process and launch of the SCATHA satellite is expected in early 1977.

ELECTRICAL PROCESSES RESEARCH

In the earth's upper atmosphere, from a few hundred kilometers out to interplanetary space, the dominant constituents are charged particles consisting of equal numbers of electrons and positive ions. All energy flow into, or out of, the lower ionosphere is a function of the motion of this plasma. Atmospheric electrical processes begin to play a dominant role in the ionospheric E-region, from 90-150 km. The work of the Electrical Structure Branch is directed toward studies of the dynamics of low energy plasmas in the range 0-200 eV, and electric fields in this ionosphere-plasmasphere-magnetosphere system. The effort is carried out by experimental rocket and satellite investigations and theoretical studies which include the modeling of outer atmosphere dynamics and the analytical foundation of new instrumental techniques.

Instrumentation development is continuing for flights aboard the SCATHA satellite, meteorological satellites, and two other Air Force satellites. These measurements will include the first three-axis measurements of the ambient electric field where wire booms of 60 feet in length are deployed by the spinning vehicle, direct measurement of the plasma bulk flow by utilizing greatly improved sensors of the type originally flown aboard the Gemini X and XII spacecraft, and measurement of satellite electrical charge build-up at synchronous altitudes.

IONOSPHERIC IRREGULARITIES: Data from the first year of operation of the thermal ion probe flown on the polar orbiting ISIS-I spacecraft have been used to study small scale irregularities. Statistical studies of the boundaries and morphology, utilizing data from more than 3,000 orbits, have yielded variations with season, local time and magnetic activity. Significant differences are found in the distributions derived from northern and southern hemispheres. On most transpolar passes irregularities were found to extend across the pole, rather than exhibiting a poleward boundary,

The irregularities have also been examined using the technique of power spectrum analysis. Power spectra from data both inside and outside the dayside cleft region (a region where the terrestrial magnetic field configuration permits penetration of significant energetic charged particle flux) have been obtained and compared. In the altitude range from 575 to 3525 km, it is found that the irregularity scale size varies from 0.2 to 100 km in latitudinal extent. An order of magnitude enhancement in the amplitude exists within

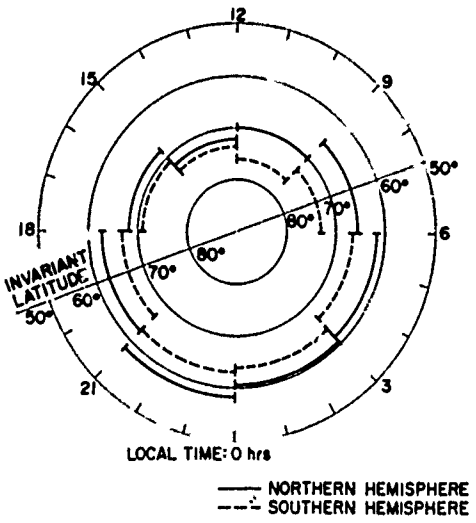

Equatorial boundaries of the high-latitude irregularity zones in the Northern and Southern Hemispheres.

the cleft as compared to lower latitude measurements outside this region. The spectral power variation is found to obey a law of the form $p = p_0^{\beta}$ where β increases from 1.8 to 2.1 with increasing magnetic activity utilizing Kp as a measure. These data have been compared with simultaneous scintillation data, obtained at AFCRL, to determine scale size responsible for scintillations which degrade UHF communications systems.

Although the ion probe results were obtained in the topside ionosphere, extensive comparisons with simultaneous on-board topside sounder measurements show that, down to the minimum scale size which can be observed with the sounder (approximately 18 km), the irregularities map down magnetic field lines to the peak of the F-region. These results thus represent a statistical mapping of ionospheric characteristics of the F-region.

ROCKET ELECTRIC FIELD MEASUREMENTS: Dipole electric field and plasma measurements have been made on two rockets flown in the E-region at Fort Churchill, Canada, at altitudes up to 165 km. The first flight, 1½ hours before local midnight, was made under quiet conditions in the presence of a weak, stable auroral arc. The second flight was flown about 2½ hours before local midnight in the break-up phase of a storm after a 700 gamma negative bay.

The first set of measurements shows that the vector electric field was directed southward with a component perpendicular to the magnetic field between 35 and 40 mv/meter. The component along the magnetic field was originally -17 mv/meter at 130 km, changing sign in mid-flight and became +6 mv/meter between 155 and 135 km on the descent. The plasma data show enhanced ionization and electron temperature, 1100° K in the altitude range 120 to 165 km. These relatively high electric fields contribute to the energy input to the upper atmosphere through Joule heating.

The measurements on the second flight are remarkably different. The rocket passed through a rapidly moving, irregular auroral patch with intensity peaks of over 80 kilorayleighs. In the altitude range of 105 to 130 km the plasma density was $6 \times 10^9/m^3$ with a peak of $1.3 \times 10^{10}/m^3$. Above 130 km, perhaps the upper boundary of the auroral form, the ionization decreased gradually with increasing altitude to $3 \times 10^9/m^3$ at apogee (150 km) and remained constant back down to 120 km. The electron temperature peaked at 1100° K coincident with the lower edge of the enhanced ionization. The ascent temperatures are approximately 200° K above the descent values which compare favorably with expected neutral gas temperatures (CIRA 1965). The vector electric fields were small and irregular having an average value near zero. The direction of the total field changed sign at the upper boundary of the enhanced ionization and showed values above this boundary of 38 mv/meter directed west of north.

The results of both flights confirm the great variability of electric fields and the plasma, over short intervals of time, over short distances, and under different

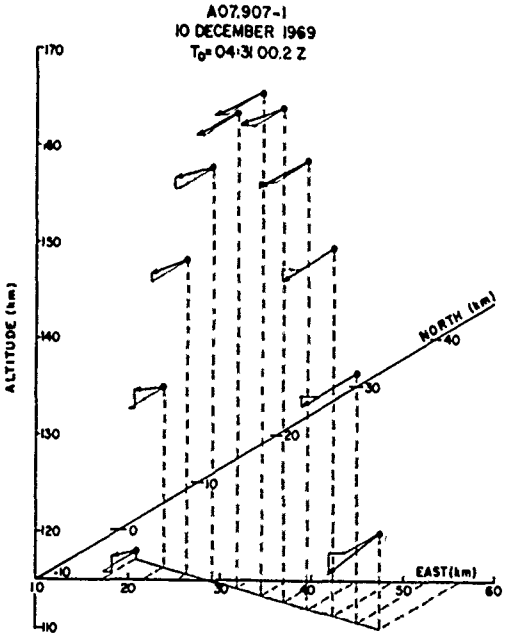

Electric field components measured by a Nike-Iroquois rocket fired into a diffuse aurora from the Fort Churchill Rocket Range, Canada.

geophysical conditions which may be encountered in the auroral zone E-region. They also illustrate that parallel electric fields of magnitudes great enough to energize low energy plasma particles are an important particle acceleration mechanism under quiescent auroral conditions. This constitutes a significant contribution to the understanding of high latitude current systems.

SATELLITE PLASMA STUDIES: Data from thermal ion and electron sensors aboard the OV3-1 satellite have been studied in the altitude range 3000 to 5700 km. During magnetically quiet periods the ionization density is characteristically found to decrease monotonically with increasing L. Between L = 2 and L = 3, a dependence of average density on longitude is found with a maximum between April and August occurring at 150 degrees E and the minimum at 300 degrees E. At L < 4, major charge density irregularities are found on 30 percent of the orbits. Comparison of density profiles obtained on the same day at different longitudes shows the irregularities to be of limited longitudinal extent. It is suggested that the depletions result from inward shifts of sectors of the plasmapause to lower L shells through the combined actions of electric and magnetic fields.

A study of the effect of five magnetic storms was made in the vicinity of the plasmapause utilizing data from ion and electron sensors flown on the Injun V and OGO-III satellites. It was found that as the plasmapause moves equatorwards during the early stages of a storm, the thermal density gradients at the plasmapause increase. Ion and electron temperatures poleward of the boundary increase above pre-storm values by 2000 to 6000° K. At the same time, temperatures within the plasmasphere increase some 1000° K over a latitude of 10 degrees equatorward of the boundary. The decrease in density of low energy particles at the boundary coincides with an increase in hyperthermal particle flux. These observations and the magnitude of energy transfer across the boundary is in substantial agreement with recent theoretical developments of Cornwall and Cole which indicate that the interaction of ring current particles with the relatively low energy cold magnetosphere plasma can produce an ion cyclotron damping mechanism for heating environmental electrons and ions in the vicinity of the plasmapause.

The data obtained from the ISIS-I satellite mentioned under "Ionospheric Irregularities" was also used to study the mid-latitude trough. Frequency of occurrence distributions of the latitude of the trough have been obtained as a function of local time and season in the Northern and Southern Hemispheres. The maximum frequency of occurrence of 60 percent is observed shortly after midnight and the minimum of 2 percent near local noon. The average trough width at half-depth is 4 ± 2 degrees of latitude. The trough is found to

be basically a nighttime phenomenon in the total electron content. Knowledge of the density gradients, width and dependence of trough characteristics on altitude, season, and local time is of fundamental importance to OTH and UHF systems operation.

GEOMAGNETISM

Magnetic activity levels control the maximum and minimum usable frequencies of a high frequency communications network, and advance assignment of a given channel requires a knowledge of the expected activity levels. Aeromagnetic detection systems, perimeter safeguards and other magnetic devices must be operated at reduced sensitivity when their detection bandwidth corresponds to the natural frequency components of magnetic disturbances. Another example of the effects of geomagnetic activity is the variation in atmospheric drag experienced by artificial satellites which is related to enhanced levels of activity. As a consequence, the orbital parameters of the satellites can be changed significantly, thus changing the predicted position of the satellite as a function of time.

Geomagnetism research is divided into two parts: measurements, both ground-based and space; and theory and analysis. Particles and field measurements are made using suitably instrumented rockets launched from Fort Churchill, Canada, during magnetic storms. Ground measurements will be obtained from a magnetometer network now being established within the United States. Theoretical models of geomagnetic phenomena are constructed to aid in the interpretation of the data. Advanced methods of data assimilation, especially high resolution spectral techniques, are developed and applied to analyze the observations.

MAGNETIC ACTIVITY ANALYSIS AND THEORY: Several indicators of geomagnetic activity are being studied: auroral activity, standard magnetic indices, and geomagnetic pulsations.

Auroral activity is an obvious manifestation of magnetospheric disturbances. The Defense Meteorological Satellite Program (DMSP) provides photographs covering a portion of the auroral oval. These are being utilized to verify and extend an empirical formula currently used by the Air Weather Service to specify the location of the entire oval. As input data, the formula can use either an index related to the general level of geomagnetic activity or the specific location of the aurora in a portion of the oval. Extension of the formula will include the possibility of using photographic data on Southern Hemisphere auroras as input for specifying the Northern Hemisphere oval. This would be necessary during the northern summer when auroral data are not available from this hemisphere. The photographs of the aurora are also being used to determine the effect of variations in interplanetary parameters such as solar wind velocity and interplanetary magnetic field direction on the size of the auroral oval.

Among the many indicators of geomagnetic activity are the indices scaled from the magnetograms of selected geomagnetic stations. Several standard indices which are being intensively studied are K_p, A_p, and C_i. K_p is a quasi-logarithmic index designed to measure world-wide variations in geomagnetic activity. It is well correlated with solar-wind speed and with the variability and magnitude of the interplanetary magnetic field. The A_p index, derived from K_p, provides a linear measure of daily magnetic activity. The C_i index, called the international daily character figure, is also a daily index but is available for all days since 1884, whereas K_p and A_p are available only since 1932.

A_p and K_p have been analyzed statistically to yield a geomagnetic climatology which is used by the Air Weather Service in forecasting magnetic activity. Studies have shown that the A_p and K_p distributions shift to-

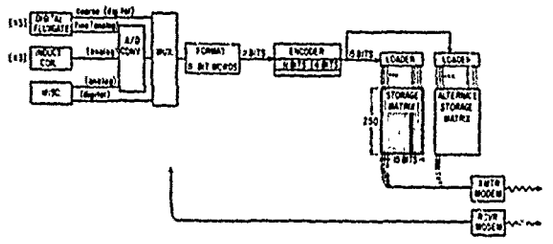

Geomagnetic data collection platform for measurement of the X, Y, and Z components of the earth's magnetic field and their time derivatives. All data are digitized, multiplexed, encoded and loaded into a storage matrix for transmission, on command to AFCRL.

ward higher levels when sunspot counts are high. Accounting for this change in frequency distribution from the quiet to the active portion of the solar cycle improves the climatology.

In recent years a new index of the polar magnetic daily variation has come into use. This index, called AC, has been used to infer the sector structure of the interplanetary magnetic field originating at or quite near the sun. Cross correlation and superposed epoch analysis have shown that, prior to 1960, sectors inferred to be away from the sun were associated with low geomagnetic activity as measured by C, and low solar activity as measured by the sunspot number, whereas sectors inferred to be toward the sun exhibited significantly enhanced geomagnetic and solar activity. The correlation after 1960 dropped to low values and has remained essentially zero since. These recent results indicate the inaccuracy of the earlier inferred sector structure.

Geomagnetic pulsations have special importance in characterizing magnetic activity. Current research involves the development of techniques for analyzing pulsation signatures, particularly power spectral estimates, and theoretical modeling of the complex phenomena displayed by magnetic pulsations.

Geomagnetic pulsations are low frequency magnetic signals with periods ranging from seconds to minutes. In the magnetosphere these pulsations must propagate as a form of electromagnetic radiation called hydromagnetic waves. The propagation of hydromagnetic waves within the plasma of the magnetosphere depends strongly on the characteristics of the earth's magnetic field and the plasma in which it is embedded. The typical time required for a hydromagnetic wave to traverse the magnetosphere is of the order of a minute. The resonant modes of the magnetosphere must have the same time scale. For this reason, magnetic pulsations are considered to be manifestations of the natural vibrations of the magnetosphere and its several structural components, such as the plasmasphere, the inner magnetosphere and the geomagnetic tail.

Geomagnetic pulsations are observed throughout the magnetosphere. However,

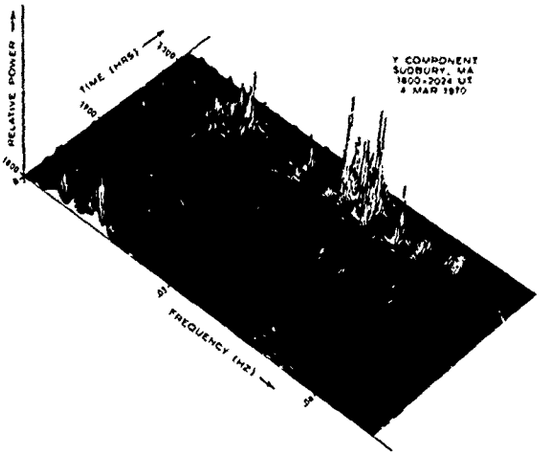

The variation in time of a geomagnetic pulsation power spectrum provides an example of the complex changes exhibited by geomagnetic pulsations. These spectral estimates were calculated by a new high resolution technique called the maximum entropy method. The burst of activity beginning at 1940 hours is a micropulsation event indicating the occurrence of a magnetospheric substorm.

their properties can be measured more conveniently and economically by ground-based magnetometers than by satellite systems. The analysis of experimental pulsation data and the conclusions based on theoretical models of hydromagnetic wave propagation suggest that geomagnetic pulsations are a sensitive indicator of the changing state of the magnetosphere.

Since magnetic pulsations often appear to be periodic, an important aspect of the analysis is the precise determination of the component frequencies. The principal method of determining these frequencies is called power spectrum analysis, which gives the power associated with the component frequencies. Conventional methods of spectral analysis have been found to be inadequate in providing sufficient detail. Research is underway to define the properties of a new method of spectral analysis called the maximum entropy method (MEM). Current results have shown that MEM produces much higher resolution than is attainable with conventional spectral estimates. The spectra obtained thus far reveal structure that has never before been resolved. Such structure gives more information about the pulsations and is important in evaluating in-house theoretical models which have predicted complex multiplet spectra. The results of these models are consistent with current observations and offer a quantitative explanation to the latitudinal variation of polarization parameters and the latitude-frequency distribution of magnetic energy.

GROUND MAGNETIC MEASUREMENTS: The specification of magnetic activity levels in real time and the prediction of magnetic activity several hours into the future require the construction of a system for the collection of terrestrial data from a number of observing sites and the transmission of this data to a central collection and analysis facility. Site selection, testing, and site-use

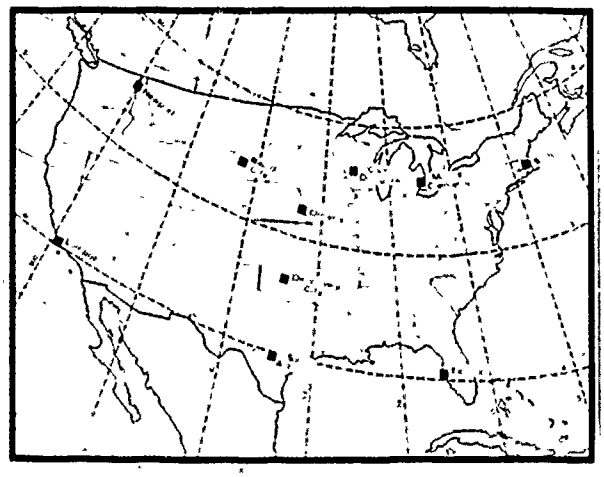

Geomagnetic micropulsation data collection and transmission network across the northern United States and the proposed N-S and southern E-W nets. All station locations are on government-owned land and each net lies on a parallel of magnetic latitude or on a magnetic meridian.

agreements have been completed for a five-station East-to-West network extending from Sudbury, Mass., to Newport, Wash., along a line of nearly constant magnetic latitude. The initial East-to-West network is scheduled for completion during FY-1975 and an additional five-station array N-S and E-W is planned for implementation during Fiscal Years 1976 and 1977. Fluxgate and induction coil magnetometer systems and an encoding, conversion, and multiplexing system will produce digital data at each site which will then be sent via phone lines to the data acquisition center at AFCRL where it will be processed, recorded and displayed in near real time.

Design of the fluxgate and induction coil magnetometer systems, the digital interfaces, the instrument shelters, the pier covers and the data acquisition station has been completed. Six fluxgate magnetometer systems have been built, tested, and calibrated. Six induction coil systems have been finished and tested and the digital data collection and acquisition prototypes have been operated successfully. Construction of the sensor piers, instrument shelter

foundations, and installation of power and signal conduits have been completed at the Selfridge ANG Base site at Mt. Clemens, Mich., and construction is in progress at the Newport, Wash., site. The computer and the discs, disc controller, tape recorder and tape controller, printer-plotter and teletype for the data acquisition center have been received and acceptance and qualification tests completed. The master time clock, WWV receiver and receiver antenna have also been received. Data transmitters and receivers (modems) have been installed at AFCRL and at the Newport, Wash., site and have been connected via full duplex data phone links. Line equalization has been completed and bit and block error rates measured.

Each magnetic observatory has been designed to operate as an unmanned station through a sophisticated control and communications system. This system is quasi-synchronous with the sampling and transmission times of each data collection platform (DCP) controlled by signals transmitted from the data acquisition stations (DAS). Each DCP has its own microprocessor which samples the various sensors, converts them to the required digital form and then stores the data briefly in a standard format. Every ten seconds a data frame is sent to the DAS. A redundant error-correcting code is incorporated together with a row entry, column read-out scheme that spreads burst errors over a number of individual words increasing reliability by orders of magnitude. About 20 percent of the data-return capability has been reserved as spares to serve future instrumentation.

Transmissions from up to ten stations pass through hubs where they are selected to arrive in sequence on a single line at the DAS. This line is fed into a computer which decodes, reformats, makes corrections (e.g., for temperature, etc.), converts to engineering units, computes averages and performs other related functions. The computer output is fed to archive tapes, real-time display, and plot storage.

ROCKET AND SATELLITE MEASUREMENTS: Magnetic substorms at high latitudes, long associated with communications disruptions, are generally accompanied by a marked increase in auroral activity as well as an intensification of ionospheric currents. The latter, known as the auroral electrojet, typically form an East-West oriented current band whose magnitude may be on the order of a million amperes. Convection patterns limited to the ionosphere alone, such as those which give rise to the dynamo currents in the mid-latitude region and account for the solar quiet day variation in the geomagnetic field, are not energetic enough to produce the current intensity of the auroral electrojet. Thus, with no source directly available in the polar ionosphere, the real current system associated with polar substorms is now believed to be a three-dimensional one, where the driving potential is generated deep in the magnetosphere and is transferred to the ionosphere via the highly conducting path along the lines of force of the geomagnetic field. Implicit in this circulation system would be a pattern of line currents, or current sheets, both upward and downward, aligned with the earth's magnetic field. Line currents to the east and west of the electrojet would argue for its being a Pedersen current; sheet currents to the north and south of the auroral band would be consistent with the more likely model of the electrojet as a Hall current.

A composite experiment designed to measure the particle fluxes and magnetic and electric fields associated with magnetic substorms has been constructed and integrated into an Air Force satellite which will be placed in a polar orbit. (The electric field experiment was described previously.) Electron fluxes will be measured in 32 discrete energy channels in the range 0.5 keV

to 20 keV with an electrostatic analyzer (ESA). This range includes the electrons responsible for the production of aurora as well as the leading candidates for the current carriers feeding the electrojet. The axis of the instrument is mounted perpendicular to the spacecraft spin axis, which is itself to be oriented normal to the orbital plane. Thus the ESA will sample electrons through all possible pitch angles in the altitude range 240 to 1200 km. The field-aligned currents will be detected indirectly by measuring the magnetic field they create. This will be normal to the much larger ambient geomagnetic field in the subpolar region, and an accurate vector measurement of the magnetic field will be required for its definition. To accomplish this a triaxial fluxgate magnetometer will be used in conjunction with an automatic ranging current source which will incrementally bias out the major portion of the background magnetic field in 128 discrete steps. This will allow measurements of high resolution without limiting dynamic range. The sensor of the magnetometer is mounted on a boom which will extend it 20 feet out from the spacecraft after it achieves orbit. Spurious magnetic fields from the satellite will thus be attenuated to a tolerable level, less than 10 gammas, while maintaining a fixed relationship between sensor and spacecraft coordinates.

Satellite photograph of aurora over central USSR. The expansive phase of an auroral substorm in the pre-midnight portion of the auroral oval is shown. The bright lights south of the aurora are individual towns along the network of railways. The large bright spots surrounded by halos are oil well burn-offs from several large oil fields.

The satellite which will carry this experiment is essentially complete now, and is scheduled for launch in 1975. Its high-inclination orbit will eventually carry the particle and field experiments over the auroral electrojet at all local-time periods. The simultaneous measurements they will provide of electron flux, field-aligned currents and electric fields will aid greatly in resolving the physical model of geomagnetic substorms.

The interaction of electrons with the earth's atmosphere was studied, formulated, and applied to the calculation of auroral absorption (30 MHz) from electron energy spectra (10-200 keV). The spectra were determined from electron data acquired in rocket experiments flown into substorm events at Fort Churchill, Canada. These results have been compared with ground observed riometer data. The relationship developed by Jelly, *et al,* who showed that the absorption is related to the square root of the electron flux above 40 keV, at night, with little sensitivity to spectrum shape, was confirmed. It was also shown that for energies of 150 keV and up, the relation of absorption to electron flux is not sensitive to spectrum shape during the daytime.

An analytic function was developed to calculate the ionization due to direct impact of electrons and to Bremsstrahlung. This allowed a calculation of riometer absorption. Since absorption, optical and particle measurements and electrojet location must

satisfy a given ionospheric model, the resolution of the Bremsstrahlung contribution provides useful information with regard to the proper ionospheric model.

POLAR UPPER ATMOSPHERIC RESEARCH

The objective of the polar atmospheric research program is to provide the basic environmental data and physical understanding needed to support Air Force systems operating within or traversing the polar cap region. To accomplish these tasks, ground-based measurements are conducted with a variety of sensor systems at the AFCRL Geopole Observatory in Thule, Greenland. The multi-sensor approach was developed because each sensor provides a specific piece of information relating to the state of the polar upper atmosphere, so that certain combinations of data could be used to gain insight into specific problem areas. The gathering methods at the station have been updated to include digital data recording systems which make all but the very fast sampled data available on computer compatible digital magnetic tapes.

The table below lists the major sensor systems presently being operated at the Observatory. Very low frequency (VLF) phase and amplitude are both recorded with the phase data being referenced to a rubidium frequency standard at the station. The VLF paths from the various transmitters are such that azimuthal dependence of disturbance effects can be detected. The low frequency (LF) receivers were installed in October 1973 in response to a request from the Electronic Systems Division (ESD), Hanscom AFB, Mass., to determine quiet level signal strengths for the Air Force transmitters at Silver Creek, Neb., and Hawes, California.

The riometer program has been ongoing for many years as the riometers are good detectors of PCA events. The 30 and 40 MHz riometer data along with the X and Z magnetometer data and cosmic ray neutron monitor data are sent out real time on a 10-channel communicator to Anchorage, Alaska, where they are computer reduced and forwarded to Global Weather Central (GWC).

The magnetometer is an Air Weather Service unit which was moved up to the Geopole Station from Thule Air Base about two years ago in anticipation of the Air Weather Service pullout from Thule. The X coil is aligned approximately with the horizontal field so the X value is ≃ H.

The photometers and other optical instruments are run only during the optical observing season — that is, when the sun is

GEOPOLE SENSORS

VLF	GBR	Rugby, England	16.0 kHz
	NLK	Jim Creek, Washington	18.6 kHz
	NDT	Yosami, Japan	17.4 kHz
	NOVIK	Norway	16.4 kHz
	NAA	Cutler, Maine	17.8 kHz
LF	WWBV	Fort Collins, Colorado	60.0 kHz
		Silver Creek, Nebraska	34.5 kHz
		Hawes, California	37.2 kHz
Riometer		26.3 MHz, 30 MHz, 40 MHz, 50 MHz	
Magnetometer		X, Y, & Z Components (X H)	
Photometer		3914 Å, 5577 Å, 6300 Å (2-second Data)	
Polarimeter		Equivalent Vertical Total Electron Content	
Field Mill		Near Earth Electric Field	
Scanning Spectrometer		Visible Spectrum (3900 Å to 6600 Å)	
Scanning Spectrometer		Dual Channel (3880 Å to 3950 Å and 7760 Å to 7900 Å)	
All Sky Camera			

more than 6 degrees below the horizon. The photometer data are recorded at second intervals and are a good indicator of auroral activity, both visual and subvisual. The polarimeter, operated for another branch at AFCRL, basically gives an equivalent vertical total electron content (TEC) at the sub-ionospheric point (400 km point) along the path from the receiver to the transmitter aboard a synchronous satellite. The subionospheric point for the Thule receiver is in the southern part of Greenland approximately halfway between Godhavn and Narssarssuaq. The electric field mill is run for the University of Minnesota at Duluth and is an indicator of world-wide thunderstorm activity.

A new system, a visible scanning spectrometer, will become operational in the Fall of 1974. It scans the wavelength region from about 3900 to 6600 angstroms once every ten minutes. The dual channel scanning spectrometer will also become operational in the fall of 1974. It was developed to support an Air Force Tactical Air Command research effort with the expectation that the data obtained will experimentally verify in a real atmosphere some of their theoretical models of atmospheric emissions in the near infrared. The all sky camera is used mainly to determine whether auroral changes as recorded by the photometers are spatial or intensity changes and to determine the alignment of auroral forms in the polar cap.

When several optical instruments are used, one of the usual practical difficulties is an apparent disagreement in the measurements. Such disagreement can be due to two sources: 1) natural changes occurring in the phenomena under observation, and 2) changes in the measuring instruments. It is essential to eliminate the second source. A controlled in-house laboratory experiment was conducted to determine various factors which lead to apparent disagreements. The results of this investigation have been published ("Calibration of Airglow Photometers and Spectrometers," *Applied Optics*).

ENERGETIC PARTICLE PRECIPITATION EFFECTS ON VLF: Since 1971 a number of energetic particle events have been recorded on the VLF receivers at Thule, Greenland. We have chosen to use the term "energetic particle event" rather than the more commonly used "polar cap absorption event" since the VLF often shows the effects of precipitation not intense enough to produce ionosonde blackout over the entire polar cap. Both the phase and amplitude of the VLF signal are affected, and the paths over the Greenland ice cap are affected to a greater extent than other paths.

During 1972 particle precipitation effects on the VLF signals were recorded on 17 different occasions.

The first eight months of 1972 were active compared to the rest of the year. During the major solar particle events in August 1972, the effects on the NLK signal were greater than any that had been recorded at Thule since the VLF program was initiated in 1966. The October 29, 1972 disturbance occurred after new receivers and a digital tape system had been installed. In addition to providing an overall picture of the event, a detailed closeup of the precipitation onset was obtained. The particle effects showed up on four of the VLF paths at times differing by up to 50 minutes, indicating the possibility of inhomogeneous precipitation over the polar cap at the onset of the event.

During 1973 energetic solar particle precipitation events were recorded on only five occasions, reflecting the minimum of solar activity during the year.

AURORAL SUBSTORM ACTIVITY

In addition to the solar particle events the effects of lower energy particle events were

reflected in VLF data, particularly around October 29 and December 22, 1973. These events produced a less drastic and shorter-lived effect on the VLF/LF propagation than the strong solar particle events, and occurred during active magnetic periods. In general, these disturbances are caused by particle precipitation in the auroral oval regions through which all propagation paths to Thule must pass. The lack of riometer absorption at Thule during most of these type events indicated little, if any, particle precipitation in the deep polar cap. However, at times there appears to be a poleward expansion of these disturbances, and at such times the riometer, magnetometer, photometer, and the VLF data show a burst of particle precipitation in the vicinity of Thule. These substorm effects are currently under more intensive study.

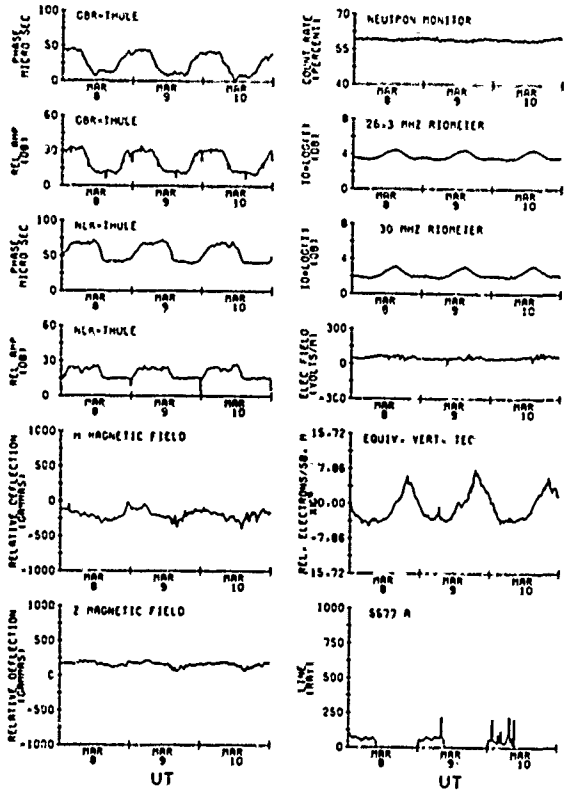

Computer plots of selected data from a 40-channel digital recording system at Thule, Greenland, for three successive days in a relatively quiet period in March of 1974. The data are 10-minute averages of samples taken every 30 seconds.

QUIET TIME STUDIES: The major polar atmospheric research effort is the study of manifestations in the polar cap of phenomena such as quiet time energy input and output, auroras, magnetic storms, and seasonal variations, which are studied in the auroral oval, mid-latitudes, and low latitudes as well as in the polar cap. The emphasis has been on the understanding of behavior during quiet times and during periods of minor and moderate disturbances since these conditions prevail most of the time. Nevertheless, large and spectacular disturbances are important and are frequently investigated as targets of opportunity. In this context, pulsating auroras measured at Bedford, Mass., during the world-wide geomagnetic storm of March 23-24, 1969 were analyzed for comparison with pulsating auroras customarily observed in the auroral oval. Several geophysical quantities, such as electrojet behavior, relative position of the proton and electron aurora, riometer absorption, and ionospheric quantities measured by ionosondes were similar to typical behavior in the auroral oval. This was interpreted as showing that the auroral oval had expanded to a geomagnetic latitude of 55 degrees from its more usual location at 65-70 degrees and not anomalous behavior at mid-latitudes occurring simultaneously with the auroral oval remaining at 65-70 degrees. These measurements of the characteristic period of the pulsating auroras at Bedford are the only known measurements at such a low latitude. The characteristic period of 7.2 seconds is unchanged from the 6-10 second period usually found by pulsating auroras in the unexpanded oval. The fact that the characteristic period of the pulsating aurora is unchanged despite the considerable

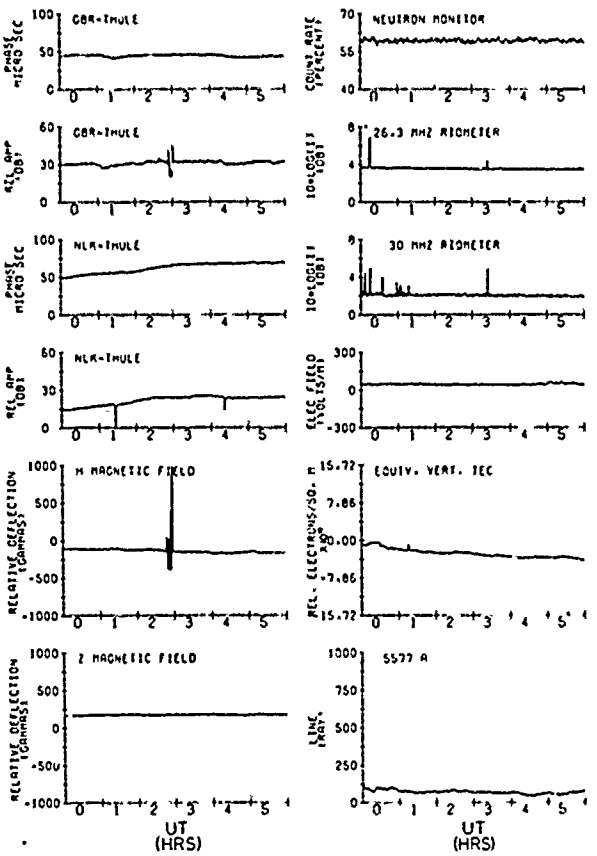

An expanded scale plot of the first six hours of March 8, 1974. Here, all the data points are plotted. This and the previous figure illustrate the capabilities of the system, and show the behavior to be expected from the basic geophysical parameters under quiet conditions.

expansion of the oval to 55 degrees geomagnetic latitude can be used as a test for theories concerning the excitation of pulsating and other types of auroras.

In mid-latitudes energy dissipation from the magnetosphere also produces an auroral arc. These latter are called Stable Red Auroral Arcs (SAR) and are not normally visible to the naked eye. One of the important factors needed in the study of either arc is the location: latitude, longitude and altitude of the arc. This information can be obtained by conducting simultaneous observations from two stations separated by several hundred kilometers. This demands planning, coordination and favorable weather conditions at both the observing stations. A lengthy graphical method has been known for determining the position of an arc from observations from a single station. With the aid of a computer these equations can be solved for a faster determination of the location of the arc.

In the construction of atmospheric models for the altitude region from 80 to 110 km, information on one of the most abundant and reactive species — atomic oxygen — is badly needed. In particular, no data at all exist in the polar cap region. Satellites obtain data at higher altitudes, so that rockets must be used for this region. Finally, at the beginning of this work, no experimental method had yet been proved to be reliable for such measurements.

Atomic oxygen profiles in the altitude region from 80 to 110 km can be determined from rocket measurements of the (OI) 5577 angstroms emission, provided one assumes that this emission, in the altitude region of study, is of chemical origin, and is predominantly due to the Chapman three-body collision excitation mechanism. The rate coefficients for excitation and quenching for this mechanism are known from the laboratory measurements. Simultaneous rocket observations were conducted to allow a comparison with other independent methods, the neutral mass spectrometer and chemical release of nitric oxide, in the ALADDIN II series from Eglin AFB, Florida, in April 1972. Preliminary results from these different methods indicate that all measurements are reasonably compatible with each other. Thus, this method of determining atomic oxygen from optical measurements is shown to be reliable.

An effort is now being made to measure in the real atmosphere spectroscopic parameters that have proved difficult to measure adequately in the laboratory. Measurements in the laboratory of the lifetime and collisional deactivation rates of

the N_2^+ A state, the upper level state for N_2^+ Meinel band emissions, have shown unacceptably large differences. The collisional deactivation of N_2^+ is important because as much as 61 percent of N_2^+ can be in the Meinel upper level A state. Collisional deactivation of this metastable state of N_2^+ is a possible important energy source for other atmospheric molecules which could emit infrared radiation. Uncertainties in the N_2^+ Meinel band collisional de-excitation processes therefore could lead to large uncertainties in evaluating excitation mechanisms for the possible IR emitters.

A special purpose dual channel scanning spectrometer has been assembled and field tested which will simultaneously measure the N_2^+ 7852 angstrom Meinel band and the N_2^+ 3914 angstrom first negative band, whose spectroscopic parameters have been more firmly established. The unique location of the AFCRL Geopole Observatory deep in the polar cap at Thule AB, Greenland, clearly separated from the auroral oval, will be used to measure these optical emissions when they are produced by energetic solar protons during solar particle events, and by auroral electrons during the occasional auroras which occur at Thule. The auroral electrons excite the Meinel and first negative bands at altitudes where the collisional de-excitation is minor. However, the energetic solar protons with energies greater than 1 MeV, present during a solar particle event, will excite the band emissions at altitudes where collisional de-excitation of the Meinel bands is significant. The energy of the solar protons, measured by satellite particle detectors, determines the altitude and pressure where the N_2^+ is produced. The ratio of the intensity of the Meinel bands relative to the intensity of the first negative bands when compared to the ratio during auroras, where collisional de-excitation is minor, can be converted to values of lifetime and collisional de-excitation rates. Here, the polar cap atmosphere provides a wall-less reaction vessel for determining spectroscopic quantities more commonly measured in the laboratory.

One of the basic problems of the polar cap region is the question of the homogeneity of effects over the entire region. Aircraft provide a suitable platform for studying this question. A series of aircraft flights during January 1974 provided the means for investigating the atmospheric z nith airglow and auroral intensities over paths which traversed the auroral oval and the polar cap. Among the measurements were zenith intensities of two emission lines of atomic oxygen (5577 angstroms and 6300 angstroms) which are commonly found in the night airglow and the aurora.

Enhanced levels of emission were found equatorwards of the afternoon sector of the oval, large intensities were encountered in the oval, and generally quiet airglow levels within the polar cap (contained within the oval). On January 26, at approximately 0642 UT, the aircraft passed under a sun-aligned arc whose red to green intensity ratio was about 0.1. On the 29th of January, the aircraft passed under another sun-aligned arc at 0800 UT with a red to green intensity ratio of about 0.5. The more intense arc had the smaller red to green ratio — an indication of more energetic particle precipitation.

The generally quiet airglow levels detected in the polar cap by the aircraft are reflected in the zenith intensities of these same emissions by instrumentation at the Geopole Observatory, Thule Air Base, Greenland, which is situated just 4 degrees from the geomagnetic pole. Even though Geomagnetic Activity Index (K_P) measurements for the two flights indicated magnetically disturbed days, the magnetometer at Geopole was very quiet.

On the 29th of January at 0750 UT, photometers at Geopole detected the sun-aligned arc which appeared over the aircraft at 0800 UT (some 600 km distant). All

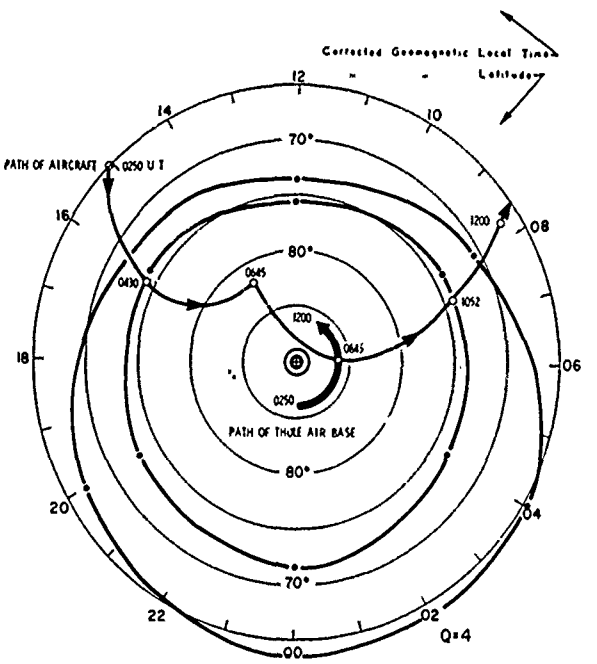

Path of the aircraft in corrected geomagnetic coordinates for the joint experiment between the Flying Laboratory and the Thule, Greenland, station on January 29, 1974.

sky camera pictures from the aircraft show a poleward motion of the arc which is compatible with the elapsed time between the ground and the aircraft observations.

From a comparison of the zenith intensities of the red and green lines of atomic oxygen observed at a deep polar cap station and an aircraft which traversed the polar cap, it has been shown that K_p is not a reliable indicator of polar cap magnetic or auroral activity and that transient discrete auroras are observed in the polar cap under quiet magnetic conditions as measured by a polar cap magnetometer even though K_p measurements indicate disturbed magnetic conditions.

SECTOR STUDIES: Associated with the rotation of the sun are sectors, so called because of a predominant direction of the interplanetary magnetic field, either away from or toward the sun. Characteristic features of the daily variations of the geomagnetic field in high latitudes were observed by Svalgaard and Mansurov to be associated with each sector type. An examination of 38 years of the planetary K_p index indicated a greater occurrence of higher K_p values or geomagnetic disturbance within the toward-the-sun sectors. Relative to expectation on a random basis, there were 175 percent of the disturbed days (average K_p of 5 or more) in the toward sector but only 40 percent of expectancy in the away sector. As the earth crossed from one sector type to another the changes in K_p level corresponded to the character of the respective sectors, a change previously thought to be unidirectional.

The higher values of K_p had the optimum association with the toward-the-sun sectors during years of sunspot maximum, years of the ascending part of the solar cycle, months of high sunspot latitude and during the equinoctial months. For these K_p or subauroral zone indices the maximum association of high K_p toward the sun and low K_p with away from the sun occurred during the times when the earth's heliocentric latitude was most southerly. A nearly similar association appeared in the southern solstitial season.

The three-hour K_p and A_p indices, a type of range indicator, have some limitations in their characterization of geomagnetic activity. Accordingly, examination was made of several years of the hourly variability of the geomagnetic component intensities for application to phenomena and problems at higher latitudes. To examine the possibilities of such extrapolation, 25 annual means of the variability of the D, H, and Z components for Sitka and College, Alaska, were compared. At College, H and D were approximately twice as variable as at Sitka while Z was only one and a half times as variable. A higher linear correlation existed between these annual means also, best for D, decreasing very little to Z and then less to

H. The Sitka variability annual means correlated very well with A_p also, best for Z and least for H. On the other hand, the Sitka geomagnetic variability correlation with the Zurich sunspot number was very poor compared with that at an equatorial station at Huancayo, Peru. Thus, the indication of solar activity, represented by sunspot number, is applied more effectively to equatorial than to subauroral zone geomagnetic manifestations.

ENERGY CONVERSION

Satellites make meteorological observations, relay communications, and maintain surveillance. All these activities require electrical power to operate on-board instruments and to telemeter data.

The energy conversion program studied both the production of this electrical power and efficient use of the primary energy sources available to a space vehicle. Space power must come primarily from the sun, either as light or heat energy, or from batteries and fuel cells, which rely on chemical energy carried on board the spacecraft. Solar energy can generate electricity directly in solar cells, or the sun's heat can be concentrated and used in a thermal energy conversion scheme such as a thermionic converter. Also, solar cells are used to recharge secondary batteries which then serve as primary power supplies.

The solar cell program was directed at improving the quality of state-of-the-art silicon solar cells and developing new, low-cost solar cells based on organic charge-transfer complexes.

Silicon solar cells are used for on-board primary electrical power generation in almost all satellites launched to date. These solar cells are exposed to X-rays, gamma rays, electrons, and protons both in the radiation belts surrounding the earth and in the solar wind. These radiations gradually degrade cell performance and thus force designers to deploy excess power generation capability on the spacecraft to meet mission power requirements at the end of the spacecraft life.

To overcome the degradation process, new techniques of controlled doping of solar cells have been investigated. It has long been realized that radiation damage can be alleviated by introducing lithium metal into the cell. The lithium reduces the ability of a radiation-induced defect to trap charge carriers. The removal of charge carriers by such traps is a major source of solar cell power loss. To act effectively as a trap inhibitor, the lithium must be concentrated near the solar cell junction. However, the ability of lithium to migrate to defect sites to reduce their trapping effects also allows the lithium to migrate far from the junction site. To prevent this, ion implantation was used to deposit a phosphorus barrier layer to block the migration of the lithium from the junction region. Results indicated that this phosphorus counter-doping technique can be successfully used for lithium location control.

Organic materials might be used in solar cells if their high resistivity could be overcome. Charge transfer complexes offer one technique for reducing this resistivity since in a one-to-one molecular complex, the number of high resistance electrical paths through the bulk material is reduced by a factor of 2. A number of such complexes have been assembled and tested and improvements in conductivity of two orders of magnitude have been achieved relative to a single-molecular species type of substrate. However, further work is needed before organic materials become competitive with silicon for solar energy conversion because although they are much less expensive than silicon, they have efficiencies two to three orders of magnitude less than the best silicon cells.

A valuable offshoot of the organic solar cell effort was the development of a variety of transition metal-organic salts which have demonstrated potential for use in metal-vapor lasers.

H. The Sitka variability annual means correlated very well with A_p also, best for Z and least for H. On the other hand, the Sitka geomagnetic variability correlation with the Zurich sunspot number was very poor compared with that at an equatorial station at Huancayo, Peru. Thus, the indication of solar activity, represented by sunspot number, is applied more effectively to equatorial than to subauroral zone geomagnetic manifestations.

ENERGY CONVERSION

Satellites make meteorological observations, relay communications, and maintain surveillance. All these activities require electrical power to operate on-board instruments and to telemeter data.

The energy conversion program studied both the production of this electrical power and efficient use of the primary energy sources available to a space vehicle. Space power must come primarily from the sun, either as light or heat energy, or from batteries and fuel cells, which rely on chemical energy carried on board the spacecraft. Solar energy can generate electricity directly in solar cells, or the sun's heat can be concentrated and used in a thermal energy conversion scheme such as a thermionic converter. Also, solar cells are used to recharge secondary batteries which then serve as primary power supplies.

The solar cell program was directed at improving the quality of state-of-the-art silicon solar cells and developing new, low-cost solar cells based on organic charge-transfer complexes.

Silicon solar cells are used for on-board primary electrical power generation in almost all satellites launched to date. These solar cells are exposed to X-rays, gamma rays, electrons, and protons both in the radiation belts surrounding the earth and in the solar wind. These radiations gradually degrade cell performance and thus force designers to deploy excess power generation capability on the spacecraft to meet mission power requirements at the end of the spacecraft life.

To overcome the degradation process, new techniques of controlled doping of solar cells have been investigated. It has long been realized that radiation damage can be alleviated by introducing lithium metal into the cell. The lithium reduces the ability of a radiation-induced defect to trap charge carriers. The removal of charge carriers by such traps is a major source of solar cell power loss. To act effectively as a trap inhibitor, the lithium must be concentrated near the solar cell junction. However, the ability of lithium to migrate to defect sites to reduce their trapping effects also allows the lithium to migrate far from the junction site. To prevent this, ion implantation was used to deposit a phosphorus barrier layer to block the migration of the lithium from the junction region. Results indicated that this phosphorus counter-doping technique can be successfully used for lithium location control.

Organic materials might be used in solar cells if their high resistivity could be overcome. Charge transfer complexes offer one technique for reducing this resistivity since in a one-to-one molecular complex, the number of high resistance electrical paths through the bulk material is reduced by a factor of 2. A number of such complexes have been assembled and tested and improvements in conductivity of two orders of magnitude have been achieved relative to a single-molecular species type of substrate. However, further work is needed before organic materials become competitive with silicon for solar energy conversion because although they are much less expensive than silicon, they have efficiencies two to three orders of magnitude less than the best silicon cells.

A valuable offshoot of the organic solar cell effort was the development of a variety of transition metal-organic salts which have demonstrated potential for use in metal-vapor lasers.

Satellites must maintain their temperature within the range in which their electronics will operate. As a satellite passes from sunlight into the earth's shadow, the vehicle experiences wide temperature swings which can exceed the allowable operating limits for temperature-sensitive satellite components.

A program was developed to specify a combination of a high melting-point solid and a canister to contain it, to assist in a satellite temperature control.

During the sunlit portion of a satellite's orbit, an optical concentrator focuses sunlight on the canister, melting the solid inside it. During shaded portions of the orbit, the molten material freezes, giving its heat to the temperature-sensitive components to maintain a proper temperature balance. Aluminum and alkali fluorides were studied as possible heat absorbing solids, and Inconel canisters as containers for the solid. Also, a variety of heat pipe designs were evaluated for transfer of the heat from the freezing molten material to the subsystems requiring thermal control.

Electrochemical batteries and fuel cells are widely used for energy storage on aircraft and balloons. Rechargeable batteries provide energy storage for longer duration missions where the primary power source may be the vehicle's engine or a solar cell panel. Conventional cells using aqueous electrolytes are close to the limits of development. Consequently, research toward higher performance batteries is directed to nonaqueous electrolytes which permit the use of highly active electrode materials such as the alkali metals.

The Laboratory program was primarily concerned with some fundamental problems of ambient temperature nonaqueous electrolytes and the problem of containing chemical reactions with standard free energies in the 100 Kcal/mole range. The problem of direct chemical reaction of the constituents of the cell is related to the thermodynamics of the system and the rates of the various reactions involved. The presence of trace impurities, especially water, is an important determinant of corrosion rates. Consequently, much effort has been devoted to purification and analysis techniques and the manipulation of solvents and solutions in a dry atmosphere. A major difficulty raised by almost all nonaqueous electrolytes is low conductance which limits the discharge rate of a battery. Conductance mechanisms are immensely complex, involving such related properties as viscosity, dielectric constant, molecular association and ion-solvent interactions. The dielectric properties of a large number of electrolytes in various organic solvents including propylene carbonate, butyrolactone, and dimethyl sulfoxide have been measured. The effects of electrolyte type and concentration and the frequency dispersion of the dielectric constant provide insight into the structure of the solution. Other problems addressed included the mechanism of the lithium electrode reaction under various conditions and finding viable positive electrodes. The lithium electrode is generally satisfactory in a clean system. Transition-metal halides are generally unsatisfactory because of their solubility and high sensitivity. However, this problem has been largely circumvented by the recent development of inorganic electrolyte cells where the positive electrode reactant is the solvent itself.

SPACE FORECASTING

The Space Forecasting Program was initiated at AFCRL in the mid-1960's to develop techniques to observe, specify and predict solar-related changes in the earth's upper atmosphere and near-space environment that impact on Air Force operations. This interdisciplinary program draws on most of the environmental sciences—radio and optical solar astronomy, astrophysics, radio propagation physics, and the physics and chemistry of

the upper atmosphere. Its very nature requires participation by specialists in a variety of technical fields, such as energetic particles, ionospheric physics, solar physics, geomagnetism and atmospheric density.

From its inception, the Space Forecasting Program has focused strongly on the operational problems related to changing space environmental conditions. To provide a convenient mechanism for coordinating the efforts of some 12 to 15 scientists, the Space Forecasting Coordination Group, now directed from staff level, was established in 1966. This group, which meets three to four times a year, provides an ideal forum for exchanging technical information, for coupling research products with operational requirements, and for directing and coordinating the efforts of in-house scientists and contractors working in a broad spectrum of related scientific disciplines. In addition to the AFCRL task scientists, representatives from Air Weather Service, NOAA, NRL, ESD, SAMSO, and NELC are periodically invited to participate at these meetings to coordinate related activities within their organizations.

Space forecasters are faced with the task of predicting the occurrence of bursts of electromagnetic radiation and energetic particles from the sun, and specifying the effects of these bursts on the earth's atmosphere. These effects include absorption of radio waves in the ionosphere, geomagnetic disturbances, auroral activity, enhanced airglow levels, and atmospheric density variations.

Through the efforts of the Space Forecasting Coordination Group, specific problem areas related to existing and planned operational space environmental support requirements are identified and programs initiated to solve them. The results of some of these efforts are outlined elsewhere in this report within the various participating laboratories' program descriptions.

PLASMA PHYSICS

The work of the Plasma Physics Branch centered on the production, heating and confinement of plasmas by high intensity magnetic fields and the flow properties of partially ionized gases using a shock tube. As both projects require input from high energy storage capacitors, effort was applied to improving dielectrics for capacitor use.

Tormac (TORoidal MAgnetic Cusp) is the acronym for a series of AFCRL experiments leading to the heating and confinement of plasmas of thermonuclear interest. In the last version investigated in detail, Tormac III, a toroidally symmetric six-pole cusp magnetic field was crossed with a toroidal magnetic field. The plasma achieved values of density and temperature of 10^{16} particles/cm^3 and 15 eV, respectively, and exhibited a decay time constant of greater than 200 microseconds.

Plasma loss due to toroidal effects can be prevented by using only two ring cusps, both having the same major radius as the toroid. This concept led to the bi-cusp, the newest version of Tormac in which a combination of toroidal and poloidal magnetic fields form a cusp. The cusp conditions of requiring the magnetic field on the plasma surface to be isogaussic and convex are met with the plasma exhibiting a shield-shaped cross section. Magnetic field design was aided with the use of an electrolytic plotting tank. Theoretical studies have shown toroidal drift to be minimal and that the bi-cusp is not vulnerable to the many types of instabilities investigated.

The first version of the bi-cusp, known as Shaker (because plasma heating is achieved with multiple shock waves), was constructed and operated in the collisionless regime. The heating or Shaker field is an 0.6 MHz signal superimposed on the principal poloidal field component. Preliminary

measurements using various optical spectroscopic methods have shown that even with a modest energy input, both electron and ion temperatures of 30 to 50 eV (over 300,000° to over 500,000°) are achieved. In addition to fusion-related studies, the boundary layer in supersonic ionized flow over a flat plate was measured using a two-color laser interferometer. This study constitutes the first quantitative measurement of a boundary layer in an ionized gas flow.

A theoretical study of the high-frequency Stark effect in pydrogenic plasmas due to plasma turbulence was performed, taking into account both static and dynamic fields, with consideration of resonant effects.

A high-power laser concept utilizing dissociating states of diatomic molecules was investigated both theoretically and experimentally. The initial gas studied was molecular hydrogen in H_2-Ar mixtures. The stimulated emission cross section of the hydrogen continuum, and the photoionization of excited H_2 molecules was one major study area. Another was the various types of gas discharges in H_2-Ar mixtures with the object of obtaining sufficiently uniform and dense plasmas for use in lasers. A pulsed electron beam configuration was found to provide the densest uniform plasmas, and gain studies were carried out using this method. Utilizing a multipass chamber, gain was measured in H_2-Ar mixtures excited by an electron beam. A strong absorption in Ar was found, which leads to net absorption for the H_2-Ar mixture. The H_2 laser buffered by Ar was shown to be unsuitable for lasing; however, the principle of electron beam excitation and the development of a gain measuring system make it attractive to explore the laser possibilities of other diatomic molecules with dissociating states.

A group of polar organic liquids were investigated for applications in liquid dielectric high energy density capacitors. These liquids showed a substantial improvement both in energy density and storage time compared to dielectric liquids presently being used. Liquid dielectric capacitors offer a promising approach to the Air Force requirement for lightweight pulse power sources in airborne applications.

RESEARCH ON SOLAR DYNAMICS

Research continued during this period on three main areas: The Solar General Circulation, Theoretical Studies of Solar Terrestrial Relations, and Physical Processes in Solar Phenomena. These areas of research result from the need to understand the development and decay of solar active regions, the need to determine the mechanisms causing the emissions and radiation from these regions, and the need to develop the calibration constants for solar measurements.

The variable solar emissions typically associated with solar active regions produce many effects in the upper terrestrial atmosphere, on the terrestrial magnetic field, and in the surrounding space. Operation of Air Force systems in each of these regions gives rise to a need to predict the effects of solar emissions on their environment, and ultimately, on the systems themselves.

SOLAR ACTIVE REGIONS: The most extensive history of the birth, growth, and decay of solar active regions that exist in the world has been compiled on tape. Sunspots have been grouped according to size, shape, and resident latitude and their motions analyzed. An investigation of the contribution of meridional cells to the solar energy balance has shown that these cells are not of primary importance.

The experiment to obtain standardized flare observations has been completed successfully. A computer program is now being written to produce an objective method for determining the area and integrated light deficits of sunspots. The suc-

cess achieved in standardizing flare observations has led to the decision to design and build five matched solar telescopes and deploy them around the world in a Solar Optical Observing Network (SOON) System for the Air Weather Service.

RADIO BURSTS: Investigation of plasma radiation processes occurring in solar flares and radio bursts developed from a major theoretical effort into one involving experiment as well.

A solar flare will produce supra-thermal electrons and protons, which will interact with the coronal plasma to produce Cerenkov plasma waves. The phase velocity of the plasma waves emitted by this process always falls between the stream velocity and the electron thermal velocity. However, as the phase velocity approaches the electron thermal velocity, the damping decreases. As a result, weakly damped large amplitude long plasma waves can propagate in the corona when the frequency of the plasma wave is slightly larger than the electron plasma waves.

A homogeneous and fully ionized hot plasma will always contain ion and electron density fluctuations which will be independent of each other. These fluctuations separately scatter incident longitudinal plasma waves, at least partially, into electromagnetic radiation of different intensity. The scattered intensity depends on the amplitude of the incident wave field and on the amplitude of each type of fluctuation. Non-thermal fluctuations may be much larger than thermal density fluctuations.

When an electron plasma wave is scattered by an ion density fluctuation (oscillating at the ion plasma frequency which is much smaller than the frequency of the incident wave), the frequency of the scattered wave remains nearly the same as that of the incident wave. This is the Rayleigh scattering process in the plasma. The scattered wave consists of a longitudinal wave that cannot leave the plasma volume, and a transverse electromagnetic wave that radiates out of it, yielding the Rayleigh scattered power at approximately the plasma frequency of the medium. Theoretical calculations have shown that the ratio of the intensity of Rayleigh scattered longitudinal wave to that of the transverse electromagnetic wave is very large, normally at least 1000.

However, when the propagating plasma wave is scattered by an electron density fluctuation (oscillating at the electron plasma frequency, which is comparable to the frequency of the incident plasma wave) the frequency of the scattered wave is strongly modulated by the frequency of the electron density fluctuation. Consequently, the scattered wave contains the sum and difference frequencies, and their hybrid overtones. Usually, however, the scattered wave has only one dominant component which is transverse electromagnetic and this is the sum frequency. This is the Raman scattering process.

As mentioned earlier, the major component of the Rayleigh scattered wave is longitudinal, coherent, and incapable of leaving the plasma volume; it will interact resonantly with the charge density fluctuations in the plasma, raising their level far above that of purely thermal charge density fluctuations. Consequently, Raman scattering of an incident, coherent plasma wave is coherently enhanced. It has been shown that this mechanism can cause the Type III radio noise bursts from the sun. In addition, by tailoring the plasma parameters in a DC discharge tube, radiated power from Raman scattering can be augmented by many orders of magnitude. It was also calculated theoretically, that the energy in the incident wave must exceed a certain threshold if enhanced coherent Raman emission is to occur.

The strength of the emission, the threshold required, its frequency, and its angular distribution was found to agree with the theory when tested in a DC discharge tube at AFCRL. In addition, far infrared radiation from a helium plasma and

microwave emission from a DC discharge in an argon plasma noted by other investigators were explained. The possible use of this phenomenon as a laser mechanism will be investigated, in addition to its possibilities in clarifying the relationships of solar noise bursts and solar flares.

ABSOLUTE F-VALUES: Absolute transition probabilities (f-values) are needed for the determination of species concentrations and temperatures in plasma diagnostics, and solar and stellar abundances in astrophysics. The pressure-driven shock tube is a preferred thermal light source for f-value measurements since the shock-heated gas is in a well defined equilibrium state over a wide range of controllable operating conditions and uniform in the line of sight.

The AFCRL shock tube uses argon or neon carrier gas in the driven section to which a trace of the gas to be investigated is added. High pressure helium gas drives the tube. Temperatures behind the reflected shock can be varied from 3,000 to 10,000 degrees K. Spectral radiation from atoms, ions, and molecules is recorded photographically and photoelectrically from steady states of known population in local thermodynamic equilibrium. Correlation of the observed spectral intensities with the measured temperature, pressure, and concentration of the gas allows the absolute f-values of the transitions to be determined.

Previously measured spectra of Cr and Fe f-values have made it possible to correct f-values for these elements, which in turn, resolved the paradox of the iron group elements being deficient by an order of magnitude in the solar photosphere relative to the corona and meteorites. Known f-values can be used to infer plasma characteristics of nuclear detonations, fireballs, reentry sheaths and wakes, and chemical releases. To allow the precise determination of conditions in sunspots, a study of Ti I, Ti II and TiO f-values was begun. Absolute f-values for 7 Ti I lines were determined in addition to the 90 reported in the last *Report on Research.* Twenty more Ti II f-values brought the total to 30. Absolute f-values were also measured for 11 Alpha bands of TiO. Manganese carbonyl in argon was used to measure 40 lines of Mn I in the range from 3800 to 5500 Å. Exploratory work was also done on f-values for Mn II, Si I and Si II.

The Energy Conversion, Space Forecasting, Solar Plasma Dynamics, and Plasma Physics Branches were terminated at the end of this reporting period.

JOURNAL ARTICLES
JULY 1972 - JUNE 1974

BARTHOLOMA, K. P., ENGE, W. (Inst. fur Reine und Angewandte Kernphysik, Univ. of Kiel, Ger.), and FUKUI, K.
Charge Separation and Flux Measurement in the Region of the Iron Peak
Proc. of the 8th Intl. Conf. on Nuc. Photog. and Solid State Track Detectors, Bucharest, Rom., Vol. 1 (July 1972)

BOOZER, A. H., CAPT., and LEVINE, M. A.
Particle Trapping in Magnetic Line Cusps
Phys. Rev. Ltrs., Vol. 30 (November 1973)

COHN, A.
Photo-Ionization of Excited H_2 Molecules
J. of Chem. Phys., Vol. 57, No. 6 (15 September 1972)

COHN, A., and BAKSHI, P., KALMAN, G. (Boston Coll., Mass.)
Linear Stark Effect Due to Resonant Interactions of Static and Dynamic Fields
Phys. Rev. Ltrs., Vol. 29, No. 6 (7 August 1972)
Hydrogenic Stark-Zeeman Spectra for Combined Static and Dynamic Fields
Phys. Rev. Ltrs., Vol. 30 (31 December 1973)

COHN, A., and MARCUCCI, M., CAPT. (Aerosp. Instmn. Lab.)
Stimulated Emission Cross-Section of H_2 Dissociation Transition
J. of Appl. Phys., Vol. 44, No. 4 (April 1973)

DORMAN, L. I., GUSHCHINA, R. T. (The Inst. of Terrestrial Mag., Iono. and Propagation of Radiowaves of the USSR), SHEA, M. A., and SMART, D. F.
Cosmic Rays Effective Cut-off Rigidities
Book, Pub. by Publishing House NAUKA, Moscow, USSR (1972)

EARNSHAW, W., and FUJIMORI, E.
Dark Bleaching of Rhodopsin by Organic Mercurial
FEBS Ltrs., Vol. 34 (1973)

FILZ, R. C.
Corpuscular Photographic Observations of Energetic Particles in Space
Proc. of 8th Intl. Conf. on Nuc. Photog. and Solid State Track Detectors, Bucharest, Rom., 10-15 July 1972 (1972)

FILZ, R. C., KATZ, L., ROTHWELL, P. L., and SELLERS, B., HANSER, F. A. (Panametrics, Inc., Waltham, Mass.)
Observation of 5-45 Me V Protons at $L \leq 3$ $L \geq 7$
Space Res. XIV, Akademie-Verlag, Berlin, Ger. (1974)

FILZ, R. C., MC NULTY, P. J., and DAVIS, A. F. (Franklin Pierce Coll., Rindge, N. H.)
Use of Plastic Detectors to Confirm the Acceleration of Argon Nuclei to Relativistic Velocities at the Princeton Particle Accelerator
Proc. of 8th Intl. Conf. on Nuc. Photog. and Solid State Track Detectors, Bucharest, Rom., 10-15 July 1972 (1972)

FOUGERE, P. F.
Dependence of Geomagnetic and Solar Activity Upon Solar Magnetic Sector Structure
Proc. of Chapman Mem. Symp. on Magneto. Motions, 18-22 June 1973 (1973)
Cross Correlation of the Inferred Solar Sector Structure with Solar and Magnetic Activity
EOS, Trans. of Am. Geophys. Union, Vol. 54, No. 4 (1973)
Dependence of Inferred Magnetic Sector Structure Upon Geomagnetic and Solar Activity
Planetary and Space Sci., Vol. 22 (1974)
Maximum Entropy Power Spectrum of Solar Activity
EOS, Trans. of Am. Geophys. Union, Vol. 55, No. 4 (April 1974)

FOUGERE, P. F., RADOSKI, H. R., and ZAWALICK, E. J.
Comparison of Power Spectral Estimates: III. Indices of Magnetospheric Activity
EOS, Trans. of Am. Geophys. Union, Vol. 54, No. 11 (December 1973)

FUJIMORI, E.
On the Fluorescence of Indole Compounds Induced by Ketone-Sensitized Photoreactions
Photochem. and Photobiol., Vol. 16 (1972)
Carotenoid Chromophore Length and Protection Against Photosensitization
Photochem. and Photobiol., Vol. 19 (1974)
Quenching of Biacetyl Phosphorescence by Indole and Methionine. Solvent Effects
Mol. Photochem., Vol. 6 (1974)

FUKUI, K., and YOUNG, P. S. (Miss. State Univ.)
Low Energy Iron Group Nuclei Observed in 1968 with Nuclear Emulsion
Proc. of the 8th Intl. Conf. on Nuc. Photog. and Solid State Track Detectors, Bucharest, Rom., Vol. 1 (July 1972)

GALLAGHER, C. C., and LEVINE, M. A.
Balmer Line Anomalies in a Turbulent Plasma
Phys. Rev. Ltrs., Vol. 30, No. 19 (7 May 1973)

HANSER, F. A., SELLERS, B. (Panametrics, Inc., Waltham, Mass.), and VANCOUR, R. P.
The Real-Time Determination of Ionospheric Current Parameters During a Substorm
J. of Geomag. and Geoelect., Vol. 25 (1973)

ISAILIN, M. V., SCHIMMERLING, W., VOSBURGH, V. G., WHITE, M. G. (Princeton Particle Accelerator, Princeton, N. J.), and FILZ, R. C., MC NULTY, P. J.
Acceleration of Argon Ions to 11.7×10^9 Electron Volts
Sci., Vol. 177 (4 August 1972)

KATZ, L., ROTHWELL, P. L., and YATES, G. K.
Simultaneous Observations of Proton and Alpha Fluxes During the Period 29 October - 3 November 1972
Correlated Interplanetary and Magneto. Obsns., D. E. Page, Ed., D. Reidel Pub. Co., Dordrecht, Holl. (1974)

KELLEY, J. G., and SELLERS, B., HANSER, F. A. (Panametrics, Inc., Waltham, Mass.)
Energy Loss and Stopping Power Measurements Between 2 and 10 MeV/amu for ^{12}C, ^{14}N, and ^{16}O in Silicon
Phys. Rev. B, Vol. 8, No. 1 (July 1973)

LEIBY, C. C., JR.
A Circulating Pump for Ultra-Pure or Toxic Gases
Rev. of Sci. Instms., Vol. 43, No. 8 (August 1972)

LIM, Y. K. (Univ. of Singapore), and FUKUI, K.
Trident Mean Free Paths of Positrons
J. of Singapore Natl. Acad. of Sci., Vol. 3, No. 2 (1973)

LIM, Y. K. (Univ. of Singapore), FUKUI, K., and YOUNG, P. S. (Miss. State Univ.)
Tridents Produced by 1-4 GeV Positrons
Phys. Rev. D1-1 (February 1974)

LINCOLN, J. V. (NOAA, Boulder, Colo.), and SHEA, M. A.
Cosmic Ray Data in World Data Centers
13th Intl. Cosmic Ray Conf., Conf. Papers, Vol. 2, 17-30 Aug. 1973 (August 1973)

MACKEN, N. A., BESSE, A. L., and LEVINE, M. A.
Shock Tube Boundary Layers in Argon-Helium Mixtures
AIAA J., Vol. 10 (August 1972)

Mc Clay, J. F.
On the Asymmetric Nature of Micropulsations. I. The Spectrum
Planetary and Space Sci., Vol. 21, No. 12 (December 1973)

Mc Nulty, P. J., and Filz, R. C.
Interactions of Energetic Neon with Emulsion Nuclei
Proc. of 8th Intl. Conf. on Nuc. Photog. and Solid State Track Detectors, Bucharest, Rom., 10-15 July 1972 (1972)

Mukherjee, T. K., Dimond, N. A., and Pittman, C. U., Jr., Sasaki, Y. (Univ. of Ala.), Cowan, D. O., Park, J. (Johns Hopkins Univ., Baltimore, Md.)
Semiconducting Polymers Mixed Valence Ferrocene-Ferricinium Polymers
J. of Am. Chem. Soc., Vol. 94 (1972)

Payne, R.
The Study of the Ionic Double Layer and Adsorption Phenomena
Techniques in Electrochem.: Electrode Processes (Book), Vol. 1 (1972)
Adsorption of Inorganic Anions on a Mercury Electrode from Solutions in Formamide II. Adsorption of Chloride and Nitrate Ions and
The Electrical Double Layer: Problems and Recent Progress
J. of Electroanalyt. Chem., Vol. 41 (1973)
Double Layer at the Mercury-Solution Interface
Chap. in Book, Prog. in Surface and Membrane Sci., Vol. 6 (1973)
Adsorption of Amides at the Mercury-Solution Interface
J. of Electroanalyt. Chem., Vol. 47 (1973)
The Electrical Double Layer in Organic Solvents
Phys. Chem. of Organic Solvent Sys., Plenum Press (Fall 1973)

Payne, R., and Theodorou, I. E.
Dielectric Properties and Relaxation in Ethylene Carbonate and Propylene Carbonate
J. of Phys. Chem., Vol. 76 (1972)

Podsiadlo, R. T.
An Objective Baseline for Flare Prediction
Space Res. XIII, Vol. 1, Akademie-Verlag, Berlin, Ger (1973)

Prasad, B.
The Coherent Amplification of Radio Emission in Type III Bursts
Bull. of Am. Astronom. Soc., Vol. 5, No. 2 (1973)

Quinlan, K. P.
Reversible Spectrophotometric Changes Accompanying the Light-Induced Proton Uptake of Porphyrin-Benzoquinone Systems
Photochem. and Photobiol., Vol. 267 (1972)

Radoski, H. R.
The Effect of Asymmetry on Toroidal Hydromagnetic Waves in a Dipole Field
Planetary and Space Sci., Vol. 20 (1972)
Hydromagnetic Propagation in the Magnetosphere: A Mechanical Analogue for the Study of the Initial Value Problem of Coupled Modes
J. of Geomag. and Geoelect., Vol. 25 (1973)
A Theory of Latitude Dependent Geomagnetic Micropulsations: The Asymptotic Fields
J. of Geophys. Res., Vol. 79, No. 76 (1 February 1974)

Radoski, H. R., Zawalick, E. J., and Fougere, P. F.
A Comparison of Power Spectral Estimates: I. Theory and Synthetic Signals
EOS, Trans. of Am. Geophys. Union, Vol. 54, No. 11 (November 1973)

Rothwell, P. L.
Comparison of Electron Fluxes with the Whistler Self-Excitation Limit During a Magnetic Storm
Annales de Geophys., Vol. 29, No. 3 (1973)

Rothwell, P. L., and Katz, L.
Enhancement of 0.24-0.96 MeV Trapped Protons During the 25 May 1967 Magnetic Storm
J. of Geophys. Res., Vol. 78, No. 25 (1 September 1973)

Rothwell, P. L., Katz, L., and Sellers, B., Hanser, F. A. (Panametrics, Inc., Waltham, Mass.)
Upper Limits to Flare-Produced Deuterium and Tritium
Phys. Rev. Ltrs., Vol. 31, No. 6 (6 August 1973)

Sellers, B., Hanser, F. A. (Panametrics, Inc., Waltham, Mass.), and Kelley, J. G.
Energy Loss and Stopping Power Measurements Between 2 and 10 MeV/amu for ^3He and ^4He in Silicon
Phys. Rev. B (1 July 1973)

Sellers, B., Hanser, F. A., (Panametrics, Inc., Waltham, Mass.), and Vancour, R. P.
An Instrument for Real-Time Determination of Polar Electrojet Position and Current Parameters
The Rev. of Sci. Instms., Vol. 44, No. 7 (July 1973)

Shea, M. A.
Cosmic-Ray Data for the August 1972 Solar Events
Collected Data Rpts. on Aug. 1972 Solar-Terrestrial Events, World Data Ctr. A for Solar Terrestrial Phys., Rpt. UAG-28, Part I, Boulder, Colo. (July 1973)

Shea, M. A., and Smart, D. F.
Cosmic-Ray Trajectory Calculations for Selected High Latitude Stations Appropriate for the Solar Cosmic-Ray Event in 1971
Data on Solar Geophys. Activity Assoc. with the Major Ground-Level Cosmic Ray Events of 24 Jan. and 1 Sep.

1971 (UAG Rpt., NOAA, Boulder, Colo.), UAG-24, Part I (December 1972)

Prediction of the End of Solar Proton Events
Space Res. XIII, Akademie-Verlag, Berlin, Ger. (1973)

Asymptotic Directions for Selected High Latitude Stations Appropriate for the August 1972 Ground Level Cosmic-Ray Events
Collected Data Rpts. on Aug. 1972 Solar-Terrestrial Events, World Data Ctr. A for Solar Terrestrial Phys., Rpt. UAG-28, Boulder, Colo. (July 1973)

A Composite Catalog of Ground-Level Cosmic-Ray Increases
Cosmic Ray Conf., Conf. Papers, Vol. 2, 17-30 Aug. 1973 (August 1973)

The Response of the Deep River Neutron Monitor to an Anisotropic Flux of Solar Cosmic Rays
J. of Geophys. Res., Vol. 79 (1 June 1974)

The Value of Multi-Spacecraft Measurements
Correlated Interplanetary and Magneto. Obsns., D. E. Page, Ed., D. Reidel Pub. Co., Dordrecht. Holl. (1974)

SHEA, M. A., SMART, D. F., and MOOMEY, W. R., 2ND LT.

Transmittance Functions for Defining the Response of a Cosmic-Ray Detector in the Geomagnetic Field
13th Intl. Cosmic Ray Conf., Conf. Papers, Vol. 2, 17-30 Aug. 1973 (August 1973)

SHIVPURI, R. K., CRUTY, M. R. (Clarkson Coll. of Technol., Potsdam, N. Y.), and MC NULTY, P. J.

The Suitability of Nuclear Emulsion for Nuclear Structure Studies at a High Energy Muon Facility
Phys. Rev. D. Vol. 8, No. 7 (1 October 1973)

SILVERMAN, J., KRUKONIS, A. P., and YANNONI, N. F.

2H, 5H-Octachloro-p-Xylene, $C_8H_2Cl_8$
Cryst. Structure Comm. (Pama, Italy), Vol. 2 (1973)

The Crystal Structures of 9-Dicyanomethylenefluorene
Acta Crystallographica, Vol. B29 (1973)

SMART, D. F., and SHEA, M. A.

The Daily Variation of Electron and Proton Geomagnetic Cutoffs Calculated for Fort Churchill, Canada
J. of Geophys. Res., Vol. 77, No. 25 (September 1972)

An Empirical Method of Estimating Cutoff Rigidities at Satellite Altitudes
13th Intl. Cosmic Ray Conf., Conf. Papers, Vol. 2, 17-30 Aug. 1973 (August 1973)

Significant Problems in Identifying Solar Particle Increases
Space Res. XIV, Akademie-Verlag, Berlin, Ger. (1974)

WARD, F. W., JR.

The Latitudinal Motion of Sunspots and Solar Meridional Circulations
Solar Phys., Vol. 30, No. 1 (June 1973)

WARD, F. W., JR., and CARNEVALE, R. F.

The Promise of Self-Consistent Flare Data
Bull. of the Am. Astronom. Soc. (March 1973)

WARD, F. W., JR., CARNEVALE, R. F., and HENDL, R.

Solar Flare Observations from a Pair of Matched Instruments
Solar Phys., Vol. 31, No. 1 (July 1973)

WHITE, M. L.

Jet Streams and the Development of the Solar System
(Ltr. to Ed.) Nature, Vol 238, No. 85 (14 August 1972)

A Physical Mechanism for the Production of Solar Prominences
Bull. of the Am. Astronom. Soc., Vol. 5, No. 2 (1973)

WOLNIK, S. J., and BERTHEL, R. O.

Shock-Tube Measurements of Absolute gf-Values for Ti I and Ti II
The Astrophys. J. (Ltrs.) (15 January 1973)

YANNONI, N. F.

Photovoltaic Effects in Organic Materials
NAS Rpt., Solar Cells: Outlook for Improved Efficiency (1972)

YATES, G. K., KATZ, L., and SELLERS, B., HANSER, F. A. (Panametrics, Inc., Waltham, Mass.)

Proton and Alpha Particle Fluxes Observed Aboard OV5-6 in August 1972
Collected Data Rpts. on Aug. 1972 Solar-Terrestrial Events, World Data Ctr. A for Solar Terrestrial Phys., Rpt. UAG-28, Part II, Boulder, Colo. (July 1973)

Interplanetary Particle Fluxes Observed by OV5-6 Satellite
Correlated Interplanetary and Magneto. Obsns., D. E. Page, Ed., D. Reidel Pub. Co., Dordrecht, Holl. (1974)

YATES, G. K., KELLEY, J. G., and SELLERS, B., HANSER, F. A. (Panametrics, Inc., Waltham, Mass.)

Proton and Alpha Particle Fluxes Measured Aboard OV5-6
Data on Solar Geophys. Activity Assoc. with the Major Ground-Level Cosmic Ray Events of 24 Jan. and 1 Sep. 1971 (UAG Rpt., NOAA, Boulder, Colo.), UAG-24, Parts I and II (December 1972)

YOUNG, P. S. (Miss. State Univ.), and FUKUI, K.

Prediction of Observing Light Flashes on SST Planes Due to Alpha-Particle Flux
Nature, Vol. 241 (12 January 1973)

Probability of Observing Light Flashes by the Passengers on SST Planes
Proc. of 8th Intl. Conf. on Nuc. Photog. and Solid State Track Detectors, Bucharest, Rom., Vol. 1 (July 1972)

ZAWALICK, E. J., FOUGERE, P. F., and RADOSKI, H. R.

A Comparison of Power Spectral Estimates: II. Long Period Micropulsations
EOS, Trans. of Am. Geophys. Union, Vol. 54, No. 11 (November 1973)

PAPERS PRESENTED AT MEETINGS JULY 1972 - JUNE 1974

BOOZER, A. H., CAPT.
Fusion Using Line Cusps
Fusion Theory Mtg., Berkeley, Calif. (3-5 April 1974)

BOOZER, A. H., CAPT., and LEVINE, M. A.
The Entrapment of Particles in a Magnetic Line Cusp
Am. Phys. Soc. Plasma Phys. Mtg., Monterey, Calif. (13-16 November 1972)
Equilibrium in a Toroidal Line Cusp (The Tormac)
Ann. Mtg. of the Am. Phys. Soc., Div. of Plasma Phys., Philadelphia, Pa. (31 October - 3 November 1973); Columbia Univ., N. Y., N. Y. (19 November 1973)

CARRIGAN, A. L., and CASTELLI, J. P. (Iono. Phys. Lab.)
Solar Activity in McMath Region Number 10789 During Disk Passage, June 12-15, 1970
Mtg. of the Com. of Eur. Solar Radio Astron. (CESRA). Obsv. of Univ. of Bordeaux, Bordeaux, Fr. (20-23 September 1972)

CHATTERJEE, S., and KWALWASSER, W. D. (AMP, Inc., Harrisburg, Pa.)
Studies of Naphthoquinone Electron Acceptors
Am. Chem. Soc. Fall Mtg., Chicago, Ill. (26-31 August 1973)

CHERNOSKY, E. J.
Geomagnetic Component Variability at High Latitudes
55th Ann. Spring Mtg. of the Am. Geophys. Union, Wash., D. C. (8-12 April 1974)

COHN, A., and BAKSHI, P., KALMAN, G. (Boston Coll., Mass.)
Determination of High Frequency Electric Fields in Plasmas from the Hydrogen Spectrum
26th Ann. Gaseous Elect. Conf., Univ. of Wis., Madison, Wis. (17-19 October 1973)

FILZ, R. C., and HOLEMAN, E. (Franklin Pierce Coll., Rindge, N. H.)
Development of Unidirectional Trapped Proton Flux Models
Fall Ann. Mtg. of the Am. Geophys. Union, San Francisco, Calif. (4-7 December 1972)

FILZ, R. C., KATZ, L., and HOLEMAN, E. (Emmanuel Coll., Boston, Mass.)
High Accuracy Directional Trapped Proton Flux Measurements Below 760 Km
Am. Phys. Soc. Mtg., Chicago, Ill. (4 February 1974)
55th Ann. Spring Mtg. of the Am. Geophys. Union, Wash., D. C. (8-12 April 1974)

FILZ, R. C., KATZ, L., and HOLEMAN, E. (Franklin Pierce Coll., Rindge, N. H.), SELLERS, B., HANSER, F. A. (Panametrics, Inc., Waltham, Mass.)
Observation of Omnidirectional Trapped Proton Energy Spectra Measured in Late 1972 Below 750 Km Altitude
1973 Ann. Am. Geophys. Union Mtg., Wash., D. C. (16-20 April 1973)

FILZ, R. C., KATZ, L., ROTHWELL, P. L., and SELLERS, B., HANSER, F. A. (Panametrics, Inc., Waltham, Mass.), HOLEMAN, E. (Franklin Pierce Coll., Rindge, N. H.)
Observation of Trapped Solar Particles Since 2 October 1972
16th Plenary Mtg. of COSPAR, Konstanz, Fed. Rep. of Ger. (23 May - 6 June 1973)

FILZ, R. C., and MC NULTY, P. J. (Clarkson Coll. of Technol., Potsdam, N. Y.), DAVIS, A. F. (Franklin Pierce Coll., Rindge, N. H.)
Use of Plastic Detectors to Confirm the Acceleration of Argon Nuclei to Relativistic Velocities at the Princeton Particle Accelerator
8th Intl. Conf. on Nuc. Photog. and Solid State Track Detectors, Bucharest, Rom. (10-15 July 1972)

FOUGERE, P. F.
Cross Correlation of the Inferred Solar Sector Structure with Solar and Magnetic Activity
1973 Ann. Am. Geophys. Union Mtg., Wash., D. C. (16-20 April 1973)
Dependence of Geomagnetic and Solar Activity Upon Solar Magnetic Sector Structure
Chapman Mem. Symp. on Magneto. Motions, ERL/NOAA, Boulder, Colo. (18-22 June 1973)

FOUGERE, P. F., RADOSKI, H. R., and ZAWALICK, E. J.
Comparison of Power Spectral Estimates: III. Indices of Magnetospheric Activity
1973 Ann. Fall Mtg. of the Am. Geophys. Union, San Francisco, Calif. (10-14 December 1973)

FOUGERE, P. F., and ZAWALICK, E. J.
Power Spectrum of the Svalgaard-Mansurov Index of Polar Magnetic Variations
Fall Ann. Mtg. of the Am. Geophys. Union, San Francisco, Calif. (4-7 December 1972)

FUKUI, K., and ENGE, W., BEAUJEAN, R. (Institut fur Reine und Angewandte Kernphysik, Univ. of Kiel, Kiel, Ger.)
Isotopic Components of Light Nuclei in the Low Energy Cosmic Radiation Medium and Heavy Cosmic Ray Nuclei Measured on Board of Apollo 16
13th Intl. Cosmic Ray Conf. (IUPAP), Denver, Colo. (17-30 August 1973)
Isotopic Components of Light Nuclei Detected with Plastic Detector
Am. Nuc. Soc. Mtg., Philadelphia Elec. Co., Pa. (23-28 June 1974)

FUKUI, K., and YOUNG, P. S. (Miss. State Univ.)
Low Energy Iron Group Nuclei Observed in 1968 with Nuclear Emulsion
8th Intl. Conf. on Nuc. Photog. and Solid State Track Detectors, Bucharest, Rom. (10-15 July 1972)

GALLAGHER, C. C., and LEVINE, M. A.
Plasma Turbulence in the Tormac Geometry
Am. Phys. Soc. Plasma Phys. Mtg., Monterey, Calif. (13-16 November 1972)

Tormac IV, A Toroidal, Bi-Cusp Containment Device
Ann. Mtg. of the Am. Phys. Soc., Div. of Plasma Phys., Philadelphia, Pa. (31 October - 3 November 1973)

GOLUBOVIC, A., and DIMOND, N. A.
Photoconductive and Photovoltaic Properties of Large Symmetrical Quinoxalines
164th Natl. Mtg. of the Am. Chem. Soc., N. Y., N. Y. (27 August - 1 September 1972)

HALL, W. N.
Energetic Solar Particle Contribution to the Energetics of the High Latitude Thermosphere
55th Ann. Spring Mtg. of the Am. Geophys. Union, Wash., D. C. (8-12 April 1974)

HENDL, R. G., CAPT., CARNEVALE, R. F., and WARD, F. W., JR.
Standardization of Solar Flare Observations
1972 AFSC Sci. and Engrg. Symp., San Antonio, Tex. (17-19 October 1972)

LEIBY, C. C., JR.
2 ω_p-Radiation from DC Discharges in the Noble Gases
Ann. Mtg. of the Am. Phys. Soc., Div. of Plasma Phys., Philadelphia, Pa. (31 October - 3 November 1973)

LEVINE, M. A.
Cusp Containment and Thermonuclear Reactors
AF Wpn. Lab., Kirtland AFB, Albuquerque, N. M., and Los Alamos Sci. Lab., Los Alamos, N. M. (16 21 July 1972)
The Bicusp A New Magnetic Configuration for Thermonuclear Reactors
Am. Phys. Soc. Plasma Phys. Mtg., Monterey, Calif. (13-16 November 1972)
Plasma Containment in Cusp Geometries
Sem. at Stevens Inst. of Technol., Hoboken, N. J. (8 March 1973)

LEVINE, M. A., BOOZER, A. H., CAPT., and GALLAGHER, C. C.
Containment Time in Tormac
Ann. Mtg. of the Am. Phys. Soc., Div. of Plasma Phys., Philadelphia, Pa. (31 October - 3 November 1973)

LINCOLN, J. V. (NOAA, Boulder, Colo.), and SHEA, M. A.
Cosmic Ray Data in World Data Centers
13th Intl. Cosmic-Ray Conf., Denver, Colo. (17-30 August 1973)

MAPLE, E., and FREY, J. H., FISCHER, W. L. (Sci. Resources Fdn., Watertown, Mass.)
Auroral-Oval Micropulsations at a Sub-Auroral Zone Station
1973 Ann. Am. Geophys. Union Mtg., Wash., D. C. (16-20 April 1973)

MUKHERJEE, T. K.
Conductivity Changes by Charge Transfer Reaction
3rd Intl. Symp. on Chem. of the Organic Solid State, Univ. of Strathclyde, Scot. (16-22 September 1972)

PAVEL, A. L., CAPT., and DEGROOT, J. S. (Univ. of Calif. at Davis)
High Power Microwave Absorption and Plasma Heating
Ann. Mtg. of the Am. Phys. Soc., Div. of Plasma Phys., Philadelphia, Pa. (31 October - 3 November 1973)

PAVEL, A. L., CAPT., KATZ, L., and YATES, G. K.
Cosmic Gamma Ray Bursts
Am. Phys. Soc. Spring Mtg., Wash., D. C. (22-25 April 1974)

PEACOCK, D. S. (Univ. of Denver, Colo.), GOLD, R. E. (Univ. of N. H.), SHEA, M. A., and SMART, D. F.
An Extended Set of Variational Coefficients
55th Ann. Spring Mtg. of the Am. Geophys. Union, Wash., D. C. (8-12 April 1974)

PRASAD, B.
Enhancement of Raman Scattering in the Presence of Rayleigh Scattered Plasma Waves
Am. Phys. Soc. Plasma Phys. Mtg., Monterey, Calif. (13-16 November 1972)
The Coherent Amplification of Radio Emission in Type III Bursts
Solar Phys. Div. Mtg. of Am. Astronom. Soc., Las Cruces, N. M. (8-10 January 1973)
A Classical "MASER" Action in a Hot Uniform Plasma
Ann. Mtg. of the Am. Phys. Soc., Div. of Plasma Phys., Philadelphia, Pa. (31 October - 3 November 1973)

RADOSKI, H. R.
Coupled Hydromagnetic Modes: Initial Value Problems
Fall Ann. Mtg. of the Am. Geophys. Union, San Francisco, Calif. (4-7 December 1972)
A Mechanical Analogue for the Study of Hydromagnetic Propagation in the Magnetosphere
1973 Ann. Am. Geophys. Union Mtg., Wash., D. C. (16-20 April 1973)

RADOSKI, H. R., FOUGERE, P. F., and ZAWALICK, E. J.
A Comparison of Power Spectral Estimates: I. Theory and Synthetic Signals
1973 Ann. Fall Mtg. of the Am. Geophys. Union, San Francisco, Calif. (10-14 December 1973)

ROTHWELL, P. L.
Comparison of Electron Fluxes with the Whistler Self-Excitation Limit During a Magnetic Storm
Fall Ann. Mtg. of the Am. Geophys. Union, San Francisco, Calif. (4-7 December 1972)
The Sun and Solar Flares
(Inv. Sem.), Wesleyan Univ., Middletown, Conn. (4 April 1974)
Flare-Produced d and ^{3}He
Am. Phys. Soc. Spring Mtg., Wash., D. C. (22-25 April 1974)

ROTHWELL, P. L., KATZ, L., YATES, G. K., and SELLERS, B., HANSER, F. A. (Panametrics, Inc., Waltham, Mass.)
Proton Energy Spectra Observed During October 29 -

November 3, 1972
55th Ann. Spring Mtg. of the Am. Geophys. Union, Wash., D. C. (8-12 April 1974)
Interpretation of Flare-Produced Proton Spectra
1974 Intl. Symp. on Solar Terrestrial Phys./17th Plenary Mtg. of COSPAR, Sao Paulo, Brazil (17 June - 1 July 1974)

ROTHWELL, P. L., YATES, G. K., KELLEY, J. G., and SELLERS, B., HANSER, F. A. (Panametrics. Inc., Waltham, Mass.)
Polar Particles Measured During the 30 October - 2 November 1972 Solar Event
1973 Ann. Am. Geophys. Union Mtg., Wash., D. C. (16-20 April 1973)

SAGALYN, R. C., WILDMAN, P., SMIDDY, M., and RAO, L. D. V. (Regis Coll., Weston, Mass.)
Stormtime Behavior of Low Energy Charged Particles in the Vicinity of the Plasmapause
AGU Conf. on Magneto.-Iono. Coupling, Yosemite, Calif. (6-8 February 1974)

SELLERS, F. B. (Panametrics, Inc., Waltham, Mass.), VANCOUR, R. P., and HANSER, F. A. (Panametrics, Inc., Waltham, Mass.)
Observed Auroral Absorption Compared with Calculations Based on Rocket-Measured Electron Spectra
1973 Ann. Fall Mtg. of the Am. Geophys. Union, San Francisco, Calif. (10-14 December 1973)

SHEA, M. A.
Introduction to Solar Terrestrial Physics
(Inv. Paper) X Gen. Asbly. of the Pan Am. Inst. of Geog. and Hist. and Pan Am. Mtgs. of Consultation on Geophys., Panama, Pan. (22 April - 9 May 1973)

SHEA, M. A., and SMART, D. F.
The Value of Multi-Spacecraft Measurements
7th ESLAB Symp., Saulgau, W. Ger. (22-25 May 1973)
Significant Problems in Identifying Solar Particle Increases
16th Plenary Mtg. of COSPAR, Konstanz, Fed. Rep. of Ger. (23 May - 6 June 1973)
A Composite Catalog of Ground-Level Cosmic-Ray Increases
13th Intl. Cosmic Ray Conf. (IUPAP), Denver, Colo. (17-30 August 1973)
Increase in the Neutron Monitor Counting Rate Resulting from Secular Changes in the Geomagnetic Field
55th Ann. Spring Mtg. of the Am. Geophys. Union, Wash., D. C. (8-12 April 1974)
Solar Particle and Related Interplanetary Observations During the Campaign for Integrated Observations of Solar Flares (CINOF)
1974 Intl. Symp. on Solar Terrestrial Phys./17th Plenary Mtg. of COSPAR, Sao Paulo, Brazil (17 June - 1 July 1974)

SHEA, M. A., SMART, D. F., and MOOMEY, W. R., 1ST LT.
Transmittance Functions for Defining the Response of a Cosmic-Ray Detector in the Geomagnetic Field
13th Intl. Cosmic Ray Conf. (IUPAP), Denver, Colo. (17-30 August 1973)

SHEA, M. A., SMART, D. F., and TANSKANEN, P. J. (Univ. of Oulu, Oulu, Finland)
Recent Small Ground-Level Solar Cosmic-Ray Increase
1973 Ann. Fall Mtg. of the Am. Geophys. Union, San Francisco, Calif. (10-14 December 1973)

SILVERMAN, J., KRUKONIS, A. P., and YANNONI, N. F.
The Molecular Structure of 2H, 5H-Octachloro-p-Xylene
9th Intl. Cong. and Gen. Asbly. of the Intl. Union of Cryst., Kyoto, Jap. (26 August - 4 September 1972)
The Crystal Structure of Terephthaldehydene Bis Malononitrile (TPM)
Am. Cryst. Assoc. Mtg., Storrs, Conn. (18-22 June 1973)

SMART, D. F., and SHEA, M. A.
Comment on the Detection of Small Proton Events Inside and Outside the Magnetosphere
1973 Ann. Am. Geophys. Union Mtg., Wash., D. C. (16-20 April 1973)
An Empirical Method of Estimating Cutoff Rigidities at Satellite Altitudes
13th Intl. Cosmic Ray Conf. (IUPAP), Denver, Colo. (17-30 August 1973)
A Technique for Evaluating Mathematical Models of the Magnetosphere
1974 Intl. Symp. on Solar Terrestrial Phys./17th Plenary Mtg. of COSPAR, Sao Paulo, Brazil (17 June - 1 July 1974)

SMART, D. F., SHEA, M. A., and GOLD, R. E., NOLTE, J. T., ROELOF, E. C. (Univ. of N. H.)
Coronal Structure Associated with Solar Particles from McMath 9740
55th Ann. Spring Mtg. of the Am. Geophys. Union, Wash., D. C. (8-12 April 1974)

WARD, F. W., JR., and CARNEVALE, R. F.
The Promise of Self-Consistent Flare Data
Solar Phys. Div. Mtg. of the Am. Astronom. Soc., Las Cruces, N. M. (8-10 January 1973)

WHITE, M. L.
A Physical Mechanism for the Production of Solar Prominences
Solar Phys. Div. Mtg. of Am. Astronom. Soc., Las Cruces, N. M. (8-10 January 1973)

WILDMAN, P. J. L., SAGALYN, R. C., and AHMED, M. (Regis Coll., Weston, Mass.)
Midlatitude Trough Characteristics Based on ISIS-I Thermal Ion Data
55th Ann. Spring Mtg. of the Am. Geophys. Union, Wash., D. C. (8-12 April 1974)

YANNONI, N. F., SILVERMAN, J., and KRUKONIS, A. P.
Intermolecular Interactions in Polar Organic Crystal Structures

Conf. on Mol. Interactions and Elect. Density in Solids, Bordeaux, Fr. (4-8 September 1973)

YATES, G. K., KATZ, L., and SELLERS, B., HANSER, A. F. (Panametrics, Inc., Waltham, Mass.)
Interplanetary Particle Fluxes in August 1972
Fall Ann. Mtg. of the Am. Geophys. Union, San Francisco, Calif (4-7 December 1972)
Interplanetary Particle Fluxes Observed by OV5-6 Satellite
7th ESLAB Symp., Saulgau, W. Ger. (22-25 May 1973)

YOUNG, P. S. (Miss. State Univ.), and FUKUI, K.
Nuclear Interactions in Emulsion by Oxygen at 2.1 BeV/n
Intl. Conf. on Reactions Between Complex Nuclei, Nashville, Tenn. (10-14 June 1974)

ZAWALICK, E. J., FOUGERE, P. F., and RADOSKI, H. R.
A Comparison of Power Spectral Estimates: II. Long Period Micropulsations
1973 Ann. Fall Mtg. of the Am. Geophys. Union, San Francisco, Calif. (10-14 December 1973)

TECHNICAL REPORTS
JULY 1972 - JUNE 1974

CAGE, A. L., CAPT., and ZAWALICK, E. J.
A Discussion of the Geomagnetic Indices Kp and ap, 1932 to 1971
AFCRL-72-0693 (27 November 1972)

CARRIGAN, A. L., and CASTELLI, J. P. (Iono. Phys. Lab.)
Solar Activity in McMath Region 10789 During Disk Passage, 12 to 15 June 1970
AFCRL-72-0669 (16 November 1972)

COHN, A., RUBIN, A. G., and BESSE, A. L.
The Hydrogen Dissociation Laser
AFCRL-TR-74-0110 (5 April 1974)

FOUGERE, P. F.
Simultaneous Solar Wind Observations
AFCRL-TR-73-0044 (12 January 1973)

FUKUI, K.
Use and Processing of Nuclear Emulsions as Particle Detectors
AFCRL-72-0613 (12 October 1972)

GALLAGHER, C. C., and LEVINE, M. A.
Design and Construction of Tormac IV, A Toroidal, Bi-Cusp Plasma Containment Device
AFCRL-TR-74-0122 (6 March 1974)

GOLD, R. E. (Univ. of N. H.), PEACOCK, D. S. (Univ. of Denver, Colo.), SHEA, M. A., and SMART, D. F.
An Extended Set of Cosmic-Ray Variational Coefficients
AFCRL-TR-74-0063 (4 February 1974)

HENDL, R. G. CAPT., and SKRIVANEK, R. A.
Statistical Analysis of Shortwave Fadeout Occurrence for the Years 1955 to 1969
AFCRL-TR-73-0385 (28 June 1973)

KATZ, L.
Galactic Cosmic Ray Considerations
Envmt. Spec. in Support of the Def. Satellite Comm. Sys., AFCRL-TR-74-0182 (8 April 1974)

KELLEY, J. G.
Accidental Coincidences in the Electron Spectrometer on Satellite OVI-13
AFCRL-72-0592 (10 October 1972)

KELLEY, J. G., and SELLERS, B. (Panametrics, Inc., Waltham, Mass.)
Specific Ionization in the Polar Atmosphere Due to Precipitating Heavy Particles
AFCRL-TR-73-0672 (2 November 1973)

KNECHT, D. J.
The Geomagnetic Field (A Revision of Chapter 11, Handbook of Geophysics and Space Environments)
AFCRL-72-0570 (26 September 1972)

LEIBY, C. C., JR., and RYAN, T. G.
Thermophysical Properties of Thermal Energy Storage Materials – Aluminum
AFCRL-TR-73-0421 (18 July 1973)

MAPLE, E.
Micropulsation Observations of the Auroral Oval Boundary
AFCRL-TR-74-0054 (28 January 1974)

MC NULTY, P. J. (Clarkson Coll. of Technol., Potsdam, N. Y.), and FILZ, R. C.
Interactions of Energetic Neon with Emulsion Nuclei
AFCRL-72-0607 (12 October 1972)

PAVEL, A. L., CAPT.
SCATHA Satellite
Envmt. Spec. in Support of the Def. Satellite Comm. Sys., AFCRL-TR-74-0182 (8 April 1974)

PAZICH, P. M.
Ground-Based Magnetometer Measurements
Chap. 6 in Envmt. Spec. in Support of the Def. Satellite Comm. Sys., AFCRL-TR-74-0182 (8 April 1974)

PODSIADLO, R. T.
An Objective Baseline for Flare Prediction
AFCRL-72-0414 (14 July 1972)
Correlations of Solar and Geophysical Parameters – Shortwave Fadeouts and Solar Optical Features
AFCRL-TR-73-0411 (12 July 1973)

QUINLAN, K. P.
Photosynthetic Energy Conversion: The Effect of Oxygen on the Light-Induced Proton Uptake Capability of Chloroplasts
AFCRL-TR-74-0024 (10 January 1974)

RADOSKI, H. R.
Coupled Hydromagnetic Modes: Initial Value Problems
AFCRL-72-0747 (29 December 1972)
A Mechanical Analogue for the Study of Hydromagnetic Propagation in the Magnetosphere
AFCRL-TR-73-0278 (30 April 1973)

RADOSKI, H. R., FOUGERE, P. F., and ZAWALICK, E. J.
A High Resolution Power Spectral Estimate: The Maximum Entropy Method
AFCRL-TR-74-0088 (13 February 1974)

ROTHWELL, P. L., and KATZ, L.
Enhancement of 0.24-0.96 MeV Trapped Protons During the May 25, 1967 Magnetic Storm
AFCRL-72-0416 (17 July 1972)

ROTHWELL, P. L., and MOOMEY, W. R., 2ND LT.
Calibration of a Magnetic Spectrometer Designed to Measure 0.1- to 1.0-MeV Electrons in Space
AFCRL-72-0710 (6 December 1972)

SEN, H. K., PRASAD, B., and BAKSHI, P. M., KALMAN, G. (Boston Coll., Mass.)
Nonlinear Theory of Electron Oscillations of a Collisionless Plasma in a Uniform Magnetic Field
AFCRL-72-0526 (5 September 1972)

SHEA, M. A.
Ground-Based Cosmic-Ray Instrumentation Catalog
AFCRL-72-0411 (17 July 1972)

SHEA, M. A., and SMART, D. F.
Theoretical Response of the Deep River Neutron Monitor to an Anisotropic Solar Cosmic-Ray Event
AFCRL-72-0456 (28 July 1972)
Tables of Asymptotic Directions, Cutoff Rigidities, and Reentrant Albedo Calculations for Palestine, Dallas, and Midland, Texas
AFCRL-TR-74-0159 (26 March 1974)
Editors, *Compilation of Solar Particle and Interplanetary Measurements Acquired During the Campaign for Integrated Observations of Solar Flares (CINOF)*
AFCRL-TR-74-0271 (19 June 1974)

SMART, D. F.
Data Acquired by the JHU/APL Solar Particle Experiments on Explorers 41 and 43 During June 1972
Compilation of Solar Particle and Interplanetary Meas. Acquired During the Campaign for Integrated Obsns. of Solar Flares (CINOF), AFCRL-TR-74-0271 (19 June 1974)

SMART, D. F., and SHEA, M. A.
Summary of Solar Particle Events During CINOF
Compilation of Solar Particle and Interplanetary Meas. Acquired during the Campaign of Integrated Obsns. of Solar Flares (CINOF), AFCRL-TR-74-0271 (19 June 1974)

STROSCIO, M. A., 1ST LT.
Positronium: A Review of the Calculations
AFCRL-TR-74-0248 (3 June 1974)

TURTLE, J. P., SILVERMAN, S. M., and MULLEN, E. G.
Geopole Observatory Data
Chap. 7 in Envmt. Spec. in Support of the Def. Satellite Comm. Sys., C. P. Pike, Compiler, AFCRL-TR-74-0182 (8 April 1974)

WARD, F.
The Latitudinal Motion of Sunspots and Solar Meridional Circulations
AFCRL-72-0499 (21 August 1972)

WARD, F., CARNEVALE, R. F., and HENDL, R. G., CAPT.
The Construction and Testing of a Pair of Matched Solar Telescopes
AFCRL-TR-73-0181 (14 March 1973)

WHITE, M. L.
A Physical Mechanism for the Production of Spot Related Solar Prominences
AFCRL-TR-74-0043 (18 January 1974)

YATES, G. K.
OV5-6 Satellite Measurements
Envmt. Spec. in Support of the Def. Satellite Comm. Sys., AFCRL-TR-74-0182 (8 April 1974)

YATES, G. K., KATZ, L., and BLAKE, J. B., PAULIKAS, G. A., VAMPOLA, A. L. (The Aerosp. Corp., Los Angeles, Calif.), SELLERS, B., HANSER, F. A. (Panametrics, Inc., Waltham, Mass.)
Energetic Particle Measurements Aboard OV5-6 and OV1-19 Satellites
Proc. of COSPAR Symp. on Solar Particle Event of Nov. 1969, AFCRL-72-0474 (11 August 1972)

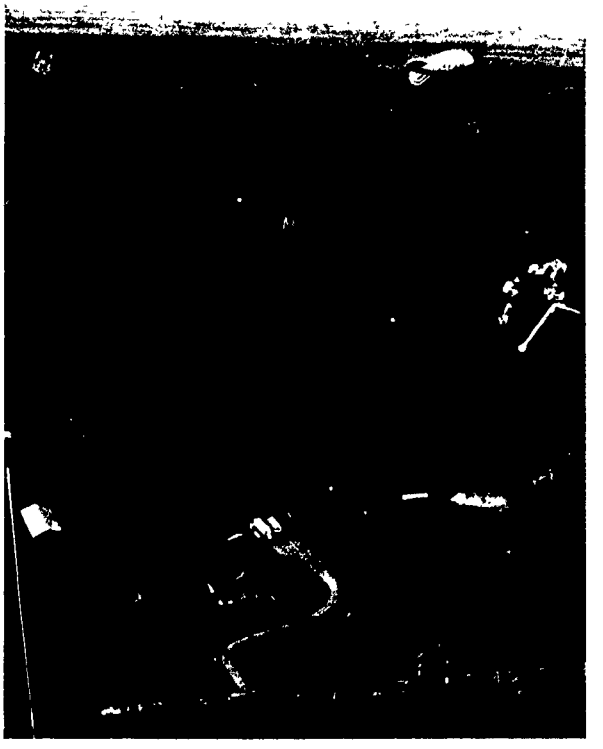

An aerial view of the AFCRL site in Minnesota used for the 1973 experiments. The site was chosen for the horizontal uniformity and unobstructed fetch it offered for boundary layer studies.

VI Meteorology Laboratory

Among the many factors which affect the efficiency and safety of man's daily activities, weather is a very important one. In carrying out its responsibilities, the Air Force, like other organizations, must contend with the impact of weather phenomena on the design, development, and operation of its systems.

It is important that some Air Force systems be operable in virtually all types of weather. To accomplish this objective, the Air Force must act on two fronts. Its first responsibility is to design systems that are operable over a broad range of weather conditions. The second is to supplement these designs by modifications of the weather affecting the success of the operations. Of course, there are many other Air Force activities which can be delayed on the basis of a weather observation or a weather prediction. But whether the deficiencies are in data needed in design, methods for significantly modifying critical weather elements, or techniques for improving observations or predictions, the need for an Air Force program in meteorological research and development has been clearly established. The major responsibility for this program rests with AFCRL's Meteorology Laboratory.

During the period covered by this report the program of the Meteorology Laboratory included the following efforts: research to improve short-range forecasting of terminal weather conditions; the modeling of large-scale atmospheric circulations; the definition of turbulent transport processes in the atmospheric boundary layer; the application of data from meteorological satellites to analysis and forecasting; and

the development of techniques for the processing and display of weather radar data to facilitate the study of thunderstorm development and motion. The program also included the development of techniques of fog dissipation and techniques for the remote recognition of potentially hazardous areas of electrical activity in convective storms.

While much of the instrumentation developed by the Meteorology Laboratory has been in support of its in-house research investigations, other instrumentation has been and is being developed for eventual use at stations of the Air Weather Service and at the Air Force's test ranges. Instrumentation in the latter category includes radiosondes with improved humidity sensors, dropsondes for determining winds below an aircraft, and new devices for the measurement of ceiling and visibility.

A significant effort has been devoted to the definition of the physical nature of the cloud and precipitation particles through which test nosecones have been flown. In another effort techniques are being developed to modify the aerospace environment through the use of artificial aerosols.

Although all of the permanent quarters of the Meteorology Laboratory are located within 15 miles of Hanscom AFB in Bedford, Massachusetts, climatic factors and the existence of unique support facilities elsewhere have led Laboratory scientists and engineers to conduct field programs at distant locations, ranging from New Hampshire to Hawaii and Minnesota to Florida. These programs have been successful because of the fine support and collaboration received from many Department of Defense, National Oceanic and Atmospheric Administration, National Aeronautics and Space Administration units and a team from the United Kingdom.

SHORT-RANGE FORECASTING

It is inevitable that operational demands for improved weather warnings and forecasts will continue to be concerned primarily with rare weather events having small space-time scales. The reason, of course, is that most Air Force systems are designed, to the extent considered practicable, to operate without serious degradation over the usual range of weather conditions. The unusual or rare events that do have serious impact on operational effectiveness and safety are difficult to resolve because they typically occur on a scale that is much smaller than the existing spacing of weather observing stations. Thus, a prerequisite for progressive improvement in the detection and short-range prediction of significant local weather events is an observational capability that is commensurate in space and time with a scale of the significant weather activity. The technology necessary for a substantial upgrading of the present observing system has advanced very rapidly in recent years and can be exploited extensively if the benefits justify the cost of the system components.

A systematic assessment of the practical operational benefits to be derived from automated mesoscale observing and forecasting techniques is the central objective of an experimental program undertaken by the Meteorology Laboratory. A fully automated field test facility has been established for this purpose in the vicinity of Hanscom AFB, Massachusetts. The Hanscom mesoscale observing network consists of a dense network of remote surface weather stations, an instrumented tower and a digital weather radar capability. The overall program includes: the development and evaluation of weather sensors suitable for use in completely automated surface weather observing systems; the development of methods of automated data proc-

essing and display for real-time operational needs; development of improved methods of short-range (0- to 3-hour) terminal weather forecasting based upon automated Mesonet observations, and operational field tests to explore the practical value of advanced observing and forecasting systems.

THE MESONET: The network of automated observing stations extends over a radius of 50 km from Hanscom. The 25 remote stations have a variable spatial density ranging from about 1 km near Hanscom to roughly 15 km at the outer edge. The individual sensors automatically report visibility, wind direction and speed, temperature, dew point, and precipitation rate. In addition, vertical profiles of these measurements, except precipitation, are reported from an instrumented tower located 600 meters from the central runway at Hanscom. The other important features of the observing network are the two radars. The FPS-77 surveys the entire Mesonet and well beyond. The vertically pointing TPQ-11 provides a continuous record of cloud structure directly overhead.

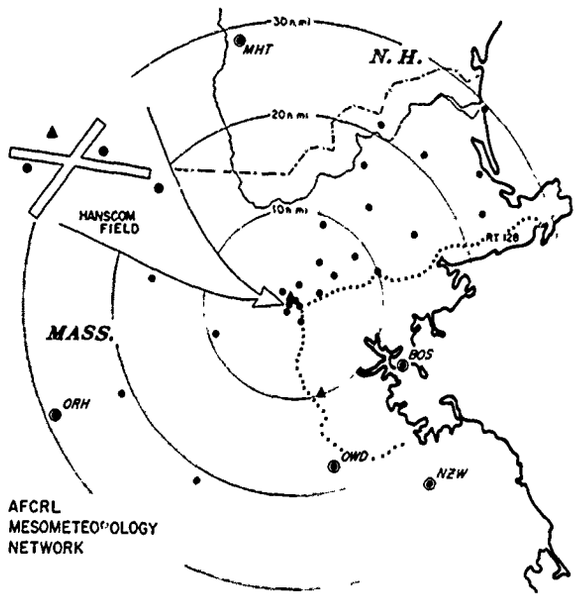

The Hanscom Mesonet: Small solid circles denote locations of surface weather stations. The triangle in the exploded view shows the location of the instrument tower at Hanscom AFB. Large circles give locations of conventional observing stations.

The basic functions of the Mesonet—collecting, processing and displaying the data—are controlled by a computer. All sensors in the network are scanned once every 10 seconds, with decisions as to the mode of processing the responsibility of the human operator. For example, station data can be displayed as maps of either 1-minute or 5-minute running averages.

THE STATIONS: Sensors used in the Mesonet are usually commercially available devices which were selected after careful testing and intercomparison rather than those used by the weather services for standard observations. They are packaged in a rugged and weatherproof station mounted on a telephone pole 25 feet above the ground. This design makes the station easily movable, reasonably vandal-proof, and readily accessible from a cherry-picker for maintenance.

The device used to measure visibility is the most radical departure from standard instrumentation. Instead of the conventional airport visibility instrument which senses transmittance in paths in excess of 200 feet, a short-path length forward scatter meter was developed for use in the Mesonet. Several years of experimentation have shown it to be a rugged and extremely accurate instrument with exceptional calibration stability and capable of high resolution over a very broad range of visibility.

THE RADAR: An important part of the Mesonet forecast experiments is the introduction of digital radar information. During periods of precipitation an FPS-77 weather radar transmits radar data by microwave to a radar pulse integrator and

then into the Mesonet computer. Periodically, digital maps representing range-normalized radar reflectivity are printed out and made available to forecasters and researchers. These maps are proving useful in forecasting onset and ending of periods of low visibility during heavy precipitation. Studies are under way to relate the reflectivity to rainfall rate, visibility, and wind gusts for particular application to forecasting severe thunderstorm conditions. Techniques are being developed to obtain the motion of precipitation patterns automatically from successive digital maps and produce guidance forecasts as additional computer output.

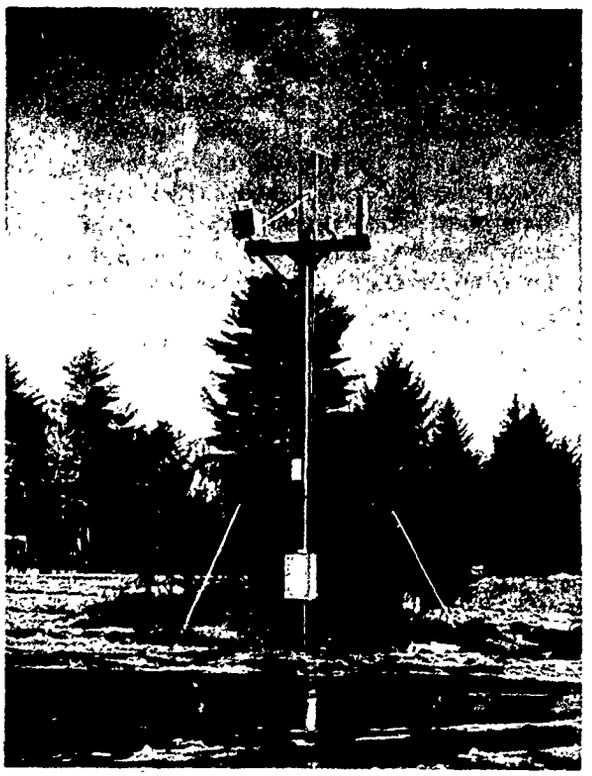

A Mesonet Station — The sensors from left to right measure visibility, wind direction and speed, temperature and dew-point, and precipitation rate.

FORECASTING TECHNIQUE DEVELOPMENT: The rationale for the development of objective short-range forecasting techniques using Mesonet observations is twofold. On the one hand, techniques which will make the best use of both the forecaster's skill and the computer's speed and memory are being sought. Alternatively, consideration is being given to the development of fully automated objective procedures which would eliminate the role of the human forecaster in short-range terminal forecasting. An evaluation of the accuracy of techniques developed herein compared to the skill of the subjective forecaster not provided with objective guidance will make available to Air Weather Service planners substantive information to weigh the alternatives of manned versus unmanned base weather stations as manpower authorizations continue to be reduced.

The Hanscom Mesonet is primarily a surface network. All observations are made close to the ground with the exception of the radar and instrumented tower observations. Because of this limitation, the focus in technique development has been towards statistical models rather than numerical mesoscale models which would require detailed information throughout the lower few thousand feet of the atmosphere. Also, deterministic numerical models have not advanced to the point where sensible weather parameters such as cloud ceiling and visibility can be accounted for with sufficient accuracy or in a manner which yields timely short-range (0-to 3-hour) predictions which would be operationally useful to forecasters and/or users.

Shortly after the Mesonet forecasting experiments started in September 1972, a single-station conditional climatology model was formulated and parameterized from a historical set of prevailing visibility observations at Hanscom. The objective stochastic model was refined after the first year's operation of the network using the continuous data collected during forecast episodes. Since its inception the output of

the model has been provided to the subjective forecaster for guidance in preparation of his short-range visibility forecasts. It also has been evaluated as a control technique in the forecast experiments.

Short period fluctuations in airport visibility result primarily from the translation of mesoscale disturbances, and from growth and decay within the disturbances. Technique development thus far has concentrated on translation. Procedures have been formulated to deduce the motion vector due to translation from an analysis of time-lag correlation data for selected pairs of stations in the Mesonet. The motion vector, so determined, would then identify the locations "upstream" from which future (up to three hours later) airport visibility will be translated. Procedures of optimum interpolation determine the forecast value at the locations from surrounding mesonet observation points, and an analysis of the spectrum of the current and recent visibility field in the network will define inputs to the visibility probability forecast procedure. Other procedures which determine forecast values from regression equations relating observations from individual stations in the network to the runway observations based on space- and time-lag correlations are also being evaluated. A critical operational problem, the initial onset of severely reduced visibility, is not handled well by either of these procedures and will be given special consideration during the next year.

Radiation (ground) fog, very common to Hanscom and many other inland airfields located in valleys, presents a special detection and prediction problem because of its highly variable and patchy nature. Since such fogs form on clear and calm nights, there is generally little organized motion or translation to the fog. As a result, technique development is concentrating on the formulation of stepwise regression equations which relate space-smoothed predictors combining the effects of two or more observation points to runway visibility. Consideration is also being given to temperature measurements just inches off the ground near the runway to measure radiation flux during the fog formation and dissipation periods.

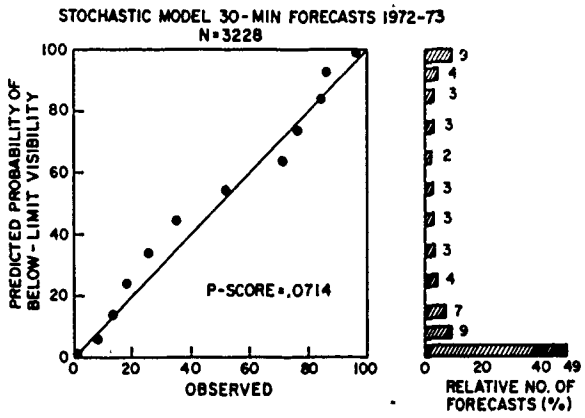

Experimental Forecasting Results — The probability of below limit visibility predicted by the stochastic model versus the corresponding frequency of occurrence.

The goal in forecast technique development is to assess the practical limitations of fully automated forecast systems as compared to a man-machine mix or a totally manual forecast system. While it would be unrealistic to expect that the Hanscom Mesonet results would apply precisely to other locations with markedly different climatic or local influences, they would establish guidelines of general validity.

ATMOSPHERIC MODELING

The atmosphere is a complex fluid system capable of sustaining motions on a whole spectrum of time and space scales from very short, rapidly moving sound waves to ultra-long, quasi-stationary planetary scale waves. There are important nonlinear interactions or feedbacks among many of these differing scale sizes such that changes

on one scale affect both longer and shorter scales and, in turn, are affected by both these and other scales.

Progress in understanding such a large and complex nonlinear system, and therefore improved predictability, largely depend on our ability to formulate valid, but much simpler, analogues (models) of the complete system. Ideally, such models should take into account the important parameters and should be amenable to controlled experimentation. Mathematical models of the atmosphere, based upon the laws of fluid dynamics, meet these requirements and are widely used in atmospheric prediction. There are, however, some problems with mathematical models which cause the time development of the model to diverge from the time development of the real atmosphere and therefore degrade the quality of the prediction. The goal of AFCRL's efforts in mathematical modeling is to minimize the sources of model error, which include inadequate representation of relevant physical processes, incomplete description of the initial state of the prognostic parameters, and imperfect representation of differential equations by finite-difference approximations.

RESEARCH ON NUMERICAL PROCEDURES: The current practice of all operational numerical weather prediction groups makes use of the space network approach in the solution of the system of equations which constitute the mathematical model. In this approach, observations of the dependent variables are interpolated onto a regular array of gridpoints in space, and differential quantities are represented by finite difference approximations. Since the entire system of equations must be solved at each gridpoint before the variables can be extrapolated in time, the limits of the capacity of the computer and the time available for the forecast restrict the number of gridpoints in the network. Naturally, the fewer the number of gridpoints, the greater the growth of error due to truncation and lack of resolution.

If there are no restrictions in computer capacity and time, a straightforward method of improving the quality of the model forecast would be to reduce the distance between gridpoints. In principle, the only limitation is that the grid distance must not be smaller than some critical value below which the underlying model assumptions are no longer valid. Another approach, and in theory a more efficient one, is to increase the order of accuracy of the finite difference approximation. For example, experience in simple advection-type model studies has shown that for satisfactory overall results, second-order accuracy schemes require about 20 gridpoints per wavelength, while fourth-order accuracy schemes require about ten.

Current operational large-scale models such as the Macro-scale Model of the Air Force Global Weather Central at Offutt AFB, Nebraska, have a grid distance of about 400 km. With a second-order scheme, these models can confidently handle only atmospheric waves with wavelengths longer than about 8,000 km. In the real atmosphere, waves associated with day-to-day weather phenomena have wavelengths between 3,000 and 6,000 km. From the point of view of accuracy, it is therefore desirable either to halve the currently adopted grid distance or to increase the order of accuracy of the numerical schemes.

At AFCRL, we have conducted comparison case studies using both approaches. Results show that the latter is more desirable because, for example, an overall 8 percent reduction in the error field of a three-day forecast can be achieved with substantial changes in neither time nor storage requirements in the computer. For the former to achieve this, not only does the computer time requirement have to be increased by a factor of 10, but also a fourfold increase in computer storage requirement is needed.

NOISE AND THE TREATMENT OF DIFFUSION: A fundamental problem in atmospheric modeling arises from a two-headed dilemma: noise and subgrid-scale processes. Noise in solutions of numerical models arises from errors in the initial data, from model inadequacies, from improper treatment of both real and contrived boundaries, and from inadequate resolution of important components of the system. If noise is not controlled in the numerical solution, it will not only produce inaccurate forecasts and limit the time range for which forecasts can be made, but may also cause the solution to become unstable and completely meaningless.

Noise in the real atmosphere is kept under control by small-scale diffusion and viscous dissipation, which is the final stage in the transfer of kinetic energy from larger to smaller scales. In numerical modeling, this diffusion process which occurs in the atmosphere on a microscopic scale must be represented in the model or parameterized in terms of scale sizes which are many orders of magnitude larger. While it may help somewhat to reduce the grid size of the model, thus increasing the resolution of smaller scales of motion, we can never expect to treat atmospheric diffusion explicitly no matter how much we reduce the grid size. Furthermore, as has already been indicated, we are limited by time, economics and machine capacity in the extent to which grid size can be reduced. Even where the capacity of the computer permits a halving of the grid distance, the increase in computer cost is at least a factor of 16 for a model with three space dimensions. Thus, the parameterization of diffusion in numerical models of the atmosphere is required to accomplish the representation of physical diffusion which takes place in the atmosphere as well as the control of numerical noise in the model. The principal shortcoming of conventional methods of representing diffusion in large-scale NWP (Numerical Weather Prediction) models, those that are operational as well as general circulation models, is that the meteorologically important cyclone-scale waves in the model are damped along with the computationally produced two-grid-interval noise. As a consequence, the predictions are too smooth and fail to forecast adequately newly developing disturbances. What is needed is a means of representing viscous dissipation that is very strong for the short wavelength noise and very weak for the larger, meteorologically important waves.

We have devoted considerable attention to this problem and have devised a digital filter which appears to have just the right properties to control noise, represent atmospheric diffusion, yet not suppress physically meaningful information in the model. The filter is actually a flexible sequence of filters varying from three-point operators in one dimension when applied near boundaries to high-ordered operators in the interior of the grid intervals. The filter has now been applied in a variety of numerical models varying from fine-mesh limited area models and channel models with solid walls to large-scale general circulation models. In all cases the filter behaves as anticipated: it controls the growth of noise and maintains computational stability and at the same time preserves the proper distribution of energy among the various scale sizes in the model as compared with observed atmospheric spectra.

FINE-MESH MODELING: The shortest wave that can be resolved in a numerical model has a length of two grid intervals. However, such waves and even those that are four to five times longer are poorly represented in numerical models, partly as a result of truncation and numerical procedures and partly as a consequence of the fact that the basic observational network is itself rather coarse. Fronts and other phenomena directly associated with clouds and precipitation occur on scale sizes which are poorly

handled by large-scale numerical models. This difficulty can be alleviated, if not circumvented, by reducing the grid size. However, as we have already indicated, this approach is very costly in computer time and is impractical for a global or hemispheric model. Nevertheless, over limited areas, this approach is both feasible and appropriate, especially for regions with greater than average observational density.

A new and serious difficulty is introduced in trying to limit the area of solution —namely, the treatment of the artificial, internal, lateral boundaries. For certain relatively simple models the appropriate physical boundary conditions are well understood and their numerical treatment presents no serious problem. Unfortunately, this is not generally the situation in practice. Therefore, means must be devised to prevent the solution from becoming contaminated by noise. We have devised a new kind of high-ordered interpolation procedure for handling the boundary problem. We have adopted the customary procedure of carrying out a large-scale solution of the model with a coarse network covering a global or hemispheric domain and using the coarse mesh solution to supply boundary information for the fine-mesh domain. It is in the process of interpolation from the coarse to fine mesh that we make use of our high-ordered interpolation which is based upon the concept of restoring information which is lost in the process of two-point linear interpolation. The effectiveness of the high-ordered interpolation is illustrated in the accompanying figures which show comparative solutions for the zonal wind at a typical lower level (level 14 is at a pressure of 812.5 mb) in a multi-level, primitive equation fine-mesh model. The solutions are obtained from identical models with identical initial conditions. The only difference between them concerns the method of interpolation from the coarse-mesh solution to the fine-mesh boundaries, which produces a dramatic difference in the smoothness of the results.

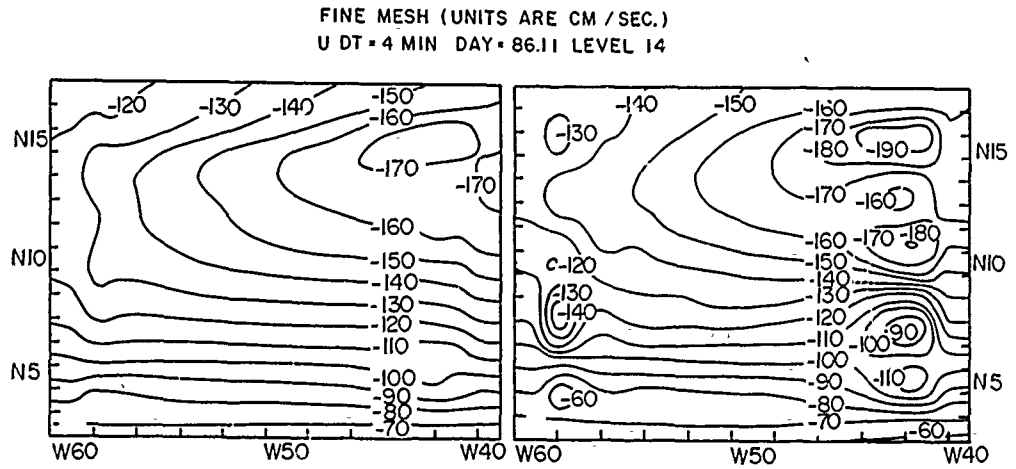

Solutions for zonal wind (u) at level 14 after 1,000 4-min. time steps. Boundary information is supplied by (a) 8-point interpolation; (b) 2-point linear interpolation. Units are centimeters per second. Contours indicate winds from the east.

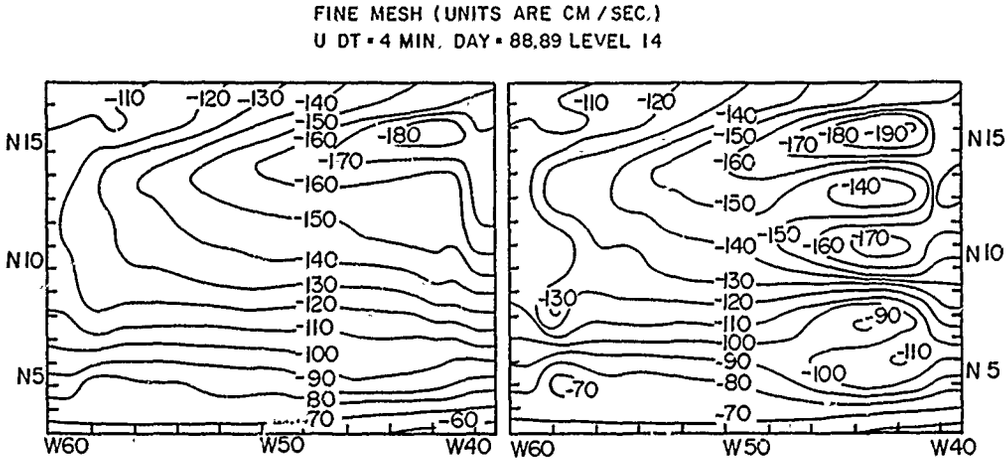

Solutions for zonal wind (u) at level 14 after 2,000 4-min. time steps. Boundary information is supplied by (a) 8-point interpolation; (b) 2-point linear interpolation. Units are centimeters per second. Contours indicate winds from the east.

ATMOSPHERIC BOUNDARY LAYER

The atmospheric boundary layer is that portion of the atmosphere where the frictional effects of the earth's drag on the air's motions, and turbulent mixing between the surface layers and the upper atmosphere are as important as the pressure gradient forces, and the earth's rotation forces are in the "friction-free" atmosphere. It is a layer that drastically changes character from a deep (1-3 km) well-mixed, turbulent layer during the daytime to a shallow (0.2-0.5 km) decoupled layer during nighttime. Until recently, research studies of the boundary layer have been restricted to the so-called surface layer, the first 40 ( ) meters of the atmosphere. Much has been learned about the characteristics of this layer with a concomitant increase in our ability to improve performance of Air Force systems and operations largely confined to, or strongly affected by, surface layer turbulence. Within the last five years, however, research efforts have been directed towards an understanding of the physics of the entire boundary layer.

Many Air Force systems are operated within the boundary layer and are frequently dependent during the design stage and eventual operational stage on the degree to which meteorological parameters in the boundary layer can be specified or predicted. In addition, those systems which operate in the free atmosphere above the boundary layer frequently require weather forecasts for periods greater than 24 hours. For such forecasts to be effective, the numerical weather forecasting models used in operational forecasting must incorporate the effects of processes occurring within the planetary boundary layer.

RESEARCH RESULTS: In 1973 a series of experiments was conducted in Minnesota to obtain detailed data on turbulent transport of momentum and heat throughout the boundary layer. This was a joint program involving research teams from the Meteorology Laboratory and the Aerospace Instrumentation Laboratory of AFCRL and the Meteorological Research Unit, RAF, Cardington, England. The British scientists had developed a technique

for mounting turbulent wind and temperature sensors on the tethering cable of large captive balloons. Earlier joint experiments had established that balloon movements did not significantly affect the measurements by the cable-mounted sensors. For the Minnesota experiments, five of the British probes were flown at heights ranging from 200 to 4,000 feet. The Meteorology Laboratory team provided detailed measurements of the turbulent transport processes in the surface layer with tower-mounted sensors. The Aerospace Instrumentation Laboratory team provided and operated the captive balloon, a 45,000 cubic foot balloon identical to the barrage balloons flown over London during World War II, one which displays exceptional aerodynamic stability and free lift. Detailed analyses of the resulting data will be directed towards a search for similarity features of the turbulent exchange processes and for relationships between boundary-layer processes and the forcing conditions imposed by the underlying surface and the free atmosphere above the boundary layer. At present, data reduction efforts have been devoted to establishing proper mathematical filters to obtain statistically stable descriptions of the transport processes. This effort has been just recently successfully completed and the similarity analyses are under way.

Captive balloon used in Minnesota being prepared for launching. Inflation of the balloon is done under near-calm conditions. After inflation, balloon can be tethered safely in winds up to 40 mph.

An effort parallel to this experimental study has been the development of a numerical model of the planetary boundary layer. This is a model designed to predict actual turbulent parameters, given the large-scale imposed boundary conditions. The opportunity for interplay between the experimental program and the modeling effort is self-evident. However, the model has far-reaching practical value in itself since it provides a means to specify turbulent processes under a wide range of conditions without the need for frequent and expensive field experiments.

Finally, a new experimental technique for probing the boundary layer with acoustic radars is being pursued. Two types of radar are being used One detects regions of fluctuating temperature activity to heights of about 2,000 feet. The other, with a height range of 600 feet, measures Doppler frequency shift of the scattered acoustic energy which is directly proportional to the wind speed of the scattering volume. These remote probe devices show outstanding potential for either research or practical application purposes and are being thoroughly studied at the present time.

Mounting of a British turbulence probe and its associated electronics on the tethering cable, Minnesota experiments, 1973. Signals from the five probes were radioed to the ground where they were recorded and processed by AFCRL's computer-controlled data acquisition system.

AIR FORCE APPLICATIONS: In April of 1973, the Air Force Flight Test Center, Edwards AFB, California, formally accepted a computer-controlled data acquisition system to measure wind and temperature variations along the 15,000-foot runway at Edwards. The system is used by AFFTC to obtain environmental data in support of various aircraft performance tests conducted there. Design, construction, and installation of the system was accomplished by AFCRL's boundary-layer scientists. Their experience in boundary-layer experiments was directly applicable to such problems as determination of number of stations to observe significant variations along the runway, data handling techniques, design of accurate, dependable sensors, etc.

At the present time, in-house scientists are deeply committed to the ARPA/RADC Compensated Imaging Program, a program to develop techniques to compensate for atmospheric distortion of images of objects in outer space. The AFCRL input to this program is to provide expertise in observation of temperature fluctuations within the boundary layer since the near-field turbulence in the vicinity of observatory telescopes is responsible for roughly 80 percent of the atmospheric distortion on the average. The program will use tower-mounted temperature sensors as well as the back-scatter acoustic radar mentioned earlier. Observations are scheduled for the ARPA Maui Optical Site (AMOS) in Hawaii, as well as the RADC observatory at Griffiss AFB, New York.

SATELLITE METEOROLOGY

During the last two years, Air Force interest in satellite research and development has steadily expanded. This reflects both the rapid increase in routine data collected from military meteorological satellites and the application of these data to an expanding set of Air Force problems. There is, in addition, the long-term expectation that satellite measurements can replace not only many conventional meteorological measurements, but also yield data not available by other means. The confluence of technological expectations and military requirements has resulted in considerable pressure to expand the scope of satellite meteorology research and applications. This has led to a steady proliferation of activities, some of which are discussed in this report.

DIRECT READOUT DATA OPTIMIZATIONS: The capability to receive satellite data directly at remote sites continues to receive high interest in the Air Weather Service. Direct readouts from both NOAA and the recently declassified Defense Meteorological Satellite Program (DMSP) vehicles are used at various Air Force and Navy sites. Developments in both hardware and software have contributed to the improved utilization of the data from these satellites.

Hardware changes were needed to accommodate the new NOAA operational satellites introduced late in 1972. The switch from vidicon to scanning radiometer sensing and the provision for the transmission of both video and infrared data during daytime made modification of ground equipment desirable. Electronics were developed which give the best image possible within the limitations of the recorder marking capabilities.

The transmission of alternating scans of visual and infrared data "confused" existing recorders, which tried to phase both portions of the signal under certain conditions. In addition, it was difficult for the operator to positively select between the visual or infrared image. A stripped-down model of the device that adjusts for the signal range also corrects the scanning difficulties. This model has been purchased by the Air Weather Service. These units contain conversion modules which can be predefined for various satellites, sensors and/or enhancement schemes.

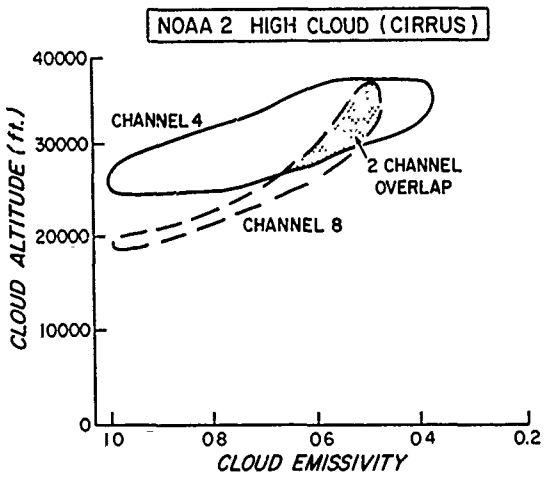

Model clouds corresponding to radiances observed by a Vertical Temperature Profile Radiometer on board the NOAA 2 satellite on September 17, 1973. Channels 4 and 8 measure atmospheric and terrestrial infrared radiation at two different wavelengths. Only a small subset of the array of model clouds satisfies both channels. Further discrimination is achieved by the use of more than two channels. On this particular day, independent observations had cirrus clouds at 30,000 feet.

In response to complaints from field sites about shortcomings in the DMSP overlay grids, an investigation uncovered significant errors, and a new set of grids for both standard and expanded displays was generated. These grids are now used at all DMSP local read-out sites. For the NOAA satellite data, more accurate grids were also generated. In addition, a program was developed to prepare grids with geographic features superimposed. Approximately 100 grids are needed for each station for each satellite. A set was prepared for Patrick AFB to support the missile and space programs, and Air Weather Service has requested sets for eight other key stations around the world.

WATER AND ICE CONTENT OF CLOUDS: In support of weather erosion programs, existing satellite measurements are being analyzed to determine the ice and water content of clouds. Substantial progress has been made in one aspect of the program—namely, the estimation of the total ice content of cirriform clouds. The method requires measurements from a Vertical Temperature Profile Radiometer (VTPR) on board a satellite. The method has been tested directly by aircraft observations underneath satellite passes. All VTPR instruments measure various wavelengths of infrared radiant energy from the earth's surface and atmosphere. The ordinary application of the VTPR is an inversion of the radiances for clear or partly cloudy areas to estimate the vertical temperature profile.

The new application combines observed radiances for a cloudy area with a known temperature profile in order to estimate cloud characteristics.

The first step in the method is to select the best cloud from an array of model clouds. Each cloud is characterized by two parameters, a cloud-top altitude and a cloud emissivity. The emissivity is the fraction of infrared radiation which is absorbed and reemitted by the cloud particles. It is also the fractional extent to which the cloud behaves as a black body. When more than one VTPR channel is considered, a joint estimate of cloud altitude and emissivity is possible.

During the winter and spring of 1974, ten successful aircraft flights were obtained in clouds underneath satellite passes. The primary aircraft were C-130 models operated by the Air Force Special Weapons Center for AFCRL. These aircraft are equipped with optical array spectrometers to measure the size distribution as well as the ice and water content of cloud particles. The aircraft flights confirmed the ability of the VTPR method to estimate cloud altitudes and the total ice content of cirriform clouds.

THE MC IDAS SYSTEM: A Man-computer Interactive Data Access System (McIDAS) was delivered to AFCRL in June 1974. With this system an analyst at a TV console exercises judgment in selecting imagery and has the capability to rapidly process this imagery with a digital computer. The analyst selects the processing operations to execute, and the computer does the analysis. This analysis can be done on full resolution digital data and returned to the analyst for his evaluation and use in the form of TV display, print-out, or magnetic tape.

Data from a live or taped source are fed through a computer to a digital disk which stores all information to 8-bit accuracy. The key to the system is the TV processor, which controls many functions in the interaction

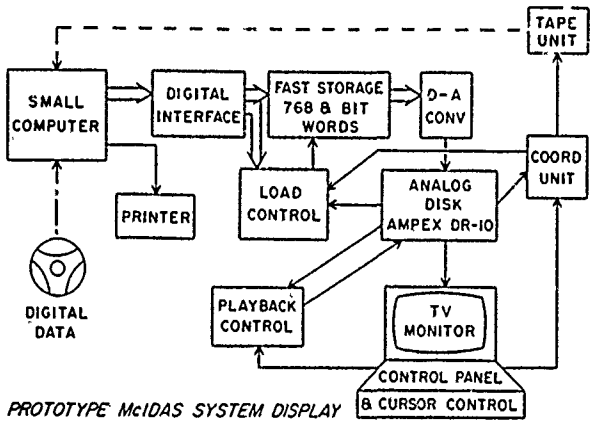

Simplified schematic of McIDAS system. It is a system which allows an analyst at a TV console to combine experienced judgment in selecting and processing meteorological satellite imagery.

between the digital and analog (TV) domains. The system establishes a unique relationship between the location of a piece of information on the digital disk and the TV disk which feeds a picture into the TV monitor. The operator selects a point or area on the TV screen for processing, and selects a processor function from a teletype keyboard. The results are recorded, as appropriate, on the TV, line printer or digital tape.

The system has several uses: McIDAS assigns geographic coordinates to the data very efficiently and accurately by adjusting the nominal satellite orbital and attitude parameters with the known position of landmarks. Because the system permits magnification of the image to the point where each image scan line and picture element occupy many TV scan lines and elements, the location of a landmark can be specified perfectly within the image system. This provides the basis for the accurate measurement of cloud motions, from which winds can be inferred. Once the geography is established and a series of pictures loaded on the digital disk, winds can be computed very rapidly.

Once the navigation for a particular day has been completed, the navigation information resides permanently within the computer memory and can be recalled any time data from that day are to be examined. A one-stroke command can be used to display the latitude and longitude of any point on the picture, or another command can be used to position a cursor over a selected geographic location.

Animated sequences of up to 250 frames can be made and displayed at any rate from 1 to 30 frames per second.

Various black-and-white or color enhancements can be generated in response to the input signal level. These enhancements can be saved for future reference and an animated sequence can be enhanced in a selected format by simply directing the comment to one frame.

Data can be degraded in the system if, for example, one is interested in experimenting with relationships between image resolution and information, or is interested in g ss cloud features over a large area.

Brightness or temperature distributions can be generated for an area of a size and shape defined by the operator.

Although it has been designed for the GEOS satellite, McIDAS can also process data from other satellites, such as DMSP, NOAA or ERTS. The system is not limited to meteorological satellite data but can be used in any field in which quantitative analysis of imagery data, requiring frequent human decisions in the analysis process, is necessary.

THE USE OF MICROWAVES: Studies at AFCRL have shown that it is possible to infer atmospheric structure from measurements of microwave energy emitted, absorbed and scattered by the atmosphere, and that such measurements would have considerable advantages over those presently in use. The strong microwave absorption spectra of water vapor and oxygen in the 15-200 GHz region (2 cm-0.15 cm wavelengths) are utilized to determine temperature, pressure and humidity profiles, cloud water content and hydrometeor size. Clouds and water are semi-transparent to radiation in this region of the spectrum, allowing atmospheric soundings in both clear and cloudy areas. The microwave temperature sounder, advanced by AFCRL, is to be flown on board the Defense Meteorological Satellite System (DMSS) satellite.

WEATHER RADAR TECHNIQUES

The weather radar program of the Meteorology Laboratory is directed toward development of instrumentation and techniques which can contribute to the solution of operational Air Force problems, such as hazardous weather warning and specification of meteorological environments which adversely affect communications. This research effort is based at a field site in Sudbury, Massachusetts, where state-of-the-art processing and display equipment converts data from four weather radars to formats adapted for study of convective processes and widespread precipitation systems. Three of the radars originated in standard Air Force inventory, but have been extensively modified to meet the needs of the research program. These include the FPS-6, a 10-cm height finder; the CPS-9, a 3-cm storm detector, and the TPQ-11, a 1-cm cloud base and top indicator. The most advanced radar, the 5-cm Porcupine Doppler, is a non-standard, continuously evolving assembly of experimental equipment for measuring the radial velocity structure as well as the reflectivity of storms. A fifth radar, the 5-cm FPS-77 located at Hanscom AFB, has been modified to produce digital reflectivity information for the Hanscom Mesonet described previously.

Weather radar data for specialized programs are also acquired at several sites op-

erated by other agencies. Most of this cooperative work is carried out at the NASA radar station at Wallops Island, Virginia. The radars at Wallops feature enormous antenna sizes, up to 60 feet in diameter, and have ultrasensitive probing capability at various wavelengths covering the range from 3 to 71 cm. Excellent observations of refractivity structures of the atmosphere associated with clear-air turbulence have been accomplished with the Wallops Island radars, and they are now employed in quantitative studies of precipitation erosion. A powerful, high-resolution 5-cm radar at the Kwajalein Missile Range also provides meteorological data for the erosion program.

TORNADO OBSERVATION BY DOPPLER RADAR: During the past two years, two tornadoes have occurred while their attendant thunderstorms were under surveillance by Doppler radar. The Brookline, Massachusetts, tornado of August 9, 1972 was observed by the Porcupine Doppler radar at the Sudbury field site. A large tornado which devastated the town of Union City, Oklahoma, on May 24, 1973 was recorded on a Plan Shear Indicator during a cooperative program with NSSL.

The Brookline tornado observations demonstrated in dramatic fashion the enhanced value of Doppler radar for identifying a dangerous storm and pin-pointing the area of dangerous winds within the storm. The indices of severe weather obtainable by conventional radar were lacking. The storm echo was neither especially tall nor unusually intense for a thunderstorm, and displayed no hook during the 30-minute period prior to the descent of the tornado funnel. However, analysis of the Doppler velocity field revealed two striking singularities. One of these was a couplet of extrema in mean velocities, arranged in a manner strongly suggestive of a vortex. This pattern was first noted 20 minutes before the tornado. It is not possible, using a single Doppler radar, to state with certainty whether or not a vortex is present, because the Doppler radar cannot sense motions across the antenna beam. In this case, persistence of the pattern and its extension over a considerable height range helped to validate its interpretation as a vortex: it was verified by three independent observers who reported a cyclonically rotating cloud base around the tornado.

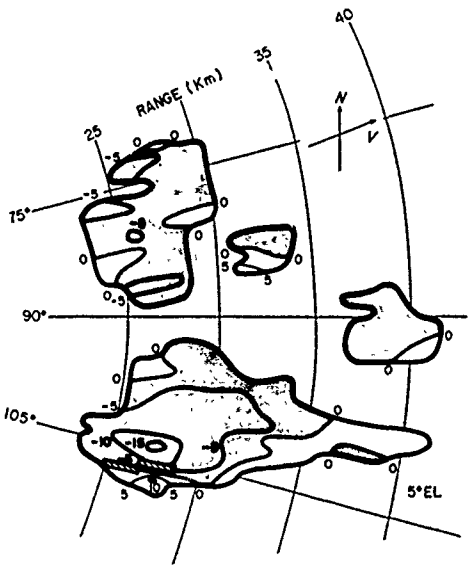

Radial velocity pattern of thunderstorms observed by the Porcupine Doppler radar while a tornado was on the ground at Brookline, Mass. Contours of velocity are given in meters per second and refer to flow relative to the storm along the radar beam. Negative numbers and shaded areas indicate motion toward the radar; positive numbers and clear areas show motion outbound from the radar. The hatched portions in the southern storm represent areas where the spread of velocity was so great that a mean velocity was unmeasurable. Straddling the hatched region, where the tornado occurred, is a couplet of velocity extrema. The maximum flow toward the radar (westward) is located north of the peak flow away from the radar, consistent with the counter-clockwise rotation or a cyclonic vortex. Since the antenna beam is tilted at an elevation of 5 degrees, the active end (velocity couplet and hatched region) of the southern storm from which the tornado descended is represented here at heights of 2 to 3 km above the ground.

The other singularity in the velocity pattern of the storm which spawned the Brookline tornado was a small region of an extremely wide spectrum of velocities, located about midway between the peaks of the velocity couplet. The spread of velocities was so great in this small region that a mean velocity could not be read. Such a region could be caused by a small high-speed vortex located entirely within the angular resolution capacity of the radar, by extreme wind shear of non-rotating form occurring within similar small confines, by extreme turbulence, or by a combination of these phenomena. In any case, the region of abnormally wide velocity spectra indicates, with precision, a dangerous hazard. When wide spectra are used in combination with the velocity couplet, good evidence is provided to show that Doppler radar can be used to advantage over conventional radar as a tool for severe storm identification and warning.

Observations of the Union City tornado demonstrated once again how Doppler radar can provide reliable warnings of major destructive storms with unprecedented accuracy. The participation of Laboratory scientists in acquiring Oklahoma tornado data was made possible by the courtesy of the Director, National Severe Storms Laboratory. During a cooperative program in the spring of 1973, the Plan Shear Indicator (PSI) developed earlier at AFCRL was successfully mated to the Doppler radar operated by NSSL.

The PSI is a primitive but very effective real-time analog device for analysis and display of Doppler velocities. Until very recently, the PSI was the only means available for diagnosis of the velocity fields within convective storms at a rate commensurate with their development. The PSI depicts storm echoes in plan view as a series of many concentric arcs, with the spacing between arcs reserved for velocity indication. A uniform or gradually changing velocity field is indicated by smooth, evenly spaced arcs. However, pronounced shear or veloc-

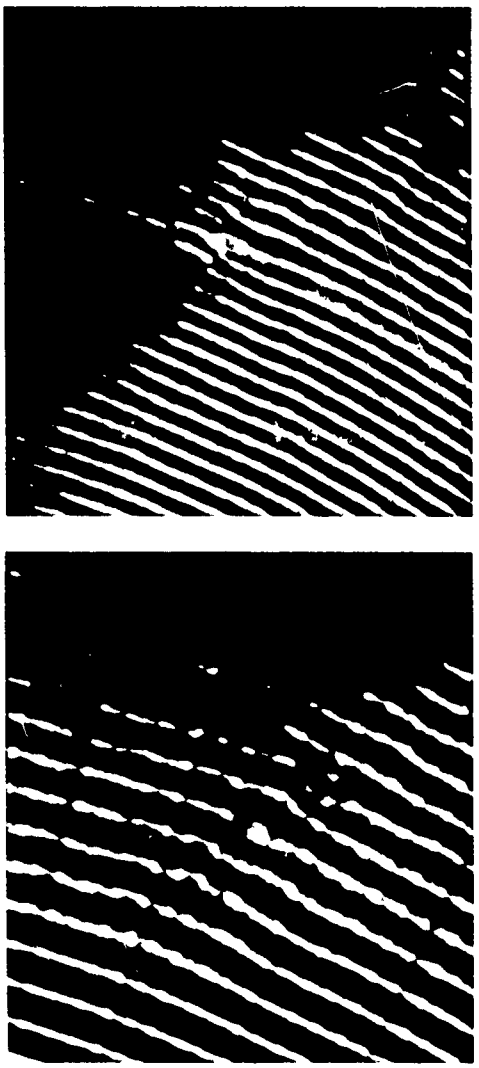

Plan Shear Indicator (PSI) displays of a small portion of the Union City tornadic storm. The bright arcs, representing range gates spaced 855 meters apart, outline the storm echo. The space between arcs is used to indicate variations in Doppler velocity of up to 50 meters per second. In the upper picture, taken four minutes before initial tornado damage at an elevation angle of 2 degrees, the disturbed area of arcs near the center of the picture represents the lower part of the descending tornado vortex, at a height of 2 km. In the lower picture, taken at near-horizontal elevation while the tornado was inflicting damage on Union City, the split arc a little to the right and above the center of the picture shows an extreme spread of velocities (at least 50 meters per second) in a small region, coincident with a small but intense cyclonic vortex.

ity gradients show up strikingly as irregularities in the arc pattern. A vortex is revealed by a unique PSI signature.

A weak but well defined vortex, rotating cyclonically, was first detected by PSI at heights of 5 to 8 km in the Union City Storm, some 40 minutes before the initial wind damage and 47 minutes before tornado touchdown. At heights below 5 km there was no hint of a severe storm; the velocity field was unruffled. Subsequent to this observation the vortex intensified and gradually descended toward the ground. As the giant tornado churned its devastating path through the town, it picked up debris and swirled it about, providing radar-detectable tracers of its violent rotation. The Union City tornado continued to be identifiable by Doppler PSI until it ceased its damage and receded into the cloud base.

PULSE-PAIR PROCESSOR: The coarse but definitive warnings of tornadoes and other severe wind disturbances in convective storms provided by PSI have encouraged the development of real-time digital methods for the quantitative determination of the velocity structure within these storm systems. The digital analysis techniques previously available were simply not fast enough to follow the rapid developments throughout a convective storm. Although a limited sampling of velocity spectra was possible in real time, the extraction of the mean and variance information from these spectra has been out of the question. Recently, however, Laboratory and contractor scientists, working in association, have developed a revolutionary Doppler processing scheme, called the pulse-pair technique, which enables calculation of Doppler spectral moments at approximately 10,000 times the speed of the fastest Fourier transform technique. Moreover, the simplicity of the logic allows these calculations to be made in real time at a small fraction of the cost of devices relying on fast Fourier transform or an analog spectral analysis. The contractor has delivered an instrument which is in the final stages of installation in the Porcupine Doppler radar.

The pulse-pair processor computes the mean and spectral width, or variance, of velocity spectrum directly, performing relatively simple operations on the complex Doppler time series. The processor has a speed comparable with the PSI, but it has the great advantage of a digital output of velocity mean as well as variance, and so has the versatility to feed a variety of display systems as well as yield an output amenable to computer processing. The pulse-pair technique offers, for the first time, the possibility of digital parameterization of the velocity fields for efficient and reliable objective identification and short-term forecasting of severely destructive storms.

COLOR DISPLAY: The conventional white-on-black display of weather echoes, used for many years on radar plan-position indicators (PPI) and Range-Height Indicators (RHI), has very limited capability to reveal the internal structure of storms. At various times attempts have been made to portray a third dimension of intensity on the two-dimensional scope by producing several shades of gray to represent quantized levels. Even with the most sophisticated integration techniques, these attempts have had only marginal success, for two basic reasons. First, the brightness on the display is a function not only of signal amplitude, but also depends on the length of time that the sweep dwells on a given area. This will cause white areas near the center of a radar scope to become gray at its perimeter, and vice versa. Compensation for this effect is extremely troublesome and unreliable. The other difficulty is the limited ability of an observer to distinguish among three or four shades of gray, especially in real time, during the fade of an echo until the sweep covers it anew.

The problem has been solved successfully by development of a color display

which converts the polar-coordinate outputs of a weather radar and integrator to cartesian coordinates, contours the video signal according to a desired, predetermined scheme, and stores the resulting data as one of 16 color-coded levels in four independent image-oriented memories, each of which refreshes one raster-scan color television monitor. The most significant advantage of this system over conventional monochrome scopes lies in the ability of the operator to unambiguously recognize 16 color-coded levels of signal intensity. Stored images can be retained indefinitely, updated, or erased independently of each other. In addition to having both an RHI and PPI capability, the system can also be used, with an appropriate antenna scanning sequence, to generate a constant altitude PPI (CAPPI) display for each of four selectable altitudes. There is also versatility in distance scaling, off-centering, and range and (for RHI) altitude marker spacing. Along the right edge of each indicator there is a display of the selected colors and their corresponding threshold levels, as well as housekeeping parameters such as antenna angle, time, and marker spacing.

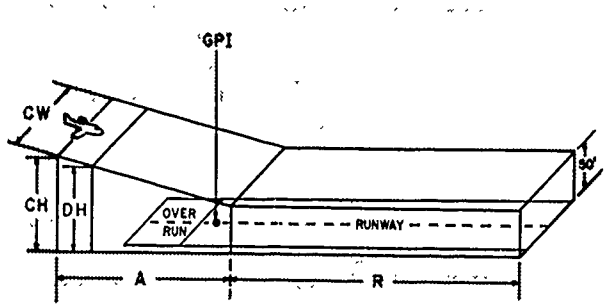

Clearing Geometry — The clearing zone produced by a typical system will extend to a Clearing Height (CH) of 236 feet from a point 5 seconds upstream of the approaching pilot's Decision Height (DH) location to a point 1500 feet beyond the Ground Plane Indicator (GPI) or Touchdown Point, and to a depth of 50 feet over the remaining length of the runway. The deeper clearing, Region A, is intended to allow the landing aircraft to acquire the field on final approach and to accomplish touchdown. The shallower clearing, Region R, is intended to aid the pilot during rollout.

WARM FOG DISSIPATION

Throughout the history of the Air Force, fog has had a very significant impact on airport operations. The numerous aircraft delays, diversions, and cancellations that result from the presence of fog reduce the effectiveness with which the major operating commands of the Air Force can accomplish their assigned missions. Cold fog dispersal operations have been highly successful, producing significant benefits wherever they have been employed. Cold fog, however, accounts for only 5 percent of the total fog encountered on a world-wide basis. Warm fog accounts for the other 95 percent. The direct application of heat from a well engineered ground-based system is the most practical and most reliable technique for dissipating warm fog at airports where the volume of traffic or urgency of mission accomplishment justify its installation.

The use of heat to dissipate warm fog from runways is not a new concept. It is, in fact, the only operationally proven technique of warm fog dissipation. Thermal fog dispersal systems were employed during World War II under the name of FIDO, an acronym for Fog Intensive Dispersal Of. These, however, were crude, inefficient and too expensive to warrant implementation at airports following the war. In 1970 AFCRL conducted a state-of-the-art review of the situation and found that the increasing traffic density of larger and costlier jet aircraft had made thermal fog dispersal systems economically more attractive. A program was therefore initiated in the spring of 1971 to develop a safe, efficient, and pollution-free system through the application of modern meteorological and heat engineering technology.

In 1972 AFCRL conducted a series of heat tests at Vandenberg AFB using a pilot scale experimental heat system to deter-

mine the configuration and heat output of passive burners required to clear fog under various fog and wind conditions. Operationally useful clearings were consistently and reliably produced in every fog for which the experimental system was designed. Data from this program provided systems design criteria and proved that turbulence generated by the heat would not be a problem to aircraft operations. It was shown that, over the range of fog densities likely to be encountered, a minimum of 2° C temperature rise is necessary to evaporate the fog droplets sufficiently to raise the visibility to the 1/2-mile level normally required for airport operations. The minimum temperature rise is directly proportional to the fog liquid water content and inversely proportional to the travel time of the fog droplets in the heated air. The latter factor is directly related to the wind speed and the distance from the heaters to the runway. It was also shown that whenever the wind was less than three knots, momentum would have to be introduced into the heated plume in order to insure that the clearing remains in contact with the ground over the runway. As a result of this last conclusion, it was recommended that the use of momentum-driven heat sources be explored as a means of possibly improving the cost effectiveness of the system by making maximum use of the generated heat, especially under light wind conditions. This was followed by a design engineering evaluation in 1973 which identified those components of the system in which improvements would result in additional increases in cost effectiveness and fuel consumption efficiency. In 1974, design optimization experiments were conducted at Irvine, California, with a subscale heat/momentum system to determine the optimum configuration, spacing, and heat and momentum output of combustors required to clear fog over airports under various cross-runway wind conditions. It was found that the plumes from individual combustors without horizontal or vertical

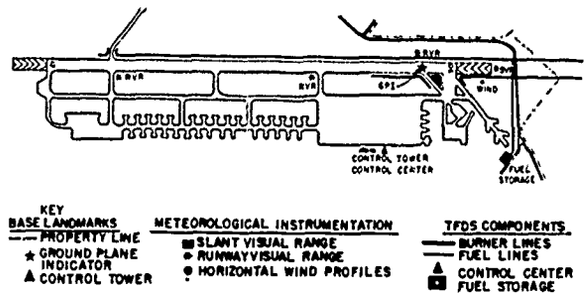

Schematic Representation of a typical Thermal Fog Dispersal System (TFDS).

diffusers merge and act as a line source at a down plume distance that is three times the separation distance between combustors. It was shown that augmenting the heat sources with only modest amounts of momentum improves the controllability of the system and, thereby, improves its fuel consumption efficiency.

A conceptual design of a modern thermal fog dispersal system has evolved from these studies. It will consist of three major subsystems: the burners alongside the runway and in the approach zone, the fuel storage and distribution system, and the control system which consists of a control center and the meteorological measurement system on which it is keyed. Each subsystem will be designed with due consideration given to energy, safety, and pollution guidelines. The system design will be compatible with existing electronic navigational guidance systems and will be capable of aiding both take-offs and landings.

Instead of a combustor that has been designed to heat homes or fly airplanes, a burner will be specifically designed to meet the requirements of fog dispersal. It is envisioned to be a combustor with low exhaust velocity and temperature but high mass flow. Where necessary, the combustor will be installed in protected underground chambers to avoid accidents should an aircraft stray off the runway. The relatively low exhaust temperature will minimize the risk of external fuel ignition in case of fuel spillage from a ruptured aircraft. Flame

and fuel flow detectors will automatically shut off a burner in case of malfunction. Flames from the burners will not be visible from approaching aircraft. The combustors will be designed to operate on aviation fuel and satisfy the air and noise quality standards established by EPA for the 1980's.

Operation of the system will be automatically controlled to produce and maintain the required clearing to assist aircraft landings and takeoffs. The wind profile in the approach zone will be remotely and automatically monitored and serve as the basis for determining the spatial distribution of heat required to produce the clearing. Slant visual range and runway visual range will also be remotely and automatically monitored to ensure that the operational weather minima have been met.

The clearing zone produced by a typical system should provide sufficient clearing to allow Category I landing operations. (Category I landing minima require a visibility or runway visual range of ½ mile and a ceiling of 200 feet). Take-offs will be possible in either direction with an adequate margin of safety for the landing aircraft. The clearing is produced within one minute after the thermal fog dispersal system is activated and persists for at least one minute after the system is deactivated.

These advances in the technology of fog dissipation by ground-based heating under AFCRL's basic and exploratory research programs have provided the basis for a proposed program for the engineering development of a Thermal Fog Dispersal System that will significantly improve the all-weather capability of the Air Force and, at the same time, result in substantial cost savings. Development of the thermal fog dispersal system is planned as a six-year program. It will consist of three phases. The first year of the program will be devoted to the development of a combustor for the system. During the next two years a pilot scale system along 2,000 feet of a simulated runway layout will be tested to verify hardware configuration concepts and to develop automatic control procedures. A fully automatic prototype system will be installed and tested during the final three years of the program. It will then be possible to design an operational system for any of the more than 22 candidate air bases that have been identified by the major operating commands. The resultant cost savings to the Air Force will be from $0.8 to $3.0 million per Air Force base each year.

THUNDERSTORM ELECTRICITY

Advanced aircraft and avionics systems become increasingly vulnerable to the effects of lightning and static electricity hazards as the use of non-conducting structures and digital systems increases. New techniques utilizing fiber-optics data and control transmission links may eventually alleviate some of the hazards. However, a need continues to exist for improved data on lightning characteristic source waveforms, rise-times, current magnitudes, charge magnitudes, aircraft attachment points and durations of swept-strokes. Existing aircraft and systems will benefit from in-flight avoidance of lightning zones, if possible. Isolated strikes to aircraft, which occur when the aircraft enters an apparently inactive cloud are known as "triggered" strikes, and are the most frequent type experienced in commercial and military flight activity. A very spectacular example of the phenomenon was provided by the two strikes to the Apollo 12 spacecraft during launch. AFCRL's effort has been directed toward improved measurement techniques for monitoring and obtaining quantitative data on lightning waveforms originating within about 100 km of an observation site, and in the development of equipment and techniques for airborne recognition and avoidance of specific cloud regions that present a potential triggered lightning hazard. Waveform sensors and waveform

analysis equipment and techniques are being developed to receive and rapidly process waveform data in the ELF-VLF and UHF frequency range. If successful, the final equipment should provide coordinates and charge magnitudes for individual cloud-ground lightning events and also indicate if each lightning bolt has some cloud-ground channels or if only cloud-cloud components are involved.

For more immediate airborne use, a system of electric field sensors was developed and installed on a C-130A aircraft. This system will determine the three components of field due to cloud charges, stabilize the components with respect to aircraft pitch and roll, and provide indications of maximum charge areas, thus indicating locations of possible triggered lightning activity. The same system can be used in a research mode to locate lightning areas for further airborne studies of lightning strike characteristics.

METEOROLOGICAL INSTRUMENTATION

The Meteorology Laboratory has responsibility for the development of meteorological instrumentation to support the operational needs of the Air Force. These developments are intended to improve the state of the art in the area of sensors and observing techniques for both surface and vertical sounding applications. Some of the major efforts of the meteorological instrumentation program are discussed in the paragraphs which follow.

WINDSONDE: The dropsonde currently in operational use by the Air Weather Service in its reconnaissance program transmits thermodynamic data (temperature, pressure and humidity) but does not have the capability of providing highly desirable wind information. This is due to the fact that the aircraft does not represent a sufficiently defined spatial reference for use in the measurement of the dropsonde velocity. A technique of utilizing Navigational Aid signals, both Loran and Omega, which are received by the dropsonde and retransmitted to the aircraft has been under investigation. The results of a series of flight tests in which the wind measurement accuracy of this technique was evaluated in comparison with data obtained from a high precision AN/FPS-16 tracking radar have recently been published. The results indicate that a system using Loran signals is capable of providing winds with a vector error of less than 1 m/sec, when speeds are determined from two-minute displacements of the sonde. Unfortunately, Loran signals cannot be received worldwide and are available at the present time only along the East Coast of the United States and in tactical situations. However, they should be available in the Gulf states in the near future and on the West Coast in the next few years.

The results with Omega retransmission signals indicate an accuracy of about 1.7 m/sec when a three-minute interval is used for measuring the wind. The Omega re-

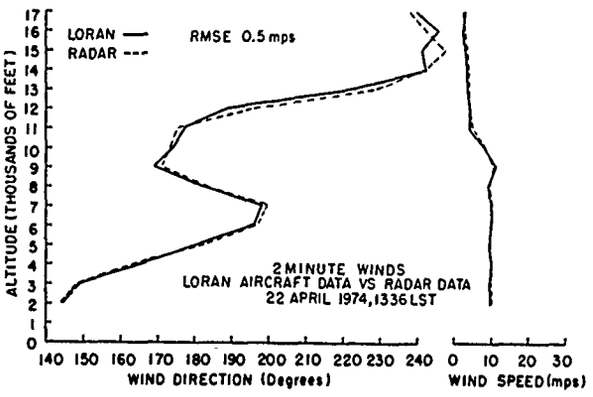

Comparison of wind measurements derived from re-transmitted Loran signals and from AN/FPS-16 radar data. The Loran signal was re-transmitted from a sonde and received aboard an AWS C-130 reconnaissance aircraft. The ground-based AN/FPS-16 radar tracked the same sonde.

sults are preliminary in nature since seasonal and geographic effects have not yet been considered and the Omega ground stations used in the test were not at operational power levels. The advantage of the Omega system is that it is essentially worldwide in operation. In addition, Omega stations are currently being upgraded to provide significantly increased signal strength.

HUMIDITY SENSING: A critical study by this Laboratory of the balloon-borne radiosonde system had revealed that gross errors existed in the measurement of humidity. Various modifications to the radiosonde which were suggested by AFCRL to minimize these errors were incorporated into a redesign of the National Weather Service radiosonde which is used operationally by the Air Force and virtually all other U.S. agencies as well. Major features of the modified sonde included a reconfigured air duct and an improved technique for mounting the humidity sensing element. Recognizing the desirability of evaluating this redesigned instrument, the Laboratory initiated an extensive series of field tests to pinpoint any additional error sources. These sources were identified and quantified for a number of parameters, including solar angle, pressure altitude, cloud cover and ventilation rate. Methods for rectifying routine radiosonde flight data were formulated and recommended to the using agencies.

Current efforts in humidity measurement are being focused upon the feasibility of upgrading the inherent accuracy of the humidity sensor itself (i.e., the carbon hygristor) for special non-routine applications, such as support of the Air Force missile development program and observations in extremely dry areas.

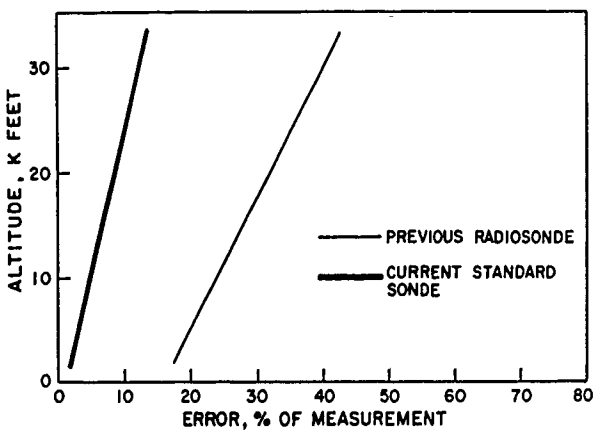

Comparison of insolation-induced humidity errors in the old and modified radiosondes.

MEASUREMENT OF CEILING AND VISIBILITY

In 1970 a study was initiated to establish a theoretical and practical basis for measuring slant visual range in the approach zone of airfields with the backscatter signal of a pulsed lidar. Preliminary field tests established the feasibility of determining visibility from a consideration of the "slope" of the amplitude of the lidar atmospheric return with distance. In January 1973 a unique field experiment was conducted at Travis AFB, California, to establish the validity and accuracy of the lidar technique. Simultaneous lidar and transmissometer atmospheric measurements were obtained along elevated, adjacent paths which approximated a pilot's line of sight during his approach. In the visual range interval from 70 to 350 meters, the lidar data correlated very well with the transmissometer data, but were consistently higher. It was concluded that the over-prediction was caused primarily by large multiple scatter of the laser beam. However, it was shown that the multiple scatter effect in the lidar measurement could be accounted for empirically. The results of these experiments demonstrated that the lidar technique has good potential for use as a practical system for the measurement of slant visual range for aircraft landing operations. The development of an experimental lidar slant

visual range measuring system has been initiated.

Lidars can also be used to determine cloud height by measuring the transit line of the laser pulse to the cloud layer and its return. Previous experimentation with a ruby laser system demonstrated that a lidar ceilometer is superior to the standard rotating beam ceilometer (RBC) as a cloud-height measuring device. However, the ruby laser constitutes an eye hazard, which would preclude its routine use at airfields. An experimental eye-safe erbium lidar was field tested to determine its applicability as a lidar ceilometer. The erbium system operated satisfactorily and compared very well with the ruby lidar ceilometer and the RBC. A prototype erbium lidar ceilometer is now being fabricated. Methods of automatically determining and displaying the cloud-height information are being developed.

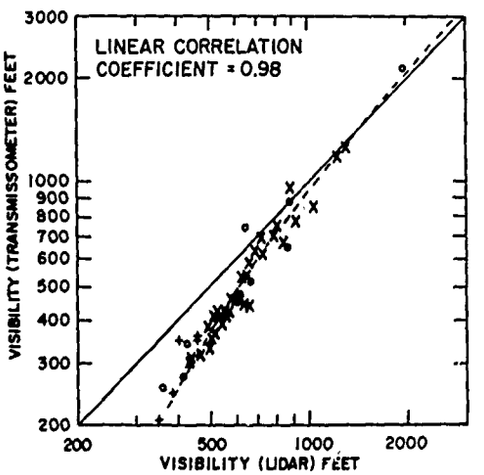

Scatter diagram and linear line of regression (dashed line) between visibility computed from single-ended lidar data and simultaneous transmissometer measurements of visibility.

WEATHER EROSION PROGRAMS

The extent of the erosion of the nosecone of a missile is a complicated function of vehicle speed, severity of cloud or weather encountered, and nosecone material. For competent design of advanced reentry vehicles it is essential that this function be well defined, since erosion alters the drag coefficient of the vehicle, and thereby affects its point of impact. During the past two years the Meteorology Laboratory has continued to support the Air Force's Space and Missile Systems Organization (SAMSO) in its field test of nosecone erosion. Most of these tests were conducted at NASA's Wallops Island range in Virginia, but starting in the summer of 1973 additional tests have been conducted at the Kwajalein Missile Range in the western Pacific Ocean.

In all such tests the role of AFCRL's scientists and technicians has been to document the clouds and precipitation through which the test nosecone passes. This is accomplished through coordinated measurements made with an ultra-sensitive ground-based radar and from aircraft specially instrumented with cloud microphysical sensors. This experimental procedure was developed specifically for the erosion tests. The radar scans the trajectory of the nosecone at the time of its passage. Simultaneous measurements are made with both radar and aircraft as close in time and space to the trajectory as is feasible. These coordinated measurements allow the radar-only trajectory to be interpreted in terms of desired cloud microphysical parameters: particle water content, particle size spectrum, and whether the particle is in a water or ice state.

The 10-cm radar used at Wallops Island is one belonging to the joint NASA-AFCRL radar facility there. At Kwajalein the radar is a 5-cm ALCOR, one of the radars operated by Lincoln Laboratory. A wide variety of cloud physics aircraft has been used in these tests, including a WB-57, a Cessna Citation and Piper Navajo. AFCRL itself

An ICBM behaves like a fiery meteor on reentering the earth's atmosphere.

mans the instruments aboard a C-130A and a C-130E. Both of these are used at Wallops while the C-130E, which was added to the program in early 1974, is also used at Kwajalein. The instrumentation aboard these aircraft is continually updated as the state of the art progresses. The sensors and recording systems are designed for digital data processing.

AEROSOL TECHNIQUES

AFCRL is deeply involved in the modification of the aerospace environment through the use of artificial aerosols. Accurate measurements of the changes induced by the aerosols require development of methods to reproducibly inject controlled amounts of relatively monodisperse aerosols into the atmosphere. Because most applications involve airborne dispensing, system weights must be kept to a minimum. However, in spite of significant advances in aerosol dispensing technology, the maximum amount of powder suspended in freon mixtures is no more than about 20 percent by weight.

To reduce the weight of aerosol dispensers, and also to minimize any possible effects of the propellant on the system being modified, great stress has been placed on the development of techniques to dispense a powder directly. This is accomplished by fluidization of the powder bed so that the powder will flow like a liquid. Fluidization has been used previously for large, regularly shaped particles. The particles of interest in our aerosol studies range in diameter from 0.1 to 1.2 micrometers and have extremely irregular surfaces. Both the size and the irregularity have contributed to the high surface area per unit mass of these particles. As the ratio of surface to volume of a particle increases, the surface becomes more active and the particle increases its tendency both to absorb foreign materials on its surface and to agglomerate.

In order to overcome the surface forces between particles and achieve good fluidization, work was conducted on the development of deagglomerating agents. The material which gives the best results is a fumed silica with a uniform negative charge. Because of the extremely small size of the silica, it is able to penetrate the interstices of irregular particles and effectively simulate smooth, spherical particles. The uniform negative charge imparted to the particles acts as a repulsive force between them and further prevents agglomeration. Nitrogen, under pressure, is then used to fluidize the powder bed.

Once a powder bed is fluidized, conditions must be chosen to allow the powder to flow freely from its container through an injection system. Tubing parameters must be matched to nitrogen pressure. Without careful system matching, spurting occurs. This spurting is due to saltation, which occurs when the fluid velocity in the tubing decreases momentarily from steady state conditions. When this occurs, the particle velocity also decreases and the particle density in the tubing increases. As the velocity decreases, the particles tend to settle to the bottom of the tube. At the saltation velocity, the number of particles per unit volume of fluid becomes too great to sustain flow. As more particles settle out in the tube, the pressure drop increases rapidly and the

velocity then increases because the fluidizing gas is now flowing through a restricted opening. When this velocity exceeds the initial equilibrium velocity, there is a rapid discharge of particles and the tube is emptied. Then the process is repeated. The rapid change of velocity from above to below equilibrium causes the spurting phenomenon.

After a material is fluidized and the proper flow system parameters have been chosen to allow smooth flow, a means must be found to control the rate of aerosol dispensing. This is accomplished by the selection of the proper nozzle size. In general, for any powder type and size a system can be designed to give linear flow over a wide range of flow rates. As nozzle diameter is increased beyond these limits, the flow no longer is linear. When the nozzle size becomes too small, clogging occurs.

Self-contained aerosol dispensers have been designed which are filled with a powder, pressurized with nitrogen, and actuated by opening a solenoid valve. Flow rates as low as 4 oz/sec have been achieved. For good aerosol distribution, the fluidized powders can be dispensed through multi-nozzle systems. Systems containing up to four nozzles per dispenser have been successfully tested. To achieve flow rates greater than the limits of a single aerosol dispenser, two or more dispensers connected in parallel are used. Using these techniques, it is possible to dispense measured amounts of sized powders into the atmosphere using lightweight, efficient equipment designed for airborne use.

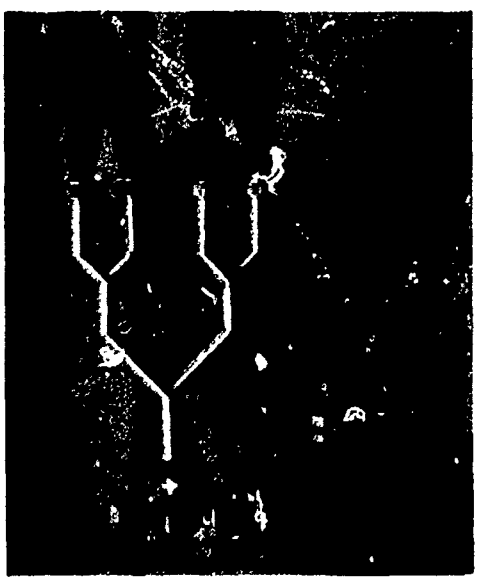

Aerosol discharge through a four-nozzle dispensing system.

JOURNAL ARTICLES
JULY 1972 - JUNE 1974

ARMSTRONG, G. M., and DONALDSON, R. J.
Plan Shear Indicator for Real-Time Doppler Radar Identification of Hazardous Storm Winds
Selected Met. Papers, 2nd Ser., Met. Soc. of Jap. (December 1972)

BARNES, A. A., JR.
Status Report on Radar, Wind and Density Measurements
Bull. of Am. Met. Soc., Vol. 54, No. 9 (September 1973)

BERKOFSKY, L.
Tropospheric Wave Motions with Baroclinic Basic Flow in Equatorial Latitudes
Tellus, Vol. 24, No. 4 (October 1972)

BOUCHER, R. J.
History of a Small Patch of Clear Air Turbulence
J. of Appl. Met., Vol. 12, No. 50 (August 1973)

CONOVER, J. H.
Weather and Equatorial Waves Over Southeast Asia During the Summer Monsoon
J. of Appl. Met., Vol. 12, No. 2 (March 1973)
Orographic Fibrous Plumes Over New England
Mo. Wea. Rev., Vol. 101, No. 11 (November 1973)

DONALDSON, R. J.
Radar Reflectivity Profiles in Thunderstorms
Methods for Identifying Severe Thunderstorms by Radar: A Guide and Bibliography and
Resolution of a Radar Antenna for Distributed Targets
Selected Met. Papers, 2nd Ser., Met. Soc. of Jap. (December 1972)
NSSL and AFCRL Observation Program of Severe Storms
Bull. of Am. Met. Soc., Vol. 54, No. 2 (February 1973)

GLOVER, K. M.
Radar Observation of Insects in Free Flight
Selected Met. Papers, 2nd Ser., Met. Soc. of Jap. (December 1972)

HARDY, K. R.
Unusual Radar Echoes
Book, Phys. and Psychol. of UFO's. UFO's - A Sci. Debate (December 1972)

HARDY, K. R., and FUKUSHIMA, M. (Rad. Res. Labs., Min. of Posts and Telecomm., Tokyo, Jap.), LESTER, P. F. (San Jose State Coll., Calif.), STEWART, R. H. (Scripps Inst. of Oceanog., Univ. of Calif.)
On the Prediction of Turbulence in Baroclinic Zones
Boundary-Layer Met., Vol. 5, No. 1/2 (April 1973)

HARDY, K. R., and REED, R. J. (Univ. of Wash.), MATHER, G. K. (Sierra Res. Corp., Boulder, Colo.)
Observation of Kelvin-Helmholtz Billows and Their Mesoscale Environment by Radar, Instrumented Aircraft, and a Dense Radiosonde Network.
Qtr. J. of the Royal Met. Soc., Vol. 99, No. 420 (April 1973)

HARDY, K. R., and SMITH, P. L., JR. (S. D. Sch. of Mines and Technol., Rapid City, S. D.), GLOVER, K. M.
Applications of Radar to Meteorological Operations and Research
IEEE Proc. Sp. Issue on Modern Radar Technol. and Appl. (June 1974)

HERING, W. S., BROWN, H. A., and MUENCH, H. S.
Mesoscale Forecasting Experiments
Bull. of Am. Met. Soc., Vol. 53, No. 12 (December 1972)

KAIMAL, J. C.
Turbulence Spectra, Length Scales, and Structure Parameters in the Stable Surface Layer
Boundary-Layer Met., Vol. 4, No. 1-4 (April 1973)
Translation Speed of Convective Plumes in the Atmospheric Surface Layer
Qtr. J. of the Royal Met. Soc., Vol. 100, No. 423 (January 1974)

KAIMAL, J. C., NEWMAN, J. T., and BISBERG, A., COLE, K. (EG&G, Waltham, Mass.)
An Improved Three-Component Sonic Anemometer for Investigating Atmospheric Turbulence
FLOW - Its Meas. and Control in Sci. and Ind. (Pt. 1), Instm. Soc. of Am., Pittsburgh, Pa. (1974)

KAIMAL, J. C., WYNGAARD, J. C., IZUMI, Y., and COTE, O. R.
Spectral Characteristics of Surface Layer Turbulence
Qtr. J. of the Royal Met. Soc., Vol. 98, No. 417 (July 1972)

KLEIN, M. M
Scattering of Microwaves by a Stratified Overdense Plasma at High Collision Frequencies
J. of Appl. Phys., Vol. 44, No. 1 (January 1973)

KRAUS, M. J.
Doppler Radar Observations of the Brookline, Massachusetts, Tornado of 9 August 1972
Bull. of Am. Met. Soc., Vol. 54, No. 6 (June 1973)

KUNKEL, B. A.
A Statistical Approach to Evaluating Fog Dispersal Operations
J. of Appl. Met., Vol. 12 (August 1973)

LEVITON, R.
The International Meteorological Rocket Comparison Program
World Met. Orgn. Bull., Vol. 22, No. 1 (January 1973)
Final Report on Sensors and Telemetry for Meteorological Rockets
Proc. of 6th Quadrennial Session of the WMO Comsn. for Instm. and Methods of Obsn., Helsinki, Finland, 6-17 Aug. 1973, CIMO-VI/Document 10 (19 November 1973)

METCALF, J. I.
22° Solar Halo and Tangent Arc
Bull. of Am. Met. Soc., Vol. 54, No. 12 (December 1973)
On the Origin and Structure of Radar Echo Layers in the Clear Atmosphere
Ph.D. Dissertation, The Univ. of Chicago, Ill. (March 1974)

METCALF, J. I., and ATLAS, D.
Microscale Ordered Motions and Atmospheric Structure Associated with Thin Echo Layers in Stably Stratified Zones
Boundary-Layer Met., Vol. 4 (1973)

MORRISSEY, J. F.
Atmospheric Temperature Measurements Using Balloons and Rockets
Temp. - Its Meas. and Control in Sci. and Ind. (Bk./1972)

MUDRICK, S. E.
A Numerical Study of Frontogenesis
J. of Atm. Sci., Vol. 31, No. 4 (May 1974)

OTTERSTEN, H. (Res. Inst. of Natl. Def., Stockholm, Swed.), HARDY, K. R., and LITTLE, C. G. (NOAA, Boulder, Colo.)
Radar and Sodar Probing of Waves and Turbulence in Statically Stable Clear-Air-Layers
Boundary-Layer Met., Vol. 4 (1973)

RAO, K. S., WYNGAARD, J. C., and COTE, O. R.
The Structure of Two-Dimensional Internal Boundary Layer Over a Sudden Change of Surface Roughness
J. of Atm. Sci., Vol. 31, No. 3 (April 1973)

SHAPIRO, R.
A Comparison Between the Effects of Fourier Truncation and a Class of Linear Digital Filters
J. of Atm. Sci., Vol. 29, No. 5 (July 1972)
Information Loss and Compensation in Linear Interpolation
J. of Comp. Phys., Vol. 10, No. 1 (August 1972)
A Test of an Apparent Response of the Lower Atmosphere to Solar Corpuscular Radiation
J. of Atm. Sci., Vol. 29, No. 6 (September 1972)
Reply to Comments on "A Test of an Apparent Response of the

Lower Atmosphere to Solar Corpuscular Radiation"
J. of Atm. Sci., Vol. 30, No. 4 (May 1973)
Geomagnetic Activity in the Vicinity of Sector Boundaries
J. of Geophys. Res., Vol. 79, No. 1 (January 1974)
On the Response of the Lower Atmosphere to Solar Variability
Proc. of the Symp. on Solar Corpuscular Effects on the Tropo. and Strato. (IUCSTP) (April 1974)

SILVERMAN, B. A., and GLASS, M.
A Numerical Simulation of Warm Cumulus Clouds: Part I. Parameterized Vs. Non-Parameterized Microphysics
J. of Atm. Sci., Vol. 30, No. 8 (November 1973)

STOLOV, H. L. (The City Coll., N. Y., N. Y.), and SHAPIRO, R.
Investigation of the Responses of the General Circulation at 700 MB to Solar-Geomagnetic Disturbance
J. of Geophys. Res., Vol. 79, No. 15 (April 1974)

VALOVCIN, F. R.
Quantitative Temperature Data from Direct-Readout Infrared (DRIR) Pictures
J. of Appl. Met., Vol. 11, No. 8 (December 1972)

WEINSTEIN, A. I.
Comments on: "Computer Model Determination of Convective Cloud Seeded Growth Using Project Whitetop Data"
J. of Appl. Met., Vol. 12, No. 2 (February 1973)
Comments on: "On the Freezing of Liquid Water in a Cloud"
J. of Appl. Met., Vol. 12, No. 8 (December 1973)

WEINSTEIN, A. I., and SILVERMAN, B. A.
A Numerical Analysis of Some Practical Aspects of Airborne Urea Seeding for Warm Fog Dispersal at Airports
J. of Appl. Met., Vol. 12, No. 5 (August 1973)

WYNGAARD, J. C.
On Surface Layer Turbulence
Chap. 3 in Wkshp. in Micromet. (Am. Met. Soc.) (June 1973)

WYNGAARD, J. C., and ARYA, S.P.S. (Univ. of Wash.), COTE, O. R.
Some Aspects of the Structure of Convective Planetary Boundary Layers
J. of Atm. Sci., Vol. 31, No. 3 (April 1974)

WYNGAARD, J. C., and COTE, O. R.
Cospectral Similarity in the Atmospheric Surface Layer
Qtr. J. of the Royal Met. Soc., Vol. 98, No. 417 (July 1972)

WYNGAARD, J. C., and IZUMI, Y.
Comments on "Statistical Characteristics of Reynolds Stress in a Turbulent Boundary Layer"
Phys. of Fluids, Vol. 16, No. 3 (March 1973)

WYNGAARD, J. C., and TENNEKES, H. (Penn. State Univ.)
The Intermittent Small-Scale Structure of Turbulence: Data-Processing Hazards
J. of Fluid Mech., Vol. 55, No. 1 (12 September 1972)

YANG C-H. and SHAPIRO, R.
The Effects of the Observational System and the Method of Interpolation on the Computation of Spectra
J. of Atm. Sci., Vol. 30, No. 4 (May 1973)

PAPERS PRESENTED AT MEETINGS JULY 1972 - JUNE 1974

BARNES, A. A., JR.
Using VHF Radars to Probe the Atmosphere
15th Radar Met. Conf., Champaign-Urbana, Ill. (10-12 October 1972)
A Review of the AFCRL Radar Meteor Trail Program
Aeronomy Lab. Sem., Univ. of Ill., Urbana, Ill. (13 October 1972)
KREMS and the Aggravated Erosion Project
Sem., Lincoln Lab., Lexington, Mass. (22 January 1974)

BERKOFSKY, L.
Parameterization of Cumulus Convection for Inclusion in a Tropical Operational Forecast Model
Sec. Conf. on Numerical Simulation, Monterey, Calif. (1-4 October 1973)

BIRSTEIN, S. J.
The Successful Testing of an Infrared Suppression System for Jet Aircraft
AIAA/SAE/Jt. Army-Navy-NASA-Air Force Prpln. Mtg., Las Vegas, Nev. (8 November 1973)

BOLLERMANN, B. (Space Data Corp., Phoenix, Ariz.), and WRIGHT, J. B.
Super-LOKI Meteorological Rocket Systems
AIAA 3rd Sounding Rocket Technol. Conf., Albuquerque. N. M. (7-9 March 1973)

BOUCHER, R. J.
Life Cycle of Brief CAT Episodes Determined by Mesoscale Analyses
15th Radar Met. Conf., Champaign-Urbana, Ill. (10-12 October 1972)
Weathercasting in Eastern Massachusetts
5th Conf. on Weathercasting (Rad. & TV), Wychmere Harbor Club, Cape Cod, Mass. (9 June 1973)

BROWN, H. A.
A Comparison of Mesoscale Precipitation and Visibility Observations with Radar Echoes
5th AMS Conf. on Wea. Forecasting and Analys., St. Louis, Mo. (4-8 March 1974)

CHISHOLM, D. A., and KRUSE, H. (Mil. Geophys. Off., Fed. Rep. of Ger.)
The Mesoscale Variability of Visibility in Time and Space

5th AMS Conf. on Wea. Forecasting and Analys., St. Louis, Mo. (4-8 March 1974)

COLLIS, R. T. H., VIEZEE, W., OBLANAS, J. (Stanford Res. Inst., Menlo Pk., Calif.), and SILVERMAN, B. A.
Lidar Evaluation of Fog Dissipation Techniques
Fall Ann. Mtg. of Am. Geophys. Union, San Francisco, Calif. (4-7 December 1972)

CONOVER, J. H.
Specification of Current and Future Cloud Ceilings from Satellite Data
5th AMS Conf. on Wea. Forecasting and Analys., St. Louis, Mo. (4-8 March 1974)

DONALDSON, R. J., JR.
Doppler Radar Evidence for Anticyclonic Circulation in a Severe Convective Storm
8th Conf. on Severe Local Storms, Denver, Colo. (15-17 October 1973)

DONALDSON, R. J., JR., ARMSTRONG, G. M., BANIS, K. J., and DYER, R. M.
Measurement of Wind Gradients in Convective Storms by Doppler Radar
15th Radar Met. Conf., Champaign-Urbana, Ill. (10-12 October 1972)

DYER, R. M.
Radar Studies of Precipitation and Their Application to Air Force Problems
AFSC Sci. and Engrg. Symp., Kirtland AFB, N. M. (2-4 October 1973)

DYER, R. M., and FALCONE, V. J. (Microwave Phys. Lab.)
Variability in Rainfall Rate-Attenuation Relations
15th Radar Met. Conf., Champaign-Urbana, Ill. (10-12 October 1972)
Effect of Drop-Size Distributions on Rainfall Rate-Attenuation Relations
1973 Intl. IEEE/G-AP Symp. and USNC/URSI Mtg., Univ. of Colo., Boulder, Colo. (21-24 August 1973)

FITZGERALD, D. R.
Observed Relations of Thunderstorm Dynamics to the Polarity of Upper Storm Regions
Fall Ann. Mtg. of Am. Geophys. Union, San Francisco, Calif. (4-7 December 1972)

GLOVER, K. M.
A Precision Digital Radar Video Integrator
15th Radar Met. Conf., Champaign-Urbana, Ill. (10-12 October 1972)

HARDY, K. R.
Remote Sensing II: Earth Planetary Atmospheres
17th Gen. Asbly. of URSI, Warsaw, Pol. (21-29 August 1972)
Radar and Aircraft Investigations of Clear Air Turbulence
Natl. Severe Storms Lab., Norman, Okla. (20-21 November 1972);
Sem., NASA Goddard Space Flt. Ctr., Greenbelt, Md. (5 January 1973)

HARDY, K. R., and REED, R. J. (Univ. of Wash.)
Wave Patterns and Clear Air Turbulence
15th Radar Met. Conf., Champaign-Urbana, Ill. (10-12 October 1972)

HAUGEN, D. A., KAIMAL, J. C., and READINGS, C. J., RAYMENT, R. (Brit. Met. Off., Bedford, Eng.)
An Evaluation of Balloon-Borne Vs. Tower-Mounted Wind and Temperature Sensors
53rd Ann. Am. Met. Soc. Mtg., St. Petersburg, Fla. (29 January 1973)

HAUGEN, D. A., PELLEGRINI, J., 1ST. LT., and READINGS, C. J., BUTLER, H. E. (Brit. Met. Off., Bedford, Eng.)
Comparison of Balloon-Borne and Tower-Mounted Turbulent Wind and Temperature Sensors
7th AFCRL Sci. Balloon Symp., Wentworth-By-The-Sea, Portsmouth, N. H. (25-27 September 1972)

HERING, W. S.
Operational Implications of a Mesoscale Aviation Weather Forecasting Experiment
Mil. Ops. Res. Symp. (MORS), U. S. Naval Postgrad. Sch., Monterey, Calif. (14-16 November 1973)
Hanscom Mesoscale Field Test Facility
5th AMS Conf. on Wea. Forecasting and Analys., St. Louis, Mo. (4-8 March 1974)

HERING, W. S., and QUICK, D. L., MAJ.
Hanscom Visibility Forecasting Experiments
5th AMS Conf. on Wea. Forecasting and Analys., St. Louis, Mo. (4-8 March 1974)

KRAUS, M. J.
Calculating Airflow from Single Doppler Radar Velocity Components
8th Conf. on Severe Local Storms, Denver, Colo. (15-17 October 1973);
Sem., McGill Univ., Montreal, Quebec, Can. (14 January 1974)

KUNKEL, B. A., SILVERMAN, B. A., and WEINSTEIN, A. I.
Results of Some Thermal Fog Dispersal Experiments
1973 Ann. Fall Mtg. of Am. Geophys. Union, San Francisco, Calif. (10-14 December 1973)

LEVITON, R.
Final Report on Sensors and Telemetry for Meteorological Rockets
6th Quadrennial Session of the WMO Comsn. for Instm. and Methods of Obsn., Helsinki, Finland (6-17 August 1973)

MOROZ, E. Y., and SEGRE, J. P., TRUSCOTT, N. R. (Am. Opt. Corp., Res. Lab., Framingham, Mass.)
An Eye Safe 1.54 μm Erbium Q-Switched Laser Ceilometer
1973 IEEE/OSA Conf. on Laser Engrg. and Appl., Wash., D. C. (30 May - 1 June 1973)
Design and Testing of an Erbium Laser Rangefinder for Use as a Ceilometer
5th Conf. on Laser Radar Studies of the Atm., Williamsburg, Va. (4-6 June 1973)

MUDRICK, S.
Numerical Simulation of Upper Level Frontogenesis
Sec. Conf. on Numerical Simulation, Monterey, Calif. (1-4 October 1973)

MUENCH, H. S.
Accuracy of the Forward Scatter Visibility Meter
5th AMS Conf. on Wea. Forecasting and Analys., St. Louis, Mo. (4-8 March 1974)

RAO, K. S., WYNGAARD, J. C., and COTE, O. R.
Modeling Local Advection and Atmospheric Turbulence Structure Over Changes in Terrain Conditions
26th Mtg. of Am. Phys. Soc. Fluid Dyn. Div., Yale Univ., New Haven, Conn. (19-21 November 1973)

SHAPIRO, R.
A High-Ordered Interpolation Procedure for Use in Fine-Mesh Limited-Area Models
Symp. on Mesoscale Repn. and Fine-Mesh Modeling, Reading, Eng. (14-18 May 1973)

SILVERMAN, B. A.
Design of a Modern Thermal Fog Dissipation System for Airports
WMO/IAMAP Intl. Conf. on Wea. Mod., Tashkent, USSR (1-7 October 1973)

SILVERMAN, B. A., and GLASS, M.
A Numerical Simulation of Warm Cumulus Clouds
Intl. Cloud Phys. Conf., London, Eng. (21-26 August 1972)

STOLOV, H. L. (The City Coll., N. Y., N. Y.), and SHAPIRO, R.
Investigation of the Responses of the General Circulation at 700 MB to Solar-Geomagnetic Disturbance
1973 Ann. Am. Geophys. Union Mtg., Wash., D. C. (16-20 April 1973)

WEINSTEIN, A. I.
Weather Modification Activities at the Air Force Cambridge Research Laboratories
7th Ann. Wea. Mod. Symp., Naval Weap. Ctr., China Lake, Calif. (11-13 April 1973)

WYNGAARD, J. C.
Model Studies of the Convective Planetary Boundary Layer
Jt. Sem., Depts. of Aerosp. Engrg.and Met., Penn. State Univ., Univ. Pk., Pa. (18 October 1973)
An Emerging Need for Planetary Boundary Layer Measurement
Sem., NOAA Wave Propagation Lab., Boulder, Colo. (14 November 1973)
Numerical Simulation of the Evolution of a Convective Planetary Boundary Layer
Sem., Drexel Univ., Philadelphia, Pa. (21 February 1974)
Simulation of a Growing Convective Planetary Boundary Layer with a Higher-Order-Closure Turbulence Model
Sem., Natl. Ctr. for Atm. Res., Boulder, Colo. (19 March 1974)
Numerical Simulation of a Growing Convective Planetary Boundary Layer
Sem., Dept. of Met., Mass. Inst. of Technol., Cambridge, Mass. (9 April 1974)

WYNGAARD, J. C., COTE, O.R., and RAO, K. S.
Modeling the Atmospheric Boundary Layer
Am. Phys. Soc. Fluid Dyn. Div. Ann. Mtg., Boulder, Colo. (20-22 November 1972);
(Inv.) 2nd IUTAM-IUGG Symp. on Turbulent Diffusion in Envmt. Pollution, Charlottesville, Va. (8-14 April 1973)
Numerical Studies of the Convective Planetary Boundary Layer
26th Mtg. of Am. Phys. Soc. Fluid Dyn. Div., Yale Univ., New Haven, Conn. (19-21 November 1973)

TECHNICAL REPORTS
JULY 1972 - JUNE 1974

BERKOFSKY, L.
Parameterization of Cumulus Convection for Inclusion in a Tropical Operational Forecasting Model
AFCRL-TR-74-0089 (13 February 1974)

BROUSAIDES, F. J.
An Assessment of the Carbon Humidity Element in Radiosonde Systems
AFCRL-TR-73-0423 (18 July 1973)

BROUSAIDES, F. J., and MORRISSEY, J. F.
Residual Temperature-Induced Humidity Errors in the National Weather Service Radiosonde. Part I.
AFCRL-TR-73-0214 (5 April 1973)
Residual Temperature-Induced Humidity Errors in the National Weather Service Radiosonde, Final Report
AFCRL-TR-74-0111 (28 February 1974)

BUNTING, J.T.
Time Series Analysis of Southwest Monsoon Data from Southeast Asia
AFCRL-TR-73-0085 (29 January 1973)

CHISHOLM, D. A., and KRUSE, H. (Mil. Geophys. Off., Fed. Rep. of Ger.)
The Variability of Airfield Visibility: A Preliminary Assessment
AFCRL-TR-74-0027 (15 January 1974)
The Variability of Visibility in the Hanscom Mesonetwork: A Preliminary Assessment
AFCRL-TR-74-0265 (13 June 1974)

CHURCH, J. F., LT. COL., and PEIRCE, R. M.
Flight Testing of a Cryogenically Cooled Hygrometer
AFCRL-TR-73-0292 (4 May 1973)

GEORGIAN, E. J.
A Solid-State Commutator Design for the Radiosonde Set ANIAMQ-9
AFCRL-TR-73-0224 (12 April 1973)

HAUGEN, D. A., PELLEGRINI, J., CAPT., and READINGS, C. J., BUTLER, H. E. (Met. Res. Unit, RAD Cardington, Bedford, Eng.)
Comparison of Balloon-Borne and Tower-Mounted Turbulent Wind and Temperature Sensors
Proc., 7th AFCRL Sci. Balloon Symp.,
AFCRL-TR-73-0071 (3 January 1973)

KRAUS, M. J.
Doppler Radar Investigation of Flow Patterns Within Severe Thunderstorms
AFCRL-TR-73-0153 (8 March 1973)

KUNKEL, B. A., SILVERMAN, B. A., and WEINSTEIN, A. I.
Thermal and Chemical Fog Dissipation – Results of Field Experiments at Vandenberg AFB, California, During July 1972
AFCRL-TR-73-0502 (8 August 1973)

MOROZ, E. Y., LAWRANCE, C. L., and TRAVERS, G. A.
Laser Ceilometers - Results of Comparison Testing of an Erbium and a Ruby Laser Ceilometer with a Standard Rotating Beam Ceilometer
AFCRL-TR-73-0751 (13 December 1973)

MUENCH, H. S., MOROZ, E. Y., and JACOBS, L. P.
Development and Calibration of the Forward Scatter Visibility Meter
AFCRL-TR-74-0145 (18 March 1974)

MYERS, R. F.
Test and Calibration of the AFCRL Raindrop Spectrometer
AFCRL-TR-74-0006 (7 January 1974)

PAULSEN, W. H., and PETROCCHI, P. J.
K_a Band Radar Weather Detection
AFRCL-TR-73-0407 (11 July 1973)

PEIRCE, R. M., and CHURCH, J. F., LT. COL.
An Expendable, Remote-Operating Weather Station (EROWS)
AFCRL-72-0501 (21 August 1972)

PETROCCHI, P. J., and PAULSEN, W. H.
Lightning Warning Set Test Report
AFCRL-TR-73-0370 (18 June 1973)

SHAPIRO, R.
A High-Order Interpolation Procedure for Use in Fine-Mesh Limited-Area Models
AFCRL-TR-73-0543 (21 August 1973)
Assessment of the Impact of the B-1 Exhaust Emissions on Local and Global Changes in Weather
Envmt. Impact of B-1 Emissions in the Strato., C. G. Stergis, Ed.
AFCRL-TR-73-0608 (10 October 1973)

SILVERMAN, B. A., and WEINSTEIN, A. I.
Fog Modification – A Technology Assessment
AFCRL-TR-73-0159 (12 March 1973)

THOMPSON, G. J., CAPT.
Atmospheric Mesostructure and Clear Air Turbulence
AFCRL-TR-73-0082 (26 January 1973)
The Nature of the Mesoscale Wind and Temperature Structure During a Case of CAT
AFCRL-TR-73-0222 (17 April 1973)

TOUART, C. N.
On the Operational Value of Terminal Weather Forecasts
AFCRL-72-0719 (12 December 1972)
Synthetic Verification Matrices – I
AFCRL-TR-73-0158 (13 March 1973)

WEINSTEIN, A. I.
Thermal Warm Fog Dissipation – Heat Requirements and Projected Utilization of a System for Travis AFB, California
AFCLR-TR-0367 (18 June 1973)

Y. K. YEE, S.
Photochemical Models of Stratospheric Ozone – A Review
AFCRL-TR-74-0098 (12 February 1974)

VII Sacramento Peak Observatory

The geophysical effects of solar activity were first detected about a century ago when variations in geomagnetic storms were observed to parallel variations in solar activity. The telescopes and magnetometers required for this discovery were relatively simple tools by modern standards. As the technology of observation advanced, more and more features of the solar-terrestrial relation became apparent. The invention of the optical spectroheliograph and the development, in the 1920's, of radio communications revealed the tendency of large flares, "chromospheric eruptions," to cause radio blackouts. More recently, space science confirmed the existence of the solar wind, the magnetosphere and the geomagnetic effects of their interaction. A particularly important discovery was that fast streams of solar wind particles originated from vast voids in the corona which were promptly named "coronal holes." Technological progress has advanced our knowledge, but has also exposed us to more and more practical problems due to the geophysical responses to solar influences. Radio blackouts, and more recently, variations in the density of the upper atmosphere have become important, and as the technology continues to advance, other Air Force activities will encounter other environmental factors controlled and perturbed by the sun.

Within AFCRL, the Aeronomy Laboratory, the Sacramento Peak Observatory, the Optical Physics Laboratory, the Microwave Physics Laboratory, and the Ionospheric Physics Laboratory study the sun's electromagnetic radiations all the way from

high-energy X-rays to the longest radio waves that can penetrate the earth's atmosphere. The Sacramento Peak Observatory is responsible for solar research in the optical band of the solar spectrum.

The Observatory, located near Alamogordo, New Mexico, at an altitude of 9200 feet in the Sacramento Mountains, began operations as an in-house AFCRL solar observatory in 1952. It was, and remains, the Air Force response to the need for knowledge about the sun which will allow prediction of solar geophysical disturbances that impede Air Force operations. While there is no prospect of suppressing the disturbances, foreknowledge prepares mission planners for problems, and often permits them to avoid or mitigate the effects.

The link between solar disturbances and the earth are the X-rays and energetic particles emitted by solar flares and flare-related phenomena, and the relatively low-energy particles of the solar wind and the embedded interplanetary magnetic field. Sporadic variations in these radiations produce changes in the ionosphere and magnetosphere. From these come the operational problems.

Degradation or complete blackout of long distance radio propagation is accompanied in extreme instances by surges on hard wire communications systems that completely garble messages. Severe clutter on OTH radar systems either drowns the signals or produces signatures difficult to distinguish from those of ballistic missiles. Perturbations of ballistic and satellite orbits produce targeting and surveillance position errors, and grossly affect predicted and planned reentry times and coordinates. Temporary blackouts of satellite surveillance equipment due to showers of energetic particles last for several hours in the most extreme cases. Space monitors of surreptitious nuclear activity can be confused by bursts of X-rays and particles. Finally, the evidence for the influence of solar variations on global weather patterns is now fairly definite, although the nature of the interaction is still a complete mystery.

The objective of the Observatory is to identify the solar origins of, and devise methods for predicting, solar geophysical disturbances that lead to these operational problems. The approach is to study every aspect of the physics of the sun, combining optical observations from the Observatory with solar radio data from the Ionospheric Physics Laboratory and other sources, and also XUV observations from space. Each of these techniques provides information obtainable in no other way, and all are necessary for understanding the physics of the sun.

Current research is directed toward the solution of two fundamental problems. The first is the nature and mechanisms of the solar input to the interplanetary medium, both the solar wind and sporadic bursts of energetic particles and X-rays. The solar features involved are the magnetic and dynamic characters of spicules, sunspots, flares, prominences, plages and the corona. The second is the mechanism for the steady, upward non-thermal transport of energy through the solar atmosphere. This involves theoretical models of the inhomogeneous solar atmosphere, and the magnetic and dynamic characters of granulation, supergranulation, and the oscillating elements at all heights.

THE SUN

The sun is a typical star, near the mean for all classes of stars in mass, size and luminosity. It is a gaseous globe 7×10^5 km in radius, powered by the nuclear conversion of hydrogen to helium in the central core. The surface temperature is about 6,000° K, and its total radiation is about 3.9×10^{23} kW, or about 6.4 kW/cm^2.

Although the sun has no liquid or solid surface, there is an optical boundary below

which the solar interior is completely inaccessible to direct observation. It is the outer limit of a shell of negative hydrogen ions, which are opaque. This boundary is termed the floor of the observable atmosphere. It is the top of a convective layer about a hundred thousand kilometers deep.

Everything above the granular floor is the solar atmosphere, the origin of all the radiations that cause geophysical effects. More than 99 percent of this atmosphere is in a steady state of considerable dynamic activity, statistically uniform from one area of the "quiet sun" to another. The vertical structure of the average solar atmosphere is divided (for historical reasons) into three layers. The first 300 km above the granulation floor is the photosphere. The temperature in this layer decreases with height from 6000 to perhaps 5500° K. Most of the dark lines of the solar spectrum are absorbed by atoms in this layer. Next is the chromosphere, in which the temperature first declines to a minimum of 4200° K at a height of 500 to 600 km above the floor, and then rises gradually through the next 1000 km to the very irregular transition layer. Here the temperature rises abruptly through a few hundred kilometers to about a million degrees with a corresponding decrease in density. Above the chromosphere is the tenuous hot corona with a temperature of about 1.5×10^{6}° K, that extends outward from the sun as the solar wind to merge with the interstellar medium somewhere past the orbit of the earth. Thus, we can think of the earth as immersed in the solar corona at a place where its temperature is on the order of 400,000° K. This high temperature has a negligible effect on the temperature of the earth because of the exceedingly low coronal density, approximately 10 atoms per cm^3.

The increase in temperature with height in the upper chromosphere and corona presents one of the fundamental problems of solar physics. Any thermal process feeds energy down along the thermal gradient.

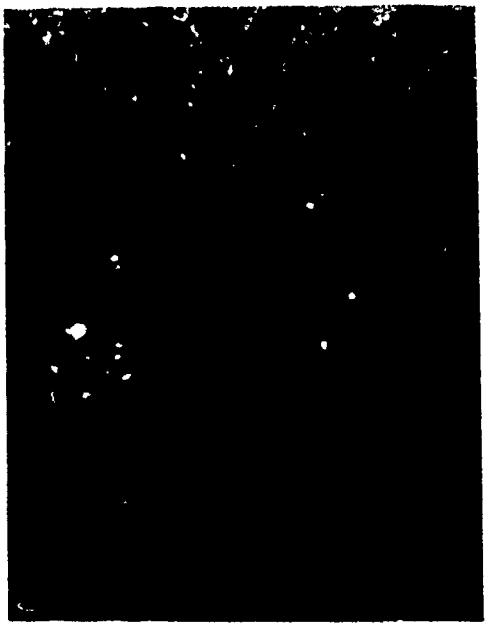

A typical simple sunspot, with the dark central umbra, the radially filamentary penumbra, and the necklace of bright points marking concentrations of magnetic field. According to recent theory, the spot radiates the same energy as the undisturbed solar surface, but most of this energy is converted by the strong magnetic field into invisible hydromagnetic waves. Hence, there is less light, and the spot appears dark.

The only source of energy external to the sun, accretion of interplanetary matter, is totally inadequate to heat the corona. Thus, the energy must come from inside the sun, and it appears that the only processes available are mechanical. The qualitative concept is that the kinetic energy of mechanical motion is carried up and converted to random thermal motions by impact on the stationary material of the chromosphere and corona. This dissipation process is not simple, and probably involves magnetic fields in ways which are presently conjectural. It is evident, however, that mass motions are important in the solar atmosphere.

The dynamics of the quiet solar atmosphere are still far from thoroughly under-

stood. The most prominent feature is a vertical oscillation with a 5-minute period extending upward from the floor to at least the middle chromosphere. In 1972, Sacramento Peak astronomers found that the oscillations are progressive pressure waves which at low levels carry enough mechanical energy to heat the chromosphere and corona. Before they reach the high temperature levels, however, their energy is largely dissipated by damping. If the oscillations do provide the energy for the upper chromosphere, there must be some presently unrecognized intermediate mechanical or magnetic process. One of the most pressing problems is to define the magnetic field in the quiet sun, because it could have a profound effect on the dynamics. Initial measurements 20 years ago, with poor spatial resolution, suggested a randomly variable field with rms field strength of the order of 1 gauss. Since then, steady improvements in resolution have shown smaller and smaller knots of flux with higher and higher field strengths, and not very much in between. The vital question now is the strength and structure of the weak fields between the magnetic knots, and the actual field strength in the knots. Sacramento Peak astronomers are now planning approaches to this problem.

At any time, the steadily stormy monotony of the quiet sun is interrupted by a few regions of more vigorous activity—the active centers. Their distinguishing feature is a strong but invisible magnetic field over an area typically 30,000 to 100,000 km in diameter. Field strengths range from 1000 to 4000 gauss. These fields are the ultimate source of both energy and geometrical constraints that shape the spectacular phenomena of solar activity. The highly conductive solar material can move freely only along the field lines, and any forced transverse motions induce strong electric currents like those in an electric generator, creating a counter force opposing the motion. The combination of gas pressure and magnetic guidance produces a variety of visible features.

The most conspicuous are the sunspots, areas on the sun that are dark because they are hundreds of degrees cooler than the surrounding area. The accepted theory that the cooling results when magnetic fields shut off the upwelling convective energy has serious problems. It has recently been challenged by a more promising hypothetical refrigeration by the radiation of hydromagnetic waves. This process must still be investigated observationally. The sunspots occur in all sizes from the smallest detectable (called pores) to giants 100,000 km in diameter. They tend to occur in pairs of opposite magnetic polarity or less frequently in more complex groups with highly irregular magnetic fields. Large ones often endure for months, though the pores may last only a few hours.

All other active center features are invisible to the unassisted telescope. They are well seen, however, through filters that transmit only the light of a strong spectral line, usually hydrogen alpha. The most spectacular features are the solar flares. An irregular bright patch, comparable in size to a sunspot, suddenly appears in the active center. In a few minutes it grows and brightens to an intensity of perhaps twice the background brightness. A large flare normally takes the form of two irregular ribbons symmetrically placed on either side of a magnetic inversion line dividing positive from negative fields. It may take an hour or two to fade away, often leaving a system of bright loops straddling the inversion line. Such flares are of particular interest to solar physicists because they are the sources of the most disruptive geophysical effects. A long-standing problem has been that of reliably predicting their occurrence, an empirical art that is gradually evolving at Sac Peak toward a scientific procedure based on physical cause and effect.

Greater understanding of flares and other active center phenomena requires a study of their basic magnetic causes. Magnetic fields cannot be seen directly, but they can be mapped by analyses of the polariza-

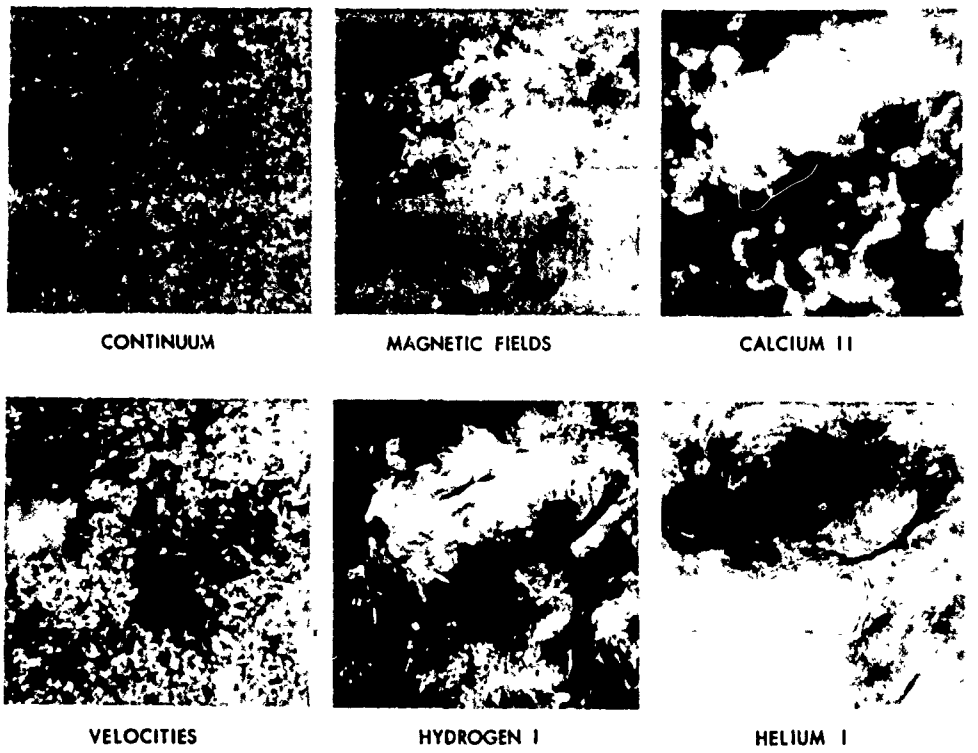

Six computer generated pictures derived from a single scan of the solar surface by the Sacramento Peak Observatory Diode Array processed in different ways. Bright and dark markings in the magnetic field and velocities frames map the locations of upward and downward directed magnetic field and mass motions.

tion profiles of certain sensitive lines in the solar spectrum. The Observatory has developed increasingly sophisticated and efficient optical accessories for this work during the past 15 years. The tower telescope with its echelle spectrograph feeding the new diode array will be a very powerful tool for defining the magnetic activity that powers the catastrophic flares and ejects the geophysically active radiations.

NEW INSTRUMENTS AT SACRAMENTO PEAK

Two new accessories for the AFCRL Vacuum Tower Telescope at the Sacramento Peak Observatory have substantially increased its observational capability. They are the Diode Array (formerly called the Multi Channel Magnetograph) and the Universal Birefringent Filter.

The diode array is a versatile set of light detectors that can be arranged in a great variety of configurations to measure simultaneously a number of different luminous signals from many elements of area on the sun. Its virtues are its quantitative digital output and its speed in mapping the measured parameters on large areas of the sun with spatial resolution down to ½ arc second (360 km on the sun). The hardware was complete by July 1972. The software required to make it a useful operating instrument reached a stage of limited useful-

ness in the fall of 1972, and has steadily improved in reliability and versatility since then. The instrument has been in full operation for more than a year.

The Diode Array consists of 512 photo diode detectors arranged in 16 linear blocks of 32. The blocks can be arranged in any desired configuration in the focal plane of the Echelle Spectrograph of the Tower Telescope. Signals from all of the diodes are stored separately in a high-speed tape recorder or disk 20 times per second, a data

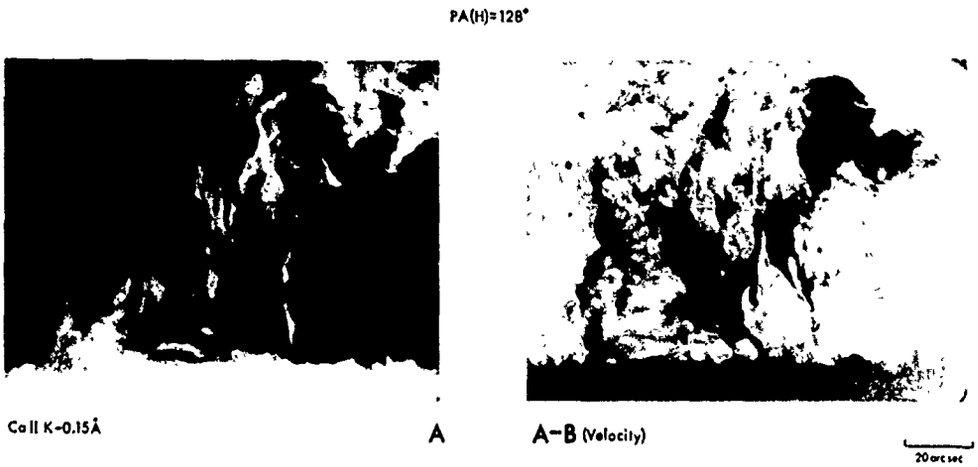

Mapping sightline velocities in a prominence by photographic subtraction. Frames A and B taken in light from either side of the strong K line of ionized calcium are the original data. Subtraction is performed by printing through a negative of B superposed on A. A prominence point with a velocity of approach will appear brighter in A and in the negative of B because of the Doppler shift in the line. This results in a bright point in the velocity picture. Similarly, a velocity of recession appears dark. The intensity frame is produced by superposing positions of both A and B, thus averaging the two.

rate of about 2.3 x 10^5 bits/second. In a typical setup, the blocks are placed to record simultaneously—at 64 points along the spectrograph slit—the magnetic field intensity, the sightline velocity, the brightness at the centers of three spectrum lines of special interest, and in the continuum between lines. A quantitative two-dimensional mapping of all these parameters is stored by scanning the solar image across the slit. Data can then be presented in any of several forms. The most useful is a video display that can be photographed either as half-tone pictures or contour maps of the various parameters. This instrument has added enormously to the observational capability at Sacramento Peak.

The world's first Universal Birefringent Filter (UBF) was delivered to Sacramento Peak in December 1972. It transmits monochromatic images of the sun for photography in the light of chosen spectral lines excluding all other wavelengths. To this end the width of the spectroscopic passband is less than the line widths. The unique feature of the UBF is tuning of the passband to any wavelength in the visible spectrum, a capability that is lacking in the fixed band filters of the past. The theoretical possibility of tuning birefringent filters was recognized over 20 years ago at Sacramento Peak, but its realization was delayed until the necessary achromatic retardation plates were made.

The UBF is a complicated mechanism which requires a computer interface for expeditious tuning, and a carefully tailored optical interface to utilize the solar image of the tower telescope. These are complete, and the system has been in research operation since August 1973. The output consists of photographs which show solar details with the highest resolution and which can be processed to show the distributions of magnetic fields and sightline velocities over the surface of the sun. For guidance of the observer, all three aspects are displayed in real time by a video system, but with somewhat less resolution than that of the photographs.

The UBF pictures of magnetic and velocity fields are, in fact, pictures of the differences in light intensity between two photographs taken in different polarizations or in slightly different wavelengths. This image subtraction is accomplished photographically by superposing the positive of one picture on the negative of another and printing through the two, a process that is very difficult to reduce to practice. The Observatory has assembled standard cinematographic components to accomplish this image subtraction for time-lapse footage of the magnetic and velocity fields. Motion picture records can now be produced in several hours instead of several months.

Superficially it may appear that the Diode Array and UBF serve the same purposes. Qualitatively, this is true, but their capabilities are complementary. The Diode Array provides quantitative digital data on light intensities, magnetic fields, and velocity distributions, with spatial resolution limited by the instrument itself. Under ordinary conditions, it retrieves all the information present in an average tower telescope solar image. Under the best seeing conditions, however, the image is much sharper, and may contain four to six times as much information as the Diode Array can accept. In these circumstances the UBF is more powerful. It records all the information in the sharper image in the form of excellent photographs with resolution at the theoretical limit of the telescope when the seeing is at its best.

SOLAR OPTICAL OBSERVING NETWORK (SOON) PROJECT: The Air Weather Service (AWS) is responsible for operational forecasting of the several types of solar geophysical disturbances of importance to the Air Force. They utilize solar and geophysical data from many sources, including optical solar data derived from their network of five stations distributed around the world to provide 24-hour-a-day monitoring of solar activity. The network

has operated since 1967. Each station has a small telescope equipped with a birefringent filter and 35-mm camera for photographing the whole sun at 1-minute intervals during clear daylight hours.

The more sophisticated solar forecasting methods developed at Sacramento Peak require much more information than these simple instruments provide. To meet this requirement, AFCRL and the AWS jointly developed specifications for a suitable optical observing system, to be produced in five identical instruments for operation at the AWS observing sites. About $5 million have been programmed for this Solar Optical Observing Network (SOON) project. The Electronic Systems Division (ESD) assumed responsibility for its implementation. At their request, AFCRL undertook the design and construction of a preproduction model at Sacramento Peak. This was nearly complete by July 1, 1974 and is due for tests by ESD in October.

The system consists of a fixed vacuum telescope of 25-cm aperture with accessories which photograph the whole solar disk on 70-mm film in the light of the hydrogen alpha line, record and display in real time the distribution of brightness of all flares, map magnetic fields in active centers, make time lapse video tapes of activity (flares particularly) that can be played back rapidly to show the evolution over the preceding several hours, and show real-time high-resolution video pictures of the active centers.

The Observatory will assemble the four remaining SOON instruments from contracted parts, test, and install them at their AWS observing sites. The project should be finished by June 1978, in time for the next sunspot cycle maximum.

Solar Optical Observing Network (SOON) telescope consisting of a fixed tube, supported by an A-frame. This is an equatorial mount in which the rotating telescope tube is parallel to the earth's axis. Sunlight enters through the tracking turret at the upper end.

Observer in the Solar Optical Observing Network (SOON) laboratory operating the system. The optical analyzing system is on the bench in the left rear of the picture. Light from the telescope enters through the box at the left end of the bench.

RESEARCH RESULTS

The most important research results at the Sacramento Peak Observatory during the reporting period are essentially progress milestones, since all the conclusions suggest further steps toward the solutions of broader solar problems.

GRANULATION: The heat generated by nuclear reactions in the sun's interior is transmitted to the visible surface by radiation, conduction and convection. The latter phenomenon is the most important in the "convection zone" of the sun, which extends outward to the photosphere from a depth of perhaps, 150,000-200,000 km (≈ ¼ of the solar radius). The granules seen in white light photographs of the quiet sun are thus presumed to be the tops of convection cells, plumes or bubbles. An understanding of granules is most important in resolution of the puzzling question: How are the outer layers (chromosphere and corona) of the sun heated? During the past two years, a study of granular velocities was completed which concluded that vertical motions in granules decrease with height in the solar atmosphere in the manner expected from a convective flow pattern, confirming the hypothesis that granules represent convective motions. In addition, when the brightness (temperature) of an element was correlated with its velocity, it was found that low in the atmosphere, hot elements are rising, while higher up, these rising elements cool and become darker, again giving a picture consistent with that of convective elements rising from the unstable convection zone (with its superadiabatic temperature gradient) into the stable photosphere (subadiabatic gradient).

Granules are not all alike. While the majority have polygonal or rounded shapes, bright at the center with dark boundaries, and remain essentially stationary during their lifetimes of 5 to 30 minutes, less than 10 percent grow much brighter and larger, then fracture into smaller granules which form into the shape of a ring. Such an "exploding granule" goes through this metamorphosis in 2 to 3 minutes, then returns to the appearance of a normal static granule. However, it is likely to explode again in 10 to 15 minutes, and may repeat this behavior three or four times. To simulate this behavior in the Laboratory, a convection experiment was performed at Sacramento Peak in which a few drops of cold milk were dropped into a tank of water. When the milk fluid hit the bottom of the tank, it formed into a ring which expanded along the base of the tank, much like a moving smoke ring which collides with a solid surface. Numerical calculations were then made to analyze the behavior of a convective element running to a barrier. Laboratory experiments and theoretical computations lead to the conclusion that as an exploding granule rises from the convection zone and penetrates into the stable photosphere, it is stretched out horizontally and its internal motions, through conservation of angular momentum, change its form into a vortex ring which expands until small-scale turbulence breaks the ring into small fragments.

The central upward velocity in the ring of an exploding granule is greater than in a normal granule. This suggested that spicules (upward-moving jets of gas seen higher in the atmosphere in the hydrogen alpha line) might have their origin in exploding granules. Since it is known that spicules appear preferentially along the chromospheric network where magnetic fields are concentrated, a search was made to determine if exploding granules also occur mainly at the network boundaries. This was found to be not true. The exploding granules appear to form at random sites on the solar surface, and do not appear to be the key to the origin of the energy being transferred by the spicules into the chromosphere and corona.

An investigation of the form and structure of granules during their lifetimes has

shed new light on the nature of granulation. Researchers in the past have estimated granule lifetimes at 8-10 minutes, but by using a superb sequence of frames obtained at the Vacuum Tower Telescope, Sacramento Peak scientists have observed some granules lasting for over 30 minutes. They have learned that most granules disappear, not by fading away or by being replaced by newly formed granules, but through fragmentation into smaller granules (similar to the exploding granule described earlier but not into the ring structure). Some of the observed fragments are at the limit of resolution ($\approx$ 0.2 arc sec) and are thus as small as filigree elements. Although most granules remain essentially fixed in location, a few migrate up to 2,500 km (two or three times their diameter) at speeds of 2-3 km/sec during their lifetime. In addition, granules interact strongly with small pores (dark regions with large magnetic fields), changing the shape, size, and even completely destroying the pores. This phenomenon is being investigated, since it gives clues as to the relative pressures exerted by the moving gas and the magnetic field, and thus to the hydromagnetic forces interacting in the solar atmosphere.

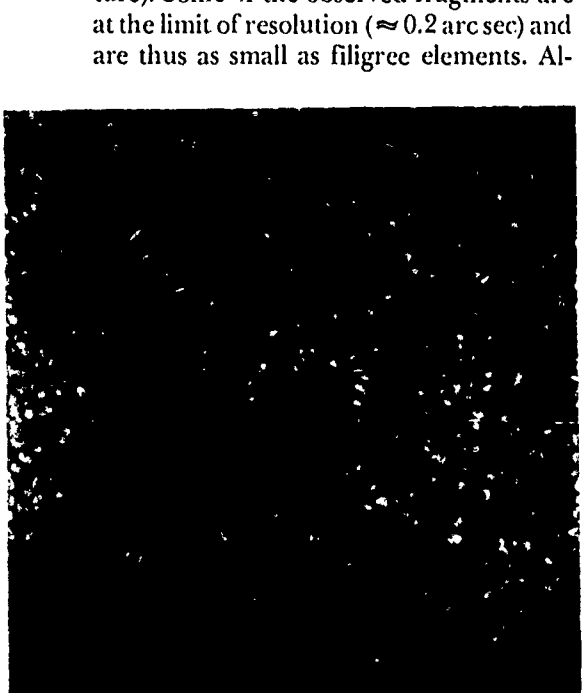

Large scale photograph of the solar surface showing the granular structure. Each bright granule is the top of a convective column, typically about 1,000 km in diameter. The convective energy of the granules is transferred by poorly understood processes through the lower solar atmosphere to heat the overlying chromosphere and corona.

Observations of the velocities in granules depend upon the Doppler effect which shifts the wavelength of a spectral line toward the blue or the red if the absorbing gas is moving toward or away from the observer, respectively. The analysis of these wavelength shifts is, however, not simple or unambiguous. A theoretical study has pointed out the effects of limited spectral and spatial resolution on a proper interpretation of the measured Doppler shifts, and has determined physical conditions under which meaningful results can be obtained.

FILIGREE, FACULAE, AND SMALL MAGNETIC FEATURES: Since the discovery of the "solar filigree" at Sacramento Peak in 1971, considerable work has been done to define the characteristics of this phenomenon. The filigree consists of tiny bright dots which are observed on filtergrams in light originating in the low photosphere, and have typical observed dimensions of 150-250 km. Since such small sizes are right at the limit of the tower telescope resolution under the best seeing (atmospheric turbulence) conditions, the actual sizes of filigree elements (called "crinkles") are still smaller. Sacramento Peak scientists have learned that the filigree tends to lie in the dark intergranular lanes, not superposed on the bright granules themselves, and that the crinkles are probably cospatial with tiny bright facular elements. Such faculae had previously been observed as brighter than

average features in continuum photographs near the solar limb. Researchers using a broad-band (16-60 angstroms wide) filter, centered in the ionized calcium "K" line at 3934 angstroms in the ultraviolet, have seen facular dots with the same dimensions as crinkles at disk center. Both the filigree and the faculae are much more numerous in active regions and at the boundaries of the chromospheric and photospheric networks, than on quieter parts of the solar surface. Since it is known that magnetic fields are associated with the network and with solar activity, attempts are being made to determine whether the filigree is the locus of very strong magnetic flux tubes of extremely small spatial extent. The inhibition of convection and the transfer and dissipation of energy by Alfven waves or shocks along such strong magnetic field lines may turn out to be a significant factor in the heating of the chromosphere and corona.

In one study, a number of high-resolution spectra were analyzed for correlations between intensity, velocity, and magnetic field observed at a number of points (quiet and active) on the solar surface. Although the spatial resolution was not quite sufficient to resolve the filigree, the magnetic field patches appeared to be larger than the corresponding intensity or velocity features. This implies that while the bright crinkles (less than 0.5 arc sec) may be at the centers of magnetic flux tubes, the magnetic field probably extends over a larger area (1 to 2 arc sec). On the other hand, the facular observations and the best filter photographs made with the Universal Birefringent Filter give some indication that the magnetic flux tubes may be as small as the crinkles. Resolution of this issue must wait until magnetic field observations (thus far limited by seeing to about 0.75 arc sec) become available with sufficient resolution (0.2 to 0.3 arc sec) to permit comparisons between simultaneously recorded crinkles, faculae, magnetic fields and velocities. If such strong magnetic field points do exist in the filigree, it is estimated that their field strengths would be in the 2000 to 3000 gauss range, perhaps even higher. Such strong fields have never been observed on the sun outside of sunspot umbrae.

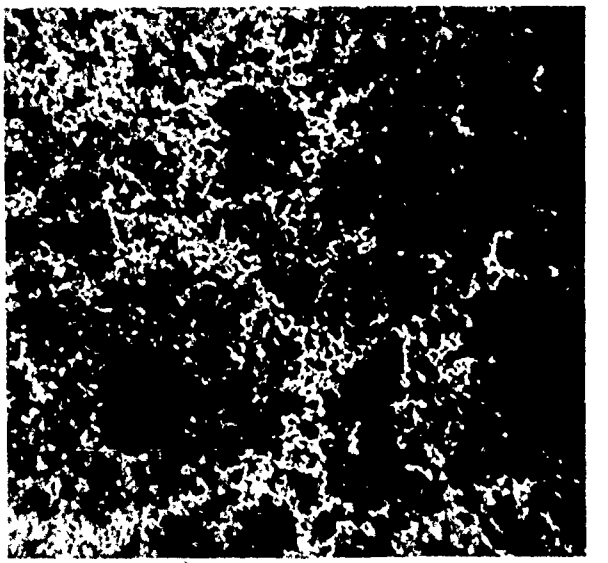

Bright photospheric faculae surrounding a small sunspot are markers for concentrated magnetic knots. Note the relatively field free "moat" around the spot. Photographed in a strong Mg line through the Universal Birefringent Filter and tower telescope at Sacramento Peak Observatory.

ENERGY TRANSPORT BY OSCILLATIONS AND NON-PERIODIC DISTURBANCES: The most commonly assumed source of heating of the solar chromosphere and corona is the dissipation of mechanical energy. A number of sources of mechanical energy are available in the photosphere such as the convection-like motions associated with the photospheric granulation or the 300-second-period gravity (and perhaps sound) waves which have been observed to exist over the entire solar surface. Both have been suggested as sources for chromospheric heating but observational

evidence does not support these hypotheses or distinguish between them.

A critical examination was made at the Observatory of the amount of mechanical energy deposited in the chromosphere by the 300-second-period waves. The result almost completely excludes a direct heating of the chromosphere by these waves since the measured amount of energy deposited at chromospheric levels fails to match that required for the heating by more than three orders of magnitude. At lower levels in the solar atmosphere, the amount of energy dissipated is, however, substantially larger, enough to match the chromospheric requirement. Therefore, one cannot definitely exclude the 300-second oscillations as the ultimate source of chromospheric energy if an intermediate mode of energy transport can be found to carry the mechanical flux from these lower levels up to the chromosphere.

The discovery of upward-propagating disturbances in the wings of the very strong H and K lines of ionized calcium may provide us with new clues to the heating of the chromosphere. Observations show that these disturbances, called "whiskers" after their appearance in these lines, propagate upwards through the solar photosphere with velocities of about 12 km per second. Some 100 seconds later they turn up as patches of strong emission in the solar chromosphere, visible in the centers of the H and K lines. The emission patches have a spectral profile very much like what one might expect if the mechanical motions cause shock waves, which can readily dissipate into thermal motions, heating the chromosphere. At present the nature of these rising disturbances is unclear.

MAGNETIC FACULAE: During the last decade it has become increasingly evident that the magnetic field on the solar surface is made very inhomogeneous by fragmentation resulting from photospheric and subphotospheric convection currents. In 1967, the magnetic knots were discovered at the Sacramento Peak Observatory. These regions, barely resolvable with the telescopes available at the time, have magnetic fields as high as 1,500 gauss concentrated in areas with diameters as small, or smaller, than 500 km. The existence of those regions has since been confirmed elsewhere, although there is some disagreement as to the size and magnitude of these magnetic field bundles.

The Universal Birefringent Filter (UBF) provides a new way of looking at the sun. Since it is tunable to any wavelength, the filter transmission can be selected to coincide in wavelength with solar absorption lines which are exceedingly sensitive to the presence of magnetic fields on the solar surface. The Zeeman effect causes most solar absorption lines to widen and split when a magnetic field is present on the sun. The light in the components of these split lines is highly circularly polarized. This causes polarization in those parts of the solar image where a magnetic field exists if this image is observed through the UBF, tuned to the wing of one of these lines. One of these very Zeeman-sensitive lines is the strong b_2 line of magnesium at 5172 angstroms. This line originates moderately high in the solar atmosphere and shows phenomena which we normally associate with the chromosphere or upper photosphere, like solar flares and faculae. Observations with the UBF made at times when the atmospheric seeing permits the highest image resolution show these faculae resolved in elements with diameters as small as 400 km. Each of these elements coincides precisely with a region of strong circular polarization in the b_2 line from which one concludes that these faculae represent regions of strongly bundled magnetic fields.

Observations with the UBF have now also firmly established that these faculae overlie the much smaller elements (~200-km diameter) of the photospheric filigree about 50-100 km lower in the solar atmo-

sphere. From this a picture is suggested in which the strong magnetic field associated with the faculae converges even more to form very tight bundles in the elements of the photospheric filigree where the field may reach a strength of thousands of gauss. Attempts to confirm this hypothesis by direct observations are now underway.

FLARES AND MAGNETIC FIELDS: Solar flares radiate strongly throughout the electromagnetic spectrum, from the longest detectable radio waves to cosmic rays. Sacramento Peak Observatory's research to gain an understanding of the physical conditions and processes leading to the solar flare itself and of the propagation of the disturbance to the vicinity of the earth has always begun with optical observations of the sun before, during, and after the flare. Other laboratories within AFCRL observe in other wavelength ranges. The optical range offers the advantage of high spatial resolution; the most reliable immediate flare precursor, motions of solar atmospheric matter, can readily be monitored in real time from Sacramento Peak. Only in the optical range can the magnetic field strength be measured down to several gauss at many levels in the solar atmosphere. The magnetic field of an active region is acknowledged as the most probable source of flare energy. Sacramento Peak research has steadily improved the ability to relate the probability of flare occurrence to the magnetic field patterns acquired by the Observatory or with the telescopes of the SOON system.

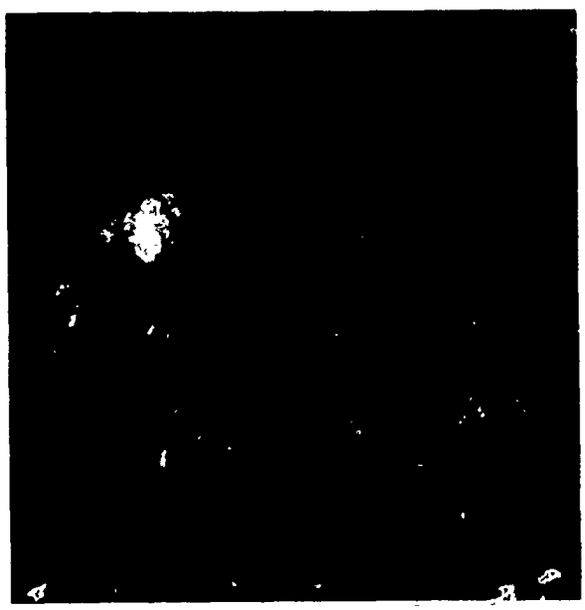

The great flare of August 7, 1972 photographed in the light of the hydrogen alpha line. This flare was one of the very few that was also visible in white light, and geophysically was the most active of the sunspot cycle now ending.

The great solar flares of August 2, 7, and 11, 1972 produced many noticeable effects on the earth. All three flares were anticipated at Sacramento Peak, and all of the Observatory instruments were ready and waiting.

The Observatory measured magnetic field, mass motions, temperature, density and position before, during, and after the August 7 flare. Several different solar telescopes, each designed for a special purpose, were used.

Two telescopes at the Hilltop Dome are operated on a patrol basis. These patrol telescopes photograph the full solar disk, with less resolution than the Tower Telescope, but at regular closely spaced intervals throughout the day. The 4-inch telescope provides the real-time television images that alert observers throughout the facility to the coming of a major flare. In addition to the continuous real-time television coverage, this system obtains the standard full-disk hydrogen-alpha photographs that form the basis of comparison with data from observatories throughout the world. These photographs are taken through a highly selective, narrow passband filter. The passband of the filter can be tuned to different wavelengths in and near the hydrogen-alpha line at 6563 angstroms to reveal the three-dimensional

structure of the flare wherever the temperature of the flare is within a factor of 2 of 10,000° K. Flares are easily detected and spectacular when observed through this system. In an observation of the August 7 flare at 15:34 Universal Time (UT), the flare was seen to cover more than ½ percent of the area of the solar disk—an exceptionally large event by solar standards. The maximum total brightness of the flare (brightness times area in hydrogen-alpha is the conventional measure of the size of the flare) was reached at 15:29 UT. The rise to maximum at 15:29 and the subsequent decay are well documented on the patrol films; the time resolution in the high-speed mode, which was operative during the August 7 flare, was 5 seconds. The value of these photographs to the research scientist is due in part to this time resolution, which permits accurate comparison of the occurrence of brightenings in the 10,000° K temperature regime to those of much different temperatures, such as the multimillion-degree X-ray range at higher levels in the solar atmosphere.

The 6-inch Hilltop Dome telescope also provided uniquely useful information. The passband of its filter is 175 angstroms wide, centered on 5900 angstroms in the orange light of the bright continuum between the dark absorption lines in the solar spectrum. Usually this "white-light" system documents only the passage and development of sunspot groups across the disk, but the August 7 flare was visible in the continuum. Such a "white-light" flare has been photographed fewer than a dozen times since the first such flare was observed visually in 1859. Any flare seen by the white-light patrol is immediately known to be in the extremely energetic great-flare category for which major terrestrial repercussions must be expected. Photographs were obtained with this system every 2 minutes. These data, combined with data from other instruments, gave the first high-quality light curves ever obtained for a white-light flare.

The large (30-inch aperture) Vacuum Tower Telescope was also in full operation. At 15:20 UT, almost 10 minutes before flare maximum in hydrogen-alpha light, the first exposure in a series of what may be the first white-light flare photographs in existence was obtained. The passband of the filter for these photographs was also broad-band, but was centered in the blue-green, rather than the orange, where the patrol passband was centered. The films were carefully calibrated, and the difference in brightness between the background and the flare was determined from the difference in brightness in the two colors. This could not have been done with only a single color, because the light shining through the flare from below was unknown.

The results revealed an unexpected characteristic of the flare. The motion picture made from the series of pictures showed hot, bluish "knots" coinciding with bright points in the hydrogen-alpha pictures and, in addition, a yellowish "wave" which appears to move out from the original flare knots at approximately 40 km/second. The knots were about 12,000° K and the waves, about 8,000° K. When the time history of the brightness of the knots was compared with that of X-rays observed from the European Space Research Organization TD-1A satellite in the 60-87 keV range, a very good correlation was found between the X-rays and the white-light knots. This suggests that the X-rays and the white-light emission may come from the same location, which the white-light observations place in the middle atmosphere, somewhat below the height of origin of most of the hydrogen-alpha radiation. This supports the hypothesis that both radiations may result from beams of high-energy electrons speeding down into the sun from a point higher in the atmosphere, suggesting that the acceleration region is higher in the atmosphere and may be discernible in the ultraviolet.

At the Big Dome, magnetic field meas-

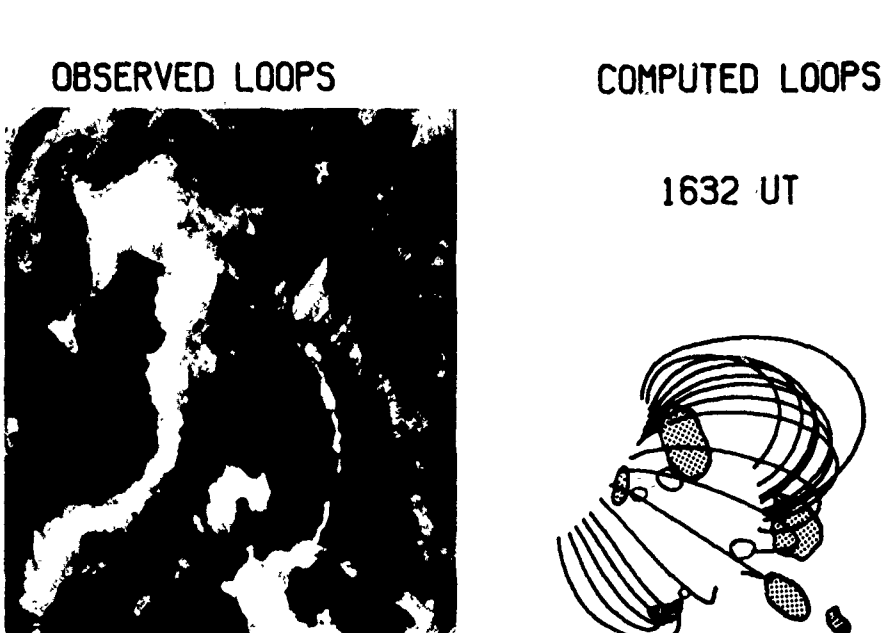

Details of the August 7, 1972 flare showing typical dark loops between the two bright flare ribbons (and obscuring a part of the right-hand ribbon). To the right is a perspective view of the three-dimensional field calculated from a magnetic map on the assumption that there were no electric currents in the material. The observed loops are obviously sheared, indicating that there are in fact very strong currents.

urements were made during the flare itself. From these measurements, maps of the distribution of the sight-line component of the magnetic field are constructed. Maps, or magnetograms, can be generated by the SOON equipment, and working rules for interpreting magnetograms have been developed. These rules permit estimation of the flare-production potential of an active region. They relate two characteristics of the active region, the principal inversion line and satellite sunspots, to the likelihood of a flare. The principal inversion line was a very convoluted, closed circle. Most of the sunspots were located in a region of positive polarity which was of limited size and was tightly surrounded by a negative field. The rules for flare production state that large flares are likely if the inversion line is convoluted, and when it runs in an east-west direction, major proton flares are likely. This led to prediction of a flare in the active region that produced the August 7 flare.

Magnetograms made after a flare can be checked to determine if the magnetic field changes during a flare. During the August 7 flare, magnetograms obtained each 6 minutes showed no sudden changes in field strength, at least in the observable atmospheric level. This is true for flares in general; only relatively slow changes, taking place on the scale of hours and tens of hours, occur. These do not relate directly to the change in magnetic energy during the

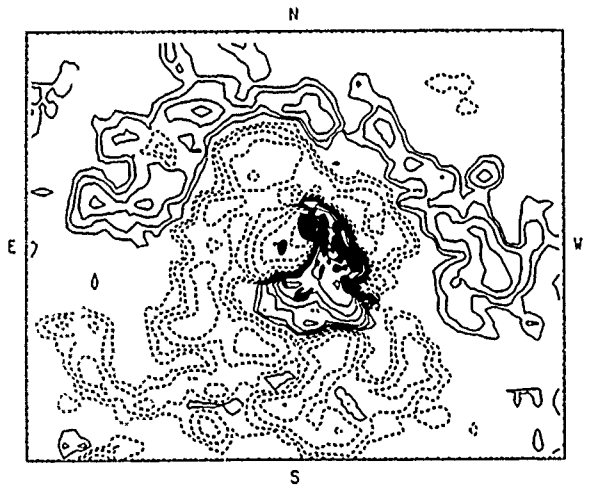

Magnetic contour map of the area around the flare of August 7, 1972. Positive and negative fields are indicated by solid and dashed contours. This is a spectacular configuration, an island of positive field around the flare completely surrounded by negative field, the presence of which gave certain warning of the coming flare several days in advance.

flare itself, since their time scale is much longer than that of the flare. However, analysis of Sacramento Peak magnetograms has shown that these slower changes apparently are necessary if a flare is to occur. The flare seems to start at the spot where the change is taking place, usually near the magnetic inversion line. This implies that the change in the field configuration due to the new magnetic flux tends to produce an unstable situation when that change occurs near the inversion line, and on the scale of a few hours.

The Diode Array and the Universal Birefringent Filter have improved the understanding of the role of magnetic fields. Although no sudden changes occur in the strength of the magnetic field in observable levels of the atmosphere, the magnetograms can be used as a basis for computing theoretical field lines in regions where the field cannot be directly observed, but where the changes are thought to take place. Presently, three-dimensional field lines can be computed from magnetograms at Sacramento Peak only in the current-free approximation. However, comparison of observed post-flare loops with field lines calculated by the current-free approximation shows little or no agreement. Since the loops do not outline the magnetic field, which they would do if ionized material moved only along the field lines, the conclusion that electrical currents are flowing in the flare region follows. The appearance of the observed loops supports this idea, since they show a structure that is shifted, or sheared, relative to the lower energy field lines computed in the current-free approximation.

The failure of the current-free theory to match the observations helps to explain the fact that no sudden change occurs in the observed fields in the lower atmosphere. It now seems quite likely that the strong heating and particle acceleration of the flare

The small flare of September 10, 1974 photographed through the Universal Birefringent Filter in the light of the hydrogen beta line.

occurs at the expense of fields in the upper solar atmosphere, and probably comes from the relaxation of current systems and fields to current-free configuration from other, higher energy systems.

DEUTERIUM IN THE SUN: Most of the deuterium atoms in the matter that formed the sun were destroyed as it contracted into a star. Many astrophysicists believe that the deuterium abundance in interstellar matter, about 1 part in 60,000, is an important clue in cosmology. Others believe that it is created in violent events such as solar flares. Gamma radiation from the creation of deuterium was observed during the giant August 1972 flares. Also, cosmic rays emitted after flares showed deuterium to be as abundant as 1 part in 10,000 in flares. For this reason, deuterium abundance in the sun is important not only in understanding flares, but also in astrophysics.

The same flare in the light of the sodium D_2 line, which originates at a lower level than the hydrogen lines.

The large coronagraph of the Sacramento Peak Observatory was used, with a specially constructed filter which suppressed the nearby bright hydrogen alpha line, to measure the Balmer alpha line of deuterium in solar prominences. The intensity was below the observational threshold, less than one millionth of the brightness of the adjacent equivalent hydrogen lines. No actual value could be calculated, but the previous upper limit was decreased by a factor of 20 to 1 part in 4 million, which indicates that deuterium destruction was very efficient during the contraction of the sun into a star and that violent explosive events such as flares have not replenished the solar deuterium to any significant degree.

EUV HEIGHTS: Various EUV lines originate in plasmas at different temperatures, and the temperature of the solar atmosphere increases with height from a minimum in the lower chromosphere. Therefore, it has been universally assumed that the different lines show the solar features at different heights. Sacramento Peak observers have confirmed this theoretical assumption by a purely geometrical method in two separate studies. The first, described in the *Report on Research* of 1972, was based on relatively crude OSO-IV data. It showed that a series of five EUV lines originated at heights between zero and 17,000 km in the expected order. The second study utilized a very much larger body of data from the Naval Research Laboratory's ultraviolet spectroheliograph, which achieved better spatial resolution by at least a factor of 20.

The study uses the fact that a solar image made with light from a line emitted high in the solar atmosphere is slightly larger than an image made with light from a line emitted lower in the atmosphere. The difference in apparent solar radius is equal to the difference in height. The difference in levels can be determined by measuring this

factor of expansion. The spectroheliograms showed hundreds of bright points on the sun. Their positions were measured in lines spanning the temperature range from that of the middle chromosphere at about 10,000° K to that of the corona, about 1,500,000° K. A statistical analysis gave a much more accurate determination of relative heights than had been possible with the OSO-IV data. The most interesting result was the positive identification of the sharp chromosphere-corona transition region. The theoretical evidence for an increase in the temperature from about 20,000 to 1,000,000° K within 1500 km is very strong, but this geometrical confirmation is an important assurance of the validity of the theory.

Post flare loops, September 10, 1974 taken in the hydrogen alpha line two hours after the preceding photographs. The loops trace the structure of the magnetic field over the flare region.

THE TEMPERATURE OF THE SOLAR CORONA: Most of the energy which originates in the core of the sun escapes in the form of visible radiation when it reaches the solar surface. But a small fraction is converted to other forms. Some is stored in twisted magnetic fields which may eventually lead to solar flares and some travels outward as violent mass motions, eventually causing shock waves which then dissipate to heat the corona. The physical conditions in the corona are extremely important to an understanding of the mechanisms involved in this dissipation of mechanical energy. Knowledge of these conditions is also required to understand the transition of the solar corona to the solar wind and to predict the effects on the earth environment caused by changes in the energy input at the base of the solar corona resulting from coronal holes and solar flares.

The most important unknown physical parameter in the corona has been the temperature. The only unambiguous method to measure the temperature was recently developed at Sacramento Peak Observatory. It is based on a discovery during the 1970 solar eclipse which showed that the corona emits the hydrogen Lyman-alpha resonance radiation at 1216 angstroms very strongly. Even at temperatures of 1 to 2 million degrees, enough hydrogen remains in the atomic un-ionized state to cause the corona to be very bright because of this resonance scattering. Because the neutral hydrogen atoms scattering the radiation have small mass, their thermal motion at the high temperature of the corona averages about 200 km/sec, well above the magnitude of any other motions. Thus, measurement of the broadening of the Lyman-alpha line due to the Doppler shift caused by thermal motion is a very precise measure of coronal temperature, undiluted by the random mass motions. Unfortunately, this line can be observed only from space.

Jointly, with the University of Colorado and the Los Alamos Scientific Laboratories,

Sacramento Peak astronomers developed a rocket-borne telescope-spectrograph system to measure coronal temperatures in this way. Rocket failures prevented the acquisition of data during the June 1974 eclipse. Another rocket flight is planned during the solar eclipse of October 1976. Other ways of measuring the coronal Lyman-alpha line width are being developed, including an externally occulted ultraviolet coronagraph which could observe the solar corona continuously from a satellite, instead of on a rocket "snapshot" basis during a solar eclipse.

SOLAR ORIGINS OF SUDDEN COMMENCEMENT MAGNETIC STORMS: Space observations of the solar particles that rain on the terrestrial magnetosphere have greatly clarified the physical relations between solar wind perturbations and certain forms of geomagnetic disturbances. This new knowledge has given renewed impetus to the Sacramento Peak Observatory effort to define the solar causes of geomagnetic disturbances. More than any other solar terrestrial phenomenon, geomagnetic disturbances produce secondary effects in the ionosphere which can hamper Air Force activities. Two lines of investigation have begun to produce results.

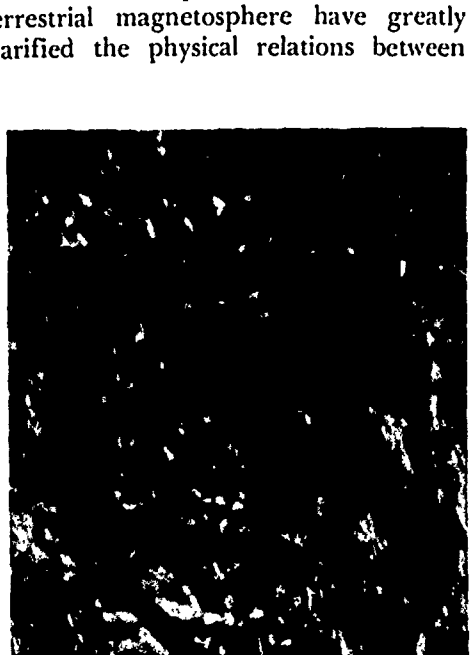

An extraordinary circular filament showing either a strong lengthwise shear or a helical structure, either of which indicates a magnetic field with strong electric currents.

Both space observation and theory unambiguously attribute the sudden commencement (SC) magnetic storms to the impact of interplanetary shock waves (IPSW's) on the magnetosphere. Solar flares have always seemed the source of IPSW's. However, the sun to earth travel time of the shock waves appears to vary between 1½ and 4½ days, and during times of high flare activity, clear associations of shocks arriving at the earth with particular solar flares become quite uncertain. Any flare within the three-day period could be responsible, and many large flares do not excite IPSW's. Sacramento Peak investigators showed that most IPSW's have origins other than flares. The most direct evidence is the great disparity between the variation in numbers of flares and SC's through the solar cycle. The flares vary in numbers in step with the sunspot cycle, while the number of SC storms is practically constant, with a very slight minimum during the years of flare minimum. In fact, during years of flare minimum, there were more SC's than large flares. The contrast between the counts of flares and SC's was even greater when the small flares were included. The flares decreased by a factor of 10 from maximum to minimum, while the SC's decreased by the barely significant factor of 1.2. Unless flares are very much more effective in producing IPSW's and SC's during solar minimum, there must be other and more important causes. One of these is the coronal holes, but even coronal holes and flares together cannot account for all the SC storms.

NASA Skylab observations of the optical corona at the solar disk limb disclosed a hitherto unsuspected form of coronal activity which appears to generate IPSW's. Once every few days a large bubble of coronal material expands radially outward at 600 to 1200 km/sec, passing out of the coronagraph field with undiminished velocity at a height of 9 million km. During the Skylab flight the astronauts photographed over 60 such events. From the ground, simultaneous monitoring by Sacramento Peak and other solar observatories provided an excellent record of surface activity on the sun. About 15 percent of the coronal bubbles started wtih large flares. Another 80 percent originated with some large prominence eruptions, some of which were of the energetic surge type. No visible activity could be associated with the remaining 5 percent.

Although it is not yet definite that all IPSW's start as coronal bubbles, it is clear that some originate in eruptive prominences. Since eruptive prominences are readily observed near the center of the solar disk, where their coronal bubbles would expand toward the earth, a useful predictor of SC geomagnetic storms is available.

CORONAL HOLES: The recurrence of magnetic storms with a period of 27 days was noted many years ago. Because this is the rotation period of the sun, the storms were attributed to the successive rotational passages of some long-lived but unidentified solar feature, named an "M Region." Comparisons of the M-region storms with every conceivable form of solar activity failed to uncover the M regions, and their nature remained a mystery until they were identified independently by several investigators, including the Sacramento Peak Observatory, in 1974. Observations of the sun from spacecraft, particularly Skylab, in the light of all X-ray and EUV high temperature lines that originate in the corona, showed vast voids—"coronal holes"—where the coronal brightness was a factor of 5 or more less than average. These holes normally persist for several solar rotations, and (in all cases examined at Sacramento Peak) whenever a hole rotated through or near the sub-terrestrial point, it was followed in three to five days by an increase in the planetary geomagnetic index, A_p. The coronal holes are the M regions.

The general nature of the physical connection is fairly clear. A coronal hole is obviously a region of low coronal density, and probably low magnetic field strength with a simple configuration of open flux tubes leading out into interplanetary space. These are the conditions for unimpeded flow of the solar wind, and space observations confirm that the holes are the sources of abnormally fast solar wind streams that distort the earth's magnetosphere. In some instances, interplanetary shock waves (IPSW's) develop along the interface between the fast stream and surrounding normal solar wind, and the impact on the magnetosphere then results in sudden commencement (SC) magnetic storms. However, the gradual commencement storms are more common.

The identification of the M regions as coronal holes is important for the prediction of disruptive geomagnetic activity, but since continuous monitoring of the sun from space cannot be expected, it will be useful only when means for observing the coronal holes from the ground are devised. The Sacramento Peak Observatory has now accomplished this. The 40-cm coronagraph at Sacramento Peak shows the lower corona in the 5303 angstrom green line of Fe XIV, which should carry the same information as the X-ray and EUV lines that show the holes projected on the solar disk. However, the green corona is detectable only at the solar limb, where the line of sight through the corona is very long. The observed intensity is the sum of the bright and dark features along this line of sight, and since coronal holes are typically bordered by abnormally bright regions, they are usually

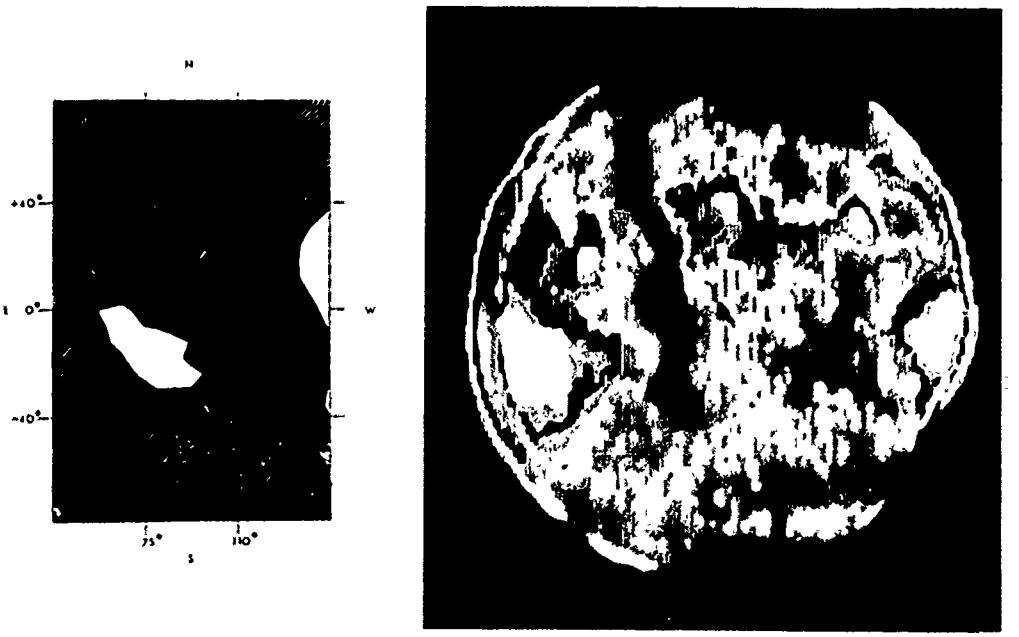

Comparison of a computer-generated image (left) of a coronal hole (at 110° longitude) derived from coronal observations at Sacramento Peak Observatory with an extreme ultraviolet image from a spacecraft (right). The horizontal scale of the Sacramento Peak Observatory image is distorted by the projection coordinate used, but the correspondence of the outline with that of the extreme ultraviolet image is apparent.

not detectable as a definite decrease in the observed brightness of the limb corona. This is overcome by taking advantage of the fact that the sun, with the corona, rotates 13 degrees per day. Thus, each day, the corona is seen from a different direction. When four or five days of coronal brightness measurements are combined in a deconvolution procedure, details along the line of sight can be resolved in a manner similar to perception of depth by stereoscopic vision, and the coronal holes can be mapped as they rotate past the limb. For the prediction of geomagnetic disturbances, this method has the advantage of lead time of about ten days. Seven days after limb passage the hole reaches the neighborhood of the sub-terrestrial point where its solar wind stream is directed toward the earth. The particles then travel the 150 million km to the earth in about three days.

Five instances were found for which both space observations of holes and adequate Sacramento Peak green line data existed. In each case, analysis of the ground data correctly showed the position, size and shape of the hole, and all five produced geomagnetic disturbances.

The Kitt Peak National Observatory has announced a second method for observing

the coronal holes from the ground. They are visible on the solar disk as areas of abnormal surface structure in pictures made with light from the strong infrared helium line at 10830 angstroms. Sacramento Peak observers have confirmed this finding with the tower telescope and diode array, and explained why chromospheric structures are affected by variations in the corona which is about 1,000 times less dense and situated about 30,000 km higher. In the 1960's, Sacramento Peak observers found that helium emission was confined to a narrow layer high in the chromosphere, unlike that of any other atom. This suggested that the helium emission was excited by ionizing radiation from the corona (the Lyman continua of both hydrogen and helium) which was completely absorbed in the narrow helium emitting layer high in the chromosphere. The reflection of coronal holes in the chromospheric helium emission confirms this theory.

The coronal green line and the helium line observations provide two methods for defining the coronal holes from the ground. The Sacramento Peak Observatory is presently preparing the special equipment required to monitor the sun in both lines, and will shortly begin reporting coronal holes and expected geomagnetic disturbances to the Air Force Global Weather Central.

Sacramento Peak scientists have also been working toward attaining a better understanding of the behavior of coronal holes. Using EUV data supplied by NASA's Goddard Space Flight Center from the spectroheliograph aboard OSO-VII, coronal hole areas have been determined for 18 months prior to and during the Skylab mission. The most unexpected discovery has been that coronal holes do not participate in the differential rotation shown by virtually all other solar surface phenomena. Thus, at latitudes away from the equator, coronal hole regions move westward with respect to the general solar atmosphere. This relative motion is as great as 50 degrees of solar longitude per rotation at 50 degrees latitude. Studies of the effects of coronal hole migration continue, especially with respect to the inevitable sweeping-up of the slower rotating active regions. Coronal holes, because of their rotational characteristics, would appear to be related to the interplanetary magnetic field, which also rotates as a rigid body.

The great size and lifetime of coronal holes indicate that they are related to a basic internal magnetohydrodynamic phenomenon of the sun. From May 1972 to November 1973, coronal holes appeared predominantly at four equatorial solar longitudes almost at 90-degree angles to each other. Data obtained in late 1974 from the Sacramento Peak Observatory coronagraph revealed only two coronal holes separated by 180 degrees in longitude. This alternation between quadrupole and dipole structures recalls a similar behavior in the sector structure of the interplanetary magnetic field. Both may be intimately linked with the 11-year cycle of solar activity.

JOURNAL ARTICLES
JULY 1972 - JUNE 1974

ALTROCK, R. C.
The Formation of Mg I 4571 Å in the Solar Atmosphere. IV. Empirical Vs. Synthetic Analyses
Solar Phys., Vol. 34 (1974)

ALTROCK, R. C., and CANNON, C. J. (Univ. of Sydney, Austl.)
The Formation of Mg I 4571 Å in the Solar Atmosphere. I. A Model Analysis of the One-Dimensional Static Atmosphere
Solar Phys., Vol. 26 (1972)
The Formation of Mg I 4571 Å in the Solar Atmosphere. II. The Effect of One-Dimensional Macroscopic Velocity Fields
Solar Phys., Vol. 29 (1973)
The Formation of Mg I 4571 Å in the Solar Atmosphere. III. The Holweger Solar Model
Solar Phys., Vol. 30 (1973)

BECKERS, J. M.
The Response of the Helium Triplet Radiation in Prominences to an Increase In Ultraviolet Flux Resulting from Solar Flares
Bull. of the Am. Astronom. Soc., Vol. 4 (1972)

The Sacramento Peak Observatory Universal Birefringent Filter
Bull. of Am. Astronom. Soc., Vol. 5 (1973)
The Next Decade in Observational Solar Research
IAU Highlights of Astron. (1973)
A Fully Tunable Lyot-Ohman Filter
J. of the Opt. Soc. of Am., Vol. 63 (1973)

BECKERS, J. M., and CHIPMAN, E. (Univ. of Colo.)
The Profile of the Coronal Lyman-Alpha Line
Bull. of the Am. Astronom. Soc., Vol. 5 (1973)
The Profile and Polarization of the Coronal Lyman-Alpha Line
Solar Phys., Vol. 34 (1974)

BECKERS, J. M., DUNN, R. B., and LYNCH, D. K. (Univ. of Tex.)
A Morphological Study of Spicule Filtergrams
Solar Phys., Vol. 30 (1973)

BECKERS, J.M., MAUTER, H.A., MANN, G. R., and BROWN, D. R. (Univ. of Colo.)
High Resolution Spectroscopy of the Disk Chromosphere. I. Observing Procedure
Solar Phys., Vol. 25 (1972)

BECKERS, J. M. and SCHULTZ, R. S. (High Alt. Obsv., Boulder, Colo.)
Oscillatory Motions in Sunspots
Solar Phys., Vol. 27 (1972)

BECKERS, J. M., and SCHULTZ, R. S. (High Alt. Obsv., Boulder, Colo.), WHITE, O. R.
High Spatial and Temporal Resolution Observations of the Magnetic Field in a Sunspot
Bull. of the Am. Astronom. Soc., Vol. 5 (1973)

BECKERS, J. M., and WILSON, F. R., REES, D. E. (Univ. of Sydney, Austl.), BROWN, D. (Jt. Inst. for Lab. Astrophys., Univ. of Colo.)
High Resolution Spectroscopy of the Disk Chromosphere II. Time Sequence Observations of Calcium II H and K Emissions
Solar Phys., Vol. 25 (1972)

BECKERS, J. M., WORDEN, S. P., and HIRAYAMA, T. (Tokyo Astronom. Obsv., Mitaka, Jap.)
The He^+ λ4686 Line in the Low Chromosphere
Solar Phys., Vol. 28 (1973)

CANFIELD, R. C.
Observations of the Variation of Temperature with Latitude in the Upper Solar Photosphere II. Magnetic Field Comparison, Implications for Solar Oblateness Measurements and Harmonic Analysis
The Astrophys. J., Vol. 179 (1973)
Theoretical Chromospheric Flare Spectra. II: Hydrogen Equilibrium for Brown's (1973) Models for Heating by Non-Thermal Electrons
Solar Phys., Vol. 34 (1974)

CANFIELD, R. C., and ATHAY, R. G. (High Alt. Obsv., NCAR, Boulder, Colo.)
Theoretical Chromospheric Flare Spectra. I. Hydrogen Equilibrium for the Kinematic Flare-Shock Models of Nakagawa, Wu and Han (1973)
Solar Phys., Vol. 34 (1974)

CANFIELD, R. C., and MEHLTRETTER, J. P.
Fluctuations of Brightness and Vertical Velocity at Various Heights in the Photosphere
Solar Phys., Vol. 33 (1973)

CANFIELD, R. C., and MUSMAN, S. A.
Vertical Phase Variation and Mechanical Flux in the Solar 5-Minute Oscillation
Astrophys. J. Ltrs., Vol. 184 (1973)
Observation and Interpretation of Phase Lags in the Five-Minute Oscillation
Bull. of the Am. Astronom. Soc., Vol. 5 (1973)

DE MASTUS, H. L., WAGNER, W. J., and ROBINSON, R. D. (Univ. of Colo.)
Coronal Disturbances I. Fast Transient Events Observed in the Green Coronal Emission Line During the Last Solar Cycle
Solar Phys., Vol. 31 (1973)

DONNELLY, R. F., BERGER, E. L. (NOAA Space Envmt. Lab., Boulder, Colo.), BUSMAN, J.D. (NOAA Comsnd. Corps., Boulder, Colo.), HENSON, B. (NASA, George C. Marshall Space Flt. Ctr., Huntsville, Ala.), JONES, T. B. (Univ. of Leicester, Eng.), LERFALD, G. M. (NOAA Wave Prop. Lab., Boulder, Colo.), NAJITA, K. (Univ. of Haw.), RETALLACK, W. M. (NOAA Space Envmt. Lab., Boulder, Colo.), and WAGNER, W. J.
An Atlas of Extreme UV Flashes of Solar Flares Observed Via SFD During the ATM-Skylab Missions.
Rpt. UAG-36, World Data Ctr. A., NOAA (1974)

DUNN, R. B., MANN, G. R., and SIMON, G. W.
Cinematography of Solar Granulation
Bull of the Am. Astronom. Soc., Vol. 5 (1973)

DUNN, R. B., RUST, D. M., and SPENCE, G. E.
A 512-Channel Photodiode Array for Solar Observations
Proc. of the Soc. of Photo-Opt. Instmn. Engrs., Instmn. in Astron. II, Vol. 44, Tucson, Ariz. (4-6 March 1974)

DUNN, R. B., and ZIRKER, J. B. (The Univ. of Haw.)
The Solar Filigree
Solar Phys., Vol. 33 (1973)

EVANS, J. W.
Glass, Polarizing and Interference Filters
Sec. in Am. Inst. of Phys. Hdbk. (1972)

EVANS, J. W., and CATALANO, C. P., LT.
Observed Oddities in the Lines H, K, B and H
Solar Phys., Vol. 27 (1972)

FISHER, R. R.
The Loop Prominence of 11 August 1972: A Coronal Continuum Event
Solar Phys., Vol. 35 (1974)
The Fe XIV Brightness Measurements: 30 June 1973
Solar Phys., Vol. 36 (1974)

LIEBENBERG, D. H., HOFFMAN, M., SANDERS, W. M. (Los Alamos Sci. Lab., Univ. of Calif., Los Alamos, N. M.), and BECKERS, J. M.
Airborne Video Recorded Coronal Emission Line Profiles of λ 5303 at the 10 July 1972 Total Solar Eclipse
Bull. of the Am. Astronom. Soc., Vol. 5 (1973)

MEHLTRETTER, J. P.
Studies of Granular Velocities. III. The Influence of Finite Spectral and Spatial Resolution Upon the Measurement of Granular Doppler Shifts
Solar Phys., Vol. 30 (1973)

MUSMAN, S. A.
A Mechanism for the Exploding Granule Phenomena
Solar Phys., Vol. 26 (1972)
The Dynamics of Solar Granulations
Bull. of the Am. Astronom. Soc., Vol. 5 (1973)
Measurements of Solar Convective Turbulence
Am. Phys. Soc. Bull., Ser. II, Vol. 18 (1973)
The Origin of the Solar Five-Minute Oscillation
Solar Phys., Vol. 36 (1974)

MUSMAN, S. A., and ALLEN, M. S. (Univ. of Mich.)
The Location of Exploding Granules
Solar Phys., Vol. 32 (1973)

ROY, J. R.
The Magnetic Configuration of the 18 November 1968 Loop Prominence System
Solar Phys., Vol. 26 (1972)

ROY, J. R. (Univ. of West. Ont., Can.), and RUST, D. M.
Solar Surges I. Their Magnetic Properties
Solar Phys., Vol. 28 (1973)

RUST, D. M.
Flares and Changing Magnetic Fields
Solar Phys., Vol. 25 (1972)
Real-Time Analysis of Flare-Associated Photospheric Magnetic Field
Bull. of the Am. Astronom. Soc., Vol. 4 (1972)
The Great Flares of August 1972
Sky and Telescope, Vol. 44 (1972)
Magnetic Fields in McMath Region 11128
Data on Solar Geophys. Activity Assoc. with the Major Ground-Level Cosmic Ray Events of 24 Jan. and 1 Sep. 1971 (UAG Rpt., NOAA, Boulder, Colo.), UAG-24 (December 1972)
Analysis of the August 7, 1972 White Light Flare: Changes in the Magnetic and Velocity Fields
Solar Phys., Vol. 33 (1973)

RUST, D. M., and BAR, V. (Tel Aviv Univ., Isr.)
Magnetic Fields of the Loop Prominences of August 2, 7, and 11
Bull of the Am. Astronom. Soc., Vol. 5 (1973)
Magnetic Fields, Loop Prominences and the Great Flares of August 1972
Solar Phys., Vol. 33 (1973)

RUST, D. M., DUNN, R. B., and LINSKY, J. L. (Jt. Inst. for Lab. Astrophys., Univ. of Colo.)
Preliminary Interpretation of Diode Array Observations
Bull of the Am. Astronom. Soc., Vol. 6 (1974)

RUST, D. M., and GRAF, W. (Stanford Univ., Calif.)
Gyro-Resonance Emission Transverse to the Magnetic Field of a Large Spot Group
Bull. of the Am. Astronom. Soc., Vol. 6 (1974)

RUST, D. M., and MACHADO, M. E. (San Miguel Obsv., Arg.)
Analysis of the August 7, 1972 White Light Flare: Its Spectrum and Vertical Structure
Solar Phys., Vol. 33 (1973)
The Spectrum and Vertical Structure of the August 7, 1972 White Light Flare
Bull. of the Am. Astronom. Soc., Vol. 6 (1974)

SIMON, G. W., and NOYES, R. W. (Smithsonian Astrophys. Obsv., Harvard Coll. Obsv., Cambridge, Mass.)
Observed Heights of EUV Lines Formed in the Transition Zone and Corona
Solar Phys., Vol. 22 (1972)
Solar Rotation as Measured in EUV Chromospheric and Coronal Lines
Solar Phys., Vol. 26 (1972)

SIMON, G. W., SEAGRAVES, P. H., and TOUSEY, R. (Naval Res. Lab., Wash., D. C.), NOYES, R. W. (Ctr. for Astrophys., Cambridge, Mass.)
Rocket Spectroheliogram Observations of the Heights of Formation and Size of Bright Features in the Transition Zone
Bull. of the Am. Astronom. Soc., Vol. 6 (1974)

SIMON, G. W., and ZIRKER, J. B. (Inst. for Astron., Honolulu, Haw.)
A Search for the Roots of Photospheric Magnetic Fields
Bull. of the Am. Astronom. Soc., Vol. 5 (1973)
A Search for the Footpoints of Solar Magnetic Fields
Solar Phys., Vol. 35 (1974)

WAGNER, W. J., and HANSEN, R. T., HANSEN, S. F. (High Alt. Obsv., NCAR, Mauna Loa, Haw.)
Coronal Disturbances. II. The Fast Rearrangement of Coronal Magnetic Fields
Solar Phys., Vol. 34 (1974)

PAPERS PRESENTED AT MEETINGS JULY 1972 - JUNE 1974

ALTROCK, R. C.

Empirical Analysis of Solar Absorption Line Profiles
1973 Summer Sci. Mtg. of the Astronom. Soc. of the Pacific, Univ. of So. Calif., Los Angeles, Calif. (11-13 June 1973)

ALTROCK, R. C., and CANFIELD, R. C.

A Non-L.T.E. Analysis of the Solar Mg I Spectrum
142nd Mtg. of the Am. Astronom. Soc., Lincoln, Neb. (27-29 March 1974)

ALTROCK, R. C., and CANNON, C. J. (Univ. of Sydney, Austl.)

The Minimum Temperature in the Solar Atmosphere
138th Mtg. of the Am. Astronom. Soc., Mich. State Univ., Lansing, Mich. (16-18 August 1972)

A One-Dimensional Approximation to the Macroturbulent Velocity Field in the Solar Atmosphere
Solar Phys. Div. Mtg. of Am. Astronom. Soc., Las Cruces, N. M. (8-11 January 1973)

Model Studies of Intensity Fluctuations on the Solar Disk in Mg I 4571 Å
Intl. Astronom. Union Symp., Southport, Queensland, Austl. (7-11 September 1973)

A Two-Dimensional Analysis of Intensity Fluctuations in Mg I 4571 Å on the Solar Disk
Mtg. of the Am. Astronom. Soc., Solar Phys. Div., Honolulu, Haw. (9-11 January 1974)

BECKERS, J. M

The Sacramento Peak Observatory Universal Birefringent Filter
Solar Phys. Div. Mtg. of Am. Astronom. Soc., Las Cruces, N. M. (8-10 January 1973)

A Fully Tunable Lyot-Ohman Filter
Opt. Soc. of Am. Mtg., Denver, Colo. (13-16 March 1973)

The Next Decade in Observational Solar Research
Intl. Astronom. Union Gen. Asbly. (Symp. Cmsn. 10 and 36), Sydney, Austl. (20-30 August 1973)

Status Report of the IAU Commission 10 Working Group on Magnetograph Calibration
Intl. ATSTRONOM. Union Symp., Southport, Queensland, Austl. (7-11 September 1973)

BECKERS, J. M., and CHIPMAN, E. (Univ. of Colo.)

The Profile of the Coronal Lyman-Alpha Line
141st Mtg. of the Am. Astronom. Soc., Tucson, Ariz. (3-6 December 1973)

BECKERS, J. M., and SCHULTZ, R. B., WHITE, O. R. (High Alt. Obsv., Natl. Ctr. for Atm. Res., Boulder, Colo.)

High Spatial and Temporal Resolution Observations of the Magnetic Field in a Sunspot
140th Mtg. of the Am. Astronom. Soc., Ohio State Univ., Columbus, Ohio (21-23 June 1973)

CANFIELD, R. C.

A Scaling-Law Approach to the Calculation of Radiative Losses in Optically Thick Atmospheres
141st Mtg. of the Am. Astronom. Soc., Tucson, Ariz. (3-6 December 1973)

Theoretical Hydrogen Spectra of Chomospheric Flares
Mtg. of the Am. Astronom. Soc., Solar Phys. Div., Honolulu, Haw. (9-11 January 1974)

CANFIELD, R. C., and MUSMAN, S. A.

Observation and Interpretation of Phase Lags in the Five-Minute Oscillation
Solar Phys. Div. Mtg. of Am. Astronom. Soc., Las Cruces, N. M. (8-10 January 1973)

DEMASTUS, H. L., WAGNER, W. J., and ROBINSON, R. D. (Univ. of Colo.)

Fast Transient Events Observed in the Green Coronal Emission Line
Solar Phys. Div. Mtg. of Am. Astronom. Soc., Las Cruces, N. M. (8-10 January 1973)

DUNN, R. B., MANN, G. R., and SIMON, G. W.

Cinematography of Solar Granulation
Solar Phys. Div. Mtg. of Am. Astronom. Soc., Las Cruces, N. M. (8-10 January 1973)

DUNN, R. B., RUST, D. M., and SPENCE, G. E.

A 512-Channel Photodiode Array for Solar Observations
Sem., Instmn. in Astron.-II, Soc. of Photo-Opt. Instmn. Engr., with Am. Astronom. Soc. and Opt. Soc. of Am., Tucson, Ariz. (4-6 March 1974)

DUNN, R. B., and SPENCE, G. E.

A Multichannel Diode Array for Solar Observations
Solar Phys. Div. Mtg. of Am. Astronom. Soc., Las Cruces, N. M. (8-10 January 1973)

DUNN, R. B., and ZIRKER, J. B. (Inst. for Astron., Honolulu, Haw.), BECKERS, J. M.

Properties of the Solar Filigree Structure
Intl. Astronom. Union Symp. No. 56, Southport, Queensland, Austl. (7-11 September 1973)

FISHER, R.

The 11 August Loops, A Coronal Continuum Event
Solar Phys. Div. Mtg. of Am. Astronom. Soc., Las Cruces, N. M. (8-10 January 1973)

FISHER, R. R., and FOUCAL, P., HUBER, M., NOYES, R., REEVES, E., SCHMAHL, E., TIMOTHY, G., VERNAZZA, J., WITHBROE, G. (Harvard Coll. Obsv., Cambridge, Mass.)

Surge Observations from ATM/Skylab
55th Ann. Spring Mtg. of the Am. Geophys. Union, Wash., D. C. (8-12 April 1974)

GRAF, W. (Stanford Univ., Calif), and RUST, D. M.

Gyro-Resonance Emission Transverse to the Magnetic Field of a Large Spot Group

Mtg. of the Am. Astronom. Soc., Solar Phys. Div., Honolulu, Haw. (9-11 January 1974)

LIEBENBERG, D. H., HOFFMAN, M., SANDERS, W. M. (Los Alamos Sci. Lab., Univ. of Calif., Los Alamos, N. M.), and BECKERS, J. M.
Airborne Video Recorded Coronal Emission Line Profiles of 5303 at the 10 July 1972 Total Solar Eclipse
Solar Phys. Div. Mtg. of Am. Astronom. Soc., Las Cruces, N. M. (8-10 January 1973)

MUSMAN, S. A.
Measurements of Solar Convective Turbulence
26th Mtg. of the Am. Phys. Soc. Fluid Dyn. Div., Yale Univ., New Haven, Conn. (19-21 November 1973)
Generation of the Solar Five-Minute Oscillation
Mtg. of the Am. Astronom. Soc., Solar Phys. Div., Honolulu, Haw. (9-11 January 1974)

RUST, D. M.
Inference of the Hard X-Ray Source Dimensions in the August 7, 1972 White Light Flare
Jt. IAU-COSPAR Symp., Buenos Aires, Arg. (11-14 June 1974)

RUST, D. M., and BAR, V. (Tel-Aviv Univ., Isr.)
Magnetic Fields of the Loop Prominences of August 2, 7 and 11, 1972
Solar Phys. Div. Mtg. of Am. Astronom. Soc., Las Cruces, N. M. (8-10 January 1973)

RUST, D. M., DUNN, R. B., and LINSKY, J. L. (Jt. Inst. for Lab. Astrophys., Univ. of Colo.)
Preliminary Interpretation of Diode Array Observations
Am. Astronom. Soc. Mtg., Solar Phys. Div., Honolulu, Haw. (9-11 January 1974)

RUST, D. M., and GRAF, W. (Stanford Univ., Calif.)
Gyro-Resonance Emission Transverse to the Magnetic Field of a Large Spot Group
Mtg. of the Am. Astronom. Soc., Solar Phys. Div., Honolulu, Haw. (9-11 January 1974)

RUST, D. M., and HEGWER, F. (High Alt. Obsv., Boulder, Colo.)
Optical Emissions from the Flare of 7 August 1972
Fall Ann. Mtg. of the Am. Geophys. Union, San Francisco, Calif. (4-7 December 1972)

RUST, D. M., and MACHADO, M. E. (San Miguel Obsv., Arg.)
The Spectrum and Vertical Structure of the August 7, 1972 White Light Flare
Mtg. of the Am. Astronom. Soc., Solar Phys. Div., Honolulu, Haw. (9-11 January 1974)

RUST, D. M., and ROY, J. R. (Big Bear Solar Obsv., Hale Obsvs., Pasadena, Calif.)
The Late June, 1972 CINOF Flares
1974 Intl. Symp. on Solar Terrestrial Phys./17th Plenary Mtg. of COSPAR, Sao Paulo, Brazil (17 June - 1 July 1974)

SIMON, G. W., DUNN, R. B., and LA BONTE, B. J. (Calif. Inst. of Technol., Pasadena, Calif.)
A Phenomenological Study of High-Resolution Granulation Photographs
Mtg. of the Am. Astronom. Soc., Solar Phys. Div., Honolulu, Haw. (9-11 January 1974)

SIMON, G. W., SEAGRAVES, P. H., and TOUSEY, R. (Naval Res. Lab., Wash., D. C.), NOYES, R. W. (Ctr. for Astrophys., Cambridge, Mass.)
Rocket Spectroheliogram Observations of the Heights of Formation and Size of Bright Features in the Transition Zone
Mtg. of the Am. Astronom. Soc., Solar Phys. Div., Honolulu, Haw. (9-11 January 1974)

SIMON, G. W., and ZIRKER, J. B. (Inst. for Astron., Honolulu, Haw.)
A Search for the Roots of Photospheric Magnetic Fields
Solar Phys. Div. Mtg. of Am. Astronom. Soc., Las Cruces, N. M. (8-10 January 1973)

WAGNER, W. J., DE MASTUS, H. L., and ROBINSON, R. D. (Colo. Univ.)
An Analysis of Transient Events Observed in the Fe XIV Coronal Emission Line
Conf. on Flare-Produced Shock Waves in the Corona and Interplanet. Space, High Alt. Obsv., NCAR, Boulder, Colo. (11-14 September 1972)
Fast Transient Events Observed in the Green Coronal Emission Line
Intl. Astronom. Union Symp., Southport, Queensland, Austl. (7-11 September 1973)

WAGNER, W. J., and HANSEN, R. T., HANSEN, S. F. (High Alt. Obsv., NCAR, Mauna Loa, Haw.)
The Fast Rearrangement of Coronal Magnetic Fields
Intl. Astronom. Union Symp. on Coronal Disturbances, Southport, Queensland, Austl. (7-11 September 1973); Mtg. of the Am. Astronom. Soc., Solar Phys. Div., Honolulu, Haw. (9-11 January 1974)

TECHNICAL REPORTS
JULY 1972 — JUNE 1974

CANFIELD, R. C.
A Simplified Method for Computing Radiative Energy Loss Due to Spectral Lines. II. Programs for Solar Flare Models
AFCRL-TR-74-0158 (26 March 1974)

FISHER, R. R.
A Photoelectric Photometer for the Fe XIV Solar Corona
AFCRL-TR-73-0696 (9 November 1973)

RUST, D. M.
Estimating the Flare-Production Potential of Solar Active Regions from Analysis of Real-Time Magnetic Field Data
AFCRL-TR-73-0221 (17 April 1973)

RUST, D. M., and ROY, J. R.
The Late June 1972 CINOF Flares
AFCRL-TR-74-0201 (22 April 1974)

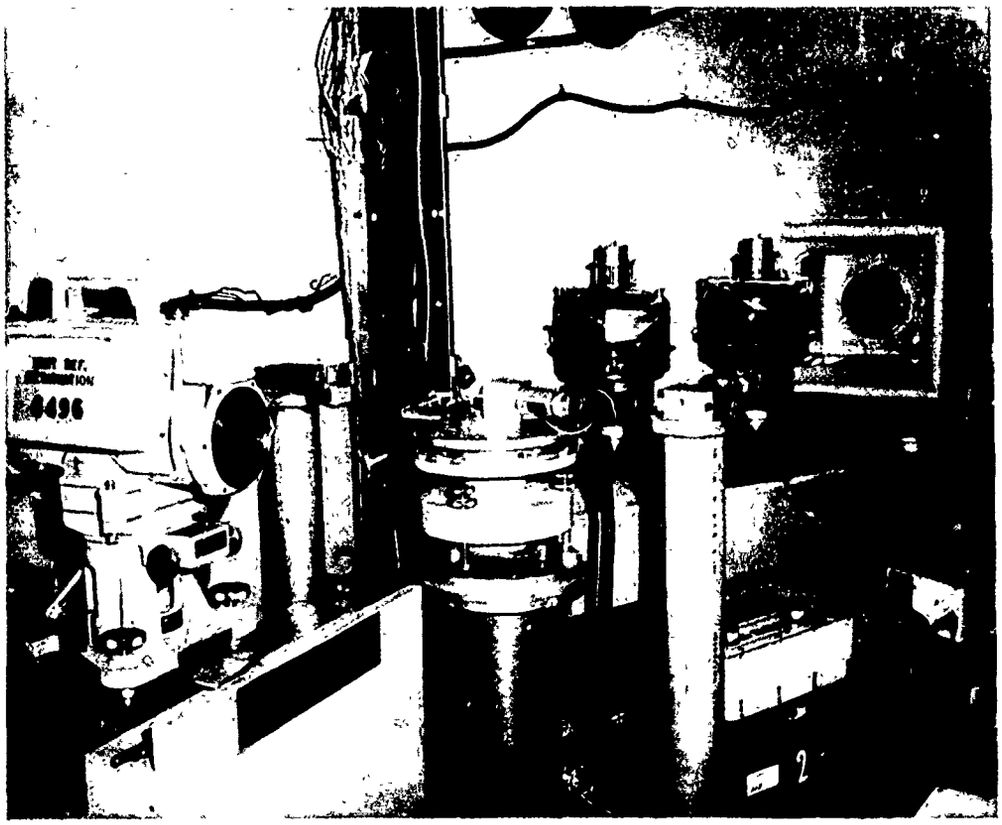

Instrumentation used to determine the effects of earth motions on guidance system alignment procedures and to measure long-term stability of a silo. Principal items and functions are: two portable gyrocompasses (dark objects in right center of picture), to provide data for establishing an azimuth standard in the silo; two tiltmeters (mounted on the gyrocompasses), to measure tilts and tilt rates affecting gyrocompass performance; and an electro-optical system (in center of picture), to measure relative movements of azimuth reference devices in the silo.

VIII Terrestrial Sciences Laboratory

The activities of the Terrestrial Sciences Laboratory cover a wide range of efforts supporting the deployment, operation,and delivery of Air Force weapons on the earth's surface, subsurface and in the near atmosphere. They comprise research, development, and testing of concepts, methods, and instrumentation to measure, model, and evaluate geophysical factors which influence the location and performance of such aerospace facilities.

Theoretical and experimental studies are conducted in the Laboratory and in the field, and aboard aircraft or satellite vehicles. Technical areas include geodesy and gravity, geokinetics, seismology, geology, and spectroscopic studies.

During the 1972-1974 period, the increasing sophistication and sensitivity of Air Force systems have necessitated advanced research on terrestrial effects constraining their use. Conversely, similar research has become necessary to forestall the effects of similar hostile systems. The Laboratory's work in geokinetics was specifically directed toward earth motion effects on inertial guidance instrumentation. Geodetic and gravimetric studies provided more accurate descriptions of the shape and surface positions of the earth and its gravity potential. Seismology and geology efforts became strongly oriented to understanding shock-wave and deformation propagation through the earth's structure. The spectroscopic studies devoted to targeting applications were transferred to another AFCRL laboratory in mid-1974, at the end of the reporting period.

GEODESY AND GRAVITY

Geodesy is concerned with the size, shape and mass distribution of the earth. The geodetic and gravimetric parameters for the earth and geodetic information for positioning are direct data inputs for missile inertial guidance systems and form the structural framework for mapping, charting and navigational aids. Knowing the size, shape, and mass distribution of the earth accurately is a necessary foundation for determining the accurate position, distance and direction between launch sites, tracking sensors and targets. Current information of this nature is often inadequate to meet the requirements of future USAF weapon systems.

The Laboratory maintains continuing research and development programs in geometric geodesy and in physical geodesy or gravity. These programs are directed towards improvement in our fundamental knowledge of earth size, shape and mass parameters, and improvements of techniques for the determination of position, distance and direction on the earth and in terrestrial and inertial three dimensional coordinate systems.

These programs require continuing cooperation and participation by AFCRL in the National Geodetic Satellite Program, together with Army, Navy, NASA, the National Oceanic and Atmospheric Administration, the U.S. Geological Survey, other civilian agencies and academic observatories. The Terrestrial Sciences Laboratory also participates with the International Gravity Commission in the development of a world-wide gravity reference network. A world-wide system of earth-tide profiles is being established in cooperation with the International Center for Earth Tides, Brussels, Belgium.

SATELLITE ALTIMETRY: The satellite altimetry technique consists of making altitude measurements with on-board altimeters in specially instrumented satellites. These altitude measurements are made over ocean areas to measure the shape of the ocean's surfaces and have applications in geodesy, geophysics and oceanography. The first on-board altimeter developed for this purpose will be on satellite GEOS-C to be launched late in 1974.

If the earth were all water, right to its center, a mean sea level would be an equipotential spheroid of revolution. However, the earth is largely solid and it can and does support density variations in continental areas and under oceans. These density variations cause mean sea level to vary scores of meters from its reference spheroid. The equipotential surface, which is the extension of mean sea level throughout the earth, is known as the geoid. The undulations of this geoid from the reference spheroid are related to the earth's gravity field, and their relationship has been the prime topic of physical geodesists who have devised means for determining the spheroid-geoid separations from gravimetric measurements. Now, by the use of satellite altimetry to measure the shape of the geoid, or an oceanic portion of it, we have a means for going in the other direction and determining or refining the earth's gravity field from spheroid-geoid separations.

The GEOS-C altimeter is designed to measure the satellite's distance above sea level to a fraction of a meter. If we assume that the satellite's orbit can be independently established from ground or satellite-to-satellite tracking to about one meter accuracy, the determination of the shape of the sea level is a straightforward procedure. Standard global tracking nets are incapable of achieving one-meter accuracy by an order of magnitude, so the burden for high precision tracking requires denser tracking nets, satellite-to-satellite tracking or other advanced tracking schemes.

AFCRL's approach to satellite altimetry has been to assume that ground tracking is only good enough to achieve orbital ac-

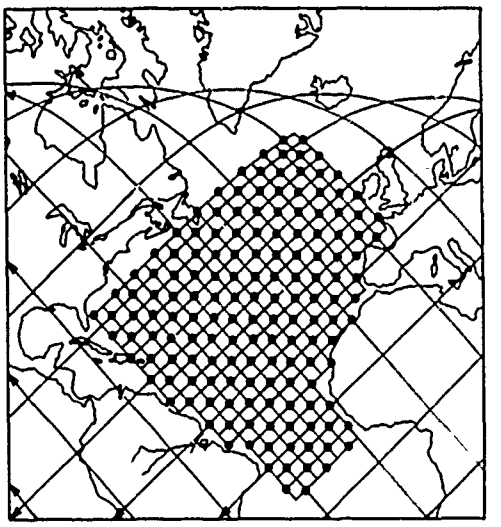

Ground tracks of every fifth pass of approximately 200 passes of GEOS-3 will be reduced in proposed short arc determination of fine structure of North Atlantic geoid. Indicated tracks generate approximate 5-degree by 5-degree cells.

curacies of about 100 meters; this is easy and routine. If we knew the state vector (position and momentum) of the satellite at any epoch, and integrated the satellite motion over a short arc (less than one quarter of a revolution), we could recover the position of the satellite to within about one meter over the entire arc. Although we do not know in advance the state vector of a short arc with adequate precision, by comparing altitudes from a number of independent, interlocking short arcs we have available data to refine all state vectors and improve our ability to determine the short arcs. Where two short arcs cross, the difference in measured altitudes to sea level is the vertical distance between the two arcs. The vertical inter-orbit ties provide a rather tight interlocking net of arcs, particularly in the most important vertical direction. Subtracting the altimeter measurements from this net gives, finally, the shape of the ocean surface.

In practice, the short arc approach to the determination of the oceanic geoid from satellite altimeter measurements is performed in one simultaneous least squares reduction. The reduction entails the estimation of geoidal parameters simultaneously with the estimation of weakly constrained orbital state vectors defining thousands of independent, interlocking short arcs. Patterned characteristics of the normal equations make such a massive solution possible. The AFCRL program for *S*hort *A*rc *R*eduction of *R*adar *A*ltimetry is dubbed SARRA. GEOS-C simulators using SARRA demonstrate that the short arc reduction of satellite altimetry is well suited to the determination of the oceanic geoid.

Once the oceanic geoid is established by satellite altimetry, AFCRL will combine this information with other existing physical geodesy material for the determination of the gravity field of the earth. The most obvious and effective supplementary observations are gravity measurements. Such observations are of greatest availability and accuracy over land—precisely where satellite altimetry is least effective. Another source of observations consists of predetermined geocentric coordinates of any satellite stations that happen to be located on a leveling net tied to mean sea level.

The utilization of altimetry by itself and in combination with existing gravity material is also being examined by developing equations that relate surface density values to geoid undulations and gravity anomalies.

Satellite altimetry is much more sensitive to the shape of the earth than gravimetry, given present levels of observational accuracy; a 1 meter rms anomaly height over an area of 1 square degree tells us more about the shape of the earth than the same square with a 3 mgal (milligal; 1 mgal = 1 cm/sec^2 or about 10^{-3}g) rms gravity anomaly. This relative information content carries over into the description of the earth's gravity field as well, and so, satellite altimetry will make significant contributions to gravity mapping.

AUTOMATED ASTRONOMIC POSITIONING SYSTEM: In the development programs of new USAF weapons systems, there is a rapid trend toward more sophisticated guidance systems, longer ranges, greater accuracies, and a concern for reduction of collateral damage.

These stringent requirements on the geodetic and geophysical error budgets of missile systems have resulted in the AFCRL geodetic instrumentation development program being directed towards more accurate automatic observing methods to acquire geodetic positioning data. An example is the Automated Astronomic Positioning System (AAPS). The AAPS consists of a vertically oriented optical system which observes the stars in zenith transit and casts these star images onto a reticle. As the earth rotates, the stars trail across slits in the reticle, producing pulse outputs from photomultipliers located behind the reticle. The output pulse and time of event are sent to an on-board computer where the stars are identified and included in an on-site determination of astronomic position. The sensor head, containing the optics, is rotated automatically about the instrument's vertical axis to cancel alignment errors. A second solution of astronomic latitude and longitude is performed with the head reversed. These two solutions are combined to form one AAPS position determination.

Field deployment of the Automated Astronomic Positioning System. The AAPS determines astronomic positions more accurately and more rapidly than conventional astronomic positioning, yet requires less operator skill.

Standard classical astronomic positioning methods require an average of 14 days to make the necessary observations at a site. It is expected that the AAPS will have a usable data rate such that it will enable the development of accurate astronomic positions from a few nights' observations per site.

Two prototypes of this system have been developed. The Defense Mapping Agency is currently testing them in extensive operations. They are proving to be automatic in operation and performing as designed. Once manual rough leveling of the instrument is completed, an automatic leveling system takes over and levels the system to the required accuracy. The fine leveling, reversing operation, recording of stellar transits, identification of stars, and the position solution are all parts of the automatic operation of the system.

The automated positioning program is also testing the concept of meridian determination by electro-optical observation of stellar transits, using an AFCRL-modified T-4 theodolite and special reticle. This is an experiment to determine the feasibility of using stellar transits of the local meridian to determine angular velocity as a function of time. These observations may also be used to determine angular resolution for determination of latitude. An important by-product of this experiment, astronomic azimuth, is the required local base reference for authenticating missile azimuth laying sets.

GEODETIC LASER RANGING: Significant advances in geodesy and geodynamics may soon result from highly accurate distance measurements between earth-based laser ranging telescopes and both the moon and

high earth artificial satellites. Centimeter-level measurements, projected for the next three years, offer the possibility of using this technique to detect solid-earth tides and continental drift, as well as to improve our knowledge of variations in the earth's rotation rate and polar motion.

AFCRL has actively participated in the NASA Lunar Laser Ranging Experiment, which has obtained since 1970 over 1500 ranges between the McDonald Observatory in Texas and four of the retroreflectors placed on the moon by the Apollo and Soviet space missions. The data from these observations have been analyzed at AFCRL using the Planetary Ephemeris Program, a large software package developed at MIT with support from AFCRL and other DoD agencies. The data analysis has produced significant improvement in the lunar orbit and physical libration, the coordinates of the McDonald Observatory, and the principal term in the earth's gravity field. The AFCRL lunar laser telescope, operated in Arizona between 1968 and 1972, is now being refurbished by Australian geodesists for operations near Canberra. The addition of laser ranges from a southern hemisphere observatory will allow analyses of the lunar data to determine separately variations in the earth's rotation and movement of the pole.

Complementing the lunar ranging experiment is an extensive NASA-DoD program for laser ranging to earth satellites. The AFCRL satellite laser at Bedford, Massachusetts, is being used to observe the GEOS-3 satellite. Launch of the high altitude, high mass density Laser Geodetic Satellite (LAGEOS) in 1976 will provide a target whose orbit is relatively free from the effects of atmospheric drag and small scale variations in the earth's gravity field, thus allowing range measurements useful for geodesy at the level of 5-10 cm.

Many geodetic parameters, such as the coordinates of observing stations and the earth's instantaneous pole of rotation, can be determined most efficiently by analyzing a combination of data types. The Planetary Ephemeris Program is capable of performing simultaneous least squares solutions for a large number of parameters using a combination of lunar and satellite laser ranging data. The results can be improved even further by including radio observations using the technique of very long baseline interferometry (VLBI), which provides angular measurements with an accuracy equivalent to centimeters on the earth's surface.

MODELS OF EARTH'S GRAVITY FIELD AND APPLICATION OF ADVANCED ADJUSTMENT TECHNIQUES: Research into the description of the gravity field of the earth encompasses the uniform combination of various heterogeneous data from physical geodesy into a parametric representation of the earth's gravity field. The parameters conventionally used for geopotential models are the coefficients of a spherical harmonic expansion of the geopotential field.

In addition to the classical least squares adjustment, least squares methods of interpolation and least squares prediction of gravity are extensively used in physical geodesy. The mathematical relation between least squares prediction and adjustment was theoretically clarified by Krarup, the Danish geodesist, by exhibiting least squares prediction as a least squares adjustment in a Hilbert space with kernel functions. Further, he generalized least squares prediction of gravity to obtain a general least squares theory for estimating any element of the terrestrial gravity field. This is the *least squares collocation.*

AFCRL simplified and applied Krarup's theory for geodetic applications. Because this development is formally very similar to the well known general case of least square adjustment, it is possible to use ordinary linear algebra, bypassing Hilbert space techniques. In a practical sense this method presents an optimal simultaneous determination of geodetic positions and of the terrestrial gravity field by combining different

data of any kinds—terrestrial angles, distances and various types of gravity measurements as well as data from advanced satellite techniques.

AFCRL is studying the application of generalized inverse theory to geopotential modeling because of its power and flexibility in solving overdetermined and underconstrained linear or quasi-linear problems. Resolution and information density matrices of generalized inverse theory promise to be of significant value in estimating parameters and selecting measurement data.

ABSOLUTE GRAVIMETRY: AFCRL is presently developing a new second generation absolute gravity measuring system. The method employed is to drop one reflector of a two-beam Michelson interferometer and to determine the distance fallen in known time intervals by direct measurements of interference fringes.

The first generation instrument was designed to be transported and was successful in that it was taken to eight different sites and, after spending between one and two weeks total set-up, operate and take down

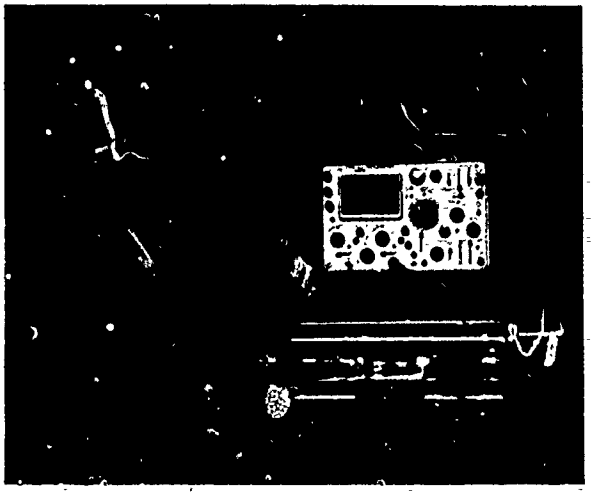

A precision laser instrument which provides wavelength reference standard for fringe measurement.

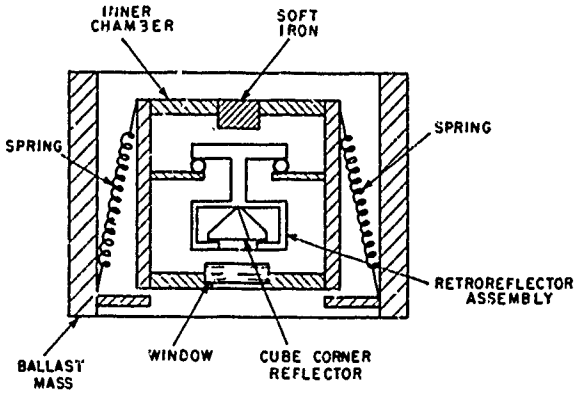

The free-falling chamber containing the cube corner reflector in the second-generation absolute gravity measuring instrument. The inner-and-outer-chamber design reduces the vacuum required to one easily attained. The springs are released at the same time as the outer chamber, pulling the inner chamber down from the retroreflector. This results in very slow rate of fall with respect to the inner chamber, allowing great accuracy.

time, absolute values with a precision of better than ±0.05 mgal were obtained at most sites. The apparatus was bulky and when packed for shipment had a total weight of about 2500 lbs. packed into about 20 shipping containers.

The aim of the new instrument is to decrease the time required to obtain an absolute value of gravity with a precision of at least as good as ±0.05 mgal to about two or three days and to reduce the total weight to at most 800 pounds. This is accomplished by making some radical changes in the mechanical design and employing present day state-of-the-art electronics and computing equipment to give rapid computation of results.

The mechanical design has evolved with the express purpose of removing the necessity of having an ultra high vacuum. This removes the approximately 100 lb. weight of the high vacuum pump and cuts the time by at least one full day besides greatly simplifying the problem of using trouble free materials in the vacuum chamber. Reliability will be increased because the tendency

for clean surfaces to stick together will not exist in the moderate vacuum required with the new design.

The main feature of the new design is that the freely falling reflector is enclosed in a small evacuated chamber which falls along with the reflector. These both fall in a larger vacuum chamber but since the air which comes into contact with the falling object is falling with the acceleration of gravity, air resistance cannot affect the measurement. The vacuum required in the outer chamber need be no better than 1 Pascal to prevent gaseous turbulence and to avoid air drag slowing its fall. The interior of the small chamber requires a vacuum of only 10^{-1} Pascal to place all possible air resistance effects beyond the level of consideration. While the mechanism required for separating the reflector from the small chamber during the fall is somewhat elaborate, it should be very reliable and able to withstand many repetitions of operation.

The electronics system makes digital time measurements between a large number (50 to 500) of interference fringes and will thus make independent measurements of g and the gravity gradient as well as detect seismic motions occurring during the fall of the object. The digital data are processed immediately by an on-line process and control mini-computer.

The future of absolute gravity instruments lies in two directions: portable instruments with precisions of between 0.01 and 0.10 mgal and fixed stations with precisions in the 0.001 mgal range. The technology for producing such portable instruments is well in hand, and the technology for 0.001 mgal precision is available.

A new low-drift gravimeter is also presently under development by AFCRL which promises to provide long-term measurements of changes in the earth's gravity field. The instrument uses a special mechanical design which is less sensitive to temperature changes and is less susceptible to drift caused by material stress than were earlier designs.

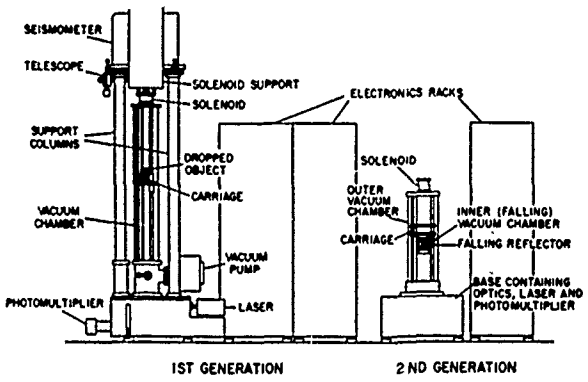

The second-generation laser interferometer absolute gravity instrument has only one electronics rack, as opposed to two in the first-generation instrument. The weight has been reduced to 800 pounds, allowing it to be moved from one location to another.

GRAVITY GRADIOMETRY: The first laboratory version of a gravity gradiometer, built b Eotvos in 1888, was a torsion balance which measured horizontal gravity gradients. Field torsion balances have since been used extensively by exploration geophysicists who found the instruments valuable for detecting density variations within the earth.

What is new about gravity gradiometry is the prospect of measuring the complete gravity gradient tensor from a moving base. The concept of an airborne gravity gradiometer is especially attractive for geodesists and geophysicists who seek to acquire high resolution gravity data over extensive areas. Airborne gravimeters have been limited in their success because aircraft accelerations cannot be discriminated from gravity accelerations, and complex data filtering techniques are required.

A properly designed moving base gravity gradiometer would not detect linear aircraft accelerations and so would be free from this important limitation of airborne gravimetry. On the other hand, gradiometers are very sensitive to rotation; but aircraft rotations can be detected by inertial instrumentation and compensated for, in

real time, to keep the orientation of a gravity gradiometer steady.

The torsion balance is a very sensitive gravity gradiometer, but is fragile, requires long measurement times to attain its high sensitivity, and is unsuitable for operations from a moving base. A number of other gravity gradiometer concepts have recently been proposed which show promise for use on a moving base with about the same sensitivity as the torsion balance—approximately 1 EU (1 Eotvos unit = 10^{-9} sec^{-2} = 1 mgal/10 km). AFCRL has sponsored research on a rotating gravity gradiometer (RGG), and a prototype of this instrument for moving base application is now being built under contract.

The basic sensor structure consists of two mass-loaded arms, pivoted freely at right angles about a common axis and connected by a stiff torsion spring. In operation, the sensor is rotated about its torsional axis at exactly half its torsional resonance frequency. Most alternating torques caused by external accelerations coupling through an imperfect mechanical system are at the spin frequency and therefore can only weakly excite the torsional resonant mode. The gravity gradient field, however, induces alternating torques at twice the spin frequency that are preferentially "amplified" by the mechanical resonance. The alternating torques are converted into measured AC voltages by piezoelectric transducers.

The phase and amplitude of the RGG sensor provides measurements of two elements of the gravity gradient tensor. Three RGG sensors, operating about mutually perpendicular axes, are required to measure the complete gravity gradient tensor.

The design of the RGG requires a consideration of all possible error sources, and methods for their elimination or minimization. The RGG system requires a state-of-the-art *V*ibration *I*solation *A*lignment and *L*eveling *S*ystem (VIALS) for support on a moving base. The RGG system's design goal is 1 EU in ten seconds.

Tests of the suitability of the RGG for operating on a moving base will be performed on laboratory simulators to define VIALS requirements and real-time compensation techniques to be used with the RGG and VIALS. Subsequently, the VIALS and compensation package will be built and integrated with the RGG. Tests of the entire system would then be performed on laboratory simulators and, finally, in actual aircraft operations.

If the RGG fulfills its promised sensitivity, it will be of enormous value in the detailed mapping of the earth's gravity field and will contribute significantly to inertial navigation and guidance.

GEOKINETICS

The observation of unexplained perturbations in early gyrocompass data raised the question of whether or not geophysical phenomena could be the underlying cause and if so, were there other degrading effects which would manifest themselves as inertial instrument sensitivity was improved? Since the resolution of these questions is highly pertinent to the accuracies obtainable with advanced inertial guidance systems, AFCRL has initiated a program to provide the needed answers. The program is concerned with the geokinetic effects on inertial instrument performance, and the motions of interest extend all the way from short-period seismic motions to long-period polar motions which may have a period of a year or more. The major emphasis is on seismic motions and tilts.

The approach which is used in the program is to first characterize the motion environment in terms of its physical and statistical properties; then estimation principles are used to predict the contribution of the motion environment to performance degradation. The research follows two courses: determining the effects of earth motions on component testing in a laboratory envi-

ronment, and examining the motional effects on systems performance in an operational environment.

COMPONENT TESTING: In collaboration with contractors, AFCRL conducted a long-term test of a gyro while monitoring the motion environment. The test, conducted at Norwood, Massachusetts, utilized the type of gyro which is used for azimuth alignment of the Minuteman guidance system and the gyro was operated in a four-position gyrocompass mode during the test. The earth motion environment was monitored by seismometers and tiltmeters.

When operated as a gyrocompass, a single-degree-of-freedom rate integrating gyro is basically an earth rotation rate sensor. The gyro responds to components of earth rate along its sensitive axis and translates these angular rates into a feedback current. This current is integrated over a period of time to obtain an average rate.

Tilting of the gyro platform during gyrocompassing is of particular concern since the tilt rates tend to mask the earth-rate component and produce erroneous gyrocompass results. The gyro is sensitive to small angular velocities and as a result, any tilt rate about the east-west axis will be interpreted as an azimuth offset. At the latitude of Norwood, Massachusetts, a tilt rate of 5×10^{-5} degrees per hour will result in a 1 arcsecond azimuth offset. The tilt rates observed during the test were equivalent to those expected at a quiet, relatively stable test facility.

In a test of the long-term accuracy of gyrocompassing, the difference between azimuth as determined by astronomical observations and that measured by gyrocompassing was ascertained and plotted. The results show significant periods of time where the residuals were quite small, i.e., less than 1 arcsecond. However, there were occasions where the residuals were in the 2 to 3 arcsecond range. Some of the discrepancies could be attributed to the tilting of the test pier.

An analysis was made of the statistical properties of the gyro when operated in a torque-to-balance mode. The output proved to be a gaussian process and as such, its random properties can be completely described in terms of second-order statistics, specifically as correlations or spectral estimates. A plot of the density distributions suggests that the output of the gyro is a non-stationary process.

Based on the properties of the gyro output and the test pad motions in the seismic regime, statistical operators were formed to predict the influence of these motions on gyro performance. The results disclosed that large distant earthquakes (earthquakes of magnitude 6 or greater) will have a significantly degrading effect on gyro output. For a magnitude 6 event, approximately 50

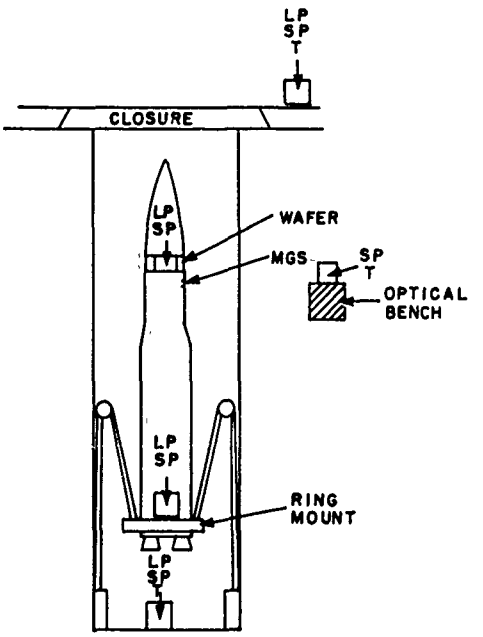

Instrumentation used to perform intra-silo motion measurements. LP indicates a Long-Period Seismometer, SP, a Short-Period Seismometer, and T, a Tiltmeter. Instrumentation is placed on the silo closure door, on an optical bench in the launch equipment room, and the base of the silo, on the missile suspension system, and in a wafer located just above the Missile Guidance Set.

percent of the low frequency output of the gyro can be attributed to the earthquake-excited motions of the test pad.

SYSTEM PERFORMANCE: An integral part of targeting a ballistic missile is to align the guidance platform with respect to some preselected reference coordinate frame. The accuracy achievable with a given guidance system will depend on the precision of the alignment of the guidance platform and on the ability to maintain this precise alignment between calibration sequences.

For the Minuteman guidance system, the reference coordinate frame is based on measurements of local vertical and azimuth. Local vertical is acquired through the use of a bubble level, and azimuth (or north) is determined by using gyrocompassing techniques. AFCRL is investigating the effects of earth motions on the precision of these measurements in a silo environment. An operationally configured Minuteman silo at Hill AFB, Utah, has been selected for the first phase of the study.

The objectives of the study being conducted at Hill AFB are threefold: 1) to characterize the total motion environment of a Minuteman silo; 2) to quantify the effects of disturbing motions on the ability to establish and maintain a stable azimuth reference, and 3) to develop techniques for predicting the motion environment within a silo from a limited set of external measurements. To achieve the objectives, the study has been segmented into four experiments: the measurement of regional, local, and intra-silo motions, and the measurement of the effects of observed motions on alignment procedures.

To establish the base level of regional motions and to ascertain their modes of propagation, a regional seismic array has been installed at Hill AFB. The array is composed of three stations, located some 3-5 km from the silo, and each station has three-component long-period seismometers installed in a buried shelter. The data from the regional stations are telemetered by radio link to the data acquisition system at the silo.

Local motion measurements are accomplished with a seismic array and a tilt array. The seismic array is composed of 21 elements (seven stations with three-component short-period seismometers) and is located approximately 200 meters from the silo. The tilt array has three stations, consisting of dual-axis borehole tiltmeters, and each station is approximately 20 meters from the silo. The tiltmeters are buried to a depth of 3 meters to eliminate surface temperature effects. By using the seismic and tilt arrays, both propagating and non-propagating motions can be measured, the response of the locality to both seismic inputs and local loading can be determined, and local motion sources can be identified and classified as typical or atypical of an operational site.

To measure the intra-silo motions, both seismometers and tiltmeters have been positioned at several points within the silo and on the missile proper. The purpose of these measurements is to characterize the motions in terms of level, mode, spatial organization, statistical class, and origin.

In addition to the instrumentation normally found in a Minuteman silo, several items of equipment have been added for the alignment experiment. The most notable additions are two portable gyrocompass devices (called Azimuth Laying Sets) and an electro-optical measuring system. The two Azimuth Laying Sets (ALS) are used to establish an azimuth standard in the silo, and the electro-optical system, consisting of an autocollimator mounted on an inductosyn table, is used to measure angular variations between the reference mirrors on the two ALS's, the mirror on the stable platform of the missile guidance system, an attached mirror on the missile's frame and the azimuth reference mirror mounted on the wall of the silo. Comparison of the positions of the various mirrors will give an indication of the precision of the azimuthal de-

terminations in the motion environment presented by the silo, and will be a measure of the long-term stability of the silo.

Also as part of the alignment experiment, raw data are being collected from the instrumentation on the inertial guidance platform–the accelerometers, the bubble level, and the gyrocompass assembly. Correlation of the data from these instruments with data from the motion sensors on the missile will give an indication of the degrading influence of the motion environment on the ability of the stable platform to maintain alignment.

CRUSTAL STABILITY: As part of the overall program in geokinetics, AFCRL is conducting experimental and theoretical studies to determine and explain the nature of long-period and aperiodic crustal deformations. The experimental investigations use borehole tiltmeter arrays and tidal gravimeters to measure and characterize these crustal motions. The theoretical investigations are directed toward predicting the response of realistic earth models to dynamic and static loading of the crust.

In the study of the temporal and spatial properties of crustal deformations, a three-element borehole tiltmeter array has been established at Bedford, Massachusetts. The instruments are buried to a depth of 20 meters and the horizontal distance between instruments is 100 meters. A similar array is planned for installation in Maynard, Massachusetts, some 25 km away, in the very near future.

Data from the Bedford tilt array have revealed that coherency between instruments is high at diurnal and semi-diurnal tidal periods but low at longer periods. At the tidal periods, the agreement is within 1 percent, a remarkable improvement over the results obtained from numerous conventional installations in tunnels. A comparison between the tilt array data and the theoretical predictions for ocean-loading tidal tilts is much better than reported from other observatories throughout the world.

SEISMOLOGY

Recent discoveries and theoretical developments in the concept of plate tectonics have improved the potential application of seismology to military objectives. It now appears that portions of the earth's crust are plates supported by a more fluid medium. This has brought an equal realization that local tectonic stress and geologic structure within a plate modify the propagation of seismic waves originating from large natural or man-made sources. The Laboratory efforts in seismology are, therefore, oriented toward refinement and test of physical and mathematical models of seismic sources and mechanisms, particularly those of earthquakes and explosions. These are combined with realistic wave propagation theory to study anomalous effects of tectonic stress, attenuation, orientation, and channeling through the earth's crust. Verification of the quantitative relationships developed is made by seismic modeling tests using real or simulated earth materials, and by analysis of seismic records from known earthquakes or explosions. This research will enable more precise de-

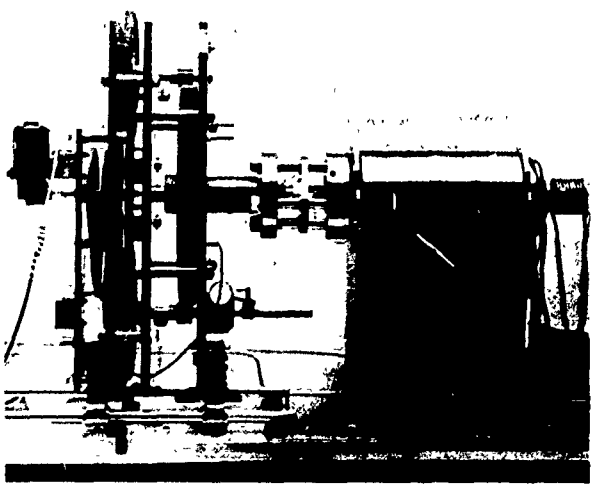

Gas high pressure apparatus which can generate a pressure of 10 kbar and simultaneous temperature of 700 degrees C.

tection and identification of unexplained seismic events for discrimination of possible clandestine underground nuclear explosions from natural earthquakes. The improved knowledge of major geologic effects on shock-wave propagation also will advance the evaluation or prediction of weapons effects on surface or subsurface military installations. The work is generally oriented toward the objectives of other DOD organizations including the Defense Advanced Research Projects Agency and the Defense Nuclear Agency.

NUCLEAR TEST DETECTION: One of the major problems in seismic discrimination between underground nuclear explosions and small earthquakes is the anomalous event–a signal presumed to have been generated by an earthquake, but one for which the ratio of body wave magnitudes to surface wave magnitudes (m_b/M_s) is similar to the ratio for explosions, or conversely a known explosion which produces an earthquake-like signature. A considerable research effort is directed toward determining the causes of such events to reduce the possibility of false identification of an earthquake as an explosion, as well as to increase the capability for identifying explosions deliberately initiated in such a way as to appear as an earthquake. It has been found that many anomalous events identified to date have a particular tectonic setting, e.g., in Tibet, along the Indus suture zone, one of active underthrusting and subduction until recent (geologic) time. Earthquakes in central Eurasia tend to give smaller M_s values for a given m_b value than earthquakes at continental margins. It has been found that when m_b is calculated from teleseismic P wave (compression wave) amplitudes and M_s is calculated from 20-second-period surface wave amplitudes using Love waves rather than Rayleigh waves, the m_b/M_s points for anomalous Eurasian events separate into two populations in the same way as events from other parts of the world. Concurrent research includes a comprehensive study of other seismic array observations to measure propagation delays and relate them to local geologic conditions. Theoretical seismic signal synthesis and comparison with actual related data, and studies to determine the most effective implementation of large aperture seismic arrays in the detection and identification of clandestine nuclear tests are conducted.

SEISMIC MODELING: Common to underground nuclear explosion detection, to assessment of shock-wave effects on subsurface installations, and to determining effects of environmental noise on missile guidance systems is the motion of the earth as it is disturbed. Since both seismic source and propagation processes occur under uncontrolled real earth conditions and nature seldom provides replication or access to the subsurface regions being disturbed, laboratory scale model studies offer another means of investigating specific aspects of seismic waves under closely controlled conditions. The Laboratory effort includes theoretical studies, field investigations, numerical simulation, and modeling. The integrated results yield a better understanding of seismic problems in source phenomena, propagation, and diffraction applicable to these military needs. A physical model of a missile silo has been fabricated. It is driven by mechanically or explosively initiated seismic waves. Strain gauge instrumentation is used to record the dynamic response of the model to various types of seismic waves generated by the source. The resulting measured motions are compared with concurrently developed elastodynamic diffraction theory. These comparisons are leading to the validation of theory and the development of analysis procedures for reducing real earth data. In another model study three dimensional model methods are being developed and applied to the problem of separating cavity-shape phenomena from tectonic prestress in the explosion source region.

This study also bears on the question of evasion and counter-evasion in detecting underground nuclear explosions.

INFRASONICS: Studies of infrasonic signals generated by large explosive events required continuous recording at a local infrasonic instrumentation array to obtain signals from all possible sources for identification and analysis. Digital computer programs were developed and used to reduce background noise, separate signal modes, and analyze frequency spectra. Environmental and climatic conditions obviously affect the propagation and reception of pertinent signals. Infrasonic generation and propagation theories were, therefore, derived and validated using realistic source mechanisms and propagation path parameters to assist in empirical analysis. A previously developed normal mode reduction program for infrasonic data was improved to include the effects of the earth's curvature on signal reception. This allowed use of data from all ranges, including observation points through and beyond the earth's antipodal point, to the source.

Photomicrograph of rock deformed at pressure and temperature simulating a depth of 20 km in the earth.

DEFORMATION AND PROPAGATION MECHANISMS: As missile guidance systems become more sophisticated and complex, they also become more susceptible to strong earth motions and shock waves propagating through deep rocks into their silos. The "hardening" of such missile installations to resist heavy attack requires knowledge of the mechanical properties and distortion or flow of rocks under extremely high pressure and temperature conditions which might result from a nuclear explosion. Information on the strength properties and failure mechanisms of the rock materials most abundant in the earth's crust can also provide more accurate criteria for the interpretation of seismic signals for determination of nuclear weapons tests and effects, their discrimination from earthquakes, and for the efficient design and operation of seismic surveillance networks.

For many years, the Laboratory has conducted tests using apparatus capable of providing static and dynamic loading conditions up to 1,000° C temperature, 100 kbar pressure, and strain rates from 10 to 10^{-8} per second on various rock and mineral material specimens. These tests duplicate deformation conditions within the depth of the earth's crust at which more than 80 percent of all known earthquakes and all man-made explosive events occur.

During the past year, a new precise triaxial loading device using argon gas pressure was used for "wet" and "dry" tests, measuring low-strength materials such as uncon solidated sediments, and attempting to recrystallize clay mineral constituents representative of the most abundant natural rocks. The device also allows introduction of pore fluids at variable pressures corresponding to natural stress states in the earth.

A large number of low pressure-temperature compression tests were run on shales and limestones typical of western U.S.A. missile installation geology. The purpose was to study deformation of clay-rich rocks exhibiting great weakness in nature. Initial test results showed that such shales have varying sensitivity depending on selective production of porewater. Initial degree of compaction, porosity, water content, and permeability also strongly controls the decrease of effective stress and strength. Initial compression experiments on a variety of natural garnet crystals have, for the first time, produced evidence of ductile behavior in this important group of rock-forming minerals abundant in the deep crust and upper mantle of the earth.

Transmission electron photomicrograph of dislocations in the mineral olivine.

Natural and experimentally deformed materials are examined with a variety of analytical techniques such as powder and single crystal X-ray diffraction, and optical and electron microscopy. Recent analysis of chain and framework silicates has established their ductile deformation modes in compression to 20 kbar pressure and simultaneous 1,000° C temperature. Transmission and polarizing electron X-ray diffraction patterns of rock materials that have undergone large displacements at high pressure may be useful indicators of peak stress levels attained in shocked materials from meteorite craters and contained nuclear explosions.

GEOLOGY

CRATERING STUDIES: The ability to compare computer simulations or models of nuclear explosions with their actual effect on earth media is constrained by international testing restrictions. An alternative means of investigating the effects of shocks at levels of stress exceeding those attainable by conventional explosions is to study materials affected by meteor impact. The collision of enormous masses with both the earth and the moon in the geologic past has produced craters several hundred kilometers in diameter. Current research conducted in the Laboratory relates the ballistic histories of material excavated by cratering events to the abrupt change in pressure and temperature experienced by material engulfed by the shock wave generated by such an event. A model has been constructed which estimates peak shock pressure, decompression temperature, and original position of material ejected from the crater, when given the size of the crater and the range at which the ejecta were deposited. Scaled experiments are conducted using surface and partially buried detonations of TNT to provide energy sources for measuring size, depth, and contour of the resulting craters and ejecta distribution

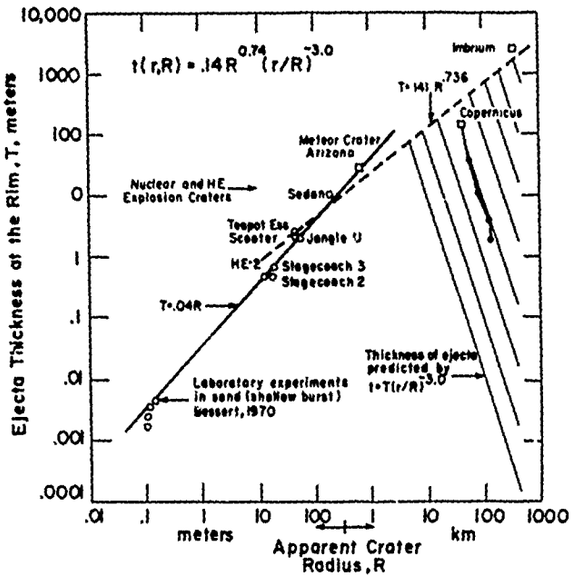

Empirical relationship between ejecta thickness and range for explosion and impact craters.

patterns. A reliable means of estimating shock stresses on the basis of such measurable physical quantities, when used in conjunction with knowledge of the ejection paths of excavated material, will permit reconstruction of the actual distribution of stresses within the ground produced by a cratering event whether it be related to meteor impact or nuclear detonation.

IN-SITU MATERIAL PROPERTY MEASUREMENT: Geophysical methods enable sampling a large volume of earth material without the usual bias introduced by point sampling techniques. This is extremely important in determining shock or blast effects on installations by analyzing the dynamic distortion or shock transmission of surrounding rock. It is generally established that the electrical conductivity of rock varies with its porosity and, hence, its strength. An effective conductivity measurement technique was developed, using a nine-electrode array in which the volume of material being measured is clearly defined by an equipotential surface within the array. Measurements were made at a 500-ton TNT explosive test in rock, with as much as 15 percent change in rock electrical conductivity found during shock-wave transit of the material. The question of interpreting the electrical observations in terms of other desired quantities remains and is being actively pursued. Field investigations are performed to identify the in situ factors controlling the electrical properties of rocks and to determine their correlations with mechanical properties determined in a variety of ways. Stochastic models of crack conductivity in rocks are being developed. Independently, a theoretical study of the relationship between strength and electrical resistivity in rock containing anisotropic crack distributions is underway. The tensor nature of electric permeability and conductivity is being determined with suitable rock models subjected to various mechanical or thermal stress distributions. Relationships between porosity, fluid content, grain size, and mineralogy on the one hand and the electrical parameters on the other are being sought as a function of frequency. The re-

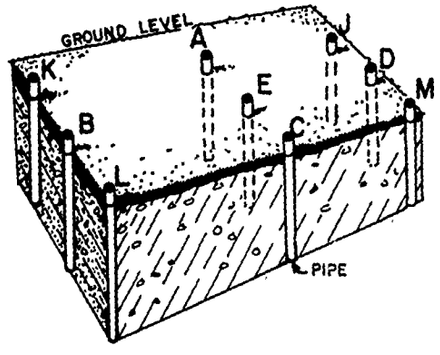

The geophysical measurement array used to determine the electrical conductivity of large volume samples *in situ* and the changes in conductivity caused by shock waves passing through the material.

sults are tested by subsurface observations in mines and quarries as well as on the surface. The fundamental basis for all of the properties of interest is also being considered from an atomic viewpoint, since the physical mechanism that lies at the basis of a connection between the electromagnetic and elastic properties of a solid is the motion of its electrons as correlated with that of its nuclei.

SOIL STABILIZATION: Chemical treatment of soft surface soil areas to stabilize and harden them for use as runways, roads, and foundations is typically approached as a civil engineering problem. Adequate research and knowledge are usually lacking on how additives, such as lime, interact with natural soil materials, principally clay, under varying moisture and temperature regimes. An in-house program was conducted to study these processes and mechanisms.

Reference clay minerals were characterized by use of a scanning electron microscope and energy-dispersive X-ray diffraction analysis. Surface area and surface roughness were found to increase with apparent decrease in crystallinity of the clay minerals. Indications are that the rough surfaces, and not the edges, of platelets of clay are the sites of reaction. This offers a partial explanation of their relative reactivity with a lime stabilizing agent. In the next stages of the study, representatives from each clay mineral group were mixed with lime in fixed percentages, aged under controlled moisture conditions, and the reaction products examined by X-ray diffraction pattern analysis. Some products observed were definitely not of the starting materials and were found to be calcite. The intermediate product, calcium aluminum carbonate hydrate, is unstable and decomposes rapidly, depending on material exposure to carbon dioxide. It was concluded that the clay-lime system creating a stabilized soil is generally produced by a chemical reaction resulting in the formation of a binder material such as a calcium silicate compound.

SPECTROSCOPIC STUDIES

REENTRY VEHICLE DECOYS: The infrared emissive behavior of materials in a space environment can be important to the missile delivery problem. One aspect of this problem worked on by AFCRL is the design of workable reentry vehicle decoys. Such decoys utilize pyrotechnic materials to simulate the infrared signature of much larger reentry vehicles. For such a technique to work properly, pyrotechnic materials that emit infrared in the appropriate region of the spectrum must be selected. AFCRL undertook this task for the Air Force Rocket Propulsion Laboratory, utilizing space simulation chambers and long-term experience in study of the infrared spectral emission of materials (including lunar soil) in a space environment. As this reporting period closed, preliminary recommendations were made to AFRPL which, if confirmed, will mean substantial changes in the current approach to decoy design.

INFRARED CALIBRATION SOURCES: Any space-based or airborne Air Force system utilizing infrared sensors requires periodic calibration, either of the system or of changing atmospheric absorption. A convenient calibration method uses planets and stars of known brightness temperature in the system field of view. One drawback in the use of planets is the inaccuracy with which their infrared spectral irradiance is known. AFCRL's 50-inch aperture balloon-borne telescope system is used to make highly accurate measurements of the infrared radiation emitted by these objects, seeking those that are best qualified to be calibration sources by the invariable (or predictably variable) nature of their emission.

Fifty-inch telescope about to be launched by nine million cubic foot balloon.

Measurements to date have been made of Venus, Mars, and Jupiter to provide a wide range of intensity levels. Venus so far appears to be a constant calibration source. Mars seems predictably variable in its irradiance, so long as large dust storms are not taking place. Jupiter, unfortunately, may be an unpredictably variable source, but additional measurements are required to confirm this view.

SPECTRAL SIGNATURES OF BACKGROUND MATERIALS: Spectral signatures of terrestrial background materials, such as rocks and soils, were determined in the visible, near-infrared and mid-infrared regions of the spectrum. Knowledge of such spectral behavior was applied to reconnaissance problems in which it was desired to use the spectral signature of a target to enhance the contrast between target and background. Knowledge of the spectral behavior of background materials was also applied to Defense Meteorological Satellite System efforts to develop techniques for remote sensing of such surface properties as soil moisture. These data were made available to the NASA ERTS program, in which they comprised the major data bank for attempts to find new earth resources.

MULTISPECTRAL SENSING: The Laboratory successfully concluded its role as technical monitor for DDR&E-sponsored research in remote sensing of earth surface conditions under Project THEMIS. The overall project was initiated by DDR&E to develop "centers of excellence" in specialties relevant to DOD interests. The work, conducted under AFCRL contract, involved advanced techniques of data collection, processing, interpretation, and enhancement. Multispectral photography and thermal infrared imagery were obtained from aircraft and surface vehicles covering representative terrains pertinent to military planning, tactical operations, and natural resource determination. The research developed significant capabilities for determining and mapping of soil type, moisture, density and thickness conditions; outlining boundaries and distribution of forest, vegetation, and water areas; and evaluating geologic landform susceptibility to landslides, cave-ins, erosion, and flooding.

JOURNAL ARTICLES
JULY 1972 - JUNE 1974

BALSAMO, S. R., CAPT., and SALISBURY, J. W.
Slope Angle and Frost Formation on Mars
Icarus, Vol. 18, No. 1 (January 1973)

BENDER, P. L. (Natl. Bur. of Stds./Univ of Colo.), CURRIE, D. G. (Univ. of Md.) DICKIE, R. H. (Princeton Univ.), and ECKHARDT, D. H., ET AL
The Lunar Laser Ranging Experiment
Sci., Vol. 182 (19 October 1973)

BLIAMPTIS, E. E.
Coupled Lenses and Their Combinations
J. of Appl. Phys., Vol. 43, No. 9 (September 1972)
Systematic Terminology for Transmission Systems
Appl. Opt., Vol. 12, No. 4 (April 1973)

CARTER, W. E., ECKHARDT, D. H., and ROBINSON, W. G.
AFCRL Lunar Laser Instrumentation Status Report
Space Res. XII, Akademie-Verlag, Berlin, Ger. (1972)

CRONIN, J. F., ROONEY, T. P., MOLINEUX, C. E. and BLIAMPTIS, E. E.
Ultraviolet Radiation and the Terrestrial Surface
Pt. 3 — Remote Sensing in the Ultraviolet, The Surveillant Sci., Book Pub. by Houghton Mifflin, Boston, Mass. (1973)

DYBWAD, J. P., and LOGAN, L. M.
Liquid Helium Cooled Photon Detectors: Cause, Prevention and Remedy of Contamination
IR Phys., Vol. 13, No. 1 (January 1973)

DYBWAD, J. P., LOGAN, L. M., and ZINNOW, K. P.
Infrared Reflection Spectroscopy of Microscopic Mineral Grains
Am. Mineralogist, Vol. 59 (May-June 1974)

DYBWAD, J. P., ZINNOW, K. P., and SALISBURY, J. W.
Microscopic Infrared Reflection Spectroscopy Applied to Qualitative and Quantitative Investigation of Petrologic Thin Sections
The Geol. Soc. of Am. Bull., Vol. 4, No. 7 (October 1972)

ECKHARDT, D. H.
Physical Librations Due to the Third and Fourth Degree Harmonics of the Lunar Gravity Potential
The Moon, Vol. 6, No. 1/2 (January/February 1973)

HADGIGEORGE, G.
The Geodetic Positioning Capability of the Geoceiver
Proc., Symp. of Satellite and Terrestrial Triangulation, Univ. of Graz, Aus., Vol. 11 (1972)

HERRING, J. C., MAJ., and CARROLL, J. E.
The Automated Astronomic Positioning System
Proc., Am. Cong. on Surveying and Mapping, 32nd Ann. Mtg., Wash., D.C., Mar. 12-17, 1972 (1972)

HUNT, G. R., LOGAN, L. M., and SALISBURY, J. W.
Mars: Components of Infrared Spectra and the Composition of the Dust Cloud
Icarus, Vol. 18, No. 3 (March 1973)

HUNT, G. R., SALISBURY, J. W., and LENHOFF, C. J., CAPT.
Visible and Near Infrared Spectra of Minerals and Rocks: VI. Additional Silicates
Visible and Near-Infrared Spectra of Minerals and Rocks: VII. Acidic Igneous Rocks
Visible and Near Infrared Spectra of Minerals and Rocks: VIII. Intermediate Igneous Rocks
Modern Geol., Vol. 4 (1973)
Visible and Near Infrared Spectra of Minerals and Rocks: IX. Basic and Ultrabasic Igneous Rocks
Modern Geol., Vol. 5 (1974)

ILIFF, R. L.
Laser-Satellite Ranging for Geodesy
Proc., Symp. on Satellite and Terrestrial Triangulation, Univ. of Graz, Aus., Vol. 11 (1972)

LOGAN, L. M., BALSAMO, S. R., CAPT., and HUNT, G. R.
Absolute Measurements and Computed Values for Martian Irradiance Between 10.5 and 12.5 m
Icarus, Vol. 18, No. 3 (March 1973)

LOGAN, L. M., HUNT, G. R., BALSAMO, S. R., CAPT., and SALISBURY, J. W.
Mid-Infrared Emission Spectra of Apollo 14 and 15 Soils and Remote Compositional Mapping of the Moon
Geochimica and Cosmochimica Acta, Vol. 3, Suppl. 3 (1972)

LOGAN, L. M., HUNT, G. R., and SALISBURY, J. W.
Infrared Emission Spectra of Apollo 15 Soils
The Apollo 15 Lunar Samples (Lunar Sci. Inst., Houston, Tex.) J. W. Chamberlain and C. Watkins, Eds. (November 1972)

LOGAN, L. M., HUNT, G. R., SALISBURY, J. W., and BALSAMO, S. R.
Compositional Implications of Christiansen Frequency Maxima for Infrared Remote Sensing Applications
J. of Geophys. Res., Vol. 78, No. 23 (August 1973)

MANGHNANI, M. H.
Pressure and Temperature Dependence of the Elastic Moduli of Na_2O-TiO_2-SiO_2 Glasses
J. of the Am. Ceramic Soc., Vol. 55, No. 7 (July 1972)

SALISBURY, J. W.
Spectroscopic Remote Sensing of Lunar Surface Composition
The Moon, Vol. 5, No. 4 (December 1972)

SALISBURY, J. W., ADLER, J. E. M., BALSAMO, S. R., DYBWAD, J. P., HUNT, G. R., LENHOFF, C. J., LOGAN, L. M., TOLENDINO, L. F., and ZINNOW, K. P.
Bibliography of Lunar and Planetary Research – Third Quarter of 1971
Icarus, Vol. 19, No. 2 (June 1973)

SALISBURY, J. W., ADLER, J. E. M., DYBWAD, J. P., HUNT, G. R., LENHOFF, C. J., LOGAN, L. M., LONG, D. A., TOLENDINO, L. F., and ZINNOW, K. P.
Bibliography of Lunar and Planetary Research – First Quarter of 1972
Icarus, Vol. 19, No. 3 (July 1973)
Bibliography of Lunar and Planetary Research – Second Quarter of 1972
Icarus, Vol. 19, No. 4 (August 1973)
Bibliography of Lunar and Planetary Research – Fourth Quarter of 1972
Icarus, Vol. 20, No. 3 (November 1973)

SALISBURY, J. W., and CHAPMAN, C. R. (Planetary Sci. Inst., Tucson, Ariz.)
Comparisons of Meteorite and Asteroid Spectral Reflectivities
Icarus, Vol. 19, No. 4 (August 1973)

SALISBURY, J. W., HUNT, G. R., and LOGAN, L. M.
Infrared Spectra of Apollo 16 Fines and Composition of Parent Material
Geochimica and Cosmochimica Acta, Vol. 3, Suppl. 4 (1973)

SZABO, B., ET AL.
The International Gravity Standardization Net 1971
Intl. Union of Geodesy and Geophys. (1974)

TERLECKY, P. M., JR., CAPT.
Mass Partition in Soil Cratering
J. of Geophys. Res., Vol. 78, No. 32 (10 November 1973)
The Origin of a Late Pleistocene and Holocene Marl Deposit
J. of Sedimentary Petrology, Vol. 44, No. 2 (June 1974)

WILLIAMS, O. W., ET AL.
Metric Conversion and the AGU
EOS, Vol. 53, No. 12 (December 1972)

WILLIAMS, J. G., SLADE, M. W. (Jet. Prpln. Lab., Pasadena, Calif.), ECKHARDT, D. H., and KAULA, W. M. (Univ. of Calif. at Los Angeles)
Lunar Physical Librations and Laser Ranging
The Moon, Vol. 8 (1973)

WILLIAMS, R. S.
IV. Terrestrial Remote Sensing: Applications of Thermal Infrared Scanners to the Geological Sciences
ISA Transducer Compendium, Pt. 3 (1972)
Thermography
Photogram. Engrg., Vol. 38, No. 9 (1972)

WU, F. T. (State Univ. of N.Y.), THOMSON, K. C., and KUENZLER, H. W., CAPT.
Stick Slip Propagation Velocity and Seismic Source Mechanisms
Bull. of the Seismolog. Soc. of Am., Vol. 62, No. 6 (December 1972)

ZINNOW, K. P., and DYBWAD, J. P.
Dynamic Readout of Weight Changes on an Ultramicrobalance System
Prog. in Vacuum Microbal. Techniques, Vol. 1, T. Gast and E. Robens, Eds., Heyden & Sons, Ltd., N.Y. (1972)

PAPERS PRESENTED AT MEETINGS JULY 1972 - JUNE 1974

BLIAMPTIS, E. E.
Soil Resistivity Measurements: Results from the MIXED COMPANY III and MIDDLE GUST V Tests
Def. Nuc. Agcy. MC/MG Results Mtg., Santa Barbara, Calif. (13-16 March 1973)
The Benioff-Gutenberg Zones in Island Arc Systems
1973 Ann. Am. Geophys. Union Mtg., Wash., D.C. (16-20 April 1973)
The Source Displacement Function Derived from the Angle Vs. Frequency Characteristic and Its Interpretation
6th GEOP Res. Conf.; Earthquake Mechanism and Displacement Fields Close to Fault Zones, San Diego, Calif. (4-5 February 1974)

CABANISS, G. H.
Secular Tilt from a Borehole Tiltmeter Cluster at Bedford, Mass.
Am. Geophys. Union Mtg., Wash., D.C. (16-20 April 1973)

CARROLL, J. E. (Control Data Corp., Minneapolis, Minn.), and HUNT, M. S.
Preliminary Results from AAPS Prototypes
55th Ann. Spring Mtg. of the Am. Geophys. Union, Wash., D.C. (8-12 April 1974)

DYBWAD, J. P., ZINNOW, K. P., and SALISBURY, J. W.
Microscopic Infrared Reflection Spectroscopy Applied to Qualitative and Quantitative Investigation of Petrologic Thin Sections
1972 Ann. Mtg. of the Geol. Soc. of Am., Minneapolis, Minn. (16 November 1972)

ECKHARDT, D. H.
Impedance Interpretation in the One-Dimensional Magnetotelluric Problem
Wkshp. on Electmg. Induction, Univ. of Edinburgh, Scot. (20-27 September 1972)
Cassini's Laws
COSPAR-IAU Colloq. on Lunar Dyn. and Observational Coordinate Sys., Lunar Sci. Inst., Houston, Tex. (15-17 January 1973)

HADGIGEORGE, G.
Simultaneous Recovery of Satellite and Station Positions Utilizing the Short Arc Method
XII Consultation on Cartog., Pan-Am. Inst., of Geog. and Hist., Panama, Pan. (22 April - 9 May 1973)

HAMMOND, J. A.
Calibration of Tidal Gravity Meters
1st GEOP Res. Conf.: Solid Earth and Ocean Tides, Ctr. for Tomorrow, Ohio State Univ., Columbus, Oh. (26-27 October 1972)
Portable Absolute Gravity Meters
Colloq., Krumb Sch. of Mines, Columbia Univ., N.Y. (4 April 1974)

HERRING, J. C., MAJ.
Techniques of Time Transfer Via Satellites and *The Automated Astronomic Positioning System*
XII Consultation on Cartog., Pan-Am. Inst. of Geog. and Hist., Panama, Pan. (22 April - 9 May 1973)

SALISBURY, J. W., and CHAPMAN, C. R. (Planetary Sci. Inst., Tucson, Ariz.)

Comparisons of Meteorite and Asteroid Spectral Reflectivities
Div. of Planetary Sci. of the Am. Astronom. Soc. Mtg., Tucson, Ariz. (5 March 1973)

SALISBURY, J. W., and HUNT, G. R.
Remote Sensing of Rock Type in the Visible and Near-Infrared
9th Intl. Symp. on Remote Sensing of Envmt., Envmt. Res. Inst. of Mich., Ann Arbor, Mich. (15-19 April 1974)

SALISBURY, J. W., HUNT, G. R. and LOGAN, L. M.
Infrared Spectra of Apollo 16 Fines and Composition of Parent Material
4th Ann. Lunar Sci. Conf., NASA Manned Spacecraft Ctr., Houston, Tex. (5-8 March 1973)

SZABO, B.
Measurement of Gravitational Gradients from Moving Platforms
Symp. on Earth Gravity Models and Related Problems, St. Louis, Mo. (16-18 August 1972)

WIRTANEN, T. E.
Field Evaluation of Time-Dependent Geodetic Data
XII Consultation on Cartog., Pan-Am. Inst. of Geog. and Hist., Panama, Pan. (22 April - 9 May 1973)

TECHNICAL REPORTS
JULY 1972 - JUNE 1974

BLIAMPTIS, E. E.
A New Method for Determining the Physical Parameters of Large Soil and Rock Samples In Situ
AFCRL-72-0734 (19 December 1972)

CABANISS, G. H., and ECKHARDT, D. H.
The AFCRL Earth Tide Program
AFCRL-TR-73-0084 (29 January 1973)

CECIL, T. E., SALISBURY, J. W., LOGAN, L. M., and HUNT, G. R.
Celestial Infrared Calibration Sources in the 8-14 Micrometer Region: Venus and Jupiter
AFCRL-TR-73-0559 (5 September 1973)

CROWLEY, F. A., and OSSING, H. A.
A Motion Study of the Frank J. Seiler Research Laboratory Guidance Test Facility
AFCRL-TR-73-0417 (16 July 1973)

CROWLEY, F. A., OSSING, H. A., and CABANISS, G. H.
Precursory Siloed Missile Geokinetic Study, Hill AFB, Utah
AFCRL-72-0531 (5 September 1972)

HADGIGEORGE, G.
Simultaneous Recovery of Satellite and Station Positions Utilizing the Short Arc Method
AFCRL-72-0748 (29 December 1972)
AFCRL Short Arc and Simultaneous Point Positioning Survey Recovery with Continuous Integrated Doppler (CID)
AFCRL-73-0513 (13 August 1973)

HAMMOND, J. A.
Some Comments on the Charged Particle Technique for Measuring Absolute Gravity
AFCRL-TR-73-0425 (18 July 1973)

HERRING, J. C., MAJ.
The Automated Astronomic Positioning System
AFCRL-TR-73-0180 (16 February 1973)
Techniques of Time Transfer Via Satellites
AFCRL-TR-73-0226 (16 February 1973)

HUNT, M. S.
The AFCRL Lunar Laser Experiment
AFCRL-TR-74-0005 (3 January 1974)

LUND, I. A. (Aeron. Lab.), and NEEDLEMAN, S. M.
Tropical Soil Moisture Estimation from Meteorological Observations
AFCRL-TR-74-0064 (1 February 1974)
Harper Lake Studies: 1. Aircraft and Ground Measurements, by ROONEY, T. P., and NEAL, J. T., MAJ. (Air Force Acad., Colo.); 2. *Micromorphology and Surface Properties,* by NEEDLEMAN, S. M.
AFCRL-72-0478 (15 August 1972)

ROONEY, T. P., and RIECKER, R. E.
Constant Strain-Rate Deformation of Amphibole Minerals
AFCRL-TR-73-0045 (12 January 1973)

THOMSON, K. C., and KUENZLER, H. W., CAPT.
Passive Test Pad Models
AFCRL-TR-73-0116 (16 February 1973)

WIRTANEN, T. E.
Field Evaluation of Time-Dependent Geodetic Data
AFCRL-TR-73-0191 (26 March 1973)
Field Results with an Automated Reticle Geodetic Theodolite
AFCRL-TR-74-0256 (7 June 1974)

IX Optical Physics Laboratory

The Optical Physics Laboratory conducts research on the sources, transmission, and detection of optical and infrared radiation and their interaction with the aerospace environment. Field measurements, laboratory studies, theoretical studies, and analyses are conducted to determine and understand the optical and infrared properties of the environment including the atmosphere and celestial sky. These determine how well the atmosphere transmits radiant energy and also how much energy the atmosphere radiates, both under natural and perturbed conditions.

Any optical or infrared detection, surveillance, reconnaissance, or weapon system that operates in or above the atmosphere must look through the atmosphere or look against a background of either atmosphere or sky. Therefore, the optical properties of the atmosphere and other environments and how they will enhance or limit the operation of these systems must be known.

The Laboratory's effort on the sources of optical/infrared radiation ranges from measurements and studies of atmospheric and stellar emission as well as missile plume radiation to research into the behavior and operation of lasers, including gas and chemical lasers.

The portion of the electromagnetic spectrum studied extends in wavelength from about 2000 angstroms in the ultraviolet to 1 millimeter where the far infrared blends into the microwave radio spectrum.

The research in the Laboratory is divided into studies of: the visible or near visible properties of the atmosphere, where aerosol and molecular scattering is the pre-

dominant mechanism of attenuation; the infrared properties of the lower atmosphere where thermal equilibrium usually prevails; the optical and infrared properties of the upper atmosphere (including auroras and airglow) where individual molecular interactions must be considered; the infrared properties of exoatmospheric sources—stars, nebulae, cosmic dust; the physics of lasers; measurements of the radiation from man-made sources such as missile plumes; and development of improved techniques for spectroscopic measurements.

A major area of investigation by the Laboratory concerns atmospheric attenuation or transmission of radiation by the atmosphere, including laser beams. Atmospheric molecules absorb optical and infrared radiation selectively at discrete wavelengths. Extensive computer programs have been developed which make use of the vast collection of spectroscopic data for molecules and which permit the calculation of this transmission, particularly for laser beams. Graphs and a computer program (LOWTRAN) have also been published and distributed widely for determining the low resolution (approximately 20 wave numbers) transmission of the atmosphere for any path through the atmosphere for a wide range of meteorological conditions. Detailed atmospheric absorption curves and tables for laser transmission have been published. The development or improvement of codes for the transmission of plume radiation through the atmosphere is underway.

Scattering by aerosols and molecules in the atmosphere also contributes both to attenuation and to reduction in the contrast of a target seen through the atmosphere. Extensive measurements from the Laboratory's C-130 flying laboratory and balloons have been made to determine the geographic, seasonal and altitude variations, as well as the optical properties of these aerosols and the effect of the underlying terrain, water surface or snow cover. The results of these measurements have been applied to several target acquisition and detection problems. As one extension of these measurements, an extensive international program of measurements is being set up in Europe.

Similarly, the emission of the atmosphere, insofar as it creates a disturbing or masking background against which a target must be located, is also a major concern of the Laboratory efforts. Such emissions represent interfering background noise superimposed on the optical/IR target signals that a surveillance system may be trying to detect. The emission of the lower atmosphere can be calculated from computer programs similar to those discussed previously. However, the emission from the upper atmosphere (above about 70 km) requires a much more detailed knowledge of the interactions and collisions among the individual molecules, many of which will be in excited states with excess energy. The amount and wavelength of the radiation resulting from this nonequilibrium chemistry, and the effects of disturbances by protons and electrons as would occur during an aurora or a nuclear burst, are also being studied. Therefore, a sizable laboratory and theoretical research program is conducted to study the physics and chemistry of the atmosphere, particularly those molecular interactions which lead to infrared emission, as well as an extensive measurement program. This includes the use of the Laboratory's NKC-135 optical/infrared flying laboratory, balloons and rockets, particularly in Alaska, where the infrared emission of the aurora is studied in the Infrared Chemistry Experiments for the Coordinated Auroral Program (ICECAP). A computer program (called OPTIR) has been developed to predict and compute the optical and IR emission of the upper atmosphere, primarily for disturbed conditions. Such background emission, particularly during disturbed

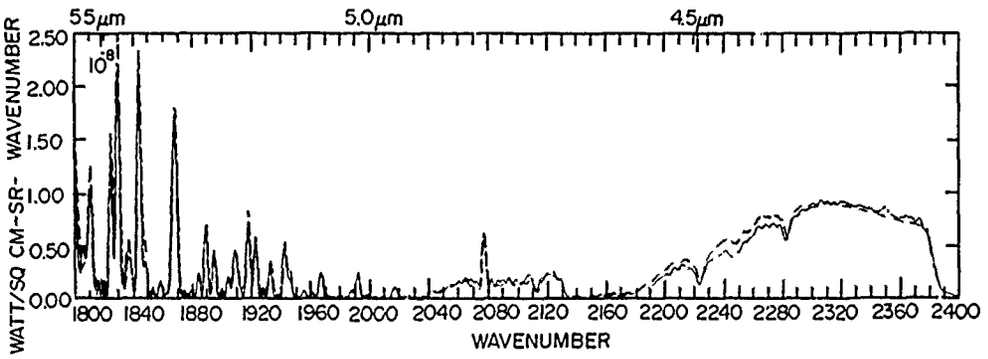

Atmospheric emission spectra as observed looking toward the zenith from a 9.45-km altitude near Hawaii on April 19, 1970, between 1219 and 1238 U. T. The dashed line is the theoretical prediction of constitutent emissions for a tropical atmosphere of H_2O, CO_2, O_3, N_2O, CO, and CH_4 for the identical aircraft geometry, showing excellent agreement with the data curve.

conditions such as auroras, could seriously impair the operation of a surveillance, tracking, or terminal guidance system. Also, the radiation profile of the horizon determines the ultimate accuracy of horizon-sensing attitude control systems on satellites.

The measurement and study of atmospheric transmission or emission also provides a method for remotely sensing atmospheric composition (including the effect of addition of contaminants, for example, from high altitude missile or jet engine exhausts) and meteorological conditions such as temperature, humidity and ozone content. The transmission codes have been extensively applied to the design and improvement of remote atmospheric sensing sensors on the Air Force meteorological satellites.

A satellite or rocket-borne infrared system looking away from the atmosphere will still see the celestial sky as a background. Consequently, the Laboratory has carried cut an extensive rocket program to survey the entire celestial sky—stars, galaxies, nebulae, etc.—in the infrared. Also, measurements of missile plumes are being obtained from rockets and aircraft. The aircraft measurements have included some of the most detailed spectroscopic data on missile plumes ever obtained.

An inseparable part of these measurements and studies is the development of more sensitive infrared sensors and spectral measuring instruments. Such a technique to which the Laboratory has contributed much is multiplex spectroscopy—all wavelengths entering the spectrometer are analyzed simultaneously. One form of multiplex spectroscopy—Fourier spectroscopy—has been studied and utilized by the Laboratory with great success for several years.

Since June 1972, in addition to the use of the two flying laboratories discussed above (an NKC-135 and a C-130A), instrumented exclusively for research by the Optical Physics Laboratory, the Laboratory has launched 32 rockets and used 24 instrumented balloon flights in its programs.

In the last 12 years, laser systems have made possible great advances in military technology. Far greater advances, both foreseen and unforeseen, can be predicted for the future. Laser physics is studied at

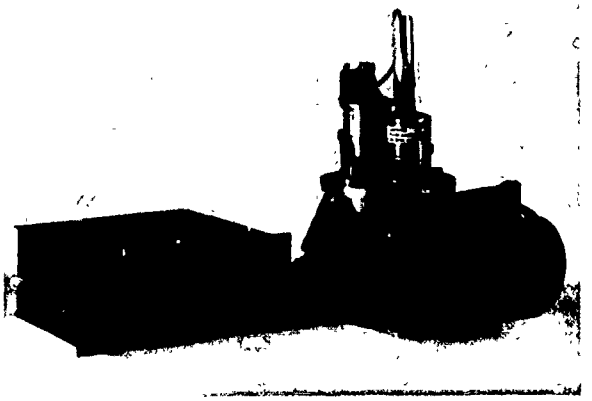

The AFCRL cold Type V Interferometer Spectrometer. Having successfully passed the airborne trial tests, the concept of operating an airborne interferometer in an environment cooled to liquid nitrogen temperature will now be expanded to include the liquid nitrogen cooled window fitted in front of the entrance aperture.

AFCRL to advance knowledge and basic technology in this vital area. Research in laser-related phenomena is initiated together with new laser applications which show potential for leading to new concept devices. Early exploratory development efforts are carried out when a research project has identified a promising new device concept. Substantial resources are also devoted to problems which have been identified in connection with existing laser systems. Exhaustive study efforts are directed toward understanding and correcting or redesigning these lase systems so that they will reliably fulfill their Air Force mission requirement.

ATMOSPHERIC OPTICS

The Atmospheric Optics program encompasses experimental and theoretical studies on the scattering and absorption properties of atmospheric aerosol particles and the scattering of light by air molecules. Molecular absorption effects are investigated under the infrared physics program. The goal of the Atmospheric Optics program is an understanding of the effects of atmospheric optical properties on the performance of various Air Force systems and the capability of predicting these atmospheric optical properties for conditions under which these Air Force systems must operate.

A primary research objective is to measure the distribution of light-scattering and absorbing aerosol particles in the atmosphere from the ground, from aircraft, from balloons and from rockets. These aerosol particles, ranging in size from clusters of molecules of less than one millionth of a millimeter in diameter to giant dust particles a fraction of a millimeter in size, scatter incident light in various directions as well as absorb some of the incident radiation. These optical properties of small particles depend on their number, size, chemical and physical composition, including refractive index, shape, and homogeneity.

The origin of these particles is as varied as the properties of the particles themselves. Many of these particles originate from solid dust particles picked up from the ground, seaspray over the oceans, or particles ejected into the atmosphere from man-made pollution sources. Others are formed in the atmosphere from gaseous contaminants by photochemical or other processes. The aerosol particles are transported over large distances by air mass movements and are carried up into the troposphere and stratosphere by convective weather systems. In addition, violent volcanic eruptions can eject large quantities of dust into the stratosphere. Their small size and weight cause these particles to remain suspended in the atmosphere for long periods of time before they fall out, are washed out, or are otherwise removed.

Because changes in the aerosols cause changes in the optical properties of the atmosphere, two kinds of questions are fre-

quently asked: What is the frequency of occurrence and the temporal and spatial distribution of various atmospheric optical conditions? And how well can one predict the atmospheric optical conditions for a given time and location? The prerequisite for answers to both questions are measurements of the various atmospheric parameters involved.

VERTICAL PROBING OF ATMOSPHERIC OPTICAL PROPERTIES: A series of three balloon flights was conducted at Holloman AFB, New Mexico, in May of 1973, using a newly developed aerosol counter. The device draws in ambient air continuously and feeds it through a one-millimeter sampling tube under laminar flow conditions. This tube is interrupted and the sensing gap thus formed is illuminated orthogonally by a helium-neon laser beam. As the aerosol particles in the flowing gas pass through the sensing gap, the scattered light is collected through two separate conical optical channels (at 10- and 30-degree angles) and detected by two photomultiplier tubes. A pair of electrical pulses is generated for each detected aerosol particle. They are processed by special on-board electronic circuitry and recorded on magnetic tape in digital format. The system output is a histogram of particle sizes with a sizing accuracy of 10 percent over a range of diameters from one micrometer to 0.1-0.2 micrometer. The particle concentration for the flight on May 24, 1973 exhibits the well known Junge layer which, during this flight, extended over the altitude range, 12 to 20 km. It appears that this layer is mainly due to particles larger than 0.5 micron.

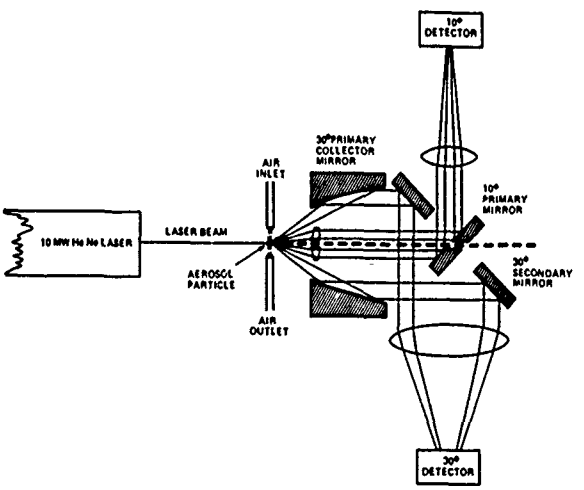

Schematic of balloon-borne optical aerosol counter.

Separate particle size distributions were obtained for the three highest segments of the downleg portion of the May 24 flight, and showed very distinct evidence of an effect not discernible when integral counting techniques are used. The size distribution of the aerosol particles can be characterized by a single exponential parameter. However, the value of the parameter differs considerably between 21 and 26 km. This behavior was also noted on the upleg portion of the flight several hours earlier, as well as on the third flight, although on the third flight intermittent interruptions of equipment function prevented the collection of data on the upleg. The particles above the 23-km level are unmistakably different from those at lower altitudes, at least under the stratospheric conditions that prevailed over Holloman AFB during the latter part of May 1973.

The optical properties of aerosol particles depend not only on their size and number density, but also on properties such as shape and refractive index, which are much more difficult to measure directly in the free atmosphere. To measure the optical scattering directly, a large polar nephelometer, constructed at AFCRL, measures the angular variation of light scattered out of a light beam. The scattered light intensity is measured at various wavelengths. A successful flight with this balloon instrument, which was previously flown in 1970, was conducted in June 1974, at Holloman AFB.

During the past two years, the development of a new instrument to measure at-

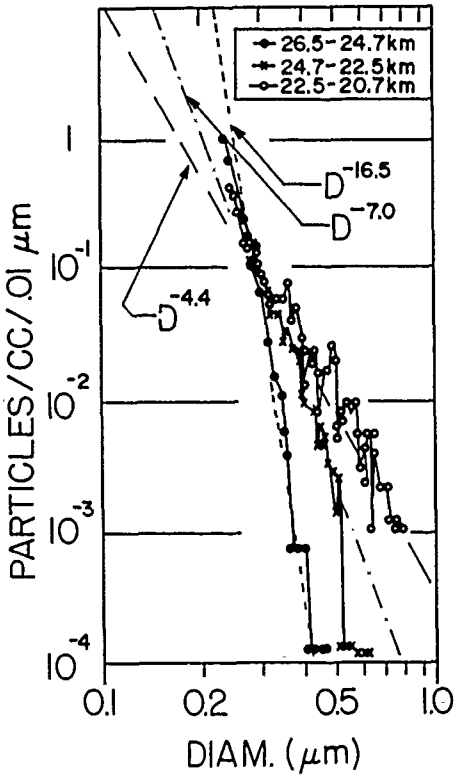

Aerosol size distributions at three different altitude intervals during the May 24, 1973 balloon flight.

mospheric light extinction was completed. This extinction coefficient sonde weighs only about 20 pounds and is therefore suitable for routine measurements on tethered balloons. It has a very high light collection efficiency because of its unique optical system. Recent test and calibration measurements in the laboratory have shown that the instrument is sensitive enough to detect the scattered light from a pure molecular atmosphere, despite the fact that the light source is only a 5-watt automobile light bulb. Tethered balloon flights with this extinction coefficient sonde will be conducted in the near future.

Although balloon-borne experiments can measure various optical or aerosol parameters directly at various altitudes, it requires many balloon flights before one can derive a reliable picture of the temporal and geographical variations. To monitor the long-term variability of the optical properties of the atmosphere, it is important to have a means of remotely measuring some atmospheric optical quantities from the ground. This is especially of significance for stratospheric altitudes since the time variations of aerosols in the stratosphere is of the order of months and years, rather than days as in the lower troposphere.

For more than ten years, AFCRL has been operating a searchlight probing experiment in New Mexico to monitor stratospheric and tropospheric aerosol attenuation coefficients. An intense searchlight beam is projected up into the night sky from White Sands and a receiver system, located 30 miles away on Sacramento Peak, scans the searchlight beam up to altitudes of 40 km and higher. The received intensity of backscattered light out of the searchlight beam is then converted to vertical profiles

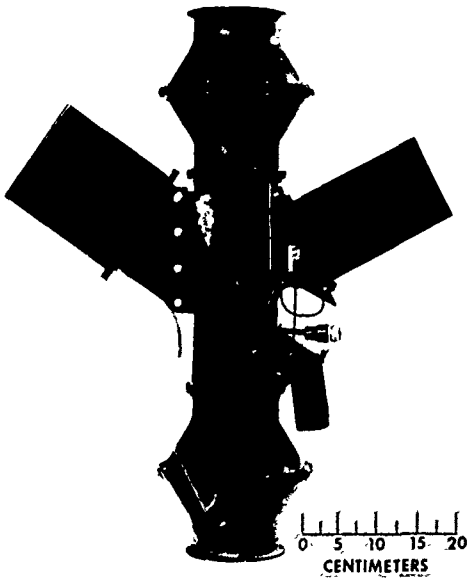

Extinction coefficient sonde.

of the aerosol attenuation coefficient or the ratio of aerosol to molecular extinction.

AIRCRAFT MEASUREMENT PROGRAM: For many tactical Air Force problems the altitude range of concern is from the surface up to 5 to 10 km altitude. An aircraft measurement program has been conducted for several years to collect data on various atmospheric optical parameters which cause the reduction in contrast between various objects and their surrounding background. The instrumented C-130A Hercules flying atmospheric optics laboratory has, over the past several years, been collecting data on atmospheric scattering coefficients, sky and terrain radiance, path radiance and various other parameters. These measurements have been taken in a variety of geographical areas and during different seasons and environmental conditions.

Comparisons of the data collected in different areas reveal some rather consistent characteristic features. For instance, in the more densely populated areas of Central Europe or the United States the atmospheric scattering coefficient has a distinct low level maximum with a rather sharp top between 1 and 2 km altitude, and the values in the lower troposphere even under fairly clear conditions are approximately three to four times higher than in the desert regions of the southwest United States. The results also show the strong dependence of contrast reduction on the illumination conditions and observer viewing angle.

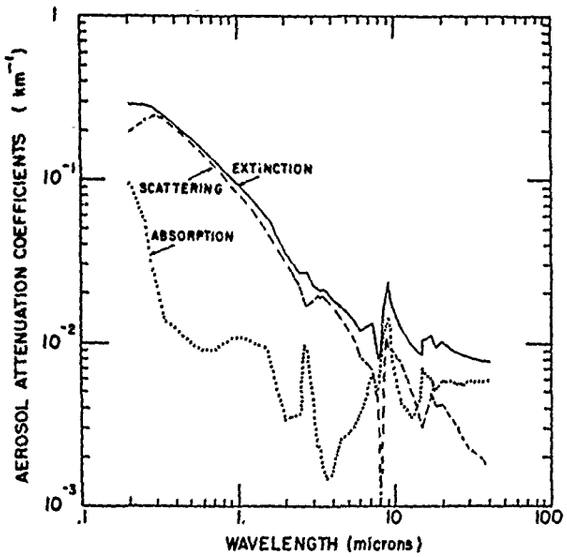

Model aerosol scattering, absorption and extinction coefficients as a function of wavelength.

ATMOSPHERIC OPTICAL MODELS: One of the major objectives of atmospheric optics research is to develop models which can be used to evaluate the performance of electro-optical military systems under average, optimum and worst conditions. Such models, therefore, must describe the values and their variance of such quantities as aerosol particle concentration, size, refractive index, and so forth.

The results from all the measurement programs form the basis for these atmospheric optical models. Models for the different aerosol distributions in continental, maritime and urban environments have been developed for the whole atmosphere from the surface to 100 km altitude. These aerosol models then can be used to calculate the scattering, absorption, and extinction properties and also such quantities as transmittance, sky background radiance, or contrast reduction.

INFRARED PHYSICS

The infrared physics program includes research on, and measurements of, the mechanisms of attenuation, absorption, transmission, and emission of infrared radiation in the aerospace environment. This includes infrared background emitted by the atmosphere and celestial sky. It also includes the attenuation by the atmosphere of the infrared radiation from natural sources, natural or man-made disturbances, or targets such as missile plumes.

The results of these efforts, in addition to the data measured directly, are models and computer codes which allow the prediction of this infrared emission and transmission for any situation. Also, improved spectroscopic measurement techniques are developed.

ATMOSPHERIC TRANSMISSION-EMISSION MODELS: Models of the transmittance and emission properties of the atmosphere have been developed. Two basically different transmittance models exist: One is a low resolution (20 wave numbers spectral resolution) model and covers the range from 0.25 micrometer to 28 micrometers. This model is described in *Optical Properties of the Atmosphere, Third Edition* (AFCRL-72-0497), and a computer version of the model in *Atmospheric Transmittance from 0.25 to 28.5 Micrometers: Computer Code LOWTRAN 2* (AFCRL-72-0745). This model includes effects of both molecular and aerosol scattering on atmospheric transmittance over the entire spectral range.

The second transmittance model uses the absorption profiles of individual molecular absorption lines and averages over these (the so-called line-by-line calculations). This approach results in synthetic spectra at either high or low resolution depending on the desired averaging spectral interval. This is the only approach capable of computing very high resolution spectra for the transmittance of laser beams through the atmosphere. It should also yield more accurate low resolution calculations when appropriately averaged over wavelength. During this past year, there has been a great increase in the development of lasers in the infrared. A frequently asked question is: "What laser frequencies are attenuated the least by the atmosphere?" This question has been answered for carbon monoxide, hydrogen fluoride, and deuterium fluoride laser systems in a summary report on laser transmittance (AFCRL-TR-74-0003). In addition to addressing the problem of laser propagation of these specific laser systems, the summary report provides synthetic spectra for the entire spectral region from 0.76 micrometer to 31.25 micrometers, thereby allowing a quick estimate of atmospheric attenuation for laser propagation throughout this entire portion of the infrared. The compilation of atmospheric absorption lines used as a basis of much of our work is described in the *AFCRL Atmospheric Absorption Line Parameters Compilation* (AFCRL-73-0096). Since the publication of this report in early 1973, we have made available over 100 copies of these data on magnetic tape. Detailed information on over 110,000 spectral lines in the spectral region from 0.76 micrometer to the microwave region are contained on this tape. Atmospheric species included in the compilation are: H_2O, CO_2, O_3, N_2O, CO, CH_4 and O_2.

Current efforts involve improving the data base, both by correcting existing data and adding new material. New material to be added includes weak absorption features of the major atmospheric absorbing gases as well as absorption parameters for trace atmospheric and pollutant gases. Additional gases on which some work is cur-

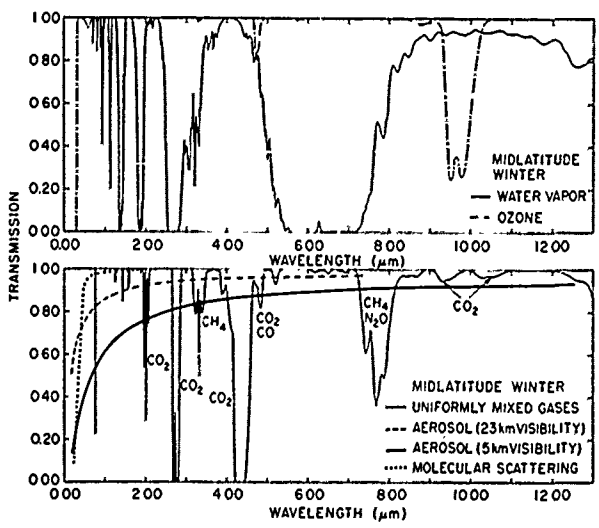

Atmospheric transmission along a vertical path from sea level to space.

rently in progress include NO, NO_2, HNO_3 and SO_2.

During the past two years, a great deal of the modeling effort has been directly in response to specific application requirements. The development of the LOWTRAN 2 code was spurred by such a requirement, and an improved version of this low spectral resolution transmittance code with substantially increased flexibility is being developed. This model will be called LOWTRAN 3. Substantial effort has gone into checking the model by comparing its rsults directly with laboratory absorption measurements. Some modifications in the basic spectral data contained in the model have been made as a result.

Another application of the transmission modeling activity is the problem of the satellite remote sensing of meteorological variables. The Line Parameters Compilation has been used as a data base for such calculations to determine the spectral channels most suitable for use in satellite sensor design. In addition, transmittance calculations performed with these models are being used in the development of software packages for the reduction of satellite-measured radiances in terms of the three-dimensional structure of temperature and moisture.

The Line Parameters Compilation has also been applied to the understanding of the signature of a hot gas (e.g., the exhaust plume of an aircraft) as viewed through a colder intervening atmosphere. Our objective is to evaluate the accuracy of applying a low spectral resolution transmittance code to remove the atmospheric effects from such measurements. We can evaluate the error by synthetic generation of the signatures with our molecular absorption compilation and comparison with the results obtained through application of the LOWTRAN code.

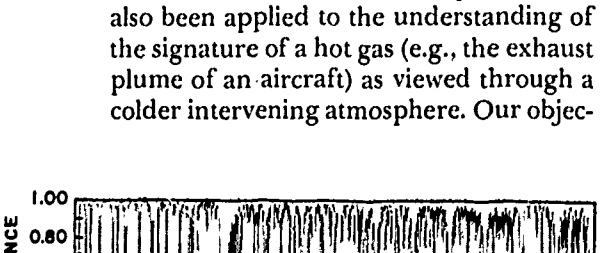

Atmospheric infrared transmission 10-km horizontal path at 12-km altitude.

MULTIPLEX/HIGH-THROUGHPUT SPECTROSCOPY: Some systems require specific detailed spectral measurements of atmospheric transmission or absorption and background radiance for optimum performance. High resolution data on atmospheric constituents must be obtained to allow generating high confidence models of these atmospheric parameters, especially when laser propagation or narrowband detection is involved; for such applications, line strengths, positions and shapes must be known to high resolution. Many of the required measurements must be made with multiplex or high-throughput systems because conventional techniques are inadequate.

The throughput of a spectrometer is a measure of its light-gathering capability. A multiplex system measures all the radiation of interest throughout the measuring time. This multiplex advantage, coupled with the throughput advantage (when using an interferometer for Fourier spectroscopy), can yield increased efficiency, or gain, in measurement time, over conventional techniques of as much as 10^8. This increase in efficiency can be applied to increase the signal-to-noise ratio of a measurement, increase the speed of measurement, or to obtain more detailed structural information (better resolution).

Research on improved spectrometric techniques is being done in-house as well as by contractual efforts. A two-meter path difference interferometer is being developed which will be capable of a resolution of 0.005 wave numbers (after smoothing out the diffraction pattern, which de-

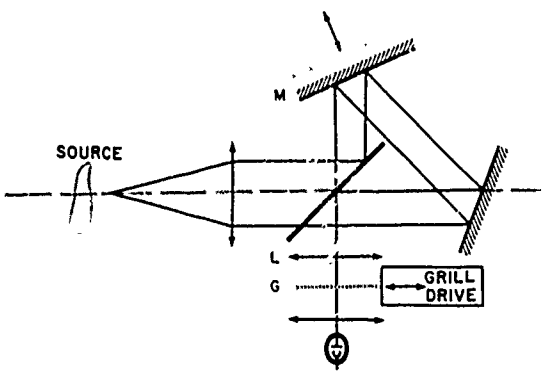

Optical schematic of high-throughput *SIMS* instrument.

creases the resolution). The instrument is nearly complete, and has yielded spectra to 0.0075 wave number resolution. The plane mirrors of the Michelson interferometer-spectrometer have been replaced by cat's eye mirrors for ease of alignment, and the interferometer operates in a step-integrate mode. The instrument will be used to obtain high resolution absorption and emission spectra of atomic molecules at various temperatures and should be capable of yielding accurate line shapes as well as line positions and strengths. In this country, this combination of high resolving power and large spectral coverage is found only in this Laboratory.

A preliminary study of a new high-throughput spectroscopic technique has been completed. Although it does not have the multiplex gain, it has the advantage of yielding the spectrum directly without any transformation. The technique is called Selective Interference Modulation Spectroscopy (SIMS). The extremely large throughput of the SIMS technique coupled with a real-time output and a simple, rugged instrument design make it a serious candidate for aircraft, balloon and rocket measurement programs. The technique seems best suited for medium resolution measurements of weak or rapidly varying spectra where detector noise-limited systems must be employed.

Work on a singly encoded coolable Hadamard transform spectrometer for the 9-14-micrometer region is in progress. It is hoped that this instrument will meet the need for a flyable instrument capable of faster scan rates and improved resolution compared with the present airborne instrumentation. This instrument will be capable of achieving a resolution of 0.15 wave number and scan rates up to one scan per second.

INFRARED HORIZON STUDIES

The infrared radiance of the earth's upper atmosphere is one of the natural background phenomena that enters into the design of infrared optical systems. The atmosphere causes two effects. First, the average value of the atmospheric radiance generates random noise at the system detector output, and this effectively determines the range at which a target can be detected. Second, fluctuations in the atmospheric radiance generate false target signals. The radiance from this region, however, is largely unmeasured. As a result, a reliable physical model from which we could calculate these effects is not available.

The Laboratory has undertaken a horizon measurements program involving the use of rocket probes to measure the vertical distribution of high altitude infrared radiance. Radiance from several atmospheric emission bands were observed up to tangent heights of 60 km. We are presently developing a program to extend these measurements up to the 200-km region using more sensitive instrumentation and covering the 3 to 25 micron spectral range.

The development of a high altitude infrared radiance model to estimate infrared radiation arising from active molecular gases and particulate material is being carried out as a parallel effort to the rocket

probe measurements. The work is currently directed toward determining the effects of vertical transport by molecular diffusion and eddy mixing on the abundance of minor species. In addition, modeling of vibrational bands is being carried out to refine the radiative transfer calculations.

INFRARED CELESTIAL MEASUREMENTS: The Air Force needs to detect infrared emitting targets at the greatest possible range. If these targets are viewed against the background of celestial sources, knowledge of the infrared characteristics of the background is necessary to permit discrimination of the target from the background.

A payload was developed to survey the sky at several wavelengths in the infrared from vertical sounding rockets. To obtain precise coordinates of the celestial objects observed, the scan axis of the payload is locked to a pre-selected star transiting near the zenith at the time of the launch. The infrared telescope is positioned at various angles with respect to the scan axis and held at this position while the rocket performs the scan maneuver. The position of the telescope along the scan plane is measured by observing star transits with a visual star aspect sensor.

Portions of the sky observable from the Northern Hemisphere have now been scanned in several infrared bands. The sources detected are not uniformly distributed throughout the scanned area but show a concentration toward the galactic plane. This concentration of sources near the plane becomes more marked at longer infrared wavelengths. Thus, one can conclude that the majority of the infrared sources observed are members of the Milky Way with very few extragalactic objects being detected

The infrared sky survey is now being extended to the Southern Hemisphere. The ultimate goal is a complete set of sky maps at wavelengths in the near, intermediate, and far infrared regions. These data will form the basis for statistical models of the galactic stellar distribution.

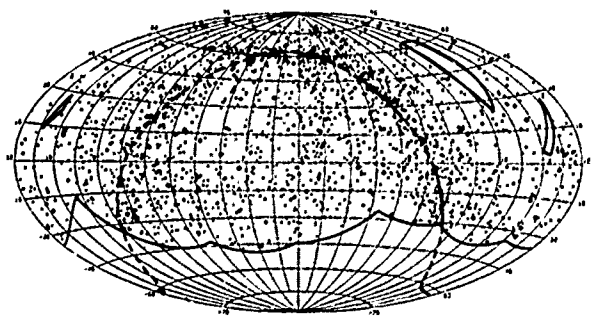

Infrared stellar sources observed at a wavelength of 4 micrometers using a rocket-borne telescope. The dotted line delineates the galactic plane.

THE REMOTE INFERENCE PROBLEM: The first meteorological satellites were designed to transmit cloud pictures. It was soon realized that the atmospheric emission in the far infrared region of the spectrum was related to the temperature of the atmosphere, so that remote passive temperature sensing was possible.

However, using this information to determine the temperature at each level in the atmosphere proved to be very difficult. All levels of the atmosphere contribute to each particular frequency, so that the radiance sensed by the satellite is a mixture of thermal information from all levels. Probing different frequencies merely weights radiation according to height, depending on the transmittance of the atmosphere.

Mathematically, the radiation is expressible as an integral transform of the temperature-related Planck intensity summed over the atmosphere. Typically, the radiances are observed over six to eight different frequency channels. The vertical temperature distribution is then recoverable as an inverse transform of the radiance profile, hence, the name inversion given to this particular inference problem. The heart of the problem is that the vertical temperature distribution is deduced from

intensity differences between neighboring frequency channels, a second order effect.

The incomplete character of the data causes two types of problems. First, a continuous function over all frequencies is required to generate a unique inversion. Given only the finite number of observations, an infinite manifold of temperature profiles can be found which are formal solutions to the problem. Most of these solutions are nonsensical physically, with negative temperatures and oscillating lapse rates. Thus, the fragmentary data force us to introduce external and subjective constraints to specify a unique solution from the many solutions possible.

Second, the data are beset with inherent, irreducible noise error. Most inversion methods use some *a priori* algorithm in an attempt to smooth out the noise. This runs the risk of discarding information on the thermal structure as noise.

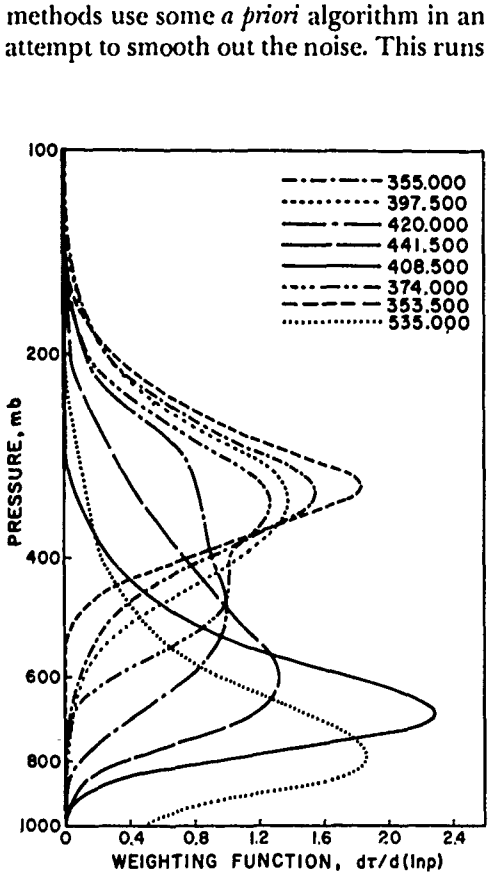

Weighting functions for sensing vertical distribution of water vapor from satellite.

To overcome these problems, subjective information is added to the fragmentary data to assure uniqueness, and information is subtracted by discarding intensity irregularities presumably due to noise. Although these procedures lead to an impressively smooth profile, it is almost impossible to separate the atmospheric features genuinely inferred by inversion from climatological features unwittingly inserted in the processing.

The algorithm used to process the data should extract all the temperature information, but nothing more. Furthermore, it should use raw data, noise and all, without smoothing. Finally, it should not require any climatological information. The optimal interpolation formula must be flexible but smooth, for the inversion grossly distorts structure. The Padé approximant is attractive because of its extreme smoothness. These approximants are used in physics as efficient approximations to complicated functions for digital computers and to fit resonances, phase changes, and other curves exhibiting mild singularities.

The Padé approximant, which is a quotient polynomial, is completely specified by the positions of its poles and their residues. Given 2N arbitrarily sensed intensities, the nonlinear exponential algorithm developed in the Laboratory determines the unique Padé approximant of N poles and residues which fits the observations. For noise-free data, the poles are clustered in the negative half-plane of the complex frequency plane. The corresponding temperature profile is represented by a sum of nonlinear exponential functions. Noise will generate a pole displaced to the real frequency axis to fit the aberrant radiance value, precisely indicating the errant channel as well as the percentage error in the channel reading.

The profile inferred by the nonlinear exponential algorithm is the smoothest consistent with the observed radiances.

Physically, it is known that the natural state of the atmosphere has properties which are constant or change in a uniform manner with altitude over an altitude range, and then change to a different type of uniform change over the next altitude range. Ramp functions are used to approximate inversions, isothermal layers, and moist adiabatic lapse rates. The nonlinear exponential algorithm is being modified to infer the unique set of N ramps associated with 2N radiance values. It is expected that the nonlinear ramp algorithm will infer, objectively, the temperature and height of the tropopause as well as the lower stratospheric and tropospheric lapse rates.

RADIATION EFFECTS

The primary research of this segment of the Laboratory is the optical/infrared properties of the upper atmosphere, both under normal conditions and when it is disturbed by auroras or nuclear weapons. At the altitudes considered, thermal equilibrium usually does not exist, and it is necessary to consider the collisions or interactions of individual pairs or triads of molecules, one or more of which may be in an excited state (i.e., with excess internal energy). Extensive Laboratory and theoretical studies, as well as rocket, balloon and aircraft measurements of upper atmospheric optical/infrared phenomena are carried out. The results of these Laboratory studies and aircraft measurements also apply to missile or jet engine plume infrared radiation, which have also been measured. As in the infrared physics program, the goal of the research is to generate both directly measured data and also models and computer codes which permit the prediction of the optical/infrared emission of the upper atmosphere, particularly under disturbed conditions. Such data and codes are particularly applicable to surveillance and detection systems operating in space or near space.

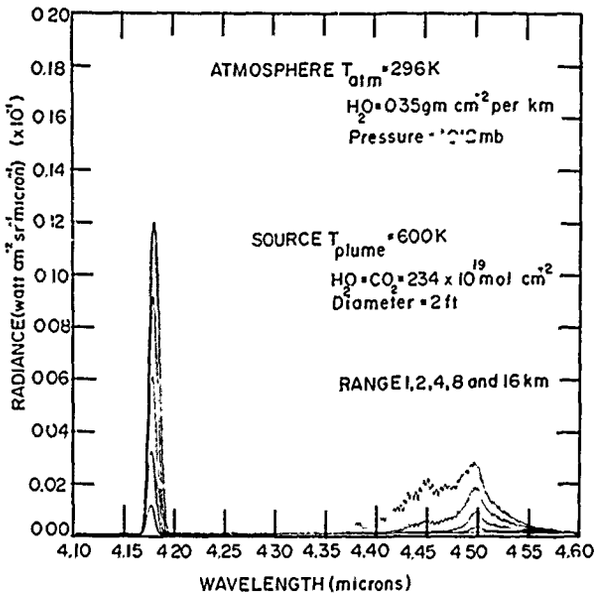

Hot plume signature as viewed through the atmosphere in the 4-micrometer region.

OPTICAL/INFRARED (OPTIR) CODE DEVELOPMENT: OPTIR is a computer code which develops mathematical and physical models to calculate the optical/infrared radiation resulting from natural or artificial stimulation of the atmosphere. The code is designed to model nuclear detonations in the atmosphere and predict their effects on optical and infrared systems.

Routines describing strong and moderate shock propagation and attendant flow fields required to describe shock-induced optical/IR radiation modification have been integrated into the OPTIR code during the reporting period. A working routine of atmospheric heave or uplift resulting from energy deposition in high altitude nuclear bursts has also been developed. Other progress on the OPTIR code during the period includes: development of an auroral version of the OPTIR code OPTAUR, obtained by deleting the artificial stimulation routines from OPTIR; improvement of the debris air-piston

model to allow for expansion in an arbitrary atmosphere: incorporation of a prompt fluorescence model; modification of the debris package using essentially RANC III and WEPH IV code phenomenology: addition of an auxiliary program to compute atmospheric refraction; inclusion of an improved ozone model below 50 km describing latitudinal and seasonal variations: development of a routine which permits calculations of chemiluminescent radiation for an arbitrary set of chemical reactions, and development of an overlayed version of OPTIR which substantially reduces core memory requirements.

Mathematical improvements have been made in the solution of differential equations having rapidly varying parameters which require time steps much smaller than would be required by the reaction rates in the actual equation. Numerical solutions of equations for hydrodynamic motion were also improved. Superior models for solving fourth order accuracy difference equations have been identified to remedy a serious defect in the coding methods used by large magnetohydrodynamic codes.

Advanced versions of the OPTIR code, including OPTIR III A (1973) and OPTIR III B (1974), have been developed and documented. These versions incorporate the most recent modeling and coding improvements as well as the accumulated experience and development of previous versions of OPTIR.

Applications of the code, in addition to direct systems calculations, include: OPTAUR calculations of profiles of neutral and ionic species and visible/SWIR radiation as seen by an ICECAP rocket payload penetrating an auroral arc; energy deposition profiles and concentrations of various chemical species following the turning-on of various exoatmospheric electron spectra; a study of shock wave contributions to chemiluminescence, and the effects of delayed beta deposition in conjunction with high altitude debris patches.

AIRCRAFT PROGRAM: The AFCRL Infrared/Optical Flying Laboratory is an NKC-135 aircraft, recently modified to provide a more efficient array of 53 viewing ports behind which a matrix of spatial mappers, radiometers, and interferometer-spectrometers are operated. The aircraft measurement program has provided the day and night infrared sky background signal levels against which specific targets of systems interest have been analyzed.

Airborne measurements of atmospheric transmission from 1 to 6 micrometers and emission from 1 to 13 micrometers have been used to revise specific constituent parameters in the AFCRL LOWTRAN-2 transmission/emission prediction code, and excellent agreement exists between predicted and observed data looking upward from aircraft altitudes. The more complicated viewing geometries are being analyzed.

Additional hydroxyl (OH) emission measurements from mid-latitude survey flights confirmed transition anomalies suspected earlier. These will be monitored on future flights, both in the auroral zone and lower latitudes, for geographic and time dependence.

Measurements made both with airborne instrumentation and instrumentation on the ground, close to the source, served as the basis for substantial instrumentation improvements. These data, with re-analysis of previous data handled by new techniques, have provided an infrared data base heretofore unavailable. Increases in radiometric sensitivities, the introduction of multiple mapper coverage of the infrared scene, and the first test flights of the prototype airborne interferometer in which the detector is cooled with liquid helium and the instrument is cooled to liquid nitrogen temperatures were accomplished. The latter opens the way to the next generation of fully cold interferometers viewing through frost-free windows cooled to liquid nitrogen temperatures.

Software development has enhanced both radiometer and interferogram data reduction and handling so much that laboratory calibration and optimization of interferometers is handled by near real-time monitoring of output spectra. The ability to search past data rapidly and decide if it is useful allows efficient analysis of selected past data.

ICECAP: (Infrared Chemistry Experiments for the Coordinated Auroral Program) is an integrated rocket and ground measurements program on the quiet and aurora-excited ionosphere to investigate infrared and optical sky backgrounds. The program uses the natural charged-particle bombardment that produces visible aurora to study the spectral, spatial and temporal behavior of atmospheric infrared emissions, identify the critical radiation-related species and reactions, and to provide rate coefficient information and bench marks for computer codes that predict the background radiances. Of significant importance in the program is the development of new instruments and experimental techniques for upper atmosphere research—cryogenic (helium and nitrogen cooled) spectrometers for measurements in the infrared region from 1 to 20 micrometers.

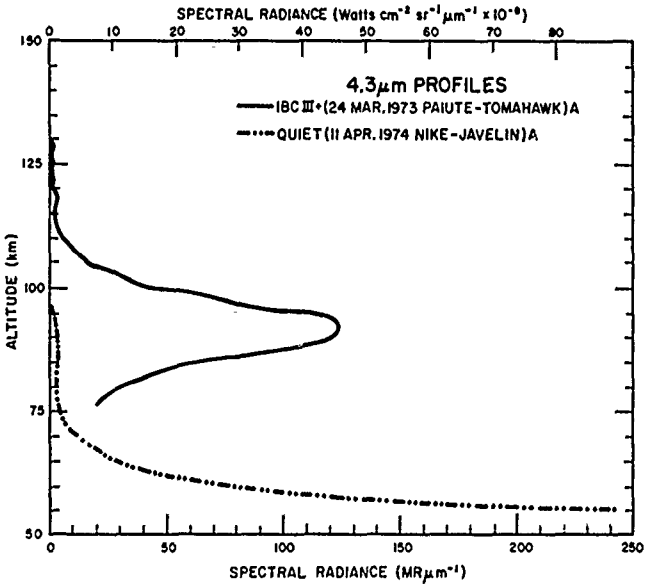

Peak spectral radiance (MR/micrometer) at 4.3 micrometers as a function of altitude from two rocket flights showing the significant enhancement in a class III+ aurora (ICECAP 73A) compared to a quiet night measurement (ICECAP 74A).

To date, five ICECAP programs have been conducted at Poker Flat, Alaska, with a toal of 22 launches (11 major rocket payloads and 11 supporting on small rocket payloads). Every flight of the major rockets obtained new, useful and significant data, and only one rocket vehicle failed in the entire program. Of particular importance, recovery of expensive payloads and instrumentation was successful on the nine major rocket launches when it was attempted, so that all recovered instruments could be and have been reflown in the program.

Much of the ICECAP data is still in an early state of reduction and analysis, but some of the results are of immediate use. For example, the first enhancement at 4.3 micrometers due to auroral deposition has been observed. There are two possible competing molecular species, CO_2 and NO^+, which can emit at 4.3 micrometers, and our spectral resolution to date is not sufficiently high to distinguish between the two. Under the assumption that CO_2 is the only radiator and is excited by vibrational transfer from electron excited $N_2^{\ddagger}$ (the double dagger indicates an excited state), the calculation using the ICECAP 72A data yielded between 3 and 7 vibrational states of N_2 excited per ion pair produced. In ICECAP 73A, good data were obtained at 4.3 micrometers under three separate auroral conditions: a stable arc was penetrated on ascent; the arc was overflown and descent occurred in a quiet atmosphere; and an SWIR spectrometer (Paiute Tomahawk) was flown into a fantastic auroral breakup with more than 200 kiloRayleighs of 3914 angstrom radiation. These data

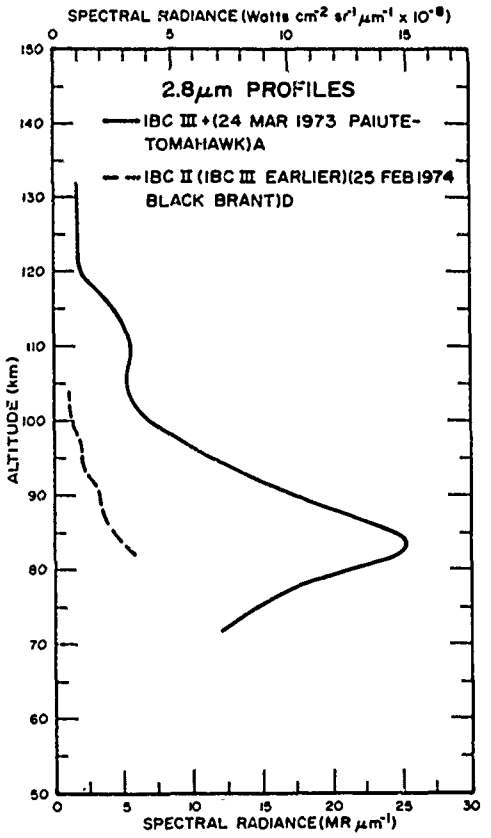

Peak spectral radiance (MR/micrometer) at 2.8 micrometers as a function of altitude from rocket flights into class III$^+$ and class II auroras.

need correction for aspect, and analysis requires details of the time and altitude of energy deposition. However, the large magnitude of the auroral enhancement observed at 4.3 micrometers is of interest. It was observed simultaneously with approximately 200 kiloRayleighs of 3914 angstrom emission, a class III$^+$ auroral event. The peak altitude of both emissions occurred near 90 km. Preliminary results from the Stanford Research Institute incoherent radar show electron densities of almost 2 x 10^6 per cubic centimeter, also peaking at 90 km during the ascent portion of this flight.

The theory for $NO^\ddagger$ is not as good even though enhanced 5.3 and 2.8 micrometer emissions were also obtained during four separate auroral conditions. There are three fundamental problems: the source production of metastable N atoms by electron deposition is not known; the initial vibrational state distribution of the $N(^2D) + O_2 \rightarrow NO^\ddagger + O$ reaction is not known, and a good dipole moment function for these high vibrational states is not yet available but is being calculated. In addition, a practical limitation has been that the measurements have only covered a small portion (5 to 5.4 micrometers) of the sequence which could extend to about 7 micrometers if $v=16$ is populated. Despite this, theoretical approximations have been made against the data available and at least there is confidence that $N(^2D)$ chemistry can explain the arc observations and that indeed NO chemiluminescence (infrared) from the excited state chemistry has been observed for the first time.

Preliminary data of 2.8 micrometer emission observed during the Paiute Tomahawk flight show 9 megaRayleighs (MR) per micrometer (vertical) peaking at 85 km which, coupled with a similar altitude profile for 5.3 micrometer emission, leads to the conclusion that $NO^\ddagger$ is the responsible emitting species. Previous 2.7 micrometer data obtained under less intense auroral

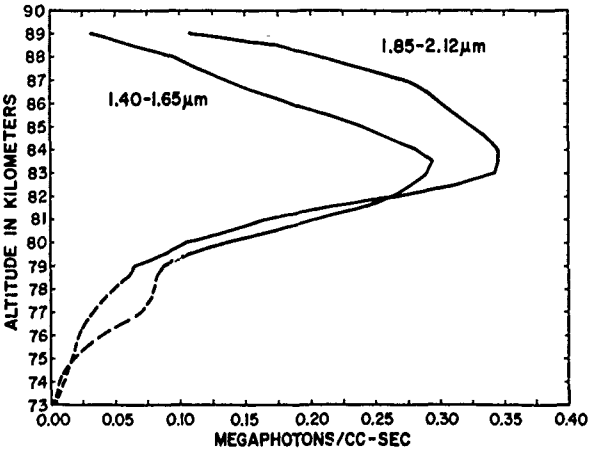

Volume emission profile (megaphotons/cc-sec) of hydroxyl from a rocket flight at Poker Flat, Alaska.

excitation were on the order of 1 megaRayleigh per micrometer or less which could be attributed primarily to hydroxyl airglow emissions.

Altitude and volume emission profiles of the hydroxyl molecule have been obtained in the polar and mid-latitude regions. The hydroxyl molecule is the principal infrared observable in the short wavelength region of the atmosphere and is known to have large natural perturbations. The energy balance and dynamics of other molecules like ozone, atomic oxygen and water may be determined through monitoring the hydroxyl molecule. From the results shown in the figure, the altitude profile of atomic oxygen has been derived for the polar regions which extends to lower altitudes than in midlatitudes.

The first fully successful flight of the LWIR circular variable filter (CVF) spectrometer (helium cooled) which was launched into a post-auroral breakup condition occurred on March 22, 1973. As viewed from the ground stations, an extended Class IBC II auroral breakup condition was penetrated by the rocket. The 3914 angstrom N_2^+ brightness was about 8 kiloRayleighs and the 5577 angstrom O I brightness was about 13 kiloRayleighs. At the time of the launch, the measurements from backscatter radar at Chatanika, Alaska, indicated a relatively low altitude electron density profile. The peak concentration was about 3.5×10^5 electrons per cubic centimeter at 92 km. The magnetometer network of the College Observatory at the University of Alaska indicated the passage of a 1600 gamma negative magnetic bay at the time of the launch of the Black Brant.

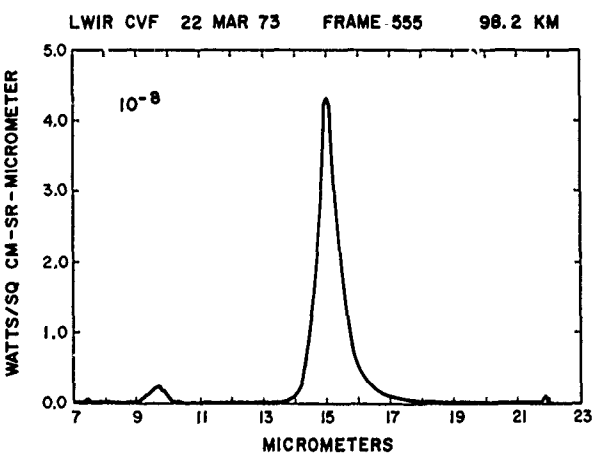

LWIR spectrum obtained at 98.2 km from a rocket-borne circular variable filter spectrometer (helium cooled) launched into a post-auroral breakup.

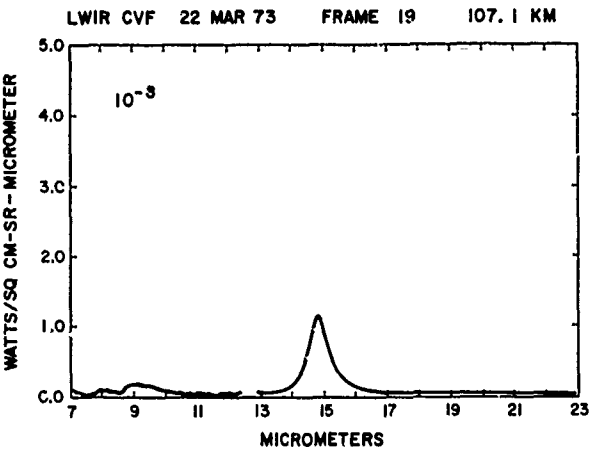

LWIR spectrum obtained at 107.1 km from a rocket-borne circular variable filter spectrometer (helium cooled) launched into a post-auroral breakup.

The infrared data from this flight are in an early and preliminary state of reduction as far as absolute units are concerned. However, as an example of this new LWIR atmospheric data, a spectrum obtained at 96.9 km during the March 1973 flight shows the dominant features to be due to O_3 at 9.6 micrometers and CO_2 at 15 micrometers. This is typical of all the lower altitude spectra obtained down to approximately 50 km. At higher altitudes (around 110 km) an unresolved feature at 9.2 micrometers can clearly be differentiated from the 9.6 micrometer ν_3 band of O_3 which may have disappeared completely. This is more apparent in the spectra at even

higher altitudes where the principal emitter is centered around 9.2 micrometers. By 150 km, the CO_2 band at 15 micrometers is no longer observable.

Comparison at 60 km, where collisional excitation is the dominant process (LTE), is in reasonable agreement with the prediction. However, at increasingly higher altitudes, as earthshine fluorescence becomes more and more important (at 140 km it is 85 percent of the excitation mechanism), there is a two-order of magnitude discrepancy. The experimental error is considered to be less than a factor of 2. There is some uncertainty in the concentration of CO_2 versus altitude, but CO_2 has been measured by helium cooled mass spectrometer and shown to be in diffusive equilibrium relative to argon. The CO_2 concentration needed for the theoretical model to produce enough intensity to fit the measured signal seems to be unreasonably large. It is difficult to find an effective mechanism to transfer energy in an aurora to radiation in the 15-micrometer band, and contributions from chemical reactions are not expected to be significant. The conclusion is that the model needs revision in the calculations of the earthshine resonance scattering to agree with the data.

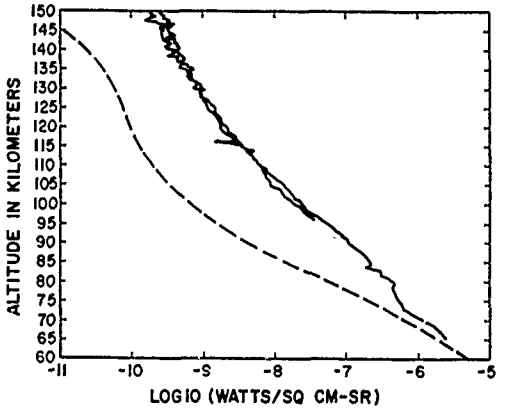

The 15-micrometer CO_2 radiance versus altitude profile from a rocket flown into a post-auroral breakup compared with the prediction of the earth limb radiance model. The dashed line is one model calculation and the solid curves the ascent and descent data.

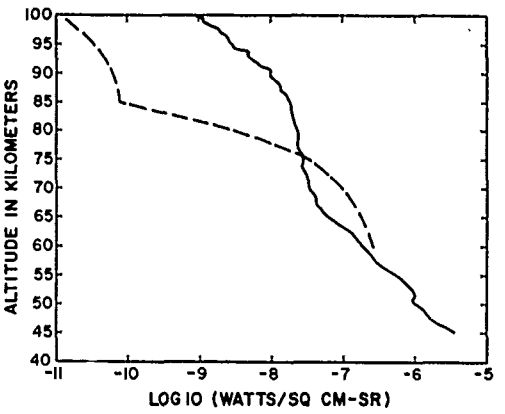

The 9.6-micrometer O_3 radiance versus altitude profile from a rocket flown into a post-auroral breakup compared with the prediction of the earth limb radiance model. The dashed line is one model calculation and the solid curve is the rocket descent data.

A similar comparison of the altitude profile of the 9.6-micrometer O_3 emission data with the same model shows that the O_3 data deviate from the theory by two orders of magnitude—this time at 95 km. However, O_3 in contrast to CO_2, is strongly dependent upon photochemistry. Although improvements in earthshine calculations may prove to be sufficient, the data above 80 km seem to require contributions from increased O_3 concentrations.

LABORATORY COLD INFRARED CHEMILUMINESCENCE EXPERIMENTS: To predict background radiance perturbations which may result from natural or artificial atmospheric disturbances and help assess their resulting impact on defense systems, it becomes necessary to specify those chemical interactions which are important sources of atmospheric radiation, and to determine the efficiency with which it is produced, redistributed spectrally and degraded. The Laboratory has nearly completed construction of a new and unique facility designed to address just such questions in a con-

trolled laboratory environment for the first time.

A new half-kilowatt closed-cycle helium gas refrigeration system supplies cryogenic power to provide both an environment of 20° K which completely eliminates thermal background effects on infrared instrumentation and a substantial cryopumping capability within a closely temperature-controlled chamber. The cryopumped chamber serves as a wall-less reaction volume within which chemical interactions are initiated and observed under the low density conditions they would encounter high in the atmosphere without introduction of spurious laboratory effects like wall collisions. Actual observation of the resulting infrared radiation is possible only because of the many orders of magnitude infrared detectivity improvement resulting from the 20° K environment.

The initial application for this facility, called COCHISE (COld CHemi-excited Infrared Simulation Experiments), is in the direct study of infrared radiation-emitting processes themselves. It is, in addition, an ideal tool for investigating relevant atmospheric environmental problems.

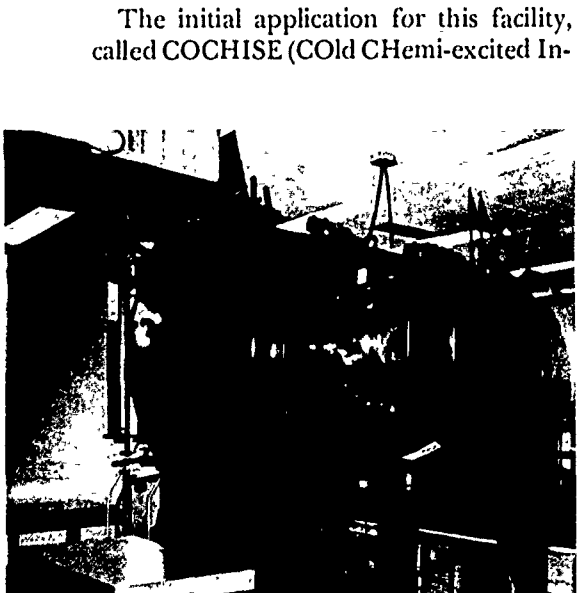

General view of the COCHISE facility showing main vacuum chamber in foreground and closed cycle helium refrigerator at rear.

Its present unique combination of controlled chemistry and enhanced infrared diagnostic capability, augmented by universal detection and fluorescence monitoring now being developed for ionic and non-radiating species, will allow the Laboratory to make a unified approach to problems requiring detailed study. In its first assignment, this facility will be used to provide a complete account of the infrared radiation emitted by vibrationally excited ozone molecules fomed in oxygen atom recombination, and to assess the contribution that metastable nitrogen atoms make to the generation of atmospheric nitric oxide radiation.

INFRARED RADIATION FROM AIR EXCITED BY ELECTRON DEPOSITION: The excitation source used in the experiment has been a 50 kilovolt, 5 milliampere electron beam interacting with target gas at pressures from a few torr to a few hundred torr and a hollow cathode discharge in the 1-10 torr region at a few hundred volts and currents up to 2 amperes. The source was pulsed in both experiments to simulate the electrical effect of the deposition of prompt X-rays in the atmosphere.

Previous spectral observations of the NO produced in such sources had not been time resolved so that the displayed spectra showed all the features which appeared during the experiment. Overlapping of features appearing in the same spectral region but at different times made analysis very uncertain. This has now been overcome by passing the signal through an electronic gate which can be opened and closed as desired. The timed portion of the received signal is averaged in an integrator and generates an interferogram as the observing interferometer-spectrometer is scanned.

The vibrational distribution of NO depends on whether it was formed as a result of the interaction of the ground state, where levels up to v=6 are possible or from the metastable levels at 2.4 eV and at 3.6 eV which have sufficient energy to excite levels up to v=18 and 21 respectively.

Resolving power limitations with the spectrometer make it necessary to observe the overtone region to investigate the vibrational levels formed. So far, levels up to v= 12 can be reasonably identified. Further work will be required to enhance the signal-to-noise ratio so that the presence or absence of higher levels can be established. Work is proceeding on calculation of the transition probabilities of the bands so that the concentrations can be found from the measured intensities.

The rates of disappearance of the metastable N atoms formed in the discharge have been measured by an absorption measurement in the vacuum UV. At high pressure (>3 torr) the rates in air become too fast for the present signal averager and further work will be performed with a faster instrument. In conjunction with the time-resolved IR spectroscopy, these measurements should allow more complete understanding of the photochemistry.

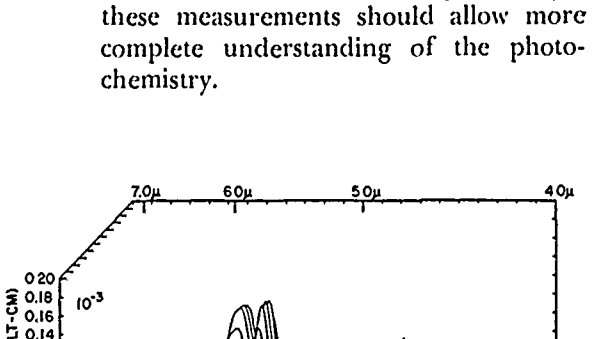

Time history from 3 ms pulse from 50 KV gun, 5 ma, into 150 torr N_2 plus 15 torr O_2. Shows buildup and decay of NO at 1800 cm^{-1} and N_2O at 2200^{-1} cm.

Low pressure, cooled background tank for air studies.

By studying the steady state intensity and decay of the NO emission of the fundamental, the vibrational quenching rate of NO has been found with O_2, N_2 and air. These are important results needed in the prediction of the NO signature expected in atmospheric disturbances.

The major feature of the late events occurring in the experiments is the appearance of N_2O. It appears to rise as the NO falls, but the mechanism is not understood. Since it is the dominant feature of the spectrum at both times, it will receive further study.

To study these reactions at low pressure (<1 torr), a 4½-foot-diameter tank 15 feet long has been installed. It is equipped with a low energy (300 eV up to 2 kV and 2 milliampere) electron gun. To reduce the infrared background to levels comparable with expected signal strengths, the entire tank is lined with a liquid N_2 cooled shroud. A liquid N_2 cooled Czerney-Turner monochromator is being installed and special high sensitivity low noise cooled amplifiers have been developed.

THEORETICAL PROGRAM: During the past two years, substantially higher quality field and laboratory-simulated spectral data of both ambient and disturbed atmospheres

have been obtained. For example, the ICECAP auroral program has provided the first high altitude infrared measurements in excited atmospheric conditions. Laboratory simulation of excited conditions in the LABCEDE program has produced high resolution infrared spectra of air excited by energetic electrons. Information obtained in these experiments has led to continuing refinements in computer codes such as OPTIR, which model the physics and chemistry of atmospheric radiative processes. This rapid sophistication has presented workers in both the data acquisition and modeling efforts with a new requirement for quantitative information regarding microscopic properties of many atmospheric molecular species.

In response to this need, a theoretical program has been initiated at AFCRL which makes use of the most sophisticated *ab initio* quantum mechanical techniques currently available for the calculation of molecular wave functions, energies and properties. The quantum mechanical capability resides chiefly in the application of Multiconfiguration Self-Consistent-Field (MCSCF) techniques to generate accurate electronic wave functions and properties followed by numerical solution of the vibration-rotation Schrödinger equation yielding observables for specific vibration-rotation states of a molecule.

The current emphasis of this theoretical effort is focused on obtaining accurate absolute intensities for the vibration-rotation transitions in important infrared-emitting atmospheric diatomics. These intensities, or Einstein coefficients as they are commonly called, determine the observed intensity of radiation emitted by molecules, and especially for highly reactive or excited species, they are exceedingly difficult to measure in the laboratory. The modeling codes which predict radiation intensity and also the analysis of atmospheric spectra critically depend on accurate values for these quantities.

A more pressing need in this area has been affected by the ICECAP and LABCEDE programs which obtain spectra under conditions where reactions involving metastables, radicals, and other species occur to form molecules in high vibrational and rotational states. The cascade from these states produces much of the infrared radiation observed in the aurora and following nuclear detonations. Proper treatment of these chemiluminescent reactions requires Einstein coefficients for specific vibration-rotation transitions up to high vibrational states which are simply unavail-

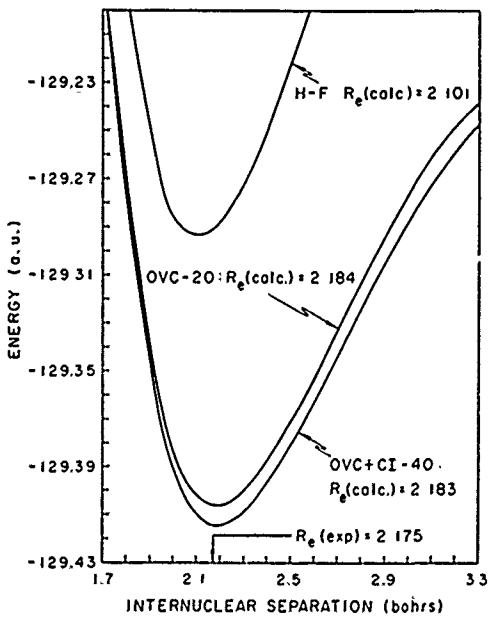

Potential curves for the ground state NO calculated at various levels of accuracy, proceeding from the least accurate single configuration Hartree-Fock (H-F) curve, to a 20-configuration MCSCF (OVC-20) function, and finally to the most accurate curve (OVC+CI-40) obtained from a 40-configuration MCSCF and configuration interaction calculation. The equilibrium internuclear separations (R_e) calculated from each curve are indicated and compared to the experimental quantity. These curves allow direct determination of rotation-vibration energies and wavefunctions for NO.

able or poorly estimated for many of the important atmospheric species.

The theoretical approach to the calculation of these quantities requires an accurate representation of the molecular electronic dipole moment as a function of internuclear separation and accurate vibration-rotation wave functions. The MCSCF techniques discussed above may be employed to satisfy both these requirements.

To date, specific vibration-rotation Einstein coefficients and infrared line positions to high vibrational levels have been calculated within this framework for CO, NO^+, OH, and NO. The results have led to a significant increase in understanding of the radiative processes associated with these molecules and provide a quantitative route to concentrations, rate constants and other properties of excited species in the atmosphere.

Future plans center around an *a priori* treatment of the primary processes governing the radiation observed following impact of energy on the atmosphere. Heavy and light particle scattering cross sections are needed for many molecules as well as intermediate excited and final state potential curves.

PARTIAL RATE CONSTANTS FOR THE NITROGEN-OXYGEN REACTION: The study of the chemiluminescent reaction $N+O_2$ which leads to the formation of NO molecules in the vibrationally excited ground electronic state was continued to obtain partial rate constants for each level. The overtone band of NO, which was formerly obtained through a circular variable filter, was measured at higher resolution by use of an interferometer-spectrometer. Detailed study of this band as a function of O_2 pressure exhibited features due to molecules other than NO. Further investigation showed that spurious signals due to N_2O molecules occurred in the overtone region of NO. Experiments indicated formation of N_2O in its ground state through three-body reaction of $N_2 + O + M \rightarrow N_2O + M$. It was established that the source of vibrational energy for N_2O was exchanged with vibrationally excited N_2 formed in the microwave discharge. Consequently, to obtain pure NO overtone spectra, vibrationally excited N_2 molecules were eliminated by insertion of sufficient glass wool in the discharge tube. Experimental spectra were then matched to theoretically constructed ones and steady-state densities for each level of NO were derived for levels 2 through 7. Final results of this experiment is a set of partial rate constants for formation of NO for these levels.

As an extension of this experiment, an NO overtone signal was obtained as a function of O_2 pressure beyond the point where quenching of vibrationally excited NO by O_2 comes into play. It was found that the results can be interpreted with a quenching rate constant k_q for 1-0 transition of approximately 10^{-14} cubic centimeters per second.

LASER PHYSICS

MOLECULAR ENERGY TRANSFER STUDIES: An understanding of energy transfer processes among excited molecular states is fundamental to understanding the operation of gas lasers of high or low energy. Such processes directly affect laser power, efficiency and size, and determine optimum design parameters such as pressures, mixture ratios, temperature and flow speeds. Energy transfer also governs phenomena in the upper atmosphere and is of basic significance in combustion phenomena, such as in jet engine exhausts.

Lasers have provided revolutionary new means for understanding molecular energy transfer. The narrow spectral widths achievable with lasers allow individual excited states to be populated. Owing to the high power densities achievable, large excited state populations can be achieved, making the evolution and redis-

tribution of the excitation energy easy to follow by various means.

The Laser Physics Branch has made numerous contributions to the development of laser techniques for molecular energy transfer measurements. The Branch has pioneered in the application of tunable lasers, which makes it possible to excite arbitrary molecular states at will. A novel application of integrating spheres has been introduced to serve the dual purpose of efficiently exciting a weakly absorbing molecular transition, and efficiently collecting fluorescence subsequently emitted. Another novel technique introduced by the Branch involves the use of carefully controlled multiple laser wavelengths to populate excited states which otherwise are inaccessible.

Molecules which have been studied include CO, HF and DF. Each of these is an active material in a highly important laser being developed at the Air Force Weapons Laboratory, Kirtland AFB, New Mexico. The energy transfer rates we have measured, using techniques described above, are a crucial component of computer models being used to understand the performance and optimize the design of these lasers.

Experiment to measure vibrational energy transfer rates in gases. Gas residing in dimpled gold integrating sphere is excited by optical parametric oscillator in foregound. Detector above sphere measures fluorescence, detector behind oscillator registers input power and electronics normalizes all measurements to input power.

INFRARED MOLECULAR GAS LASERS: A number of molecular gas lasers are being developed because of their potential for high output energy. However, there exist needs in many areas for infrared lasers of lower energy but with special characteristics, such as compactness, efficiency and specific wavelength. There are also regions of the infrared spectrum, notably at very long wavelengths, where fruitful applications have been speculated, but where even preliminary technology to test concepts was unavailable. Our infrared molecular gas laser activity has addressed these needs and opportunities.

The submillimeter region of the spectrum is one which until recently had been little explored. Important applications, such as weapons effects diagnostics, exist, and others, such as secure communications and all-weather-landing radar, have been conjectured. Scientific applications abound. An important advance in the technology of submillimeter waves was the demonstration of an optically pumped submillimeter laser at Bell Telephone Laboratories, where a CO_2 laser was used to pump a molecular gas, stimulating it to emit in the submillimeter. Following that initial demonstration, we have made several important advancements in the technology. In prior work it was necessary for the pump laser frequency to overlap a molecular absorption line of the gas being pumped. This restricted the systems to which the technique could be applied. We have demonstrated two ways in which this restriction can be overcome. One, the "off resonant optical pumping" technique suitable for pulsed systems, relies on the fact that molecular absorption lines are broadened by a high intensity infrared pump. The

other, suitable for CW or pulsed systems, uses a dc electric field to tune an absorption line into coincidence with the pump laser frequency. An important aspect of the latter work was the use of waveguide modes of the two plates through which the dc field was applied, to propagate the generated submillimeter radiation. This demonstration of a two-plate waveguide laser will be much more generally useful: for example, it could lead to compact, high repetition rate hybrid chemical lasers.

The optically pumped submillimeter lasers work by creating a population inversion and lasing between pure rotational transitions. These transitions can produce laser wavelengths as short as about 50 micrometers. We have demonstrated a closely analogous optical pumping technique wherein the lasing takes place between vibrational states. This technique is generally applicable at shorter infrared wavelengths. Our technique is a general means of converting the wavelength of a good existing laser into a more favorable wavelength because of propagation or application-motivated factors. We are currently investigating the use of optical pumping techniques to generate useful lasers in the 3-5 micrometer spectral region.

LASER INDUCED DAMAGE: Pulsed laser systems are the basis for recent radical advances in Air Force weapons delivery capabilities. In extensions of this capability, numerous requirements exist for higher laser power and more compact devices than currently exist. The most serious problem limiting the power or size of many pulsed laser devices is damage to optical components caused by the laser radiation itself. This problem has been under investigation here for several years. AFCRL scientists have made major advances in diagnosing and understanding the physical causes of laser-induced damage under many different conditions. Over the years, an experimental diagnostic procedure, known as the "survival time curve" method, has been developed in-house. It is uniquely capable of telling what mechanism is causing damage to a given specimen under given conditions. The survival time technique cannot only tell damage mechanism, but can also measure with great sensitivity the parameters associated with each mechanism. This provides an invaluable feedback to the component producer so that he may improve his processing to alleviate damage problems. In addition to studying basic causes and cures for laser-induced damage, we have provided, as a service to various other DOD agencies, an assessment of the damage characteristics of materials in which they had special interest.

Thin film dielectric coatings used for mirrors, or anti-reflective coatings, are often the weakest link in a pulsed laser system. For this reason, understanding and improving the damage properties of films has been a focus of our efforts. We have investigated mirrors made by many commercial suppliers and have shown that in most of these, bulk absorption is not a significant factor. The damage almost always occurs due to the presence of absorbing defects in the dielectric film. Currently, we

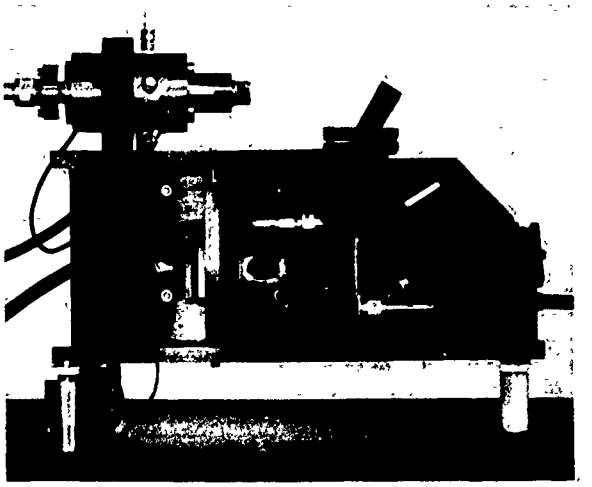

A laser triggered switch built for in-house laser-induced damage experiments. Rise and fall times of 0.7 ns have been achieved.

are working with several coating experts to eliminate or minimize the problems caused by those defects. By focusing the laser beam to spot sizes small enough so that the spot irradiated almost never includes an absorbing defect, we have shown that the next most damaging mechanism is due to electron avalanche, and that laser intensities about ten times greater are allowed before this kind of damage occurs.

Although the work in laser-induced damage to films was motivated by laser problems, the sensitivity with which the technique measures various coating parameters offers promise that it can be used to learn about films meant for other purposes—for example, electronic components. This progress represents a considerable understanding of laser-induced damage, and some understanding of how to combat it.

NEW LASER CONCEPTS: Some of the many new concepts and inventions introduced at AFCRL have been described in previous sections; some will be described here.

A novel laser configuration was invented, capable of producing intense pulses of continuously variable duration from about 0.1 to 1.5 nanoseconds. This had been a particularly awkward temporal region, with mode locking producing shorter pulses and Q-switching longer ones. The technique uses a simple switch in connection with an interferometer as one laser end reflector. The pulse duration is determined by the (variable) spacing of the interferometer. We have investigated experimentally three types of switches—an amplitude switch, a phase switch, and a "self" switch—whereby the laser beam is focused into a gas cell and its transmission is terminated due to breakdown of the gas. The latter has the virtue that it requires no additional active elements.

A pulsed laser configuration in which the active medium is annular in shape and pumped by a flashlamp within it was invented and experimentally characterized within the Branch. This geometry allows for uniform, efficient pumping of the active medium. It allows for efficient heat removal from a large, useful volume of active material.

A technique was invented for stabilizing the frequency of a wideband tunable laser (such as a capillary laser) at an arbitrary value. The technique uses the molecular Stark effect to shift the frequency of an absorbing gas to the desired value. The laser frequency is then locked to the center of the absorption line. There are many important uses for capillary lasers which require such careful frequency control.

JOURNAL ARTICLES
JULY 1972 - JUNE 1974

BENDOW, B., GIANINO, P. D. (Solid State Sci. Lab.), HORDVIK, A., and SKOLNIK, L. H. (Solid State Sci. Lab.)
Theory of Thermally Induced Interference and Lensing in Transparent Materials
Opt. Comm., Vol. 7, No. 3 (March 1973)

BILLINGSLEY, F. P., II
Calculations of the Absolute Infrared Intensities for the 0-1, 1-2 Vibration-Rotation Transitions in the Ground State of NO^+
Chem. Phys. Ltrs. Vol. 23 (1973)

BILLINGSLEY, F. P., II, and HAYES, L. J. (Air Products and Chem., Inc., Allentown, Pa.), TRINDLE, C. (Univ. of Va.)
INDO Molecular Orbital Study of Alpha Heteroatom Nitrenes
The J. of Organic Chem., Vol. 37 (1972)

BILLINGSLEY, F. P., II, and KRAUSS, M. (Natl. Bur. of Stds., Wash., D.C.)
Coupled Multi-Configurational Self-Consistent Field Method for Atomic Dipole Polarizabilities. I. Theory and Application to Carbon
The Phys. Rev., Vol. A6 (1972)
Quadrupole Moment of Co, N_2 and NO^+
The J. of Chem. Phys., Vol. 60, No. 7 (1 April 1974)
Multi-Configuration Self-Consistent-Field Calculation of the Dipole Moment Function of CO
The J. of Chem. Phys., Vol. 60, No. 11 (June 1974)

BILLINGSLEY, F. P., II, and STEVENS, W. J. (Argonne Natl. Lab., Argonne, Ill.)
Coupled Multi-Configurational Self-Consistent Field

Method for Atomic Dipole Polarizabilities. II. The First Row Atoms Lithium Thru Neon
The Phys. Rev., Vol. A8 (1973)

BILLINGSLEY, F. P., II, and TRINDLE, C. (Univ. of Va.)
A Mixed-Basis Scheme for the Rapid Computation of Molecular Electronic Energy in the SCF-LCAO-(STO)-MO Formalism, and Its Application to the Lithium Super-Oxide Molecule
The J. of Phys. Chem., Vol. 76 (1972)

BLISS, E. S., MILAM, D., and BRADBURY, R. A.
Dielectric Mirror Damage by Laser Radiation Over a Range of Pulse Durations and Beam Diameters
Appl. Opt., Vol. 12, No. 4 (April 1973)

CLOUGH, S. A., ROTHMAN, L. S., and BEERS, Y., KLEIN, G. P. (Natl. Bur. of Stds., Boulder, Colo.)
The Dipole Moment of Water from Stark Measurements of H_2O, HDO, and D_2O
J. of Chem. Phys., Vol. 59, No. 5 (1 September 1973)

CONLEY, T. D.
Mesospheric Positive Ion Concentrations, Mobilities and Loss Rates Obtained from Rocket Borne Gerdien Condenser Measurements
Radio Sci., Vol. 9, No. 6 (June 1974)

DEL GRECO, F. P.
Kinetics of Atmospheric Radiation
DNA Reaction Rate Handbook, Sec. Ed. (1972)

ELTERMAN, L., TOOLIN, R. B., and ESSEX, J. D.
Stratospheric Aerosol Measurements with Implications for Global Climate
Appl. Opt., Vol. 12 (February 1973)

ERNST, K. (Mass. Inst. of Technol.), OSGOOD, R. M., JR. (MIT Lincoln Lab., Lexington, Mass.), JAVAN, A. (Mass. Inst. of Technol.), and SACKETT, P. B.
Measurement of the Vibrational-Vibrational Exchange Time (v=2) for DF Gas
Chem. Phys. Ltrs., Vol. 23, No. 4 (15 December 1973)

FAIRBAIRN, A. R.
Radiative Lifetime of O_2^+
J. of Chem. Phys., Vol. 60 (1974)

FENN, R. W.
Atmospheric Effects
Adv. Scanners and Imaging Sys. for Earth Obsns., NASA SP-335 (1973)

FENN, R. W., and AGAZARIAN, K. (Met. Lab.)
Atmospheric Haze Models for Contrast Transmittance Calculations
Proc. of the Ann. Electro-Opt. Sys. Design Conf. — 1972

FETTERMAN, H. R. (MIT Lincoln Lab., Lexington, Mass.), SCHLOSSBERG, H. R., and PARKER, C. D. (MIT Lincoln Lab, Lexington, Mass.)
CW Submillimeter Laser Generation in Optically Pumped Stark Tuned NH_3
Appl. Phys. Ltrs., Vol. 23, No. 2 (15 December 1973)

FETTERMAN, H. R. (MIT Lincoln Lab., Lexington, Mass.), SCHLOSSBERG, H. R., and WALDMAN, J. (Lowell Technol. Inst., Mass.)
New Tools for Submillimeter Spectroscopy
Laser Focus, Vol. 8, No. 9 (September 1972)
Submillimeter Lasers Optically Pumped Off Resonance
Opt. Comm., Vol. 6, No. 2 (October 1972)

GARING, J. S., and MCCLATCHEY, R. A.
Atmospheric Absorption Line Compilation
Bull. of the Am. Met. Soc. (September 1973): (Ltr. to the Ed.) Appl. Opt., Vol. 12, No. 11 (November 1973)

GARING, J. S., and SCHURIN, B. D.
Infrared Observations of the Earth's Upper Atmosphere
Proc. of Summer Adv. Study Inst. on Phys. and Chem. of Upper Atm., Orleans, Fr., 31 July - 11 Aug. 1972, Ed. by B.M. McCormac, D. Reidel Pub. Co. (1973)

GRIENEISEN, H. P., GOLDHAR, J., KURNIT, N. A., JAVAN, A. (Mass. Inst. of Technol.), and SCHLOSSBERG, H. R.
Observation of the Transparency of a Resonant Medium to Zero Degree Optical Pulses
Appl. Phys. Ltrs., Vol. 21, No. 11 (December 1972)

HORDVIK, A., and SACKETT, P. B.
Characteristics of the Optical Parametric Oscillator and Its Use for Selective Excitation
Appl. Opt., Vol. 13, No. 4 (May 1974)

HORDVIK, A., and SCHLOSSBERG, H.
Reply to "Comment on Luminescence from $LiNbO_3$"
J. of Appl. Phys., Vol. 44, No. 1 (January 1973)

HUPPI, E. R., ROGERS, J. W., and STAIR, A. T., JR,
Aircraft Observations of the Infrared Emission of the Atmosphere in the 700-2800 cm^{-1} Region
Appl. Opt., Vol. 13, No. 6 (June 1974)

HUSHFAR, F., ROGERS, J. W., and STAIR, A. T., JR.
Further Comments on the Chemiluminescent Reaction $N + O_2 \rightarrow NO + O$ and Its Overtone Photon Efficiency
Appl. Opt., Vol. 11 No. 7 (July 1972)

KENNEALY, J. F., and DEL GRECO, F. P.
The Kinetics of Atmospheric Radiative Processes in the Infrared
Chap. II of DNA Reaction Rate Handbook, Sec. Ed. (1972)

LOEWENSTEIN, E. V.
Far Infrared: Applications in Remote Sensing and Materials Research
Opt. Spectra (September 1972)

LOEWENSTEIN, E. V., and SMITH, D. R.
Far Infrared
Section in Am. Inst. of Phys. Handbook (1972)

LOEWENSTEIN, E. V., SMITH, D. R., and MORGAN, R.
Optical Constants of Far Infrared Materials. II. Crystalline Solids
Appl. Opt., Vol. 12 No. 2 (February 1973)

LOGGINS, A. B., MAJ., and EPPS, J. B., FERRY, D. K., SEAGAT, R. H. (Tex. Tech. Univ.)
Development of a Dynamic Model for Turbulence Effects on a Fighter Aircraft
Proc. of the 6th Gdnce. Test Symp., Holloman AFB, N.M., Oct. 4-6, 1972 (AFSWC TR 72-34)

MILAM, D.
Brewster-Angle Pockel's Cell Design
Appl. Opt., Vol. 12, No. 3 (March 1973)

MILAM, D., and BRADBURY, R. A.
Laser Damage in Dielectric Mirrors
Laser Focus, Vol. 9, No. 12 (December 1973)

MILAM, D., BRADBURY, R. A., and BASS M. (Univ. of So. Calif.)
Laser Damage Threshold for Dielectric Coatings as Determined by Inclusions
Appl. Phys. Ltrs., Vol. 23, No. 12 (15 December 1973)

MILAM, D., BRADBURY, R. A., HORDVIK, A., SCHLOSSBERG, H. R., and SZOKE, A. (Hebrew Univ., Tel Aviv, Isr.)
Production of Intense Subnanosecond Pulses by Cavity Dumping
J. of Quantum Elect., Vol. QE-10, No. 1 (January 1974)

MILAM, D., GALLAGHER, C. C., BRADBURY, R. A., and BLISS, E. S.
Switching Jitter in Spark Gap Triggered by a TEM_{00}-Mode Mode-Locked, Ruby Laser
Rev. of Sci Instm., Vol. 43, No. 10 (Octol 72)

MILAM, D., HORDVIK, A., and STAHL, H. (Pitney-Bowes, Inc., Norwalk, Conn.)
Comments on: A Brewster-Angle Pockel's Cell
Appl. Opt., Vol. 12, No. 6 (June 1973)

MILAM, D., and SCHLOSSBERG, H. R.
Long-Pulse Emission Characteristics of a Tube-Shaped Laser Oscillator
J. of Appl. Phys., Vol. 44, No. 5 (May 1973)

MURPHY, R. E.
Nuclear Weapon Optical-Infrared Phenomena and Their Effects on Air Force Systems
AF Sys. Command Manual 500-5 (1972)
Measurements of OH in the Auroral Zone
J. of Geophys. Res., Vol. 78 (1973)

NADILE, R.
High Altitude Spectral Measurements in the LWIR
M^3 Meas. Proc. (March 1973)
Radiation Enhancement Program III
JANNAF Enhancement Program Paper (9 May 1973)

NAGARAJA RAO, C. R., TAKASHIMA, T. (Univ. of Calif. at Los Angeles), and TOOLIN, R.
Measurements and Interpretation of the Polarization of Radiation Emerging from the Atmosphere at an Altitude of 28 Km Over Southwestern New Mexico (USA)
Qtr. J., Royal Met. Soc., Vol. 99, No. 420 (April 1973)

O'NEIL, R. R., and PENDLETON, W. R., JR.
Departure of N_2^+ Vibrational Population from Franck-Condon Predictions in the Case of Energetic e-N_2 Collisions
J. of Chem. Phys., Vol. 56 (1972)

O'NEIL, R. R., PENDLETON, W. R., JR., HART, A. M., and STAIR, A. T., JR.
Vibrational Temperature and Molecular Density of Thermospheric Nitrogen Measured by Rocket-Borne Electron Beam Induced Luminescence
J. of Geophys. Res., Vol. 79 (April 1974)

PICARD, R. H., and WILLIS, C. R. (Boston Univ., Mass.)
Coupled Superradiance Master Equations: Application to Fluctuations in Coherent Propagation of Radiation in Resonant Media
Coherence and Quantum Opt., Ed. by L. Mandel and E. Wolf, Plenum Press, N. Y. (1973)
Coupled Superradiance Master Equations
Phys. Rev. A, Vol. 8, No. 3 (September 1973)
Time-Dependent Projection-Operator Approach to Master Equations for Coupled Systems
Phys. Rev. A, Vol. 9, No. 3 (March 1974)

PRICE, S. D.
Radiative Opacity Due to the Phillips and Ballik-Ramsey Bands of C_2
Bull. of the Am. Astronom. Soc., Vol. 5, No. 3, Pt. 1 (June 1973)

RAHBEE, A.
Overtone Photon Efficiency of $N + O_2 \rightarrow NO + O$
Appl. Opt., Vol. 11 (1972)

ROGERS, J. W., MURPHY, R. E., STAIR, A. T., JR., and ULWICK, J. C. (Iono. Phys. Lab.), BAKER, K. D., JENSEN, L. L. (Utah State Univ.)

Rocket Borne Radiometric Measurements of OH in the Auroral Zone
J. of Geophys. Res., Vol. 78, No. 30 (20 October 1973)

SACKETT, P. B.
Effect of Fluorescence Observation Geometry on Lifetime Measurement, Including the Development of an Approximation to the Detector Collection Efficiency Integral
Appl. Opt., Vol. 11, No. 10 (October 1972)

SACKETT, P. B., HORDVIK, A., and SCHLOSSBERG, H. R.
Measurement of the V-V Energy Transfer Rate from CO(V=2) Using Tunable Parametric Oscillator Excitation
Appl. Phys. Ltrs., Vol. 22, No. 8 (15 April 1973)

SANCHEZ, A., and SMALL, J. G., ELCHINGER, G. M., JAVAN, A. (Mass. Inst. of Technol.), BACHNER, F. J., SMYTHE, D. L. (MIT Lincoln Lab., Lexington, Mass.)
A.C. Electron Tunneling at Infrared Frequencies: A Thin Film MOM Diode Structure with Broad-Band Characteristics
Appl. Phys. Ltrs., Vol. 24 (15 March 1974)

SCHLOSSBERG, H. R., and KELLEY, P. L.
Using Tunable Lasers
Phys. Today, Vol. 25, No. 7 (July 1972)

SHARMA, R. (Avco-Everett Res. Lab., Everett, Mass.) and SCHLOSSBERG, H. R.
On the Assumption Underlying the Near-Resonant Theory of Energy Transfer
Chem. Phys. Ltrs., Vol. 20, No. 1 (1 May 1973)

SKOLNIK, L. H. (Solid State Sci. Lab.), HORDVIK, A., and KAHAN, A. (Solid State Sci. Lab.)
Laser Doppler Interferometry for Measuring Small Absorption Coefficients
Appl. Phys. Ltrs., Vol. 23, No. 8 (15 October 1973)

STAIR, A. T., JR. and BAKER, D. J., STEED, A. (Utah State Univ.)
Ground Observations of Resolved Hydroxyl ($\Delta v = 2$) Airglow
J. of Geophys. Res., Vol. 78, No. 36 (1973)

STAIR, A. T., JR., WHEELER, N. B., and BAKER, D. J., WYATT, C. L. (Utah State Univ.)
Cryogenic IR Spectrometers for Rocket-Borne Measurements
NEREM '73 Record, Vol. 15, IEEE Catalog (7-9 November 1973)

VANASSE, G. A.
Fourier Spectroscopy: A Critical Review
(Inv. Paper) CRC Critical Rev. in Solid State Sci., Vol. 4, Issue 1 (December 1973)
Hadamard Matrices in Spectroscopy
(Inv. Paper) Textbook, Appl. of Walsh Functions (December 1973)

VANASSE, G. A., and DESPAIN, A. M. (Utah State Univ.)
Walsh Functions in Grille Spectroscopy
Proc. of 1972 Walsh Function Symp. (1972)

VOLZ, F. E.
IR Optical Constants of Ammonium Sulphate, Sahara Dust, Volcanic Pumice, and Flyash
Appl. Opt., Vol. 12, No. 3 (March 1973)
Note on Satellite Remote Sensing of Atmospheric Aerosol
J. of Air Pollution Control Assoc. (APCA), Vol. 23, No. 6 (April 1973)
The Stratospheric Dust Event of October 1971
J. of Geophys. Res., Vol. 79, No. 3 (20 January 1974)

WESTON, E. B.
The Main Sequence of the H-R Diagram: Its Significance and Role in Stellar Evolution
Proc. of 1972 Summer Sci. Mtg. of the Astronom. Soc. of the Pacific, Vol. 84 (October 1972)

PAPERS PRESENTED AT MEETINGS JULY 1972 - JUNE 1974

BAKER, D. J., KEMP, J. C. (Electro-Dyn. Lab., Utah State Univ.), BRUCE, M., and ULWICK, J. C. (Iono. Phys. Lab.)
Rocket Measurements of Near Infrared Auroral Spectra
1973 Ann. Am. Geophys. Union Mtg. Wash., D. C. (16-20 April 1973)

BENDOW, B., SKOLNIK, L. H., GIANINO, P. D. (Solid State Sci. Lab.), HORDVIK, A., and CROSS, E. F. (Aerosp. Corp., Los Angeles, Calif.)
Laser-Induced Interference and Thermal Lensing in Transparent Materials
1973 IEEE/OSA Conf. on Laser Engrg. and Appl., Wash., D. C. (30 May-1 June 1973)

DUCAS, T. W., 2nd LT., and JAVAN, A. (Mass. Inst. of Technol.)
Measurement of Microwave Fine Structure in OH Infrared Transitions Using Frequency Mixing with Metal-to-Metal Infrared Diodes
1972 Fall Mtg. of the Opt. Soc. of Am., San Francisco, Calif. (17-20 October 1972)

ECKBERG, E. E.
Thin Film Vacuum Depositioning and Ion Plating for the Scientific Glassblower
Am. Sci. Glassblowers Soc. Ann. Symp., Denver, Colo. (11-15 June 1973)

ELTERMAN, L., ESSEX, J. D., and TOOLIN, R. B.
Trends in Stratospheric Aerosol Levels
1972 Fall Mtg. of the Opt. Soc. of Am., San Francisco, Calif. (17-20 October 1972)

FENN, R. W., DEARBORN, F. K., and MIRANDA, H., DULCHINOS, J. (GCA Corp., Bedford, Mass.)
Balloon-Borne Aerosol Particle Concentration and Size Distribution Measurements
7th AFCRL Sci. Balloon Symp., Wentworth-By-The Sea, Portsmouth, N. H. (25-27 September 1972)

FETTERMAN, H. R. (MIT Lincoln Lab., Lexington, Mass.), and SCHLOSSBERG, H. R.
Development and Applications of Optically Pumped Submillimeter Lasers
(Inv.) Intl. Conf. on Submm. Waves and Their Appl., Atlanta, Ga. (5-7 June 1974)

GARING, J. S., and SCHURIN, B. D.
Infrared Measurements of the Earth's Upper Atmosphere
Summer Adv. Study Inst. on Phys. and Chem. of Upper Atm., Orleans, Fr. (31 July - 11 August 1972)

GIBSON, F. W.
Balloon-Borne Measurements of the Atmospheric Optical Scattering Parameters
Old Dominion Univ., Norfolk, Va. (21 July 1972)

GITELSON, S., NEWBURGH, R. G. (Microwave Phys. Lab.), and SAKAI, H.
A Polarization Sagnac Interferometer
1972 Fall Mtg. of the Opt. Soc. of Am., San Francisco, Calif. (17-20 October 1972)

GOLUBOVIC, A., EWING, W. S., BRUCE, J., COMER, J. (Solid State Sci. Lab.), and MILAM, D.
A Comparison of 10.6 μ m Laser Damage in Sputtered Vs. Electron Beam Deposited Ge-Coated KCl
ASTM Mtg., Natl. Bur. of Stds., Boulder, Colo. (22-23 May 1974)

HORDVIK, A.
Tunable Lasers and Some of Their Applications
Colloq., Dept. of Elec. Engrg., Univ. of R. I., Kingston, R. I. (2 May 1973)

HORDVIK, A. and SKOLNIK, L. (Solid State Sci. Lab.)
Laser Induced Thermal Distortion of CO_2 Laser Window Materials.
1972 AFSC Sci. and Engrg. Symp., San Antonio, Tex. (17-19 October 1972)

KENNEALY, J. P.
Outline of Ozone Measurements Program in the COCHISE Facility
ARPA/DNA/DDR&E Planning Mtg., Wash, D.C. (9 May 1973)
Project COCHISE – Status and Outlook
NWER Council Mtg., Albuquerque, N. M. (22 January 1973)

LOGGINS, A. B., LT. COL., and FERRY, D. K., SEAGAT, R. H. (Texas Tech. Univ.)
Modified Wiener-Bose Modeling Applied to Dynamic Vibration Response of Large Aircraft
IEEE Circuit Theory Mtg., Soc. for Ind. and Appl. Math., Univ. of Waterloo, Waterloo, Ont., Can. (12-13 April 1973)

MC CLATCHEY, R. A.
Molecular Absorption Parameters in Atmospheric Modeling
UCLA Intl. Conf. on Radn. and Remote Probing of the Atm., Los Angeles, Calif. (28-30 August 1973)
The Determination of Atmospheric Transmittance for Remote Sensing
24th Intl. Astro. Fedn. Cong., Azerbaijan SSR Acad. of Sci., Baku, USSR (8-15 October 1973)
Report of the IAMAP Radiation Commission Working Group on a Standard Radiation Atmosphere
Intl. Assoc. of Met. and Atm. Phys., Melbourne, Aust. (12-27 January 1974)

MILAM, D.
Recent Progress in Variable-Duration Short-Pulse Lasers at AFCRL
Sem. at Lawrence Livermore Labs., Livermore, Calif. (14 January 1974)

MILAM, D., BLISS, E. S., CAPT., BRADBURY, R. A., and GALLAGHER, C. C.
Generation, Selection and Amplification of Mode Locked Ruby Laser Pulses
1972 AFSC Sci. and Engrg. Symp., San Antonio, Tex. (17-19 October 1972)

MILAM, D., and BRADBURY, R. A.
Double-Pulse Damage Experiments: A Technique for Detecting Damage Due to Absorption
1973 Laser Damage Conf., Natl. Bur. of Stds., Boulder, Colo. (15-16 May 1973)

MILAM, D., BRADBURY, R. A., and BASS, M. (Raytheon Res. Div., Waltham, Mass.)
The Principal Cause of Laser Damage to Optical Coatings
1973 IEEE/OSA Conf. on Laser Engrg. and Appl., Wash., D. C. (30 May - 1 June 1973)

MILAM, D., BRADBURY, R. A., PICARD, R. H., and BASS, M. (Univ. of So. Calif., Los Angeles, Calif.)
Statistical Technique for Detecting Inclusion Damage
1973 Conf. on High Power IR Laser Window Mats., Hyannis, Mass. (12-14 November 1973)
Difference Between Breakdown and Inclusion Laser Damage Statistics
Gordon Res. Conf. on Nonlin. Opt. and Lasers, Santa Barbara, Calif. (7-11 January 1974)
Laser-Damage-Mechanism Identification by the Measurement of Survival Times
1974 Symp. on Laser Induced Damage in Opt. Mats., Natl. Bur. of Stds., Boulder, Colo. (22-23 May 1974)

MILAM, D., and SCHLOSSBERG, H.
Tube-Shaped Laser Oscillators for Efficient Cooling and Excitation

1972 Fall Mtg. of the Opt. Soc. of Am., San Francisco, Calif. (17-20 October 1972)

MILAM, D., SCHLOSSBERG, H., and SZOKE, A. (Mass. Inst. of Technol.)
Modified Cavity Dumping Technique for the Production of Intense Nanosecond Duration Pulses
Elect. Devices Conf., Wash., D. C. (4-6 December 1972)

MURCRAY, D. G. (Univ. of Denver, Colo.), and LOEWENSTEIN, E. V.
Enhanced LWIR Emission from the Auroral Zone
High Alt. Nuc. Eff. Symp. (DNA), San Diego, Calif. (9-13 April 1973)

MURCRAY, D. G. (Univ. of Denver, Colo.), ET AL, and LOEWENSTEIN, E. V.
Temporal Variations in the Atmospheric Radiance as Observed at High Altitudes
Midcourse Meas. Mtg., Monterey, Calif. (22 January 1973)

MURPHY, R. E., ROGERS, J. W., STAIR, A. T., and ULWICK, J. C. (Iono. Phys. Lab.)
Rocket-Borne Radiometric Hydroxyl Observations
DNA Atm. Eff. Symp., San Diego, Calif. (9-13 April 1973)

O'NEIL, R. R., PENDLETON, W. R., JR. (Utah State Univ.), HART, A. M., and STAIR, A. T., JR.
Vibrational Temperature of Thermospheric Nitrogen Measured by Electron Induced Luminescence
Int. Assoc. for Geomag. and Aeron., Kyoto, Jap. (9-21 September 1973)

PICARD, R. H.
Master Equations in Quantum Optics and Kinetic Theory
Phys. Sci. Sem., U. S. Army Missile Res., Dev. and Engrg. Lab., Redstone Arsenal, Ala. (13 December 1973)

POSEN, H., BRUCE, J. (SolidState Sci. Lab.), and MILAM, D.
10.6 μm Laser Damage in ZnSe
ASTM Mtg., Natl. Bur. of Stds., Boulder, Colo. (22-23 May 1974)

PRICE, S. D.
Radiative Opacity Due to the Phillips and Ballik-Ramsey Bands of C_2
140th Mtg. of the Am. Astronom. Soc., Ohio State Univ., Columbus, Ohio (25-28 June 1973)

ROGERS, J. W., MURPHY, R. E., STAIR, A. T., JR., and ULWICK, J. C. (Iono. Phys. Lab.), BAKER, K. D., JENSEN, L. L. (Utah State Univ.)
Rocket Borne Radiometric Measurements of OH in the Auroral Zone
Intl. Assoc. for Geomag. and Aeron., Kyoto, Jap. (9-21 September 1973)

OSGOOD, R. M., JR., JAVAN, A. (Mass. Inst. of Technol.) and SACKETT, P. B.
Vibration-Vibration Transfer Rate Out of the Third Vibrational Level in Hydrogen Fluoride Gas
Middle Atlantic Regional Mtg. of the Am. Chem. Soc., Wash., D. C. (14-17 January 1973)

SACKETT, P. B.
Measurement of the V-V Energy Transfer Rate from CO(V=2) Using Tunable Parametric Oscillator Excitation
Am. Phys. Soc. Mtg., Wash., D. C. (23-26 April 1973)

SANDFORD, B. P.
Review of AFCRL Infrared Spectral and Spatial Observations of Apollo and Titan Plumes
ARPA Sec. Plume Phys. Prog. Mtg., and the 19th Midcourse Meas. Mtg., AF Acad., Colorado Springs, Colo. (24 April 1973)

SANDOCK, J. A.
D and E Region Effective Recombination Coefficients from Daytime Auroral Absorption Measurements
55th Ann. Spring Mtg. of the Am. Geophys. Union, Wash., D. C. (8-12 April 1974)

SCHLOSSBERG, H.
Tunable Lasers and Some Applications
Colloq., Case West. Reserve Univ., Cleveland, Ohio (7 December 1972)

SCHLOSSBERG, H. R., and FETTERMAN, H. R., PARKER, C. D. (MIT Lincoln Lab., Lexington, Mass.)
Optically Pumped Vibrational Transition Laser in the Far Infrared
8th Intl. Quantum Elect. Conf. — 1974, San Francisco, Calif. (10-13 June 1974)

SCHLOSSBERG, H. R., and KELLEY, P. L., KILDAL, H. (MIT Lincoln Lab., Lexington, Mass.)
Highly Selective Excitation of Atoms and Molecules Using Two Photon Processes
8th Intl. Quantum Elect. Conf. — 1974, San Francisco, Calif. (10-13 June 1974)

SCHLOSSBERG, H., and SACKETT, P. B.
Infrared Laser Studies of Vibrational Energy Transfer
AF Off. of Sci. Res. Contr. Mtg. on the Kinetics of Energy Conversion, Newton, Mass. (23-24 August 1973)

SELBY, J. E. A.
Atmospheric Transmittance
1973 Ann. Mtg. of the Opt. Soc. of Am., Rochester, N. Y. (9-12 October 1973)
Atmospheric Transmittance Predictions for System Applications
IRIS Imaging Gp. Mtg., Tex. Instm., Inc., Dallas, Tex. (22-25 January 1974)

SHETTLE, E. P.
Atmospheric Aerosol Models
22nd Natl. IRIS Mtg., Specialty Gp. on IR Backgrounds and Atm. Phys., AF Avionics Lab., Dayton, Ohio (21-23 May 1974)

SKOLNIK, L. H., BENDOW, B., GIANINO, P. D. (Solid State Sci. Lab.), and HORDVIK, A.
Interference and Lensing Effects in the Transmission of High Power Laser Beams Through Infrared Windows
Conf. on High Power IR Laser Window Mats. — 1972, Hyannis, Mass. (30 October - 1 November 1972)

SKOLNIK, L. H., KAHAN, A., (Solid State Sci. Lab.), HORDVIK, A., and CLARK, O. M. (Solid State Sci. Lab.)
A Doppler Shift Interferometric Technique for Measuring Small Absorption Coefficients
1973 Conf. on High Power IR Laser Window Mats., Hyannis, Mass. (12-14 November 1973)

STAIR, A. T.
High Altitude Spectral Measurements in the LWIR
Midcourse Meas. Mtg. (ARPA), Inst. for Def. Analys., Arlington, Va. (7 November 1973)
Analysis of 4.3 μ m ICECAP Data
High Alt. Nuc. Eff. Symp. (DNA), San Diego, Calif. (9-13 April 1973);
19th Midcourse Meas. Mtg., AF Acad., Colorado Springs, Colo. (24 April 1973)
Rocket Measurements of Arc Emissions and Near Infrared Auroral Spectra, ICECAP 72
High Alt. Nuc. Eff. Symp. (DNA), San Diego, Calif. (9-13 April 1973);
Am. Geophys. Union Mtg., Wash., D. C. (16-20 April 1973)

STAIR, A. T., and ULWICK, J. C. (Iono. Phys. Lab.)
IR Measurements in Auroras
2nd Conf. of Appl. of Chem. to Nuc. Wpn. Eff., Inst. for Def. Analys., Arlington, Va. (12-14 September 1972)

STAIR, A. T., WHEELER, N. B., and BAKER, D. J., WYATT, C. L. (Utah State Univ.)
Cryogenic IR Spectrometers for Rocket-Borne Measurements
IEEE Northeast Elect. Res. and Engrg. Mtg., Boston, Mass. (9 November 1973)

STAIR, A. T., JR., and WYATT, C. L. (Utah State Univ.)
Rocket Borne Measurements of Infrared Emission of O_3 and CO_2 in the Auroral Zone
Intl. Assoc. for Geomag. and Aeron., Kyoto, Jap. (9-21 September 1973)

TOOLIN, R. B., and POIRIER, N. C. (Northeastern Univ., Boston, Mass.)
Observations of Gondola Motions for High Altitude Flight Systems
7th AFCRL Sci. Balloon Symp., Wentworth-By-The Sea, Portsmouth, N. H. (25-27 September 1972)

VANASSE, G. A.
Novel Spectrometric Techniques
(Inv. Talk) Phys. Dept., Univ. of Laval, Quebec City, Can. (20 Feburary 1974)
Hadamard Matrices in Spectroscopy
(Inv. Paper) Symp. on Appl. on Walsh Functions, Wash., D. C. (18-20 March 1974)

VOLZ, F. E.
Return of Normal Stratospheric Turbidity and a New Short Dust Event During October 1971 and
The Complex Index of Refraction of Aerosol from 0.2 to 40 μ m
Conf. on Atm. Radn., Ft. Collins, Colo. (7-9 August 1972)
On Background Conditions of Stratospheric Aerosol from Recent Twilight Measurements
5th Conf. on Laser Radar Studies of the Atm., Williamsburg, Va. (4-6 June 1973)

WODARCZYK, F. J.
Laser Studies of Molecular Kinetics
Opt. Phys. Lab. Sem., Natl. Bur. of Stds., Wash., D. C. (17 April 1974)

TECHNICAL REPORTS
JULY 1972 - JUNE 1974

BLISS, E. S., CAPT., MILAM, D., and BRADBURY, R. A.
Laser Induced Damage to Mirrors at Two Pulse Durations (Technical Report No. 2, Period 31 December 1971 to 30 June 1972)
AFCRL-72-0423 (25 July 1972)

CONDRON, T. P.
Calibration of a Liquid Helium Cooled CVF Radiometer in a Warm Environment
AFCRL-TR-73-0480 (31 July 1973)

FENN, R., and DULCHINOS, J., MIRANDA, H. (GCA Corp., Bedford, Mass.)
Balloonborne Aerosol Particle Concentration and Size Distribution Measurements
Proc., 7th AFCRL Sci. Balloon Symp., AFCRL-TR-73-0071 (3 January 1973)

HORDVIK, A., and MILLER, H.
A Twyman-Green Electro-Optic Light Modulator
AFCRL-TR-73-0375 (26 June 1973)

MCCLATCHEY, R. A., and BENEDICT, W. S. (Univ. of Md.), CLOUGH, S. A., and BURCH, D. E. (Philco Corp.), CALFEE, R. F., FOX, K. (Univ. of Tenn.), ROTHMAN, L. S., and GARING, J. S.
AFCRL Atmospheric Absorption Line Parameters Compilation
AFCRL-TR-73-0096 (26 January 1973)

McCLATCHEY, R. A., FENN, R. W., SELBY, J. E. A., VOLZ, F. E., and GARING, J. S.
Optical Properties of the Atmosphere (Third Edition)
AFCRL-72-0497 (24 August 1972)

McCLATCHEY, R. A., and SELBY, J. E. A.
Atmospheric Transmittance, 7-30 μ m: Attenuation of CO_2 Laser Radiation
AFCRL-72-0611 (12 October 1972)
Atmospheric Attenuation of Laser Radiation from 0.76 to 31.25 μ m
AFCRL-TR-74-0003 (3 January 1974)

MILAM, D., BRADBURY, R. A., and GALLAGHER, C. C.
Evaluation of Three Techniques for Producing Laser Pulses of Nanosecond Duration, Technical Report No. 3
AFCRL-73-0007 (9 January 1973)

MILAM, D., BRADBURY, R. A., PICARD, R. H., and BASS, M. (Raytheon Res. Div., Waltham, Mass.)
Laser Damage in Dielectric Coatings
Identification of Inclusions as the Limiting Damage Mechanism and First Observation of Intrinsic Damage in Dielec. Coatings, AFCRL-TR-73-0406 (10 July 1973)

MURDOCK, T. L., 1st LT.
The Contribution of Asteroids to the Infrared Astronomical Sky Survey
AFCRL-TR-73-0514 (9 March 1973)

O'NEIL, R. R., LEE, E. T. P., HUPPI, E. R., and STAIR, A. T., JR.
Project EXCEDE: SWIR Experiment
AFCRL-TR-73-0152 (5 March 1973)

PRITCHARD, J. (Idealab, Inc., Franklin, Mass.), SAKAI, H., and VANASSE, G.
Two-Meter Path Difference Interferometer for Fourier Spectroscopy
AFCRL-TR-73-0223 (11 April 1973)

SANDFORD, B. P.
Optical Airborne Measurements During 2-3 November 1969
Proc. of COSPAR Symp. on Solar Particle Event of Nov. 1969, AFCRL-72-0474 (11 August 1972)

SELBY, J. E. A., and McCLATCHEY, R. M.
Atmospheric Transmittance from 0.25 to 28.5 μ m: Computer Code LOWTRAN 2
AFCRL-72-0745 (29 December 1972)

SKOLINK, L. H., KAHAN, A. (Solid State Sci. Lab.), HORDVIK, A., and CLARK, M. (Solid State Sci. Lab.)
A Doppler Shift Interferometric Technique for Measuring Small Absorption Coefficients
AFCRL-TR-74-0001 (20 December 1973)

STREED, E. R., VLIET, G. C. (Lockheed Missile and Space Co., Inc., Palo Alto, Calif.), CONDRON, T. P., and SULLIVAN, J. C.
Operation of a Cryogenically Cooled Infrared Radiometer from a Balloon Platform
Proc., 7th AFCRL Sci. Balloon Symp.,
AFCRL-TR-73-0071 (3 January 1973)

TOOLIN, R. B., and POIRIER, N. C. (Northeastern Univ., Boston, Mass.)
Observations of Gondola Motions for High Altitude Flight Systems
Proc., 7th AFCRL Sci. Balloon Symp.,
AFCRL-TR-73-0071 (3 January 1973)

VANASSE, G. A.
Multiplex Techniques in Spectroscopy
AFCRL-72-0412 (19 July 1972)

X Ionospheric Physics Laboratory

For communication, detection, and navigation, it is vital for certain Air Force operations to transfer information quickly from one location to another, or detect reflections. Radio transfers information by coupling electromagnetic energy into the surrounding medium, such as the atmosphere, ionosphere or magnetosphere by means of antennas. In these media, electromagnetic signals propagate, but the quality of the information conveyed can vary depending on the temporal and spatial structure of the propagation medium. This structure varies in a poorly understood manner although it is known that solar, earth-induced and atmosphere-induced driving forces are at work. The ionosphere, which helps guide a frequency band of radio signals over large distances, is particularly sensitive to changes in solar radiation. Such changes alter the propagation conditions for electromagnetic waves. The capability for predicting these changes and their effects on radio waves is presently limited. The causes underlying the behavior of the ionosphere, the response of the interactive magnetosphere-ionosphere-atmosphere system to solar radiation and its changes, as well as the coupling between these subregimes, must be better understood to aid Air Force missions more effectively.

There are two classes of solar radiation: waves and particles. The waves that produce and modify the ionosphere have wavelengths below 200 nanometers and thus contain extreme ultraviolet, X-ray and gamma-ray radiation. This radiation directly affects the daylight portion of the earth's atmosphere and is particularly effective in changing the ionosphere at low and middle latitudes. Corpuscular radia-

tion consisting of energetic charged particles changes the ionospheric characteristics at high latitudes as earth-bound solar particles are deflected toward the polar regions through the influence of the earth's magnetic field. A second set of less energetic particles is contained in the solar wind. These particles enter the earth's magnetosphere through the magnetosheath. By still unknown processes they are accelerated from a few 100eV to keV and even MeV energies and precipitate into the high latitude ionosphere causing extreme and rapidly changing electron density distributions in association with auroral displays. The most severe ionospheric modifications occur during large-scale dynamic events known as substorms. In the ionospheric response to all these modifying influences, propagation conditions for electromagnetic waves change.

To minimize or eliminate the potential degradation of communication, surveillance, detection and navigation systems resulting from solar disturbances, the Air Force has established a Research Objective directing a study of the ionospheric environment to assess and predict the radio frequency effects that can be expected in the course of varying solar activity on a short-term and long-term basis. These directives resulted in the conception and implementation of a variety of research programs within the Ionospheric Physics Laboratory whose ultimate purpose serves to overcome the deficiencies likely to be encountered. Some of these deficiencies are in the fields of ionospheric absorption and under blackout conditions: signal delays imposed by the ionosphere causing range errors: field-aligned irregularities in the ionosphere causing undesirable radar clutter and scintillations of trans-ionospheric radio signals; wave-like disturbances causing global ionospheric changes, multipath, and refraction errors: regional depletion of ionization associated with the ionospheric trough; inadequacy of ionospheric models and ray-tracing computer programs; existing shortcomings in efficient automation of ionospheric data reduction and processing for ionospheric specification, mapping and prediction schemes. Efforts are also directed to define, in order to exploit, the most effective and reliable transmission mode for low frequencies propagating in the earth-ionosphere waveguide. Solar radio emissions are monitored on a world-wide basis and analyzed to improve the early detection of solar events likely to cause disruption in the performance of vital Air Force functions.

TRANS-IONOSPHERIC PROPAGATION STUDIES

VHF radio beacon signals from low altitude and synchronous satellites, as well as from radio stars, are used to study the effects of the ionosphere in both producing signal amplitude fluctuations and rotating the plane of polarization of linearly polarized signals. The amplitude fluctuations of the signals are produced by ionospheric irregularities at F-layer heights, particularly at high latitudes and the equator. The Faraday rotation of the plane of polarization is used to study the total electron content of the ionosphere, a parameter of importance in correcting radar range and navigation errors.

TOTAL ELECTRON CONTENT: The total electron content (TEC) of the earth's ionosphere is defined as the total number of electrons contained in a column of unit cross-sectional area extending from the ground to a height of approximately 2,000 km. Typical TEC values vary from 10^{16} to 10^{19} electrons in a column one square meter in area, the exact value depending on geographic location, local time, season, solar extreme ultraviolet flux, and geomagnetic activity. This variation affects any system which uses radio waves that propagate through the ionosphere. The electrons distributed along the radio ray path produce a retardation in the velocity at which the information is carried by the

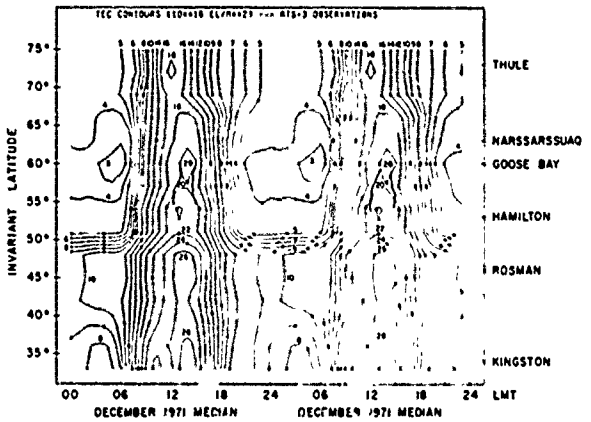

A contour map of total electron content of the northern mid-latitude ionosphere, constructed from observations of the ATS-3 satellite, during December 1971. The sub-ionospheric points shown for each station are relative to the ATS-3 satellite. The contours are multiples of 10^{16} electrons in a column 1 square meter in area.

signal. The phenomenon is called the "ionospheric group path delay." If the signal's time of arrival is important, as in a radar system or a navigational satellite's position-fixing system, the trans-ionospheric group delay can cause timing errors (and therefore position errors) of significant proportions, especially if the overall accuracy desired is of the same order as the ionospheric delay. A typical time delay for a radar operating at 430 MHz might range from 10 to 1,000 nanoseconds (10^{-8} to 10^{-6}) for a target at the zenith, corresponding to a positional error of 3 to 300 meters.

The practical value of TEC data lies in its ability to provide continuous information about the ionospheric plasma along specific earth station-to-satellite paths. During solar and geomagnetic disturbances, TEC measurements provide a widely available description of the often drastic effects which occur.

AFCRL has constructed a network of TEC (137 MHz) observing sites spanning polar to equatorial latitudes. AFCRL stations in Thule and Narssarssuaq, Greenland, monitor the high latitude ionosphere while observations from Goose Bay, Labrador, and Sagamore Hill, Massachusetts, measure the TEC at upper mid-latitudes. On occasion, sites in Rosman, North Carolina: Cape Canaveral, Florida: Kingston, Jamaica; and Huancayo, Peru, are used to extend TEC coverage to low and equatorial latitudes.

The first preliminary multi-station analysis of TEC obtained from the AFCRL network showed the dominant solar control of the ionosphere during the daytime, and the influence of geomagnetic processes which cause a trough (or minimum) in the nighttime TEC near 60 degrees latitude. TEC measurements have several direct uses: they can be converted to ionospheric group-delay corrections at various radio

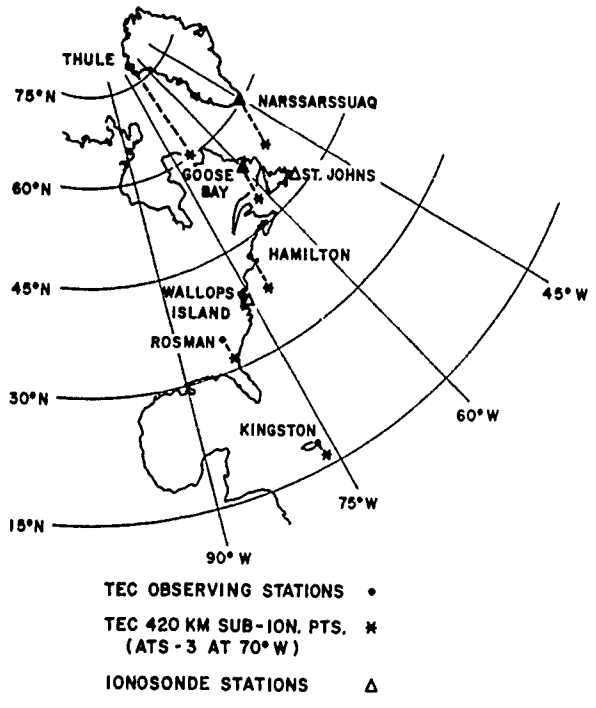

Observing stations for determining total electron content. The sub-ionospheric points are the points where the line of sight to the ATS-3 satellite, in synchronous orbit at 70° west longitude, crosses 420 km altitude.

frequencies: they are used to generate and test global ionospheric models which specify propagation conditions, and detailed observations of the latitudinal and local time structure apply directly to theoretical studies of ionospheric processes.

The AFCRL network of TEC observatories is also being used to examine the large ionospheric perturbations which accompany geomagnetic storms. A technique for iso-TEC contouring has recently been used to examine the ionospheric response to both global magnetic storms and the more temporally and spatially isolated magnetospheric substorms. Investigations of magnetic storm effects on ionospheric electron content measured from Sagamore Hill have revealed the storm-time variations at mid-latitudes. Thus, the extension of this work towards polar regions will help unify current understanding of the global characteristics of ionospheric storms.

PHASE STUDIES USING INTERFEROMETER AND DIFFERENTIAL PHASE SYSTEMS: A 137 MHz interferometer has been in operation at various locations since 1970. The interferometers have a 300-meter baseline on Sagamore Hill, Hamilton, Massachusetts; a 10-km baseline between North Ipswich and Sagamore Hill: a 50-km baseline between Durham, New Hampshire, and Sagamore Hill; and a 3-km baseline at Goose Bay, Labrador. At each site the 137-MHz signal from a geostationary satellite was the source of the probe frequency.

The interferometer is used to make precise measurements of the apparent angular position of the satellite. Refraction effects, which vary with time, cause small deviations which appear as phase changes of the probing frequency at the baseline terminals.

The measurements have revealed pronounced diurnal and seasonal variations in the amount of refraction. The diurnal variation in refraction has a maximum near local noon and appears to be partly controlled by the normal diurnal variation of integrated ionospheric electron content. Quasi-periodic variations, usually between 5 and 100 minutes, are attributed to traveling ionospheric disturbances which appear to be caused by the propagation of internal gravity waves in the neutral thermospheric gas. The power spectrum shows that the periods of most fluctuations range from 20 to 40 minutes and that very few are less than 14 minutes. Goose Bay, Labrador, appears to be on the fringe of the region where the gravity waves are generated, since the data from this site show the effect to be minimum.

Fast phase fluctuations of the 137 MHz signal along each baseline were generally, but not always, correlated with amplitude scintillations.

The interferometer measurements are presently being terminated and emphasis is placed on a differential phase system. The launching of ATS-6, a geostationary satellite with several coherent probing frequencies available, provides the means for making nearly absolute phase measurements. (The interferometer is limited to phase measurements along its baseline.) The system is extremely sensitive and the ionospheric phase data, unlike the interferometer, are not contaminated by relative position changes of the satellite.

Useful information provided by a differential phase system includes: the diurnal variation of the electron content in the medium all the way to the satellite: measurement of essentially absolute ionospheric phase on the 40 MHz satellite frequency when compared against the coherent 360 MHz frequency, which in turn allows measurement of the variable refraction pattern: extreme sensitivity in detecting traveling ionospheric disturbances: and with three sites, the opportunity to determine the direction, speed and height of the T.I.D.s, as well as the direction of the variable refraction angle; and extreme sensitivity in detecting fast phase scintillations with the opportunity to correlate them with amplitude scintillations, and to determine their effect on communications.

SCINTILLATIONS AND MORPHOLOGY: Amplitude fading of signals from HF to

microwaves traversing the ionosphere has recently been studied by many radio propagation research teams. Both deep fluctuations on microwave signals received through the equatorial ionosphere and deep fading at frequencies in the 130-400 MHz region at auroral and polar latitudes have been noted. Both are caused by small irregularities at 200-600 km altitude.

Skin tracking radar signatures of missiles or satellites lose clarity when they pass through small-scale ionospheric irregularities. Air-to-satellite-to-ground communications systems experience deep fading during magnetic storms when the signals traverse the high latitude disturbed ionosphere.

Recent concentrated scintillation studies at AFCRL took observations at a chain of stations between the 45th and 75th meridians from Thule, Greenland, to Huancayo, Peru. During severe magnetic storms (the worst problem for user organizations), distributions of fading have been measured as well as the morphology of the irregularity regions. During the magnetic storms of August 4-10, 1972, intense scintillations were noted even during the daylight hours at latitudes as far south as Washington, D.C. The magnetic storms of 1972 and 1973 have been studied to determine the rate at which the high latitude intensity irregularity region expands and the depths of fading reached during various times.

The intensity of the small-scale irregularities is being correlated with DMSP auroral photographs. At auroral latitudes, signals begin fading four to five degrees south of the latitudes at which the aurora is seen. The aurora, predominantly at 100 km altitude, is narrower in height than the F-layer irregularity zone. However, many of the characteristics of the two are the same. During magnetic storms the intensity of the aurora increases and the luminosity expands both equatorward and poleward. The intensity of the small-scale irregularities (typically 500 meters to several kilometers in length and aligned along the earth's magnetic field) also increases, and the F-layer irregularity region expands even more toward the pole and the equator than the aurora.

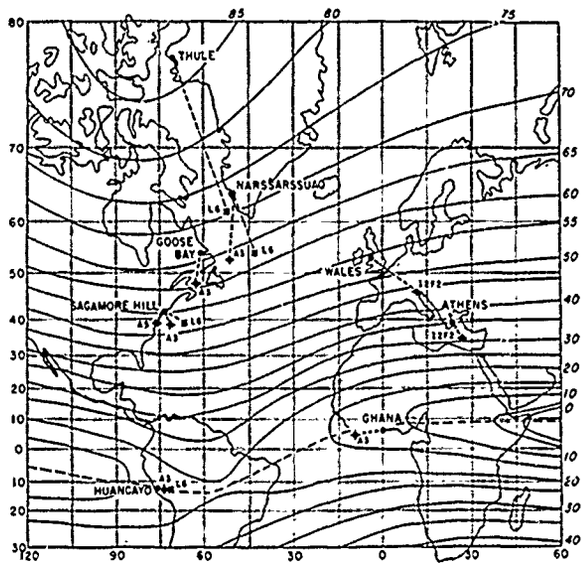

Stations observing satellite signals and the satellites they observed to analyze the global effects of scintillations during the magnetic storms of August 1972. Invariant latitudes at 300 km altitude, as well as geographic coordinates, are indicated.

A statistical model of F-layer irregularities at high latitudes has been published. It integrated observations for both magnetically quiet and disturbed periods, allowing the systems designer to understand the latitudinal effect and magnetospheric physicist to explain the interaction between magnetic fields and the irregularity generation mechanisms.

Future work in this area will include correlations with clutter in HF backscatter as well as a program with high altitude satellites (DNA and AFSATCOM) transmitting over high latitude stations.

SIGNAL STATISTICS: Various scintillation indices have been used to describe the depth of amplitude fluctuations caused by

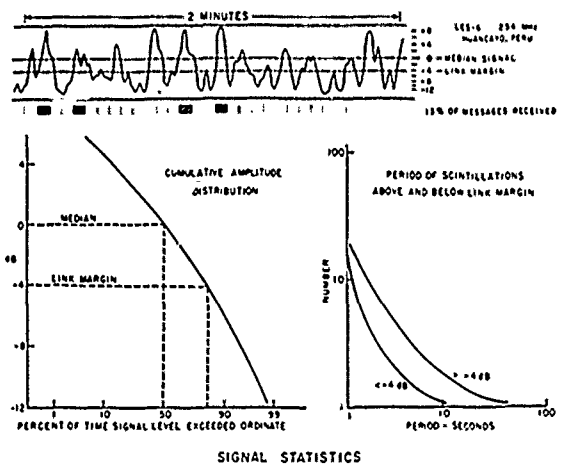

SIGNAL STATISTICS

Signal statistics for messages transmitted at 254 MHz by the LES-6 satellite, to the station at Huancayo, Peru. The 2-minute graph of fading shows that for a message requiring 4 seconds to transmit, only 13 percent of the messages would be received, even though the signal was above the fade margin almost 80 percent of the time (shows effects of period of scintillations). If the fades had been of shorter period, all of the messages would have been lost. The graph at the lower right shows the relative number of fades of any duration. The severity of the problem is indicated by the fact that the majority of the fades are greater than the fade margin.

ionospheric irregularities. Scintillation index does not describe precisely the fading characteristics of the signal in sufficient detail for either the engineer interested in propagation effects, or for the physicist interested in determining scattering mechanisms for the signal. Information on the fade margin, which specifies the amount of increased power necessary to overcome ionospheric scintillations as a function of local time, latitude, season, and magnetic index, is usually required for a complete evaluation of the expected performance of trans-ionospheric communication systems.

Amplitude distributions were related to scintillation indices and a technique for converting archive data to a cumulative amplitude distribution was developed. Ionospheric scintillations in the VHF band were shown to closely follow the Nakagami m distribution. Simultaneous distributions for two frequencies were measured and the frequency dependence of scintillations was evaluated. The spectral index was related to the m parameter, allowing the prediction of scintillation effects in other frequency bands of interest.

In conjunction with the amplitude distribution, the fading rates of scintillations determine the message reliability. The amount of time the signal is above the margin specifies statistics of good signal level and is useful in choosing data frame formats. The statistics of fades are useful in selecting coding and time-diversity techniques. The study is continuing with emphasis on particular Air Force satellite communications systems.

SOLAR RADIO ASTRONOMY RESEARCH

Research has shown that one of the best tools for studying solar activity is the radio emission. Apart from the spectrally narrow optical region, radio offers the only other spectral window for solar observations from the ground. Its quantitative data provide reliable predictors for geophysical phenomena. Continuing research provides an increasing number of associations, which help in understanding the mechanisms of the sun.

A balanced program of research satisfies operational needs by providing significant observational data and by investigating how the data are correlated with ionospheric and geophysical parameters. Patrol-type (low angular resolution) measurements of the quiet sun and bursts, and high resolution measurements of active regions are made in the solar radio astronomy research program.

Absolute accuracy in the measurement of quiet-sun radio emission has become an operational necessity. The slowly varying component of solar radio emission relates well to atmospheric neutral density, which

causes drag on space vehicles; therefore, radio data provide an input to satellite position calculations. Recent results indicate that longer or shorter wavelength data may, at certain periods of the solar cycle, lead to better neutral-density predictions than the use of the traditional 10-cm wavelength data. Quiet-sun radio data are widely used for calibration of DOD telemetry-range antenna systems on a routine basis. For this application, day-to-day consistency of patrol data is required and maintained.

The Air Weather Service, through its Space Environmental Support System (SESS), is the agency through which data are disseminated. We work closely with AWS in both operational and research applications. Sagamore Hill is the principal station of the Air Force solar radio network, continuously developing techniques and providing calibration for the other stations. A second generation solar radio network (RSTN) is in the procurement stage, with AFCRL responsible for engineering direction. Partly completed stations of the network at Manila, Athens, and Hawaii (all instrumented by AFCRL) now complement the Sagamore Hill station.

The radiation from the sun (both quiet and disturbed) comes from different solar altitudes for different wavelengths, thus requiring multifrequency measurements. The radio patrol provides spectral information with an overall accuracy of roughly 5 percent. Recently, absolute calibration measurements were made at 15.4 GHz using a precisely constructed optimum-

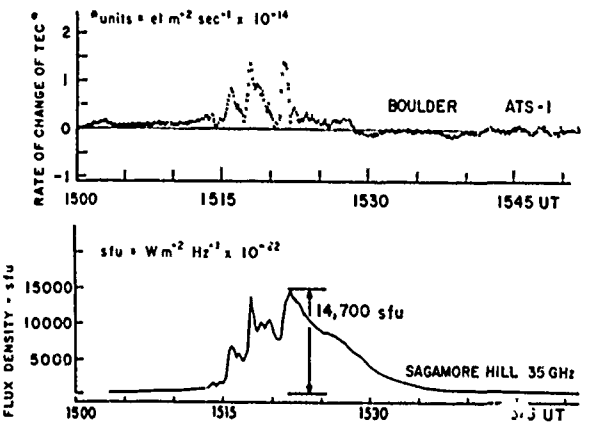

GREAT BURST OF 7 AUGUST 1972 AND ITS EFFECT ON IONOSPHERIC TOTAL ELECTRON CONTENT

A comparison of the time profiles of the rate of change of total electron content (measured at Boulder using the 136 MHz transmission from ATS-1) and the 35 GHz solar flux density measured at the Sagamore Hill Radio Observatory for the great burst of August 7, 1972. The change in TEC, occurring in the E and F regions, is caused by solar EUV radiation from the burst; this EUV emission is thus shown to be well represented by ground-level cm and mm wavelength radio emission data.

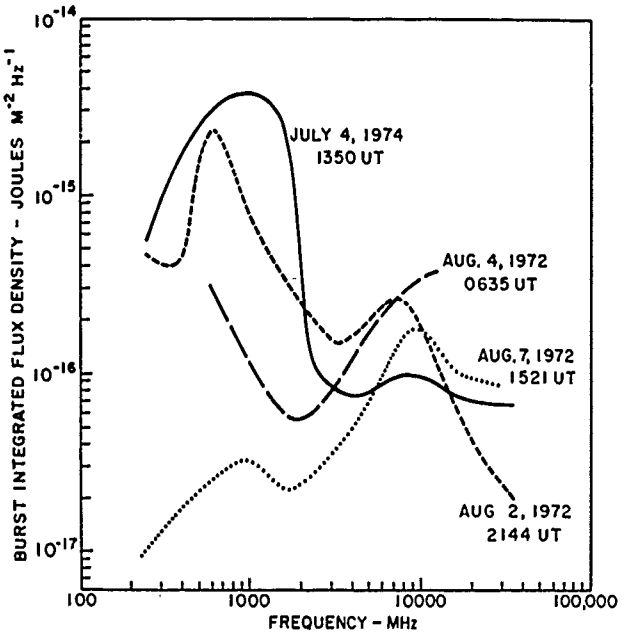

Comparison of burst integrated flux density spectra for events of August 1972 and July 1974. The shot centimeter wavelength flux densities correlate well with PCA's and >10 MeV protons, where $\sim 10^{-17}$ joules is the approximate threshold of particle detection. Note that the July 4, 1974 event had a high integrated flux density (and energy) over the *meter-decimeter* band. Large quantities of *low* energy protons were observed for this event.

gain horn. The results confirmed the absolute accuracy of the Sagamore Hill patrol at 15.4 GHz whose original calibration was based on lunar observations.

The U-Shape spectral signature is working well as a yes-no predictor of catastrophic proton events. NORAD has requested immediate reporting of solar outbursts occurring at decimeter wavelengths. Burst integrated flux density provides a reliable predictor of the magnitude of a PCA event that begins soon after the burst. Future research will concentrate on predicting from radio data the probable time of onset and the probable duration of proton events. The integrated flux density of a radio burst at centimeter wavelengths may offer a more reliable indication of the proton flux at energies greater than 10 MeV than the flux density at longer wavelengths which seems better correlated with the flux of lower energy solar protons.

The burst spectrum above the frequency of maximum emission relates to the energy distribution of the radiating electrons. Extremely hard (flat) spectra have been found to be well correlated with white-light flares and ground-level events. A remarkable similarity of structure has been noted between temporal behavior of hard X-rays (greater than 20 keV) and short, cm-wavelength microwave bursts. The similarity of the spectral index variations in these two wavelength regions during the burst suggests that the same electrons produce both types of emission. Also, remarkable agreement between short impulsive microwave bursts and XUV bursts has been noted for the first time. The range of frequencies enclosed within the "U" for U-shaped bursts has been studied to determine its exact correlation with proton energy distribution. A broad "U" is indicative of a hard proton energy distribution (high particle energies), while a narrow "U" suggests a soft (low particle energies) particle energy distribution.

A data automation system has been developed and tested at Sagamore Hill to allow more accurate and more nearly real-time reporting of burst activity. Automation can make various types of burst spectral information available quickly and in a form well suited for statistical studies.

Radio studies of individual solar active regions were conducted on the NEROC 120-foot Haystack radio telescope to find precursor activity which would give advance warning of flares on the sun. Temperature (T) and polarization (p) characteristics of the 3.8 cm radio emission were monitored with a narrow 4.4 arc-minute antenna beam. A number of regions displayed not only temperature variations minutes to hours before the flare, but also had strong polarization variations which suggest significant magnetic field changes occur prior to the flare. The (T) and (p) variations for several events were time-series analyzed for possible periodicities in the power spectrum. Large power components were found with periods from 250 to 380 seconds. Similar periodicity (five-minute periods) has been noted by several optical and radio observers at photospheric and chromospheric levels. Since the 3.8-cm emission comes from the transition zone (between the chromosphere and corona) where flares are thought to originate, it provides what appears to be a very sensitive indicator of impending solar eruptions.

Active regions have also been studied at 8-mm wavelength in an attempt to identify proton-flare regions long before catastrophic activity begins. Although the technique does not produce any "false alarms," there may be "misses" for very hot localized regions of small angular extent that cannot be resolved with the 2-4 arc-minute beamwidths used in the studies.

The influence of the magnetic field on the polarization of bursts is also being studied. The identification of spectral signatures in the temperature profiles of radio bursts is also being attempted through polarization studies. The AFCRL 5 GHz polarimeter, which measures all four Stokes parameters, has been completed,

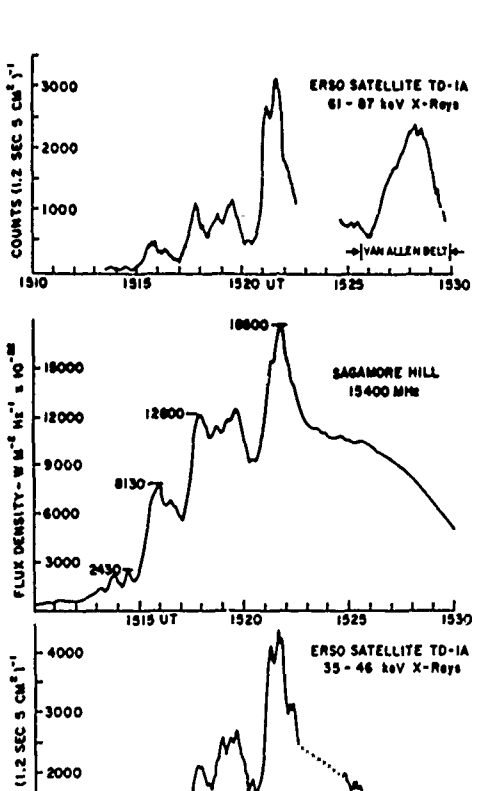

Burst profiles of August 7, 1972, event at selected radio and hard X-ray regions of the spectrum. Note the remarkable agreement in the fine-scale variations. Two components of emission are apparent: 1) gradual (dashed line), and 2) impulsive (solid). The similarity of microwave and hard X-ray spectral variations during the burst suggests that the same electrons produce both types of radiation.

and numerous bursts have been recorded in circular polarization. Polarization data for comparison of radio bursts at 7.0 GHz and 9.4 GHz are being obtained through AFCRL-funded grants with Mackenzie University and Instituto Geofisico del Peru.

That meter-decimeter solar Type II and Type III bursts, consisting of fundamental and harmonic bands, may be caused by Raman scattering has been confirmed by laboratory-controlled experiments at AFCRL using direct-current gas discharge tube methods. A pseudo-harmonic band has been reproduced in the laboratory at approximately twice the plasma frequency (similar to a Type II solar radio burst) along with its characteristic spatial directivity and band splitting. This experiment confirms the fact that the intensities of the fundamental and harmonic bands are comparable and that no bands higher than the second harmonic are emitted. Scaling the laboratory results to coronal conditions will help define known (as well as new) aspects of solar radio bursts. These scattering processes may even apply to cm-band radiation, which would challenge the current view that the gyro-synchrotron mechanism causes the microwave bursts emitted by the sun.

GLOBAL IONOSPHERIC FLUCTUATIONS

Since 1967, AFCRL has monitored the very stable high frequency signals transmitted by CHU—the time station of the Dominion Observatory of Canada at Ottawa. These signals reach the receiver by reflection from the ionosphere, and any disturbance of the ionosphere in a vertical direction changes the phase of the received signal. The rate of change of this phase is a frequency, which is recorded with great precision and sensitivity. This Doppler frequency, usually varying in time, can be used to determine the changes in the propagation path, and these, in turn, can be related to variations of ionospheric reflection height.

Analysis of ionospheric Doppler data obtained from these transmissions led to the conclusion that height variations of global extent were associated with oscillations in the magnetic field with a period of eight minutes. Similar oscillatory disturbances with much shorter periods have previously been related to ionospheric radio absorption and optical emissions. However, this is probably the first observation of this

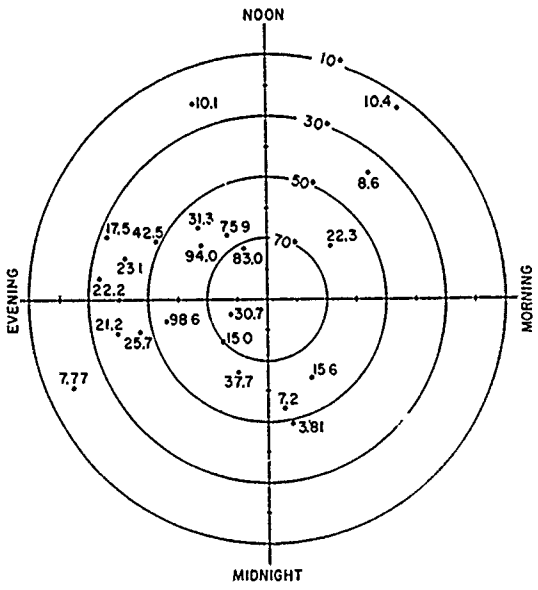

Peak-to-peak excursion in gammas of the horizontal component of the magnetic field disturbance vector for the October 10, 1969 magnetic disturbance from 0006 until 0022 Universal Time. The map is a polar plot in geographic coordinates.

eight-minute periodicity in F-region height variations and its global extent.

The global variations of the size of the horizontal component of the magnetic disturbance, determined for more than 25 observatories, were strongest at about 65 degrees geomagnetic latitude and in the noon-evening sector. Near synchronism was noted for ionospheric variations for at least two probing locations separated by more than 2,000 km. At mid-latitudes, a change of 10 gammas in the magnetic disturbance could be associated with a change of 1 km in ionospheric height. No changes in amplitude and phase of the 100 kHz Loran C signals transmitted from the station at Cape Fear, North Carolina, were detectable in Colorado, during a disturbance monitored on October 10, 1969. Correlation with the disturbance of fluctuations in amplitude and phase of the 13.6 kHz Omega emission from Trinidad, West Indies, as received at Table Mountain, Colorado, was not possible, but could not be ruled out. Analysis of Extremely Low Frequency noise data, recorded by the University of Rhode Island, showed variations of the fundamental earth-ionosphere cavity resonance frequency (Schumann resonance) from about 8.4 to about 8.2 Hz. This decrease coincided with a lowering of the F region by approximately 3 km. The shift in resonance frequency during the lowering of the F region seems to imply that the effect of the hydromagnetic wave on the ionosphere was not confined to the F region—observed by means of the high frequency transmission —but may have extended to the E or D region.

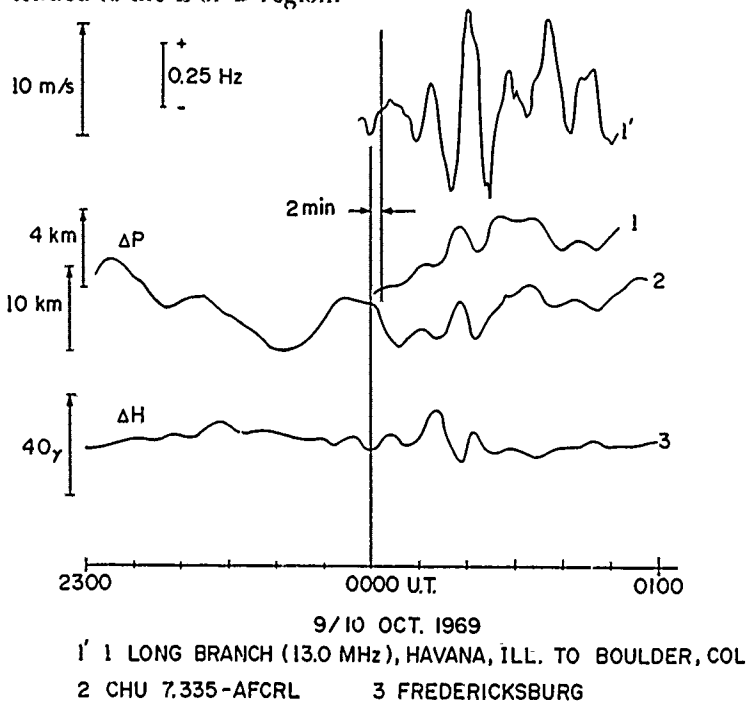

The top trace shows the variation in frequency of the 13.0 MHz signal transmitted from Havana, Illinois, as received at Boulder, Colorado. The change in frequency implies a velocity of the ionospheric reflecting layer, as indicated in the outer scale on the left. Curves 1 and 2 are the changes in total path length between Havana and Boulder, and CHU and AFCRL, respectively. Curve 3 is the H-component of the magnetic field measured at Fredericksburg, Virginia.

Further analysis of this and similar events may provide more detailed information on one of several sources of ionospheric perturbations that change the conditions for radio wave propagation.

AURORAL INVESTIGATIONS

The Ionospheric Physics Laboratory utilizes a uniquely instrumented NKC-135 Airborne Ionospheric Observatory in an extensive program of auroral and ionospheric research. Numerous expeditions in this program have provided ionospheric and optical surveys over large portions of the arctic region. Also, the Ionospheric Physics Laboratory and the Air Weather Service are cooperating in the Auroral Data Program which has established a new

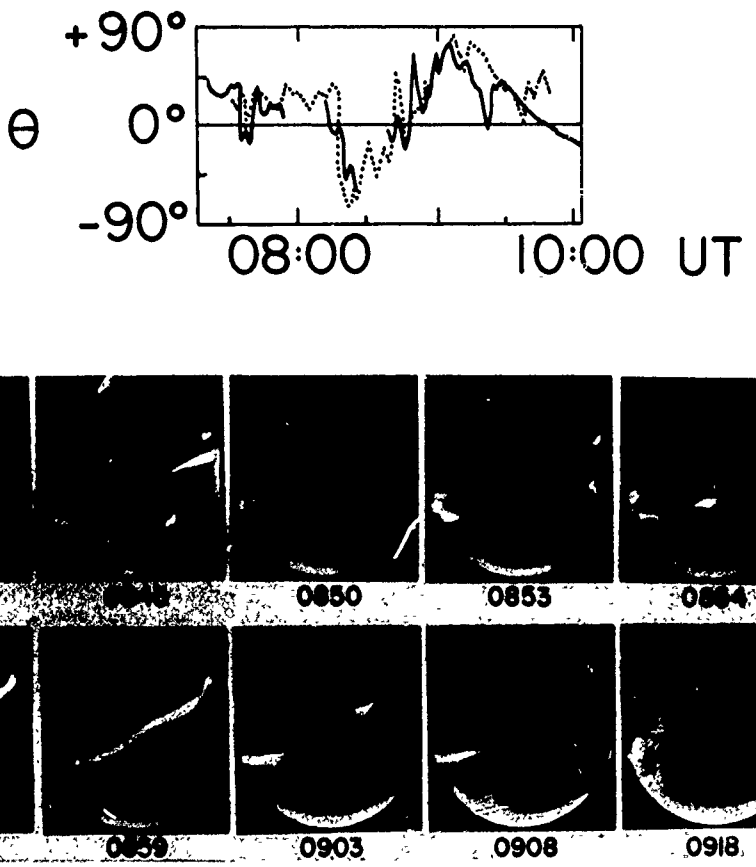

Latitude component (θ) of IMF vector as a function of universal time (UT) compared to simultaneous airborne all-sky camera pictures. A positive angle θ corresponds to a northward field, while a negative angle θ corresponds to a southward field. North is at the top of the all-sky photos and east is to the right. This figure demonstrates the control of the IMF over the midday auroras. It shows the dramatic change in the latitude, character and intensity of the midday aurora due, apparently, to the steep southward turning of the IMF at 0820 UT.

technology—the ability to specify the auroral ionosphere on a global scale by means of auroral photographs obtained from the Defense Meteorological Satellite Program (DMSP).

These research efforts seek a better understanding of ionospheric structure and dynamics, so that this knowledge can be incorporated into studies and verification testing which support Air Force communication, surveillance, and detection systems. These research programs also enhance the operational effectiveness of the Space Environmental Support System of the Air Weather Service which, in turn, supports a variety of Air Force users.

The intimate connection between magnetosphere, solar wind and ionosphere has required the scope of investigations to be extended to space measurements as well. This has been rewarded in the area of observing auroral ionospheric variations in terms of the interplanetary magnetic field (IMF), and conversely, monitoring satellite space environment via auroral observation, the latter having direct systems application.

The Airborne Ionospheric Observatory, a versatile system with unique capabilities, is instrumented with a digital ionospheric sounder, photometers, spectrometers, all-sky cameras, and HF and VHF receivers. With the Airborne Observatory, the midnight sector or any other sector of the auroral oval can be observed continuously for extended periods of time by flying westward, opposite to the direction of the earth's rotation. On the other hand, by flying eastward, in the direction of the earth's rotation, local time is accelerated, and the entire auroral oval can be circumnavigated in a single aircraft flight.

DAY SECTOR: Research flights of the Airborne Ionospheric Observatory in the daytime sector of the auroral oval revealed for the first time the existence in this sector of three ionospheric regimes which are produced by precipitation of auroral electrons. These ionospheric regimes reveal a progressive poleward decrease in the energy of auroral electrons. The southernmost regime is associated with enhanced D-region ionization; next is a regime of auroral E-layer ionization, and the northernmost regime shows the presence of F-layer irregularities. Patch-type auroras are associated with the D-region ionization, and the continuous aurora is associated with the auroral E layer. A region of enhanced 6300 angstrom emission ("red band") is collocated with the F-layer irregularity zone (FLIZ). The "red band" and the FLIZ extend continuously across the geomagnetic day sector from 0800 to 1730 corrected geomagnetic time. The "red band" has a width of 2 to 5 degrees in latitude and occurs between 75 and 80 degrees corrected geomagnetic latitude. Dayside discrete auroras occur within the "red band," which bridges time sectors in which discrete auroras are temporarily absent. The "red band" and the FLIZ result from precipitation of low energy electrons of magnetosheath origin down through the polar cusp into the upper atmosphere.

INTERPLANETARY MAGNETIC FIELD (IMF): The airborne all-sky camera and the ionospheric sounder have been used to follow the time history of the equatorward boundary of the auroral oval and the FLIZ. A dependence of the equatorward boundary of the FLIZ on corrected geomagnetic local time and on magnetic activity was demonstrated. Meridional motions of the equatorward boundary of the auroral oval and the FLIZ were found to correspond to variations in the interplanetary magnetic field.

QUIET PERIODS: Airborne Ionospheric Observatory data taken during magnetically quiet periods were correlated with data from ground stations in Alaska to derive a basis for understanding more disturbed conditions. It has been found that during quiet magnetic periods there are two circumpolar zones of E-region ioniza-

tion with different characteristics. The first zone is a particle-produced auroral E-layer band that has previously been found to be identical with the continuous aurora. The second is a zone of sporadic E which is collocated with the discrete aurora and is observed poleward of the first band.

During quiet magnetic periods, the main trough, constituting a regime of depleted ionization, is a prominent feature of the night-sector F region. This trough is most pronounced in depth in the early morning. It is bounded on the poleward side by a well defined "wall" of F-region ionization. The night-sector poleward-trough wall is located approximately three degrees of latitude equatorward of the discrete auroral oval. A plateau of F-region ionization extends from the poleward trough wall to the auroral oval. These results suggest that during exceptionally quiet periods the polar ionosphere is dominated by quasi-stationary circumpolar patterns that undergo relatively minor temporal variations.

MIDNIGHT SECTOR: Ionospheric and auroral phenomena in the midnight sector of the auroral oval have been observed simultaneously by coordinated aircraft, satellite, and ground-based measurements. By combining these measurements, the principal auroral and ionospheric features were continuously mapped before, during, and after magnetospheric substorms. Measurements indicate the presence of a wide band of continuous aurora, such as auroral E layer, which persists at all times and is observed even at very quiet times, during which discrete auroral forms are absent. At other times, the discrete auroral forms appear embedded in the continuous aurora or located just poleward of the band of continuous aurora. On the nightside, the "red band" contains both discrete auroras and the continuous aurora. During auroral substorms, the "red band" varies in latitudinal width from three degrees near substorm onset, to greater than ten degrees during the maximum of the expansive phase of a substorm. An F-layer irregularity zone (FLIZ) associated with the "red band" is observed to be a regular feature of the nightside ionosphere, and may be caused by precipitation of low energy electrons from the plasma sheet. The poleward wall of the main F-layer trough coincides with the equatorward edge of the "red band" and FLIZ.

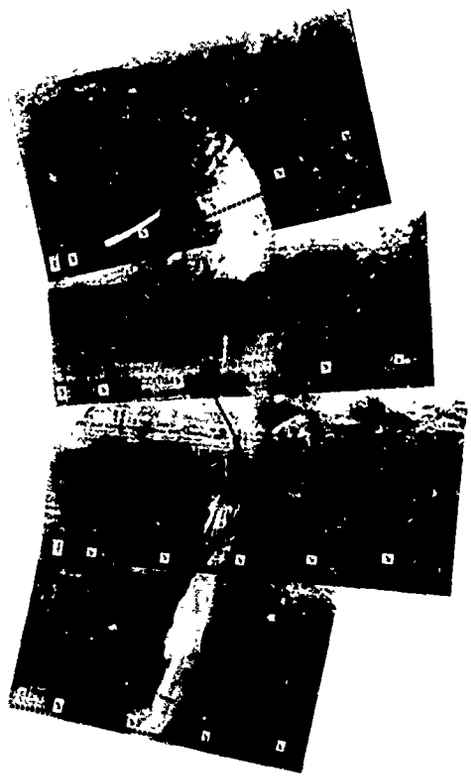

A montage of DMSP auroral photos, recorded near midnight on four consecutive satellite orbits. The bright band seen on the top of each photo is the instantaneous position of the auroral oval. The ground projections of the ISIS satellite tracks are noted on each photo. The ISIS satellite measured precipitating particles, which produced the aurora seen in the photo, and measured the topside ionosphere. The flight route of the Airborne Observatory is noted across the auroral photos by a diagonally dashed line. The Airborne Observatory measured the structure of the bottomside ionosphere in the region of the auroral features seen in the photos.

AURORAL DATA PROGRAM: An achievement of the Auroral Data Program was the initial demonstration of the feasibility of providing near real-time ionospheric data on a semi-global scale to Air Weather Service customers by using the Defense Meteorological Satellite Program (DMSP) satellites' auroral images to infer the structure of the auroral ionosphere. The Auroral Data Program has subsequently enhanced the operational use of the DMSP satellite auroral data, and present work is focused on technique development to allow optimizing future DMSP satellite sensors.

The initial data base for the Auroral Data Program resulted from a series of simultaneous measurements between the International Satellite for Ionospheric Studies (ISIS), the AFCRL Airborne Ionospheric Observatory, and the Defense Meteorological Satellite Program satellite. The DMSP satellite photographed the aurora while passing over it and the ISIS satellite measured the precipitating particles, which produced the aurora, and the topside ionosphere. The Airborne Ionospheric Observatory measured the structure of the bottomside ionosphere in the region of the auroral features.

A "DMSP Auroral-Ionospheric Interpretation Guide" is being assembled to enable users to infer ionospheric structure from auroral patterns. Auroral patterns, representative of impending substorm activity and of the stages of auroral substorms, can be visualized in time sequence. The ionospheric structure most likely to be associated with a a particular auroral feature is identified by a label on each photograph in the guide. Observers can be trained in pattern recognition to relate ionospheric features to auroral patterns.

ENVIRONMENTAL DATA PROGRAM: An in-depth analysis of the environment for periods during which the Defense Satellite Communications System (DSCS) satellites experienced anomalies was made by AFCRL. The DSCS satellites are located in geosynchronous orbit. The geomagnetic field lines and the particle flux regions which intersect DSCS ultimately extend down to the ionosphere in the region of the

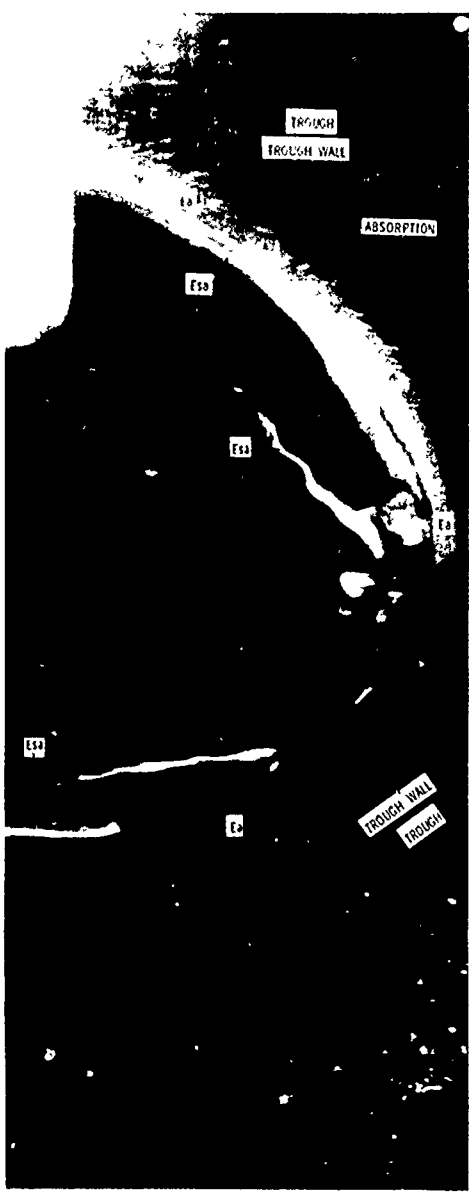

A DMSP photo typifying patterns seen in the aurora. The ionospheric structure expected to be associated with a particular auroral feature is identified by a label which is affixed to the photo.

aurora. Environmental conditions prevailing at satellite altitude were inferred by interpreting DMSP auroral photos, data from the AFCRL Airborne Ionospheric Observatory, and data from ionospheric ground stations. The analysis suggested that environmental disturbances were a factor in producing the satellite anomalies. Results of the study effort along with recommendations concerning follow-on DSCS satellites were forwarded to the DSCS Program Office, and engineering corrections to preclude effects of the environment on the satellite systems were recommended. These corrections included grounding of spacecraft surfaces and adding mechanical relays. The spacecraft-charging-at-high-altitude (SCATHA) satellite is now proposed to directly measure the environmental parameters affecting the operation of geosynchronous satellites.

PROPAGATION STUDIES

The unique capability of the Airborne Ionospheric Observatory to map the ionosphere over large areas has also made it a very important tool in support of various over-the-horizon (OTH) radar efforts in Europe and the United States, especially in determining the effects of the high latitude ionosphere on OTH propagation.

The extremely strong horizontal electron density gradients found above approximately 50 degrees corrected geomagnetic latitude make it mandatory to specify the ionosphere as accurately as possible to interpret correctly the observations made by OTH systems.

Even the high speed and maneuverability of the aircraft is not sufficient to produce an instantaneous picture of those portions of the ionosphere necessary to the detailed interpretation of complicated propagation phenomena observed by the OTH systems. Thus, the results of years of airborne research were combined into a morphological model of the high latitude ionosphere giving the location and variability of the boundaries of the morphological structure of the ionosphere. This model, together with airborne ionosoundings, satellite measurements and DMSP satellite photos, was used to produce large-scale, three-dimensional quasi-instantaneous descriptions of segments of the arctic ionosphere through which OTH signals propagate.

OTH RADAR STUDY: In a joint effort by AFCRL and the MIT Lincoln Laboratory, Lexington, Massachusetts, during the Polar Fox II OTH experiments it was determined that inconsistencies in path loss derived from transponder and ground-backscatter data were mainly due to lack of proper three-dimensional models of the propagation environment.

To test the effects of the large-scale horizontal electron density gradients, a sample ionosphere was constructed, using a large data base accumulated by the aircraft, the DMSP satellite and the ISIS 2 topside sounder on December 9, 1971 around 0400 UT. Samples of the resulting ionospheric cross sections clearly depict the extremely different ionospheres seen in different directions from the selected origin (Polar Fox II site, Caribou, Maine).

Three-dimensional ray tracing was done using this sample ionosphere, and the effects on HF communications systems, OTH detection and direction finding were evaluated. The results showed large deviations for a 6 MHz signal encountering the strong electron density gradients across the initial plane of propagation.

Efforts are underway to improve means of providing these large-scale, typical ionospheric descriptions for use in further evaluation of propagation problems. Furthermore, theoretical efforts will determine the sensitivity of the initial results to changes in the gradients to define the accuracy requirements of the description of the environment.

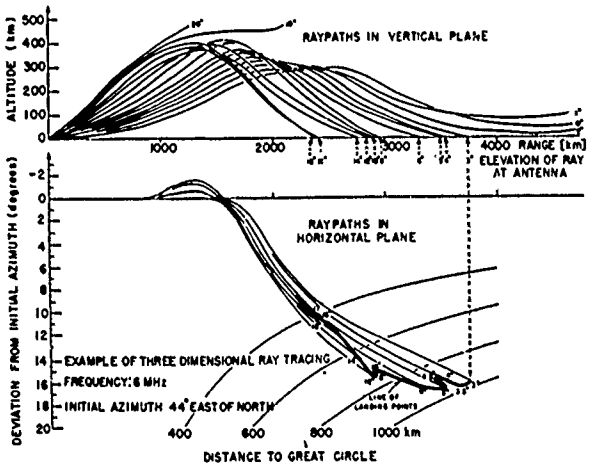

Example of Three-Dimensional Ray Tracing. Top shows projection of ray paths into vertical plane of initial azimuth. Bottom shows projection into the horizontal plane.

GOOSE BAY IONOSPHERIC OBSERVATORY: Since January 1974, the AFCRL Goose Bay Ionospheric Observatory has become a part of the AWS Space Environmental Support System (SESS). Routinely throughout each night it reports to Air Force Global Weather Central vital parameters derived from ionosonde, riometer, total electron content, and scintillation measurements of the high latitude ionosphere on an hourly basis and during auroral events. Airborne measurements, supported by many other inputs, have put a certain degree of order into the previou., ather chaotic appearance of the high latitude ionosphere. The morphological model which evolved from these investigations led to the concept that with proper understanding of specific signatures in vertical and backscatter soundings, one could monitor the high latitude and the auroral ionosphere with very few stations.

The AFCRL Goose Bay Ionospheric Observatory, located at 65 degrees corrected magnetic latitude, provides an ideal site to sense, in range, ionospheric irregularities associated with the auroral oval. This allows one to determine the general state and the size of the oval long before it appears in the zenith at Goose Bay. The large-scale structure of the high latitude ionosphere, intimately tied to the oval, can then be inferred, using an ionospheric model. Additional investigations are necessary, however, before a definitive oval monitoring capability can be developed. One such study is the ordering of oblique echo ranges, observed with a northward pointing backscatter system, as a function of the magnetic activity over the 12 hours prior to local midnight. With increased magnetic activity the auroral oval enlarges and the oblique echoes are seen earlier and arrive over Goose Bay earlier. At present, joint experiments between aircraft and ground backscatter systems are underway to uniquely identify the nature of the scatterers and to relate them to the oval, thus providing the input parameter needed for the control of the model.

DIGITAL IONOGRAM COMPRESSION: To speed up the data reduction of Goose Bay ionograms and other ionograms, to provide for the possibility of surveying long-term ionospheric trends, and to aid in real-time assessment of ionospheric conditions, computer programs have been developed which allow the transformation of digital ionograms into so-called "characteristics." The characteristics include the backscatter echo ranges, the dynamics and structure of the layers of the overhead ionosphere, and the behavior of the overhead E layer. An electronic test system has been built to provide these characteristics in real time. It works so well that an improved version of this "Automatic Ionogram Compression" System is planned at Goose Bay for data transmission via teletype line to AFCRL. Success for the real-time assessment of the high latitude ionosphere as a vital input to the planned OTH system is anticipated.

OBLIQUE PROPAGATION STUDY: The digital sounders operating at Goose Bay, Labrador, and Maynard, Massachusetts,

and in the Airborne Ionospheric Observatory are ideally suited for oblique propagation experiments. Vertical soundings at two sites, combined with the information about the midpoint ionosphere derived from the oblique ionograms, are an extremely valuable tool to describe the ionosphere over a large area. With one terminal of this sensing system on board a moving aircraft, three-dimensional ionospheres can be described with a high degree of accuracy. The system allows assessment of the useful frequency band available over a fixed or changing path and is extremely useful in determining effects of auroral activity on propagation conditions. Frequency windows have been determined and communication maintained between the ground station and the aircraft over distances up to

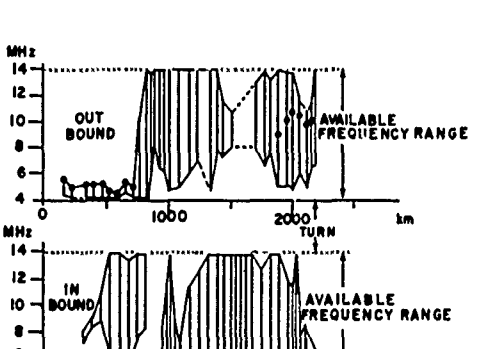

Frequency windows in which communication was maintained between Goose Bay and the aircraft over distances up to 2,000 km.

2,000 km. On one flight, except for a short interruption on the inbound leg at about 900 km distance, communication was maintained continuously within the available 4-14 MHz frequency band. Results of seven initial flights indicate that using the sweep frequency mode, HF contact between aircraft and ground stations was nearly routinely maintained over distances of 2,000 km during disturbed ionospheric conditions. Phase measurements demonstrated that information can be transmitted in this disturbed environment using proper phase codes and pulse-modulated step-frequency transmission. The ongoing flight program will provide, for selected paths, propagation data for the investigation of mode and frequency availability as a function of season, local time, auroral and geomagnetic activity.

These flight tests provide the background for a planned joint AFCRL-ESD-Mitre study to determine the feasibility of using HF swept-frequency techniques for radio communication through a disturbed ionosphere on an operational basis.

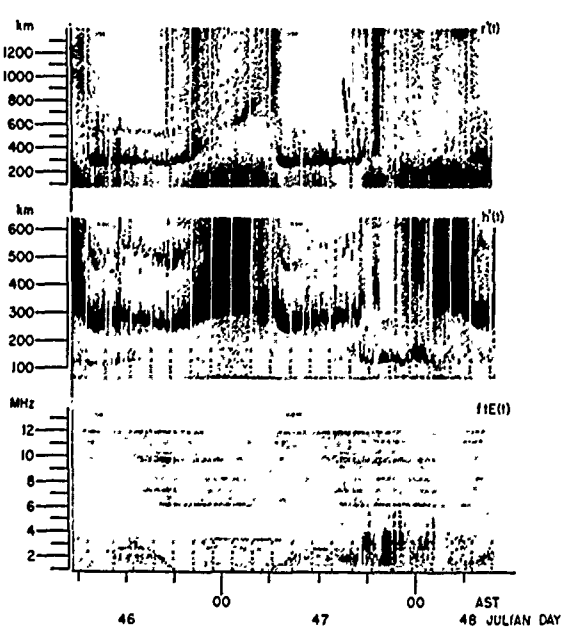

Three characteristics: backscatter echo range (r'(t), virtual height h'(t), top frequency for E layer ftE(t), recorded over a period of three days. They are the result of computer processing reformatting of 600 ionograms, or 10^7 data points, into this unique presentation produced by a Digicoder/electrostatic printer system.

LIGHTNING WARNING AND SUPPRESSION

AFCRL's involvement with missile and rocket launch problems originated when an

early prediction that a rapidly rising rocket might initiate a lightning stroke was dramatically confirmed during the launch of Apollo 12. The prediction had been based on a previous demonstration that thin steel wires, rapidly paid out from grounded reels and carried to altitudes of less than 2,000 feet by miniature rockets, could trigger lightning strokes, if the atmosphere were properly electrified.

Laboratory scientists initiated a project to evaluate the lightning threat, and , if possible, find ways to reduce it. One technique could be to deploy long wires along the planned trajectory to drain off electric charge, making a "window" through which the rocket can be launched.

To evaluate the effectiveness of any countermeasure, a statistical determination is needed of the percentage of rocket launches which might trigger lightning strokes. Launching large rockets for this purpose would be too expensive, so long conducting wires are used to simulate the rocket plumes. The previous technique, however, cannot be extended to higher altitudes, because the higher velocities required generate aerodynamic drag forces which exceed the strength of available materials.

Three new approaches were tried. First, a fine wire cable was stored on a bobbin in the nose of a Little John rocket. A flight test showed that several thousand feet of wire could be paid out from the bobbin during flight. A second approach was to drop a canister containing several thousand feet of wire from a high altitude airplane, using a standard flare dispenser. A small parachute slowed the canister, and gravity caused the wire to deploy. Field tests showed the system was mechanically feasible, and provided C- and S-band radar reflections in clear air, but rain masked any returns when they were dropped into precipitation clouds.

A third scheme used 1,000-foot lengths of metallized Mylar tape wound into compact shapes and stored in the nose of a small sounding rocket. The tapes were ejected at the desired altitude, and aerodynamic forces rapidly slowed and unwound the tapes. In November 1972, standard 2.75-inch diameter air-to-air rockets were fired from the ground to test this less expensive method of deployment. Difficulties were encountered in detecting the tape deployment, whether by C-band radar, S-band radar, or visually. Weak but definite echoes were seen by the S-band radar.

The radar cross section of the conductor could be enhanced, and at the same time, the cloud returns could be reduced, if a much longer wavelength radar were used. In preliminary tests at Ipswich, Massachusetts, a VHF (30 MHz, 60 MHz) radar tracked balloon-borne half-wave dipoles in clear air out to distances approaching 100 miles. Since a VHF radar is also capable of detecting the ionized paths produced by lightning strokes, the sudden appearance of such a signal, simultaneously with the disappearance of the dipole return would provide evidence of a triggered lightning stroke. A VHF radar has recently been acquired, and will be used in further tests of this tracking technique.

A corollary problem is the detection and measurement of the degree of electrification in thunderstorm clouds. Traditionally, the ambient electrostatic field strength is measured on the ground in a number of locations by so-called "field mills" and the data are analyzed to try to determine an effective charge center. However, resolving the position and magnitude of individual charge centers within clouds requires a detailed knowledge of the field on the ground and very large number of field mills.

A new method is based on the theory that low level electrical discharge activity occurring in cloud charge centers produces VHF radio noise. In a joint project with NASA, AFCRL scientists utilized directional antennas at Kennedy Space Center during August 1971 to passively detect radio emissions from storm clouds in the frequency range between 100 and 1,000 MHz. The

tests showed that clouds emit very short pulses of VHF and UHF radio noise for a considerable time period. The noise was detected at ranges of 50 miles or more and could be mapped in two dimensions with a scanning antenna. In August 1972, an experiment at Kennedy Space Center used two NASA antennas with coincidence circuits in an attempt to map charge centers in three dimensions. This experiment confirmed the basic principle, but signals detected by the side lobes of the antenna patterns interfered with the signals from the main beams for certain antenna orientations. The search for an antenna with narrow beamwidth and low side-lobe sensitivity resulted in the fabrication of new antennas following an AFCRL design. One of these antennas, mounted with its axis vertical, monitors a volume directly above it. The antenna, in a sandbag pit for shielding against signals arriving from the side, has been in operation since April 1974 on Reservoir Hill, Bedford, Massachusetts. Tests in frontal storms, which passed over the antenna, showed that this antenna system can register storms without responding to automobile ignition and other side-lobe interference.

This work shows that a combination of the techniques investigated may provide a true lightning warning system for fixed ground installations.

IONOSPHERIC WAVEGUIDE

The ionosphere is a transmission medium for high frequency and medium frequency waves. But at the very-low-frequency (VLF) end of the radio frequency spectrum, the ionosphere is primarily a reflector. In combination with the earth's surface, it forms, essentially, a giant waveguide through which VLF waves propagate in various modes with little loss. Each mode can be thought of as a combination of ascending and descending plane waves whose phases and amplitudes are primarily determined

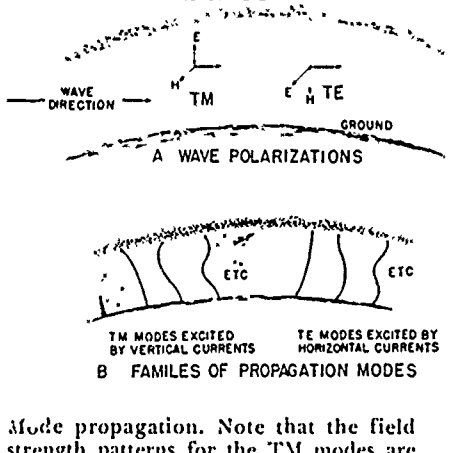

Mode propagation. Note that the field strength patterns for the TM modes are strongest at the earth's surface, where the TE modes are weakest.

by the properties of the earth-ionosphere boundaries.

VLF waves propagate to great distances, can be received beneath the surface of the sea, are highly stable, and are relatively little affected by either natural or man-made ionospheric disturbances. However, prediction of VLF propagation and efficient design of VLF systems have been hampered by the lack of information on the reflective properties of the lower ionosphere. The usual probing techniques involving transmission and reception of pulses cannot readily be extended to these low frequencies. The relatively long pulses generated by conventional VLF transmitters allow the reflected (skywave) pulse to arrive at the transmitter before the direct (groundwave) pulse has ended. This superposition of signals contaminates the skywave and makes it impossible to deduce ionospheric properties.

SHORT PULSE IONOSOUNDER: AFCRL has developed a unique high resolution 5 to 100 kHz ionosounder which radiates VLF pulses so short that, even at ranges of 400 km, the ground-wave pulse has ended before the sky-wave pulse arrives. Reflection coefficients and heights can now be derived

by Fourier analyzing the two pulses and comparing the amplitudes and phases. The transmitter can utilize any conventional, base-insulated VLF antenna tower, or can also be equipped with a 1,000-meter balloon-supported vertical wire antenna. This feature is particularly useful for short-term measurements in remote locations, as it is transportable and requires very little land area.

The azimuthally uniform radiation pattern from either type of antenna allows measurements to be made simultaneously over propagation paths with different orientations relative to the earth's magnetic field.

In 1970, the ionosounder was operated in southern California to study mid-latitude ionospheric reflectivity. In May 1971, in a cooperative program with the Brazilian Air Force, it was set up on the geomagnetic equator in Brazil and used to study ionospheric reflectivity associated with a horizontal geomagnetic field.

From January 1972 to January 1973, the ionosounder was used in a long-term study of diurnal variations in ionospheric reflection coefficients at low and very low frequencies. The signals were transmitted from an RADC 600-foot vertical antenna at Camden, New York, and were received in Bethel, Vermont, over a 260-km magnetically west-to-east propagation path.

The data obtained in these measurement programs covered a wide range of frequencies, magnetic azimuths, angles of incidence, and geomagnetic field conditions. The reflection coefficients calculated from the measurements are used as input parameters for a recently developed VLF propagation computer program. Called POWERFLUX, this program uses a relatively simple integral formulation based on incoherent power addition to calculate the average VLF radio-wave power propagating within the curved earth-ionosphere waveguide. Using this formulation, average field strength versus distance curves can be obtained with a small computer or even a desk calculator.

The VLF ionosounding program has now been extended to the arctic to observe high latitude ionospheric effects. Even under normal ionospheric conditions, the reflectivity of the D region is strongly influenced by the strength and orientation of the geomagnetic field relative to the propagation path. The arctic measurements provide the first high resolution VLF—LF data on ionospheric reflectivity as influenced by a near-vertical magnetic field. The arctic also provides a unique opportunity to study transient events of solar origin such as polar cap absorption, magnetic disturbances, and auroral activity, which significantly affect VLF and LF systems. High altitude nuclear explosions can also produce ionospheric disturbances which critically affect VLF and LF systems. The natural phenomenon which most closely simulates a nuclear event is the Polar Cap Absorption event (PCA). The arctic observations of these transient phenomena will provide data with sufficient accuracy to permit a quantitative understanding of their effects on ionospheric reflectivity.

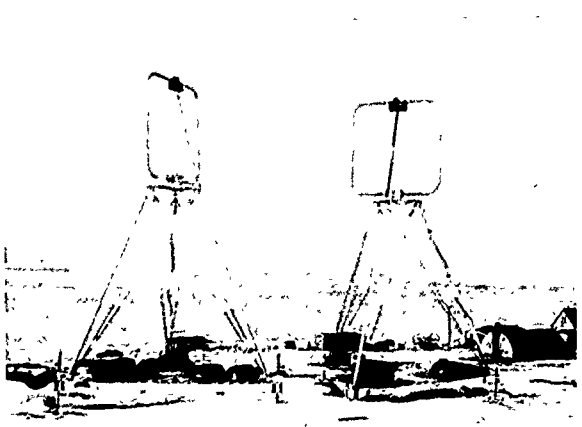

High-precision VLF/LF ionosounder receiving antennas at Qanaq, Greenland.

The data will be analyzed to provide the propagation information required to evaluate VLF and LF systems in a disturbed environment.

For the current ionosounding experiment, the transmitter is located at Thule AB, Greenland. Arrangements have been made with the Danish Meteorological Institute to receive and record the pulses at their Ionospheric Observatory at Qanaq, 100 km north of Thule. The data are recorded automatically on digital magnetic tape for computer processing at AFCRL.

Since September 1973, the transmitter has been operated with an existing 1,200-foot Air Force antenna on a very limited, time-shared basis. Although most measurements were made during normal ionospheric conditions, the January 1974 measurements included a reflection anomaly, the start of which correlated with a magnetic perturbation observed by the Danish Meteorological Institute in Qanaq.

To increase the operating time, a 400-foot antenna tower is being erected at Thule, and should be available for full-time use in the fall of 1974.

LONG-PATH STUDIES: In addition to the ionosounding technique, which produces short-path, one-hop measurements of local ionospheric conditions, the Laboratory is also studying long-path propagation. An X-ray detection and warning study was recently completed for the Air Weather Service (AWS).

Because X-ray events cannot be forecast accurately, AWS has identified the need for continued availability of timely X-ray data as a high priority item within the Space Environmental Support System. AFCRL responded by searching for an alternative method which would provide information on X-ray flux at lower costs than those resulting from the use of X-ray satellites.

X-rays are absorbed in the ionosphere at D-layer height. Furthermore, long-path VLF signals propagate by "bouncing" back and forth between the D layer and the earth, the two surfaces acting as walls of a waveguide. Thus, if one wall of the waveguide, the D layer, were lowered as a result of X-ray induced ionization, then the character of the VLF signal would be significantly changed. It was this change, a phase advance and an amplitude increase or decrease that was used to specify the X-ray flux. A two-year sample of VLF data, covering 130 VLF paths, was used. In all, the data sample included 141,180 events.

The first part of this study demonstrated that VLF can be used to reliably detect the occurrence of an X-ray event. This study also related the magnitude of the VLF phase changes to the instantaneous X-ray flux in the 1-8 angstrom region. To account for the varying conditions that prevailed on different paths, it was necessary to normalize the data. The important factors in the normalizations were found to be VLF frequency, path length, percent of path illuminated by sunlight, and average solar zenith angle along the path.

An extremely accurate and reliable method was developed and tested. At frequencies above 16 kHz, the event signatures are particularly dramatic, resembling

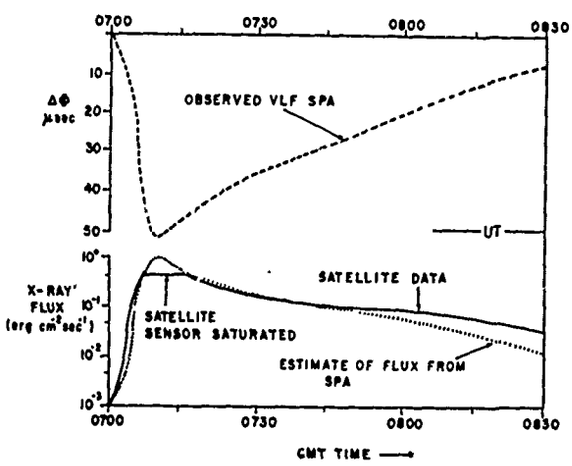

Trace of VLF Sudden Phase Anomaly (SPA) caused by a solar X-ray event, with the derived flux estimate compared to satellite observations.

arrowheads when the amplitude trace is recorded above the phase trace. Such a signature indicates, with practically no uncertainty, that an X-ray event is in progress. The study has also demonstrated that VLF paths can be calibrated so that real-time evaluations of the severity of the event can be obtained almost directly from the observed VLF phase anomaly.

For fully illuminated, low latitude VLF paths, such evaluations can be very accurate. Recently the AWS has adopted this technique and is establishing a suitable world-wide VLF network to detect and evaluate X-ray events on a round-the-clock basis.

PROPAGATION MODE STUDIES: VLF transmitters use the Transverse Magnetic (TM) mode. A vertical antenna will excite this mode in the earth-ionosphere waveguide. For some time, the Laboratory has been studying VLF transmissions for the Transverse Electric (TE) mode, which would be excited by a horizontal antenna. TM waves are easily excited and received at the earth's surface, but TE waves are essentially shorted out by the ground, making them difficult to excite and weak for reception. Above the surface of the earth, as in air-to-air communication, the situation changes, and theoretical considerations indicate that the TE mode may propagate with less loss than the TM mode, especially under highly disturbed ionospheric conditions.

As a part of the Air Force support to the Minimum Essential Emergency Communications Network (MEECN), AFCRL has been exploring the use of this mode. Instrumentation developed here provides a means for conducting high altitude measurements. The present system consists of a package which is dropped from altitudes of 70,000 feet or more by a weather balloon. The payload is dart-shaped and stabilized aerodynamically so that signals from TE and TM polarizations can be received individually as the dart falls. This provides information on signal strength versus altitude for both modes. Preliminary tests at Swan Island (near Honduras) showed that TE atmospheric noise is 15-20 dB less than TM noise.

In August 1972, the existence of man-made VLF TE signals was first demonstrated. Basic antenna theory indicates that a horizontal trailing wire antenna, such as the one used by the Air Force for the ARC-96 transmitter, radiates a wave which is primarily TE. The slight vertical droop of the antenna is expected to provide a small TM component, but the TE component of the signal should be much stronger than the TM component.

In this experiment, a dart package dropped over Fort Churchill, Canada, received a VLF signal from an aircraft using a trailing wire antenna. Data from the falling dart showed that radiation from this trailing wire antenna was essentially TE, and was much stronger at high altitudes than near the ground. As expected, the TM signal, radiated from the slightly drooping portion of the antenna, was extremely weak and became even weaker at high altitudes. Further experiments at Canton Island in the Pacific confirmed the results of the Fort Churchill test.

The first of several additional projects uses the high altitude capabilities of the Air Force's U-2 aircraft to make TE measurements as a function of altitude and range. Preliminary tests with this type of aircraft in association with trailing wire transmissions have begun, and although the program is still in its infancy, these tests have yielded very encouraging results.

A second project is an attempt to generate TE signals using a long horizontal antenna on the ground. This experiment utilizes an abandoned power line at Thule AB, Greenland, and takes advantage of the very poor ground conductivity in the Arctic which is especially favorable for the generation of TE waves using a ground-based transmitter. A preliminary experiment using this power line has been encouraging.

This attempt, if successful, will enable long-term TE data to be gathered under both normal and disturbed ionospheric conditions.

LORAN ACCURACY: In response to a request by the Electronic Systems Division, AFCRL reviewed current techniques for predicting and measuring LORAN navigation coordinates. Positional information is derived from the time difference between the reception of ground-wave pulses from two synchronized transmitters. Ultimate location accuracy depends on such factors as system geometry, pulse-processing techniques, ground-wave propagation velocity, proximity of local scattering sources, and receiver altitude. The contributions of such factors to the time difference error were estimated, and methods were suggested for experimental verification. A technique for reducing errors due to terrain irregularities, by measuring both the electric and magnetic fields, was proposed.

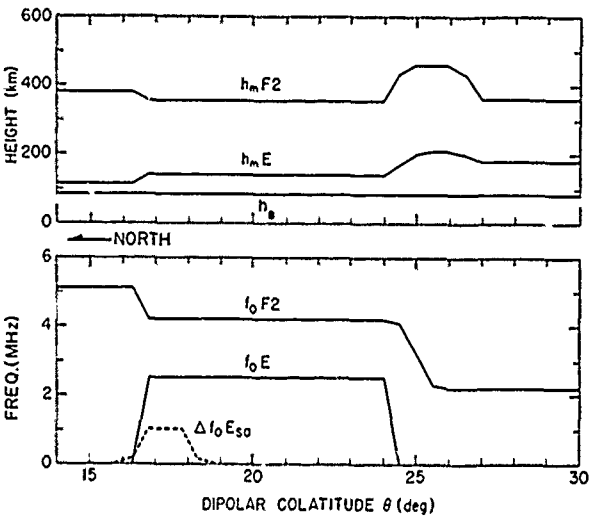

Idealized variation with dipolar colatitude of the heights and critical frequencies of the E and F_2 layers, and the top frequency of sporadic E near the 70-degree West meridian and local midnight, 8 December 1971.

IONOSPHERIC MAPPING AND POLAR MODELING

System design and efficient operation require extensive simulation of ionospheric propagation, which in turn requires accurate mathematical models of the polar ionosphere which reproduce its essential features—spatial and temporal variability and the influence of solar and geomagnetic activity.

Although much is now known of the physics of the ionosphere, it is still not possible to construct a predictive model, based on physical principles, which is sufficiently accurate for most modern system simulation studies This is especially true in the polar regions, where the ionosphere is influenced by many complex interacting processes. Empirical models have been constructed at AFCRL which reproduce, in a statistical manner, many of the observed features of the polar ionosphere. These models are tailored to meet specific system needs and are, in most cases, adequate for that purpose. They have been formulated as computer programs which are readily coupled to propagation simulation (ray-tracing) programs for estimation of such effects as refraction, radar range error, Doppler shift, and so on. In particular, emphasis recently has been placed on the modeling of small-scale auroral irregularities, the simulation of auroral clutter in backscatter radars, and oblique scatter propagation at high frequencies.

The ionospheric mapping effort has yielded a scheme whereby observations of ionospheric parameters can be used to produce a realistic three-dimensional global ionospheric model. A first-guess ionospheric structure is updated using actual observations to provide a series of correction factors. These correction factors are used to modify the initial ionospheric structure to produce a statistically optimum representation of the ionosphere for a given instant of time. The parameters em-

ployed in the updating scheme are the F2 region critical frequency and the height of the F2 region maximum electron density ($h_m F2$). The parameters can be either observations at specific locations, or predictions valid for different regions of the globe.

From the results of the mapping and modeling scheme, ionospheric structure maps of height versus latitude have been prepared with the critical frequency as a parameter. Using similar results from adjoining longitudes in conjunction with a three-dimensional ray-tracing program, an assessment can be made of the changes in HF radio-wave propagation that result from changes in the structure of the ionosphere.

An application of ionospheric modeling and ray tracing is to the problem of determining the source of auroral clutter observed by an OTH backscatter radar. Range-azimuth plots showing contours of the angle between the geomagnetic field at ionospheric altitude and the refracted radar beam have been prepared. Because of the aspect sensitivity of ionospheric irregularities, the backscatter is a maximum when this angle is 90 degrees. A certain kind of auroral irregularity occurs most frequently at the equatorward boundary of the auroral oval. The points where this boundary crosses the 90-degree contour are the locations in space of the major clutter-producing irregularities.

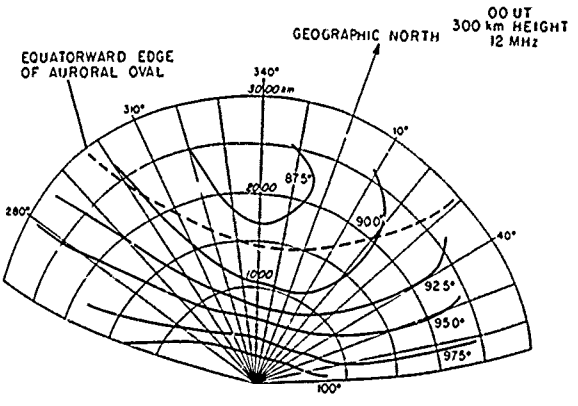

A Range-Azimuth plot showing contours of the angle between the geomagnetic field at ionospheric altitudes, and the refracted radar beam.

Another application of the AFCRL polar ionosphere prediction and ray-tracing computer programs is a special adaptation to the peculiar requirements of a fast-moving aircraft for analysis of Doppler data and mode structure as well as for flight planning.

POLAR IONOSPHERIC SCATTERING: Off-great-circle propagation of communication and radar signals is the result of scattering from electron density irregularities aligned along the magnetic field lines. These field-aligned irregularities can be of natural origin as in auroras or man-made as caused by a nuclear device. When the direction of propagation is approximately perpendicular to the lines of force of the earth's magnetic field, the radio waves are scattered back in the direction of the radiating source. The effect is referred to as backscatter. When the direction of propagation is not perpendicular to the field-aligned ionization, the radiation undergoes forward scattering. It is assumed that the forward-scattered signal is oriented in the direction which satisfies the condition for specular reflection for a particular path, i.e., the angle of incidence to the ionization column is equal to the angle of reflection.

Utilizing computer programs developed at AFCRL to generate a model for the polar ionosphere and perform three-dimensional ray-tracing calculations for radio waves, the possible forward-scatter areas have been determined. These can be superimposed on a map to determine if field-aligned irregularities exist in this area and to assess the probability of receiving a reflected signal.

Ray-tracing studies have been made of HF propagation effects under the conditions of realistic electron-density distributions in the polar ionosphere, and work has

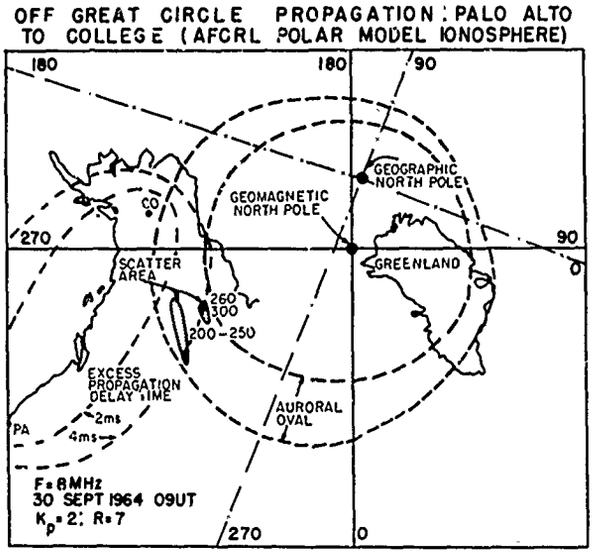

Radio waves can propagate along paths other than the great circle if they are reflected or scattered off irregularities which occur in the auroral oval.

begun on the important problem of converting backscatter radar ionograms into electron distributions in the sector of radar surveillance. From these electron distributions, the ionospheric effects on the performance of OTH radars can be computed or predicted. An accurate geomagnetic field model has been incorporated into the AFCRL ray-tracing program for computing the aspect angle between the ray direction and the direction of field-aligned ionization at all points along a ray trajectory. The regions of clutter can now be specified more realistically, thus providing better predictions.

A method has been developed for conveniently representing arbitrary three-dimensional electron distributions for ray computations. Studies are being made to determine the effects on swept-frequency backscatter-radar ionograms by systematically altering the heights and critical frequencies of ionospheric layers in all three dimensions. The effects computed so far are generally sensitive to alterations of the layers. However, whether the effects will be sufficient to enable the electron distribution to be inferred reliably from backscatter ionograms by iterative ray-tracing schemes still remains to be determined.

IONOSPHERIC EXPERIMENTAL STUDIES: Radio waves passing through the ionosphere suffer absorption or attenuation. The amount of degradation this causes in communication circuits depends on the operating frequency and on the electron density profile of the ionosphere for the particular geographical area.

Riometers (Relative Ionospheric Opacity meters) are instruments used to investigate ionospheric absorption by continuous ground-based absorption measurements utilizing cosmic noise signals emitted from our Galaxy.

Since 1972, the emphasis of the riometer investigations has shifted to the polar region to study Polar Cap Absorption (PCA) and auroral zone absorption events. The riometer located at Thule, Greenland, has been instrumental in obtaining information of importance to system designers and operational personnel, such as the behavior of PCAs, and in relating this information to solar flare effects, geomagnetic disturbances, and other ionospheric phenomena.

A study utilizing ten years of riometer data from Thule (1962-1972) and the detailed investigations of 53 events have helped to answer such questions as occurrence frequency, duration and severity of PCAs. The study revealed that the mean duration of PCAs is 63.6 hours, the mean magnitude is 4 dB, and that large events (greater than 10 dB) were observed only during 1966, 1969, and 1972.

A Digisonde has been in operation at Maynard, Mass., since mid-1971, as part of the global ionospheric sounder network. The Digisonde, developed and built under AFCRL sponsorship, derives its name from the use of digital integration, storage and processing of coded pulses and pulse coherent detection. These techniques yield

better ionosonde records including a significant improvement of the signal-to-noise ratio. This provides better reception of echoes in the presence of interfering noise, thereby making it possible to extend the operation to lower frequencies.

Modifications and improvements since 1972 include the addition of a crossed-loop receiving antenna system providing a better signal-to-noise ratio as well as the ability to separate right- and left-hand polarizations. This gives a means of distinguishing the ordinary from the extraordinary echoes for later use in automating ionogram reduction.

Automatic, objective processing of vertical HF ionograms has been needed for several years. The recent developments in digital ionospheric sounders have made it possible to automate ionogram reduction systems.

The method of automatic processing of digital ionograms developed at AFCRL has application in: elimination of the need to train data technicians in the interpretation of ionograms: storage of data on magnetic tape so that specific information can be easily recalled to meet the needs of various users: remote operation of the sounder permitting data to be fed over telephone lines to a center (command or forecast) for near real-time information concerning the state of the ionosphere; and in high compression of raw data by storing only the actual echoes. Since the original ionogram has more than 20,000 points, of which there are generally no more than 200 echo points, the compression ratio is about two orders of magnitude, yielding a considerable saving in storage.

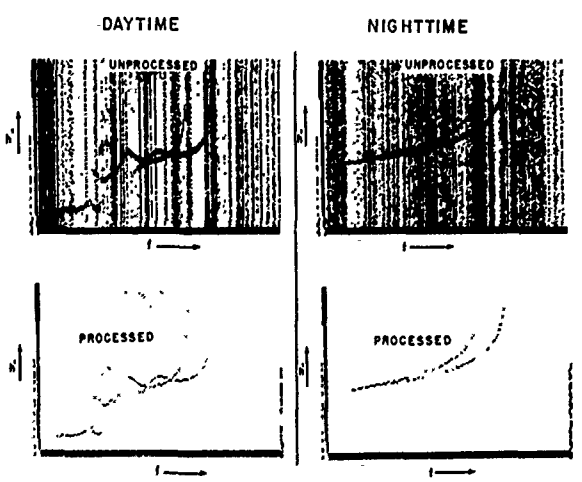

Computer processing of ionograms greatly simplifies the interpretation.

Conventional over-the-horizon radio propagation at high and medium frequencies is often inhibited for extensive periods during ionospheric disturbances by magnetic storms (particularly in the polar regions). At these times, electron densities in the absorbing D region are greatly increased, resulting in high attenuation of the signals normally reflected back to the earth from the E and F regions. A study was conducted to investigate a predicted reduction in losses at very steep angles to the ionospheric D region.

A low-loss (long-range) propagation phenomenon called "Whispering Gallery Mode" is the result of focusing by the lower boundary of the curved ionospheric D region at medium frequencies, together with a large reduction in reflection loss at near-grazing incidence angles, which are achievable only at high altitudes. It can be considered as an "earth-detached" mode in the earth-ionosphere waveguide, occurring at frequencies (200 to 2,000 kHz), where the familiar VLF mode is normally unusable due to prohibitive ground reflection losses. Theory and calculations indicated an expected enhancement of this ambient earth-detached mode during ionospheric disturbances and suggested a feasibility test.

A low power transmission experiment lasting over 30 hours was successfully conducted between balloons separated by 1,000 miles at an altitude of 35 km, on 220 and 440 kHz. Signals were received over the balloon path during most of the day and night. Total path attenuations varied from

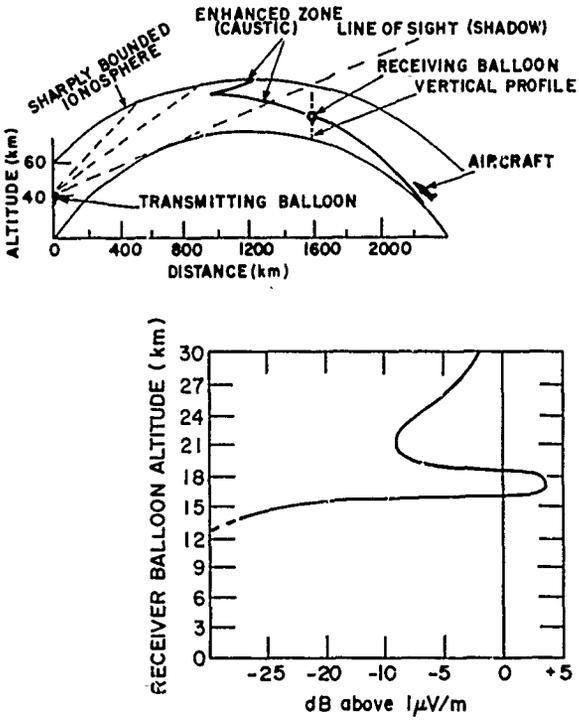

Focusing along the lower edge of the ionosphere causes a zone of signal enhancement (caustic). The upper diagram shows the receiving balloon passing through the caustic. The graph below shows the variation of signal strength with altitude above the receiving site with the transmitting balloon fixed at a height of 37 km, and beyond the line of sight, at a distance of 1,000 km.

as little as 3 to 30 dB more than that of a free space path. Maximum signal height-gains ranging from 40 to 60 dB (normalized relative to an equivalent ground-to-ground path) were measured. An enhanced zone or caustic of about 13 dB was observed as predicted from geometric optics at about 19 km altitude of the receiving balloon. This measurement appears to agree with the vertical profile of signal strength expected for the earth-detached whispering gallery mode.

The potential for long distance reliable communication using modest power and manageable antennas is indicated. Advantages are seen for this form of propagation because of inherently low transmission losses, particularly during radio blackouts and independence from effects of the earth's surface.

GOOSE BAY OBSERVATORY: To investigate the effects of auroral irregularities on backscatter and forward-scatter radio signals an experimental radar system has been established at the Goose Bay Ionospheric Observatory, Goose Bay, Labrador. This system, referred to by the acronym DAASM (Doppler-Arrival Angle Spectral Measurements), utilizes a highly versatile pulsed transmission system and a large multi-element receiving array. The recorded radio signals are either forward propagation from the AFCRL KC-135 aircraft or direct backscatter from aurora using the DAASM transmitting system.

The analysis of these signals involves both time and space transforms, resulting in a two-dimensional map of the radio signals as perturbed by the auroral ionosphere. These maps, where the coordinates are Doppler frequency and azimuthal arrival angle, provide a high resolution description of the structure of auroral irregularities as seen by radio waves in the HF band. It is through the analysis of these maps that the degrading effect of auroral clutter on an OTH radar system can be minimized, provided that the intensity of the clutter exhibits spatial variations that could be exploited by placing nulls of antenna patterns in specific directions.

The DAASM system also provides data on the temporal and spatial coherence of the radar signals and will provide the necessary data for optimum design and operation of an OTH radar system in the auroral environment. Fundamental design parameters such as antenna size and integration times result from this research.

The DAASM system has been in operation for approximately six months and some six aircraft flights have been carried out. The results indicate a variety of unusual effects of the polar ionosphere on the aircraft signal. These effects range from

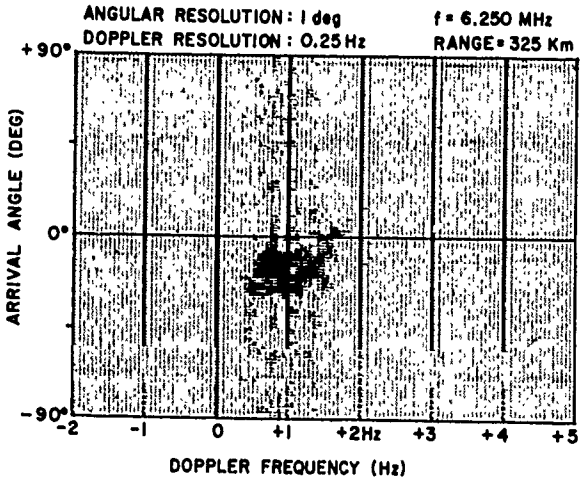

A typical map of Doppler frequency versus arrival angle when a 6.25 MHz signal is reflected by auroral backscatter 325 km distant.

minor to severe, such as large Doppler spreads and angular deviations.

A riometer site was established at the Goose Bay Observatory to investigate the morphology of auroral substorms. This site is unique in that, in addition to the zenith antenna, a four-corner reflector antenna is employed to observe auroral absorption events at four different azimuths from one location, thus covering a large geographical area with minimum logistical support. This system gives information concerning azimuth from the site to the maximum absorption observed, and allows locating the auroral oval with respect to Goose Bay. The oval is observed to the north of the site during quiet magnetic periods and to the south during periods of severe geomagnetic activity (neglecting the diurnal variation). Also, events seen at some azimuths with the new antenna were not observed with the vertical antenna.

JOURNAL ARTICLES
JULY 1972 - JUNE 1974

AARONS, J.
A Descriptive Model of F Layer High Latitude Irregularities as Shown by Scintillation Observations
J. of Geophys. Res., Vol. 78, No. 31 (November 1973)

The Effect of Magnetic Storms on Scintillation at Sub-Auroral and Auroral Latitudes
Proc. of the Jt. Satellite Studies Gp. Tech. Mtg., Lannion, Fr., 28 Jan. - 2 Feb. 1974 (January 1974)

AARONS, J., ET AL
Total Electron Content and Scintillation Studies of the Ionosphere
AGARD-OTAN, Electmg. Wave Propagation Panel, Paris, Fr., AGARD-AG-166 (March 1973)

AARONS, J., ALLEN, R. S., and WHITNEY, H. E.
Observations of Scintillations of Two Satellite Beacons Near the Boundary of the Irregularity Region
Planetary and Space Sci., Vol. 20, No. 7 (July 1972)

AARONS, J., and MARTIN, E. (Emmanuel Coll., Boston, Mass.)
Satellite Scintillation Observations at Sagamore Hill, Mass., and Narssarssuaq, Greenland, During the Solar Events of August 3-10, 1972
Collected Data Rpts. on Aug. 1972 Solar-Terrestrial Events, World Data Ctr. A for Solar Terrestrial Phys., Rpt. UAG-28, Pt. II, Boulder, Colo. (July 1973)

AARONS, J., MULLEN J. P., WHITNEY, H. E. and STEENSTRUP, F. (Danish Met. Inst., Copenhagen, Denm.)
Seasonal, Diurnal, and Magnetic Dependence of Ionospheric Scintillation at 64° Invariant Latitude
Planetary and Space Sci., Vol. 20, No. 7 (July 1972)

AKASOFU, S.-I., KIMBALL, D. S. (Univ. of Alaska), BUCHUA, J., and GOWELL, R.
Alignment of Auroral Arcs
J. of Geophys. Res., Vol. 77, No. 22 (August 1972)

ALLEN, R. S.
Evaluation of Models of Electron Density Profiles
Proc. of the Jt. Satellite Studies Gp. Tech. Mtg., Lannion, Fr., 28 Jan. - 2 Feb. 1974 (January 1974)

BARRON, W. R.
Radio Burst Observations of 24 January 1971 Solar Proton Flare
(Pub. in Pt. I of Rpt.)
September 1, 1971 Solar Radio Burst Observations
(Pub. in Pt. II of Rpt.)
Data on Solar Geophys. Activity Assoc. with the Major Ground-Level Cosmic Ray Events of 24 Jan. and 1 Sep. 1971 (UAG Rpt., NOAA, Boulder, Colo.), UAG-24 (December 1972)

BASU, S.
Spectral Characteristics of Solar Radio Bursts Associated with the Emission of Energetic Electrons from the Sun
Indian J. of Radio and Space Phys., Vol. 3 (March 1974)

BASU, S., and VESPRINI, R. L. (Emmanuel Coll., Boston, Mass.), AARONS, J.
Field-Aligned Ionospheric E-Region Irregularities and Sporadic E
Radio Sci., Vol. 8, No. 3 (1973)
F-Layer Irregularities as Determined by Backscatter Studies at 19 MHz Over Half of a Solar Cycle
Radio Sci., Vol. 9 (March 1974)
Study of Field-Aligned Ionospheric E-Region Irregularities and Sporadic E at HF
Indian J. of Radio and Space Phys., Vol. 3 (March 1974)

BEWERSDORFF, A. B. (Regis Coll., Weston, Mass.), and SAGALYN, R. C.
Spatial and Temporal Variations of the Thermal Plasma at 3000-5700 Km within the Plasmasphere
J. of Geophys. Res., Vol. 77 (September 1972)

BUCHAU, J., GASSMANN, G. J., PIKE, C. P. WAGNER, R. A., and WHALEN, J. A.
Precipitation Patterns in the Arctic Ionosphere Determined from Airborne Observations
Annales de Geophys., Vol. 28, No. 2 (1972)

CARRIGAN, A. L. (Space Phys. Lab.) and CASTELLI, J. P.
Solar Activity in McMath Region Number 10789 During Disk Passage, June 12-15, 1970
Proc. of the 3rd Mtg. of the Com. of Eur. Solar Astron. (CESRA), Bordeaux, Fr., 21-22 Sep. 1973 (1973)

CASTELLI, J. P.
Investigation of Solar Radio Burst Parameters at AFCRL
Proc. of the 3rd Mtg. of the Com. of Eur. Solar Radio Astron. (CESRA), Bordeaux, Fr., 21-22 Sep. 1973 (1973)
Report of Observatories. Sagamore Hill Radio Observatory, Air Force Cambridge Research Laboratories, L. G. Hanscom Field, Bedford, Mass.
Bull. of Am. Astronom. Soc., Vol. 5 (January 1973)

CASTELLI, J. P., BARRON, W. R., and BADILLO, V. L. (Manila Obsv., Manila, Phil.)
Highlights of Radio Activity During Disk Passage of McMath Plage No. 11976
Collected Data Rpts. on Aug. 1972 Solar-Terrestrial Events, World Data Ctr. A for Solar Terrestrial Phys., Rpt. UAG-28, Pt. I, Boulder, Colo. (July 1973)

CASTELLI, J. P., and CARRIGAN, A. L. (Space Phys. Lab.), KO, H. C. (Ohio State Univ.)
Spectral Association of the 7 August 1972 Solar Radio Burst with Particle Acceleration
Coronal Disturbances, Proc. of IAU Symp. #57, Gordon Newkirk, Jr., Ed., D. Reidel Pub. Co., Dordrecht, Holl. (1974)

CASTELLI, J. P., GUIDICE, D. A., and FORREST, D. J. (Univ of N. H.), BABCOCK, R. R.
Solar Bursts at λ = 2cm on 31 July 1972
J. of Geophys. Res.. Vol. 79, No. 7 (1 March 1974)

CASTELLI, J. P., GUIDICE, D. A., STRAKA, R. M., and AARONS, J.
The Solar Radio Patrol Network of the USAF and Its Application
Proc. of the IEEE, Vol. 61, No. 9 (January 1974)

CONLEY, T. D.
Mesospheric Positive Ion Concentration, Mobilities, and Loss Rates Obtained from Rocket-Borne Gerdien Condenser Measurements
Radio Sci., Vol. 9 (June 1974)

CORMIER, R. J.
Polar Riometer Observations During August 1972
Collected Data Rpts. on Aug. 1972 Solar-Terrestrial Events, World Data Ctr. A for Solar Terrestrial Phys., Rpt. UAG-28, Pt. III, Boulder, Colo. (July 1973)

GASSMANN, G. J.
High Latitude Ionosphere
1972 McGraw Hill Yrbk. of Sci. and Technol. (1972)

GASSMANN, G. J., and WAGNER, R. A.
Visible Light Flux Affecting the D-Layer
Radio Sci., Vol. 7, No. 5 (1972)

GUIDICE, D. A.
Report of Observatories: Sagamore Hill Radio Observatory
Bull. of the Am. Astronom. Soc., Vol. 6, No. 1 (January 1974)

GUIDICE, D. A., and CASTELLI, J. P.
Spectral Characteristics of Microwave Bursts
Proc. of NASA Symp. of High Energy Phenom. on the Sun, X-693-73-193 (May 1973)

HARVEY, R. B., and LEWIS, E. A.
Radio Mapping of 250- and 925-Megahertz Noise Sources in Clouds
J. of Geophys. Res., Vol. 78, No. 12 (April 1973)

JOHLER, J. R., (Inst. for Telecomm. Sci., Boulder, Colo.), and HOROWITZ, S.
Propagation of the LORAN C Ground and Ionospheric Wave Pulses
Inst. for Telecomm. Sci. Rpt. (January 1973)
Reflection Coefficients for the Computer Simulation of LORAN C/D Pulse Propagation Transforms
Inst. for Telecomm. Sci. Rpt. (May 1973)

KLOBUCHAR, J. A.
Polarization of VHF Waves Emitted from Geostationary Satellites
Addendum to the Jt. Satellite Studies Gp. Rpt. No. 5
CNET, Lannion, Fr. (January 1974)

KLOBUCHAR, J. A., and AARONS, J.
Numerical Models of Total Electron Content Over Europe and the Mediterranean and Multi-Station Scintillation Comparisons
AGARDograph (November 1973)

KLOBUCHAR, J. A., and TAVES, E. H., MENZEL, D. H. (Harvard/Smithsonian Natl. Geog. Expedition, Cambridge, Mass.)
Ionospheric Total Electron Content Measurements from Mauritania During the Total Solar Eclipse of June 30, 1973
Addendum to the Jt. Satellite Studies Gp. Rpt. No. 5 CNET, Lannion, Fr. (January 1974)

KOSSEY, P. A., RASMUSSEN, J. E., and LEWIS, E. A.
VLF Pulse Ionosounder Measurements of the Reflection Properties of the Lower Ionosphere
Space Res. XIV, Akademie-Verlag, Berlin, Ger. (1974)

LEWIS, E. A., RASMUSSEN, J. E., and KOSSEY, P. A.
Measurements of Ionospheric Reflectivity from 6 to 35 kHz
J. of Geophys. Res., Vol. 78, No. 19 (July 1973)

MENDILLO, M., and EVANS, J. V. (Lincoln Lab., Lexington, Mass.)
Incoherent Scatter Observations of the Ionospheric Response to a Large Solar Flare
Radio Sci., Vol. 9, No. 2 (February 1974)

MENDILLO, M., and KLOBUCHAR, J. A.
Synoptic F-Region Studies Using Contour Mapping Techniques
Addendum to the Jt. Satellite Studies Gp. Rpt. No. 5 CNET, Lannion, Fr. (January 1974)

MENDILLO, M., KLOBUCHAR, J. A., ET AL
The Behavior of the Ionospheric F-Region During the Great Solar Flare of 7 August 1972
J. of Geophys. Res., Vol. 79, No. 4 (February 1974)

MENDILLO, M., KLOBUCHAR, J.A., and D-H. CHUNG, (Weston Obsv., Weston, Mass.)
Ionospheric and Geomagnetic Behavior at Mid-Latitudes During the Solar Events of August 1972
Collected Data Rpts. on Aug. 1972 Solar-Terrestrial Events, World Data Ctr. A for Solar Terrestrial Phys., Rpt. UAG-28, Pt. II, Boulder, Colo. (July 1973)

MENDILLO, M., KLOBUCHAR, J. A., and HAJEB-HOSSEINIEH, H. (Boston Univ., Mass.)
Ionospheric Disturbances: Evidence for the Contraction of the Plasmasphere During Severe Geomagnetic Storms
Planetary and Space Sci., Vol. 22 (1974)

MENDILLO, M., PAPAGIANNIS, M. D. (Boston Univ., Mass.), and KLOBUCHAR, J. A.
The Average Behavior of the Mid-Latitude F-Region Parameters N_t, N_{max}, and τ During Geomagnetic Storms
J. of Geophys. Res., Vol. 77, No. 25 (1 September 1972)

MULLEN, J. P.
Sensitivity of Equatorial Scintillation to Magnetic Activity
J. of Atm. and Terrestrial Phys., Vol. 35, No. 6 (June 1973)
Activities Report . May 1973 - 31 December 1973, Radio Astronomy Branch, Air Force Cambridge Research Laboratories, Bedford, Massachusetts 01730
Addendum to the Jt. Satellite Studies Gp. Rpt. No. 5 CNET, Lannion, Fr. (January 1974)

MULLEN, J. P., and WHITNEY, H. E.
Equatorial Scintillation Measurements Using the LES-6 and ATS-3 Satellite Beacons
Jt. Satellite Studies Gp. Rpt. No. 5 CNET, and Addendum to this Rpt., Lannion, Fr. (January 1974)

NIELSEN, E. (Bartol Res. Fdn., Swarthmore, Pa.), and AARONS, J.
Satellite Scintillation Observations Over the Northern High Latitude Regions
J. of Atm. and Terrestrial Phys., Vol. 36 (1974)

PAPAGIANNIS, M. D., ARORA, K., KOGUT, J. (Boston Univ.), and STRAKA, R. M.
Polarization Observations of Solar Active Regions at 7.875 GHz
Bull. of the Am. Astronom. Soc., Vol. 5, No. 4, Pt. 1 (1973)

PFISTER, W.
Critical Survey of Electron and Ion Temperatures Measured with Probes
Space Res. XII, Akademie-Verlag, Berlin, Ger. (1972)

PFISTER, W., and BIBL, K. (Lowell Technol. Inst. Res. Fdn., Lowell Mass.)
A Modernized Technique for Ionospheric Drifts with Spectral Analysis
Space Res. XII, Akademie-Verlag, Berlin, Ger. (1972)

PIKE, C. P.
Equatorward Shift of the Polar F-Layer Irregularity Zone as a Function of the Kp-Index
J. of Geophys. Res., Vol. 77, No. 34 (1972)
DAPP Satellite Observations of Auroras
EOS Trans. of the Am. Geophys. Union, Vol. 55, No. 6 (June 1974)

PIKE, C. P., and WHALEN, J. A.
Satellite Observations of Auroral Substorms
J. of Geophys. Res., Vol. 79, No. 7 (July 1974)

REINISCH, B. W. (Lowell Technol. Inst. Res. Fdn., Lowell, Mass.), and SALES, G. S.
Multifrequency Long Wave Vertical Sounding of the Lower Ionosphere

Space Res. XIV, Akademie-Verlag, Berlin, Ger. (1973)

RICHMOND, A. D.
Equatorial Electrojet – I. Development of a Model Including Winds and Instabilities
J. of Atm. and Terrestrial Phys., Vol. 35, No. 6 (June 1973)

ROGERS, J.W., MURPHY, R.E., STAIR, A.T. (Opt. Phys. Lab.), ULWICK, J.C., and BAKER, K.D., JENSEN, L.L. (Utah State Univ.)
Rocket Borne Radiometric Measurements of OH in the Auroral Zone
J. of Geophys. Res., Vol. 78, No. 30 (20 October 1973)

RUSH, C. M.
Some Effects of Neutral Wind Changes on the Low Latitude F Region
J. of Atm. and Terrestrial Phys., Vol. 34, No. 8 (August 1972)
Some Effects of Neutral Air Wind Changes on the Low Latitude F Region
Proc. of the 4th Intl. Symp. on Equatorial Aeron., Ibadan, Nig., 4-11 Sep. 1972, Ed. by Ebun Oni, Univ. of Ibadan (1973)

RUSH, C. M., and MILLER, D. (Arcon Corp., Wakefield, Mass.)
Some Aspects of the Day-to-Day Variability of the Equatorial Anomaly: American and Japanese Sectors
Radio Sci., Vol. 1, No. 12 (December 1972)

RUSH, C. M., and RICHMOND, A. D.
The Relationship Between Day-to-Day Changes in the Strength of the Equatorial Electrojet and the Structure of the Appleton Anomaly
J. of Atm. and Terrestrial Phys., Vol. 35, No. 6 (June 1973)
The Relationship Between the Structure of the Equatorial Anomaly and the Strength of the Equatorial Electrojet
Proc. of the 4th Intl. Symp. on Equatorial Aeron., Ibadan, Nig., 4-11 Sep. 1972, Ed. by Eban Oni, Univ. of Ibadan (1973)

SAGALYN, R. C., ET AL
ISIS-I Observations of the High-Latitude Ionosphere During a Geomagnetic Storm
J. of Geophys. Res., Vol. 77, No. 31 (November 1972)

SAGALYN, R. C., and BEWERSDORFF, A. B. (Regis Coll., Weston, Mass.)
Spatial and Temporal Variations of the Thermal Plasma Between 3000 and 5700 Kilometers and L = 2 to 4
J. of Geophys. Res., Vol. 77, No. 25 (September 1972)

SINGLETON, D. A.
The Dependence of High-Latitude Ionospheric Scintillations on Zenith Angle and Azimuth
J. of Atm. and Terrestrial Phys., Vol. 35 (1973)

Power Spectra of Ionospheric Scintillations
J. of Atm. and Terrestrial Phys., Vol. 36 (1974)

SLACK, F. F.
Quasiperiodic Scintillation in the Ionosphere
J. of Atm. and Terrestrial Phys., Vol. 34 (1972)

SNYDER, A. L. (AF Global Wea. Cent., Offutt AFB, Neb.), AKASOFU S.-I. (Univ. of Alaska), and PIKE, C.P.
The Day-Sector Polar F Layer During a Magnetospheric Substorm
Planetary and Space Sci., Vol. 21, No. 3 (March 1973)

SNYDER, A. L. (AF Global Wea. Cent., Offutt AFB, Neb.), BUCHAU, J., and AKASOFU, S.-I. (Univ. of Alaska)
Formation of Auroral Patches in the Midday Sector During a Substorm
Planetary and Space Sci., Vol. 20. No. 7 (July 1972)

TANAKA, H. (Nagoya Univ., Toyokawa, Jap.), CASTELLI, J. P. and COVINGTON, A. E. (Natl. Res. Council, Ottawa, Can.), KRUGER, A. (Heinrich-Hertz-Inst., Berlin-Adlershof, D.D.R.), LANDECKER, T. L. (Univ. of Sydney, Aust.), TLAMICHA, A. (Acad. of Sci., Ondrejov, Czech.)
Absolute Calibration of Solar Radio Flux Density in the Microwave Region
Solar Phys., Vol. 29, No. 1 (1973)

ULWICK J. C.
Eclipse Rocket Measurements of Charged Particle Concentrations
J. of Atm. and Terrestrial Phys. Vol. 34 (1972)
Steady State Coefficients in the D-Region During Solar Particle Events
Space Res. XIII, Akademie-Verlag, Berlin, Ger. (1973)
Analysis of HAES Results: ICECAP 72
Final Rpt., DNA 3247F (1974)
Ion Composition in an IBC Class II Aurora I Measurements
J. of Geophys. Res., Vol. 79, No. 19 (1974)
Altitude Profiles of Infrared Radiance of O_3 (9.6 μ m) and CO_2 (15 μ m)
Geophys. Res. Ltrs., Vol. 1, No. 3 (1974)

WAGNER, R. A. and SNYDER, A. L. (AF Global Wea. Cent., Offutt AFB, Neb.), AKASOFU S.-I. (Univ. of Alaska)
The Structure of the Polar Ionosphere During Exceptionally Quiet Periods
Planetary and Space Sci., Vol. 21, No. 11 (November 1973)

WHALEN J. A. and PIKE, C. P.
F-Layer and 6300 Å Measurements in the Day Sector of the Auroral Oval
J. of Geophys. Res., Vol. 78, No. 9 (July 1973)

WHITNEY, H. E.
Notes on the Relationship of Scintillation Index to Probability Distributions and Their Uses in System Design
Addendum to the Jt. Satellite Studies Gp. Rpt. No. 5
CNET, Lannion, Fr. (January 1974)

WHITNEY, H. E., AARONS, J., ALLEN, R. S., and SELMANN, D. R.
Estimation of the Cumulative Amplitude Probability Distribution Function of Ionospheric Scintillations
Radio Sci., Vol. 7, No. 12 (December 1972)

PAPERS PRESENTED AT MEETINGS JULY 1972 - JUNE 1974

AARONS, J.
F-Layer Irregularities During the August Events
Fall Ann. Mtg. of the Am. Geophys. Union, San Francisco, Calif.
(4-7 December 1972)
The Effect of Magnetic Storms on Scintillation at Sub-Auroral and Auroral Latitudes
Jt. Satellite Studies Gp. Tech. Mtg., Lannion, Fr.
(28 January - 2 February 1974)

AARONS, J., and MARTIN, E.
(Emmanuel Coll., Boston, Mass.)
A High Latitude F-Layer Irregularity Model and the August 1972 Magnetic Storms
1973 Intl. IEEE/G-AP Symp. and USNC/URSI Mtg., Univ. of Colo., Boulder, Colo. (21-24 August 1973)

AARONS, J., MENDILLO, M., and KLOBUCHAR, J.A.
Studies of the Ionospheric F-Region Near the 70° W Meridian
55th Ann. Spring Mtg. of the Am. Geophys. Union, Wash., D.C. (8-12 April 1974)

ALLEN, R.S.
Evaluation of Models of Electron Density Profiles
Jt. Satellite Studies Gp. Tech. Mtg., Lannion, Fr.
(28 January - 2 February 1974)

ALTSHULER, E.E., WULFSBERG, K.N. (Microwave Phys. Lab.), and KALAGHAN, P.M.
Atmospheric Emission Statistics at 35 GHz
IUCRM Colloq. on the Fine Scale Structure of Precipitation and EM Propagation, Observatoire de Nice, Fr. (23-31 October 1973)

BAKER, D. J., KEMP, J. C. (Electro-Dyn. Lab., Utah State Univ.), BRUCE, M. (Opt. Phys. Lab.), and ULWICK, J. C.
Rocket Measurements of Near Infrared Auroral Spectra
1973 Ann. Am. Geophys. Union Mtg., Wash., D. C.
(16-20 April 1973)

BASU, S.
Spectral Characteristics of Solar Radio Bursts Associated with the Emission of Energetic Electrons from the Sun
Symp. on Near Space Envmt. and Radio Comm. (NSERC), New Delhi, India (14-20 February 1973)

BASU, S., AARONS, J., and VESPRINI, R. L. (Emmanuel Coll., Boston, Mass.)
Field-Aligned Ionospheric E-Region Irregularities and Sporadic E
Symp. on Near Space Envmt. and Radio Comm. (NSERC), New Delhi, India (14-20 February 1973)

BIBL, K. (Lowell Technol. Inst. Res. Fdn., Lowell, Mass.), PFISTER, W., and REINISCH, B. W. (Lowell Technol. Inst. Res. Fdn., Lowell, Mass.), SALES, G. S.
Velocities of Small and Medium Scale Ionospheric Irregularities Deduced from Doppler and Arrival Angle Measurements
1974 Intl. Symp. on Solar Terrestrial Phys./17th Plenary Mtg. of COSPAR, Sao Paulo, Brazil (17 June - 1 July 1974)

BIBL, K., REINISCH, B. W. (Lowell Technol. Inst. Res. Fdn., Lowell, Mass.), PFISTER, W., and SALES, G. S.
Radio Doppler Probing of Ocean Surface
1973 Intl. IEEE/G-AP Symp. and USNC/URSI Mtg., Univ. of Colo., Boulder, Colo. (21-24 August 1973)

BUCHAU, J., PIKE, C. P., and WONG, M.
Detailed Specification of the Arctic Ionosphere and an Application to Three-Dimensional Ray Tracing
OHD Tech. Rev. Mtg., Colorado Springs, Colo.
(2-3 May 1973)
A Case Study of 3-Dimensional Ray Tracing in the Arctic Nighttime Ionosphere
1973 Intl. IEEE/G-AP Symp. and USNC/URSI Mtg., Univ. of Colo., Boulder, Colo. (21-24 August 1973)

BUCHAU, J., and WAGNER, R. A.
Extended Observations of Discrete and Continuous Aurora in the Oval Midnight Sector
1973 Ann. Am. Geophys. Union Mtg., Wash., D. C.
(16-20 April 1973)

CASTELLI, J. P.
Investigation of Solar Radio Burst Parameters at AFCRL
Mtg. of the Com. of Eur. Solar Radio Astron. (CESRA), Obsv. of Univ. of Bordeaux, Fr.
(20-23 September 1972)

CASTELLI, J. P., BARRON, W. R., and AARONS, J.
Solar Radio Burst Spectra and Flux Densities for the Proton Flares of Early August 1972
Fall Ann. Mtg. of the Am. Geophys. Union, San Francisco, Calif. (4-7 December 1972)

CASTELLI, J. P., and CARRIGAN, A. L. (Space Phys. Lab.), KO, H. C. (Ohio State Univ.)

Spectral Association of the 7 August 1972 Solar Radio Burst with Particle Acceleration
IAU Symp., Southport, Queensland, Aust. (7-11 September 1973)

CASTELLI, J. P., GUIDICE, D. A., and KALAGHAN, P. M.
Millimeter Wave Solar Observations
1974 IEEE G-MTT Intl. Symp. and USNC/URSI Mtg., Ga. Inst. of Technol., Atlanta, Ga. (11-13 June 1974)

CORMIER, R. J.
Ionospheric Physics Laboratory Research Programs and Their Potential Benefit to Polar Cap III
(Inv.) Test Planning Mtg. for Polar Cap III, Griffiss AFB, Rome, N. Y. (11 July 1972)
Riometer Observations During the August 1972 Polar Cap Absorption Events
Fall Ann. Mtg. of the Am. Geophys. Union, San Francisco, Calif. (4-7 December 1972)

ELKINS, T. J.
Empirical Model of Topside F-Region
Empirical Model of High Latitude E and F1 Regions
AFCRL Electron Density Data Base
ARPA-Sponsored Mtg. on Iono. Modeling, NOAA, Boulder, Colo. (31 October - 2 November 1972)
A Model of the Polar E and F_2 Layers
Fall Ann. Mtg. of the Am. Geophys. Union, San Francisco, Calif. (4-7 December 1972)
Empirical Model of the Polar Ionosphere
1973 Ann. Am. Geophys. Union Mtg., Wash., D. C. (16-20 April 1973)

GUIDICE, D. A., and CASTELLI, J. P.
Spectral Characteristics of Solar Microwave Bursts
NASA High Energy Phenom. on the Sun Symp., NASA Goddard Space Flt. Ctr., Greenbelt, Md. (28-30 September 1972)

GUIDICE, D. A., and FERIOLI, C. P.
Separation and Determination of Gain Boresight and Beamwidth Differences in Dual Beam Antennas
IEEE/G-AP Intl. Symp., Williamsburg, Va. (11-14 December 1972)

HARRISON, R. P.
Demonstration of Transverse Electric (TE) Mode Radio Propagation in the Earth-Ionosphere Waveguide
AFSC Sci. and Engrg. Symp., Kirtland AFB, N. M. (2-4 October 1973)

HAWKINS, G. S.
Ionospheric Electron Content and Radio Scintillations During Magnetospherically Quiet Periods in 1970-71
55th Ann. Spring Mtg. of the Am. Geophys. Union, Wash., D. C. (8-12 April 1974)

HECKSCHER, J. L.
Rocket Plume DC Electrical Properties
1972 AFSC Sci. and Engrg. Symp., San Antonio, Tex. (17-19 October 1972)

HOROWITZ, S., and JOHLER, J. R. (Inst. for Telecomm. Sci., Boulder, Colo.)
Results of a Computer Simulation of the LORAN-C Radio Pulse Employing Full Wave Propagation Theory
1973 Intl. IEEE)G-AP Symp. and USNC/URSI Mtg., Univ. of Colo., Boulder, Colo. (21-24 August 1973)

HUMPHREY, L. C. (Gen. Elec. Co., Syracuse, N. Y.), TOMAN, K., and ROBERTS, C. R. (Gen. Elec. Co., Syracuse, N. Y.)
High Altitude Focusing by Earth Detached Modes Below the D Region
1973 Intl. IEEE/G-AP Symp. and USNC/URSI Mtg., Univ. of Colo., Boulder, Colo. (21-24 August 1973)

JOHLER, J. R. (Inst. for Telecomm. Sci., Boulder, Colo.), and HOROWITZ, S.
Propagation of the LORAN Pulse Over Irregular Inhomogeneous Ground
AGARD Electmg. Wave Propagation Panel XX Mtg., The Netherlands (25-29 March 1974)

KALAGHAN, P. M.
Spectral Characteristics of Solar Active Regions in the 9.1 cm to 3.4 mm Wavelength Range
140th Mtg. of the Am. Astronom. Soc., Ohio State Univ., Columbus, Ohio (25-28 June 1973)
Solar Limb Brightening at λ 8.6 mm
1973 Intl. IEEE/G-AP Symp. and USNC/URSI Mtg., Univ. of Colo., Boulder, Colo. (21-24 August 1973)

KLOBUCHAR, J. A.
Polarization of VHF Waves Emitted from Geostationary Satellites
Jt. Satellite Studies Gp. Tech. Mtg., Lannion, Fr. (28 January - 2 February 1974)

KLOBUCHAR, J. A., and MENDILLO, M.
Behavior of Equivalent Slab Thickness at a Northern Mid-Latitude Station
1973 Ann. Am. Geophys. Union Mtg., Wash., D. C. (16-20 April 1973)

KLOBUCHAR, J.A., and TAVES, E. H., MENZEL, D. H. (Harvard/Smithsonian Natl. Geog. Expdn., Cambridge, Mass.)
Ionospheric Total Electron Content Measurements from Mauritania During the Total Solar Eclipse of June 30, 1973
Jt. Satellite Studies Gp. Tech. Mtg., Lannion, Fr. (28 January - 2 February 1974)

KOSSEY, P. A., RASMUSSEN, J. E., and LEWIS, E. A.
VLF Pulse Ionosounder Measurements of the Reflection Properties of the Lower Ionosphere

16th Plenary Mtg. of COSPAR, Konstanz, Fed. Rep. of Ger. (23 May - 6 June 1973)

MAHAN, H. P. (Univ. of Mass.), SMIDDY, M., and SAGALYN, R. C.
Parallel B Electric Fields Between 120 Km and 165 Km
1973 Ann. Am. Geophys. Union Mtg., Wash., D. C. (16-20 April 1973)

MENDILLO, M., and KLOBUCHAR, J. A.
Preliminary Results of a Multi-Station Analysis of Total Electron Content Variations During Geomagnetic Storms
1973 Ann. Am. Geophys. Union Mtg., Wash., D. C. (16-20 April 1973)
Synoptic F-Region Studies Using Contour Mapping Techniques
Jt. Satellite Studies Gp. Tech. Mtg., Lannion, Fr. (28 January - 2 February 1974)

MENDILLO, M., KLOBUCHAR, J. A., CASTELLI, J. P., ET AL
Total Electron Content Increases During the Great Solar Flare of 7 August 1972
1973 Intl. IFEE/G-AP Symp. and USNC/URSI Mtg., Univ. of Colo., Boulder, Colo. (21-24 August 1973)

MENDILLO, M., KLOBUCHAR, J. A., and CHUNG, D. H. (Boston Coll./Weston Obsv., Mass.)
Ionospheric and Geomagnetic Observations During the August 1972 Solar-Terrestrial Events
Fall Ann. Mtg. of the Am. Geophys. Union, San Francisco, Calif. (4-7 December 1972)

MENDILLO, M., KLOBUCHAR, J. A., and CONWAY, E. (ACSI, Burlington, Mass.)
A 5-Year Summary of Ionospheric Storm Effects at a Mid-Latitude Site
55th Ann. Spring Mtg. of the Am. Geophys. Union, Wash., D. C. (8-12 April 1974)

MULLEN, J. P.
Sensitivity of Equatorial Scintillation to Magnetic Activity
4th Intl. Symp. on Equatorial Aeron., Univ. of Ibadan, Ibadan, Nig. (4-11 September 1972)

MULLEN, J. P., and WHITNEY, H. E.
Equatorial Scintillation Measurements Using the LES-6 and ATS-3 Satellite Beacons
1st Lloyd V. Berkner Symp. on Irreg. in the Equatorial Iono., Univ. of Texas at Dallas (14-17 May 1973); Jt. Satellite Studies Gp. Tech. Mtg., Lannion, Fr. (28 January - 2 February 1974)

MURPHY, R. E., ROGERS, J. W., STAIR, A. T., JR. (Opt. Phys. Lab.), and ULWICK, J. C.
Rocket-Borne Radiometric Hydroxyl Observations
DNA Atm. Eff. Symp., San Diego, Calif. (9-13 April 1973)

PAPAGIANNIS, M. D., ARORA, K., KOGUT, J. (Boston Univ. Mass.), and STRAKA, R. M.
Polarization Observations of Solar Active Regions at 7.875 GHz
141st Mtg. of the Am. Astronom. Soc., Tucson, Ariz. (3-6 December 1973)

PFISTER, W.
Drift Measurement with Spectral Analysis During Period of Chemical Releases into the Ionosphere
16th Plenary Mtg. of COSPAR, Konstanz, Fed. Rep. of Ger. (23 May - 6 June 1973)

PHELPS, A. D. R., and SAGALYN, R. C.
Power Spectra of Plasma Density Irregularities in the Topside Ionosphere
1973 Ann. Am. Geophys. Union Mtg., Wash., D. C. (16-20 April 1973)

PIKE, C. P.
F-Layer Irregularity Zone Observations in the Midnight Sector of the Auroral Oval
1973 Ann. Am. Geophys. Union Mtg., Wash., D. C. (16-20 April 1973)
Airborne and Satellite Observations of the Auroral Oval and the High-Latitude Ionosphere
Inv. Sem., Univ. of Texas at Dallas (1 May 1973)
Cleft Dynamics Inferred from Airborne Ionospheric and Optical Observations
(Inv.) AGU Magneto. Cleft Symp., Dallas, Tex. (1-3 November 1973)

PIKE, C. P., and WHALEN, J. A.
Relationship Between Discrete-Oval Auroras, Continuous Aurora, and Red (6300A) Band Near Midnight
1973 Ann. Fall Mtg. of the Am. Geophys. Union, San Francisco, Calif. (10-14 December 1973)

PIKE, C. P., WHALEN, J. A., BUCHAU, J., and WAGNER, R. A.
Relationship Between Discrete, Oval Auroras, the Continuous Aurora, and the Red Band During Auroral Substorms
Electrodyn. of Substorms and Mag. Storms Mtg., Basye, Va. (11-14 June 1974)

PIKE, C. P., WHALEN, J. A., and SNYDER, A. L. (AF Global Wea. Cent., Offutt AFB, Neb.)
Observed Correlations Between Interplanetary Magnetic Field Variations and the Dynamics of the Auroral Oval and High-Latitude Ionosphere
Fall Ann. Mtg. of the Am. Geophys. Union, San Francisco, Calif. (4-7 December 1972)

REINISCH, B. (Lowell Technol. Inst. Res. Fdn., Lowell, Mass.), and SALES, G. S.
Multifrequency, Long Wave, Vertical Sounding of the Lower Ionosphere

16th Plenary Mtg. of COSPAR, Konstanz, Fed. Rep. of Ger. (23 May - 6 June 1973)

RICHMOND, A. D.
A Study of the Equatorial Electrojet with a Model Including Winds and Instabilities
4th Intl. Symp. on Equatorial Aeron., Univ. of Ibadan, Ibadan, Nig. (4-11 September 1972)

ROGERS, J. W., MURPHY, R. E., STAIR, A. T., JR. (Opt. Phys. Lab.), ULWICK, J. C., and BAKER, K. D., JENSEN, L. L. (Utah State Univ.)
Rocket Ba Radiometric Measurements of OH in the Auroral Zo.
Intl. Assoc. for Geomag. and Aeron., Kyoto, Jap. (9-21 September 1973)

RUSH, C. M.
Some Effects on Neutral Air Wind Changes on the Low Latitude F Region
4th Intl. Symp. on Equatorial Aeron., Univ. of Ibadan, Ibadan, Nig. (4-11 September 1972)

RUSH, C. M., and RICHMOND, A. D.
The Relationship Between Day-to-Day Changes in the Strength of the Equatorial Electrojet and the Structure of the Appleton Anomaly
4th Intl. Symp. on Equatorial Aeron., Univ. of Ibadan, Ibadan, Nig. (4-11 September 1972)

SAGALYN, R. C., and PHELPS, A. D. R.
Irregularity Scale Sizes in the Dayside Polar Cleft
AGU Magneto. Cleft Symp., Dallas, Tex. (1-3 November 1973)

SAGALYN, R. C., WILDMAN, P. J. L., BREDESEN, S. C., and RAO, L., AHMED, M. (Regis Coll., Weston, Mass.)
Topside Ionosphere Irregularities at High Latitudes
1973 Ann. Am. Geophys. Union Mtg., Wash., D. C. (16-20 April 1973)

SALES, G., VIDEBERG, J., and HUMPHREY, L. (Gen. Elec. Co., Syracuse, N. Y.)
Multihop Caustics at Oblique Angles in Long Range D-Region Propagation
1973 Intl. IEEE/G-AP Symp. and USNC/URSI Mtg., Univ. of Colo., Boulder, Colo. (21-24 August 1973)

SANDOCK, J. A., ULWICK, J. C., and GRIEDER, W. F. (Utah State Univ.)
E Region Effective Recombination Coefficients from Auroral Measurements
1973 Ann. Am. Geophys. Union Mtg., Wash., D. C. (16-20 April 1973)

STAIR, A. T., JR. (Opt. Phys. Lab.), and ULWICK, J.C.
IR Measurements in Auroras
2nd Conf. of Appl. of Chem. to Nuc. Wpn. Eff., Inst. for Def. Analys., Arlington, Va. (12-14 September 1972)

TOMAN, K.
The Pc5 Event of 9-10 October 1969
Fall Ann. Mtg. of the Am. Geophys. Union, San Francisco, Calif. (4-7 December 1972)
Hydromagnetic Pumping of the Ionosphere
Fall URSI Mtg., Williamsburg, Va. (11-15 December 1972)
On Wavelike Perturbations in the Ionosphere
1973 Intl. IEEE/G-AP Symp. and USNC/URSI Mtg., Univ. of Colo., Boulder, Colo. (21-24 August 1973)

TOMAN, K., and MARTINE, J. E. (Boston Coll., Mass.)
Study of Source Location Error by Computer Simulation
1973 Intl. IEEE/G-AP Symp. and USNC/URSI Mtg., Univ. of Colo., Boulder, Colo. (21-24 August 1973)

ULWICK, J. C.
Effective Recombination Coefficients and Lumped Parameters in the D Region During Solar Particle Events
2nd Conf. of Appl. of Chem. to Nuc. Wpn. Eff., Inst. for Def. Analys., Arlington, Va. (12-14 September 1972)

ULWICK, J. C., and HEGBLOM, E. R. (Boston Coll., Mass.), REIDY, W. P. (Visidyne, Inc., Burlington, Mass.), BURT, D. A. (Utah State Univ.)
Production Rates, Ionization and Effective Recombination Coefficients in a Class II Aurora
DNA Atm. Eff. Symp., San Diego, Calif. (9-13 April 1973)

ULWICK, J. C., and MANLEY, D. P., SMITH, H., CARPENTER, J. W. (Visidyne Corp., Burlington, Mass.)
Comparison of Rocket Measurements with Code Results
1973 Ann. Am. Geophys. Union Mtg., Wash., D. C. (16-20 April 1973)

VIDEBERG, J., SALES, G., and ROBERTS, C. (Gen. Elec. Co., Syracuse, N. Y.), TOMAN, K.
Low-Loss MF Transmission Via Whispering Gallery Modes in the D Region
1973 Intl. IEEE/G-AP Symp. and USNC/URSI Mtg., Univ. of Colo., Boulder, Colo. (21-24 August 1973)

WHALEN, J. A.
Coordinated Observations in the Midnight Sector of the Auroral Oval
1973 Ann. Am. Geophys. Union Mtg., Wash., D. C. (16-20 April 1973)
Ionospheric Effects of Substorms
(Inv.) AGU Conf. on Magneto.-Iono Coupling, Yosemite, Calif. (6-8 February 1974)

WHITNEY, H. E.
Notes on the Relationship of Scintillation Index to Probability Distributions and Their Uses in System Design
Jt. Satellite Studies Gp. Tech. Mtg., Lannion, Fr. (28 January - 2 February 1974)

WINNINGHAM, J. D. (Univ. of Texas at Dallas), and PIKE, C. P.
Dynamic Behavior of the Dayside Cleft and the Nightside Distribution of Low Energy Particle Precipitation
(Inv.) Intl. Union of Geod. and Geophys. Gen. Asbly., Kyoto, Jap. (9-21 September 1973)

WONG, M. S.
Ionospheric Ray Tracing and Off-Great-Circle HF Propagation
1973 Intl. IEEE/G-AP Symp. and USNC/URSI Mtg., Univ. of Colo., Boulder, Colo. (21-24 August 1973)

WONG, M. S., and VANGURI, K.-S., FRIEDMAN, M. P. (Arcon Corp., Wakefield, Mass.)
Use of an Accurate Geomagnetic Field for Three-Dimensional Ray Tracing
1973 Intl. IEEE/G-AP Symp. and USNC/URSI Mtg., Univ. of Colo., Boulder, Colo. (21-24 August 1973)

TECHNICAL REPORTS
JULY 1972 - JUNE 1974

AARONS, J., WHITNEY, H. E., ALLEN, R. S., and SEEMANN, D. R.
High Latitude Models, Observations, and Analysis of Ionospheric Scintillations
AFCRL-TR-73-0048 (12 January 1973)

BAKER, D. J., WYATT, C. L., PENDLETON, W. R., JR. (Utah State Univ.), and ULWICK, J. C.
High Altitude Effects Simulation (HAES) Program, Report No. 1: Rocket Launch of a SWIR Spectrometer into an Aurora (ICECAP 72)
AFCRL-TR-74-0077 (5 February 1974)

BUCHAU, J.
Environmental Specification in Support of Defense Satellite Communications System — Ionosonde Measurements
AFCRL-TR-74-0182 (8 April 1974)

BUCHAU, J., PIKE, C. P., and WONG, M.
Detailed Specification of the Arctic Ionosphere and an Application to Three-Dimensional Raytracing
AFCRL-TR-73-0726 (27 November 1973)

CARRIGAN, A. L. (Space Phys. Lab.), and CASTELLI, J. P.
Solar Activity in McMath Region 10789 During Disk Passage, 12 to 15 June 1970
AFCRL-72-0669 (16 November 1972)

CASTELLI, J. P., BARRON, W. R., and AARONS, J.
Solar Radio Activity in August 1972
AFCRL-TR-73-0086 (24 January 1973)

CASTELLI, J. P., and GUIDICE, D. A.
The Radio Event Associated with the Polar Cap Absorption Event of 2 November 1969
Proc. of COSPAR Symp. on Solar Particle Event of Nov. 1969, AFCRL-72-0474 (11 August 1972)

CONLEY, T. D.
Positive Ion Concentrations in the Lower D Region During the November 1969 Solar Particle Event Measured by a Rocket-Borne Gerdien Chamber
Proc. of COSPAR Symp. on Solar Particle Event of Nov. 1969, AFCRL-72-0474 (11 August 1972)

CORMIER, R. J.
PCA Behavior as Observed on Riometers
Proc. of COSPAR Symp. on Solar Particle Event of Nov. 1969, AFCRL-72-0474 (11 August 1972)
Thule Riometer Observations of Polar Cap Absorption Events (1962-1972)
AFCRL-TR-73-0060 (30 January 1973)
Goose Bay Riometer Observations
AFCRL-TR-74-0097 (19 February 1974)
Riometer Measurements
Envmt. Spec. in Support of the Def. Satellite Comm. Sys., AFCRL-TR-74-0182 (8 April 1974)
Thule Riometer Observations During May and June 1972
Compilation of Solar Particle and Interplanetary Meas. Acquired During the Campaign for Integrated Obsns. of Solar Flares (CINOF), AFCRL-TR-74-0271 (June 1974)

ELKINS, T. J.
A Model of Auroral Substorm Absorption
AFCRL-72-0413 (18 July 1972)
Editor, *An Empirical Model of the Polar Ionosphere*
AFCRL-TR-73-0331 (23 May 1973)

FORBES, J. M., CAPT. (Aeron. Lab.), and STRAKA, R. M.
Correlations Between Exospheric Temperature and Various Indicators of Solar Activity
AFCRL-TR-73-0378 (21 June 1973)

GASSMANN, G. J.
Analog Model 1972 of the Arctic Ionosphere
AFCRL-TR-73-0151 (2 March 1973)

GASSMANN, G. J., and BUCHAU, J.
Analysis of Simultaneous Polar Fox II Backscatter and Ionospheric Sounding Data
AFCRL-72-0432 (July 1972)

GASSMANN, G. J., GOWELL, R. W., PIKE, C. P., and WAGNER, R. A.
Airborne Determination of Arctic Ionosphere Cross Sections
AFCRL-72-0525 (5 September 1972)

HARVEY, R. B., HARRISON, R. P., FIELDS, V. C., CAPT., HIRST, G.C., CAPT., KOSSEY, P. A., and LEWIS, E. A.
Rocket Investigations of the VLF Ionospheric Transmission Window
AFCRL-TR-73-0293 (7 May 1973)

HAWKINS, G. S.
Ionospheric Electron Content and Radio Scintillations During Magnetospherically Quiet Periods in 1970-71
AFCRL-TR-74-0160 (28 March 1974)

HAWKINS, G. S., and KLOBUCHAR, J. A.
Seasonal and Diurnal Variations in the Total Electron Content of the Ionosphere at Invariant Latitude 54 Degrees
AFCRL-TR-74-0294 (28 June 1974)

HECKSCHER, J. L., and PAGLIARULO, R. P.
Measurement of Ionic Conductivity and Temperature in the Apollo 15 Plume
AFCRL-TR-73-0124 (26 February 1973)

KALAKOWSKY, C. B., HIRST, G. C., CAPT., and LEWIS, E. A.
Tests of Long Wire Deployment from Supersonic Rockets
AFCRL-TR-73-0553 (28 August 1973)

KALAKOWSKY, C. B., WHIDDEN, R. W., and LEWIS, E. A.
Experiments in Small Rocket Deployment of 1000-Foot-Long Electrically Conducting Filaments
AFCRL-TR-73-0408 (10 July 1973)

KLOBUCHAR, J. A., ET AL
Total Electron Content Studies of the Ionosphere
AFCRL-TR-73-0098 (1 February 1973)

MENDILLO, M.
Magnetospheric Convection at Ionospheric Heights
AFCRL-TR-73-0358 (12 June 1973)

MENDILLO, M., and EVANS, J. V. (MIT Lincoln Lab., Lexington, Mass.)
Millstone Hill Incoherent Scatter Observations of the Ionospheric Response to the Solar Flare of 7 August 1972
AFCRL-TR-73-0686 (6 November 1973)

MENDILLO, M., and KLOBUCHAR, J. A.
An Atlas of the Midlatitude F-Region Response to Geomagnetic Storms
AFCRL-TR-74-0065 (6 February 1974)

NEWELL, D. T., CAPT.
Forecasting Peak Proton Flux and PCA Event Magnitudes Using "Flash-Phase" Integrated Radio-Burst Flux Density
AFCRL-72-0543 (23 August 1972)

PFISTER, W.
Pulse Sounding with Closely Spaced Receivers as a Tool for Measuring Atmospheric Motions and Fine Structure in the Ionosphere. V. Period of Chemical Releases as Example of Spectral Analysis
AFCRL-TR-74-0105 (22 February 1974)
Pulse Sounding with Closely Spaced Receivers as a Tool for Measuring Atmospheric Motions and Fine Structure in the Ionosphere. VI. Spectral Analysis of Interlaced Sets of Data
AFCRL-TR-74-0125 (7 March 1974)

PIKE, C. P., Compiler
Environmental Specification in Support of the Defense Satellite Communications System
AFCRL-TR-74-0182 (8 April 1974)
Results of the Environmental Data Program
Envmt. Spec. in Support of the Def. Satellite Comm. Sys., AFCRL-TR-74-0182 (8 April 1974)

PIKE, C. P., and SNYDER, A. L. (AF Global Wea. Cent., Offutt AFB, Neb.)
Satellite Observations of Auroras
Envmt. Spec. in Support of the Def. Satellite Comm. Sys., AFCRL-TR-74-0182 (8 April 1974)

REINISCH, B. W. (Lowell Technol. Inst. Res. Fdn., Lowell, Mass.), and SALES, G. S.
Multifrequency, Long Wave, Vertical Sounding of the Lower Ionosphere
AFCRL-TR-74-0002 (20 December 1973)

RICHARDS, D. W., CAPT.
Twenty-Element Receive Array for the DAASM Experiment
AFCRL-72-0475 (15 August 1972)

RICHMOND, A. D.
Numerical Model of the Equatorial Electrojet
AFCRL-72-0668 (16 November 1972)

RUSH, C.M., and GIBBS, J. (Arcon Corp., Wakefield, Mass.)
Predicting the Day-to-Day Variability of the Mid-Latitude Ionosphere for Application to HF Propagation Predictions
AFCRL-TR-73-0335 (23 May 1973)

RUSH, C. M., and MILLER, D. (Arcon Corp., Wakefield, Mass.)
A Three-Dimensional Ionospheric Model Using Observed Ionospheric Parameters
AFCRL-TR-73-0567 (10 September 1973)

SAGALYN, R. C., BREDESEN, S. C., and WILDMAN, P. J. L.
Mapping of High Latitude Ionospheric Characteristics
Chap. 2 of An Empirical Model of the Polar Iono., AFCRL-TR-73-0331 (23 May 1973)

SANDOCK, J. A.
Ion Measurements Made by Collapsing the Space Charge Sheath on a Spherical Rocket Probe
Proc. of COSPAR Symp. on Solar Particle Event of Nov. 1969, AFCRL-72-0474 (11 August 1972)

SHANKLAND, D. G., LT. COL.
Fast Spectral Analysis of Linearly Swept Signals
AFCRL-TR-73-0121 (27 February 1973)

TOMAN, K., and MARTINE, J. E. (Boston Coll., Mass.)
Study of Source Location Error by Computer Simulation
AFCRL-TR-73-0684 (6 November 1973)

ULWICK, J. C., Editor
Proceedings of COSPAR Symposium on Solar Particle Event of November 1969
AFCRL-72-0474 (11 August 1972)

Comparison of Black Brant Rocket Measurements of Charged Particle Densities During Solar Particle Events and *Effective Recombination Coefficients and Lumped Parameters in the D Region During Solar Particle Events*
Proc. of COSPAR Symp. on Solar Particle Event of Nov. 1969, AFCRL-72-0474 (11 August 1972)

ULWICK, J. C., and BLANK, C. A. (Def. Nuc. Agcy., Wash., D.C.;)
Summary of Operation PCA 69
Proc. of COSPAR Symp. on Solar Particle Event of Nov. 1969, AFCRL-72-0474 (11 August 1972)

VIDEBERG, J. I., and SALES, G. S.
Long Range Survivable MF Radio Communication Study Using High Altitude Whispering Gallery Modes
AFCRL-TR-73-0552 (28 August 1973)

WHALEN, J. A., WAGNER, R. A., and HONES, E. W., JR., (Univ. of Calif. at Los Alamos, N.M.)
A Case Study Using Aircraft, Satellite and Ground Observations
Envmt. Spec. in Support of the Def. Satellite Comm. Sys., AFCRL-TR-74-0182 (8 April 1974)

WHITNEY, H. E.
Notes on the Relationship of Scintillation Index to Probability Distributions and Their Uses for System Design
AFCRL-TR-74-0004 (3 January 1974)

WONG, M .S
On Signal Decrease in HF Circuits During PCA Events
AFCRL-TR-73-0289 (2 May 1973)

WONG, M. S., and VANGURI, K. -S., FRIEDMAN, M. P. (Arcon Corp., Wakefield, Mass.)
Geomagnetic Field Models for Ray Tracing
AFCRL-TR-73-0294 (8 May 1973)

XI Solid State Sciences Laboratory

Reconnaissance satellites and "smart" bombs are already in the Air Force inventory. High power lasers and high power microwave devices are being developed, as well as materials and devices that can withstand high radiation doses with little or no performance degradation, and infrared sensors of controlled uniformity that can operate in extreme environments and at longer wavelengths. But the optical components for the high power lasers, the radiation-resistant devices, the high power microwave devices, and the improved infrared sensors depend on electromagnetic materials and the sophisticated exploitation of their properties through new device concepts and technologies.

The mission of the Solid State Sciences Laboratory to engage in research on electromagnetic materials and the phenomena they exhibit, and to exploit these phenomena for Air Force use, has been directed in recent years to three major areas: electromagnetic materials research, infrared detector research, and radiation effects and device hardening. Additionally, programs to improve device processing technology, and to apply this technology to primary laboratory goals, have been pursued at a lower level of effort. To conduct these programs, the Laboratory is organized into the Preparation and Growth, Materials Characterization, Opto-Electronic Physics, Device Physics, and Radiation Effects Branches. Each of the major efforts, however, cuts across organizational lines to involve several Branches.

During the reporting period, increased emphasis has been placed on making the Laboratory expertise available to the Air

Force product divisions, particularly the Space and Missile Systems Organization (SAMSO). New emphasis has been placed on consulting within the Air Force and much greater attention given to insuring that the results will meet important needs of today's and tomorrow's Air Force.

The Laboratory is now the principal laboratory within the Air Force and Department of Defense in the fields of electromagnetic materials and radiation hardening, and it has a significant role in advanced detector research. These programs require extensive and unique facilities. The Laboratory can produce almost any optical, semiconductor, or magnetic crystal, either in bulk or single crystal thin film form. Coupled closely with the materials preparation facilities are analytical techniques for determining structure, purity, and properties of these materials. Facilities are also available for fabricating, and then evaluating, prototype devices.

Recent significant advances in semiconductor devices have, unfortunately, been somewhat offset by a greater sensitivity to radiation. To study the effects of ionizing radiation on materials and devices, AFCRL operates an irradiation facility with a wide variety of radiation sources and related analytical facilities.

When polished, this single crystal of rutile was almost clear, with only a slight reddish coloration. Rutile is normally dark brown or black when grown, but this crystal is clear because it was grown in a pure oxygen atmosphere in AFCRL's Thermal Imaging Furnace.

Traditionally, the bulk of the Laboratory's work has been in-house. Because it must maintain extensive in-house facilities and is oriented toward basic research, the Laboratory has used relatively little contract assistance. The need to exploit this research rapidly for military use has caused a large increase in contractual support, particularly for the high power IR laser window and radiation hardening programs. This expansion has been financed by the Laboratory's customers: the Space and Missile Systems Organization (SAMSO), the Air Force Weapons Laboratory (AFWL), the Defense Nuclear Agency (DNA), and the Defense Advanced Research Projects Agency (ARPA).

ELECTROMAGNETIC MATERIALS

An electromagnetic material is one which can usefully manipulate electromagnetic energy. Matter can exist as a gas, liquid, or solid, but our attention is almost totally directed toward the solid state. Enormous payoff continues to result from solid state research, but manipulation of sound and light or phonons and photons in solids is growing in importance to challenge manipulation of electrons. The AFCRL program will continue to capitalize on the numerous characteristics and capabilities of EM materials, and to produce and measure materials which display electronic, acoustic and optical phenomena, and their combinations.

HIGH TEMPERATURE GROWTH METHODS: High quality single crystals have made possible countless solid state devices ranging from transistors to solid state lasers. Many of these devices are household and commercial items. Although the material used in commercial equipment is satisfactory, military equipment requires material that can withstand far more extreme conditions than found in the average household. For this reason, new materials must be de-

veloped for these applications, materials which frequently cannot be produced in single crystal form by conventional methods. Major limitations in single crystal growth are the lack of satisfactory temperature sources and materials in which the molten material can be contained. Three new growth techniques are being investigated at AFCRL in an attempt to overcome this problem.

Thermal imaging has been under investigation for several years. This technique uses mirrors to collect the energy from a high power light source (a xenon lamp) and refocus this energy on the top of a sintered compact of the material to be grown. This creates a molten area on the top of the compact. A seed (small single crystal) of the same material is then dipped into the melt and slowly withdrawn, with the result that the molten material freezes out in single crystal form on the seed as it is withdrawn. This is the Czochralski (pulling) growth method. Under proper condition, temperatures as high as 3,000° C can be reached in this apparatus. Present work is on rutile (TiO_2), a potential polarizer material for high power laser applications. Crystals of this material grown by the usual methods are deeply colored and unusable. The rutile produced by the thermal imaging technique is transparent.

The AFCRL Thermal Imaging Furnace. Light from a high-pressure xenon arc lamp in the lower portion of the furnace is focused by parabolic mirrors onto the material to be melted, in the upper portion. The molten material is shown on the TV monitor to the left of the furnace. The rod in the upper half of the TV picture is pulled upward to remove it from the heated zone, and thereby make the material crystallize. The electronics rack on the right controls the arc lamp current, the rate of rotation of the crystal as it is pulled, and the rate of pulling of the crystal. The gauges in front of the rack meter the flow of gas through the furnace.

A second high temperature growth method is an adaptation of a technique known as skull melting. It uses induction heating to melt the charge in a manner similar to that in which silicon is prepared. However, cooling coils are added to the system. They cool the outer surface of the melt enough to prevent the outer skin of the charge from melting, while the charge inside this skin (or skull) does melt. Thus, the melt is contained within a skin of the same material with the result that there is no hot container, a major source of impurities, in contact with the melt. The apparatus is presently being constructed with the aim of fitting it inside a standard crystal grower so that the atmosphere can also be controlled.

The third technique under investigation is the use of a new material as the heating element in a standard resistance heating mode. Most resistance heating elements are unstable in air above 1800° C. The new material is stable in air to 2200° C and possibly to 2400° C. This should facilitate the growth of several oxides which have melting points in this range. The apparatus is presently being designed.

While not a novel device, a high pressure furnace installed at AFCRL is capable of crystal growth at 100 atmospheres. This can be used for liquid encapsulation growth wherein a molten liquid (B_2O_3) over the melt prevents vaporization of the melt.

Since this encapsulant can be backed by pressures up to 100 atmospheres, highly volatile materials can be grown from the melt. Crystals grown thus far include gallium phosphide, indium phosphide and zinc selenide.

UNIDIRECTIONAL SOLIDIFICATION OF EUTECTICS (USE): Most electromagnetic applications require single crystal material. However, in some recent applications, specially tailored materials involving two separate phases have exhibited properties unobtainable in single crystals. These materials can be formed by the careful solidification of a eutectic, which is the concentration at which a minimum melting temperature is found in a phase diagram. The result on cooling a melt of this concentration is the formation of two well defined phases. If the eutectic occurs in a certain concentration region, well formed thin rods of one phase will occur in a matrix of the second material.

This technique is being employed at AFCRL to produce conducting fibers. In this technique, chromium or molybdenum filaments (thin rods) are produced in a matrix containing aluminum and nickel. The aluminum-nickel matrix is then etched away, producing well formed filaments of chromium or molybdenum.

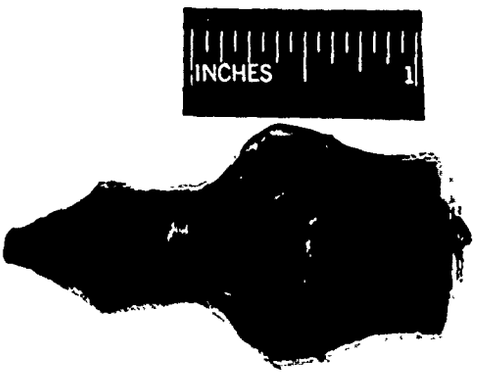

Gallium phosphide crystal grown by a liquid-encapsulated high pressure Czochralski technique.

The scanning electron microscope has proved invaluable in delineating surface topography at the micron level, using its enhanced depth of field, and with the attached non-dispersive X-ray system, has permitted *in situ* qualitative chemical analysis of selected areas three micrometers in diameter. While the microscope is used in other programs, its most striking use was the characterization of the morphology and chemistry of the chromium fibers produced by the USE method.

It is believed that there are many other applications for the USE technique: for example, production of an optical filter by this technique is being considered. Specific examples and applications of this technique and others are illustrated by AlN, ZnSe, and alkali halide growth.

ALUMINUM NITRIDE GROWTH: Aluminum nitride is believed to be an outstanding material for microwave acoustic devices such as surface wave acoustic delay lines, signal correlators and filters. While poor quality films of aluminum nitride have been produced, large single crystals of the material have never been obtained. These crystals are necessary for a true evaluation of the figure of merit calculations which indicate AlN is a potentially efficient SAW material. Two types of crystal growth are being attempted. The first method is solution growth. Calcium nitride has been found to dissolve the material and temperature versus solubility curves have been determined. Well formed crystals larger than a millimeter have been produced and the investigation is continuing. Recently, sublimation has also been employed to grow crystals of aluminum nitride. Early experiments have produced platelets up to 5 mm in length and 2 mm across. These are presently being characterized prior to evaluation of their acoustical properties.

GROWTH OF ZINC SELENIDE: Zinc selenide may be useful both as a transparent high

A high-quality single crystal of zinc selenide grown by chemical vapor transport can be seen at the bottom of the other crystals. This crystal was large enough so that measurements of intrinsic properties could be made, unaffected by the boundaries between crystals of polycrystalline materials.

power laser window and as a semiconductor. While crystals of this material are available, the quality is poor with a tendency for twinning in the crystal. Scientists at AFCRL have attempted a low temperature growth scheme to overcome this problem. This is the chemical vapor transport technique in which a carrier gas reacts with the starting material at one temperature to form a volatile intermediate which is decomposed to form a crystal when it passes from the first temperature zone to a second temperature zone where the intermediate is unstable. Iodine is usually used for this system and was employed for the transport of zinc selenide. Well formed crystals approaching a cubic centimeter have been produced by the technique. Both their optical and semiconductor properties are being evaluated.

HALIDE IR WINDOWS: The increasingly higher power of conventional lasers continues to produce increased demands both on the laser itself and on the supporting equipment. One such supporting element, the window between the laser system and the environment, continues to receive major emphasis at AFCRL. The major objectives are to produce a material that is exceedingly transparent in the IR and yet is high in mechanical strength. Prime materials for this application still appear to be the alkali halides since these are among the only materials with sufficiently low absorption to act as a satisfactory window. The attempts to improve the mechanical strength of the material continue in two directions: alloying and grain boundary introduction. Several materials have been alloyed with potassium chloride (KCl) which continues to be the most promising candidate. The addition of small amounts (in the range of 1 percent) of rubidium chloride has been most successful. This material will harden KCl without adversely affecting its optical properties.

Alloying with rubidium chloride by itself will not produce the mechanical strength necessary for a window. In addition, crystals of sufficient size for this application are not available. Thus, a second process, hot forging, is being investigated, both to improve the strength and to increase the size of the window blank. For the research phase of the work a new hot forging unit has been installed at AFCRL. Work with this unit has produced strengthened alkali halides, principally alloyed KCl, without any loss of optical quality. Alkaline earth fluorides are also being investigated by this technique.

POLYCRYSTALLINE MATERIALS: Practical applications of electro-optic materials such as laser windows, mirrors, and IR domes require sizes and strength available only from polycrystalline materials. As a consequence, our interests have expanded to include polycrystal material. This reorientation has required consideration for the first time of effects of grain boundaries and sub-boundaries other than their resistance

Hot-forging apparatus used for preparation of strengthened alkali halide materials.

to dislocation travel, which is used to strengthen the material. The good and bad effects of grain boundaries acting as diffusion pipes, electrical traps, or as collectors of impurities must be considered when making polycrystalline electromagnetic materials.

The method used to produce polycrystalline material is important because it can produce variations in strength with direction. For example, the CVD process of producing ZnSe results in a material in which the grain boundaries are preferentially oriented along the (111) plane of each crystal. This gives a plate of ZnSe a higher yield strength normal to the plane of the plate than in the plane of the plate. Thus the plate would fail by having layers flake off it, rather than by having a crack go through the thickness of the plate.

SURFACES AND COATINGS: Surface phenomena and thin film coatings are increasingly important as parts of laser systems, integrated optical systems, and the large-scale integrated circuits, so necessary to the complex Command, Control and Communications requirements of modern Air Force technology.

Methods of surface preparation and surface states are studied by a variety of advanced technologies such as Auger spectroscopy and scanning microscopy coupled with non-dispersive X-ray facilities and phase contrast microscopy.

During the past year, a broad spectrum capability for the deposition of thin films for a variety of devices has been established in the Laboratory. A typical example of this part of the program is the study and development of ion beam polishing techniques which illustrated for the first time that the polishing rates will be affected by the individual grain orientations, even when ion polishing is used. However, an appropriate combination of ion rate and incident angle can provide an overall optical figure commensurate with low scattering and low surface absorptance needed for optical elements to be used at high power densities.

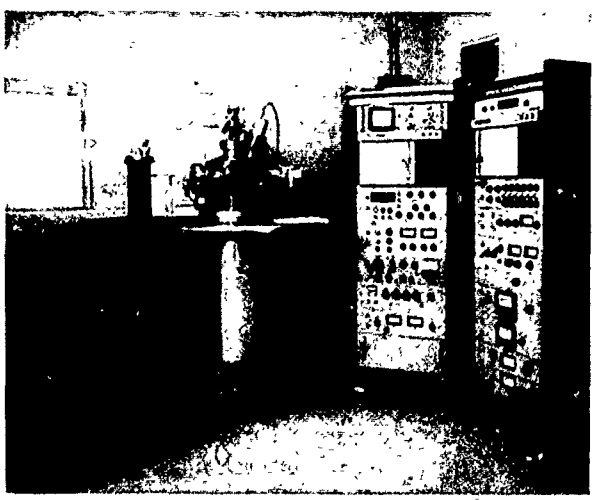

The Auger spectrometer, part of the expanded and continuing interest of the Solid State Sciences Laboratory in surfaces and interfaces, which are important both optically and for evaluating surface, optical, and chemi-absorption, and determining the local chemistry of interfaces, in relation to processing steps. The ability of the system to look at the first five or six atomic layers, coupled with argon sputtering, can give profiles of the chemistry every five atoms in depth, on a continuing basis.

Auger depth profiling has proven a particularly useful tool in evaluating dielectric coatings used in reflective optics for high power laser systems. We can delineate the individual coating species and their thicknesses and then correlate these with anomalously low reflectivities or low damage thresholds.

Much of our surface and thin film work has studied the damage process when "real" conditions were simulated, and thereby improved either the processing or material selection. A typical example of such an integrated study was our comparative evaluation of the damage thresholds at 10.6 micrometers of germanium coated potassium chloride, which clearly showed that the damage threshold of the sputtered coating was significantly higher than that of the typical evaporated coating.

OPTICAL EVALUATION OF LASER WINDOWS: An increasing number of Air Force systems use lasers, particularly infrared lasers. To ensure aerodynamic stability and to help maintain a suitable physical environment for laser operation, windows are needed. Optimum characteristics for a laser window, in addition to physical strength and resistance to severe climatic conditions, include optical performance which minimizes alteration of the laser beam. Defocusing and beam wander are particularly troublesome. However, the minute absorption of the beam by even the best window materials causes heating of the window. This heating is non-uniform over the window area because the intensity profile of the beam is usually Gaussian, and is never uniform. Heating of the window leads to variable changes of the refractive index and non-uniform thermal expansion of the window itself. Beam spreading and degradation of the intensity profile attenuate the beam.

A major element of the Solid State Sciences Laboratory program uses both theory and experiment to specify the most suitable window materials and evaluate their optical performance when used as windows for a variety of lasers.

THEORETICAL ANALYSIS: Almost all the failure modes of laser windows are initiated by the weak residual infrared absorption in these materials. The principal mechanism for this absorption in perfect crystals is multiphonon lattice processes, where many vibrational quanta of the solid are excited by the incident laser beam. Before high power IR lasers became feasible, there was little interest in IR absorption by very transparent materials, and so new theoretical approaches had to be developed at AFCRL to treat the problem. Using many-body physics techniques, a theory was developed to account for the observed frequency and temperature dependence of absorption in typical window materials. The theory successfully accounted for the observations of nearly exponential frequency dependences and temperature dependences weaker than those previously predicted for absorption in a variety of materials.

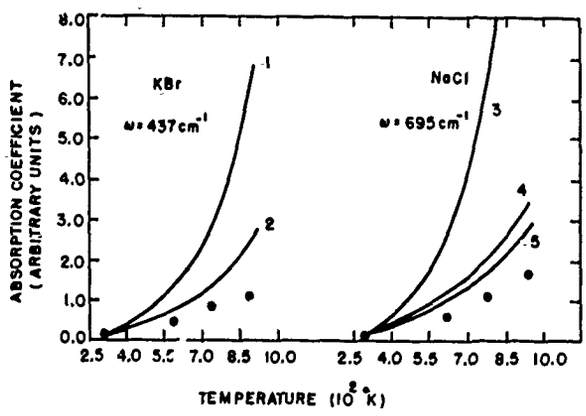

Temperature dependence of multiphonon absorption. The predictions of the older theory of absorption are given by the upper curves (1 and 3), while the predictions of newer theories developed at AFCRL are given by curves 3, 4, and 5, showing a marked improvement in agreement with the experimental data indicated by the dots.

The rate at which the refractive index changes with temperature is a measure of the potential for thermal distortion of laser beams traversing material windows. Observations revealed a wide range of magnitudes and both positive and negative signs for this rate of change in different materials, but no quantitative explanation of the data was available. A theory was developed which was the first to provide a detailed understanding of the principal mechanisms causing the refractive index to change with temperature. It predicted values of refractive index versus temperature which agreed very well with experiments for a wide variety of materials. The theory was based on calculating changes both in energy levels and oscillator strengths of the optical transitions (both lattice and electronic) of the material.

Photoelasticity is the change in refractive index induced by pressure or stress, and is important in predicting the behavior of laser windows due to thermal stresses, or externally applied stresses. Virtually no calculations or experimental data were available in the infrared for laser window materials. For this reason, refinement of a recent theory was pursued which enabled detailed predictions of the IR frequency dependence of the elasto-optic constants for typical window materials.

INFRARED SPECTROSCOPY AND LASER CALORIMETRY

Because of its very low absorption at 10.6 micrometers, potassium chloride (KCl) is an attractive laser window material. It is known that trace impurities contribute significantly to increases in absorption. A study of the wavelength dependence of IR absorption of KCl selectively doped with a variety of impurities known to occur frequently in KCl crystals has determined the effect of hydroxyl and carbonate ions on KCl absorption at 10.6 micrometers. The strongest bands in the spectrum are caused by chlorate ions, indicating that oxygen, probably in the form of the Cl-O structure, is an important contributor to the 10.6 micrometer absorption.

Laser calorimetry is an experimental technique in which a window sample is irradiated by a laser, and the increase in temperature is measured by thermocouples placed on the perimeter of the sample. From such measurements, the absorption of the sample at the wavelength of the laser light can be determined. This technique has shown that adding rubidium chloride to potassium chloride, which improves the mechanical strength of KCl, does not cause a significant increase in absorption. Laser calorimetric experiments, as well as emittance spectroscopy, have been used to establish the effects on optical absorption caused by a variety of surface conditions. Samples used in the experiments were well polished, poorly polished and cleaved crystals. Results indicate that absorption determined by emittance techniques is less sensitive to surface conditions than calorimetry and that surface roughness can enhance scattering and increase absorption.

PHYSICAL OPTICS OF LASER WINDOWS: The first detailed experimental evidence of thermal lensing phenomena in a variety of candidate laser window materials has been demonstrated by using a unique far infrared vidicon system to provide real-time evaluation of transmitted laser beam spatial distribution. Materials studied included zinc selenide (ZnSe), barium fluoride, silicon (Si), cesium bromide and KCl. While some of these materials exhibited the expected thermal lensing behavior, others did not. For example, ZnSe showed predominantly a self-induced interference effect, while silicon exhibited a combination of lensing, interference, and beam oscillation. KCl, a prime candidate for a high power 10.6 micron laser window, showed an off-axis beam wander effect which could result in a time dependent boresight error

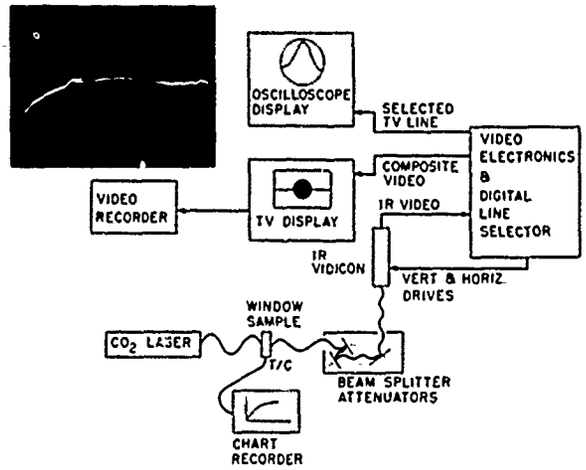

The IR Vidicon system allows observation of the degradation of the laser beam as it happens. The television camera is an IR vidicon with attenuators to prevent TV camera burnout. A videotape can be made so that parameters such as the length of time it takes the window to degrade can be measured for any particular power level.

in systems employing this type of window.

Thermal distributions developing in CO_2 laser-irradiated windows have also been measured on a real-time basis by using a mid-infrared vidicon system sensitive in the 2-5 micrometer range to record thermal re-radiation emitted from the window. It has been shown that scattering of incident laser radiation can result in significant deviations from the expected radial heat distributions in centrally irradiated windows. This problem may have implications in design of edge cooling schemes for high power applications. In addition, the mid-IR vidicon has been used to measure absorption in germanium coatings on KCl windows.

A new laser Doppler interferometric (LDI) calorimeter has been developed for measuring small absorption coefficients in low loss optical materials. This instrument allows the determination of the absorption coefficient in far less time than that required by conventional thermocouple calorimetry and in addition, the data are unaffected by laser beam scattering effects. The LDI has also been used for measuring the temperature change of the refractive index and to provide the thermal profiles in laser window materials. Further, the Doppler shift interferometer has provided optical path length homogeneity data on large size chemical vapor deposited (CVD) ZnSe sheets. The LDI is completely automated and employs an on-line minicomputer for data analysis and graphical data display.

The temperature dependence of the absorption coefficient can be useful for determining whether a material has been purified to its intrinsic limit. This property has been determined at 10.6 micrometers in state of the art and in high resistivity Gallium Arsenide (GaAs) by using laser calorimetry. GaAs showed intrinsic-like behavior in the low temperature region but the absorption increased rapidly above 500° K, perhaps indicating the presence of a deep trap near 0.37 eV. CVD ZnSe did not exhibit intrinsic behavior and hence this material still appears to be surface loss or impurity dominated.

REFRACTIVE PROPERTIES OF LASER WINDOW MATERIALS: The heating of laser window materials caused by optical absorption causes physical swelling of the window, a "lensing" effect, as well as temperature-dependent changes in refractive index. A detailed knowledge of photoelastic and refractive window properties is required for a logical selection of an optimum window material. An experimental program has been established to measure refractive index, its temperature dependence, and stress-optic coefficients at various wavelengths and temperatures of interest. The program has provided data on ZnSe, potassium bromide and lithium fluoride in several crystallographic orientations. Measurements are presently underway on a series of alkali halides and their alloys.

LASER HARDENED MATERIALS RESEARCH: High power lasers can physically damage

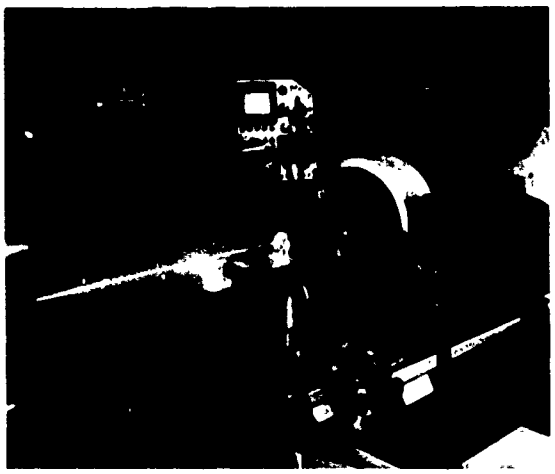

Experimental arrangement for measurement of the wavelength and intensity of the laser-induced fluorescence of impurities in optical components.

any aircraft or missile skin, structural member, control or guidance system. A new element of the Laboratory program studies the protection of a variety of sensitive systems and components from undesirable laser interaction. Airborne IR sensors are of particular interest because a laser beam that is not powerful enough to destroy the sensor can still cause spurious signals so strong that the sensor cannot operate.

This program studies techniques to reflect, attenuate, or absorb selected radiation from a variety of lasers, for particular critical opto-electronic systems and components. Laboratory experiments have shown that tough, highly reflective coatings can be applied to radome materials, and a theoretical effort has been undertaken to specify film thickness and refractive properties of multilayer optical coatings.

RADIATION EFFECTS AND DEVICE HARDENING

During the past two decades, the use of solid state device technology has increased component reliability and decreased component size, both by orders of magnitude. These advances have made space and missile borne computer systems possible. Unfortunately, these solid state devices are also extremely sensitive to radiation of all kinds. Semiconductor devices are sensitive to radiation because their operation depends on a delicate charge balance or high crystalline perfection, both of which are altered at relatively low radiation levels. Temporary or permanent failures will occur at much lower radiation levels than those which would immediately incapacitate a man. Fortunately, almost all of the low level radiation problems are easily solved, as long as their possible existence is known. The AFCRL radiation effects and device hardening program provides information for predicting the effects of radiation on materials and devices and developing radiation hardened devices.

RADIATION-INDUCED TRANSPORT PHENOMENA: When electron beams, X-rays, or gamma rays penetrate materials, they impart sufficient energy to atomic electrons to eject them from their bound states and drive them far from the site of the initial interaction. In this process the electrons lose energy along their entire path and carry charge some distance from the parent atom. This transport of energy and charge produces dose enhancement effects in solid state devices, noise in optical sensors, charge buildup in dielectric components, severe voltage pulses in cables, and destructive electromagnetic signals known as system generated electromagnetic pulses (SGEMP). The prediction uncertainties associated with these phenomena have been typically greater than a factor of 10. An AFCRL study of several transport phenomena was undertaken to reduce uncertainties to acceptable levels.

X-ray photoemission is an example of one of the charge transport phenomena studied at AFCRL. The problem arose in connection with estimating the electron

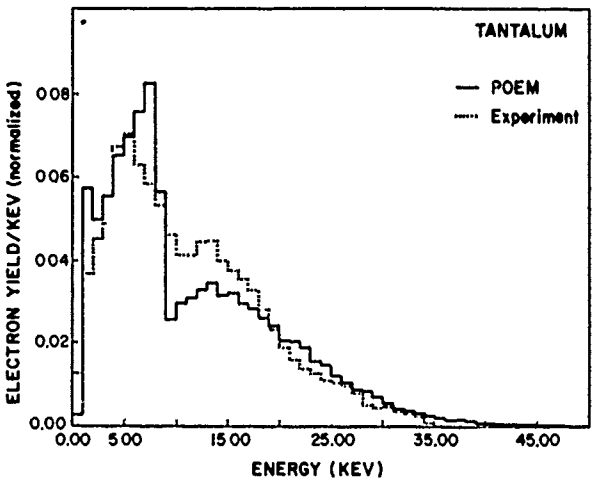

A comparison of the measured energy distribution from tantalum with a distribution computed using the POEM Monte Carlo code. The continuum above 10 keV is largely a reflection of the input photon spectrum shifted down in energy by binding and transport energy losses. The prominent peak at 7 keV is due to Auger emission. The general features of this emission spectrum and the degree of agreement between experiment and theory are typical of results obtained on a number of elements.

currents emitted from the walls of irradiated aerospace systems. Prior to AFCRL's involvement, theoretical models had been tested at gamma ray energies, but there were reasons to doubt their validity when extrapolated to the X-ray regime, and no reliable data were available to test them. Information was needed on the absolute yield of secondary electrons as a function of emission energy and angle for a range of incident X-ray energies and target materials. AFCRL undertook an experimental program designed to furnish this information and modified an existing Monte Carlo electron transport code so that it could be extended to X-ray energies.

Agreement between experimental data and calculated yields as a function of emission energy and angle is satisfactory and, therefore, the experimental effort has been discontinued. There is still a need for more efficient computational methods, and work in this direction is continuing.

Dose enhancement at interfaces is an example of an energy transport phenomenon studied under this program. Ordinary experimental and theoretical methods of determining energy absorbed by irradiated materials (the dose) are not applicable to the boundary region separating materials of different atomic number. Since X-rays produce many energetic electrons in a high atomic number material, a low atomic number material adjacent to it will absorb many of these electrons and thereby experience a large dose enhancement. Solid state devices frequently incorporate high atomic number materials and are, therefore, susceptible to this effect. Factors of 10 errors are possible if the effect is ignored and conventional dosimetry techniques applied.

Experimental techniques were devised at AFCRL which enabled the precise observation of dose profiles at material boundaries and were applied to a wide range of material combinations and X-ray energies. Good agreement has been found with Monte Carlo calculations.

Both of the phenomena described are examples of electron transport phenomena, and the same basic electron transport model can be applied. Other phenomena that are being studied include: Compton photocurrents in materials, charge accumulation in dielectrics, dose fluctuations, correlation of effects, secondary emission, and microdosimetry. The ability to describe all of these effects depends upon knowledge of the electron transport process. The information and general approach which have evolved from these studies promise to bring this problem area under satisfactory control.

DISPLACEMENT EFFECTS: The effects of high energy radiation on the electrical and optical properties of solid state device materials are not only due to ionization effects, but also to displacement damage. Ioniza-

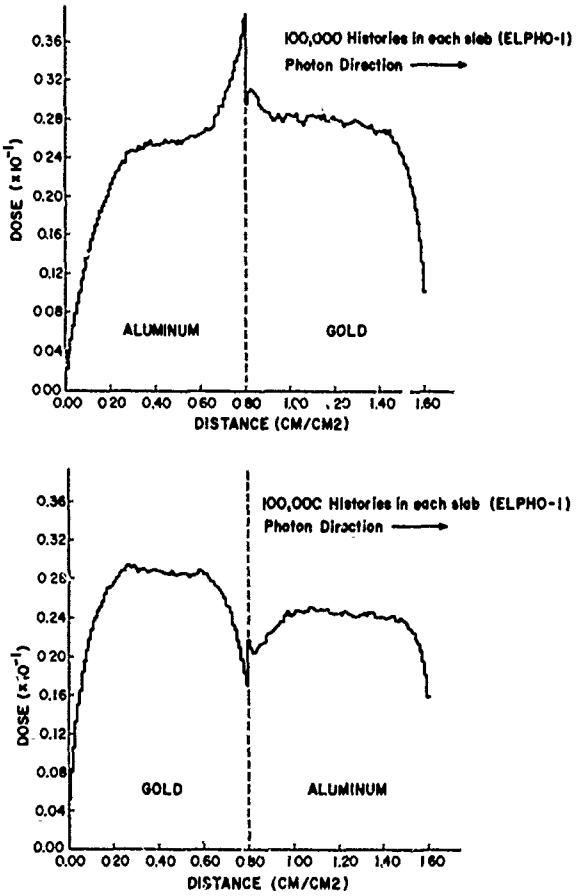

An example of the dose profiles calculated for irradiated slabs. In the upper figure, a 1.25-MeV gamma beam enters an aluminum slab from a vacuum, passes through it into a gold slab, and exits into a vacuum. The plateau regions in the aluminum and gold represent the "normal" dose. At the interface the dose is enhanced on both sides. When the beam is reversed as shown in the lower figure, the dose on both sides of the interface is reduced. For gamma rays of this energy, the effects are governed by differences in electron scattering in the two materials. At lower energies, differences in the generation of electrons control the result and the dose enhancement exceeds a factor of 10.

tion causes transient changes in material properties while displacement effects are essentially permanent, requiring thermal treatment for recovery.

Displacement damage is the physical disorder in the crystal lattice produced by knocking atoms from their normal positions to other locations in the lattice. The observed effects result from electronically active energy states introduced in a semiconductor material by lattice disorder. It is the controlled introduction of similar energy states which causes the material to function as a device. Radiation damage modifies this desired structure, radically changing the electrical properties of the material.

Radiation-induced changes in material properties which are related to the performance of solid state devices have been measured at AFCRL. In addition, the characteristics of the displacement-produced defects responsible for these changes were investigated. Knowledge of the factors influencing production and stability of radiation-induced defects is necessary for hardening existing materials and in specifying alternate materials intrinsically hard to radiation.

The introduction rates of defects, their associated energy levels and charge capture parameters were determined in n-type silicon irradiated with electrons, gamma rays, and neutrons using capacitance measurement techniques on semiconductor diodes. This revealed defect information not observable by conventional electrical and optical techniques. The role of impurities in defect production in electron- and gamma-irradiated samples was quite clearly seen. Neutron irradiation produces complex, cluster-like defect structures as compared with the simpler defects produced by electron and gamma irradiations. Several energy levels were observd in neutron-irradiated samples, and differences between materials involving different crystal growth techniques were apparent. The capacitance technique was used to follow uniquely the thermal anneal of a specific defect in phosphorous-doped, float-zone silicon. Furthermore, it permitted the determination of the role of charge state of the defect on its annealing behavior. It was found that the defect (a

phosphorous-vacancy associate) anneals more readily when neutral, and more slowly when negatively charged.

The study of interactions between radiation-produced defects and impurities in semiconductors can lead to methods for prediction and control of damaging, undesirable effects. Such an investigation of lithium-doped silicon has been completed. The role of lithium, an unconventional, but potentially beneficial dopant in silicon solar cells, has been clarified in neutron-irradiated, float-zone and crucible-grown silicon. This material has been studied by means of Hall effect, resistivity, and infrared absorption measurements. A model developed indicates a precipitation-like interaction between lithium impurities and neutron-produced clusters. It was determined that at least 200 lithium atoms per cubic centimeter are needed for every neutron per square centimeter to neutralize the damaging effects in neutron-irradiated silicon. This information has had a considerable impact on the development of radiation-hardened solar cells.

RADIATION SERVICES AND DOSIMETRY: Irradiation support for radiation effects research is provided by the AFCRL radiation facility. This facility consists of a multi-kilocurie Cobalt 60 source, 23-MeV electron linear accelerator, 3-MeV Van de Graaff generator, 2-MeV flash X-ray machine, and a 1.5-MeV Dynamitron electron accelerator. These sources supply a wide variety of radiation types including electrons, protons, gamma rays, neutrons, X-rays, and heavy ions with energies from the kilovolt range to 23 MeV and with output currents from microamperes to kiloamperes. With these radiations, it is possible to simulate many radiation effects phenomena of interest to the electronic system designer.

Irradiation support is provided, and research is conducted that is related directly to a variety of radiation effects studies by experimenters using the facility. Recent

The AFCRL 1.25 MeV Dynamitron.

examples include a study of the hardness of magnetic bubble materials and the determination of surface temperatures for heavy ion bombarded silicon and gallium arsenide.

Magnetic bubbles have shown promise for mass memory applications. Before these devices could be used in a space or nuclear environment their radiation hardness had to be determined. Consequently, several magnetic bubble material samples were exposed to 10^8 to 10^9 rad (Si) cobalt 60, and 4×10^{14} fission neutrons per square centimeter. Magnetic properties such as coercivity, wall mobility, and magnetization were measured before and after irradiation and were found to be stable at these levels. Sophisticated X-ray topographic techniques delineated the stress response to the irradiation of these bubble materials. Another radiation effect is the stability of stored information to intense pulses of ionizing radiation. It has been demonstrated that information stored in a magnetic bubble shift register is stable up to

at least 10^{12} rad (Si) per second for a 20-nanosecond pulse.

Experimenters conducting ion implantation studies must know the surface temperature during the implant to allow for annealing effects. These temperatures were measured using an infrared detector-prism system for various radiation conditions. The results showed that the surface temperature was not dependent on either the energy, current, or bombarding ion species. The temperature depended only on beam power, target material, and method of mounting the target to the cooling head. The beam power for most ion implantation applications is generally less than 1 watt per square centimeter and this would result in surface temperature increases of less than 20° C for an 0.02-cm thick silicon sample and less than 65° C for an 0.035-cm thick gallium arsenide sample.

The comprehensive nature of the AFCRL radiation facility has attracted other DOD laboratories to satisfy their irradiation requirements. Programs which have extensively utilized these facilities include the Advanced Ballistic Reentry System (ABRES), Poseidon, Advanced Minuteman (MX) and TTC-39 (radiation-hardened switch). The 23-MeV linear accelerator has been used to study transient effects on these systems and the cobalt 60 to provide the total dose requirements.

PHYSICS OF DEVICE HARDENING: The science of device hardening seeks to design devices so that they depend as little as possible on materials properties that are sensitive to radiation. The changes in operating characteristics induced by radiation vary considerably with the type of device and the nature of the radiation. AFCRL is taking both long- and short-term approaches to hardening semiconductor devices. The long-term approach seeks to modify materials and material interfaces so they are less affected by radiation. This requires a basic understanding of why material parameters are affected by radiation. The short-term approaches are to design semiconductor devices so that they are less affected by material property changes, and to find and use in circuits those semiconductor devices which are electrically useful and resistant to radiation.

To meet present and future Air Force needs, all semiconductor devices should be hardened to the maximum practical extent, or at least the theory and techniques to harden them should be developed, because the requirements may increase in the future.

Transistors can suffer all three principal types of radiation damage: displacement, ionization, and thermomechanical. The principal cause of displacement damage is fast neutrons, which remove carriers and reduce minority carrier lifetime. They also reduce mobility, a second-order effect. X-rays and gamma rays cause permanent ionization damage by causing charge to build up in insulators, and transient effects by generating photocurrents. Electronic system designers usually try to circumvent transient effects from very high dose rates. The extent of transistor degradation due to displacement and ionization depends strongly on the transistor type, while the extent of thermomechanical damage depends mainly on packaging and metallization, and not on the transistor type.

When properties of the bulk material are changed to decrease their sensitivity to radiation, changes in the geometry of the device are usually required to maintain the electrical characteristics, or at least ensure that the electrical characteristics are still useful. Fortunately, most hardening techniques harden against more than one type of radiation, and some techniques actually improve the operation of the device.

AFCRL scientists have studied the numerous radiation environments, the feasibility of shielding against some types of radiation, circumventing high dose rate induced transients, the radiation sensitivity of existing devices, and their hardening po-

The AFCRL 3 MeV Van de Graaff Generator.

tential. The most serious deficiencies found were in hardening against neutrons and gamma rays in high power and micropower devices, and in linear integrated circuits. These are still the most serious problems, but the AFCRL program has significantly lessened the deficiencies in research and exploratory development.

HARDENED CMOS/SOS: Almost all of the radiation effects and hardening efforts for complementary metal oxide-semiconductor (CMOS) structures have been devoted to problems associated with the interface between the silicon and the gate insulator. Several solutions to this problem have been demonstrated in the laboratory. The dielectric substrate/silicon interface and the gate electrode/gate insulator interface have been shown by AFCRL to be important in determining the overall radiation sensitivity of metal/insulator/semiconductor structures. The first of these interfaces is important when a device must be hardened against transient photocurrents, and the second results from the new technology utilizing polysilicon gate electrodes for increased packing density and better threshold control. Research must also be performed on "rapid anneal" effects in all three interfaces. The radiation susceptibility of CMOS devices will become more critical when large-scale integrated (LSI) circuits are used. The effects involved must be understood and adequate semiconductor process control maintained if LSI radiation hardness and manufacturability are to be achieved.

CHARGE COUPLED DEVICES (CCD): Two-phase, polysilicon/aluminum CCD shift registers, 64 and 128 stages long, with both surface p- and n-channels and buried n-channels have been irradiated by high energy electrons. The oxide charge and fast interface state levels increase as the dose levels approach 10^5 rads (Si). The most serious effect for surface-channel devices is the increased fast interface state level, since this increases the minimum

The AFCRL Multicurie cobalt-60 cell.

transfer inefficiency which can be achieved to 10^{-3}, even with a zero signal which is 30 percent of the one signal. Narrower channels aggravate this effect.

The transfer inefficiency of buried-channel devices is relatively insensitive to radiation. While some increase in inefficiency was measured, the buried-channel devices continued with inefficiency less than 10^{-4} at radiation doses as high as 5×10^5 rads (Si).

No significant changes in average dark current levels or dark current profiles were observed, especially in buried-channel devices. This indicated that no appreciable bulk damage was incurred during irradiation with 1-MeV electrons.

The maximum well size in multi-level oxide structures decreased as dose levels increased. This is predictable on the basis of surface potential calculation and the well size can be re-established by adjustment of the dc levels applied to the various gates. Incorporation of an on-chip threshold tracking circuit can automatically correct for the radiation-induced threshold shifts. This combination of a buried-channel CCD with threshold tracking should be as radiation-hard as peripheral MOS on-chip circuits commonly used to interface the CCD.

DIELECTRIC ISOLATION PROCESSES: Dielectric isolation techniques are used to reduce photocurrents in semiconductor devices and integrated circuits exposed to pulses of ionizing radiation. Three materials for dielectric isolation have given rise to isolation schemes. These are: the more conventional silicon on silicon dioxide: silicon on silicon nitride (SON) process, and silicon on sapphire (SOS). In the first two processes, the isolation dielectric is deposited or grown on the bulk silicon, polysilicon substrate material is deposited, and then most of the original silicon is removed, leaving only a thin layer of single crystal silicon. Silicon dioxide is the usual isolation dielectric, while silicon nitride (SON process) is used to harden the dielectric against total ionizing radiation. In the silicon on sapphire (SOS) process, a thin film of silicon is heteroepitaxially grown on a sapphire substrate. The quality of the thin film silicon in the first two processes is essentially the same as bulk silicon, while the quality of the SOS silicon is degraded because of lattice mismatch. However, the SOS process is simpler and easier to control.

Total ionizing radiation effects on the isolation dielectric and the interface between the isolation dielectric and semiconductor are not a significant problem for bipolar structures. For this reason, dielectric isolation has been used to harden them against transient radiation. However, exposure of n-channel MIS devices to radiation results in trapped positive charge in the isolation dielectric which may induce leakage currents. For these devices, the radiation-hardened SON process, or the SOS process, modified to minimize charge trapping in the sapphire, is needed. Radiation hardening the isolation dielectric gains the advantages of both dielectric isolation and MOS technology.

HARDENED DIFFUSED RESISTORS: Radiation normally causes large transient effects in diffused resistors, limiting their use in hardened integrated circuits. Oxide isolation will be investigated as a way to harden diffused resistors against radiation. The effects of isolation area and isolation region bias will be studied. Properties of the resistor strip such as sheet resistivities and resistor widths will also be examined.

The physics of the behavior of diffused resistors under irradiation has been reviewed and design criteria established for hardened resistors. Detailed layout of test structures which will permit a comparison of the predictions to actual device performance was made. Masks have been fabricated, and device fabrication has begun.

INFRARED DETECTOR RESEARCH

Burning fuel emits recombination radiation as well as black body thermal radiation, and both are infrared targets of military interest. Available detectors for this radiation often operate within a factor of 2 or 3 of their theoretical ideal. But future requirements for long-range, high-reliability missile detection, large forward-looking infrared (FLIR) systems, nighttime "smart" bombs, and passive detection modes for RPV's will require continued detector research. AFCRL has initiated a program to develop new detector concepts, new detector materials, and integrated optics, and to study radiation effects in detectors, and sensor hardening, to generate the technology base that will be needed.

INFRARED CAMERA: Infrared cameras are much more difficult to design than cameras for visible light. Signals from infrared scenes have low contrast and a large, uniform background component, whereas signals from visible scenes have good contrast and negligible background. An infrared camera must have a large dynamic range in order to accumulate the background signal without saturation, and at the same time, it must have sufficient sensitivity to resolve low contrast detail. In addition, there must be provision for the removal of the background signal component to obtain acceptable display contrast. Ideally, background removal should occur during the frame integration process to minimize the dynamic range requirements imposed on both the sensor surface, or retina, and its associated readout mechanism. The combination of strong background and low contrast signal conditions leads to the further requirement that the point-to-point photoresponse of the retina must be extremely uniform. Depending upon the thermal resolution required and upon the spectral range of operation, photoresponse spatial variance limits range from 0.1 to 1 percent. This requirement exceeds the limits set by variations of semiconductor composition, impurity density and minority carrier lifetime in conventional photoconductive or photovoltaic retinas. However, larger variations of photoresponse will introduce "fixed pattern" noise into the imagery.

A new type of retina is being developed at AFCRL which is based on internal photoemission from the metal photocathodes of large two-dimensional arrays of silicon Schottky diodes. The Schottky retina photoresponse is independent, to first order, of both minority carrier lifetime and impurity density. This independence, together with the exclusive use of silicon monolithic processing technology in the fabrication of Schottky retinas, is expected to lead to photoresponse uniformities that are good enough to provide a basis for a viable infrared television camera technology. It is expected that Schottky retina cameras, operating in the 3-5 micrometer spectral band, will be capable of performance comparable with state-of-the-art line

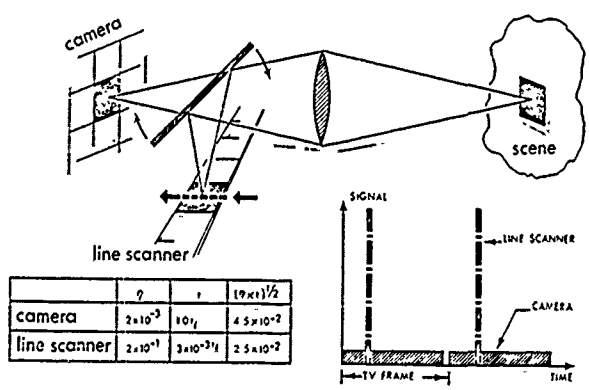

	η	τ	$(\eta\times\tau)^{1/2}$
camera	2×10^{-3}	$10\tau_f$	4.5×10^{-2}
line scanner	2×10^{-1}	$3\times10^{-3}\tau_f$	2.5×10^{-2}

Line scanner systems typically use a rotating mirror to scan across the scenes. Although a camera system using Schottky Barrier devices would have a quantum efficiency of only one one-hundredth that of the devices used in the line scanner, they would stare at the scene for the full frame time, while the scanner would look at each element in the scene for the frame time divided by the number of lines in the scene, about 300. The overall efficiency of the two systems would thus be within a factor of two.

scanners. Further, Schottky retina cameras are expected to be significantly less complex and costly than thermal imaging systems.

The basic photoresponse, contrast and noise relationships for a family of thermal imaging cameras based upon the infrared internal emission photoresponse of silicon Schottky diodes have been derived. The camera retinas consist of large-scale two-dimensional arrays of Schottky diodes operating in a charge storage mode. The measured values of quantum efficiency and uniformity lead to a prediction of performance approaching that of line scanning systems. Use of the Schottky response has led to an order of magnitude improvement in available photoresponse uniformity, an advance which will make possible the development of a viable infrared camera technology.

LWIR DETECTORS, EXTRINSIC SILICON: In the 8-30 micrometer spectral region, extrinsic silicon photoconductors are the prime candidates for high-performance detectors in a single-element or small arrays. Background limited detectivities had been achieved under a wide range of background conditions by these extrinsic silicon photoconductors. Basic detector parameters essential to high detectivity such as photocarrier lifetime and mobility were strongly dependent on compensation level which is kept as low as possible. For detectors of sizable dimensions as found in single-element or small arrays, the bulk properties can be optimized to obtain best performance (the physics and material parameters are reasonably under control). As the detector size decreases, both for integration into large dimensional arrays and for minimization of nuclear and space radiation effects, the bulk properties of the extrinsic silicon material no longer dominate and the effects of contacts cannot be neglected. Under operating conditions, where most carriers are frozen out, the carrier spillover from the accumulative regions of the ohmic contacts can change the dc conductivities by several orders of magnitude. Computer models and programs were designed to quantify the low temperature electrical and optical characteristics, taking into consideration the effects of ideal ohmic contacts. The ideal ohmic contact is defined as a high-low junction in the semiconductor in series with a tunnel-emission junction on the high dopant level side. Significant departures from bulk values were found as the distance between ohmic contacts is decreased. Many design and material parameter changes can be identified. Experimental low temperature measurements on extrinsic silicon photoconductors simulating actual operating conditions are underway to seek out the best design for integrating the detectors into large arrays and for minimizing radiation effects.

RADIATION EFFECTS IN IR DETECTOR AND SENSOR HARDENING: These studies seek to determine the mechanisms by which ionizing radiation affects detectors that operate in the 10-micrometer spectral region and the modifications in signal response caused by permanent radiation damage.

The effects of gamma-photon-induced ionizing noise in infrared sensors were modeled in such a way that methods could be recommended for improving the radiation hardness of infrared sensors, by varying geometry, electronic parameters, etc. The goal is to maintain optical performance while minimizing the gamma ray response in a given focal plane, in spite of the fact that any infrared detector is also a gamma ray detector. The model takes into account the incident gamma spectrum, both Compton events in the detector and secondary hot electrons from the metal surroundings, partial or total deposition of the initial hot electron energy, detector geometry, and preamplifier impulse response. The model as coded gives predicted pulse height distributions and, for threshold-gating type circumvention, pre-

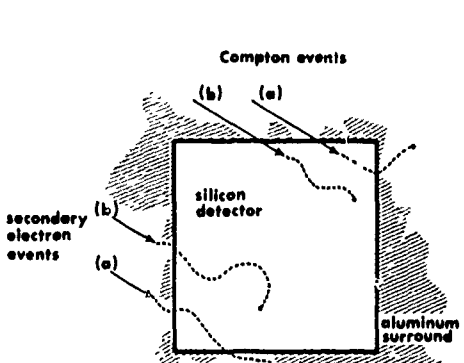

A silicon detector in an aluminum surround can have electrons knocked loose from the silicon which then either escape into the aluminum (a) or remain as locally unbalanced charges in the silicon (b). It can also be affected by electrons released from the aluminum which then deposit energy in the silicon as they pass through it (a) or come to rest in the silicon (b).

dicted duty cycles; it indicates that detector volume should be minimized. Good agreement with experimental results is achieved. In particular, signal-to-noise parameters are calculated for an extrinsic silicon infrared detector mounted on an aluminum focal-plane assembly operating at 10° K in the presence of a weapons debris gamma-ray ionizing environment. Preamplifier clamping, to truncate large ionizing radiation pulses, leads to significant increases in system sensitivity.

Upon analysis, it was found that the modifications of photoconductive response caused by permanent radiation damage in HgCdTe can be adequately described by the theory of degenerate semiconductors. The effects of irradiation in HgCdTe consist mainly of the introduction of donor defects. The filling of the conduction band states by electrons from donor defects inhibits phototransition to the conduction band edge: rather, transitions take place from the valence band to empty states near the Fermi level in the conduction band (Burstein-Moss effect). This explains the shift toward shorter wavelength in the photoconductive response peak. Moreover, the electrons from the donor defects will exhibit a large dark current which shunts the photoconductive current and decreases the overall signal response.

INTEGRATED OPTICS: Optical circuits are being considered with increasing interest for use in Air Force communications and control systems. Some of the advantages are low weight and size, security, no electromagnetic interference, and high data rate capability. This proposed use of optical circuits for data transmission has produced an increasing need for the theoretical understanding of propagation of light in dielectric structures of all kinds. The theoretical treatment of such problems is difficult since the electromagnetic field is both time varying and vectorial. Thus, problems in dielectric combine all the difficulties of scalar wave propagation in variably refracting media with the fact that an electromagnetic field has six components (three electric and three magnetic) and hence generates six simultaneous wave equations. In an attempt to overcome these difficulties, efforts have been made to isolate these two stumbling blocks of the electromagnetic case by first solving model problems in which one or the other of them is absent. Two such model problems are: the penetration of long wavelength (static) fields into dielectrics, and the scattering of scalar waves from arbitrarily shaped bodies. There is an additional interest in this strategy of attack in that the model problems themselves have intrinsic practical interest. Thus, the long wavelength problem, the electrostatics of fields in the presence of dielectrics, is important in the theory of electric or magnetic shielding. Similarly, scalar problems of scattering are widely important in acoustics, in impurity scattering in solid state theory, and in electron-atom interaction theory. Both these model problems have been successfully attacked and solved. A new technique has been devised that permits the calculation of the response of almost any dielectric

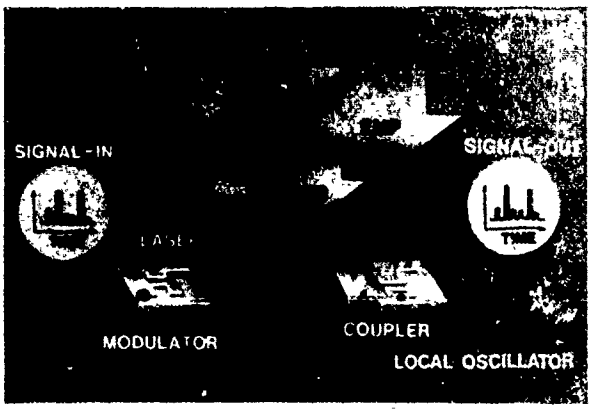

By developing integrated optics components, the Laboratory can assemble systems which, because they transmit light, usually through fiber optics connectors, are not affected by radio frequency interference, jamming, cross talk between channels, or the electromagnetic pulses from nuclear detonations.

(or permeable body) to an external field. Similarly, new formulas have been derived that permit the calculation of the scattering of scalar waves from a large class of refracting bodies. The insight gained from these model problems is now being applied to the electromagnetic dielectric waveguide propagation problem with good portents for success.

Full potential of the optical circuits can only be realized with the development of the necessary integrated optics (IO) components. These IO components perform analogous functions as IC's in electronic circuits by the manipulation of lightwave with electro-optical or acousto-optical interactions. The state of the art of solid state device processing technology must be extended to meet the novel and stringent requirements for these IO devices. New and innovative approaches must be considered to exploit various electro-optical phenomena exhibited by EM materials and to solve novel problems arising in optical circuit designs. For the hybrid circuit approach, the development of efficient coupling between optical fibers and/or thin film waveguides is paramount. In an all GaAs monolithic approach, an integrable and compatible injection laser source is the key to success.

DEVICE DESIGN: The operation and advantages of Schottky barrier diodes as infrared detectors have been discussed previously. The proven reliability of solid state components makes an integrated all solid state infrared imaging system desirable. A design which couples the Schottky barrier diode detectors to a CCD (Charge Coupled Devices) readout uses an MOS transistor transfer gate to convert a majority carrier signal, obtained from the Schottky barrier diode when infrared photons impinge upon it, to a minority carrier signal, which can be transferred along a CCD shift register.

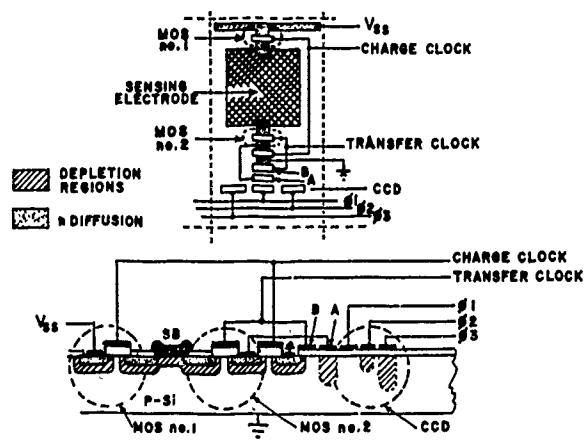

The charge coupled imaging device for use with the Schottky Barrier infrared sensing array. A pulse from the charge clock charges the Schottky Barrier through MOS No. 1 to a reverse bias potential and at the same time reduces the potential at A to ground. For a frame time, the reversed biased Schottky Barrier is discharged by IR photons. The transfer clock then turns on MOS No. 2 and transfers electrode B. This allows a charge proportional to the voltage on A to flow from the grounded source. The CCD shift register is locked so that the next pulse will transfer the charge beneath A to the closest CCD electrode, from which it travels down the CCD shift register for readout. This is the first conversion of a majority carrier to a minority carrier signal on a monolithic integrated chip.

This scheme solves, for the first time, the problem of transforming a majority carrier signal to a minority carrier signal on a monolithic integrated circuit chip. AFCRL has applied for a patent on this voltage transfer scheme and effort is underwway to reduce this scheme to practice in the laboratory. Under this same program, on contract, a slightly modified version using charge transfer rather than voltage transfer is being built. Initial results have demonstrated imaging in the infrared, reported in AFCRL-TR-74-0375. The primary difference between the voltage transfer and the charge transfer is that in voltage transfer the capacitance of the sensing element must be large in comparison to the CCD electrode capacitance, while in the case of charge transfer these capacitances should be equal. This consideration implies that for a given CCD design using voltage transfer, a larger fraction of the chip must be used for sensing, giving greater sensitivity but lower resolution than charge transfer.

DEVICE PROCESSING TECHNOLOGY

Research in solid state device technology is primarily directed either toward achieving better control over existing processes or toward developing new processes which can yield the desired improvement in control. Thus, the laboratory maintains a capability for conventional processing using a standard photographic step and repeat camera for mask making, contact exposure of photoresist, thermal oxidation, and boron or phosphorus diffusion. The fast progress of semiconductor technology requires considerable time and effort to keep abreast of the latest techniques; during this reporting period, HCl treatment of thermal oxides and plasma etching and stripping capabilities have been incorporated. At the same time, continuous research is carried out on new experimental techniques for their inherent advantages. In the latter category are ion implantation, direct projection on photoresist, and use of electron beam technology.

In previous reports, the fundamental studies undertaken on ion implantation into silicon were discussed. Once it was established that the ion-implantation-induced lattice damage could be removed by annealing to a degree where it no longer seriously degraded basic semiconductor properties such as carrier concentration, mobility, or minority carrier lifetime, attention was focused on the use of ion implantation. Implantation ions deposit their charge on the target so that by integrating the charge deposited during an implantation run, one is able to get an electronic measure of the total dose of impurity ions deposited into the target material. This fact permits at least an order of magnitude improvement in the control of the introduction of desired dopants. Invariably, ion implanted diodes show better uniformity of breakdown voltages across a slice than diffused diodes which are fabricated under otherwise similar conditions, e.g., improvement in the quality of passivating oxide and photolithographic processing. The degree of control available through ion implantation has also been applied to the fabrication of high ohms/square resistors. Diffused resistors have typical values of 250 ohms/square with 1000 ohms/square constituting a difficult-to-control upper boundary. Implanted resistors having values of 3000 ohms/square have been easily obtained. However, all high valued resistors suffer from a self-pinching effect and thus have poor voltage linearity. This problem may be overcome for implanted resistors by intentionally retaining some of the implantation-introduced damage. This possibility is the subject of our ongoing investigation. High valued resistors in integrated circuits would greatly reduce chip size, thereby increasing yield, and would permit circuit hardening through elimination of thin film resistors.

In addition to the control of the exact

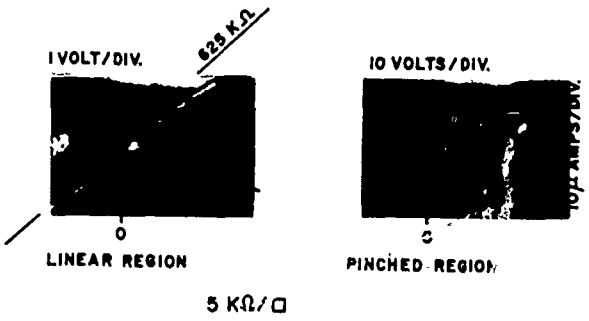

An illustration of the pinch effect in an implanted resistor, of 5,000 ohms per square. From 0 to 5 volts, the resistance is approximately constant at 625,000 ohms. However, the plot of current for voltages from 0 to 50 volts shows the current approaching a constant value, regardless of voltage — the pinching effect.

concentration of dopant impurities, the control of physical dimensions is of great interest to solid state devices. Both absolute linewidth and line edge uniformity are of importance. Experiments with direct projection of 10X master images on photoresist have resulted in substantially improved resolution of 1 micron lines with 1 micron spaces. In the quest for even greater resolution a contract has been let to build an Electron Beam Equipment with a Laser Controlled Stage which will have the capability of ±0.2 micron resolution and ±0.2 micron registration accuracy over a 10-cm x 10-cm working area. This equipment will be used in the study of high valued resistors. The width of the resistors will be reduced in an effort to experimentally verify the expected reduction in photocurrents when a given valued resistor made by this technique is exposed to pulsed gamma radiation.

Another area of processing research has been necessitated by the Laboratory's program in Schottky barrier infrared detectors. Since these Schottky barriers must be fabricated on p-type silicon to obtain sufficiently low barriers, they suffer from surface inversion problems. Through the use of a special structure, the problems arising from surface inversion have been characterized at 77° K. No information exists in the literature for low barrier Schottky junctions with surrounding oxide. Through the use of field plates it has been shown that leakage currents at 77° K for 40 mil Schottky barrier diodes can be reduced below 1 nanoampere. This experiment demonstrated that the leakage currents in low barrier Schottky junctions can be reduced so that no significant discharge occurs during integration.

GAAS IMPLANTATION: One of the limiting factors in GaAs device technology is the difficulty of forming thin heavily doped n-type regions. The high frequency performance of FET's, for example, is restricted by the series resistance of the source and drain. The solubility limit of n-type dopants in GaAs is in the mid 10^{18} atoms per cubic centimeter range and this sets the highest doping that can be anticipated. Implantation would seem particularly suitable for such layer formation and, bearing in mind the solubility limit, the highest implanted doses should be in the vicinity of 10^{14} ions per square centimeter. Such a dose averaged over ¼ micrometer is equivalent to 4×10^{18} per cubic centimeter. This contrasts with doses up to 10^{15} per square centimeter for p-type dopants and more than 10^{15} per square centimeter for silicon.

Despite the success achieved with p-type implants, results for n-type implantation have generally been disappointing. Accordingly, an investigation was undertaken in an attempt to determine the limiting factors. Possible limitations to achieving the necessary doping include: the requirement that the ion locate substitutionally and on the correct sublattice site; incomplete removal of compensating defects that result from the ion irradiation; surface degrada-

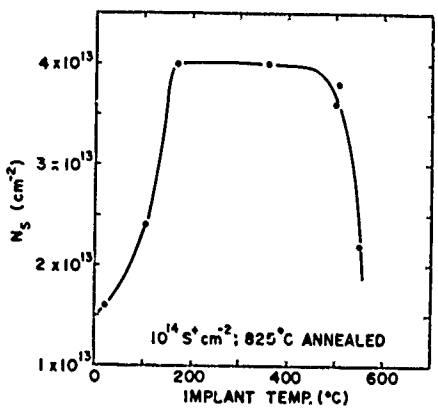

Number of sulfur atoms substituting on arsenic sites in GaAs at various implant temperatures, when implantation is followed by annealing. The electrical activity due to doping increases sharply as the implant temperature is increased from room temperature to 150° C.

tion during the thermal annealing required to satisfy the first two requirements; and loss of implanted species by out-diffusion through the GaAs surface.

In addition, the effects on GaAs of implanting at elevated temperatures are still unknown.

Because it assumes the correct lattice position with less damage to the lattice, silicon might be preferred over the group VI dopants. If the better utilization of p-type ions as dopants is due in some way to the ease with which they can assume positions on Ga sites, then n-type doping should be easier with Si, since it also should locate on Ga rather than As sites. The ability of Si to act amphoteric when used as a dopant is usually detrimental. However, GaAs requires surface encapsulation during post-implantation annealing to prevent As loss, and the technologically simpler but generally inadequate SiO_2 films might be beneficial in this instance. By allowing Ga to diffuse out, they allow creation of Ga vacancies. This is a limitation when group VI dopants are used, but it should aid Si in taking lattice positions normally occupied by Ga atoms. While doping levels up to 2.2 x 10^{13} per square centimeter have been obtained from 10^{14} per square centimeter implants, better results can be accomplished by implanting sulfur and selenium.

Considerable effort has centered on removal of defects resulting from implantation, with emphasis on determining how many defects are caused per ion implanted and learning how these defects anneal. Lighter non-dopant ions such as B and N were found to remove about 200 carriers per ion when implanted at 1 MeV. Such damage, if from a dopant ion, would have to be entirely removed before a net doping gain could result. The carrier (and mobility) annealing of a nitrogen damaged layer shows, typically, a recovery stage at 225° C from electron irradiation damage, and a stage above 600° C for damage from the ions. Such compensation studies are also useful in integrated optics where removal of the carriers causes a refractive index change which can be used to form a waveguide.

The highest doping achieved so far has been obtained using Se and S, where up to 2.9 x 10^{13} per cubic centimeter and 4 x 10^{13} per square centimeter of the 10^{14} ions per square centimeter implanted have been rendered active. Peak concentrations are approximately 1-2 x 10^{18} per cubic centimeter. Layers doped to 7 x 10^{13} per square centimeter have been obtained at higher sulfur doses and such active concentrations are significantly better than what has been previously reported. The single most important factor influencing the electrical activity of the layers is the implantation temperature. Typically, an improvement of 2½ occurs if the implantation is performed above 150° C rather than at room temperature. However, elevated temperatures do not significantly reduce compensating defect formation. It is concluded that if S or Se is implanted below 150° C, an appreciable fraction of the ions are trapped in defect complexes from which they are never released during annealing to become substitutional on the desired As sites.

JOURNAL ARTICLES
JULY 1972 - JUNE 1974

ARMINGTON, A. F., POSEN, H., and LIPSON, H. G.
Strengthening of Halides for Infrared Windows
J. of Elect. Mats., Vol. 2, No. 1 (February 1973)

BENDOW, B.
Lensing of High Power Laser Windows
AFSC Sci. & Engrg. Symp. Proc., Vol. 1, AFSC-TR-72-005 (1972)
Temperature Dependence of Intrinsic Multiphonon Absorption in Crystals
Appl. Phys. Ltrs., Vol. 23, No. 3 (1 August 1973)
Frequency and Temperature Dependence of Anharmonicity-Induced Multiphonon Absorption
Phys. Rev. B, Vol. 8, No. 12 (15 December 1973)
Optical Properties of Infrared Transmitting Materials
J. of Elect. Mats., Vol. 3, No. 1 (February 1974)

BENDOW, B., and GIANINO, P. D.
Photoelastic Constants of Infrared Transmitting Materials
Laser Induced Damage in Opt. Mats., Eds.: A. J. Glass and A. H. Guenther, NB Sp. Pub. 387, U. S. Govt. Prtg. Off., Wash., D. C. (1973)
Thermal Lensing of Laser Beams in Optically Transmitting Materials. I. General Formulation
Appl. Phys., Vol. 2, No. 1 (July 1973)
Theoretical Lower Bound on the Absorption Coefficient of Infrared Transmitting Materials
Opt. Comm., Vol. 9, No. 3 (November 1973)

BENDOW, B., GIANINO, P. D., and HORDVIK, A. (Opt. Phys. Lab.), SKOLNIK, L. H.
Theory of Thermally-Induced Interference and Lensing in Transparent Materials
Opt. Comm., Vol. 7, No. 3 (March 1973)

BENDOW, B., and HORDVIK, A. (Opt. Phys. Lab.), LIPSON, H. G., SKOLNIK, L. H.
Optical Evaluation of CO_2 Laser Window Materials at AFCRL
Proc. of the Fifth Conf. on Laser Technol., Vol. 1 (Pub.: Navy Pubs. and Prtg. Svc., Boston, Mass. — 1972)

BENDOW, B., SKOLNIK, L. H., and CROSS, E. F. (Aerosp. Corp., El Segundo, Calif.)
Investigations of Laser Induced Thermal Lensing and Interference from Infrared Transmitting Materials
Appl. Opt., Vol. 13, No. 4 (April 1974)

BENDOW, B., and YING, S. C. (Brown Univ., Providence, R. I.)
Dynamics of Adatoms on Solid Surfaces: Interaction with Phonons
Proc. of Intl. Conf. on Phonon Scattering in Solids, Ed.: H. Albany (Pub.: Documentation Francais, Paris, Fr. — 1972)
Absorption Due to Higher-Order Electric Moments in Transparent Crystals
Phys. Ltrs. A, Vol. 42A, No. 5 (1 January 1973)
Phonon-Induced Desorption of Adatoms from Crystal Surfaces: I. Formal Theory
Phys. Rev. B, Vol. 7, No. 2 (15 January 1973)

BENDOW, B., and YING, S. C. (Brown Univ., Providence, R. I.), YUKON, S. (Parke Math. Labs., Carlisle, Mass.)
Theory of Multiphonon Absorption Due to Anharmonicity in Crystals
Phys. Rev. B, Vol. 8, No. 4 (15 August 1973)

BERMAN, I., MARSHALL, R. C., and RYAN, C. E.
Annealing of Sputtered β SiC
Proc. "Silicon Carbide — 1973," Univ. of S. C. Press (1974), Ed. by R. C. Marshall, J. W. Faust, Jr., and C. E. Ryan

BOWEN, H. K., SINGH, R. N. (Mass. Inst. of Technol.) POSEN, H., ARMINGTON, A. F., and KULIN, S. A. (ManLabs, Inc., Cambridge, Mass.)
Fabrication and Properties of Polycrystalline Alkali Halides
Mats. Res. Bull, Vol. 8, No. 12 (December 1973)

BRADFORD, J. N.
Absolute Yields of X-Ray Induced Photoemission from Metals
IEEE Trans. on Nuc. Sci., Vol. NS-19, No. 6 (December 1972)
X-Ray Induced Electron Emission II
IEEE Trans. on Nuc. Sci., Vol. NS-20, No. 6 (December 1973)

BUCHANAN, B. L., SHEDD, W. M., NEAMEN, D. A., and ROOSILD, S. A.
Radiation Hardened CMOS
1974 Govt. Microcircuit Appl. Conf.

BUCKMELTER, J. R., and KENNEDY, J. K.
Electron-Microprobe Characterization of Vapor-Grown $InAs_{1-x}P_x$ Layers
J. of the Electrochem. Soc. (Tech. Note), Vol. 120. No. 1 (January 1973)

COMER, J. J.
Electron Microscope Study of Dauphine Microtwins Formed in Synthetic Quartz
J. of Cryst. Growth, Vol. 15, No. 3 (August 1972)
Clay Minerals
Encycl. of Microscopy and Microtechnique, Ed.: Peter Gray (Pub.: Van Nostrand-Reinhold Co., N. Y. — 1973)

COMER, J. J. and BERGERON, C. A.
Gold Decoration of Etched Polycrystalline KCl
31st Ann. Proc. Elect. Microscopy Soc. Am., New Orleans, La. (1973), Ed.: C. J. Arceneaux

COMER, J. J., BERGERON, C. A., and LOWE, L. F.
Effects of High-Energy Ions on Synthetic Quartz
30th Ann. Proc. of Elect. Microscopy Soc. of Am. (1972) Ed.: C. J. Arceneaux
Ion Damage in Synthetic Quartz
Mats. Res. Bull., Vol. 8, No. 5 (May 1973)

DAVIES, D. and COMER, J. J.
Damage and Penetration of Implanted Ions in SiC
Proc. "Silicon Carbide — 1973" Univ. of S. C. Press (1974), Ed. by R. C. Marshall, J. W. Faust, Jr., and C. E. Ryan

DAVIES, D. E., KENNEDY, J. K,. and YANG, A. C.
Compensation from Implantation in GaAs
Appl. Phys. Ltrs., Vol. 23, No. 11 (1 December 1973)

DAVIES, D. E., and ROOSILD, S. A.
Device Implications of Ion Implantation Damage in Silicon
1972 Govt. Microcircuit Appl. Conf. Papers (GOMAC) (October 1972)

DIEBOLD, J. W., LT. COL., DE ANGELIS, H. M., and KIMERLING, L. C., CAPT.
Specific Observations of Radiation Effects in Semiconductors by Junction-Capacitance Techniques
Radn. Damage and Defects in Semicond. (Pub.: Inst. of Phys., London, Eng. - 1973)

DUGGER, C. O.
The Synthesis of Aluminum Nitride Single Crystals
Mats. Res. Bull., Vol. 9, No. 3 (March 1974)

EULER, F. K., BOUTHILLETTE, L. O., KAHAN, A., and STEIN, H. J. (Sandia Labs., Albuquerque, N. M.)
Neutron Displacement Damage in Heavily Doped GaAs
Radn. Damage and Defects in Semicond. (Pub.: Inst. of Phys., London, Eng. - 1973)

EYGES, L.
New Method for the Band Structure Problem with Overlapping Potentials
J. of Phys.-C: Solid State Phys. (Ltr. to Ed.), Vol. 6, No. 15 (6 August 1973)
Solution of Schrodinger and Related Equations for Irregular and Composite Regions
Annals of Phys., Vol. 81, No. 2 (December 1973)

FIELD, W. G., and SAMPSON, J. L.
Growth of Rare Earth-Cobalt Single Crystals
AIP Conf. Proc., No. 10, Pt. 1 (1973), Ed.: C. D. Graham, Jr., and J. J. Rhyne (Pub.: Am. Inst. of Phys., N. Y.)

FREDERICKSON, A. R.
Hemispherical Triode: A Device and Technique for Measuring Electron Emission
Proc. of 7th Natl. Conf. on Elect. Probe Analys. (Pub.: Electron Probe Analys. Soc. of Am - 1972)

FREDERICKSON, A. R., and BURKE, E. A.
Total Electron Backscatter and Backemission Yields from Metals Bombarded at Several Angles by 0.4 to 1.4 MeV Electrons
IEEE Trans. on Nuc. Sci., Vol. NS-19, No. 6 (December 1972)

GARTH, J. C., and CHADSEY, W. C. (Sci. Appl., Inc., Arlington, Va.)
Poem Code Calculations of X-Ray Photoemission
IEMP Symp. (Proc.), 6-8 Feb. 1973 (4 June 1973), Tech. Rpt. DNA-3098P

GARTH, J. C. and O'BRIEN, J. V. (Arcon Corp., Wakefield, Mass.)
Numerical Solution of the Spencer-Lewis Equation for Kilovolt Electron Transport in Plane Slabs
IEEE Trans. on Nuc. Sci., Vol. NS-20, No. 6 (December 1973)

GIANINO, P. D., and BENDOW, B.
Optical Performance Evaluation of Infrared Transmitting Materials
J. of Elect. Mats., Vol. 2, No. 1 (February 1973)
Thermal Lensing of Laser Beams in Optically Transmitting Materials. II. Numerical Computations
Appl. Phys., Vol. 2, No. 2 (August 1973)

HORDVIK, A. (Opt. Phys. Lab.), and SKOLNIK, L. H.
Laser Induced Thermal Distortion of CO_2 Laser Window Materials
AFSC Sci. & Engrg. Symp. Proc., AFSC-TR-72-005, (1972)

HUNT, M. H., NIKULA, J. V., POSEN, H., and VICKERS, V. E.
The AFCRL Automated Photoplate Data Acquisition and Reduction System
20th Ann. Conf. on Mass Spectrometry and Allied Topics, 4-9 June 1972, Dallas, Tex. (Pub.: Am. Soc. for Mass Spectrometry - 1972)

KACHARE, A. A., SPITZER, W. G. (Univ. of So. Calif., Los Angeles, Calif.), KAHAN, A., EULER, F., and WHATLEY, T. A. (Appl. Res. Labs., Sunland, Calif.)
Ion Implanted Nitrogen in Gallium Arsenide
J. of Appl. Phys., Vol. 44, No. 10 (October 1973)

KENNEDY, J. K., and POTTER, W. D.
The Effect of Various Growth Parameters on the Formation of Pits and Hillocks on the Surface of Epitaxial GaAs Layers
J. of Cryst. Growth, Vol. 19, No. 2 (May 1973)

KIMERLING, L. C., CAPT., DRLVINSKY, P. J., and YING, S. C. (Brown Univ., Providence, R. I.)
Defect Interactions in Neutron-Irradiated, Lithium-Doped Silicon
Radn. Damage and Defects in Semicond. (Pub.: Inst. of Phys., London, Eng. - 1973)

LARKIN, J. J.
Hardening of Alkali Halides for Infrared Laser Window Applications
AFSC Sci. & Engrg. Symp. Proc., AFSC-TR-72-005, Vol. II (1972)

MAGEE, T. J., and COMER, J. J.
Controlled Sectioning Technique for Small Gallium Arsenide Samples
Rev. of Sci. Instms., Vol. 43, No. 8 (August 1972)

MARSHALL, R. C.
Perspectives on Silicon Carbide
Proc. "Silicon Carbide - 1973," Univ. of S. C. Press (1974), Ed. by R. C. Marshall, J. W. Faust, Jr., and C. E. Ryan

MARSHALL, R. C., LITTLER, J. R., RYAN, C. E., HAWLEY, J. J., BERMAN, I., and CONSIDINE, D. P.
A Unique High Temperature-High Pressure Crystal Growth System for Silicon Carbide
Proc. of Fourth All-Union Conf. on Cryst. Growth (1974)

MARSHALL, R. C., RYAN, C. E., LITTLER, J. R., and BERMAN, I.
New Growth Experiments in Alpha Silicon Carbide
Proc. "Silicon Carbide - 1973," Univ. of S. C. Press (1974), Ed. By R. C. Marshall, J. W. Faust, Jr., and C. E. Ryan

NEAMEN, D. A., SHEDD, W. M., and BUCHANAN, B. L.
Effects of Ionizing Radiation on Dielectrically Isolated Junction Field Effect Transistors
IEEE Trans. on Nuc. Sci., Vol. NS-19, No. 6 (December 1972)
Permanent Ionizing Radiation Effects in Dielectrically Bounded Field Effect Transistors
IEEE Trans. on Nuc. Sci., Vol. NS-20, No. 6 (December 1973)
Permanent Ionizing Radiation Effects in Gate and Isolation Dielectrics in FET's
1974 Govt. Microcircuit Appl. Conf.

NIKULA, J. V., and DIEBOLD, J. W., LT. COL.
The Automation of a Junction Capacitance Measurement within the LAAF System
COMMON Proc. (April 1973), Detroit, Mich., Ed.: John F. Zieserl, Jr., Upjohn Co., Kalamazoo, Mich. (Pub.: IBM)

O'CONNOR, J. J., LARKIN, J. J., POSEN, H., and ARMINGTON, A. F.
Solid Solution Halide Crystals
Mats. Res. Bull., Vol. 7, No. 12 (December 1972)

PELLEGRINI, P. W., and FELDMAN, J. M. (Northeastern Univ., Boston, Mass.)
LPE Growth of SiC Using Transition Metal-Silicon Solvents
Proc. "Silicon Carbide - 1973," Univ. of S. C. Press (1974), Ed. By R. C. Marshall, J. W. Faust, Jr., and C. E. Ryan

POSEN, H.
An Atlas of Laue Patterns of SiC Polytypes
Proc. "Silicon Carbide - 1973," Univ. of S. C. Press (1974), Ed. by R. C. Marshall, J. W. Faust, Jr., and C. E. Ryan

POSEN, H., ARMINGTON, A. F., and BRUCE, J. A.
The Selection and Improvement of Alkali Halide Materials for High Power 10.6 μm Windows
Proc. of Fifth Conf. on Laser Technol., Vol. 1 (Pub.: Navy Pubs. and Prtg. Svc., Boston, Mass. - 1972)

POSEN, H., and BRUCE, J. A.
Observation of Slip Distributions in Alpha SiC
Proc. "Silicon Carbide - 1973," Univ. of S. C. Press (1974), Ed. by R. C. Marshall, J. W. Faust, Jr., and C. E. Ryan

POSEN, H., BRUCE, J. A., COMER, J. J., and ARMINGTON, A. F.
A Study of 10.6 Laser Induced Damage in Halide Crystals
Laser Induced Damage in Opt. Mats. (1973) Eds.: A. J. Glass and A. H. Guenther, NBS Sp. Pub. 387, U. S. Govt. Prtg. Off., Wash., D. C. (1973)

RYAN, C. E., BERMAN, I., and MARSHALL, R. C.
Thin Films of Alpha and Beta Silicon Carbide Prepared by Liquid Epitaxy and by Sputtering
Proc. "Silicon Carbide - 1973," Univ. of S. C. Press (1974), Ed. by R. C. Marshall, J. W. Faust, Jr., and C. E. Ryan

RYAN, C. E., BERMAN, I., MARSHALL, R. C., and LITTLER, J. R.
The Influence of Annealing on Thin Films of Beta Silicon Carbide
Proc. of IVth All-Union Conf. on Cryst. Growth - 1974

SCHWUTTKE, G. H., BRACK, K., and GOREY, E. F. (IBM, East Fishkill Labs., Hopewell Junction, N. Y.), KAHAN, A., LOWE, L. F., and EULER, F. K.
Formation and Annealing of Isolation Regions in Silicon Through SI^+ Bombardment[1]
Physica Status Solidi (a), Vol. 14, No. 1 (16 November 1972)

SHEPHERD, F. D., Jr., and YANG, A. C.
Silicon Schottky Retinas for Infrared Imaging
1973 IEDM Technical Digest, Published by IEEE (AFCRL-TR-74-0067)

SKOLNIK, L. H., BENDOW, B., and CROSS, E. F. (Aerosp. Corp., El Segundo, Calif.)
Infrared Vidicon Technique for Measuring Thermal Lensing from Laser Windows
Appl. Opt., Vol. 13, No. 4 (April 1974)

SKOLNIK, L. H., and HORDVIK, A. (Opt. Phys. Lab.), KAHAN, A.
Laser Doppler Interferometry for Measuring Small Absorption Coefficients
Appl. Phys. Lts., Vol. 23, No. 8 (15 October 1973)

TSAY, Y. F. (Univ. of R. I.), BENDOW, B., and MITRA, S. S. (Univ. of R. I.)
Theory of the Temperature Derivative of the Refractive Index in Transparent Crystals
Phys. Rev. B, Vol. 8, No. 6 (15 September 1973)

YING, S. C. (Brown Univ., Providence, R. I.), and BENDOW, B.
Phonon-Induced Desorption of Adatoms from Crystal Surfaces. II. Numerical Computations for a Model System
Phys. Rev. B, Vol. 7, No. 2 (15 January 1973)

YUKON, S. P. (Parke Math. Labs., Carlisle, Mass.), and BENDOW, B.
Single-Particle Model for the Frequency Dependence of Weak Infrared Absorption in Crystals and Molecules at T=0 K
Opt. Comm., Vol. 10, No. 1 (January 1974)

PAPERS PRESENTED AT MEETINGS JULY 1972 - JUNE 1974

ADAMSKI, J. A., WEINER, J. R., KLAUSUTIS, N., and LARKIN, J. J.
Czochralski Growth of CdTe-CdSe
Conf. on High Power IR Laser Window Mats., Hyannis, Mass. (12-14 November 1973)

ARMINGTON, A. F.
Window Materials and Coatings
Conf. on High Power IR Laser Window Mats., Hyannis, Mass. (29 October - 1 November 1972)

ARMINGTON, A. F., and BUFORD, J. T., RISING, J. (Eagle-Picher Res. Lab., Miami, Okla.), OWNBY, D. (Univ. of Mo.)
Preparation and Properties of $B_{13}P_2$ and $B_{13}As_2$
Intl. Symp. on Boron, Georgian Acad. of Sci., Metallurgy Inst., Tbilisi, Georgia, USSR (9-15 October 1972)

ARMINGTON, A. F., KLAUSUTIS, N., and SAVAGE, J. A. (Royal Radar Establishment, Great Malvern, Eng.)
Single Crystal Zinc Selenide by Vapor Transport
Conf. on High Power IR Laser Window Mats., Hyannis, Mass. (12-14 November 1973)

ARMINGTON, A. F., POSEN, H., and LIPSON, H.
Strengthening of Halides for Infrared Windows
14th Ann. Conf. of AIME, Boston, Mass. (28-30 August 1972)

BENDOW, B.
Multibranch Polariton Light Scattering in Semiconducting Crystals
11th Intl. Conf. on Semicond., Warsaw, Poland (25-29 July 1972))
Lensing of High Power Laser Windows
1972 AFSC Sci. and Engrg. Symp., San Antonio, Tex. (17-19 October 1972)
Correlation Function Theory of Multiphonon Absorption in Laser Window Materials and *Review of Thermal Lensing from Laser Window Materials*
Conf. on High Power IR Laser Window Mats. - 1972, Hyannis, Mass. (30 October - 1 November 1972)
Optical Properties of Infrared Transmitting Materials
Elect Mats. Conf. of AIME, Las Vegas, Nev. (27-29 August 1973)

BENDOW, B., and GIANINO, P. D.
The Optics of Thermal Lensing in Solids
Opt. Soc. of Am. Mtg., San Francisco, Calif. (17-20 October 1972)
Photoelastic Constants of Infrared Transmitting Materials
1973 Laser Damage Conf., Natl. Bur. of Stds., Boulder, Colo. (15-16 May 1973)

BENDOW, B., GIANINO, P. D., and MITRA, S. S., TSAY, Y. F. (Univ. of R. I.)
Stress and Pressure Dependence of the Refractive Index of Laser Window Materials
1973 Conf. on High Power IR Laser Window Mats., Hyannis, Mass. (12-14 November 1973)

BENDOW, B., SKOLNIK, L. H., GIANINO, P. D., and HORDVIK, A. (Opt. Phys. Lab.), CROSS, E. F. (Aerosp Corp., Los Angeles, Calif.)
Laser-Induced Interference and Thermal Lensing in Transparent Materials
Conf. on Laser Engrg. and Appl., Wash., D. C. (30 May - 1 June 1973)

BENDOW, B., and YING, S. C. (Brown Univ., Providence, R. I.)
Dynamics of Adatoms on Solid Surfaces: Interaction with Phonons
Intl. Conf. on Phonon Scattering in Solids, Paris, Fr. (3-6 July 1972)

BENDOW, B., and YING, S. C. (Brown Univ., Providence, R. I.), YUKON, S. (Parke Math. Labs., Carlisle, Mass.)
Multiphonon Absorption Due to Anharmonicity in Transparent Crystals
Am. Phys. Soc. Mtg., San Diego, Calif. (19-22 March 1973)
Theory of Frequency and Temperature Dependence of Intrinsic Multiphonon Absorption in Laser Window Materials
1973 Conf. on High Power IR Laser Window Mats., Hyannis, Mass. (12-14 November 1973)
Theory of Multiphonon Absorption Due to Higher Order Electric Moments in Crystals

Mtg. of Am. Phys. Soc., Philadelphia, Pa. (25-28 March 1974)

BERMAN, I.
Preparation of a Single Crystal Thin Film Compound Semiconductor by Sputtering and Annealing
Electrochem. Soc. Mtg. San Francisco, Calif. (12-16 May 1974)

BERMAN, I., MARSHALL, R. C., and RYAN, C. E.
Annealing of Sputtered β SiC
Intl. Conf. on Silicon Carbide - 1973, Miami, Fla. (17-20 September 1973)

BERMAN, I., RYAN, C. E., and MARSHALL, R. C.
Liquid Epitaxy of Alpha Silicon Carbide
Electrochem. Soc. Mtg., Miami Beach, Fla. (8-13 October 1972)

BRADFORD, J. N.
Absolute Yields of X-Ray Induced Photoemission from Metals
1972 IEEE Ann. Conf., on Nuc. and Space Radn. Eff., Univ. of Wash., Seattle, Wash. (24-27 July 1972)
X-Ray Induced Electron Emission II
IEEE Ann. Conf. on Nuc. and Space Radn. Eff., Utah State Univ., Logan, Utah (23-26 July 1973)

BROWN, R. N.
Absorption Spectra of Irradiated a-Quartz in the 3μm Region
(Inv. Talk), Lehigh Univ., Bethlehem, Pa. (21-22 May 1973)

BROWN, R. N., and KAHAN, A.
Infrared Absorption Spectra of Irradiated a-Quartz
Am. Phys. Soc. Mtg., Wash., D. C. (23-26 April 1973)

BRUCE, J. A., COMER, J. J., COLLINS, C. V., MAJ, and LIPSON, H. G.
Effects of Ion Beam Polishing on Alkali Halide Laser Window Materials
Conf. on High Power IR Laser Window Mats., Hyannis, Mass. (12-14 November 1973)

BRUCE, J. A., POSEN, H., ARMINGTON, A. F., YANG, A. C., and BLOOM, J. H.
The Inter-Relationship of Substrate Crystal Orientation and Coating in Germanium Coated Alkali Halides
Conf. on High Power IR Laser Window Mats. - 1972, Hyannis, Mass. (30 October - 1 November 1972)

BUCHANAN, B. L., NZAMEN, D. A., ROOSILD, S. A., and SHEDD, W. M.
Radiation Hardened CMOS
Wkshp. on Radn. Eff. in MOS Technol., The Dept. Auditorium, Wash., D. C. (6-7 December 1973)

BUCHANAN, B. L., SHEDD, W. M., NEAMEN, D. A., and ROOSILD. S. A.
Radiation Hardened CMOS
1974 Govt. Microcircuit Appl. Conf., Univ. of Colo., Boulder, Colo. (25-27 June 1974)

BUCKMELTER, J., CAPT., KLAUSUTIS, N., and ARMINGTON, A. F.
Calcium Addition to Potassium Halide Crystals
Am. Assoc. for Cryst. Growth - II Mtg., Princeton Univ., Princeton, N. J. (30 July - 3 August 1972)

COMER, J. J.
The Gold Decoration Technique and Its Application
NESEM Mtg., Gen. Tel. & Elect. Labs., Waltham, Mass. (16 April 1974)

COMER, J. J., and BERGERON, C.
Gold Decoration of Etched Polycrystalline KCl
Mtg. of Elect. Microscopy Soc. of Am., New Orleans, La. (13-17 August 1973)

COMER, J. J. BERGERON, C., and LOWE, L. F.
Effects of High-Energy Ions on Synthetic Quartz
30th Ann. Elect. Microscopy Soc. of Am. Mtg., Los Angeles, Calif. (14-18 August 1972)

COMER, J. J., POSEN, H., and KULIN, S. A. (ManLabs, Inc., Cambridge, Mass.)
Deformation Structures in Pressure Induced Recrystallized (PIR) KCl
Conf. on High Power IR Laser Window Mats., Hyannis, Mass. (12-14 November 1973)

DAVIES, D. E., and COMER, J. J.
Damage and Penetration of Implanted Ions in SiC
Intl. Conf. on Silicon Carbide, Miami Beach, Fla. (17-20 September 1973)

DAVIES, D. E., and ROOSILD, S. A.
Device Implications of Ion Implantation Damage in Silicon
1972 Govt. Microcircuit Appl. Conf., San Diego, Calif. (10-12 October 1972)

DIEBOLD, J. W., LT. COL., DE ANGELIS, H. M., and KIMERLING, L. C., CAPT.
Specific Observations of Radiation Effects in Semiconductors by Junction-Capacitance Techniques
Intl. Conf. on Defects in Semicond., Univ. of Reading, Reading, Eng. (19-21 July 1972)

EULER, F. K., BOUTHILLETTE, L. O., KAHAN, A., and STEIN, H. J. (Sandia Labs., Albuquerque, N. M.)
Neutron Displacement Damage in Heavily Doped GaAs
Intl. Conf. on Defects in Semicond., Univ. of Reading, Reading, Eng. (19-21 July 1972)

EYGES, L. J.
Band Structure with Overlapping Potentials
Am. Phys. Soc. Mtg., Univ. of So. Calif., Los Angeles, Calif. (27-29 December 1972)

Scattering from a Homogeneous Object of Arbitrary Shape
Am. Phys. Soc. Mtg., N. Y., N. Y. (29 January - 1 February 1973)

FIELD, W. G.
The Lore and Science of Diamonds
Pres. Night Mtg. of the Am. Inst. of Mining, Metallurgical, and Petrol. Engrg., Wash., D. C. (11 December 1973)

FIELD, W. G., and SAMPSON, J. L.
Growth of Rare Earth-Cobalt Compounds by Thermal Imaging
Am. Assoc. for Cryst. Growth - II Mtg., Princeton Univ., Princeton, N. J. (30 July - 3 August 1972)
Growth of Rare Earth-Cobalt Single Crystals
18th Ann. Conf. on Magnetism and Mag. Mats., Denver, Colo. (28 November - 1 December 1972)

FREDERICKSON, A. R.
Hemispherical Triode: A Device and Technique for Measuring Electron Emission
7th Natl. Conf. on Elect. Probe Analys., San Francisco, Calif. (17-21 July 1972)

FREDERICKSON, A. R., and BURKE, E. A.
Total Electron Backscatter and Backemission Yields from Metals Bombarded at Several Angles by 0.2 to 1.4 MeV Electrons
1972 IEEE Ann. Conf. on Nuc. and Space Radn. Eff., Univ. of Wash., Seattle, Wash. (24-27 July 1972)

GARTH, J. C., and CHADSEY, W. C. (Sci. Appl., Inc., Arlington, Va.)
POEM Code Calculations of X-Ray Photoemission
Symp. on Internal Electmg. Pulse (IEMP), San Diego, Calif. (6-8 February 1973)

GARTH, J. C., and O'BRIEN, J. V. (Arcon Corp., Wakefield, Mass.)
Numerical Solution of the Spencer-Lewis Equation for Kilovolt Electron Transport in Plane Slabs
1973 IEEE Ann. Conf. on Nuc. and Space Radn. Eff., Utah State Univ., Logan, Utah (23-26 July 1973)

GARTH, J. C., and O'BRIEN, J. V., FRIEDMAN, M. P. (Arcon Corp., Wakefield, Mass.)
Numerical Solution of the Transport Equation for Kilovolt Electrons in Solids
Am. Phys. Soc. Mtg., San Diego, Calif. (19-22 March 1973)

GARTH, J. C., and PARKE, N. G. (Parke Math. Labs., Concord, Mass.), DI STEFANO, T. H. (IBM Res. Ctr., Yorktown Heights, N. Y.)
Anisotropic Electron-Phonon Scattering of Electrons in Lithium Fluoride
Am. Phys. Soc. Mtg., Philadelphia, Pa. (25-28 March 1974)

GIANINO, P. D., and BENDOW, B.
Optical Performance Evaluation of Infrared Transmitting Materials
14th Ann. Conf. of AIME, Boston, Mass. (28-30 August 1972)

GOLUBOVIC, A., EWING, W. S, BRUCE, J. A., COMER, J. J., and MILAM, D. (Opt. Phys. Lab.)
A Comparison of 10.6 μ m Laser Damage in Sputtered Vs. Electron Beam Deposited Ge-Coated KCl
ASTM Mtg., Natl. Bur. of Stds., Boulder, Colo. (22-23 May 1974)

HORDVIK, A. (Opt. Phys. Lab.), and SKOLNIK, L. H.
Laser Induced Thermal Distortion of CO_2 Laser Window Materials
1972 AFSC Sci. and Engrg. Symp., San Antonio, Tex. (17-19 October 1972)

KAHAN, A., LIPSON, H. G., and SKOLNIK, L. H.
The Computation of the Absorption Coefficient from Calorimetric Data
1973 Conf. on High Power IR Laser Window Mats., Hyannis, Mass. (12-14 November 1973)

KENNEDY, J. K., and POTTER, W. D.
The Effect of Various Growth Parameters on the Surface Morphology of Epitaxial GaAs
Am. Assoc. for Cryst. Growth - II Mtg., Princeton Univ., Princeton, N. J. (30 July - 3 August 1972)

KENNEDY, J. K., POTTER, W. D., and DAVIES, D. E.
The Effect of the Hydrogen Carrier Gas Flow Rate on the Electrical Properties of Epitaxial GaAs Prepared in a Hydride System
Intl. Conf. on Cryst. Growth (ICCG-4), Tokyo, Jap. (24-29 March 1974)

KIMERLING, L. C. (Bell Labs., Murray Hill, N. J.), DE ANGELIS, H. M., and DIEBOLD, J. W., LT. COL.
On the Role of Defect Charge State in the Stability of Point Defects In Silicon
Am. Phys. Soc. Mtg., Philadelphia, Pa. (25-28 March 1974)

KIMERLING, L. C., CAPT., DREVINSKY, P. J., and CHEN, C. S. (Rensselaer Polytech. Inst., Troy, N. Y.)
Defect Interaction in Neutron-Irradiated Lithium-Doped Silicon
Intl. Conf. on Defects in Semicond., Univ. of Reading, Reading, Eng. (19-21 July 1972)

KLAUSUTIS, N., HUNT, M. H., ADAMSKI, J. A., WEINER, J., and BUCKMELTER, J., CAPT.
Preparation and Growth of Indium Phosphide
Am. Assoc. for Cryst. Growth - II Mtg., Princeton Univ., Princeton, N. J. (30 July - 3 August 1972)

KULIN, S. A., KREDER, K. (ManLabs, Inc., Cambridge, Mass.), POSEN, H., and BOWEN, H. K. (Ctr. for Mats. Sci. and Engrg., Mass. Inst. of Technol., Cambridge, Mass.)
Fabrication of Large Polycrystalline Infrared Windows
Conf. on High Power IR Laser Window Mats. -1972, Hyannis, Mass. (30 October - 1 November 1972)

KULIN, S. A. (ManLabs, Inc., Cambridge, Mass.), and POSEN, H.
Texture Studies in ZnSe
Conf. on High Power IR Laser Window Mats., Hyannis, Mass. (12-14 November 1973)

LARKIN, J. J.
Hardened Alkali Halide Laser Window Materials
1972 AFSC Sci. and Engrg. Symp. San Antonio, Tex. (17-19 October 1972)

LARKIN, J. J., ARMINGTON, A. F., POSEN, H., and O'CONNOR, J. J.
Structure and Properties of Polycrystalline Sodium Chloride-Potassium Chloride Systems
Am. Ceramic Soc. BEN Jt. Div. Fall Mtg., Philadelphia, Pa. (24-27 September 1972)

LARKIN, J. J., HILTON, R., BRUCE, J. A., POSEN, H., ARMINGTON, A. F., and LIPSON, H. G.
Some Studies on the Growth of Gallium Phosphide
Am. Assoc. for Cryst. Growth - II Mtg., Princeton Univ., Princeton, N. J. (30 July - 3 August 1972)

LIPSON, H. G., LARKIN, J. J., BENDOW, B., and MITRA, S. S. (Univ. of R. I.)
Impurity Absorption in KCl Windows
1973 Conf. on High Power IR Laser Window Mats., Hyannis, Mass. (12-14 November 1973)

LIPSON, H. G., and LIGOR, P. A.
Impurity, Surface and Imperfection Effects on 10.6 Micron Absorption in Alkali Halides
Conf. on High Power IR Laser Window Mats. - 1972, Hyannis, Mass. (30 October - 1 November 1972)

LIPSON, H. G., and SKOLNIK, L. H.
Optical Properties of Laser Window Materials - A Review of the AFCRL Experimental Program
IRIS Speciality Gp. on IR Opt. Mats. Mtg., Monterey, Cali. (5-7 June 1973)

LIPSON, H. G., SKOLNIK, L. H., and STIERWALT, D. L. (Naval Elect. Ctr., San Diego, Calif.)
Small Absorption Coefficient Measurement by Calorimetric and Spectral Emittance Techniques
1973 Conf. on High Power IR Laser Window Mats., Hyannis, Mass. (12-14 November 1973)

MARSHALL, R. C.
Perspectives on Silicon Carbide
Intl. Conf. on Silicon Carbide - 1973, Miami Beach, Fla. (17-20 September 1973)

MARSHALL, R. C., LITTLER, J. R., RYAN, C. E., HAWLEY, J. J., BERMAN, I., and CONSIDINE, D. P.
A Unique High Temperature-High Pressure Crystal Growth System for Silicon Carbide
IVth All-Union Conf. on Cryst. Growth, Tsakhkadzor, Armenian SSR (16-23 September 1972)

MARSHALL, R. C., RYAN, C. E., LITTLER, J. R., and BERMAN, I.
New Growth Experiments in SiC
Intl. Conf. on Silicon Carbide - 1973, Miami Beach, Fla. (17-20 September 1973)

MITRA, S. S. (Univ of R. I.), BENDOW, B., and TSAY, Y. F. (Univ. of R. I.)
Theory of dn/dT in Crystals
Am. Phys. Soc. Mtg., San Diego, Calif. (19-22 March 1973)

MITRA, S. S., NAMJOSHI, K. V., PAUL, D. K. TSAY, Y. F. (Univ. of R. I.), and BENDOW, B.
Optical Properties of Amorphous Materials for Laser Windows
1973 Conf. on High Power IR Laser Window Mats., Hyannis, Mass. (12-14 November 1973)

MITRA, S. S., TSAY, Y. F. (Univ. of R. I.), and BENDOW, B.
Theory of the Temperature Dependence of the Index of Refraction of Laser Window Materials
Conf. on High Power IR Laser Window Mats., Hyannis, Mass. (30 October - 1 November 1972)

NEAMEN, D. A., SHEDD, W. M., and BUCHANAN, B. L.
Radiation Effects on Dielectrically Isolated Junction Field Effect Transistors
1972 IEEE Ann. Conf. on Nuc. and Space Radn. Eff., Univ. of Wash., Seattle, Wash. (24-27 July 1972)
Permanent Ionizing Radiation Effects in Dielectrically Bounded Field Effect Transistors
1973 IEEE Ann. Conf. on Nuc. and Space Radn. Eff., Utah State Univ., Logan, Utah (23-26 July 1973)
Permanent Ionizing Radiation Effects in Gate and Isolation Dielectrics in FET's
Wkshp. on Radn. Eff. in MOS Technol., The Dept. Auditorium, Wash., D. C. (6-7 December 1973)
1974 Govt. Microcircuit Appl. Conf., Univ. of Colo., Boulder, Colo. (25-27 June 1974)

NIKULA, J. V., and DIEBOLD, J. W., LT. COL.
The Automation of a Junction Capacitance Measurement Within the LAAF System
COMMON Mtg., Detroit, Mich. (24-27 April 1973)

O'CONNOR, J. J., LARKIN, J. J., ARMINGTON, A. F., POSEN, H., and PICKERING, N. E.
Solid Solution Halide Crystals
Am. Assoc. for Cryst. Growth - II Mtg., Princeton Univ., Princeton, N. J. (30 July - 3 August 1972)

O'CONNOR, J. J., LARKIN, J. J., PICKERING, N. E., and ARMINGTON, A. F.
Preparation and Properties of Rubidium Chloride Doped Solid Solutions
Conf. on High Power IR Laser Window Mats., Hyannis, Mass. (12-14 November 1973)

PELLEGRINI, P. W., and FELDMAN, J. M. (Northeastern Univ., Boston, Mass.)
LPE Growth of SiC Using Transition Metal-Silicon Solvents
Intl. Conf. on Silicon Carbide - 1973, Miami Beach, Fla. (17-20 September 1973)

PICK, M. A., SCHWUTTKE, G. H. (IBM, East Fishkill Labs., Hopewell Junction, N. Y.), LOWE, L. F., and POSEN, H.
Precision Measurement of Lattice Changes in Magnetic Bubble Garnets After High Energy H^+ Implantation
Electrochem. Soc. Mtg., San Francisco, Calif. (12-17 May 1974)

POSEN, H.
The Mechanical Strengthening of Infrared Halide Windows
Conf. on High Power IR Laser Window Mats., Hyannis, Mass. (30 October - 1 November 1972)

POSEN, H., BRUCE, J. A., COMER, J. J., and ARMINGTON, A. F.
A Study of 10.6 μm Laser Induced Damage in Halide Crystals
Symp. on Damage in Laser Mats., Natl. Bur. of Stds., Boulder, Colo. (15-16 May 1973)

POSEN, H., Bruce, J. A., and MILAM, D. (Opt. Phys. Lab.)
10.6 μm Laser Damage in ZnSe
ASTM Mtg., Natl. Bur. of Stds., Boulder. Colo. (22-23 May 1974)

POSEN, H., and KULIN, S. A., KREDER, K. (ManLabs, Inc., Cambridge, Mass.), BOWEN, H. K. (Ctr. for Mats. Sci. and Engrg., Mass. Inst. of Technol., Cambridge, Mass.)
Properties of Large Polycrystalline KCl Windows
Conf. on High Power IR Laser Window Mats., Hyannis, Mass. (30 October - 1 November 1972)

ROOSILD, S. A., SHEDD, W. M., and BUCHANAN, B. L.
High Dose Gamma Radiation Effects on Solid State Electronic Devices
1972 Govt. Microcircuit Appl. Conf., San Diego, Calif. (10-12 October 1972)

RYAN, C. E., BERMAN, I., and MARSHALL, R. C.
Thin Films of a and Silicon Carbide Prepared by Liquid Epitaxy and by Sputtering
Intl. Conf. on Silicon Carbide - 1973, Miami Beach, Fla. (17-20 September 1973)

RYAN, C. E., BERMAN, I., MARSHALL, R. C., and LITTLER, J. R.
The Influence of Annealing on Thin Films of Beta SiC
IVth All-Union Conf. on Cryst. Growth, Tsakhkadzor, Armenian SSR (16-23 September 1972)

SAHAGIAN, C. S.
Crystal Growth Technology (Inv. Lecture)
Armenian Acad. of Sci., Erivan, ASSR (23-26 September 1972)

SAMPSON, J. L., and FIELD, W. G.
Crucibleless Czochralski Crystal Growth
Assoc. for Cryst. Growth - II Mtg., Princeton Univ., Princeton, N. J. (30 July - 3 August 1972)

SHEDD, W. M., NEAMEN, D. A., and BUCHANAN, B. L.
Rapid Anneal in MIS Transistors
Wkshp. on Radn. Eff. in MOS Technol., The Dept. Auditorium, Wash., D. C. (6-7 December 1973)

SHEPHERD, F. D., VICKERS, V. E., and BURKE, E. A.
Prediction of Ionizing Radiation Noise in Infrared Sensors
IRIS Specialty Gp. on IR Detectors, Naval Res. Lab., Wash., D. C. (13-15 March 1973)

SHEPHERD, F. D., JR., and YANG, A. C.
Silicon Schottky Retinas for Infrared Imaging
1973 IEEE Intl. Elect. Dev. Mtg., Wash., D. C. (3-5 December 1973)

SKOLNIK, L. H., BENDOW, B., GIANINO, P. D., and CROSS, E. F. (Aerosp. Corp., El Segundo, Calif.)
Mid and Far Infrared Vidicon Investigations of Thermal Lensing, Interference, and Thermal Radiation from Laser Windows
1973 Conf. on High Power IR Laser Window Mats., Hyannis, Mass. (12-14 November 1973)

SKOLNIK, L. H., BENDOW, B., GIANINO, P. D., and HORDVIK, A. (Opt. Phys. Lab.), CROSS, E. F. (Aerosp. Corp., El Segundo, Calif.)
Interference and Lensing Effects in the Transmission of High Power Laser Beams Through Infrared Windows
Conf. on High Power IR Laser Window Mats - 1972, Hyannis, Mass. (30 October - 1 November 1972)

SKOLNIK, L. H., KAHAN, A., and HORDVIK, A. (Opt. Phys. Lab.), CLARK, O. M.
A Doppler Shift Interferometric Technique for Measuring Small Absorption Coefficients
1973 Conf. on High Power IR Laser Window Mats., Hyannis, Mass. (12-14 November 1973)

TING, C. S., BIRMAN, J. L. (N. Y. Univ.), and BENDOW, B.
Theory of Multiphonon Absorption Including the Impurity

Vibrational Mode for an Ionic Crystal
Conf. on High Power IR Laser Window Mats., Hyannis, Mass. (12-14 November 1973)
Theory of Multiphonon Infrared Absorption Including Impurity Vibrational Modes for Ionic Crystals
Am. Phys. Soc. Mtg., Philadelphia, Pa. (25-28 March 1974)

TSAY, Y. F., MITRA, S. S. (Univ. of R. I.), and BENDOW, B.
Pressure and Stress Dependence of the Refractive Index in Transparent Crystals
Am. Phys. Soc. Mtg., Philadelphia. Pa. (25-28 March 1974)

WILKENING, W., FRIEDMAN, J. D., and PITHA, C. A.
Measurement of Stress-Induced Birefringence in Alkali Halides
1973 Conf. on High Power IR Laser Window Mats., Hyannis, Mass. (12-14 November 1973)

TECHNICAL REPORTS
JULY 1972 - JUNE 1974

ADAMSKI, J. A., WEINER, J. R., KLAUSUTIS, N., and LARKIN, J. J.
Czochralski Growth of CdTe-CdSe
Third Conf. on High Power IR Laser Window Mats., Nov. 12-14, 1973, Vol. II: Mats., AFCRL-TR-74-0085 (II) (14 February 1974)

ARMINGTON, A. F., KLAUSUTIS, N., and SAVAGE, J. A. (Royal Radar Establishment, Great Malvern, Eng.)
Single Crystal Zinc Selenide by Vapor Transport
Third Conf. on High Power IR Laser Window Mats., Nov. 12-14, 1973, Vol. II: Mats., AFCRL-TR-74-0085(II) (14 February 1974)

BENDOW, B.
Correlation Function Theory of Multiphonon Absorption in Laser Window Materials
Conf. on High Power IR Laser Window Mats., Oct. 30, 31 and Nov. 1, 1973, Vol. I, AFCRL-TR-73-0372(I) (19 June 1973)

BENDOW, B., and GIANINO, P. D.
Optical Performance Evaluation of Infrared Transmitting Materials
AFCRL-72-0565 (19 September 1972)

BENDOW, B., GIANINO, P. D., and MITRA, S. S., TSAY, Y. F. (Univ. of R. I.)
Stress and Pressure Dependence of the Refractive Index of Laser Window Materials
Third Conf. on High Power IR Laser Window Mats., Nov. 12-14, 1973, Vol. I: Opt. Properties, AFCRL-TR-74-0085(I) (14 February 1974)

BENDOW, B., SKOLNIK, L. H., and GIANINO, P. D.
A Review of Research on Thermal Lensing from Laser Window Materials
Conf. on High Power IR Laser Window Mats., Oct. 30, 31 and Nov. 1, 1973, Vol. 1, AFCRL-TR-73-0372(I) (19 June 1973)

BENDOW, B., and YING, S. C. (Brown Univ., Providence, R. I.), YUKON, S. P. (Parke Math. Labs., Carlisle, Mass.)
Theory of Frequency and Temperature Dependence of Intrinsic Multiphonon Absorption in Laser Window Materials
Third Conf. on High Power IR Laser Window Mats., Nov. 12-14, 1973, Vol. I: Opt. Properties, AFCRL-TR-74-0085(I) (14 February 1974)

BERMAN, I., RYAN, C. E., MARSHALL, R. C., and LITTLER, J. R.
The Influence of Annealing on Thin Films of Beta SiC
AFCRL-72-0737 (19 December 1972)

BRADFORD, J. N.
Absolute Yields of X-Ray Induced Photoemission from Metals
AFCRL-72-0542 (23 August 1972)

BROWN, R. N.
The Conductivity of Quartz After Electrolysis
AFCRL-TR-73-0479 (31 July 1973)
The Analysis of Optical Surface Scattering from Epitaxial Films
AFCRL-TR-73-0728 (28 November 1973)

BROWN, R. N., and KENNEDY, J. K.
Preparation and Optical Energy Gap of Epitaxial Films of $InAs_{1-x}P_x$ Alloys
AFCRL-TR-74-0280 (20 June 1974)

BRUCE, J. A., COMER, J. J., COLLINS, C. V., MAJ., and LIPSON, H. G.
Effects of Ion Beam Polishing on Alkali Halide Laser Window Materials
Third Conf. on High Power IR Laser Window Mats., Nov. 12-14, 1973, Vol. III: Surfaces, Coatings, AFCRL-TR-74-0085(III) (14 February 1974)

COMER, J. J., POSEN, H., and KULIN, S. A. (ManLabs, Inc., Cambridge, Mass.)
Deformation Structures in Pressure Induced Recrystallized (PIR) KCl
Third Conf. on High Power IR Laser Window Mat., Nov. 12-14, 1973, Vol. II: Mats., AFCRL-TR-74-0085(II) (14 February 1974)

DE ANGELIS, H. M., DIEBOLD, J. W., LT., COL., and KOMM, D. S., 1ST. LT.,(Mass. Inst. of Technol.), NIKULA, J. V.
Charge State Effects on Annealing of Electron Irradiated Silicon
AFCRL-TR-74-0239 (22 May 1974)

DIEBOLD, J. W., LT. COL., DE ANGELIS, H. M., and KIMERLING, L. C. (Bell Labs., Murray Hill, N. J.), FITZGERALD, J. J.
Junction Capacitance Techniques to Characterize Radiation Damage in Silicon
AFCRL-TR-73-0157 (12 March 1973)

EWING, W. S.
Polishing Methods for KCl
AFCRL-TR-74-0134 (8 March 1974)

FIELD, W. G., and SAMPSON, J. L.
A Vertical Thermal-Imaging Furnace for Single Crystal Growth
AFCRL-TR-73-0386 (2 July 1973)

KAHAN, A.
Free-Carrier Optical Effects in Gallium Arsenide
AFCRL-TR-73-0122 (27 February 1973)

KAHAN, A., LIPSON, H. G., and SKOLNIK, L. H.
The Computation of the Absorption Coefficient from Calorimetric Data
Third Conf. on High Power IR Laser Window Mats., Nov. 12-14, 1973, Vol. I: Opt. Properties, AFCRL-TR-74-0085(I) (14 February 1974)

KULIN, S. A. (ManLabs, Inc., Cambridge, Mass.), and POSEN, H.
Texture Studies in ZnSe
Third Conf. on High Power IR Laser Window Mats., Nov. 12-14, 1973, Vol. II: Mats., AFCRL-TR-74-0085(II) (14 February 1974)

LIPSON, H. G., Larkin, J. J., BENDOW, B., and MITRA, S. S. (Univ. of R. I.)
Impurity Absorption in KCl Windows
Third Conf. on High Power IR Laser Window Mats., Nov. 12-14, 1973, Vol. I: Opt. Properties, AFCRL-TR-74-0085(I) (14 February 1974)

LIPSON, H. G., and LIGOR, P. A.
Impurity, Surface and Imperfection Effects on 10.6 Micron Absorption in Alkali Halides
Conf. on High Power IR Laser Window Mats., Oct. 30, 31 and Nov. 1, 1973, Vol. I, AFCRL-TR-73-0372(I) (19 June 1973)

LIPSON, H. G., SKOLNIK, L. H., and STIERWALT, D. L. (Naval Elect. Lab. Ctr., San Diego, Calif.)
Small Absorption Coefficient Measurement by Calorimetric and Spectral Emittance Techniques
Third Conf. on High Power IR Laser Window Mats., Nov. 12-14, 1973, Vol. I: Opt. Properties, AFCRL-TR-74-0085(I) (14 February 1974)

LITTLER, J. R., MARSHALL, R. C., RYAN, C. E., HAWLEY, J. J., and BERMAN, I.
A Unique High-Temperature, High-Pressure Crystal Growth System for Silicon Carbide
AFCRL-TR-73-0074 (4 January 1973)

LOWE, L. F., KENNEDY, J. K., DAVIES, D. E., DEANE, M. L., and EYGES, L. J.
Surface Temperature Measurements for Ion Bombarded Si and GaAs at 1.0 to 2.0 MeV
AFCRL-TR-73-0660 (29 October 1973)

LOWE, L. F., TURNER, C. D., and HYATT, J. R. (Tufts Univ., Medford, Mass.)
Summary Report on Magnetic Bubble Material Radiation Hardness Study
AFCRL-TR-74-0316 (16 July 1974)

LUDMAN, J. E.
Defect Levels in Neutron-Irradiated GaAs Schottky Diodes and Laser Diode Degradation
AFCRL-TR-73-0344 (31 May 1973)

MITRA, S. S. NAMJOSHI, K. V., PAUL, D. K., TSAY, Y. F. (Univ. of R. I.), and BENDOW, B.
Optical Properties of Amorphous Materials for Laser Windows
Third Conf. on High Power IR Laser Window Mats., Nov. 12-14, 1973, Vol. III: Surfaces, Coatings, AFCRL-TR-74-0085(III) (14 February 1974)

O'CONNOR, J. J., LARKIN, J. J., PICKERING, N. E., and ARMINGTON, A. F.
Preparation and Properties of Rubidium Chloride Doped Solid Solutions
Third Conf. on High Power IR Laser Window Mats., Nov. 12-14, 1973, Vol. II: Mats., AFCRL-TR-74-0085(II) (14 February 1974)

PITHA, C. A. (Editor)
Conference on High Power Infrared Laser Window Materials, October 30, 31 and November 1, 1972
AFCRL-TR-73-0372(I) & (II) (19 June 1973)

PITHA, C. A., ARMINGTON, A. F., and POSEN, H. (Editors)
Third Conference on High Power Infrared Laser Window Materials November 12-14, 1973, Vol. II: Materials
AFCRL-TR-74-0085(II) (14 February 1974)

PITHA, C. A., and BENDOW, B. (Editors)
Third Conference on High Power Infrared Laser Window Materials November 12-14, 1973, Vol I: Optical Properties
AFCRL-TR-74-0085(I) (14 February 1974)

PITHA, C. A., POSEN, H., and ARMINGTON, A. F. (Editors)
Third Conference on High Power Infrared Laser Window Materials November 12-14, 1973, Vol. III: Surfaces, Coatings
AFCRL-TR-74-0085(III) (14 February 1974)

POSEN, H., ARMINGTON, A. F., and BRUCE, J. A.
Appropriate Hardening Mechanisms in Alkali Halide Materials for High Power 10.6 μ m Windows
AFCRL-72-0434 (28 July 1972)

SHEPHERD, F. D., JR., and VICKERS, V. E.
Debris Gamma-Induced Limitations on the System Performance of an Extrinsic Infrared Sensor
AFCRL-TR-73-0537 (2 August 1973)

SKOLNIK, L. H., BENDOW, B., GIANINO, P. D., and CROSS, E. F. (Aerosp. Corp., Los Angeles, Calif.)
Mid and Far Infrared Vidicon Investigations of Thermal Lensing, Interference, and Thermal Radiation from Laser Windows
Third Conf. on High Power IR Laser Window Mats., Nov. 12-14, 1973, Vol. III: Surfaces, Coatings, AFCRL-TR-74-0085(III) (14 February 1974)

SKOLNIK, L. H., BENDOW, B., GIANINO, P. D., and HORDVIK, A. (Opt. Phys. Lab.), CROSS, E. F. (Aerosp. Corp., Los Angeles, Calif.)
Interference and Lensing Effects in the Transmission of High Power Laser Beams Through Infrared Windows
Conf. on High Power IR Laser Window Mats., Oct. 30, 31 and Nov. 1, 1973, Vol. I, AFCRL-TR-73-0372(I) (19 June 1973)

SKOLNIK, L. H., KAHAN, A., and HORDVIK, A. (Opt. Phys. Lab.), CLARK, M.
A Doppler Shift Interferometric Technique for Measuring Small Absorption Coefficients
AFCRL-TR-74-0001 (20 December 1973), Third Conf. on High Power IR Laser Window Mats., Nov. 12-14, 1973, Vol. I: Opt. Properties, AFCRL-TR-74-0085(I) (14 February 1974)

TING, C. S., BIRMAN, J. L. (N. Y. Univ.), and BENDOW, B.
Theory of Multiphonon Absorption Including the Impurity Vibrational Mode for an Ionic Crystal
Proc. of 3rd Conf. on High Power IR Laser Window Mats., Nov. 12-14, 1973, Vol. I: Opt. Properties, Ed.: C. A. Pitha and B. Bendow, AFCRL-TR-74-0085 (I) (14 February 1974)

VICKERS, V. E., SHEPHERD, F. D., Jr., and BURKE, E. A.
Ionizing Noise in Infrared Sensors
AFCRL-TR-73-0750 (13 December 1973)

WILKENING, W. W., FRIEDMAN, J. D., and PITHA, C. A.
Measurement of Stress-Induced Birefringence in Alkali Halides
Third Conf. on High Power IR Laser Window Mats., Nov. 12-14, 1973, Vol. I: Opt. Properties, AFCRL-TR-74-0085(I) (14 February 1974)

Appendix A

AFCRL PROJECTS BY PROGRAM ELEMENT

Program Element	Project Number, Title and Agency	
61101F	*IN-HOUSE LABORATORY INDEPENDENT RESEARCH*	
	ILIR Laboratory Director's Fund	
61102F	*DEFENSE RESEARCH SCIENCES*	*AFCRL*
	2153 Electromagnetics of Hypersonic Flight	
	5620 Advanced Electromagnetic Materials	
	5621 Physics of the Interaction of Energy with Solid Materials	
	5631 Ionospheric Radio Physics	
	5634 Research in Quantum Electronics	
	5635 Electromagnetic and Electroacoustic Sensors and Devices	
	5638 Research on Solid State Electronics	
	8600 Energetic Particle Environment	
	8601 Geomagnetism	
	8603 Infrared and Optical Techniques	
	8604 Meteorological Research	
	8605 Upper Atmosphere Composition	
	8607 Earth Sciences and Technologies	
	8608 Solar Plasma Dynamics*	
	8617 Electrical Structure of Aerospace	
	8620 Cloud Physics	
	8627 Spectroscopic Studies of Upper Atmospheric Processes	
	8658 Infrared Non-Equilibrium Radiative Mechanisms	
	8659 Space Power Research*	
62101F	*ENVIRONMENT*	*AFCRL*
	4603 Generation and Propagation of Low Frequency Radio Waves	
	4642 Plasma Interactions and Microwave and Laser Systems*	
	4643 Aerospace Radio Propagation	
	6665 Balloon Technology	
	6670 Atmospheric Sensing Techniques	
	6672 Weather Radar Techniques	
	6687 Stratospheric Environment	
	6688 Ultraviolet Radiation	
	6690 Atmospheric Density and Structure	
	6698 Satellite Meteorology	
	7600 Geodesy for Naviguidance	
	7601 Electric and Magnetic Fields	
	7605 Weather Modification	
	7621 Atmospheric Optics	
	7628 Geophysical and Geokinetic Effects	
	7635 Upper Atmosphere Dynamics	
	7639 Wave Propagation Studies	
	7649 Solar Environmental Effects	
	7655 Micrometeorology	
	7659 Aerospace Research Instrumentation	
	7661 Polar Atmospheric Processes	
	7663 Ionospheric Dynamics and Propagation	
	7670 IR Properties of the Environment	
	8624 Variability of Meteorological Elements	
	8628 Mesoscale Weather Forecasting	
	8666 Space Environment Observing and Forecasting Techniques*	
	8682 Tropospheric Wave Propagation	

Appendix A

AFCRL PROJECTS BY PROGRAM ELEMENT

62102F	*MATERIALS*	*AFML*
	7371 Magnetic Bubble Memory Investigation	
62204F	*AEROSPACE AVIONICS*	*AFAL*
	6096 Electronic Device and Circuitry Techniques	
	6100 Electro-Optical Technology	
62601F	*ADVANCED WEAPONS AND APPLICATIONS*	*AFWL*
	3326 Laser Application	
62702F	*GROUND ELECTRONICS*	*RADC*
	4600 Electromagnetic Radiation Techniques	
	5573 Microwave Tubes/Devices	

In addition to the above continuing Air Force funded projects, AFCRL participates in joint programs supported by the following agencies:

1) U.S. Air Force:
   - Air Force Weapons Laboratory
   - Electronic Systems Division
   - Air Force Materials Laboratory
   - Space and Missile Systems Organization
   - Air Weather Service
   - Air Force Technical Applications Center
   - Air Force Flight Test Center
2) Advanced Research Projects Agency
3) National Aeronautics and Space Administration
4) Atomic Energy Commission
5) Defense Nuclear Agency
6) Defense Mapping Agency
7) Army Materiel Command
8) Department of Transportation
9) U.S. Navy

* Terminated 30 June 1974

Appendix B

AFCRL ROCKET AND SATELLITE PROGRAM: JULY 1972 - JUNE 1974

Date	Launch Site	Vehicle	Experiment	Scientist	Results
15 Jul 72	ADTC	Black Brant VB	Solar EUV	J. Higgins	Failure (V)*
28 Jul 72	WOPS	Trailblazer II	Additives	J. L. Poirier	Success
18 Aug 72	WSMR	Aerobee 170	IR Stellar Sources	R. Walker	Success
23 Aug 72	WSMR	Aerobee 170	Solar XUV	L. Heroux	Success
24 Sep 72	CRR	Black Brant VA	PCA Study	J. Ulwick	Success
25 Sep 72	CRR	Black Brant VA	Quiet Background	J. Ulwick	Success
2 Oct 72	WTR	STP 72-1	Proton and Alpha Isotope Detector	L. Katz	Success
11 Oct 72	WTR	Aerobee 170	Chaser	R. Huffman	Success
31 Oct 72	ADTC	Niro	TMA, Ba, Na/Li	N. Rosenberg	Success
31 Oct 72	ADTC	Niro	Hibal Sphere	N. Rosenberg A. Faire	Success
1 Nov 72	ADTC	Niro	COS, Na	N. Rosenberg	Success
1 Nov 72	ADTC	Niro	Chemical Release	N. Rosenberg	Success
1 Nov 72	ADTC	Niro	Hibal Sphere	A. Faire	Success
5 Nov 72	ADTC	Nike Tomahawk	Chemical Release	N. Rosenberg	Failure (V)
6 Nov 72	ADTC	Nike Tomahawk	10" Sphere	A. Faire	Failure (V)
4 Dec 72	WSMR	Aerobee 170	IR Stellar Sources	R. Walker	Success
5 Dec 72	CRR	Black Brant VC	IR Airglow	A. T. Stair	Success
6 Dec 72	CRR	Astrobee D	IR Ionospheric Characteristics	J. Ulwick	Failure (V)
7 Dec 72	CRR	Ute Tomahawk	Neutral Mass Spectrometer	C. Philbrick J. Aarons	Success
7 Dec 72	CRR	Niro	7" Falling Sphere	A. Faire	Success
8 Dec 72	CRR	Astrobee D	IR Ionosphere Characteristics	J. Ulwick	Partial
10 Dec 72	CRR	Niro	Polar Neutral Composition	C. Philbrick	Success
10 Dec 72	CRR	Niro	7" Falling Sphere	A. Faire	Success
21 Mar 73	PFRR	Astrobee D	OH Background	A. T. Stair	Success
22 Mar 73	PFRR	Black Brant V	Auroral Emission (ICECAP)	A. T. Stair	Success
24 Mar 73	PFRR	Paiute Tomahawk	Auroral Characteristics	J. Ulwick	Success
26 Mar 73	PFRR	Black Brant VC	Ionospheric Characteristics	J. Ulwick	Success
26 Mar 73	PFRR	Paiute Tomahawk	TMA, 10" Falling Sphere	A. Faire	Partial
6 Apr 73	PFRR	Astrobee D	Enhanced OH	A. T. Stair	Success
16 Apr 73	WSMR	Ute Tomahawk	O_3 & OH & O_2 Photometers	L. Weeks	Success

WOPS — Wallops Island
WSMR — White Sands Missile Range, New Mexico
CRR — Churchill Rocket Range, Manitoba, Canada
ADTC — Armament Development Test Center, Eglin AFB, Florida
WTR — Western Test Range, Vandenberg AFB, California
PFRR — Poker Flat Rocket Range, Alaska

Appendix B

AFCRL ROCKET AND SATELLITE PROGRAM: JULY 1972 - JUNE 1974

Date	Launch Site	Vehicle	Experiment	Scientist	Results
16 Apr 73	WSMR	Ute Tomahawk	O_3 & O_2 Photometer, Geiger X-Ray	L. Weeks	Success
26 Apr 73	WSMR	Aerobee 150	UV Absorption	F. LeBlanc	Failure (P)*
25 May 73	Natal, Brazil	Castor-Lance	IR Markov Layer	R. Walker	Success
12 Jun 73	CRR	Ute Tomahawk	Mass Spectrometer, Scintillation	R. Narcisi	Success
13 Jun 73	CRR	Ute Tomahawk	Mass Spectrometer, Scintillation	R. Narcisi	Success
9 Aug 73	WOPS	Black Brant IVB Mod. I	Diagnostic	E. Mansfield	Success
10 Aug 73	WSMR	Aerobee 150	Bremsstrahlung	H. Cohen	Success
11 Sep 73	WSMR	Ute Tomahawk	Vehicle Potential Stabilization	C. Sherman	Failure (P)
18 Sep 73	PFRR	Ute Tomahawk	Polar Disturbed Ionosphere	R. Nadile	Success
18 Sep 73	PFRR	Ute Tomahawk	Polar Disturbed Ionosphere	R. Nadile	Success
26 Sep 73	Natal, Brazil	Paiute Tomahawk	O_2, O_3, X-Ray	L. Weeks	Failure (P)
26 Sep 73	Natal, Brazil	Niro	7" Sphere	A. Faire	Success
27 Sep 73	Natal, Brazil	Niro	7" Falling Sphere	A. Faire	Success
3 Oct 73	WSMR	Astrobee D	IR Detector, Radiometer	J. Ulwick	Partial
3 Oct 73	WSMR	Astrobee D	IR Detector, Radiometer	J. Ulwick	Success
3 Oct 73	WSMR	Astrobee D	IR Detector, Radiometer	J. Ulwick	Success
18 Oct 73	ADTC	Niro	TMA Release	N. Rosenberg	Success
19 Oct 73	ADTC	Nike Tomahawk	NO Release, Photometers	N. Rosenberg	Success
19 Oct 73	ADTC	Ute Tomahawk	TMA Release	N. Rosenberg	Success
19 Oct 73	ADTC	Niro	TMA Release	N. Rosenberg	Success
19 Oct 73	ADTC	Nike Tomahawk	Ba Release	N. Rosenberg	Success
19 Oct 73	ADTC	Ute Tomahawk	Al Vapor	N. Rosenberg	Success
19 Oct 73	ADTC	Nike Tomahawk	TMA Release	N. Rosenberg	Success
20 Oct 73	ADTC	Nike Iroquois	Tetra Ethyl Pb, Li	N. Rosenberg	Success
21 Oct 73	ADTC	Paiute Tomahawk	Na/Li Diborane, 7" Sphere	N. Rosenberg	Failure (V)
24 Oct 73	ADTC	Black Brant IVA	VLF Propagation	E. Lewis	Success
25 Oct 73	ADTC	Black Brant IVA	VLF Propagation	E. Lewis	Success
2 Nov 73	WSMR	Aerobee 170	EUV	L. Heroux	Success
6 Dec 73	WOPS	Trailblazer	Reentry Microwave Physics	W. Rotman	Success
10 Dec 73	CRR	Ute Tomahawk	Mass Spectrometer — O_2, O_3 — Photometers	C. Philbrick	Partial
16 Dec 73	WTR	AE-C	Tri-Axial Accelerometer	F. Marcos	Success
16 Dec 73	WTR	AE-C	EUV Spectrophotometer	H. Hinteregger	Success
8 Feb 74	PFRR	Astrobee D	TMA Tracking	J. Ulwick	Success
14 Feb 74	PFRR	Black Brant VC	CVF & Photometer	J. Ulwick	Success
14 Feb 74	PFRR	Ute Tomahawk	Density — Hibal	A. Faire	Failure (V)
16 Feb 74	WSMR	Aerobee 350	IR Steliar Sources	R. Walker	Partial
16 Feb 74	WSMR	Ute Tomahawk	Density	J. Geary	Success
21 Feb 74	PFRR	Black Brant VC	HIRIS	A. T. Stair	Success

Appendix B

AFCRL ROCKET AND SATELLITE PROGRAM: JULY 1972 - JUNE 1974

Date	Launch Site	Vehicle	Experiment	Scientist	Results
25 Feb 74	PFRR	Black Brant VC	ICECAP	J. Ulwick	Success
28 Mar 74	CRR	Ute Tomahawk	Mass Spectrometer and Langmuir Probe	R. Narcisi	Success
3 Apr 74	CRR	Ute Tomahawk	Switched Mass Spectrometer Scintillation Counter/Plasma Frequency Probe	R. Narcisi	Success
3 Apr 74	CRR	Ute Tomahawk	Negative Mass Spectrometer, Langmuir Probes	R. Narcisi	Success
9 Apr 74	CRR	Ute Tomahawk	Mass Spectrometer Scintillation (Plasma Frobe)	R. Narcisi	Success
11 Apr 74	PFRR	Astrobee D	Gerdien Condenser, Impedance Probe	J. Ulwick	Failure (P)
12 Apr 74	PFRR	Astrobee D	VLF	J. Ulwick	Success
18 Apr 74	PFRR	Paiute Tomahawk	Retarded Potential E-Field, Photometer-Electrostatic Analyzer	J. Ulwick	Success
22 Apr 74	WSMR	Aerobee 170	EUV	L. Heroux	Success
29 Jun 74	WOPS	Niro	Telemetry Test (ALADDIN)	N. Rosenberg G. Best	Success
29 Jun 74	WOPS	Aerobee 170	EUV (ALADDIN)	L. Hall	Success
29 Jun 74	WOPS	Ute Tomahawk	Neutral Mass Spectrometer, E-Field (ALADDIN)	C. Philbrick	Success
29 Jun 74	WOPS	Nike Tomahawk	10"-Sphere, Photometers (ALADDIN)	L. Weeks A. Faire	Success
29 Jun 74	WOPS	Nike Tomahawk	NO, Chemical Release, Photometers (ALADDIN)	D. Golomb R. Good	Partial
30 Jun 74	WOPS	Ute Tomahawk	Ba & TMA Release (ALADDIN)	N. Rosenberg	Success
30 Jun 74	WOPS	Ute Tomahawk	Ion Mass Spectrometers (ALADDIN)	R. Narcisi	Failure (V)
30 Jun 74	WOPS	Ute Tomahawk	Ba & TMA Release (ALADDIN)	N. Rosenberg	Failure (V)
30 Jun 74	WOPS	Ute Tomahawk	Ion Mass Spectrometer (ALADDIN)	R. Narcisi	Failure (V)
30 Jun 74	WOPS	Ute Tomahawk	Na/Li Release (ALADDIN), TMA Release	N. Rosenberg	Failure (P)
30 Jun 74	WOPS	Ute Tomahawk	TMA; Hibal & Photometers (ALADDIN)	N. Rosenberg A. Faire	Success
30 Jun 74	WOPS	Nike Tomahawk	NO Release & Photometers (ALADDIN)	D. Golomb R. Good	Success
30 Jun 74	WOPS	Ute Tomahawk	TMA Release, Photometers (ALADDIN)	N. Rosenberg D. Golomb	Partial
30 Jun 74	WOPS	Paiute Tomahawk	TMA & Ba Releases, Photometers (ALADDIN)	N. Rosenberg D. Golomb R. Good	Success
30 Jun 74	WOPS	Paiute Tomahawk	7"-Falling Sphere, Photometers (ALADDIN)	A. Faire L. Weeks	Success
30 Jun 74	WOPS	Ute Tomahawk	Na & Li Releases (ALADDIN)	N. Rosenberg G. Best	Success
30 Jun 74	WOPS	Ute Tomahawk	Na/Li Release (ALADDIN)	N. Rosenberg G. Best	Success

*(V) — Vehicle
*(P) — Payload

APPENDIX C

Air Force Cambridge Research Laboratories

L. G. HANSCOM FIELD, BEDFORD, MASS.

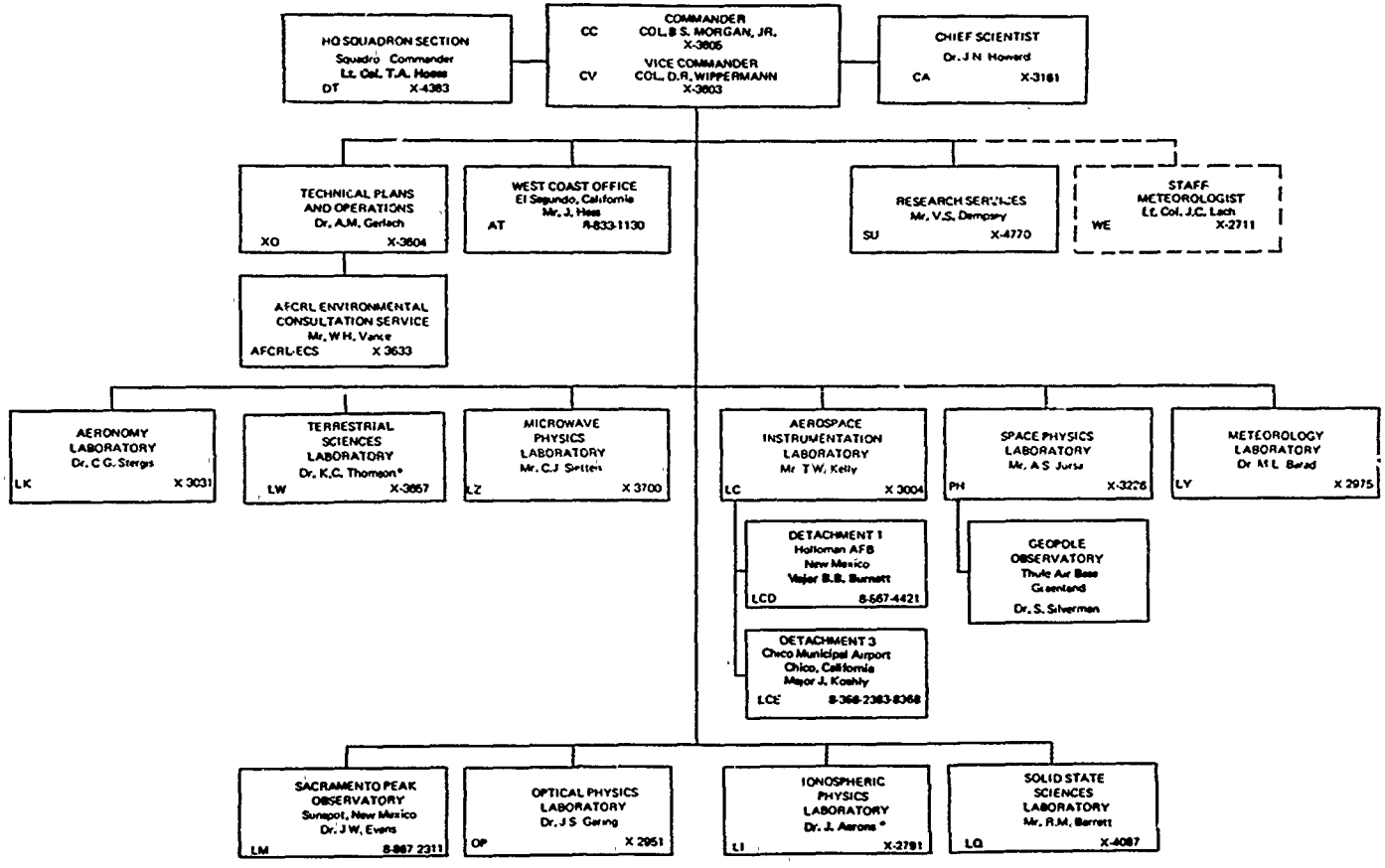

AS OF 1 MAY 1974
*ACTING

PRECEDING PAGE BLANK-NOT FILMED

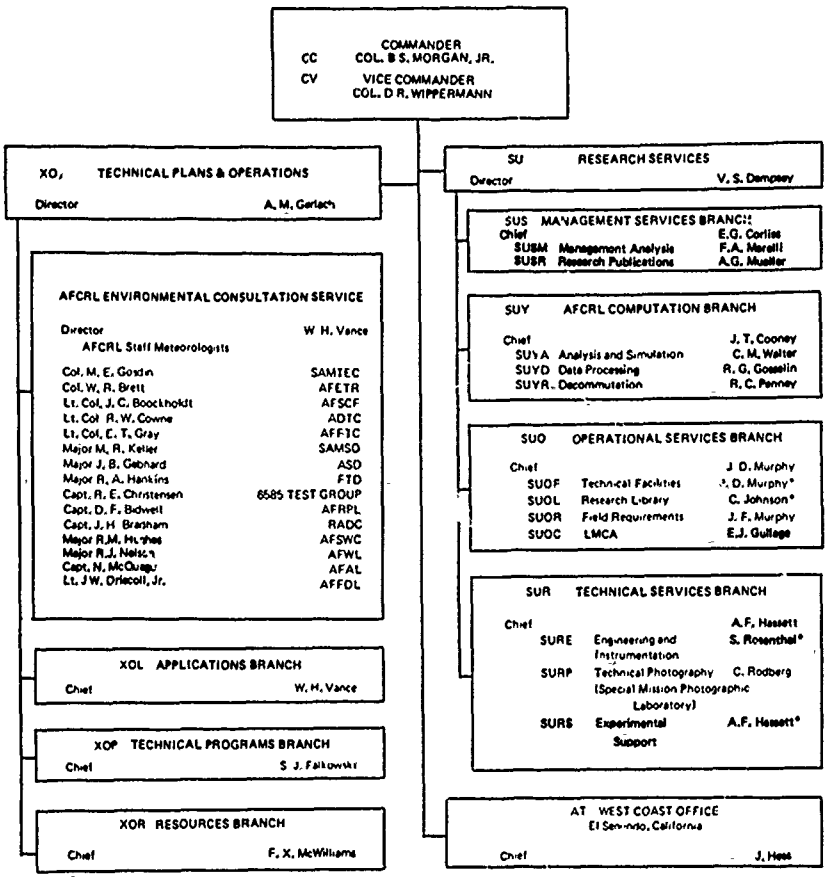

AS OF 1 MAY 1974
*ACTING

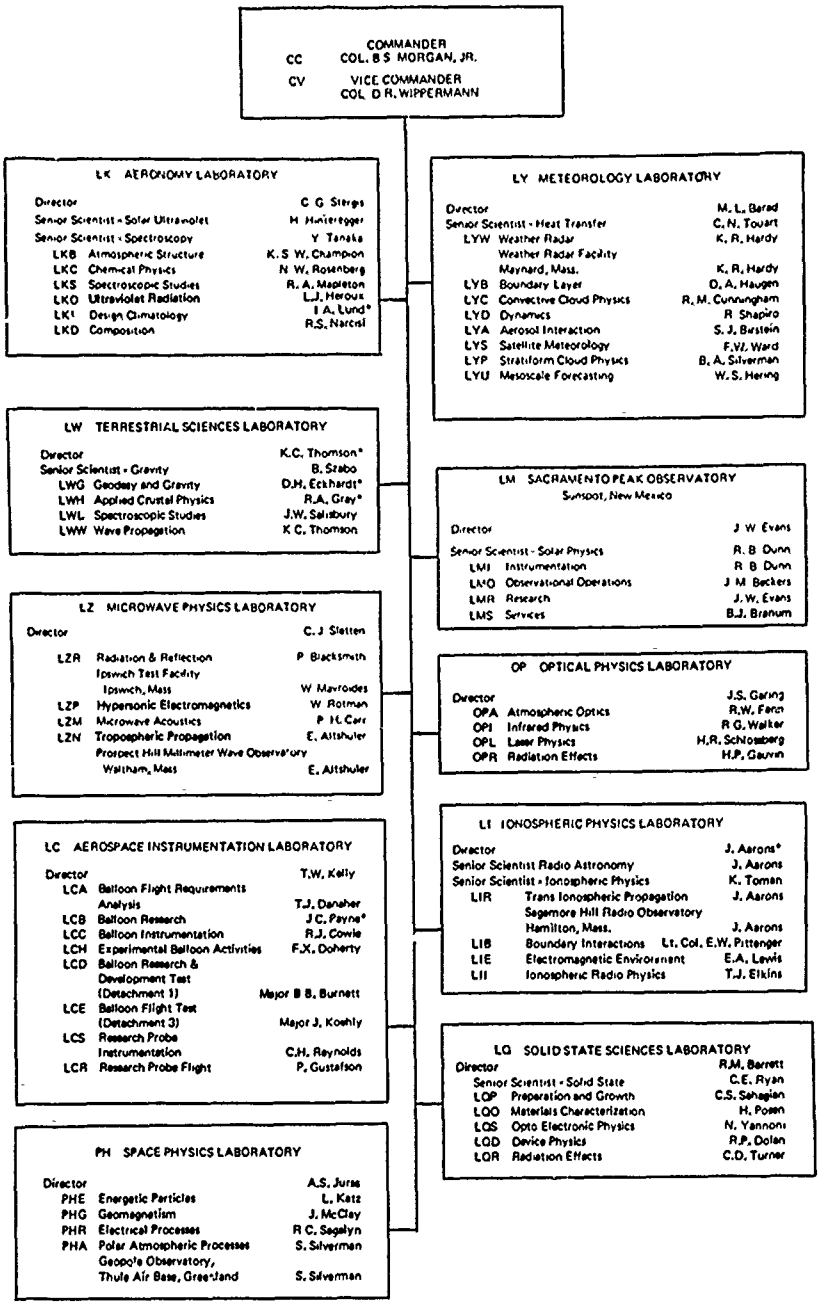

AS OF 1 MAY 1974
*ACTING

Unclassified
Security Classification

DOCUMENT CONTROL DATA - R&D

(Security classification of title, body of abstract and indexing annotation must be entered when the overall report is classified)

1. ORIGINATING ACTIVITY *(Corporate author)*
Air Force Cambridge Research Laboratories (CA)
L. G. Hanscom AFB
Bedford, Massachusetts 01731

2a. REPORT SECURITY CLASSIFICATION
Unclassified

2b. GROUP

3. REPORT TITLE
(6) AIR FORCE CAMBRIDGE RESEARCH LABORATORIES
REPORT ON RESEARCH, July 1972 - June 1974.

4. DESCRIPTIVE NOTES *(Type of report and inclusive dates)*
Scientific. Interim. July 1, 1972 through June 30, 1974

5. AUTHOR(S) *(First name, middle initial, last name)*
(10) John F. Dempsey Editor (9) Interim rept. 1 Jul 72 - 30 Jun 74

6. REPORT DATE
(11) May 1975

7a. TOTAL NO. OF PAGES
326

7b. NO. OF REFS
0

8a. CONTRACT OR GRANT NO.
N/A

b. PROJECT, TASK, WORK UNIT NOS. 9993xxxx

c. DOD ELEMENT N/A (16) AF-9993

d. DOD SUBELEMENT N/A

9a. ORIGINATOR'S REPORT NUMBER(S)
(14) AFCRL-TR-75-0288, AFCRL-SR-192

9b. OTHER REPORT NO(S) *(Any other numbers that may be assigned this report)*
Special Reports, No. 192

10. DISTRIBUTION STATEMENT
This document has been approved for public release and sale; its distribution is unlimited.

11. SUPPLEMENTARY NOTES
TECH, OTHER (12) 333 p.

12. SPONSORING MILITARY ACTIVITY
Air Force Cambridge Research Laboratories (CA)
L. G. Hanscom AFB
Bedford, Massachusetts 01731

13. ABSTRACT

This is the seventh in a series of Reports on Research at the Air Force Cambridge Research Laboratories. This report covers a two-year interval. It was written primarily for Air Force and DOD managers of research and development and more particularly for officials in Headquarters Air Force Systems Command, for the Director of Science and Technology (DL), and for the Commanders of and the Laboratories within DL. It is intended that the report will have interest to an even broader audience. For this latter audience, the report, by means of a survey discussion, attempts to relate the programs of the larger scientific field of which they are a part. The work of each of the laboratories is discussed as a separate chapter. Additionally, the report includes an introductory chapter on AFCRL management and logistic activities related to the reporting period.

DD FORM 1 NOV 65 1473

Unclassified
Security Classification

011 800 LP

PRECEDING PAGE BLANK-NOT FILMED

14. KEY WORDS	LINK A		LINK B		LINK C	
	ROLE	WT	ROLE	WT	ROLE	WT
Upper Atmosphere Physics						
Upper Atmosphere Chemistry						
Prediction of Meteorological Extremes						
Microwave Acoustics						
Millimeter Wave Propagation						
Signal Processing and Detection						
Balloon Technology						
Rocket Instrumentation						
Plasma Physics						
Energy Conversion						
Solar Plasma Dynamics						
Solar Astronomy						
Ionospheric Physics						
Trans-Ionospheric Signal Propagation						
Meteorology						
Geology						
Gravity						
Seismology						
Geodesy						
Geokinetics						
Optical Physics						
Laser Physics						
Electronic Solid State						
Radiation Damage						
Crystal Growth and Characterization						
Electromagnetic Wave Propagation						